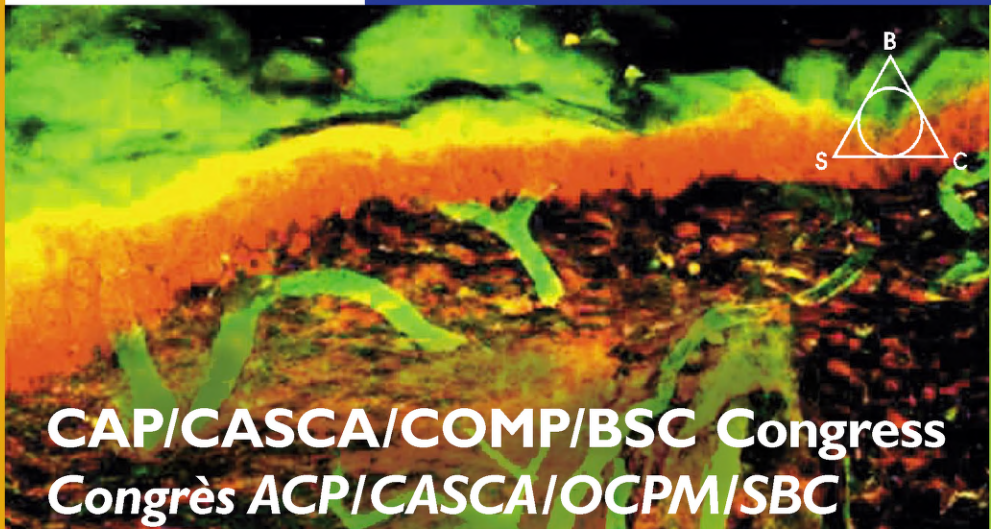
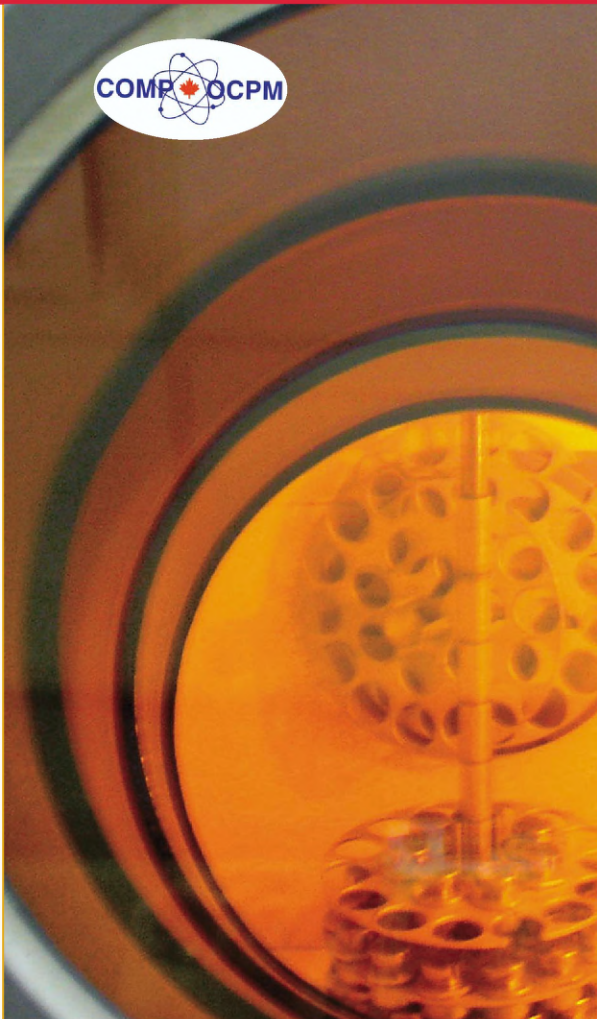




PHYSICS IN CANADA LA PHYSIQUE AU CANADA

Vol. 60 No. 3
May / June 2004
mai / juin 2004



CAP/CASCA/COMP/BSC Congress Congrès ACP/CASCA/OCPM/SBC

Hôtel Delta Hotel, Winnipeg, Manitoba
2004 June 13-16 juin 2004

Organized by the University of Manitoba
Organisé par l'Université du Manitoba

Canadian Publications Product Sales Agreement
No. 40036324 / Numéro de convention pour les
envois de publications canadiennes : 40036324

GLASSMAN HIGH VOLTAGE

DC Power Supply Solutions for Vacuum Processing Applications

For Ion Source, Electron Gun, Substrate Biasing, Magnetron Sputtering and Glow Discharge applications



KL Series 3000 watt



LH Series 5000 watt



SH Series 8-40kW



LQ Series 10,000 watt

For over 25 years, the Glassman name is synonymous with High Reliability Performance and has built its reputation as a market leader by its dedication and investment in technology development as well as after-sale customer support that is second to none in the power supply industry.

For Vacuum processing applications, Glassman's KL(3000W), LH(5000W), SH(8000W) and LQ(10kW) power supplies will meet your need for high power requirements with typical application output voltage range from 300V-10kV. All feature compact size, advanced arc management, low-stored energy and use air as the primary dielectric—**A Glassman Innovation!**

Key Features:

- Proprietary Arc Sense and Arc Quench circuitry for ultimate power supply and load protection
- High frequency technology-up to 60kHz
- Tight regulation and high stability
- Master/Slave configuration option to increase power capacity
- RS-232 serial interface option

For more information on the complete line of Glassman High Voltage power supplies, visit our website at www.glassmanhv.com or call us today at 908-638-3800.



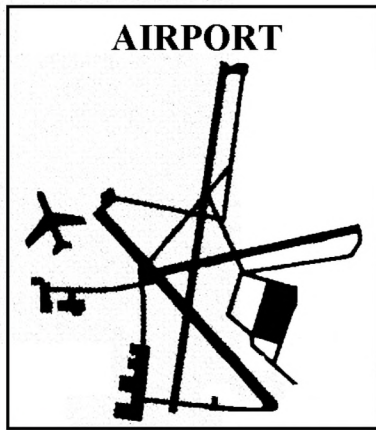
Glassman High Voltage, Inc., 124 West Main Street, PO Box 317, High Bridge, NJ 08829-0317
Phone: (908) 638-3800, FAX: (908) 638-3700

www.glassmanhv.com email: sales@glassmanhv.com

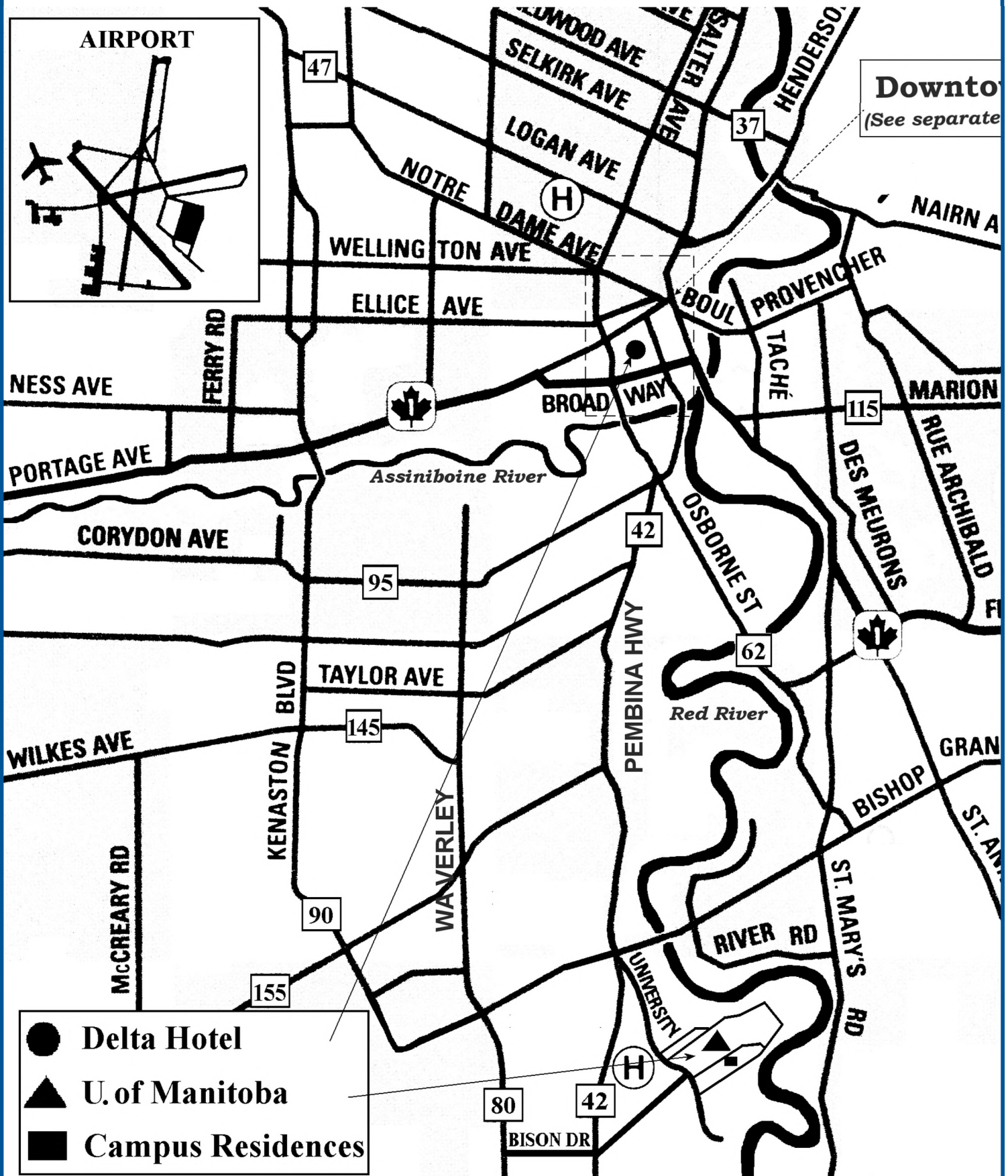
In Europe, Glassman Europe Limited (UK) +44 1256 883007, FAX: +44 1256 883017

In Asia, Glassman Japan Limited +81 45 902 9988, FAX: +81 45 902 2268

Winnipeg Map

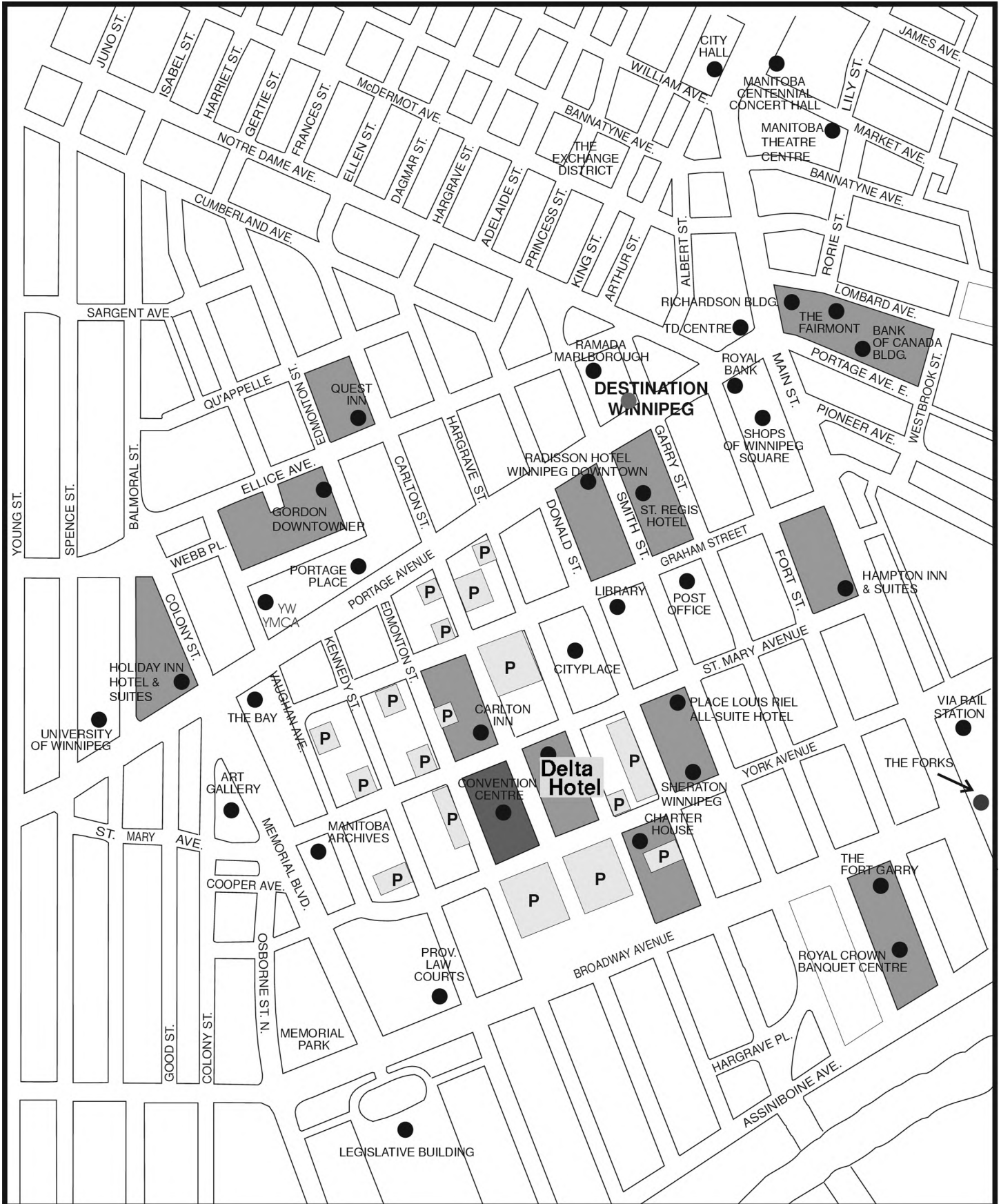


Downtown
(See separate map)



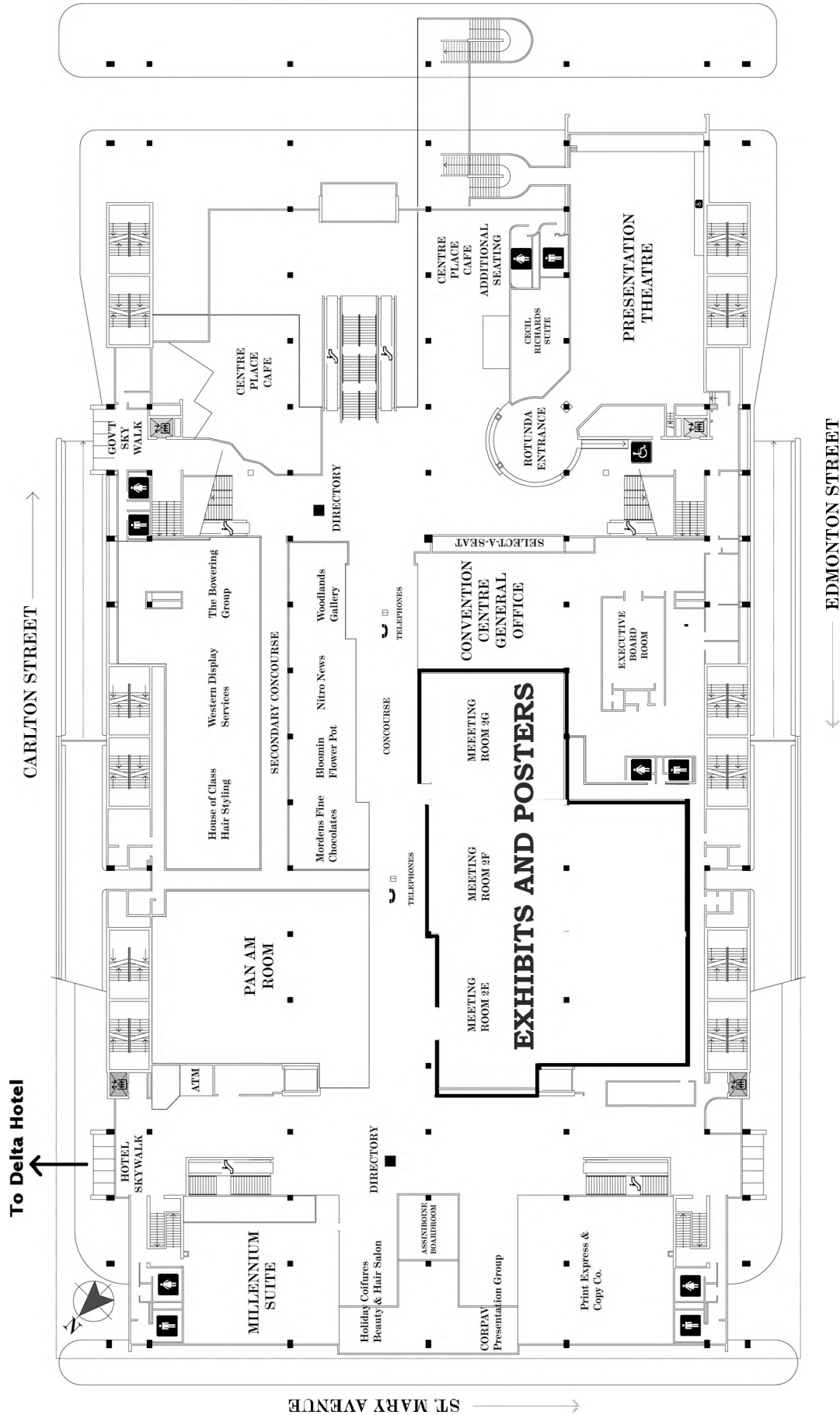
- Delta Hotel
- ▲ U. of Manitoba
- Campus Residences

Downtown Winnipeg



Winnipeg Convention Centre (Second Floor)

YORK AVENUE



ST MARY AVENUE

To Delta Hotel

CARLTON STREET

EDMONTON STREET

Delta Hotel Meeting Rooms

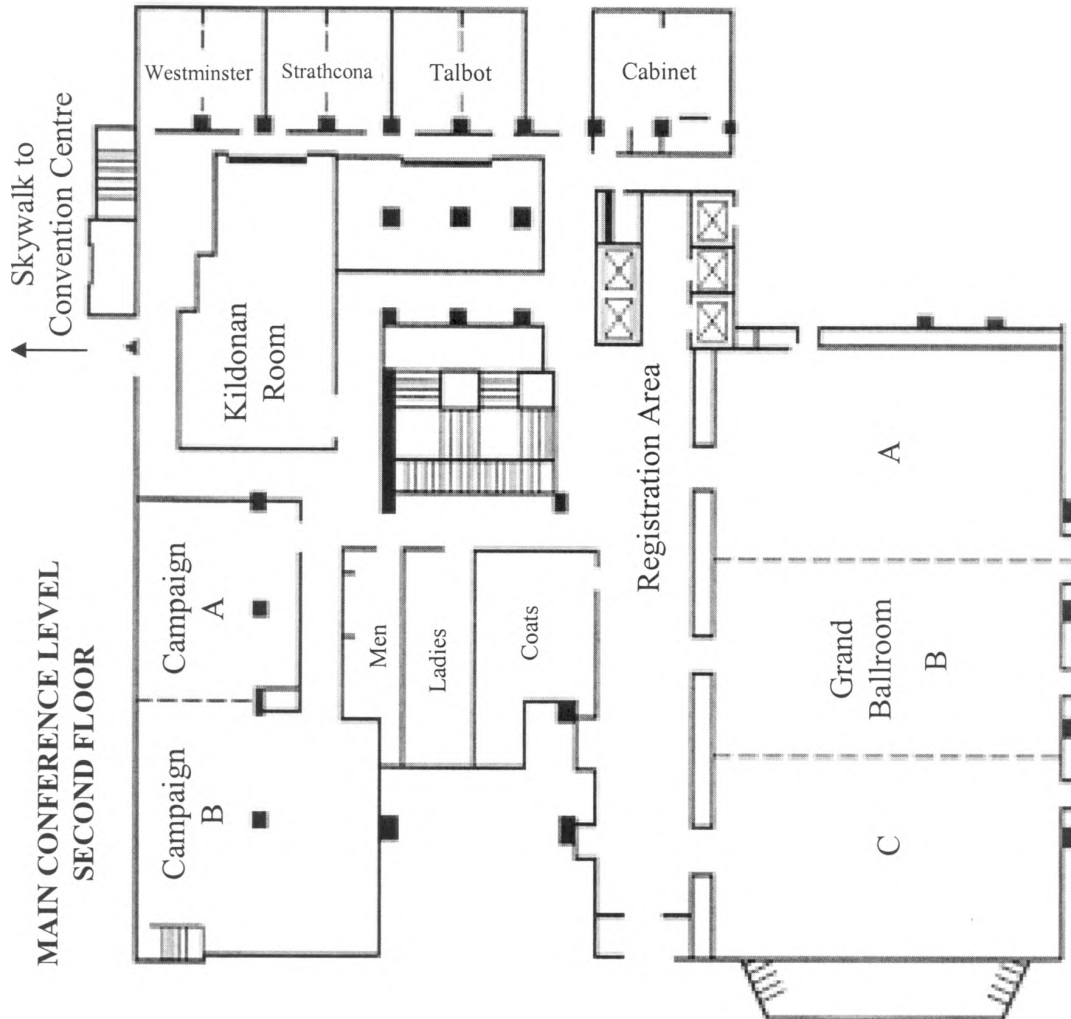
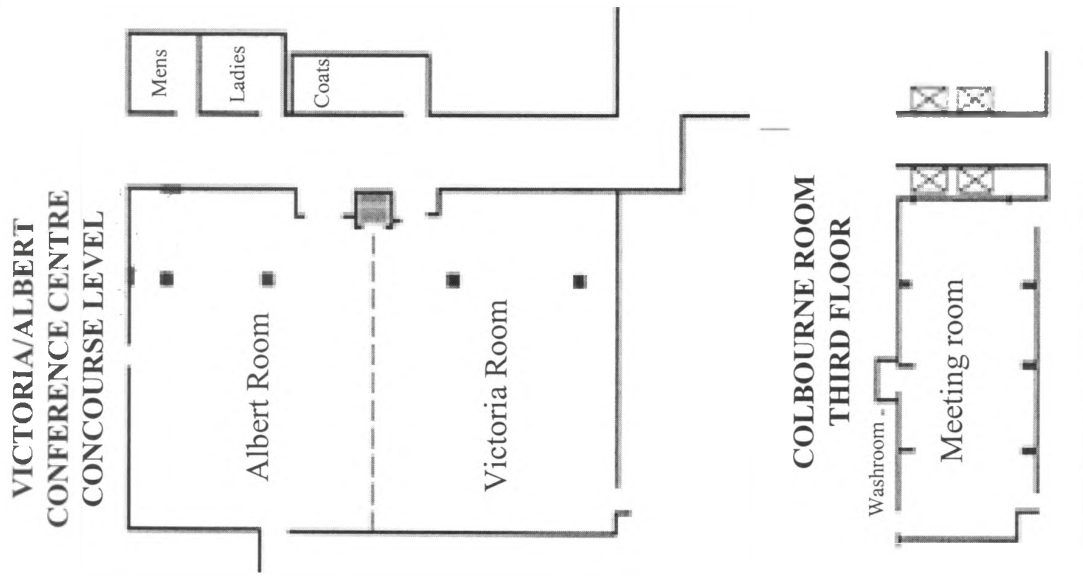




TABLE OF CONTENTS / TABLE DES MATIÈRES

| | | | |
|---|-----|--|--|
| Editorial : Tomorrow, and Tomorrow, and Tomorrow ... by J.S.C. McKee, P.Phys., Editor | 2 | 2004 CAP CONGRESS | |
| <i>Éditorial : Demain et demain et demain ...</i> par J.S.C. McKee, phys. rédacteur | 3 | CONGRÈS DE L'ACP 2004 | |
| Future CAP Conferences <i>Prochains Congrès de l'ACP</i> | 3 | Maps / Cartes | Inside Front Cover / Intérieur de la couverture avant |
| Professional Certification <i>professionnelle</i> | 4 | Technical Program Committee & Local Organizing Committee / <i>Comité du programme technique et</i> <i>Comité organisateur local</i> | 12 |
| Congratulations / <i>Félicitations</i> | 4 | Registration / <i>Inscription</i> | 13 |
| Book Review / <i>Critique de livre</i> (The Expanding World of Physics at Manitoba: A Hundred Years of Progress) | 5 | Exhibitors - Sponsors / <i>Exposants - Commanditaires</i> | 13 |
| Medallists 2004 <i>Lauréats</i> | 6 | Congress Information / <i>Renseignements sur le Congrès</i> | 14 |
| 2004 University Prize Exam Results <i>Résultats de l'examen du prix universitaire 2004</i> | 7 | Special Events / <i>Évènements spéciaux</i> | 16- 21 |
| 2003 Art of Physics Competition Winners Gagnants du Concours l'Art de la physique | 8 | Abbreviation Key / <i>Code des abréviations</i> | 22 |
| Congress Sponsors / <i>Commanditaires du Congrès</i> | 10 | Invited Speakers / <i>Conférenciers invités</i> | 23 |
| Annual General Meeting - Draft Agenda <i>Assemblée générale annuelle - Ordre du jour provisoire</i> | 19 | Congress at a Glance / <i>Sommaire du congrès</i> | 29 |
| Institutional, Sustaining, and Corporate Members <i>Membres institutionnels, de soutien et corporatifs</i> | 152 | Detailed Congress Program / <i>Programme détaillé du Congrès</i> | 32 |
| Advertisements / <i>Publicités</i> | 151 | Abstracts - Oral Sessions / <i>Résumés - Sessions orales</i> | 58 |
| | | Abstracts - Poster Sessions / <i>Résumés - Session d'affiches</i> | 127 |
| | | Author Index / <i>Index des auteurs</i> | 146 |

**Notice to
CAP Members**

Bring this free copy of the Congress issue to the Annual Congress at the Delta Hotel, Winnipeg, Manitoba. Replacement or additional copies will be available at \$10.00 each.

**Avis aux
membres de l'ACP**

Veuillez apporter cet exemplaire gratuit du programme au Congrès, à l'Hôtel Delta, Winnipeg, Manitoba. Des exemplaires de remplacement ou supplémentaires se vendront 10 \$ chaque.

Advertising Rates and Specifications (effective January 2004) can be found on the PiC website (www.cap.ca - PiC online). / *Les tarifs publicitaires et dimensions (en vigueur dès janvier 2004) se trouvent sur le site internet de La Physique au Canada (www.cap.ca - PiC Électronique).*

FRONT COVER / COUVERTURE

- CAP:** Gwyn Williams and Wei Li looking at the coldest spot in Manitoba, the dilution refrigerator in the Department of Physics and Astronomy at the University of Manitoba.
- CASCA:** The shape of this galaxy, in Stephan's Quintet, is distorted by the gravitational tug of its companions. (NASA, J. English (U.Manitoba), S. Hunsberger (PSU) and collaborators.)
- COMP:** View through the lead glass window of the shielded transfer cell during loading of the 201 cobalt-60 source capsules into the Winnipeg Gamma Knife® (Dr. Anita Berndt).
- BSC:** A laser scanning confocal microscope image of blood vessels beneath the skin of a mouse. Vessels are stained green and the surface of the skin is red, yellow and green. (Dan Dumont, University of Toronto and Sunnybrook and Women's Health Science Centre).



PHYSICS IN CANADA
LA PHYSIQUE AU CANADA

The Journal of the Canadian Association
of Physicists

La revue de l'Association canadienne des physiciens et physiciennes

ISSN 0031-9147

EDITORIAL BOARD / COMITÉ DE RÉDACTION

Editor / Rédacteur en chef

J.S.C. (Jasper) McKee, P.Phys.

Accelerator Centre, Physics Department
University of Manitoba
Winnipeg, Manitoba R3T 2N2
(204) 474-9874; Fax: (204) 474-7622
e-mail: mckee@physics.umanitoba.ca

Associate Editor / Rédactrice associée

Managing / Administration

Francine M. Ford

c/o CAP/ACP

Honorary Associate Editor / Rédacteur associé honoraire

Béla Joós, P.Phys.

Physics Department, University of Ottawa
150 Louis Pasteur Avenue
Ottawa, Ontario K1N 6N5
(613) 562-5800x6755; Fax:(613) 562-5190
e-mail: bjoos@science.uottawa.ca

Book Review Editor / Rédactrice à la critique de livres

Erin Hails

c/o CAP / ACP

Suite.Bur. 112, Imm. McDonald Bldg., Univ. of d' Ottawa,
150 Louis Pasteur, Ottawa, Ontario K1N 6N5
(403) 912-0037; Fax (403) 912-0083
e-mail: eehails@ucalgary.ca or cap@physics.uottawa.ca

Advertising Manager / Directeur de la publicité

Michael Steinitz, P. Phys.

Department of Physics

St. Francis Xavier University, P.O. Box 5000
Antigonish, Nova Scotia B2G 2W5
(902) 867-3909; Fax: (902) 867-2414
e-mail: msteinit@stfx.ca

Recording Secretary / Secrétaire d'assemblée

Rod H. Packwood, P. Phys.

Metals Technology Laboratories
E-M-R, 568 Booth Street
Ottawa, Ontario K1A 0G1
(613) 992-2288; Fax: (613) 992-8735
e-mail: packwood@magma.ca

René Roy, phys.

Département de physique, Université Laval
Cité Universitaire, Québec G1K 7P4
(418) 656-2655; Fax: (418) 656-2040
e-mail: roy@phy.ulaval.ca

David J. Lockwood, P. Phys.

Institute for Microstructural Sciences
National Research Council (M-36)
Montreal Rd., Ottawa, Ontario K1A 0R6
(613) 993-9614; Fax: (613) 993-6486
e-mail: david.lockwood@nrc.ca

Henry P. Schreimer

School of Information Technology and Engineering
University of Ottawa, 800 King Edward Ave., Room 3-034
Ottawa, Ontario K1N 6N5
(613) 562-5800 x2203; Fax: (613) 562-5664
e-mail: hschreim@site.uottawa.ca

ANNUAL SUBSCRIPTION / ABONNEMENT ANNUEL:

\$40.00 Cdn + GST or HST (Cdn addresses),

\$40.00 US (US addresses)

\$45.00 US (other/foreign addresses)

**Advertising, Subscriptions, Change of Address/
Publicité, abonnement, changement d'adresse:**

Canadian Association of Physicists /
Association canadienne des physiciens et physiciennes,
Suite/Bureau 112, Imm. McDonald Bldg., Univ. of d' Ottawa,
150 Louis Pasteur, Ottawa, Ontario K1N 6N5
Phone/ Tél: (613) 562-5614; Fax/Télex: (613) 562-5615
e-mail/courriel: CAP@physics.uottawa.ca
Website/Internet: http://www.cap.ca

Canadian Publication Product Sales Agreement No. 0484202/
Numéro de convention pour les envois de publications canadiennes:
0484202

© 2004 CAP/ACP

All rights reserved / Tous droits de reproduction réservés

WWW.CAP.CA

(select PIC online / Option : PiC Électronique)

-- EDITORIAL / ÉDITORIAL -- TOMORROW, AND TOMORROW, AND TOMORROW... DEMAIN ET DEMAIN ET DEMAIN

Science inspires us with a feeling of hopefulness and infinite possibility...the human spirit applied in the tradition of science will find a way toward the objective. Science shows that it is possible to foresee and to plan...

– Isodor I. Rabi, "Faith in Science,"

Atlantic Monthly, 187 28-30 (January 1951)

The year, 2004, sees the 100th anniversary of both the appointment of the first Professor of Physics, and the birth of the Faculty of Science at the University of Manitoba. This, the oldest university in Western Canada, is hosting the Annual Congress of the Canadian Association of Physicists from 13th to 16th June, in Winnipeg, and at this time the Department of Physics and Astronomy will look proudly at a completed century of research and teaching; at the quality of physicists it has so far produced, and at the launching pad for further discovery it has already built.

The CAP Congress gives an opportunity for physicists across Canada to share in local celebrations, and to develop further the dissemination of new knowledge, that is the life blood of the practising research scientist. Some years ago, Richard Feynman wrote, in relation to the definition of time, "it is what happens when nothing else happens", but whether this satisfies the average physicist, indicating as it does that 'time' is the distance between events, I do not know. Perhaps a corollary might be the statement [mine], that if the physicist is aware of the passage of time, he or she is not working hard enough at the business of discovery. In the words of Ralph Hodgson (1871-1962):

Time you old gypsy man,
Will you not stay,
Put up your caravan,
Just for one day?

Scientists should run out of time long before they run out of ideas!

Of course, the cost of carrying out experimental science has burgeoned over the years, and as a result scientific research and development is expensive. But as an eminent Canadian medical scientist once remarked over fifty years ago, "if you think medical research is expensive, try disease!" Not much of a choice one might think! And now, in 2004, it seems that the intimate relationship of education and research to technology, discovery, innovation, and the national economy seems suddenly to be accepted by scientists, economists and politicians alike, which is encouraging to all of us who require financial support and public enthusiasm for our success.

A hundred years ago, the slogans around scientific laboratories were restraining in the extreme. Notices trumpeting the fact that "Faraday did it on less" or Rutherford's dictum that "we haven't got the money so we have got to think", implied that rational thought should in the end solve most problems. And, in the past it sometimes did. There was often vision and imagination that generated the solution to an otherwise intractable problem, with minimal cost to scientist or institution. I think of H. Helmholtz, physicist, physiologist and psychologist, discounting the widely held belief that the speed of the nervous impulse was many times that of light, and measuring it at a party

The contents of this journal, including the views expressed above, do not necessarily represent the views or policies of the Canadian Association of Physicists. *Le contenu de cette revue, ainsi que les opinions exprimées ci-dessus, ne représentent pas nécessairement les opinions et les politiques de l'Association canadienne des physiciens et des physiciennes.*

with friends and colleagues at which using a smoked drum as a timing device he showed it to be less than that of sound. The impossibility of this technique for measuring such a phenomenon, was so well "established" by J. Müller and others that no one even thought to try it. Helmholtz did! Then at a later time, but still prior to the discovery of the electron, measurement of the size of an atom or molecule was believed impossible by almost the entire scientific community. Lord Kelvin, 'en passant' in his Baltimore lectures however suggested that a drop of oil free to flow on a flat liquid surface could spread until the pancake of oil was essentially a mere atom or molecule thick. Then, by measuring the area of the drop by a planimeter, and knowing the volume of the drop of oil, a simple calculation could yield the dimension of a molecule approximately. So, the impossible becomes possible, by rational thought and simple observation alone.

And in the field of innovation, we have the Slinky, an anti-vibration device invented by Richard James to stabilise cargo ships. It was dramatically ineffective at its proper task, but when his wife Betty observed the fact that the cylinder of coiled wire, when placed on an upper shelf in the library in their home, would roll, top over bottom and dismount the shelves to the floor, she thought to herself, here is a fine 'toy', and a means of demonstrating longitudinal wave motion. The company started 60 years ago is still functioning as a tribute to innovation and the entrepreneurial spirit that can take advantage of simple scientific observation.

In 2004, however, the climate for the funding of scientific research is now much more favourable than a century ago. Research is highly competitive, and an all-consuming activity, and physics as a discipline is changing rapidly, while still sustaining the established breadth of the subject.

Larger and larger microscopes are required for studies of the nano- and atto-scales of matter. Biophysics, the subject of a recent theme issue of *Physics in Canada*, now relates to biosystems at the molecular level, and many of the established models of nuclear and condensed matter physics are finding value in this new arena. Indeed, thinking of strands of DNA as electrical conductors, semiconductors or superconductors would have seemed unlikely, if not bizarre, only a few years ago. But physics, like time, moves forward, and the next hundred years will amaze even those scientists who are a part of it.

Physics is fun, so let us enjoy it to the full. Have a great Congress!

Jasper McKee, P.Phys.
Editor, *Physics in Canada*

NOTE: For your entertainment, the Editor has included the following exchange of comments between himself and two Editorial Board members after reading the May/June editorial.

Member one:

I enjoyed reading your editorial as usual. I was amused at the perhaps unintended pun towards the end of the editorial:

"Larger and larger microscopes are required for studies of the nano- and atto-scales of matter." Should we not call them nanoscopes or attoscopes? Actually as we know "micro" can either mean 10^{-6} of whatever, or simply "very small", so it is only a perception of obsolescence.

Editor:

Since the first photograph of a flea by Robert Hooke, equipment used to illuminate an object with smaller and smaller wavelength radiation has grown in scale inversely as the scale of the object itself; i.e. from fleas through atoms to nuclei, nucleons and now gluons?

Member two:

... walk into Paul Corkum's lab at the Steacie Institute and check out the size of his "attoscope"!

The comments of readers on this editorial are more than welcome.

DEMAIN ET DEMAIN ET DEMAIN....

La science nous inspire un sentiment d'espoir et de possibilités infinies...l'esprit humain impliqué dans la tradition scientifique trouvera son chemin vers son objectif. La science montre qu'il est possible de prévoir et de planifier...

- Isodor I. Rabi, "Faith in Science,"
Atlantic Monthly, 187 28-30 (janvier 1951)

L'année 2004 correspond au 100^e anniversaire de l'engagement du premier professeur de physique et la naissance de la faculté des sciences de l'université du Manitoba. Cette université, la plus ancienne de l'ouest canadien, est l'hôte du congrès annuel de l'Association canadienne des physiciens et physiciennes qui se tiendra du 13 au 16 juin à Winnipeg; durant cette même période, le département de physique et d'astronomie fêtera fièrement un siècle complet de recherche et d'enseignement, la qualité des physiciens qu'il a formés jusqu'à présent et les installations de lancement de découvertes ultérieures qu'il a déjà bâties.

Le congrès de l'ACP fournit l'occasion aux physiciens du Canada de prendre part à des célébrations locales et de développer davantage la diffusion des connaissances nouvelles, ce qui est le principe vital des scientifiques pratiquants. Il y a quelques années, Richard Feynman a écrit au sujet de la définition du temps : " c'est ce qui se passe lorsque rien d'autre ne se passe ", indiquant par là que le " temps " est la distance qui sépare des événements; mais je ne sais pas si cela satisfait le physicien moyen. Peut être qu'un corollaire (le mien) pourrait être que si le physicien est sensible au passage du temps, il ou elle ne travaille pas assez à faire des découvertes. D'après Ralph Hodgson (1871-1962) :

Vieux nomade Temps,
Ne resterez-vous pas,
Ne parquerez-vous pas votre roulotte,
Juste pendant une journée?

Les scientifiques devraient manquer de temps bien avant qu'ils ne manquent d'idées!

Bien sûr, le coût de la science expérimentale a beaucoup augmenté avec les années; en conséquence, la recherche et le développement scientifiques sont onéreux. Mais un scientifique médical canadien éminent a fait la remarque suivante il y a plus de cinquante ans : " si vous croyez que la recherche médicale est onéreuse, que penser de celle de la

maladie! " On pourrait penser que l'on n'a pas vraiment beaucoup de choix! Et aujourd'hui, en 2004, il semble que la relation intime entre l'éducation et la recherche d'une part, et la technologie, les découvertes, l'innovation et l'économie nationale d'autre part soit soudainement acceptée également par les scientifiques, les économistes et les politiciens, ce qui est très encourageant pour nous tous qui avons besoin d'un soutien financier et l'appui du public pour nos réussites.

Il y a cent ans, les slogans dans les laboratoires scientifiques étaient très limitatifs. Des remarques claironnant le fait que " Faraday l'a fait avec moins " ou le dicton de Rutherford disant " si nous n'avons pas d'argent, il faut que nous réfléchissions " impliquent que le raisonnement peut finir par résoudre la plupart des problèmes. Et, dans le passé, cela a été parfois vrai. Souvent, la vision et l'imagination ont généré une solution à une question autrement intraitable avec un coût minimal pour le scientifique ou l'institution. Je pense à H. Helmholtz, physicien, physiologiste et psychologue, remettant en cause l'idée largement répandue selon laquelle la vitesse de l'influx nerveux était égale à plusieurs fois la vitesse de la lumière et la mesurant lors d'une fête avec des amis et des collègues à laquelle il a utilisé un cylindre fumé comme chronomètre pour montrer qu'elle était en fait inférieure à celle du son. L'impossibilité d'utiliser cette technique pour mesurer un tel phénomène était si bien " établie " par J. Müller et autres que personne n'a même pensé à l'essayer. Helmholtz l'a fait! Plus tard, mais toujours avant la découverte de l'électron, des mesures de la taille d'un atome ou d'une molécule étaient soit-disant impossibles d'après la presque totalité de la communauté scientifique. Pendant des conférences tenues à Baltimore, Lord Kelvin a suggéré en passant qu'une goutte d'huile libre de flotter sur une surface plane d'un liquide pourrait s'étendre jusqu'à ce que la couche d'huile atteigne l'épaisseur d'un atome ou d'une molécule. Ensuite, en mesurant la surface de la goutte au moyen d'un planimètre et en connaissant son volume, un simple calcul pourrait conduire à la dimension approximative d'une molécule. Ainsi, l'impossible devient possible grâce à un raisonnement et une simple observation.

Et dans le domaine de l'innovation, nous avons le Slinky, dispositif antivibration inventé par Richard James pour stabiliser les navires de marchandises. Il était particulièrement inefficace pour cela, mais sa femme Betty a observé le fait que le cylindre de fil bobiné descendait de l'étagère supérieure de leur bibliothèque jusqu'au sol en basculant; elle s'est alors dit qu'il s'agissait là d'un beau jouet et d'un moyen de démontrer le déplacement d'une onde longitudinale. La compagnie fondée il y a 60 ans fonctionne toujours comme tribut à l'innovation et à l'esprit entrepreneurial qui peut tirer profit d'une simple observation scientifique. Toutefois, en 2004, le climat relatif au financement de la recherche scientifique est beaucoup plus favorable qu'il y a un siècle. La recherche est très concurrentielle et une activité exigeante, et la physique, en tant que discipline, évolue rapidement tout en continuant à couvrir l'ampleur établie du sujet.

Des microscopes de plus en plus gros sont nécessaires pour l'étude à l'échelle nanométrique et atométrique de la matière. La biophysique, sujet d'une édition récente de *La physique au Canada*, s'intéresse maintenant au niveau

moléculaire des biosystèmes, et un grand nombre de modèles établis de la physique nucléaire et de la matière condensée trouvent une application dans ce nouveau domaine. Finalement, penser à des brins d'ADN comme étant des conducteurs électriques, les semiconducteurs ou les supraconducteurs aurait semblé improbable, sinon bizarre, il y a quelques années seulement. Mais la physique, comme le temps, avance et les cents prochaines années étonneront même les scientifiques qui les auront vécues.

La physique est joyeuse; profitons-en pleinement. Je vous souhaite un bon congrès!

J. S. C. McKee, phys.
Éditeur, *La physique au Canada*

REMARQUE : Pour votre divertissement, l'éditeur a inclus l'échange de commentaires suivants entre lui et deux membres du bureau éditorial après la lecture de l'éditorial de mai/juin.

Membre un :

Comme d'habitude, j'ai eu du plaisir à lire votre éditorial. Je me suis amusé du calembour peut-être imprévu vers la fin de l'éditorial : " Des microscopes de plus en plus gros sont nécessaires pour l'étude à l'échelle nanométrique et atométrique de la matière. " Devrions-nous les appeler désormais des nanoscopes ou des attoscopes? En fait, micro peut signifier 10^{-6} ou simplement très petit, de sorte qu'il ne s'agit que d'une perception de la désuétude.

Éditeur :

Depuis la première photographie d'une mouche réalisée par Robert Hooke, l'échelle du matériel utilisé pour éclairer un objet à l'aide de rayons de longueur d'onde de plus en plus petite a augmentée inversement à l'échelle de l'objet lui-même, c-à-d de la mouche aux atomes et aux noyaux, nucléons et maintenant gluons.

Membre deux :

... marcher dans le laboratoire de Paul Corkum à l'Institut Steacie et jeter un coup d'œil sur la dimension de son " attoscope "!

Nous accueillons les commentaires de nos lecteurs au sujet de cet éditorial.

NOTE: *Le genre masculin n'a été utilisé que pour alléger le texte.*

FUTURE CAP CONFERENCES PROCHAINS CONGRÈS DE L'ACP

Congrès annuel 2005 Annual Congress,
June 5 - 8, 2005
University of British Columbia / Université de la Colombie
Britannique, Vancouver, BC

Congrès annuel 2006 Annual Congress,
June 11 - 14 juin, 2006 (tentative)
Université Brock University, St. Catharines, ON

WWW.CAP.CA

PROFESSIONAL CERTIFICATION *PROFESSIONNELLE*

CONGRATULATIONS TO OUR NEW LICENSEES

We are pleased to announce that 1 additional licence has been granted to :

W. James Slater

Details regarding the certification process, as well as all forms required to apply for certification, can be found in the "Professional Certification" section of <http://www.cap.ca>.

FÉLICITATIONS À NOS NOUVEAUX LICENCIÉS

Il nous fait plaisir de vous signaler que l'ACP a octroyé 1 nouveau licence à :

L'information relative au processus de certification, ainsi que les formulaires requis, sont disponibles sous la rubrique "Certification professionnelle" du site Internet de l'ACP qui se lit ainsi : <http://www.cap.ca>.

CONGRATULATIONS / FÉLICITATIONS

KILLAM RESEARCH FELLOWSHIPS

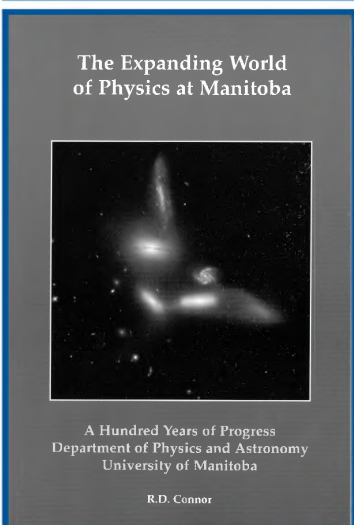
This year, only nine new Killam Research Fellowships were awarded. Of these, two went to physicists -- **Mike Thewalt, SFU** (Redefining the limits of semiconductor spectroscopy) and **Hong Guo, McGill U.** (Multi-scale modelling for nonoelectronic devices). Congratulations to both. This prestigious award brings funding to their universities to

cover two years of complete teaching and administrative relief so that Drs. Thewalt and Guo can focus on their proposed reeseach.

APS FELLOWSHIP

At the March APS Meeting, Dr. André Longtin, U. Ottawa, received an APS Fellowship. His citation was presented to him by the incoming Chair of the APS Division of Biological Physics, Denis Rousseau.

BOOK REVIEW / CRITIQUE DE LIVRE



"THE EXPANDING WORLD OF PHYSICS AT MANITOBA: A HUNDRED YEARS OF PROGRESS", DEPARTMENT OF PHYSICS AND ASTRONOMY, UNIVERSITY OF MANITOBA.

A history of the Department of Physics and Astronomy, University of Manitoba, written by Robin Connor, Dean Emeritus of Science, has been published and will be available for purchase at the 2004 Congress in Winnipeg. This book celebrates 100 years of 'The Expanding World of Physics at Manitoba' and sells for 20\$ Canadian, plus GST. Copies can also be obtained from Wanda Klassen at the Department of Physics and Astronomy Office (phone 204 474 9817); the University Bookstore (phone 204 474 8321), or McNally Robinson Booksellers (phone 204 475 0483). A book review appears below.

Une histoire du département de physique et d'astronomie de l'Université du Manitoba, écrite par Robin Connor, doyen émérite des sciences, a été publiée et pourra être achetée au congrès de Winnipeg. Ce livre célèbre 100 ans de l' "Expansion du monde de la physique au Manitoba"; son prix est de 20 \$ canadien plus la TPS. Des copies sont aussi disponibles auprès de Wanda Klassen au bureau du département de physique et d'astronomie (tél. : (204) 474 9817), à la librairie de l'Université (tél. : (204) 474 8321) ou chez McNally Robinson Booksellers (tél. : (204) 475 0483). Voir la critique du livre ci-dessous.

BOOK REVIEW / CRITIQUE DE LIVRE

"The Expanding World of Physics At Manitoba: A Hundred Years of Progress", Department of Physics and Astronomy, University of Manitoba.

by R.D. Connor, Professor Emeritus (Physics), Published by Department of Physics and Astronomy, University of Manitoba, ISBN1-895035-10-4; Soft cover 235 pages

The prologue describes the pre-history of the University and the persons engaged in its creation - literally from scratch to form the basis for a modern, comprehensive institution. The body of the text comprises six chapters; I through IV cover the growth of the Physics Department via the lives and endeavours of the staff from 1904 up until the present day. Chapter V covers the work of the major groups in the Department and VI, Accolades, outlines its fine record of accomplishment and service. Endnotes and a short biography of Prof. Connor round out the volume.

Enough of statistics, this is a splendid book, beautifully written, informative without ever being boring. Even the Endnotes are worth going through. The lives of the Physicists that were and are the Department are drawn with good humour and kindness. As for the Physics in question, time and again, ideas at the fore front of science are introduced and the reader carefully led through the general notions so as not to lose that sense of excitement that is the core attraction of the Science.

Half a million years ago as Homo sapiens' cousins first sorted through fallen branches for suitable weapons, the smarter ones undoubtedly checked the "heft" of their choice before trying it out on the nearest creature. The "Heft" test still works, even with your eyes shut, even on books. This volume feels good in your hand. The weight says that a good quality paper has been used, and the glossy finish promises, and delivers, a fine illustrated cover.

In all an excellent record of the Department's first 100 years.

Dr. R.H. Packwood, Ottawa, Ontario

Canadian Association of Physicists
Association canadienne des physiciens et physiciennes

MEDALLISTS 2004 LAURÉATS



CAP Medal for Achievement in Physics
Médaille de l'ACP pour contributions exceptionnelles en physique

Michael Thewalt
Simon Fraser University



CAP/INO Medal for Outstanding Achievement in Applied Photonics
Médaille de l'ACP-INO pour contributions exceptionnelles en photonique appliquée

Nicolas Jaeger
University of British Columbia



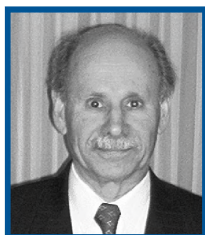
Herzberg Medal
Médaille Herzberg

Victoria Kaspi
McGill University



CAP/CRM Prize in Theoretical and Mathematical Physics
Prix ACP-CRM en physique théorique et mathématique

Jiri Patera
CRM, Université de Montréal



CAP Medal for Excellence in Teaching Undergraduate Physics
Médaille de l'ACP pour l'excellence en enseignement de la physique au premier cycle

Helmy Sherif
University of Alberta



CAP/COMP Peter Kirkby Memorial Medal for Outstanding Service to Canadian Physics
Médaille commémorative Peter Kirkby de l'ACP/OCPM pour services exceptionnels à la physique au Canada

Robert C. Barber
University of Manitoba



CAP-DCMMP Brockhouse Medal
Médaille Brockhouse de l'ACP-DPMCM

Michael Thewalt
Simon Fraser University

Canadian Astronomical Society / Société canadienne d'astronomie

MEDALLISTS 2004 LAURÉATS



Carlyle S. Beals Award / Priz Carlyle S. Beals

Ernest R. Seaquist
University of Toronto



CASCA-RAS J.S. Plaskett Medal / Médaille J.S. Plaskett de la CASCA-SRA

Jo-Anne C. Brown
University of Calgary



We are pleased to note that, in 2004, **Helen Sawyer Hogg** was inducted into the Canadian Science Hall of Fame, and was named a Great Teacher at the University of Toronto.

Canadian Association of Physicists
Association canadienne des physiciens et physiciennes

PRIZE WINNERS

University Prize Exam Results 2004 Résultats de l'examen du prix universitaire

101 students from 23 post-secondary institutions competed this year. The exam was administered by members of the Physics Department of the University of New Brunswick. The names of the first, second and third prize winners are shown, followed by the fourth to tenth ranking marks.

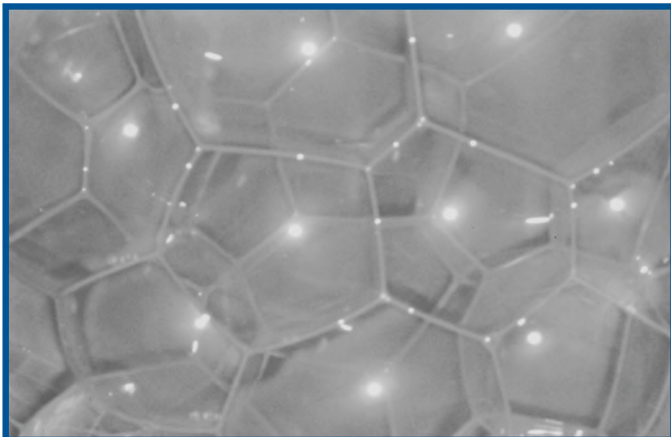
| | | | |
|----------------------------|-------------------------------------|---|-----------|
| Gary Goldstein | First Prize / Premier Prix | Univ. of Toronto / Univ. de Toronto | |
| Nicholas Gutenberg | Second Prize / Deuxième Prix | McGill University / Université McGill | |
| David Press | Third Prize / Troisième Prix | Simon Fraser University / Université Simon Fraser | |
| 4. Robert Barrington Leigh | U.Toronto | 8. Tudor Costin | UBC |
| 4. Benjamin Wilson | U.Saskatchewan | 9. Matthew Lightman | York U. |
| 6. Michael Garrett | U.Toronto | 10. Stephen Green | U.Toronto |
| 7. Rob Pitcairn | U. Manitoba | | |

TOP STUDENT IN EACH UNIVERSITY

| | | | |
|----------------------------------|---------------------|---------------------------------------|-------------------------|
| Acadia University | Aaryn Tonita | University of Lethbridge | Steven Horn |
| Bishop's University | Edward Wilson-Ewing | University of Manitoba | Rob Pitcairn |
| Carleton University | Artur Kochermin | Université de Moncton | did not participate |
| Concordia University | did not participate | Université de Montreal | Isabeau Prémont-Schwarz |
| Dalhousie University | James Cordes | University of New Brunswick | James Rioux |
| Ecole Polytechnique | did not participate | University of Northern B.C. | did not participate |
| Lakehead University | did not participate | University of Ottawa | did not participate |
| Laurentian University | Chris Pagnutti | University of Prince Edward Island | did not participate |
| McGill University | Nicholas Gutenberg | Université de Québec à Chicoutimi | did not participate |
| McMaster University | Andrew Lohn | Université de Québec à Montréal | did not participate |
| Memorial University of NFLD | did not participate | Université de Québec à Rimouski | did not participate |
| Mount Allison University | Jean-Marc Samson | Université de Québec à Trois-Rivières | did not participate |
| Queen's University | Martin Koslowsky | University of Regina | Abram Krislock |
| Royal Military College of Canada | did not participate | University of Saskatchewan | Benjamin Wilson |
| Saint Francis Xavier University | Pat Clancy | Université de Sherbrooke | did not participate |
| Saint Mary's University | did not participate | University of Toronto | Garry Goldstein |
| Simon Fraser University | David Press | University of Victoria | Daniel Roberge |
| Trent University | Tam Nhan | University of Waterloo | Michael Garrett |
| University of Alberta | Adam Rupp | University of Western Ontario | did not participate |
| University of British Columbia | Tudor Costin | University of Windsor | did not participate |
| University of Calgary | did not participate | University of Winnipeg | did not participate |
| University of Guelph | did not participate | Wilfrid Laurier University | did not participate |
| Université Laval | did not participate | York University | Matthew Lightman |

2003 ART OF PHYSICS COMPETITION WINNERS GAGNANTS DU CONCOURS L'ART DE LA PHYSIQUE 2003

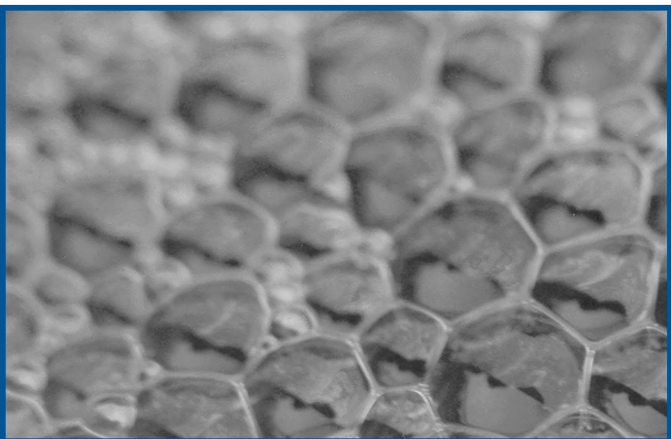
Class Project / Projet de classe



1st Prize - 1^{ier} Prix

“Kaleidoscopic Bubbles” by Matthew Kostanecki
(submitted by St. Elizabeth CHS, Toronto, Ontario)

In a kaleidoscope of orange coloured milk bubbles, it seems at first glance that there are an infinite variety of configurations that can be formed by joining milk bubbles. However, this is not the case. In reality, there are only 2 ways that milk bubbles, or any other bubbles, can physically join. When surfaces meet along curves or when curves and surfaces meet at ponts, they do so at equal angles. When three surfaces meet along a curve, they do so at an angle of 120° with respect to one another. When 4 curves meet at a point, they do so at angles of 109.47° . These principles and basic rules are credited to Frederick Almgren, Jr., and Jean E. Taylor.



2nd Prize - 2^{ième} Prix

“Thin-Film Effect” by Daven Hughes
(submitted by Fredericton High School, New Brunswick)

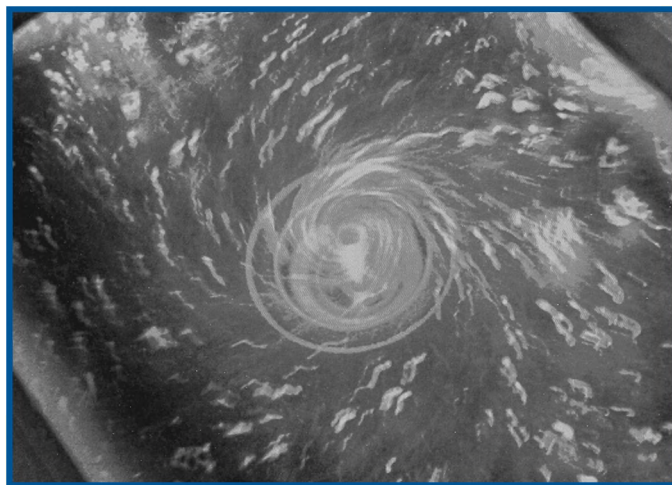
The thin-film effect is the product of a very thin layer of liquid that distorts reflected light waves. The distortion is due to the phase difference of the light waves between the outer and inner surfaces of the liquid. The thickness of the film determines the colour of the effect. Since red waves are the longest (about 700 nm), and blue waves shortest (about 400 nm), the thinner layer of liquid will be blue end of the light spectrum, the thicker layer to the red end of the spectrum. Bubbles exhibit the thin-film effect very well. All bubbles have some thickness of water which makes up their dome shape, but sometimes the surface does not noticeably diffract light into different colours. This is because the layer is either too thick or too thin, rendering infrared or ultraviolet wavelengths in the diffraction. Upon creation of the bubble, the diffracted light is visible because the layer is too thick (diffracting infrared). Over a short period of time, the layer of liquid evaporates and the diffracted wavelengths become visible. During the life of a bubble, the diffracted light colour will progress from infrared to visible ultraviolet. In my photograph the bubbles are at the right stage to diffract visible light.

High School Individual / Individuel, école secondaire

1st Prize - 1^{ier} Prix

“Vortex in a Sink” by Ian Liu
of St. Elizabeth CHS, Toronto, Ontario

This is a picture of biodegradable hairspray, illuminated by black light, flowing counterclockwise down a standard sink drain. It is believed that Coriolis force was responsible for the counterclockwise rotation of fluids in sink drains in the Northern hemisphere and clockwise rotation in the Southern Hemisphere. However, information that contradicts this belief is being presented by various sources. It is being suggested that the rotational motion of the fluids is due to the way the fluid filled the sink and that the Coriolis force is too weak to be a significant factor in causing a very small body of water to rotate in a particular direction. In several experimental trials where a rubber hose was used to direct the water flow while filling the sink, the direction of drainage was observed to be the same as the direction of filling. This suggests that the micro influences within the sink environment have a greater effect than the Coriolis force on the fluid body.

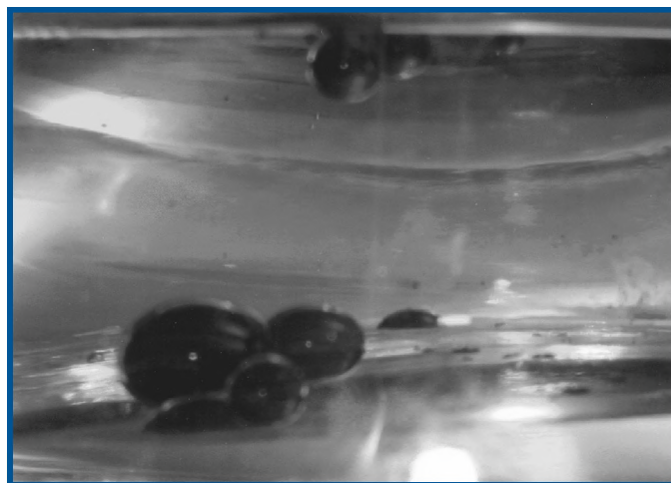


Honourable Mention / Mention honorable

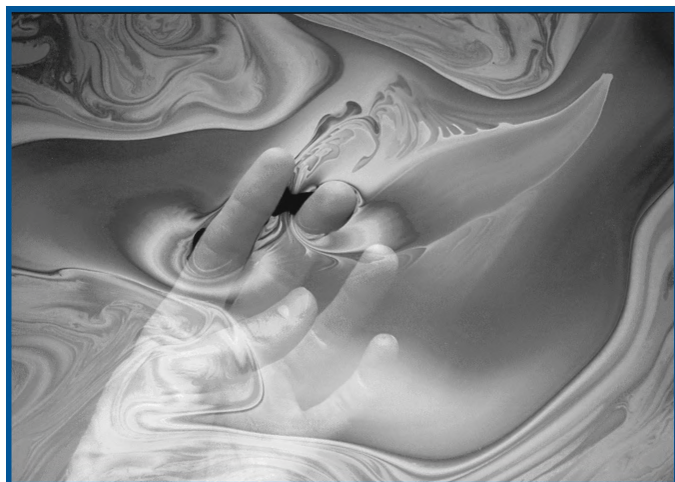
“Spheres of Water” by Matthew Kostanecki

of St. Elizabeth CHS, Toronto, Ontario

Water and oil do not form a solution that can be mixed. In most cases, you see ample amounts of water with a small surface layer of oil. However, in this reverse situation where droplets of coloured water have been placed in an oil solution, the results are depicted in the photo. The hydrophobic nature of the oil causes the coloured water to be repelled and to take on a spherical shape since this provides the least surface area to volume ratio. Since the density of water is greater than oil, the drop sink to the bottom of the container. However, a few smaller water droplets remain at the surface due to surface tension of the oil molecules. As more water droplets were added, the smaller droplets would become larger due to cohesion and would sink to the bottom.



Open Category / Catégorie ouvert



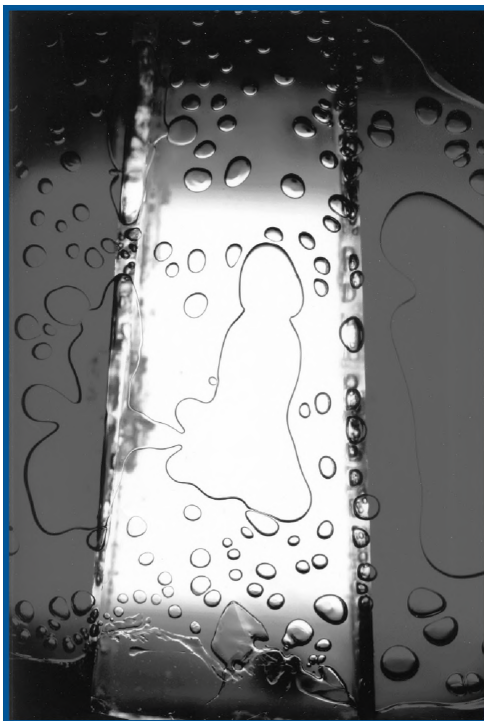
1st Prize - 1^{ier} Prix

“Hand Through a Flat Soap Bubble”

by David Elfstrom, Toronto, Ontario

A flat bubble is made from a mixture of water, dish detergent, and glycerin by dipping a wire frame into the mixture. The frame with the bubble is held above a dark surface, and a studio flask with a 'softbox' is aimed at the bubble. The camera is aimed so that the reflection of the flash will be seen over the entire surface of the bubble, and a photograph is taken of that reflection, showing a swirling pattern of colours.

Interference between the light waves reflected from the front of the film and the back create a shift in colour. Small variations in thickness of the film show up as different colours. By whetting one's fingers with the solution, it is possible to poke a finger or two through the bubble without breaking it. Oils from the skin cause the fluid to move and swirl in unpredictable ways.



2nd Prize - 2^{ième} Prix

“Surface Interface Dynamics: Methyl Benzene & Silicon Dioxide”

by Carol Pfeffer, Irvington, New York

This cameraless photograph illustrates the surface dynamics of a liquid - solid interface. The work "stops time" and allows the viewer to visually ingest the spreading coefficient. Spreading is what happens when a liquid comes into contact with a solid. In this case I chose glass, a non porous solid, to maximize spreading but used an adhesive liquid! Adhesive forces will bring a substance to a surface. It acts surfactant with impurities that reduces the surface tension or the intermolecular force of attraction between adjacent molecules that keeps the fluid together at the interface. A methyl benzene adhesive was applied between two silicon dioxide surfaces. The methyl benzene has a high viscosity, which is a measure of the resistance of the liquid to flow. This allowed me to coordinate the spreading speed with the darkroom exposure. The print is made by treating the sandwich as a film alternative. I remove the negative carrier from an enlarger and substitute the work above the condenser. This creates a projection which I then expose onto the emulsion coated surface. The print is then reversed by paper negative transfer.

Come and visit the Art of Physics exhibition on display at the 2004 Congress and see these entries in full colour. Entry forms for the 2004 competition will be available at the CAP Information Desk (deadline Dec.31/04). Winning entries will be on display during some 2005 World Year of Physics events.

CONGRESS SPONSORS / COMMANDITAIRES DU CONGRÈS

Canadian Space Agency
Varian Medical Systems
AMEC Dynamic Structures

Dean of Science, University of Manitoba
Oxford Instruments
Canadian Institute for Photonics Innovation
Elekta Canada
VP Research Administration, University of Manitoba
Canadian Institute for Photonics Innovations

NRC Institute for Biodiagnostics
Department of Physics, University of Winnipeg
Royal Bank
Travel and Conference Sponsorship Program, UMRA
CancerCare Manitoba
Ministry of Education, Citizenship, and Youth, Province of Manitoba

DraxImage
Ministry of Energy, Science and Technology, Province of Manitoba
Philips Medical Systems
Siemens Canada Limited
Vice-President Administration, University of Manitoba

Best Medical International Inc.
Computerized Medical Systems, Inc.
Dean of Science, University of Winnipeg
Dr. S. Safi-Harb
Therapy Revolution Inc.
Thomson Nelson

InfoMagnetics Technologies Corp.
Merlan Scientific
Manitoba Hydro

CASCA Student Workshop Sponsors:

Herzberg Institute of Astrophysics
Graduate Students' Association, University of Manitoba
Faculty of Graduate Studies, University of Manitoba
Faculty of Science, University of Manitoba
Physics and Astronomy Graduate Students' Association, University of Manitoba

**We would also like to thank some additional sponsors
who wish to remain anonymous / *Nous voudrions aussi remercier certains de
nos commanditaires qui veulent demeurer anonymes***

THE 59th CAP ANNUAL CONGRESS LE 59^e CONGRÈS ANNUEL DE L'ACP

INFORMATION / PROGRAMME



(See page 22 for the Session Codes / Voir page 22 pour les indicatifs des sessions)

2004 CAP CONGRESS / CONGRÈS DE L'ACP 2004

TECHNICAL PROGRAM COMMITTEE / COMITÉ DU PROGRAMME TECHNIQUE

| | | |
|---|------------------------------|---|
| Chair / Président | M. Morrow | myke@physics.mun.ca |
| CASCA Representative / Répresentant de CASCA | J. English | jayanne_english@umanitoba.ca |
| COMP Representative / Répresentant de l'OCPM | P. O'Brien | Peter.O'Brien@tsrcc.on.ca |
| BSC Representative / Répresentant de SBC | J. Lepock | chair@physics.uwaterloo.ca |
| Atmospheric & Space Physics / physique atmosphérique et de l'espace | W. Hocking | whocking@uwo.ca |
| Atomic & Molecular Physics / physique atomique et moléculaire | W-K. Liu | wkliu@uwaterloo.ca |
| Condensed Matter and Materials Physics / physique de la matière condensée et des matériaux | J. Bechhoefer | bechhoefer@sfu.ca |
| Industrial and Applied Physics / physique industrielle et appliquée | Roman Maev | maev@server.uwindsor.ca |
| Instrumentation and Measurement Physics physique des instruments et mesures | Andreas Mandelis | mandelis@mie.utoronto.ca |
| Medical and Biological Physics / physique médicale et biologique | A. Rutenberg | andrew.rutenberg@dal.ca |
| Nuclear Physics / physique nucléaire | M.D. Hasinoff | hasinoff@physics.ubc.ca |
| Optics and Photonics / physique optique et photonique | M. Campbell | mcampbel@quark.uwaterloo.ca |
| Particle Physics / physique des particules | W. Trischuk | william@physics.utoronto.ca |
| Physics Education / enseignement de la physique | Robert Hawkes | rhawkes@mta.ca |
| Plasma Physics / physique des plasmas | C. Boucher | boucher@inrs-emt.quebec.ca |
| Surface Science / science des surfaces | E.T. Jensen | ejensen@unbc.ca |
| Theoretical Physics / physique théorique | M. Shegelski M. Paranjape | mras@unbc.ca paranj@lps.umontreal.ca |

LOCAL ORGANIZING COMMITTEE / COMITÉ ORGANISATEUR LOCAL

| | | | |
|---|------------------------------------|---|---------------|
| Chair / Président | J.P. Svenne | Fundraising / commanditaires | K. Sharma |
| Vice-Chair / Vice-président | W.T.H. van Oers | Exhibits / Exposants | P. Zetner |
| Secretary / Secrétaire | J. Birchall | Poster Session / Session d'affiches | R. Roshko |
| CASCA LOC Chair | S. Safi-Harb | Webmaster / Site web | A. Aleksejevs |
| COMP LOC Chair | S. Pistorius | A-V and/et Entertainment/divertissement | J. Page |
| BSC LOC Chair | M. Jackson | Congress poster / Affiche du congrès | S. Barkanova |
| Registration / Inscription | B.W. Southern | Students, signage / Étudiants, panneaux | J. Hein |
| Head, U. Manitoba Dept. of Physics and Astronomy/ Chef, Dépt. de physique et astronomie (UManitoba) | | | G. Williams |
| Head, U. Winnipeg Dept. of Physics / Chef, Département de physique (UWinnipeg) | | | R. Kobes |
| Publicity / Publicité | J. English, R. Lamontagne, S. Page | | |
| Social Subcommittee / Souscomité des événements sociaux | A. Svenne, S. Safi-Harb, P. Loly | | |
| Grad Student's Barbeque / Barbecue des étudiants diplômés | J. West | | |

CAP OFFICE STAFF / PERSONNEL DE L'ACP

| | | |
|--|-----------|---------------------------|
| Executive Director / Directrice exécutive | F.M. Ford | CAP@physics.uottawa.ca |
| Administrative Assistant / Adjointe administrative | C. Harvey | carmen@physics.uottawa.ca |

GENERAL INFORMATION / RENSEIGNEMENTS GÉNÉRAUX

2004 CAP Congress / Congrès de l'ACP 2004
 Canadian Association of Physicists / Association canadienne des physiciens et physiciennes
 Suite/Bur. 112, Imm. McDonald Bldg. , Univ. of d'Ottawa
 150, avenue Louis Pasteur Avenue OTTAWA, ON K1N 6N5
 Tel/tél.: (613) 562-5614; Fax/télec.: (613) 562-5615; e-mail: cap@physics.uottawa.ca
 web: <http://www.cap.ca>

REGISTRATION

The registration desk is located on the Main Conference Level, second floor of the Delta Hotel, and will be staffed according to the following schedule:

| | |
|---------------------|---------------|
| Saturday, June 12th | 13h00 - 19h30 |
| Sunday, June 13th | 08h00 - 19h00 |
| Monday, June 14th | 07h30 - 17h00 |
| Tuesday, June 15th | 07h30 - 17h00 |
| Wednesday June 16th | 07h30 - 12h00 |

PARKING

Delegates staying at the Delta hotel should arrange for parking with the hotel registration desk. For those not staying at the hotel, there is a public parkade under the hotel and other parking lots and garages in the area. On-street parking is mainly at parking meters with a 1 or 2 hour limit. On Saturday there are 2 hours of free parking at meters on downtown streets; on Sundays, on-street parking is free.

E-MAIL ACCESS

For residents of the hotel, internet access is available in all rooms. In addition, there is a free email station at the concierge desk in the lobby, with limited time of access. The Congress will also provide email access, details of which will be included in the registration package.

EXHIBITORS (in alphabetical order)

Best Medical International, Inc.
 BOC Edwards
 Canberra Co.
 Channel Systems
 CMS Inc.
 Coherent Inc.
 Donaldson Marphil Medical
 Gamble Technologies Ltd.
 Harpell Associates Inc.
 John Wiley and Sons Canada Ltd.
 Kodak Canada Inc.
 Kurt J. Lesker Company
 LAP of America
 McGraw Hill
 Melles Griot Canada Inc.
 Nucletron Corporation
 Oxford Instruments
 Pearson Education Canada
 Plasmionique Inc.
 Scanditronix-Wellhofer North America
 Siemens Canada Ltd., Medical Solutions Division
 Standard Imaging Inc.
 Systems for Research
 Therapy Revolution Inc.
 Thompson Nielsen
 Varian Inc.

SPONSORS

A complete list of sponsors can be found on page 10 of the Congress program. The Congress organizers thank each of the sponsors for their generous contributions.

INSCRIPTION

Le bureau d'inscription est situé au deuxième étage de l'hôtel Delta (Main Conference Level) et sera ouvert aux heures suivantes:

| | |
|------------------|----------------|
| Samedi 12 juin | 13 h à 19 h 30 |
| Dimanche 13 juin | 8 h à 19 h |
| Lundi 14 juin | 7 h 30 à 17 h |
| Mardi 15 juin | 7 h 30 à 17 h |
| Mercredi 16 juin | 7 h 30 à 12 h |

STATIONNEMENT

Les congressistes qui logent à l'hôtel Delta doivent prendre des dispositions avec la réception de l'hôtel. Pour ceux qui ne logent pas à l'hôtel, un stationnement public est situé sous l'hôtel, ainsi que d'autres stationnements dans le quartier. Le stationnement dans la rue est limité à une ou deux heures avec des parcomètres. Le samedi, deux heures de stationnement gratuit est permis dans les rues du centre-ville; le dimanche, le stationnement dans la rue est gratuit.

ACCÈS AU COURRIER ÉLECTRONIQUE

Pour ceux qui résident à l'hôtel, chaque chambre est munie d'un accès Internet. De plus, il est possible d'accéder gratuitement à ses courriels (temps d'accès limité) au bureau du concierge d'hôtel dans le hall de l'hôtel. Le Congrès fournira l'accès aux courriels. Les détails seront compris dans la trousse d'inscription.

EXPOSANTS (en ordre alphabétique)

Best Medical International, Inc.
 BOC Edwards
 Canberra Co.
 Channel Systems
 CMS Inc.
 Coherent Inc.
 Donaldson Marphil Medical
 Gamble Technologies Ltd.
 Harpell Associates Inc.
 John Wiley and Sons Canada Ltd.
 Kodak Canada Inc.
 Kurt J. Lesker Company
 LAP of America
 McGraw Hill
 Melles Griot Canada Inc.
 Nucletron Corporation
 Oxford Instruments
 Pearson Education Canada
 Plasmionique Inc.
 Scanditronix-Wellhofer North America
 Siemens Canada Ltd., Medical Solutions Division
 Standard Imaging Inc.
 Systems for Research
 Therapy Revolution Inc.
 Thompson Nielsen
 Varian Inc.

COMMANDITAIRES

Une liste complète des commanditaires se trouve à la page 10 du programme du Congrès. Les organisateurs du Congrès remercient chacun des commanditaires pour leur généreuse contribution.

2004 JOINT CONGRESS

Welcome to the 59th Annual Congress of the Canadian Association of Physicists, held jointly with the Canadian Astronomical Society (CASCA), the Canadian Organization of Medical Physicists (COMP), and the Biophysical Society of Canada (BSC), hosted by the Department of Physics and Astronomy of the University of Manitoba and held in the Delta Winnipeg Hotel and the Winnipeg Convention Centre in downtown Winnipeg, Manitoba, the **true** Centre of Canada.

Saturday, June 12, Graduate Student Barbecue

For graduate students there will be a free barbecue on the University of Manitoba campus on the Saturday evening. For students staying at the Delta hotel, a shuttle service to the campus will be provided. Students staying at campus residences will be provided directions to the barbecue site.

Sunday, June 13, Public Lecture

A public plenary session, the Herzberg Lecture and CASCA Public Lecture will feature Dr. James E. Peebles, of Princeton University, and a University of Manitoba alumnus, speaking on *A Cosmic Picture: Images from Astronomy*. The plenary session begins at 19h00 and will be followed by a reception with cash bar.

Monday, June 14, Beer and Poster session

The Beer and Poster session will be held in the Convention Centre, accessible by a bridge from the hotel, at 19h00. One complimentary beverage ticket will be provided in your registration package.

Tuesday, June 15, Banquet and Awards

The congress banquet will be held at 19h30, at the Delta hotel. The cost is \$65 per person, including taxes and a limited amount of wine at each table. A reception and cash bar will precede the banquet starting at 19h00.

REGISTRATION INFORMATION

After May 31, 2004, delegates should register on site. Payment may be made by credit card (Visa, Mastercard only) or cheque or money order. All fees are quoted in Canadian dollars.

Cancellation policy

A full refund (less \$50 administration fee) will be issued, provided written notification is received by Dr. Juris P. Svenne, Department of Physics and Astronomy, University of Manitoba, on or before May 13, 2004. No refunds will be issued after May 13, 2004.

TRANSPORTATION TO ACCOMMODATION

Taxis are available from Winnipeg airport to downtown for a fare of approximately \$12.50-\$13.00. Car rentals from various companies are available at the airport. The City of Winnipeg has a fairly good public transit system (bus). There is also a city bus from the airport to downtown. The cash fare is \$1.80 per trip; visitors bus passes will be available for purchase at the registration desk.

ACCOMMODATION

The congress hotel is the Delta Winnipeg hotel, where all the scientific sessions will be held. The poster session, exhibitors and coffee breaks will be at the adjoining Winnipeg Conference Centre. Delegates are encouraged to stay at the Delta Hotel at the low conference rate of \$109 per day for single or double room.

The block-booked rooms will be available at this low rate until May 12, 2004. Should these fill up before this date, every effort will be made to find alternate accommodation in the downtown area. For students, a block of rooms have been reserved on the University of Manitoba campus, which is approximately 10 km away from the Delta Hotel. These are standard dormitory style rooms, not air-conditioned, with shared bathrooms. These residence rooms are available for \$38.79 single occupancy, and \$28.50 per person, double occupancy.

CONGRÈS CONJOINT 2004

Bienvenue au 59^e Congrès annuel de l'Association canadienne des physiciens et physiciennes, organisé conjointement avec la Société canadienne d'astronomie (CASCA), l'Organisation canadienne des physiciens médicaux (COMP) et la Société de biophysique du Canada (BSC), qui est présenté par le Département de physique et d'astronomie de l'Université du Manitoba à l'hôtel Delta Winnipeg et au Centre des congrès du centre-ville de Winnipeg, Manitoba, le **vrai** centre du Canada.

Samedi 12 juin, Barbecue des étudiants diplômés

Il y aura un barbecue gratuit samedi soir pour les étudiants diplômés au campus de l'Université du Manitoba. Un service de navette jusqu'au campus sera offert aux étudiants qui logent à l'hôtel Delta. Des directions sur la façon de se rendre au site du barbecue seront remises aux étudiants qui logent dans les résidences du campus.

Dimanche 13 juin, conférence publique

Une session plénière publique, la conférence Herzberg et la conférence publique CASCA, mettra en vedette le Dr. James E. Peebles, de l'Université Princeton, et ancien étudiant de l'Université du Manitoba, qui nous entretiendra sur le sujet suivant: *Une photo cosmique: Images de l'astronomie*. La session plénière débutera à 19 h 00, suivi d'un bar payant.

Lundi 14 juin, session affiches et bière

La session affiches et bière aura lieu à 19 h au Centre des congrès, accessible de l'hôtel par un pont. Vous trouverez dans votre trousse d'inscription un billet pour une boisson gratuite.

Mardi 15 juin, banquet et remise de prix

Le banquet du congrès aura lieu à 19 h 30 à l'hôtel Delta. Le prix de 65 \$ par personne comprend les taxes et une quantité limitée de vin par table. Un cocktail avec bar payant précédera le banquet, dès 19 h.

INSCRIPTION

Après le 31 mai 2004, les congressistes doivent s'inscrire sur place. Le paiement peut être effectué par carte de crédit (Visa et MasterCard seulement), par chèque ou par mandat poste. Tous les frais sont indiqués en dollars canadiens.

Politique d'annulation

Un remboursement complet (moins des frais d'administration de 50 \$) sera émis, pourvu qu'un avis écrit soit reçu par le Dr. Juris P. Svenne, Département de physique et d'astronomie, Université du Manitoba, au plus tard le 13 mai 2004. Aucun remboursement ne sera accordé après cette date.

TRANSPORT VERS L'HEBERGEMENT

Il est possible de vous rendre en taxi de l'aéroport de Winnipeg au centre-ville pour environ 12,50 \$ à 13 \$. Plusieurs compagnies de location de voitures se trouvent à l'aéroport. La ville de Winnipeg possède un service de transport en commun (autobus) assez efficace. Un autobus fait le circuit entre l'aéroport et le centre-ville. Le coût du billet est de 1,80 \$ le trajet; des cartes d'autobus pour visiteurs seront en vente au bureau d'inscription.

HEBERGEMENT

L'hôtel Delta Winnipeg est l'endroit où toutes les sessions scientifiques auront lieu. La session d'affiches, les exposants et les pauses-café auront lieu au Centre des congrès de Winnipeg adjacent. Nous invitons les congressistes à profiter du tarif congrès avantageux de 109 \$ la nuit pour une chambre simple ou double.

Les chambres bloquées au tarif réduit seront disponibles jusqu'au 12 mai 2004. Si toutes ces chambres devaient être louées avant cette date, tous les efforts seront déployés pour vous trouver une autre chambre au centre-ville. Pour les étudiants, une section de chambres a été réservée sur le campus de l'Université du Manitoba, à environ 10 km de l'hôtel Delta. Il s'agit de chambres standards de résidence étudiante, sans air climatisé, avec salle de bain partagée. Les chambres dans les résidences sont louées 38,79 \$ (occupation simple) et 28,50 \$ par personne (occupation double).

AUDIO-VISUAL EQUIPMENT

For the scientific sessions at the Delta hotel, all rooms will be equipped with a standard overhead projector and a LCD data projector for computer-based presentations. All CAP, CASCA and BSC members who plan on doing a computer-based presentation should bring their presentation on their own laptop computer, and be sure to visit the Speaker Ready Room (Talbot) beforehand to test that the presentation will run smoothly. (You may also wish to bring your presentation on viewgraphs as a back-up to your computer presentation.) At the session in which you are speaking, if you are using the LCD projector, please have your laptop turned on and ready to go. Since all talks must keep to schedule, any time lost in setting up your computer will reduce the time available for your talk, and none of us want this to happen!

In the room where most COMP presentations will be held, a computer will also be available, since this is the tradition at COMP conferences. Presenters using this facility should bring their presentations in PowerPoint format on a CD-ROM disk, with all fonts embedded in the presentation. Make sure to transfer your talk to the computer well before your session is scheduled to start.

If you need additional projection equipment, it can be rented from the A-V company servicing the meeting by contacting Kevin Wolfe at 204 989-2592 (email: kwolfe@corpav.com). The cost of additional equipment must be covered by the speaker.

RECREATIONAL FACILITIES

The Delta hotel has a well-equipped exercise facility, including two swimming pools, one indoor, one outdoor, available to hotel guests. Jogging downtown Winnipeg is easy (totally flat!), but traffic interferes. Head south from the hotel and soon you arrive at the river walk along the Assiniboine and Red Rivers, where pleasant jogging is possible.

MEALS

Bag lunches will be available in the exhibits area on Monday and Tuesday, if you have pre-ordered these. The Delta Hotel has a fine dining restaurant and a snack bar, and in the same building (not strictly part of the hotel) there is a pub. Other restaurants are within easy walking distance of the hotel, as are fast-food places in the City Place indoor mall, kitty-corner across from the hotel. A list of recommended restaurants will be included in the conference package.

GENERAL INFORMATION ABOUT WINNIPEG

Winnipeg is the vibrant capital of Manitoba, the geographic centre of Canada and North America. With a population of over 685,000 people with diverse background, there is an international, cosmopolitan flair to the city as well as a feeling of community. Winnipeg is home to 60% of Manitoba's residents. The Provincial Legislature building is near the Delta Hotel and well worth a visit. Also not far is the Winnipeg Art Gallery. The Forks Market at the historic junction of the Red and Assiniboine rivers is a little farther in the opposite direction. Winnipeg Transit operates a free shuttle bus circulating the downtown area.

The University of Manitoba is the oldest university in Western Canada. It celebrated its 125th anniversary in 2002. This year the Faculty of Science and the Department of Physics and Astronomy celebrate their 100th anniversary. The first 6 professors of science, including physicist Frank Allen, were hired in 1904. A reunion of former students, post-docs, faculty and staff of the Physics Department (Physics and Astronomy since 1999) is being held in conjunction with Congress 2004. The main reunion events will begin on Wednesday afternoon, June 16 and continue on Thursday, June 17, culminating with a banquet in the evening at the Faculty Club of the University of Manitoba.

CLIMATE

The average daily maximum and minimum temperatures in Winnipeg in June are 23°C and 10 °C. One can generally expect dry, sunny weather in the summer in Winnipeg (average precipitation for June: 84 mm).

ÉQUIPEMENT AUDIOVISUEL

Pour les sessions scientifiques à l'hôtel Delta, toutes les salles sont munies d'un rétroprojecteur standard et d'un vidéoprojecteur ACL pour les présentations informatisées. Tous les membres de l'ACP, de CASCA et de BSC qui planifient faire une présentation informatisée devraient apporter leur présentation sur leur propre bloc-notes et se rendre à la salle Talbot (Speaker Ready Room) auparavant pour tester si leur présentation se déroule correctement. (Vous pourriez aussi apporter votre présentation sur transparents comme alternatif à votre présentation informatisée.) Lors de votre propre présentation, si vous utilisez un projecteur ACL, veuillez vous assurer d'allumer votre ordinateur et d'être prêt à débiter. Puisque toutes les présentations doivent s'en tenir à l'horaire, tout temps perdu à préparer votre ordinateur sera retranché de votre temps de présentation. Nous ne désirons pas que cela arrive à qui que ce soit.

Dans la salle où la plupart des présentations de OCPM auront lieu, un ordinateur sera aussi disponible, car c'est la pratique courante dans les conférences de OCPM. Les présentateurs qui utilise ce moyen devraient apporter leurs présentations en format PowerPoint sur un CD-Rom, avec toutes les polices de caractères intégrées dans la présentation. Assurez-vous de transférer votre présentation à l'ordinateur bien avant le début de votre session.

Si vous avez besoin d'autre équipement de projection, il peut être loué de l'entreprise en charge de l'audiovisuel au Congrès en communiquant avec Kevin Wolfe au (204) 989-2592 (courriel: kwolfe@corpav.com). Le coût de l'équipement additionnel doit être payé par le présentateur.

INSTALLATIONS RÉCRÉATIVES

L'hôtel Delta possède beaucoup d'équipement sportif, dont deux piscines (une intérieure, une extérieure), disponibles aux clients de l'hôtel. Faire son jogging au centre-ville de Winnipeg est facile (tout est plat!), mais la circulation peut nuire. À partir de l'hôtel, dirigez-vous vers le sud et vous tomberez rapidement sur la piste qui longe les rivières Assiniboine et Rouge, où le jogging est très agréable.

REPAS

Lundi et mardi, des sacs à lunch seront disponibles à l'aire des exposants, si vous les avez commandés à l'avance. L'hôtel Delta possède un restaurant haut de gamme et un casse-croûte et, dans le même édifice un pub qui ne fait pas strictement partie de l'hôtel. D'autres restaurants sont à distance de marche de l'hôtel, ainsi que de la restauration rapide dans le mail intérieur de City Place, de l'autre côté de l'hôtel. Votre trousse d'inscription contiendra une liste de restaurants recommandés.

RENSEIGNEMENTS GÉNÉRAUX SUR LA VILLE

Winnipeg, capitale dynamique du Manitoba, est le centre géographique du Canada et de l'Amérique du Nord. Avec une population de plus de 685 000 habitants de cultures diverses, cette ville cosmopolite internationale est aussi dotée d'une sens de la communauté. Winnipeg accueille 60 % de la population du Manitoba. L'Assemblée législative, située tout près de l'hôtel Delta, vaut la peine d'être visitée. La Winnipeg Art Gallery se trouve aussi à portée. Le marché Forks, à la jonction historique des rivières Assiniboine et Rouge, se trouve un peu plus loin dans la direction inverse. Le transport en commun de Winnipeg offre une navette gratuite dans le centre-ville.

L'Université du Manitoba est la plus vieille université de l'ouest du Canada. Elle a célébré son 125^e anniversaire en 2002. Cette année, la Faculté des sciences et le Département de physique et d'astronomie célèbrent leur 100^e anniversaire. Les six premiers professeurs en science, dont le physicien Frank Allen, ont été engagés en 1904. Une réunion d'anciens étudiants, chercheurs post-doctoraux, professeurs et membres du personnel du Département de physique (Physique et astronomie depuis 1999) aura lieu lors du Congrès 2004. Les événements principaux entourant la réunion débiteront le mercredi après-midi 16 juin et se poursuivront le jeudi 17 juin, avec un banquet le soir au Faculty Club de l'université du Manitoba.

CLIMAT

Les températures minimales et maximales moyennes à Winnipeg en juin sont de 10 oC et de 23 oC, respectivement. À Winnipeg, le temps l'été est habituellement sec et ensoleillé (précipitations moyennes en juin: 84 mm).

CASCA GRAD STUDENTS' WORKSHOP

U. MANITOBA FORT GARY CAMPUS

Saturday, June 12, 2004**Samedi, le 12 juin 2004**

The annual CASCA Grad Students Workshop will be held on Saturday, June 12, 2004, at the University of Manitoba Fort Gary campus. The theme of the workshop this year is **Data Mining and Image Processing**.

In the afternoon, there will be a panel discussion on the Long Range Plan and the future of Canadian Astronomy, specifically its implications for current graduate students. There will be plenty of time for discussion, so come with your questions!

Schedule

| | | | |
|---------------|--|------------|-------------------------------------|
| 8:45 - 9:30 | Intro/Grad student mixer | | Beausejour Room, Univ.Centre |
| 9:45 - 11:30 | Colour image processing | J. English | Machray Hall Computer Lab |
| 11:30 - 13:00 | Lunch | | Degrees, Univ.Centre |
| 13:00 - 14:30 | CADC workshop | D. Durand | Machray Hall Computer Lab |
| 14:30 - 15:00 | Break | | |
| 15:00 - 16:30 | Panel Discussion "The Long Range Plan and the Future of Canadian Astronomy" | | Beausejour Room, Univ.Centre |
| | Panel Members: G. Fahlman, R. Taylor, and R. Pudritz | | |
| - 15:00 | opening remarks | G. Fahlman | |
| - 15:10 | opening remarks | R. Taylor | |
| - 15:20 | opening remarks | R. Pudritz | |
| - 15:30 | discussion/questions | | |
| - 16:15 | closing remarks/wrap-up | | |
| 16:30 - 17:30 | CASCA Grad Student's Meeting | | Beausejour Room, Univ.Centre |
| 17:30 - | Grad Student's BBQ | | St.John's College (to be confirmed) |

Supporters**NRC - Herzberg Institute of Astrophysics**

Graduate Students' Association, University of Manitoba

Faculty of Graduate Studies, University of Manitoba

Faculty of Science, University of Manitoba

Physics and Astronomy Graduate Students' Association, University of Manitoba

Graduate Student Barbecue des étudiants diplômés (All organizations/ Toutes les organisations)

For graduate students, there will be a free barbecue on the University of Manitoba campus on the Saturday evening. For students staying at the Delta Hotel, a shuttle service to the campus will be provided. Students staying at campus residences will be provided directions to the barbecue site.

Il y aura un barbecue gratuit samedi soir pour les étudiants diplômés au campus de l'Université du Manitoba. Un service de navette jusqu'au campus sera offert aux étudiants qui logent à l'hôtel Delta. Des directions sur la façon de se rendre au site du barbecue seront remises aux étudiants qui logent dans les résidences du campus.

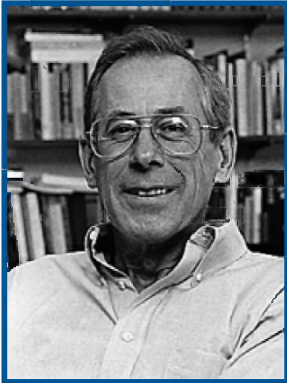
HERZBERG MEMORIAL PUBLIC LECTURE
CONFÉRENCE PUBLIQUE COMMÉMORATIVE HERZBERG

CHI-WAN YOUNG SPORTS
CENTRE

Sunday, June 13, 2004

19h00

Dimanche, le 13 juin 2004



P. James E. Peebles

DR. P. JAMES E. PEEBLES,
PRINCETON UNIVERSITY

"A Cosmic Picture Show : Images from Astronomy"

Some of the astronomical images I will present are meant to illustrate what we know about the large-scale nature of the world around us and how we have gone about discovering it; others are chosen just because they're pretty. Some of the images are close to what you can see with a pair of binoculars; others are numerical representations of what you would 'see' if you had Superman's X-ray eyes, or eyes sensitive to radio waves or neutrinos. I'll show historical examples of the learning process in astronomy, both good -- Hubble's classification of the galaxies -- and not so good -- Lowell's idea that he was seeing canals on Mars -- and illustrations drawn from current debates about what is happening on scales ranging from black holes in the centers of galaxies to the expansion of the universe.

"Présentation d'images cosmiques : Images de l'astronomie"

Certaines des images astronomiques que je vais présenter sont destinées à illustrer ce que nous connaissons de la nature du monde qui nous entoure à grande échelle et ce qui nous a conduit à la découvrir; d'autres ont été choisies uniquement en raison de leur beauté. Certaines de ces images sont proches de ce que nous pouvons voir à l'aide de jumelles; d'autres sont des représentations numériques de ce que nous pourrions voir si nous possédions la vision à rayons-X de Superman ou des yeux sensibles aux ondes radio ou aux neutrinos. Je présenterai des exemples historiques de l'évolution de la connaissance en astronomie, des bons (classification Hubble des galaxies) et des moins bons (idée de Lowell qui aurait vu des canaux sur Mars), ainsi que des illustrations réalisées à partir de discussions récentes sur ce qui se produit à des échelles allant des trous noirs aux coeurs des galaxies à l'expansion de l'univers.

BIOGRAPHY

Born April 25, 1935 in Winnipeg, Manitoba, Canada, naturalized U.S. citizen 1991. Married to Alison Peebles with three children, Lesley, Ellen and Marion, six grandchildren.

1958 BS University of Manitoba; 1962 Ph.D. Princeton University; 1961-1962 Instructor, Princeton; 1962-64 Research Associate, Princeton; 1964-65 Research Staff Member, Princeton; 1965-68 Assistant Professor, Princeton; 1968-72 Associate Professor, Princeton; 1972-84 Professor Princeton; 1984-2000 Albert Einstein Professor of Science, Princeton; 2000 Albert Einstein Professor of Science Emeritus, Princeton.

Professional Societies: Fellow, American Academy of Arts and Sciences; Fellow, American Physical Society; Fellow, Royal Society; Fellow, Royal Society of Canada; Fellow, U.S. National Academy of Sciences; Member, American Astronomical Society; Member, American Association for the Advancement of Science.

Awards: 1977, A.C. Morrison Award in National Science, NY Academy of Sciences

1981, Eddington Medal, Royal Astronomical Society
 1982, Heineman Prize, American Astronomical Society
 1986, Doctor of Science, University of Toronto
 1986, Doctor of Science, University of Chicago
 1989, Doctor of Science, McMaster University
 1989, Doctor of Science, University of Manitoba
 1992, Robinson Prize, University of Newcastle upon Tyne
 1992, Henry Norris Russell Lectureship of the AAS
 1994, Silliman Lectureship, Yale
 1994, Feshbach Lecturer, MIT
 1995, Bruce Medal, Astronomical Society of the Pacific
 1995, Lemaitre Award, Université catholique de Louvain
 1995, de Vaucouleurs Lectureship, University of Texas
 1996, McPherson Lecturer, McGill University, October

1996, Doctor of Science, Université catholique de Louvain, October
 1997, Danz Professor, University of Washington, May
 1997, Klein Lecturer, University of Stockholm, June
 1997, Jansky Lectureship, NRAO
 1997, Doctor Honoris Causa, Universidad Nacional de Córdoba, December
 1998, Gold Medal, Royal Astronomical Society, UK
 2000, Peter S. Gruber Foundation Award, September
 2001, Oort Professor, Leiden University, May
 2001, Harvey Prize Technion University, Israel
 2003, Tomalla Foundation Prize, University of Geneva, June

Fourth Annual Physics Teacher Workshop
Monday, June 14, 2004
University of Manitoba, Winnipeg, Manitoba
Delta Hotel

Monday, June 14, 2004 - **Delta Hotel**, Room TBA

8:00 am **Registration and Refreshment**

8:30 am **Keynote Lecture by Dr. Helmy Sherif**, University of Alberta, **Winner of 2004 CAP Medal of Excellence in Physics Teaching**. Dr. Sherif has been named winner of this prestigious national medal for "outstanding physics teaching at both introductory and advanced levels, and for his exemplary work as a mentor to students and to former students." He has played a pivotal role in the physics careers of many students.

9:20 am **Demonstration of computer-based physics laboratory technology** by a Merlan Scientific representative.

10:20 am **Refreshment Break**

10:35 am **Fast Optimization of the Radiation Therapy of Tumours: The Impossible Possible** by Dr. S. P. Goldman, Dept. of Physics and Astronomy, University of Western Ontario. A crucial problem in radiation therapy is to optimize hundreds of beams so that the dose distribution is uniform inside the tumours and small inside organs at risk. A system of linear algebraic equations will handle this quickly but it is *impossible* to use: it results in negative beams! Instead we are forced to *search* numerically the optimal intensities, taking long computation times and yielding sometimes incorrect results. Our new solution made the *impossible* (a linear method) *possible* on physical grounds, delivering excellent dose distributions in times orders of magnitude shorter than present search methods.

11:25 am **Distance Learning from 820 km Straight Up: The Educational Potential of the MOST Space Telescope** by Dr. Jaymie Matthews, University of British Columbia. The MOST (Microvariability & Oscillations of STars) mission is the first all-Canadian scientific satellite in over 30 years. It is a small but powerful optical telescope and photometer in polar orbit, capable of detecting variations in the brightnesses of stars down to a few parts per million. It is searching for acoustic oscillations and convection in stars, and reflected light from planets outside the Solar System. MOST offers a great opportunity to introduce a wide range of physical, astronomical, technological and even political concepts in the classroom, all packaged in a "Humble" suitcase-sized observatory!

12:05 pm **LUNCH Sponsored by Canadian Institute for Photonic Innovation CIPI with guest speaker**

1:35 pm **Lost Amongst the Stars** by Heather R. Scott, Ridley College, St. Catherine's, ON. Recent changes in the Manitoba science curriculum have placed greater emphasis on Astronomy in the Senior 1 course. For many teachers, a lack of expertise in this area of science can lead to incomplete or incorrect coverage of topics, or, in some cases, even exclusion. This workshop will address the concerns of teachers new to astronomy and provide ideas for suitable in-class projects, hands-on demonstrations and a comprehensive list of teacher resources. A question and answer session on all things astronomical will follow!

2:20 pm **Ongoing Professional Development Projects - BC Association of Physics Teachers** by Donald Mathewson, Kwantlen University College. The BC Association of Physics Teachers is a chapter of the American Association of Physics Teachers. Our membership is comprised of a wide cross-section of high school, college and university physics teachers. The BCAPT executive has recently embarked on an ambitious series of professional development projects for teachers that have been enthusiastically embraced by the physics teaching community and have positively impacted the BC physics teaching community. For those within CAP and its member institutions interested in outreach, some information about the BCAPT and its professional development programs will be presented.

2:35 pm **Refreshment and Exhibits Break**

3:00 pm **ALTA to CANALTA : Moving Towards a Canada Wide Network Of Cosmic Ray Telescopes** by Dr. Jim Pinfold, University of Alberta. The ALTA (Alberta Large Time Coincidence Array) collaboration in Alberta has developed and deployed a very large area sparse array in Alberta the scientific purpose of which is to search for a non-random high energy cosmic ray phenomena. The detectors are placed in high-schools and colleges around Alberta. One of the unique features of ALTA is its strong educational dimension due to the involvement of high-schools students and teachers. The ALTA project is presented in the talk, along with initial plans for the development of the CANALTA (CANadawide-ALTA) project across Canada.

Other Related Congress Activities

- Teachers who are planning to arrive early are invited to the public lecture "**A Cosmic Picture Show: Images from Astronomy**" given by Dr. Jim Peebles, Princeton University on Sunday, June 13 at 7:00 pm.
- There are joint CAP/CASCA/COMP sessions around the theme of Enriching Our Teaching Through Integration on Sunday, June 13.
- The Division of Physics Education is holding a series of sessions on the theme of New Directions in the Physics Curriculum on Tuesday, June 15.



Manitoba
Education, Citizenship
and Youth

Manitoba
Advanced Education
and Training



CANADIAN ASSOCIATION OF PHYSICISTS ASSOCIATION CANADIENNE DES PHYSIENS ET PHYSIENNES

ANNUAL GENERAL MEETING ASSEMBLÉE GÉNÉRALE ANNUELLE

DATE: Tuesday, June 15, 2004
Mardi, le 15 juin, 2004

TIME/HEURE: 17h00

PLACE: Room/Salle Victoria, Delta Hotel, Winnipeg, Manitoba

DRAFT AGENDA / ORDRE DU JOUR PROVISOIRE

1. Call to Order and Approval of the Agenda
2. Approval of the Minutes of the June 11, 2003 Annual General Meeting
 - .1 Matters arising from the Minutes
3. Annual Report
 - .1 Audited Financial Statements to December 31, 2003
 - .2 Membership Report
4. Appointment of Auditors
5. Report on the Activities of the Association
 - .1 Update on Engineering Acts
 - .2 Update on Professional Certification / Trademark
 - .3 Science Policy / Lobbying
 - .4 Preliminary Results from CAP Membership Survey
 - .5 Meetings with the APS
 - .6 2005 Year of Physics
 - .7 Other Matters
6. Report by the Chair of the 2004 Local Organizing Committee
7. Host Universities - Future Congresses
8. New Business
 - .1 2005 Membership Fees (R. Hodgson)
 - .2 Report of the Canadian National IUPAP Liaison Committee (H. van Driel)
 - .3 Report by the Editor of Physics in Canada (J.S.C. McKee)
 - .4 Report by the Editor of the Canadian Journal of Physics (G.W.F. Drake)
 - .5 CUPC 2004 at U. Victoria (Jennifer Barker)
9. Report of the Nominating Committee
10. Votes of Thanks and Change of the Chair
11. Date and Place of Next Meeting
12. Adjournment

IMPROVING THE CLIMATE FOR WOMEN IN PHYSICS

A special event organized by the Committee to Encourage Women in Physics

CAP Congress
 Monday, June 14; 5:00 pm
 Delta Hotel; Colbourne Room
Reception to Follow

BARBARA L. WHITTEN, Colorado College

What Works for Women in Undergraduate Physics?

The participation of women in physics has increased in recent years, but the percentage of women in undergraduate physics is still less than half that in mathematics and chemistry. This is due in large part to the "leaky pipeline"—women become more scarce in physics with every step up the academic ladder. The largest decrease occurs between high school physics and college graduation, so it is worthwhile to look at how undergraduate physics departments try to make women comfortable. With a team of women physicists, I visited nine undergraduate physics departments in the US. We compared those that are successful in producing a large percentage of women majors (about 40%) with those that are more typical of the national average (about 20%). We found that the most important factor is a warm and female-friendly department culture that reaches out to introductory students. I'll discuss the factors that make up a female-friendly culture, and describe other results of our research.

NEW FACULTY LUNCHEON / DÉJEUNER POUR LES NOUVEAUX PROFESSEUR(E)S

PRIVATE DINING ROOM, DELTA HOTEL, WINNIPEG

We extend a special invitation to new Faculty members to attend the CAP Congress, to be held at the Delta Hotel in Winnipeg, Manitoba, from the 13th to the 16th of June 2004. The CAP Congress is a unique opportunity to meet and hear colleagues from universities across Canada, and to discover a part of our country. For new Faculty members who choose to attend the Congress, we have organized a special luncheon at 12:30 p.m. on Wednesday, June 16th. This luncheon will be hosted by the CAP's Director of Academic Affairs. NSERC representatives will give a short presentation followed by a question period and a round table discussion of issues of interest to new professors.

If you would like to attend, please let us know by e-mail at cap@physics.uottawa.ca. We welcome any suggestions regarding information that you would like to obtain from NSERC, or topics that you would like to hear discussed at the round table.

I hope to see you in Winnipeg.

Mike Morrow, P.Phys.
 Vice President of the CAP

N.B. A new professor is any regular Faculty member who started after December 31st, 2002.

Nous lançons une invitation spéciale aux nouveaux professeurs d'assister au Congrès de l'ACP à l'Hôtel Delta, Winnipeg, Manitoba du 13 au 16 juin. Le Congrès de l'ACP est une occasion unique de rencontrer et d'écouter vos collègues des autres universités canadiennes, en plus de découvrir un joli coin de notre pays. Pour les nouveaux professeurs, qui assisteront au Congrès, nous avons aussi organisé un déjeuner spécial à 12h30 le mercredi 16 juin. Le déjeuner sera animé par le Directeur des affaires académiques de l'ACP. Des représentants du CRSNG vont faire une courte présentation sur les programmes disponibles aux professeurs de physique au Canada et demeureront pour répondre à vos questions. La discussion sera suivie d'une table ronde sur les sujets d'intérêt aux nouveaux professeurs.

Si vous aimeriez assister au déjeuner, veuillez nous le laisser savoir en envoyant un courrier électronique à cap@physics.uottawa.ca. Toutes les suggestions que vous auriez sur les sujets que vous aimeriez entendre discuter par les représentants du CRSNG ou à la table ronde seront bienvenues.

J'espère vous voir à Winnipeg.

Mike Morrow, phys.
 Vice-Président de l'ACP

N.B. Un nouveau professeur est tout professeur régulier qui est entré en fonction après le 31 décembre 2002.

NSERC Workshop

Monday/Lundi, June 14 juin

16h00 ; Room/salle Strathcona

Tips to Prepare Your Next Discovery Grant Application

Conseils pour l'élaboration de votre prochaine demande de subvention à la découverte

NSERC staff and Grant Selection Committee members will present an interactive overview of the peer review process, inform you of the latest changes at NSERC, give useful advice for the preparation of your next NSERC application and answer your questions on the functioning of grant selection committees. The workshop is open to all researchers. It will be particularly helpful to new faculty members and researchers likely to apply (or re-apply) in the fall.

Des employés du CRSNG et des membres des comités de sélection des subventions du CRSNG donneront une présentation en mode interactif sur le processus d'évaluation par les pairs, vous renseigneront sur les derniers changements opérés au CRSNG, vous donneront des conseils utiles pour l'élaboration de votre prochaine demande de subvention au CRSNG et répondront à vos questions sur le fonctionnement des comités de sélection des subventions. Tous les chercheurs peuvent participer à l'atelier, qui sera particulièrement utile aux professeurs et aux chercheurs récemment embauchés qui comptent soumettre une demande (ou une nouvelle demande) à l'automne.

WORLD YEAR OF PHYSICS - 2005 - ANNÉE MONDIALE DE LA PHYSIQUE



2005 has been designated the World Year of Physics. Physical societies around the globe will be arranging and/or coordinating events to celebrate the 100th anniversary of the publishing of Einstein's three famous papers. The central theme for the year is Public Outreach. Check out the CAP's WYP2005 website at <http://www.cap.ca> for more information.

Anyone who is planning a physics-related event during 2005 is invited to submit information about the event -- including date, location, and contact details for more information -- to the CAP office at cap@physics.uottawa.ca for inclusion on the central website.

In 2005, the CAP will be celebrating its 60th anniversary. Special events will be organized at the 2005 CAP Congress at the University of British Columbia to celebrate both of these special occasions.

A planning meeting of the WYP2005 Organizing Committee will be held at 3:00 p.m. on Tuesday, June 15th in the Heartland Boardroom of the Delta Hotel in Winnipeg. Anyone interested in WYP2005 events is welcome to attend.

CALENDAR / CALENDRIER

| | |
|------------------|---|
| 2004 June 6-9 | 25th Annual Conference of the Canadian Nuclear Society, Marriott Eaton Centre Hotel, Toronto, Ontario, Canada. Visit www.cns-snc.ca |
| 2004 June 10-14 | CCWEST 2004 Conference, Brock University, St. Catharines, Ontario. Visit http://www.brocku.ca/fms/ccwest2004 |
| 2004 June 21-23 | 64th Annual Physical Electronics Conference, University of California at Davis. Visit http://www.physicalelectronics.org/ |
| 2004 July 2-6 | 6th EPS Liquid Matter Conference, Utrecht. Visit www.liquids2005.nl . |
| 2004 Aug. 16-22 | 32nd International Conference on High Energy Physics (ICHEP04), Beijing, China. Visit www.ichep04.ihep.ac.cn |
| 2004 Aug. 18-21 | 2004 Crystallography at High Pressure Workshop, Canadian Light Source, Saskatoon, Saskatchewan, Canada. Visit www.lightsource.ca/iucr2004/ . |
| 2004 Sept. 6-10 | 12th International Conference on the Physics of Highly Charged Ions, Villinius, Lithuania. Visit www.itpa.IT/hci2004/ or contact hci2004@itpa.it . |
| 2004 Sept. 27-29 | Photonics North, Ottawa Congress Centre, Ottawa, Ontario. Visit www.spie.org/info/pn |
| 2005 July 11-15 | EPS13 - 13th General Conference of the European Physical Society (WYP2005 event), University of Bern, Bern, Switzerland. Visit http://www.eps13.org |

ABBREVIATION KEY / CODES DES ABBRÉVIATIONS

Organizations

| | |
|-------|--|
| BSC | Biophysical Society of Canada Société de biophysique du Canada |
| CAP | Canadian Association of Physicists Association canadienne des physiciens et physiciennes |
| CASCA | Canadian Astronomical Society Société canadienne d'astronomie |
| COMP | Canadian Organization of Medical Physicists Organisation canadienne des physiciens médicaux |

Divisions

| | | | |
|-------|---|-------|--|
| DAMP | Division of Atomic and Molecular Physics | DOP | Division of Optics and Photonics |
| DPAM | Division de physique atomique et moléculaire | | Division d'optique et photonique |
| DASP | Division of Atmospheric and Space Physics | DPE | Division of Physics Education |
| DPAE | Division de physique atmosphérique et de l'espace | DEP | Division de l'enseignement de la physique |
| DCMMP | Division of Condensed Matter and Materials Physics | DPP | Division of Plasma Physics |
| DPMCM | Division de physique de la matière condensée et matériaux | | Division de physique des plasmas |
| DMBP | Division of Medical and Biological Physics | DSS | Division of Surface Sciences |
| DPMB | Division de physique médicale et biologique | | Division de la science des surfaces |
| DIAP | Division of Industrial and Applied Physics | DTP | Division of Theoretical Physics |
| DPIA | Division de physique industrielle et appliquée | DPT | Division de physique théorique |
| DIMP | Division of Instrumentation and Measurement Physics | PPD | Particle Physics Division |
| DPIM | Division de physique des instrumentation et mesures | | Division de physique des particules |
| DNP | Division of Nuclear Physics | CEWIP | Committee to Encourage Women in Physics |
| DPN | Division de physique nucléaire | CEFEP | Comité d'encourager les femmes en physique |

Sessions

| | |
|-----------|--|
| SA-A# | Saturday A.M. Session / Session du samedi matin |
| SA-P# | Saturday P.M. Session / Session du samedi après-midi |
| SU-CHAIRS | Sunday Physics Department Heads/Chairs Workshop / Réunion des directeurs de départements de physique le dimanche |
| SU-A# | Sunday A.M. Session / Session du dimanche matin |
| SU-P# | Sunday P.M. Session / Session du dimanche après-midi |
| SU-KEY | Sunday Keynote Speaker / Session plénière publique du dimanche soir |
| MO-A# | Monday A.M. Session / Session du lundi matin |
| MO-P# | Monday P.M. Session / Session du lundi après-midi |
| MO-STUD | Monday Best Graduate Student Paper Competition / Compétition de la meilleure présentation étudiante, le lundi après-midi |
| MO-POS# | Monday evening Poster Session / Session d'affiche du lundi soir |
| TU-A# | Tuesday A.M. Session / Session du mardi matin |
| TU-P# | Tuesday P.M. Session / Session du mardi après-midi |
| WE-A# | Wednesday A.M. Session / Session du mercredi matin |
| WE-P# | Wednesday P.M. Session / Session du mercredi après-midi |

INVITED SPEAKERS / CONFÉRENCIERS INVITÉS

(in alphabetical order / selon l'ordre alphabétique)

| | | | |
|---|------------|--|------------|
| AFFLECK, Ian (DTP /DPT) University of British Columbia <i>Field-Induced Phase Transition in Anisotropic Haldane Gap Antiferromagnetic Chains</i> | [TU-P7-1] | BOCCARA, Claude (DIMP /DPIM) École supérieure de physique et chimie industrielles <i>Optical Imaging in Turbid Media: New Developments</i> | MO-P9-1] |
| ALVARADO-GIL, Juan J. (DIMP /DPIM) University of Guelph <i>Study of Blood Sedimentation by Photothermal and Optical Techniques</i> | [WE-A8-2] | BONN, Douglas (DCMMP / DPMCM) University of British Columbia <i>Dying Gasps of a d-Wave Superconductor</i> | [MO-P11-1] |
| ANDREOIU, Corina (DNP / DPN) University of Guelph <i>Doorway States in the Gamma Decay-Out of the Yrast Superdeformed Band in ⁵⁹Cu</i> | [WE-P5-3] | BRIGGS, Matthew (DIMP /DPIM) Los Alamos National Laboratory <i>Optical Velocity-Measurement Techniques for Supersonic Surfaces</i> | [WE-A12-4] |
| ANTONIOW, Jean-Stéphane (DIMP /DPIM) Reims University <i>(Photo)(Photo)Thermal Imaging Using a Modified Atomic Force Microscope (AFM) Combined with Pyroelectric Detection</i> | [WE-P6-4] | BRONSKILL, Michael (CCPM / CCPM) Sunnybrook and Women's College Health Sciences Centre/ University of Toronto <i>Imaging Physics Meets Public Perception: Is Private MRI Bad?</i> | [MO-A12-4] |
| ARKANI-HAMED, Nima (DTP /DPT) Harvard University <i>The Crises Of Frontier Physics: From The Hubble Length to the Planck Length</i> | [TU-A2-1] | BRONSKILL, Michael (DMBP /DPBM) Sunnybrook and Women's College Health Sciences Centre/ University of Toronto <i>MRI Guidance for the New Sounds of Tumour Therapy</i> | [TU-P13-1] |
| BACHER, Andrew (DNP / DPN) Indiana University/IUCF <i>Observation of Charge Symmetry Breaking in the Reaction $d-d \rightarrow ^4\text{He}-\pi^0$</i> | [MO-P8-3] | BROWN, Jeremy (DMBP /DPBM) Queen's University <i>Development and Applications of High Frequency Ultrasound Imaging Systems</i> | [TU-P13-3] |
| BAESSO, Mauro L. (DIMP /DPIM) Universidade Estadual de Maringá, Brazil <i>Time Resolved Thermal Lens for Thermo-Optical Measurements in Transparent Materials During Phase Modification</i> | [WE-A12-3] | BROWN, Jo-Anne (CASCA / CASCA) University of Calgary <i>Visualizing the Invisible Using Polarization Observations</i> | [TU-A17-1] |
| BARBER, Robert (CAP/COMP Peter Kirkby Memorial Medal winner - récipiendaire de la médaille de commémorative Peter Kirkby) University of Manitoba <i>IUPAP - A Brief Introduction</i> | [WE-P1-1] | BUYERS, Williams J.L. (DCMMP / DPMCM) National Research Council <i>Spins and Paired Carriers in a Superconductor that is Nearly an Antiferromagnet - Who Pushes Whom?</i> | [MO-P11-4] |
| BATTISTA, Jerry J. (DIAP / DPIA) London Regional Cancer Centre / University of Western Ontario <i>On-Line CT Imaging for Precision Radiotherapy</i> | [WE-P8-1] | CALAMAI, Peter (CAP / ACP) Toronto Star <i>Don't Overlook Images Created with Words</i> | [MO-P6-1] |
| BEAULIEU, Luc (DIAP-DIMP / DPIA-DPIM) Université Laval <i>Scintillating Optical Fibers as High Precision, Small Area Dosimeters in Radiation Therapy</i> | [WE-A8-4] | CARRINGTON, Margaret (DTP /DPT) Brandon University <i>Transport Theory Beyond Binary Collisions</i> | [MO-A10-1] |
| BEAULIEU, Luc (DNP / DPN) Université Laval <i>The Dynamics of Neck Formation and its Isospin Dependence</i> | [WE-P5-4] | CHAKRABORTY, Tapash (DCMMP / DPMCM) University of Manitoba <i>How to Probe a Fractionally-Charged Quasihole</i> | [TU-A13-1] |
| BENSIMON, David (DCMMP / DPMCM) École normale supérieure, France <i>The Elastic Behaviour of a Real Polymer: The Case of ssDNA</i> | MO-A5-1] | CHAPMAN, Dean (BSC / SBC) University of Saskatchewan <i>New Sources of X-ray Imaging Contrast</i> | [WE-A14-2] |
| BERNDSSEN, Aaron (DTP - PPD / DPT - PPD) CHEP/McGill U. <i>Aspects of Brane-Gas Cosmology</i> | [TU-A9-3] | CHRISTIAN, Carol (CAP / ACP) STSci <i>Putting Research Science and Education Together: Lessons Learned from HST</i> | [SU-P3-2] |
| | | CHRISTIAN, Carol (CASCA / CASCA) STSci <i>Public Impact of Scientific Images: Examples from Space Science</i> | [MO-A12-3] |

| | | | |
|---|------------|---|------------|
| CLARKE, Robert (DMBP /DPBM) Carleton University <i>High Intensity Focused Ultrasound for Non-Invasive Therapy</i> | [TU-P13-2] | FENSTER, Aaron (DMBP /DPBM) Robarts Research Institute <i>Use of 3D Ultrasound Imaging in Diagnosis, Treatment and Research: Advances and Opportunities</i> | [WE-A3-1] |
| CORRIVEAU, François (PPD / PPD) IPP/McGill University <i>Recent ZEUS Results at HERA</i> | [TU-P5-3] | FENSTER, Aaron (DIAP / DPIA) Robarts Research Institute <i>From Concept to Product: 3D Ultrasound Imaging for Diagnosis and Treatment</i> | [WE-P8-4] |
| CÔTÉ, Michel (DCMMP / DPMCM) Université de Montréal <i>Virtual Experiments: Applications of Density Functional Theory on Large-Scale Computational Facilities</i> | [TU-A7-1] | FORDE, Nancy (DCMMP / DPMCM) UC Berkeley <i>Using Optical Tweezers to Study Single-Molecule Reactions in Real Time*</i> | [SU-A4-2] |
| DAS, Saurya (DTP /DPT) University of Lethbridge <i>Black Holes in Future Colliders</i> | [WE-P10-1] | FORTIER, Tara (DAMP / DPAM) JILA, University of Colorado at Boulder <i>Carrier-Envelope Phase Stabilized Modelocked Lasers</i> | [WE-A16-1] |
| DASGUPTA, Arundhati (DTP /DPT) Université Libre de Bruxelles <i>Entropy of a Black Hole Apparent Horizon</i> | [WE-P10-5] | FRANZ, Marcel (DCMMP / DPMCM) University of British Columbia <i>Nodal Protectorate in Underdoped Cuprates</i> | [MO-P11-2] |
| DATTA, Alakabha (DTP /DPT) University of Toronto <i>Getting CP Violating Phase Information from $b \rightarrow c$ Penguins</i> | [TU-P6-4] | GALE, Charles (DTP /DPT) McGill University <i>Electromagnetic Signals from Matter Under Extreme Conditions</i> | [MO-A10-2] |
| DAVIDGE, Tim (CASCA / CASCA) National Research Council <i>Adaptive Optics Systems on Canadian Telescopes</i> | [TU-P10-1] | GALINDO-URIBARRI, Alfredo (DNP / DPN) Oak Ridge National Laboratory <i>Nuclear Spectroscopy with Radioactive Ion Beams: Latest Results from HRIBF</i> | [WE-P5-1] |
| DENNISTON, Colin (DCMMP / DPMCM) University of Western Ontario <i>Dynamic Boundaries in Complex Fluids</i> | [TU-P4-2] | GARCIA, Jose (DIMP /DPIM) PTD Inc. <i>Photo-Carrier Radiometry of Semiconductors: Instrumentation and Ion-Implantation Studies</i> | [TU-A12-1] |
| DICK, Rainer (DTP /DPT) University of Saskatchewan <i>Theoretical Aspects of Ultra-High Energy Cosmic Rays</i> | [TU-P6-5] | GRAHAM, Kevin (PPD / PPD) Queen's University <i>Recent Results from the Sudbury Neutrino Observatory</i> | [WE-A10-1] |
| DILLING, Jans (DNP / DPN) TRIUMF <i>Ion Traps in Nuclear Physics: the Ultimate Tool for Precision Experiments</i> | [WE-A11-3] | GRÉGOIRE, Thomas (DTP /DPT) CERN <i>Little Higgs Models and Electroweak Precision Measurements</i> | [TU-A9-4] |
| DRAKE, Gordon (DAMP / DPAM) University of Windsor <i>Exotic Nuclear Size Measurements from High Precision Atomic Theory</i> | [TU-P9-1] | GRIFFIN, Allan (DAMP / DPAM) University of Toronto <i>Molecular BEC Condensate vs a BCS Superfluid in a Trapped Atomic Fermi Gas</i> | [TU-A14-4] |
| DUBINSKI, John (CASCA / CASCA) University of Toronto <i>A Universe in Motion : Dynamical Evolution of Galaxies in the New Cosmological Paradigm</i> | [WE-P3-1] | GUREVICH, Yuri (DIMP /DPIM), CINVESTAV <i>The Transport of Nonequilibrium Carriers in Semiconductor Structures (New Point of View)</i> | [TU-A12-2] |
| DUTTA, Bhaskar ((DTP /DPT) University of Regina <i>Minimal SO(10) Model for Neutrinos and its Implications</i> | [TU-P6-1] | GWINNER, Gerald (DNP / DPN) University of Manitoba <i>A New Test of the Special Theory of Relativity with the Heidelberg Test Storage Ring</i> | [MO-P8-2] |
| EDERY, Ariel (DTP /DPT) Bishop's University <i>Compact Formulas for Casimir Energies in D-Dimensions via Operator Technique</i> | [TU-A8-4] | HA, Bae-Yeun (DCMMP / DPMCM) University of Waterloo <i>Statics and Dynamics of Biopolymers: Theory and Biological Relevance</i> | [SU-A4-3] |
| EMBERLY, Eldon (DCMMP / DPMCM) Simon Fraser University <i>The Smallest Molecular Switch</i> | [WE-A9-3] | | |

| | | | |
|--|------------|--|------------|
| HACKMAN, Greg (DNP / DPN) TRIUMF <i>TRIUMF-ISAC Gamma-Ray Escape Suppressed Spectrometer (TIGRESS)</i> | [WE-P5-2] | HWANG, Una (CASCA / CASCA) NASA's Goddard Space Flight Center <i>Windows into Nucleosynthesis from X-Ray Observations of Supernova Remnants</i> | [TU-A11-1] |
| HALLEN, Hans (DIMP / DPIM) North Carolina State University <i>Electron-Induced Motion of Atoms: Mechanisms and Insights about Hot Electron Transport</i> | [TU-A12-3] | JAEGER, Nicolas (CAP-INO Medal winner / récipiendaire de la médaille l'ACP-INO) University of British Columbia <i>Optical Sensors for Power Utility Applications</i> | [MO-P3-1] |
| HALLEN, Hans (DIMP / DPIM) North Carolina State University <i>Electric Field Effects in Nanoscale Raman Spectroscopy</i> | [TU-P8-3] | JAEGER, Wolfgang (DAMP / DPAM) University of Alberta <i>Spectroscopy of HeN-Molecule Clusters: A Probe of the Onset of Superfluidity?</i> | [TU-A14-2] |
| HALLIN, Emil (DIAP / DPIA) Canadian Light Source <i>The Applied Science Program at the Canadian Light Source</i> | [WE-P8-2] | JALILEHVAND, Farideh (BSC / SBC) University of Calgary <i>X-Ray Absorption Spectroscopy in Natural Sciences; Exploring New Possibilities</i> | [WE-A14-3] |
| HARRIS, Gretchen (CASCA / CASCA) Goddard University <i>CASCA 1971-2004: The Story So Far</i> | [TU-A14-1] | KAERN, Mads (DMBP-DCMMP / DPBM-DPMCM) Boston University <i>Gene Regulatory Systems: Roles of Physics in Post-Genomic Biology</i> | [MO-P13-2] |
| HASINOFF, Michael (DNP / DPN) University of British Columbia <i>A Test of Time Reversal Invariance in Stopped Kaon Decay</i> | [MO-P8-4] | KARLEN, Dean (PPD / PPD) University of Victoria <i>The Future Linear Collider Project</i> | [MO-A8-3] |
| HAUGEN, Harold (DAMP / DPAM) McMaster University <i>Selected Studies of Femtosecond Laser Ablation and Modification of Semiconductors*</i> | [TU-A10-1] | KASPI, Victoria (CAP Herzberg Medal winner / récipiendaire de la médaille ACP Herzberg) McGill University <i>Revolutions in Neutron Star Astrophysics</i> | [TU-P3-1] |
| HEPBURN, John (DAMP / DPAM) University of British Columbia <i>Spectroscopy and Dynamics of Threshold Ionization of Clusters and Small Molecules</i> | [TU-A14-1] | KEMPF, Achim (DTP / DPT) University of Waterloo <i>Towards a Notion of Qubit Density for Quantum Fields in Curved Spacetime</i> | [MO-P10-5] |
| HERBUT, Igor (DTP / DPT) Simon Fraser University <i>Theory of Underdoped Cuprates as Fluctuating d-wave Superconductors</i> | [TU-P7-2] | KILFOIL, Maria (DCMMP / DPMCM) McGill University <i>Consequences of Being Soft: Equilibrium Concepts in Nonequilibrium, Soft Materials Using Real Space Imaging</i> | [TU-P4-3] |
| HIGGS, Paul (DMBP-DCMMP / DPBM-DPMCM) McMaster University <i>Bacterial Phylogenetics and Horizontal Gene Transfer</i> | [MO-P13-5] | KNOBEL, Robert (DCMMP / DPMCM) Queen's University <i>Integrated Mechanics and Electronics at the Nanoscale</i> | [WE-A9-2] |
| HILL, Ian (DCMMP / DPMCM) Dalhousie University <i>Contact Resistance in Organic Thin-Film Transistors</i> | [TU-P4-4] | KOBES, Randy (DTP / DPT) University of Winnipeg <i>Exploring Paths in Adiabatic Quantum Computing</i> | [MO-P10-3] |
| HIROSE, Akira (DPP / DPP) University of Saskatchewan <i>Anomalous Electron Thermal Conductivity in Tokamaks</i> | [WE-P9-1] | KOLIOS, Michael (DIMP / DPIM) Ryerson University <i>Micrometer Particle Sizing Using High Frequency Ultrasound with Biological Applications</i> | [TU-P8-1] |
| HOEKSTRA, Henk (CASCA / CASCA) CITA <i>Astrophysical Evidence for Dark Matter</i> | [WE-P13-1] | KOLIOS, Michael (DMBP / DPBM) Ryerson University <i>High Frequency Ultrasound Imaging and Spectroscopy for the Imaging of Cell Damage and Death</i> | [TU-P13-4] |
| HOLDOM, Bob (DTP / DPT) University of Toronto <i>Ghostly Tales</i> | [TU-A9-1] | KORDAS, Kostas (PPD / PPD) University of Toronto <i>Recent Results from the Collider Detector at Fermilab</i> | [TU-P5-1] |
| HUSAIN, Viqar (DTP / DPT) University of New Brunswick <i>Singularly Resolution in Quantum Gravity</i> | [WE-P10-2] | | |

| | | | |
|---|------------|---|------------|
| KOTLICKI, Andrzej (DIAP / DPIA) University of British Columbia <i>Applied Research at the Structured Surface Physics Laboratory at UBC</i> | [WE-A8-3] | MARKO, John (DCMMP / DPMCM) University of Illinois at Chicago <i>Micromanipulation Study of Chromatin Fibers and Whole Chromosomes</i> | [SU-P4-1] |
| KREUZER, Jurgen (DCMMP / DPMCM) Dalhousie University <i>Stretching and Confinement of Single Polymer Molecules and the Growth of a Polymer Brush: A First Principles Theory</i> | [SU-A4-4] | MARLEAU, Luc (DTP / DPT) Université de Laval <i>Revisiting the Skyrme Model</i> | [TU-P6-2] |
| KRIEGER, Peter (PPD / PPD) University of Toronto <i>The ATLAS Detector at the Large Hadron Collider</i> | [MO-A8-2] | MARTIN, James (DAMP / DPAM) University of Waterloo <i>Dipole-Dipole Interactions between Ultracold Rydberg Atoms</i> | [WE-A11-2] |
| KRULL, Ulrich J. (DIMP / DPIM) University of Toronto at Mississauga <i>Genomic Target Identification using Imaging of Distributed Gradients of Oligonucleotide Probes in Conjunction with Microfluidics</i> | [WE-A8-1] | MARZIALI, André (DCMMP / DPMCM) University of British Columbia <i>A Single-Molecule Nanosensor For Oligonucleotide Identification</i> | [SU-P4-3] |
| KUNSTATTER, Gabor (DTP / DPT) University of Winnipeg <i>Vibrational Modes of Black Holes and their Quantum Gravitational Microstates</i> | [WE-A13-1] | MATTHEWS, Jaymie (CASCA / CASCA) University of British Columbia <i>Distance Learning from 820 km Straight Up: The Educational Potential of the MOST Space Telescope</i> | [SU-A1-7] |
| LAFLAMME, Ray (DTP / DPT) University of Waterloo <i>NMR and Quantum Information Processing</i> | [MO-P10-1] | MATTHEWS, Jaymie (CASCA / CASCA) University of British Columbia <i>Space Science in a Suitcase: Early Results from MOST</i> | [TU-A15-1] |
| LAKE, Kayll (DTP / DPT) Queen's University <i>Recent Developments in Computer Algebra Applied to General Relativity</i> | [WE-A13-5] | MATZNER, Chris (CASCA / CASCA) University of Toronto <i>Energy Feedback in Core-Collapse Supernovae</i> | [TU-A11-2] |
| LEE, Taejin (DTP / DPT) University of British Columbia <i>Free Field Representation of Rolling Tachyon</i> | [TU-A9-2] | MAZINI, Rachid (PPD / PPD) University of Toronto <i>The ATLAS Detector Physics Potential</i> | [TU-P5-2] |
| LEWIS, Randy (DTP / DPT) University of Regina <i>Lattice QCD Phenomenology and its Limits</i> | [MO-A10-3] | MICHAELIAN, Kirk (DIMP / DPIM) CANMET Energy Technology Centre-Devon <i>Dispersive Photoacoustic Spectroscopy of Hydrocarbons</i> | [WE-A12-1] |
| LOLY, Peter / STINNER, Arthur (DPE / DEP) University of Manitoba <i>Using the History of Science to Present the Evolution of Major Concepts in Physics</i> | [SU-A1-8] | MILDENBERGER, Joseph (PPD / PPD) TRIUMF <i>Latest Results from the Search for $K^+ \rightarrow \pi^+ \nu \bar{\nu}$</i> | [MO-P7-2] |
| MANDELIS, Andreas (DIMP / DPIM) University of Toronto <i>Laser Photo-Thermo-Acoustic Frequency Swept Heterodyned Lock-in Depth Profilometry for Three-Dimensional Sub-Surface Tissue Imaging</i> | [MO-P9-2] | MOORE, Guy (DTP / DPT) McGill University <i>Strong Bounds on Lorentz Symmetry Violation</i> | [MO-A10-4] |
| MANN, Robert (DTP / DPT) University of Waterloo <i>Revised Radiative Electroweak Symmetry Breaking: Further Results</i> | [MO-A10-5] | MUNGER, Rejean (DOP / CASCA) University of Ottawa Eye Institute <i>Adaptive Optics: Implications to Optical Correction of the Eye</i> | [TU-P10-3] |
| MANN, Robert (DTP / DPT) University of Waterloo <i>Mass Conjectures, Entropy Bounds and the dS/CFT Correspondence</i> | [WE-A13-2] | NG, Kenneth (BSC / SBC) University of Calgary <i>Protein Crystallography and Antiviral Drug Design</i> | [WE-A14-4] |
| MANOGUE, Corinne (DPE / DEP) Oregon State University <i>Revitalizing the Upper-Division Physics Curriculum</i> | [SU-A1-6] | NOIREAUX, Vincent (DMBP-DCMMP / DPBM-DPMCM) Rockefeller <i>From In Vitro Genetic Circuits to an Artificial Cell</i> | [MO-P13-3] |
| | | OELERT, Walter (DNP / DPN) Forschungszentrum Juelich <i>Observation of Cold Antihydrogen - Perspectives for Testing Fundamental Symmetries</i> | [MO-P8-1] |

| | | | |
|---|------------|--|------------|
| OSHIKAWA, Masaki (DTP /DPT) Tokyo Institute of Technology <i>Junctions of Three Quantum Wires and the Dissipative Hofstadter Model</i> | [TU-P7-3] | RONEY, Michael (PPD / PPD) University of Victoria <i>Recent Results from the BaBar Experiment</i> | [MO-P7-1] |
| OSER, Scott (PPD / PPD) University of British Columbia <i>Long-Baseline Neutrino Oscillations at K2K and J-PARC</i> | [MO-A8-1] | ROORDA, Austin (DOP / CASCA) University of Houston College of Optometry <i>From Telescope to Ophthalmoscopes: Adaptive Optics for Microscopic Imaging of the Living Eye</i> | [MO-A12-2] |
| OTTENSMEYER, Peter (BSC / SBC) University of Toronto <i>Images of the Invisibly Small: from Atoms to Biomacromolecular Structure and Function</i> | [MO-A12-1] | ROSEI, Federico (DCMMP / DPMCM) INRS-EMT, Université du Québec <i>Critical Issues in Ge/Si Nanostructures: Positioning, Intermixing and Ripening</i> | [WE-A9-1] |
| PAGE, Don (DTP /DPT) University of Alberta <i>Particle Production in a Tunneling Universe</i> | [WE-A13-3] | ROWE, David J. (DTP /DPT) University of Toronto <i>Quasi-Dynamical Symmetry in the Approach to a Second-Order Phase Transition</i> | [TU-A8-3] |
| PATERA, Jiri (CAP-CRM Prize winner /récipiendaire du prix ACP-CRM) Université de Montréal <i>Deterministic Aperiodic Multidimensional Point Sets, Their Properties And Exploitation</i> | [MO-P2-1] | RUTH, Thomas (DIAP / DPIA) TRIUMF <i>Production of Radioisotopes for Research in Bioscience and Physical Science</i> | [WE-P8-5] |
| PATERA, Jiri (DTP /DPT) Université de Montréal <i>Orbit Functions of Compact Lie Groups and their Applications</i> | [TU-A8-5] | SAINT-AUBIN, Yvan (DTP /DPT) Université de Montréal <i>Behavior of the Two-Dimensional Ising Model at the Boundary of a Half- Infinite Cylinder</i> | [TU-P7-5] |
| PEARSON, Mathew (DNP / DPN) TRIUMF <i>Nuclear Physics from Cold, Trapped Atoms</i> | [WE-A11-1] | SANDERS, Barry (DTP /DPT) University of Calgary <i>Quantum Information Processing with Continuous Variables</i> | [MO-P10-2] |
| PEEBLES, P. James E. (CASCA-CAP / CASCA-ACP) Princeton University <i>A Cosmic Picture Show: Images from Astronomy</i> | [SU-KEY] | SCHADE, David (CASCA / CASCA) NRC/CADC <i>Data Mining and the Virtual Observatory</i> | [WE-A6-1] |
| PERCY, John (CASCA / CASCA) University of Toronto <i>Variable Stars: Dynamic Tools for Hands-On Astronomy and Physics Education</i> | [SU-P3-3] | SCHATZ, Hendrik (DNP / DPN) Michigan State University <i>Nuclear Physics on Accreting Neutron Stars - from X-Ray Bursts to Superbursts</i> | [TU-A11-3] |
| POISSON, Eric (DTP /DPT) University of Guelph <i>The Gravitational Self-Force</i> | [WE-A13-4] | SEAQUIST, Ernie (CASCA / CASCA) University of Toronto <i>The Galaxy M82 - a Rosetta Stone for the Starburst Phenomenon</i> | [WE-A18-1] |
| POSPELOV, Maxim (DTP /DPT) University of Victoria <i>Search for Dark Matter in $b \rightarrow s$ Transition with Missing Energy</i> | [TU-A9-5] | SEVICK, Edit (DCMMP / DPMCM) Australian National University <i>The Fluctuation Theorem as a Generalised Second-Law for Nanomachines and Single Biopolymer Manipulations: Optical Tweezers Experiments and Beyond</i> | [SU-A4-1] |
| QUIRION, Guy (DCMMP / DPMCM) Memorial University of Newfoundland <i>Investigation of the Phase Diagram of UNi_2Si_2</i> | [WE-P4-1] | SHAPIRO, Evgeny (DAMP / DPAM) National Research Council <i>Arbitrary Shaping of Molecular Wavepackets by AC Stark Shifts</i> | [WE-A16-3] |
| RAGAN, Ken (PPD / PPD) McGill University <i>STACEE Continues, VERITAS Lives !</i> | [WE-A10-2] | SHEN, Jun (DIMP /DPIM) National Research Council Canada <i>Photothermal Beam Deflection Techniques Applied to the Non-Destructive Measurements of Thermophysical Properties</i> | [WE-A12-2] |
| ROGERS, David (COMP /OCPM) Carleton University <i>Monte Carlo Simulation of Electron-Photon Transport: from Particle Physics to Cancer Radiotherapy</i> | [WE-A7-1] | SHEPARD, Stephen M. (DIMP /DPIM) Thermal Wave Imaging Inc. <i>Pulsed Thermography: Perspectives on the Evolution from Qualitative to Quantitative Application</i> | [WE-P6-2] |

| | | | |
|---|------------|---|------------|
| SHERIF, Helmy (Excellence in Teaching Medal winner - récipiendaire de la médaille de l'ACP pour l'excellence en enseignement de la physique) University of Alberta <i>A Discussion of Spin: From Teaching to Research</i> | [MO-A3-1] | TROTTIER, Howard (DTP /DPT) Simon Fraser University <i>Perturbation Theory for High-Precision Lattice QCD</i> | [TU-P6-3] |
| SIPE, John (DAMP / DPAM) University of Toronto <i>Optically Injected Spin Currents in Semiconductors</i> | [TU-A10-3] | UNRUH, William (DTP /DPT) University of British Columbia <i>Dumb Holes-- Black Holes in the Lab?</i> | [WE-P10-4] |
| SLATER, Gary (DCMMP / DPMCM) University of Ottawa <i>Single-Molecule Polymer Physics: The Role of Molecular Dynamics Simulations</i> | [SU-P4-2] | VAN WIJNGAARDEN, William (DAMP / DPAM) York University <i>Bose-Einstein Condensation in a QUIC Trap</i> | [TU-A14-3] |
| SNIATYCKI, Jędrzej (DTP /DPT) University of Calgary <i>Gauge Symmetries in Yang-Mills Theory</i> | [TU-A8-2] | WADE, Gregg (CASCA / CASCA) Royal Military College <i>Imaging the Surfaces of Stars</i> | [WE-P6-3] |
| SORENSEN, Erik (DCMMP / DPMCM) McMaster University <i>Kondo Effect and Persistent Currents in Quantum Dot Systems</i> | [TU-A7-2] | WALTON, Mark (DTP /DPT) University of Lethbridge <i>Finding NIM-Reps</i> | [TU-A8-1] |
| STAMP, Philip (DTP /DPT) University of British Columbia <i>Decoherence Mechanisms and the Dynamics of Decoherence in Qubit Networks</i> | [MO-P9-4] | WESTWOOD, Tim (DMBP-DCMMP /DPBM-DPMCM) University of Toronto <i>Using DNA Microarrays for Functional Genomic Studies</i> | [MO-P13-4] |
| STINNER, Arthur/LOLY, Peter (DPE / DEP) University of Manitoba <i>Using the History of Science to Present the Evolution of Major Concepts in Physics</i> | [SU-A1-8] | WHITMORE, Mark (DCMMP / DPMCM) Memorial University of Newfoundland <i>High Performance Computing: The New and Growing Environment in Canada</i> | [TU-A7-3] |
| SUTHERLAND, Michael (DCMMP / DPMCM) University of Toronto <i>Nodal Metallic Phase in Underdoped Cuprates</i> | [MO-P10-3] | WHITTEN, Barbara (CEWIP / CEFEP) Colorado College <i>What Works for Women in Undergraduate Physics?</i> | [MO-P16-1] |
| SWAIN, Peter (DMBP-DCMMP /DPBM-DPMCM) McGill University <i>Stochastic Gene Expression in Single Cells</i> | [MO-P13-1] | WICHOSKI, Ubi (PPD / PPD) Université de Montréal <i>Status of the Dark Matter Search</i> | [WE-P13-2] |
| THEWALT, Michael (Brockhouse Medal winner / récipiendaire de la médaille Brockhouse) Simon Fraser University <i>Redefining the Limits of Semiconductor Spectroscopy</i> | [SU-P1-1] | WICKHAM, Robert (DCMMP / DPMCM) St. Francis Xavier University <i>Kinetics of Self-Assembly in Block Copolymer Melts</i> | [TU-P4-1] |
| THEWALT, Michael (CAP Medal of Achievement winner - récipiendaire de la médaille de l'ACP pour contributions exceptionnelles à la physique) Simon Fraser University <i>Optical Spectroscopy in Semiconductors</i> | [TU-A5-1] | WIEGERT, Paul (CASCA / CASCA) University of Western Ontario <i>Visualizing Dynamics in the Solar System</i> | [MO-A6-1] |
| THOMLINSON, William (BSC / SBC) Canadian Light Source <i>The Canadian Light Source: Opportunities in Biomedical Research</i> | [WE-A14-1] | WOOLGAR, Eric (DTP /DPT) University of Alberta <i>The Poincaré Conjecture, Ricci Flow, and the Renormalization Group</i> | [WE-P10-3] |
| TREMBLAY, André-Marie (DTP /DPT) Université de Sherbrooke <i>Two Ways to Destroy a Fermi Liquid</i> | [TU-P7-4] | ZETNER, Peter (DAMP / DPAM) University of Manitoba <i>Progress in the Investigation of Electron Collisions with Laser Excited Atoms</i> | [TU-P9-2] |
| | | ZHOU, Fei (DCMMP / DPMCM) University of British Columbia <i>Spin Correlated Ultra Cold Atoms</i> | [WE-A9-4] |

LEGEND/LÉGENDE

CAP Sessions *ACP*
 Joint Sessions *conjointes*
 CASCA Sessions *CASCA*
 COMP Sessions *OCPM*
 BSC Sessions *SBC*

CAP/CASCA/COMP/BSC CONGRESS / CONGRÈS DE L'ACP/CASCA/OCPM/SBC

HÔTEL DELTA HOTEL, WINNIPEG, MANITOBA

JUNE 13-16 JUIN 2004

Saturday / Samedi, June 12 juin

Unless otherwise stated all rooms are at the Delta Hotel.

| | | |
|---------------|--|------------------------------|
| all day | JCSA Meeting / Réunion de JCSA | Victoria |
| 08h30 - 17h30 | COMP Business Meetings / Réunions d'affaires de l'OCPM (SA-A1) | Talbot/Wesminster/Strathcona |
| 08h30 - 14h00 | CAP Executive Meeting / Réunion de l'exécutif de l'ACP (SA-A2) | Kildonan |
| 08h30 - 19h00 | CASCA Board and Other Meetings / Réunion du Conseil de CASCA et autres réunions (SA-A3) | Colbourne |
| 08h45 - 16h30 | CASCA Student Workshop and Registration / Atelier des étudiants et inscription CASCA (SA-A4) | Univ. of Manitoba Campus |
| 13h00 - 19h30 | Conference Registration and Information / Inscription au congrès et information | Lobby 2nd Floor |
| 14h00 - 18h00 | CAP Council Meeting (Old and New) / Réunion du conseil (ancien et nouveau) de l'ACP (SA-P1) | Kildonan |

Sunday / Dimanche, June 13 juin

| | | |
|---------------|---|------------------------------------|
| 08h00 - 19h00 | Conference Registration and Information / Inscription au congrès et information | Lobby 2nd Floor |
| 08h00 - 12h30 | Enriching our Teaching Through Integration - a.m. session / Enrichissement de notre enseignement par l'intégration - session du matin (SU-A1) -- CAP-CASCA-COMP / ACP-CASCA-OCPM | Victoria/Albert |
| 08h00 - 12h30 | COMP Business Meetings / Réunions d'affaires de l'OCPM (SU-A2) | Campaign B |
| 08h30 - 12h30 | CAP - Physics Department Heads/Chairs Workshop ACP - Réunion des directeurs de départements de physique | Paragon Restaur. then Colbourne |
| 09h00 - 12h00 | IPP Board of Trustees Meeting / Réunion du conseil d'administration de l'IPP (SU-A3) | Campaign A |
| 09h30 - 12h30 | Single-Molecule Polymer Physics: Fundamental Questions - a.m. session / Physique des polymères monomoléculaires : questions fondamentales - session du matin (SU-A4) | Ballrooms B/C |
| 13h30 - 14h15 | CAP Brockhouse Medal Winner / Récipiendaire de la médaille Brockhouse de l'ACP - MICHAEL THEWALT, Simon Fraser University (SU-P1) | Ballrooms B/C |
| 13h30 - 15h00 | Brachytherapy and Thermal Therapy / Curiothérapie et thérapie thermique (SU-P2) | Campaign B |
| 14h15 - 16h15 | Enriching our Teaching Through Integration - p.m. session / Enrichissement de notre enseignement par l'intégration - session d'après-midi (SU-P3) - CAP-CASCA-COMP / ACP-CASCA-OCPM | Victoria/Albert |
| 14h15 - 17h00 | Single-Molecule Polymer Physics: Biophysical Applications / Physique des polymères monomoléculaires : applications en biophysique (SU-P4) | Ballrooms B/C |
| 14h30 - 17h30 | IPP General Meeting / Assemblée générale (IPP) (SU-P5) | Campaign A |
| 15h30-17h00 | Radiation Treatment Devices / Appareils de radiothérapie (SU-P6) | Campaign B |
| 17h00-18h30 | CCPM Annual General Meeting / Assemblée générale (CCPM) (SU-P7) | Campaign B |
| 19h00 - 20h00 | CAP's Herzberg Memorial Lecture - CASCA's Public Lecture in Astronomy / Conférence publique commémorative Herzberg de l'ACP - CASCA's conférence publique plénière en astronomie - Dr. P. James E. Peebles, Princeton University - (SU-KEY) | Ballrooms A/B/C |
| 20h00-22h30 | Opening Reception / Réception d'accueil | Ballrooms A/B/C |

Monday / Lundi, June 14 juin

| | | |
|---------------|---|-------------------|
| 07h30 - 17h00 | Conference Registration and Information / Inscription au congrès et information | Lobby 2nd Floor |
| 07h00 - 08h30 | "Friends of CAP" Breakfast / Déjeuner des "Ami(e)s de l'ACP" (MO-A1) | Private Dining Rm |
| 08h00 - 12h05 | Registration and High School Teachers' Workshop Inscription et Atelier pour les enseignant(e)s de la physique (MO-A2) | Colbourne |
| 08h30 - 09h15 | CAP Teaching Medal Winner / Récipiendaire de la médaille d'enseignement de l'ACP - Helmy Sherif, Univ. of Alberta (MO-A3) - CAP/CASCA/BSC | Ballrooms B/C |
| 08h30 - 09h45 | Diagnostic Imaging / Imagerie diagnostique (MO-A4) | Albert |
| 09h15 - 10h00 | Plenary Session / Session plénière - DAVID BENSIMON, École normale supérieure (MO-A5) | Ballrooms B/C |
| 09h15 - 10h00 | Visualization in Planetary Sciences / Visualisation en science planétaire - PAUL WIEGERT (MO-A6) | Campaign B |
| 10h00 - 12h30 | Soft Matter / Matière molle (MO-A7) | Victoria |
| 10h00 - 12h30 | Advances in Instrumentation / Progrès en instrumentation (MO-A8) | Kildonan |
| 10h00 - 12h30 | Semiconductors / Semiconducteurs (MO-A9) | Ballroom A |
| 10h00 - 12h30 | Particle Physics I / Physique des particules I (MO-A10) | Albert |
| 10h20 - 10h30 | Opening Greetings for Imaging Session / Accueil pour la session sur l'imagerie (MO-A11) | Ballrooms B/C |
| 10h30 - 12h30 | Scientific Images in the Public Sphere / Les images scientifiques dans la sphère publique (MO-A12) | Ballrooms B/C |
| 12h30 - 13h30 | DCMMP Business Meeting / Réunion d'affaires DPMCM (with lunch / avec repas) | Victoria |
| 12h30 - 13h30 | DTP Business Meeting / Réunion d'affaires DPT (with lunch / avec repas) | Albert |
| 12h30 - 13h30 | DAMP Business Meeting / Réunion d'affaires DPAM (with lunch / avec repas) | Campaign A |
| 12h30 - 13h20 | CASCA JCMT User's Meeting / Réunion des utilisateurs du TJCM de la CASCA (MO-A13) | Campaign B |
| 12h30 - 13h30 | CAP Past Presidents' Lunch / Déjeuner des anciens présidents de l'ACP (MO-A14) | Heartland Bdrm. |
| 13h25 - 14h15 | Herschel Space Observatory Information Session / Session d'information sur l'observatoire spatial Herschel (MO-P1) | Campaign B |
| 13h30 - 14h15 | CAP-CRM Medal Winner / Récipiendaire de la médaille ACP-CRM - JIRI PATERA, CRM, Université de Montréal (MO-P2) | Ballroom A |
| 13h30 - 14h15 | CAP-INO Medal Winner / Récipiendaire de la médaille ACP-INO - NICOLAS JAEGER, University of British Columbia (MO-P3) | Victoria |

| | | |
|--------------------------------------|---|-------------------|
| 13h30 - 14h00 | Demonstration of Karma Visualzation Software / Démonstration du logiciel de visualisation Karma (MO-P4) | Strathcona |
| 13h35 - 15h30 | High School Teacher Workshop / <i>Atelier pour les enseignant(e)s du secondaire</i> (MO-P5) | Colbourne |
| 14h15 - 14h45 | Scientific Images in the Public Sphere / <i>L'imagerie scientifique dans la sphère publique</i> - Peter Calamai, Toronto Star (MO-P6) | Ballrooms B/C |
| 14h15 - 18h00 | The Precision Frontier in Particle Physics / <i>La frontière de la précision en physique des particules</i> (MO-P7) | Ballroom A |
| 14h15 - 17h00 | Symmetries in Nuclear Physics / <i>Les symétries en physique nucléaire</i> (MO-P8) | Campaign A |
| 14h15 - 17h00 | Instrumentation and Techniques in Biomedical Physics I / <i>Instrumentation et techniques en physique biomédicale I</i> (MO-P9) | Albert |
| 14h15 - 17h00 | Quantum Information Theory / <i>Théorie de l'information quantique</i> (MO-P10) | Kildonan |
| 14h30 - 17h00 | Cuprates in the Extreme Underdoped Limit / <i>Les cuprates dans la limite extrême sous-dopée</i> (MO-P11) | Campaign B |
| 14h45 - 15h45 | Panel on Scientific Images in the Public Sphere / <i>Discussion sur les images scientifique dans la sphère publique</i> (MO-P12) | Ballrooms B/C |
| 15h30 - 18h00 | Genetic Networks / <i>Réseaux génétiques</i> (MO-P13) | Victoria |
| 16h00 - 17h00 | NSERC Information Session for Existing Grant Holders / <i>Session d'information du CRSNG pour les détenteurs actuels de bourses</i> (MO-P14) | Strathcona |
| 16h15 - 17h30 | Scientific Imaging and Visualization - contributed / <i>Imagerie et visualisation scientifiques - contribuées</i> (MO-P15) | Ballrooms B/C |
| 17h00 - 19h00 | Best Student Paper Competition / <i>Compétition de la meilleure communication étudiante</i> (MO-STUD) | Albert |
| 17h00 - 19h00 | Improving the Climate for Women in Physics / <i>Amélioration du climat pour les femmes en physique</i> (MO-P16) | Colbourne |
| 17h30 - 19h00 | <i>Physics in Canada</i> Editorial Board Meeting / <i>Réunion du Comité de rédaction de La physique au Canada</i> (MO-PIC) | Westminster |
| 17h30 - 18h15 | NSERC GSC-017: Possible Change to Envelope Funding / CRSNG GSC-017 : Modification possible du financement par enveloppe (MO-P17) | Campaign B |
| 18h00 - 20h30 | CJP Editorial Board Meeting / <i>Réunion du Comité de rédaction de la RCP</i> (MO-CJP) | Heartland Bdrm. |
| 19h00 - 21h00 | Poster Session, with Beer / <i>Session d'affiches, bière servie</i> (MO-POS) CASCA (68); DASP/DPAE (2); DAMP/DPAM (10); DCMP/DPMCM (15); DNP/DPN (6); DOP (1); DPE/DEP (1); DTP/DPT (11); DIAP/DPIA (1); DIMP/DPIM (2); DMBP/DPMB (7); COMPIOCPM (25) | Conven. Centre |
| Tuesday / Mardi, June 15 juin | | |
| 07h30 - 17h00 | Conference Registration and Information / <i>Inscription au congrès et information</i> | Lobby 2nd Floor |
| 07h00 - 09h00 | Meeting of the Canadian National IUPAP Liaison Committee <i>Réunion du comité de liaison national canadien (IUPAP)</i> (TU-A1) | Private Dining Rm |
| 08h30 - 09h15 | Plenary Session / <i>Session plénière</i> - NIMA ARKANI-HAMED, Harvard University (TU-A2) | Ballroom B |
| 08h30 - 10h00 | Young Investigators in Medical and Biological Physics; Part I / <i>Jeunes chercheurs(ses) en physique médicale et biologique; partie I</i> (TU-A3) (COMP/DMBP) | Albert |
| 08h30 - 09h15 | Imaging with ALMA / Imagerie à l'aide de l'ALMA - to be announced / à venir (TU-A4) | Campaign B |
| 09h15 - 10h00 | Medal of Achievement Winner / <i>Récipiendaire de la médaille ACP</i> - MICHAEL THEWALT, Simon Fraser University (TU-A5) | Ballroom B |
| 09h15 - 09h45 | News from Space - Contributed / Nouvelles de l'espace - contribuées (TU-A6) | Campaign B |
| 10h00 - 12h30 | The Impact of High-Performance Computing on Materials Research / <i>Impact de l'informatique à haute performance sur la recherche sur les matériaux</i> (TU-A7) | Ballroom B |
| 10h00 - 12h30 | Mathematical Physics / <i>Physique mathématique</i> (TU-A8) | Westminster |
| 10h00 - 12h30 | Particles/Strings/Fields / <i>Particules/ficelles/champs</i> (TU-A9) | Kildonan |
| 10h00 - 12h00 | Coherent Interactions of Lasers / <i>Interactions cohérentes des lasers</i> (TU-A10) | Victoria |
| 10h00 - 12h30 | Novae and Supernovae / <i>Novas et supernovas</i> (TU-A11) | Ballroom C |
| 10h00 - 12h30 | Techniques and Measurements in Semiconductor Physics and Transport Phenomena / <i>Techniques et mesures en physique des semiconducteurs et phénomènes de transport</i> (TU-A12) | Campaign A |
| 10h00 - 12h30 | Correlated Electrons/Magnetism / <i>Électrons corrélés/Magnétisme</i> (TU-A13) | Colbourne |
| 10h00 - 12h30 | Atomic and Molecular Spectroscopy and Dynamics I / <i>Spectroscopie et dynamique atomique et moléculaire I</i> (TU-A14) | Ballroom A |
| 10h15 - 11h00 | News from Space - The MOST Satellite / Nouvelles de l'espace - Le satellite MOST - JAYMIE MATTHEWS, UBC (TU-A15) | Campaign B |
| 10h30 - 12h00 | Young Investigators in Medical and Biological Physics, Part II / <i>Jeunes chercheurs(ses) en physique médicale et biologique; partie II</i> (TU-A16) | Albert |
| 11h00 - 11h45 | CASCA Plaskett Lecture / Conférence Plaskett CASCA - JO-ANNE BROWN, U. Calgary (TU-A17) | Campaign B |
| 11h45 - 12h30 | Imaging in the Submillimetre Window - contributed / <i>Imagerie dans la fenêtre sous-millimétrique - contribuées</i> (TU-A18) | Campaign B |
| 12h30 - 13h30 | ALMA Information Session / Session d'information sur l'ALMA (TU-A19) | Campaign B |
| 12h30 - 13h30 | DNP Business Meeting / <i>Réunion d'affaires DPN</i> (with lunch / avec repas) | Colbourne |
| 12h30 - 13h30 | DOP Business Meeting / <i>Réunion d'affaires DOP</i> (with lunch / avec repas) | Westminster |
| 12h30 - 13h30 | DPP Business Meeting / <i>Réunion d'affaires DPP</i> (with lunch / avec repas) | Strathcona |
| 12h30 - 13h30 | DMBP Business Meeting / <i>Réunion d'affaires DPMB</i> (lunch not provided / repas non-inclus) | Campaign A |
| 13h15 - 14h15 | Radiobiology and Tissue Characterization / <i>Biologie radiologique et caractérisation des tissus</i> (TU-P1) COMP/DMBP | Albert |
| 13h15 - 14h00 | Microimaging / <i>Microimagerie</i> (TU-P2) - COMP/DMBP | Victoria |
| 13h30 - 14h15 | CAP Herzberg Medal Winner / <i>Récipiendaire de la médaille Herzberg de l'ACP</i> - VICTORIA KASPI, McGill University (TU-P3) | Ballrooms B/C |
| 14h15 - 16h45 | Young Investigators in Condensed Matter Physics I / <i>Jeunes chercheurs(ses) en physique de la matière condensée I</i> (TU-P4) | Ballrooms B/C |
| 14h15 - 17h30 | The Energy Frontier in Particle Physics / <i>La frontière de l'énergie en physique des particules</i> (TU-P5) | Campaign A |
| 14h15 - 17h00 | Particle Physics II / <i>Physique des particules II</i> (TU-P6) | Westminster |

| | | |
|----------------------|--|-----------------|
| 14h15 - 17h00 | Statistical Physics / <i>Physique statistique</i> (TU-P7) | Victoria |
| 14h15 - 16h45 | General Measurement Physics / <i>Physique des mesures générales</i> (TU-P8) | Kildonan |
| 14h15 - 17h00 | Atomic and Molecular Spectroscopy and Dynamics II / <i>Spectroscopie et dynamique atomique et moléculaire II</i> (TU-P9) | Colbourne |
| 14h15 - 16h15 | Adaptive Optics in Astronomy, Biology, Medicine, and Physics / <i>Optique adaptative en astronomie, biologie, médecine et physique</i> (TU-P10) -- DOP/CASCA | Ballroom A |
| 14h15 - 15h15 | New Directions in the Physics Curriculum / (TU-P11) | Strathcona |
| 14h15 - 14h45 | Measuring Hidden Parts of Galaxies / Mesure des parties cachées des galaxies (TU-P12) | Campaign B |
| 14h30 - 17h00 | Medical Applications of Sound: Imaging and Beyond / <i>Applications médicales du son : l'imagerie et au-delà</i> (TU-P13) - COMP/DMBP | Albert |
| 14h45 - 15h15 | CASCA Outgoing President's Talk / Conférence du président sortant de la CASCA - GRETCHEN HARRIS, U.Waterloo (TU-P14) | Campaign B |
| 15h00 - 16h30 | World Year of Physics 2005 Committee Meeting / <i>Réunion du Comité pour l'Année mondiale de la physique</i> (TU-P15) | Heartland Bdrm |
| 15h45 - 16h30 | CASCA - Long Range Plan Review / Examen du plan à long terme de la CASCA (TU-P16) | Campaign B |
| 16h30 - 18h00 | CASCA Annual General Meeting / Assemblée générale de la CASCA (TU-P17) | Campaign B |
| 17h00 - 18h30 | CAP Annual General Meeting / <i>Assemblée générale de l'ACP</i> (TU-P18) | Victoria |
| 17h00 - 18h00 | COMP Annual General Meeting / Assemblée générale de l'OCPM (TU-P19) | Albert |
| 19h00 | Banquet Reception / <i>Réception du banquet</i> | Ballrooms A/B/C |
| 19h30 | Banquet | Ballrooms A/B/C |

Wednesday / Mercredi, June 16 juin

| | | |
|----------------------|--|-------------------|
| 07h30 - 12h00 | Conference Registration and Information / <i>Inscription au congrès et information</i> | Lobby 2nd Floor |
| 07h00 - 09h00 | Meeting of the CAP-NSERC Liaison Committee / <i>Réunion du comité de liaison ACP-CRSNG</i> (WE-A1) | Heartland Bdrm. |
| 07h00 - 08h15 | DPE Business Meeting / <i>Réunion d'affaires DEP</i> (WE-A2) | Private Dining Rm |
| 08h30 - 09h15 | Plenary Session / <i>Session plénière</i> -- AARON FENSTER, Robarts Res.Inst. (WE-A3) | Ballrooms B/C |
| 08h30 - 09h00 | Portraits at Multiple Wavelengths - Contributed / Portraits à longueurs d'ondes multiples - proposée (WE-A4) | Campaign B |
| 08h30 - 10h00 | Radiation Treatment Planning / Planification d'une radiothérapie (WE-A5) | Albert |
| 09h00 - 09h45 | Data Mining and Archiving / Exploitation et archivage des données - DAVID SCHADE (WE-A6) | Campaign B |
| 09h15 - 10h00 | Plenary Session / <i>Session plénière</i> -- DAVE ROGERS, Carleton U. (WE-A7) - CAP/COMP | Ballrooms B/C |
| 10h00 - 12h30 | Instrumentation and Techniques in Biomedical Physics II / <i>Instrumentation et techniques en physique biomédicale II</i> (WE-A8) | Colbourne |
| 10h00 - 12h30 | Young Investigators in Condensed Matter Physics II / <i>Jeunes chercheurs(es) en physique de la matière condensée II</i> (WE-A9) | Ballroom A |
| 10h00 - 12h00 | Particle Astrophysics / <i>Astrophysique des particules</i> (WE-A10) | Victoria |
| 10h00 - 12h45 | Ion Traps in Atomic and Nuclear Physics / <i>Pièges à ions en physique atomique et nucléaire</i> (WE-A11) | Campaign A |
| 10h00 - 12h30 | Imaging with Photoacoustic and Photothermal NDE Techniques and Microscopies / <i>Imagerie à l'aide de techniques END et de microscopies photoacoustiques et photothermiques</i> (WE-A12) | Strathcona |
| 10h00 - 12h30 | General Relativity and Gravitation I / <i>Relativité générale et gravitation I</i> (WE-A13) | Kildonan |
| 10h00 - 12h30 | Synchrotron Biophysics: The Canadian Light Source / Biophysique au synchrotron : La source de lumière canadienne (WE-A14) | Albert |
| 10h15 - 11h00 | Imaging in Multiple Wavelengths - Contributed / Imagerie dans des longueurs d'ondes multiples - contribuées (WE-A15) | Campaign B |
| 10h30 - 12h30 | Ultrafast Laser Applications / <i>Applications des lasers ultra-rapides</i> (WE-A16) | Ballroom C |
| 10h30 - 12h30 | Radiation Dosimetry / Dosimétrie des rayonnements (WE-A17) | Ballroom B |
| 11h00 - 11h45 | CASCA Beals Award Lecture / Conférence du prix Beals de la CASCA - ERNIE SEAQUIST (WE-A18) | Campaign B |
| 11h45 - 12h30 | New Directions in Imaging - Contributed / Nouvelles orientations en imagerie - contribuées (WE-A19) | Campaign B |
| 12h30 - 13h30 | DIAP-DIMP Business Meeting / <i>Réunion d'affaires DPIA-DPIM</i> (with lunch / avec repas) | Colbourne |
| 12h30 - 13h30 | New Faculty Luncheon with NSERC / <i>Déjeuner pour les nouveaux professeurs avec le CRSNG</i> (WE-A20) | Private Dining Rm |
| 12h30 - 13h30 | CITA AGM / Assemblée générale de CITA (WE-A21) | Campaign B |
| 13h30 - 14h15 | CAP/COMP Kirkby Medal Winner / <i>Récipiendaire de la médaille Kirkby de l'ACP/OCPM</i> - ROBERT BARBER, Univ. of Manitoba (WE-P1) | Victoria |
| 13h30 - 15h00 | Radiation Treatment Delivery / Exécution de la radiothérapie (WE-P2) | Albert |
| 14h00 - 14h45 | Visualizing Theory: Simulations in Cosmology / Théorie de visualisation : simulations en cosmologie - JOHN DUBINSKI, U.Toronto / (WE-P3) | Campaign B |
| 14h15 - 16h30 | Materials and Magnetism / <i>Matériaux et magnétisme</i> (WE-P4) | Victoria |
| 14h15 - 17h00 | Radioactive Beam/Heavy Ion Physics / <i>Physique des faisceaux radioactifs/d'ions lourds</i> (WE-P5) | Ballroom C |
| 14h15 - 16h30 | Imaging in the Stars and on Earth / <i>Imagerie dans les étoiles et sur terre</i> (WE-P6) | Ballroom A |
| 14h15 - 15h00 | Photonics Devices / <i>Dispositifs photoniques</i> (WE-P7) | Campaign A |
| 14h15 - 16h45 | Industrial and Applied Physics General Session / <i>Session générale sur la physique industrielle et appliquée</i> (WE-P8) | Ballroom B |
| 14h15 - 15h30 | Plasma Physics / <i>Physique des plasmas</i> (WE-P9) | Strathcona |
| 14h15 - 17h00 | General Relativity and Gravitation II / <i>Relativité générale et gravitation II</i> (WE-P10) | Kildonan |
| 14h45 - 15h30 | Visualizing Concepts in Theory - Contributed / Visualisation des concepts théoriques- contribuées (WE-P11) | Campaign B |
| 15h30 - 17h00 | Radiation Treatment Verification / Vérification de la radiothérapie (WE-P12) | Albert |
| 16h00 - 17h30 | Dark Matter and Dark Energy / <i>Matière et énergie noires</i> (WE-P13) | Colbourne |
| 16h00 - 16h30 | Imaging the Invisible Spectrum - Contributed / Imagerie dans le spectre de l'invisible - contribuées (WE-P14) | Campaign B |
| 16h30 - 17h15 | Miscellaneous Intrigues - Contributed / Intrigues diverses - contribuées (WE-P15) | Campaign B |
| 17h00 - 18h30 | CAP Council Meeting (New and Old) / <i>Réunion du Conseil (nouveau et ancien) de l'ACP</i> (WE-P16) | Campaign A |
| 17h15 - 17h30 | CASCA Closing and Awards Given for Best Student Presentations / CASCA Clôture et remise des prix aux meilleures présentations d'étudiants (WE-P17) | Campaign B |

DETAILED CONGRESS SUMMARY PROGRAMME DÉTAILLÉ DU CONGRÈS

(SEE PG. 20 FOR DESCRIPTION OF CODES-ABBREVIATIONS / VOIR PG. 20 POUR UNE DESCRIPTION DES CODES-ABBREVIATIONS)
(ABSTRACTS START ON PAGE 50 / LES RÉSUMÉS COMMencent À LA PAGE 50)

Saturday, June 12, 2004 / Samedi, le 12 juin

08h00 - 17h30 JCSA Meeting / Réunion de JCSA
 08h30 - 14h00 CAP Executive Meeting / Réunion de l'exécutif de l'ACP (SA-A2)
 08h30 - 17h30 COMP Business Meetings / Réunions d'affaires de l'OCPM (SA-A1)
 08h30 - 19h00 CASCA Board and Other Meetings / Réunion du Conseil de CASCA et autres réunions (SA-A3)
 08h45 - 16h30 CASCA Student Workshop and Registration/ Atelier des étudiants et inscription CASCA (SA-A4)
 12h00 - 13h30 COMP lunch / Déjeuner de l'OCPM
 14h00 - 18h00 CAP Council Meeting (Old and New) / Réunion du conseil (ancien et nouveau) de l'ACP (SA-P1)

Victoria
 Kildonan
 Talbot/Westminster/Strathcona
 Colbourne
 Univ. of Manitoba Campus
 Private Dining Room
 Kildonan

Sunday, June 13, 2004 / Dimanche, le 13 juin

| TIME HEURE | Victoria/Albert | Ballrooms B/C | Other Rooms/Autres salles |
|---------------|--|--|---|
| | SU-A1 (CAP-CASCA-COMP/ACP-CASCA-OCPM) ENRICHING OUR TEACHING THROUGH INTEGRATION / ENRICHISSEMENT DE NOTRE ENSEIGNEMENT PAR L'IN- TÉGRATION Chair: J. Percy, U.Toronto | | 08h00-12h30 Campaign B COMP Business Meeting Réunion d'affaires de l'OCPM (SU-A2) |
| 08h00 | V. Milosevic-Zdjelar (c) U.Winnipeg Astronomy, Biology, Chemistry, Geology and Physics integrated in a newly developed course "Science: World Views" (SU-A1-1) | | 08h30-12h30 Paragon Rest./Colbourne (CAP-ACP) Physics Department Heads/Chairs Workshop / Réunion des directeurs de départe- ments de physique (SU-CHAIRS) |
| 08h15 | C.R. Kerton (c) Iowa State U. Integrating a Lab Experience with an Astro 101 Class (SU-A1-2) | | |
| 08h30 | W.E. Harris (c) McMaster U. The Big Questions: Integrating Science at the Undergraduate Level (SU-A1-3) | | |
| 08h45 | J. West (c) U.Manitoba Crossing the Disciplines: Using Medical Imaging Software for Teaching Astronomy (SU-A1-4) | | |
| 09h00 | RICKEY, Daniel W. CancerCare Manitoba Medical Physics at the Undergraduate and High School Levels (SU-A1-5) | SU-A4 (DCMMP/DPMCM) SINGLE MOLECULE POLYMER PHYSICS: FUNDAMEN- TAL QUESTIONS / PHYSIQUE DES POLYMÈRES MONOMOLÉCULAIRES : QUESTIONS FONDAMENTALES Chair: J. Bechhoefer, SFU | 09h00-12h00 Campaign A IPP Board of Trustees Meeting Réunion du conseil d'administration de l'IPP (SU-A3) |
| 09h30 | MANOGUE, Corinne A. Oregon State U. Revitalizing the Upper-Division Physics Curriculum (SU-A1-6) | SEVICK, EDIT M. Australian National U. The Fluctuation Theorem as a Generalised Second- Law for Nanomachines and Single Biopolymer Manipulations: Optical Tweezers Experiments and Beyond (SU-A4-1) | |
| 10h00 | Coffee Break / Pause café | ↓ | |
| 10h15 | ↓ | FORDE, Nancy UC Berkeley Using Optical Tweezers to Study Single-Molecule Reactions in Real Time (SU-A4-2) | |
| 10h30 | MATTHEWS, Jaymie UBC Distance Learning from 820 km Straight Up: The Educational Potential of the MOST Space Telescope (SU-A1-7) | ↓ | |
| 11h00 | STINNER, Art / LOLY, Peter U.Manitoba Using the History of Science to Present the Evolution of Major Concepts in Physics (SU-A1-8) | HA, Bae-Yeun U.Waterloo Statics and Dynamics of Biopolymers: Theory and Biological Relevance (SU-A4-3) | |
| 11h30 | ↓ | ↓ | |
| 11h45 | ↓ | KREUZER, Hans Juergen Dalhousie U. Stretching and Confinement of Single Polymer Molecules and the Growth of a Polymer Brush: A First Principles Theory (SU-A4-4) | |
| 12h15 | Morning Session ends / Fin de la session du matin Lunch / déjeuner | Morning Session ends / Fin de la session du matin Lunch / déjeuner | |

Sunday, June 13, 2003 / *Dimanche, le 13 juin* (cont'd / suite)

| Victoria/Albert | Ballrooms B/C | Campaign A | Campaign B | TIME HEURE |
|---|---|--|--|--------------|
| | | | SU-P2 (COMP/OCPM) BRACHYTHERAPY AND THERMAL THERAPY / CURIOTHÉRAPIE ET THÉRAPIE THERMIQUE Chair: J. Bews, CancerCare Manitoba | |
| | SU-P1 Plenary Session plénière (CAP Brockhouse Medal winner / Récipiendaire de la médaille Brockhouse de l'ACP) Chair: J. Bechhoefer, SFU MICHAEL THEWALT SFU <i>Redefining the Limits of Semiconductor Spectroscopy</i> (SU-P1-1) | | N. Blais (c) Hôpital Maisonneuve-Rosemont <i>Space Distribution Analysis of the Attenuation in Lead and Steel of the Scattered Radiation in a Maze of a High Dose Rate (Iridium 192) Brachytherapy Suite</i> (SU-P2-1) | 13h30 |
| | | | M. Al-Ghazi (c) U.California, Irvine <i>Yttrium-90 Microspheres for the Treatment of Hepatocellular Carcinoma</i> (SU-P2-2) | 13h45 |
| | | | M. Shim (c) Juravinski Cancer Care <i>Cs-137 Dosimetry Using GAFchromic® Film</i> (SU-P2-3) | 14h00 |
| SU-P3 (CAP-CASCA-COMP/ACP-CASCA-OCPM) ENRICHING OUR TEACHING THROUGH INTEGRATION / ENRICHISSEMENT DE NOTRE ENSEIGNEMENT PAR L'INTÉGRATION Chair: R. Hawkes, Mount Allison U. H. Scott (c) Ridley College <i>Bringing the Stars to the Students</i> (SU-P3-1) | SU-P4 (DCMMP/DPMCM) SINGLE-MOLECULE POLYMER PHYSICS: BIOPHYSICAL APPLICATIONS / PHYSIQUE DES POLYMÈRES MONOMOLÉCULAIRES : APPLICATIONS EN BIOPHYSIQUE Chair: J. Bechhoefer, SFU MARKO, John U.Illinois at Chicago <i>Micromanipulation Study of Chromatin Fibers and Whole Chromosomes</i> (SU-P4-1) | | G. Leclerc (c) CHUQ <i>Dynamical Post-Implant Dose Calculation for Permanent Prostate Implants: Taking Edema into Consideration</i> (SU-P2-4) | 14h15 |
| CHRISTIAN, Carol Space Tel.Sci.In. <i>Putting Research Science and Education Together: Lessons Learned from HST</i> (SU-P3-2) | ↓ | SU-P5 IPP General Meeting / Assemblée générale (IPP) (ends at 17h30/ se termine à 17h30) | L. Chin (c) Princess Margaret Hospital <i>Interstitial Optical-Based Reconstruction of Thermal Coagulation During Microwave Thermal Therapy</i> (SU-P2-5) | 14h30 |
| ↓ | ↓ | | S. Lochhead (c) Sunnybrook/UToronto <i>A Gel Phantom for MR Calibration of Thermal Therapies</i> (SU-P2-6) | 14h45 |
| Coffee Break / Pause café | Coffee Break / Pause café | | Coffee Break / Pause café | 15h00 |
| PERCY, John R. U.Toronto <i>Variable Stars: Dynamic Tools for Hands-On Astronomy and Physics Education</i> (SU-P3-3) | SLATER, Gary U.Ottawa <i>Single-Molecule Polymer Physics: The Role of Molecular Dynamics Simulations</i> (SU-P4-2) | | SU-P6 (COMP/OCPM) RADIATION TREATMENT DEVICES / APPAREILS DE RADIOTHÉRAPIE Chair: P. Dunscombe, TomBaker CancerCen. H. Johnson (c) CancerCare Manitoba <i>Licensing, Construction and Radiation Safety of Canada's First Gamma Knife®</i> (SU-P6-1) | 15h30 |
| ↓ | ↓ | | A. Berndt (c) CancerCare Manitoba <i>Gamma Knife® Commission Report</i> (SU-P6-2) | 15h45 |
| M.L. Milne (c) Centre of Universe <i>Reaching out from the Centre of the Universe: A Report from Canada's Astronomy Interpretation Centre</i> (SU-P3-4) | ↓ | | J.W. Beck (c) CancerCare Manitoba <i>An Algorithm for Independent Verification of Gamma Knife® Treatment Plans</i> (SU-P6-3) | 16h00 |
| Session ends / Fin de la session | MARZIALI, Andre UBC <i>A Single-Molecule Nanosensor for Oligonucleotide Identification</i> (SU-P4-3) | | M. MacKenzie (c). Cross Cancer Inst. <i>Initial Experiences with a Commercial Helical Tomotherapy Unit</i> (SU-P6-4) | 16h15 |
| | ↓ | | A. Gladwish (c) London Health Sciences <i>Helical Tomotherapy Fan Beams and Craniocaudal Penumbra Improvement</i> (SU-P6-5) | 16h30 |
| | ↓ | | J. Schella (c) NS Cancer Centre <i>Using Isocentre Corrections in Treatment Planning to Improve Accuracy in Stereotactic Radiosurgery</i> (SU-P6-6) | 16h45 |
| | Session ends / Fin de la session | | Session ends / Fin de la session SU-P7 CCPM AGM / Assemblée générale (CCPM) (ends at 18h30/se termine à 18h30) | 17h00 |

CAP Herzberg Memorial Public Lecture / Conférence publique commémorative Herzberg de l'ACP
CASCA Public Lecture in Astronomy / Conférence publique plénière en astronomie de CASCA

[SU-KEY]

P. James E. Peebles, Princeton University

19h00

Followed by the Opening Reception / suivi par la réception d'accueil

Ballroom A/B/C (see pg. 17 for details / voir pg. 17 pour les détails)

DETAILED CONGRESS PROGRAM - MONDAY, JUNE 14

| TIME HEURE | Other locations autres endroits | Ballroom A | Ballroom B/C | Kildonan |
|--|--|--|---|---|
| 07h30 | "Friends of CAP" Breakfast / Déjeuner des 'Ami(e)s de l'ACP' (07h30-08h30) - Private Dining Room (MO-A1) | | | |
| The all-day High School Teachers Workshop, organized by the CAP's Division of Physics Education, will be held in Colbourne starting at 08h00 L'atelier pour les enseignant(e)s de la physique, coordonnée par le Division d'enseignement de l'ACP, aura lieu dans Colbourne, commençant à 08h00 (see page 18 for details / voir page 18 pour le programme) | | | | |
| 08h30 | | | MO-A3 Plenary Session plénière (CAP/ACP) (Teaching Medal winner - récipiendaire de la médaille d'enseignement) Chair: R. Hawkes, Mount Allison U. HELMY SHERIF U. Alberta <i>A Discussion of Spin: From Teaching to Research (MO-A3-1)</i> | |
| 08h45 | | | ↓ | |
| 09h00 | | | ↓ | |
| 09h15 | | | MO-A5 Plenary Session plénière Chair: J. Bechhoefer, SFU (CAP/ACP) DAVID BENSIMON École normale supérieure <i>The Elastic Behaviour of a Real Polymer: The Case of ssDNA (MO-A5-1)</i> | |
| 09h30 | | | ↓ | |
| 09h45 | | | ↓ | |
| | | MO-A9 (DCMMP/DPMCM) SEMICONDUCTORS / SEMICONDUCTEURS Chair: M.Thewalt, SFU | ↓ | MO-A8 (PPD-DNP / PPD-DPN) ADVANCES IN INSTRUMENTATION / PROGRÈS EN INSTRUMENTATION Chair: F. Corriveau, McGill U. |
| 10h00 | | S. Webster (c) UBC <i>Dilute Nitride Multiple-Quantum-Well Light Source for Optical Coherence Tomography (MO-A9-1)</i> | Session ends / <i>La session se termine</i> Coffee Break until 10h20 / Pause café jusqu'à 10h20 | OSER, Scott M. UBC <i>Long-Baseline Neutrino Oscillations at K2K and J-PARC (MO-A8-1)</i> |
| 10h15 | | K.A.L. Shorlin (c) UWO <i>Clustering of Ga on GaAs (100) (MO-A9-2)</i> | | ↓ |
| 10h20 | | ↓ | MO-A11 (All Org.) OPENING GREETINGS BY MB MIN. TIM SALE BIENVENUE PAR LE MIN. DU MB, TIM SALE | ↓ |
| | | ↓ | MO-A12 (All Org.) SCIENTIFIC IMAGES IN THE PUBLIC SPHERE / LES IMAGES SCIENTIFIQUES DANS LA SPHÈRE PUBLIQUE Chair: M. Campbell, U. Waterloo | ↓ |
| 10h30 | | H. Rastegar-Moghaddam (c) UBC <i>Change in Photoluminescence Spectrum of Infrared Coupled Multiple Quantum Wells (MO-A9-3)</i> | OTTENSMEYER, Peter U.Toronto <i>Images of the Invisibly Small: from Atoms to Biomacromolecular Structure and Function (MO-A12-1)</i> | KRIEGER, Peter W. U.Toronto <i>The ATLAS Detector at the Large Hadron Collider (MO-A8-2)</i> |
| 10h45 | | F. Schiettekatte (c) U.Montreal <i>Controlled Modification of Quantum Heterostructures by Ion Implantation Induced Defects (MO-A9-4)</i> | ↓ | ↓ |
| 11h00 | | Coffee break / Pause café | ROORDA, Austin U.Houston <i>From Telescope to Ophthalmoscopes: Adaptive Optics for Microscopic Imaging of the Living Eye (MO-A12-2)</i> | Coffee break / Pause café |

| Campaign A | Victoria | Campaign B | Albert | TIME HEURE |
|--|---|--|---|------------|
| 07h30 | | | | |
| The all-day High School Teachers Workshop, organized by the CAP's Division of Physics Education, will be held in Colbourne starting at 08h00 L'atelier pour les enseignant(e)s de la physique, coordonnée par le Division d'enseignement de l'ACP, aura lieu dans Colbourne, commençant à 08h00 (see page 18 for details / voir page 18 pour le programme) | | | | |
| | | | MO-A4 (COMP-OCPM) DIAGNOSTIC IMAGING / IMAGERIE DIAGNOSTIQUE Chair: J.A. Rowlands, SWCHSC/U.Toronto | |
| | | | A. Kress (c) Cross Cancer Inst./ U.Alberta <i>Experimental Verification of Sinogram Merging Technique to Reduce Limited Field-of-View Artifacts in CT Imaging</i> (MO-A4-1) | 08h30 |
| | | | C. McKenzie (c) Harvard Med.School <i>Abdominal Three Point Dixon Imaging with Self Calibrating Parallel MRI</i> (MO-A4-2) | 08h45 |
| | | | A.F. Wind (c) Carleton U. <i>Pinhole SPECT with Iterative Reconstruction and the Median Root Prior Filter</i> (MO-A4-3) | 09h00 |
| | | MO-A6 (CASCA) VISUALIZATION IN PLANETARY SCIENCES / VISUALISATION EN SCIENCE PLANÉTAIRE Chair: S. Safi-Harb, U.Manitoba PAUL WIEGERT UWJO <i>Visualizing Dynamics in the Solar System</i> (MO-A6-1) | E. Van Uytven (c) CancerCare MB <i>3D Mammography: A Single Projection Compton Scatter Imaging Technique</i> (MO-A4-4) | 09h15 |
| | | ↓ | E. Galiano (c) Laurentian U. <i>Unintentional Human Skeletal Imaging with ^{99m}Tc-Methylene Diphosphonate 45 Months Beyond Expiration</i> (MO-A4-5) | 09h30 |
| | | ↓ | Session ends / Fin de la session | 09h45 |
| | MO-A7 (DCMMP/DPMCM) SOFT MATTER / MATIÈRE MOLLE Chair: B. Joos, U. Ottawa | Session Ends at 10h00 / La session se termine à 10h00 Coffee Break until 10h20 / Pause café jusqu'à 10h20 | MO-A10 (DTP/DPT) PARTICLE PHYSICS I / PHYSIQUE DES PARTICULES I Chair: R. Mann, U. Waterloo | |
| | B.J. Frisken (c) SFU <i>Temperature-Sensitive Size of Microgel Particles</i> (MO-A7-1) | ↓ | CARRINGTON, Margaret Brandon U. <i>Transport Theory Beyond Binary Collisions</i> (MO-A10-1) | 10h00 |
| | M.-P. Nieh (c) NRC <i>Spontaneous Formation of Monodisperse Small Unilamellar Vesicles - Kinetically Trapped or Thermodynamically Stable?</i> (MO-A7-2) | ↓ | ↓ | 10h15 |
| | ↓ | | ↓ | 10h20 |
| | V.A. Raghunathan (c) NRC <i>Phase Behaviour of Aqueous Solutions of Short and Long Chain Phospholipids</i> (MO-A7-3) | | GALE, Charles McGill U. <i>Electromagnetic Signals from Matter Under Extreme Conditions</i> (MO-A10-2) | 10h30 |
| | J. Katsaras (c) NRC <i>Novel Finite-Size Effects in Biomimetic Smectic Films</i> (MO-A7-4) | | ↓ | 10h45 |
| | J. Bechhoefer (c) SFU <i>Studies of Banded Spherulites in Ethylene-Carbonate-Polymer Mixtures</i> (MO-A7-5) | | LEWIS, Randy U.Regina <i>Lattice QCD Phenomenology and Its Limits</i> (MO-A10-3) | 11h00 |

| TIME HEURE | Other locations autres endroits | Ballroom A | Ballrooms B/C | Kildonan |
|------------|--|---|---|--|
| 11h15 | | | ↓ | KARLEN, Dean U. Victoria/TRIUMF <i>The Future Linear Collider Project</i> (MO-A8-3) |
| 11h30 | | M.C. Gallagher (c) Lakehead U. <i>Tailoring the Dimensionality of Gold Chains on Silicon</i> (MO-A9-5) | CHRISTIAN, Carol SpaceTel.Sci.Inst. <i>Public Impact of Scientific Images: Examples from Space Science</i> (MO-A12-3) | ↓ |
| 11h45 | | L. Pedri (c) Lakehead U. <i>STM of Gold Induced Chains at Stepped Silicon Surfaces</i> (MO-A9-6) | ↓ | D. Gingrich (c) U. Alberta/TRIUMF <i>Radiation Tolerant Microelectronics by Design</i> (MO-A8-4) |
| 12h00 | | G. Beydaghyan (c) Queen's U. <i>GISAXS Characterization of Nanostructures in Glancing Angle Deposited Films</i> (MO-A9-7) | BRONSKILL, Michael Sunnybrook/U. Toronto <i>Imaging Physics Meets Public Perception: Is Private MRI Bad?</i> (MO-A12-4) | J. Gauthier (c) U. Laval <i>BaF₂ Detector Development</i> (MO-A8-5) |
| 12h15 | | R. Karmouch (c) U. Montreal <i>Damage in Self-Implanted Si: Channeling Compared to Nanocalorimetry</i> (MO-A9-8) | ↓ | R. Roy (c) U. Laval <i>HERACLES Multidetector Calibration</i> (MO-A8-6) |
| 12h30 | MO-A14 Past Presidents' Lunch (Ends at 13h30) / <i>Déjeuner des anciens présidents (se termine à 13h30)</i> (Heartland Boardroom) | Session ends / Fin de la session | Session ends / Fin de la session | Session ends / Fin de la session |

| TIME HEURE | Other Locations Autres endroits | Ballroom A | Ballroom B | Ballroom C | Colbourne | Kildonan |
|------------|---------------------------------|---|---|------------|--|---|
| 13h25 | | | | | | |
| 13h30 | | MO-P2 Plenary Session plénière (CAP/CRM Medal winner - récipiendaire de la médaille ACP/CRM) Chair: W.J. McDonald, UAlta JIRI PATERA U. Montreal <i>Deterministic Aperiodic Multidimensional Point Sets, Their Properties and Exploitation</i> (MO-P2-1) (Session ends a 14h15 / Session Se termine à 14h15) | | | 13h35 MO-P5 High School Teacher's Workshop continues / L'atelier pour les enseignant(e)s de la physique continue | |
| | | MO-P7 (PPD) THE PRECISION FRONTIER IN PARTICLE PHYSICS / LA FRONTIÈRE DE LA PRÉCISION EN PHYSIQUE DES PARTICULES Chair: D. Karlen, U.Victoria | MO-P6 (ALL ORGS) SCIENTIFIC IMAGES IN THE PUBLIC SPHERE / L'IMAGERIE SCIENTIFIQUE DANS LA SPHÈRE PUBLIQUE Chair: J. English, U.Manitoba | ↓ | | MO-P10 (DTP-DPT) QUANTUM INFORMATION THEORY / THÉORIE DE L'INFORMATION QUANTIQUE Chair: R. Mann, U.Waterloo |
| 14h15 | | RONEY, Michael U. Victoria <i>Recent Results from the BaBar Experiment</i> (MO-P7-1) | CALAMAI, Peter The Toronto Star <i>Don't Overlook Images Created with Words</i> (MO-P6-1) (Ends at 14h45 / Se termine à 14h45) | ↓ | | LAFLAMME, Raymond Inst. for Quantum Comp. <i>NMR and Quantum Information Processing</i> (MO-P10-1) |
| 14h30 | | ↓ | ↓ | ↓ | ↓ | ↓ |

| Campaign A | Victoria | Campaign B | Albert | TIME HEURE |
|--|--|---|--|------------|
| | M. Singh (c) Queen's U. <i>Development of a GISAXS Furnace for In-Situ Polymer Film Characterization (MO-A7-6)</i> | | ↓ | 11h15 |
| | J.H. Page (c) U.Manitoba <i>Diffusion of Ultrasonic Waves in Porous Glass Bead Sinters (MO-A7-7)</i> | | MOORE, Guy McGill U. <i>Strong Bounds on Lorentz Symmetry Violation (MO-A10-4)</i> | 11h30 |
| | A. Sukhovich (c) U.Manitoba <i>Resonant Tunneling of Ultrasound in Phononic Crystals (MO-A7-8)</i> | | ↓ | 11h45 |
| | W. Hildebrand (c) U.Manitoba <i>Direct Vibrational Density of States Measurements in Strongly Scattering Media (MO-A7-9)</i> | | MANN, Robert U.Waterloo <i>Revised Radiative Electroweak Symmetry Breaking: Further Results (MO-A10-5)</i> | 12h00 |
| | A. Plyukhin (c) U.Saskatchewan <i>Nonlinear Dissipation in Brownian Motion (MO-A7-10)</i> | | ↓ | 12h15 |
| DAMP Business Mtg Ends at 13h30 <i>Réunion d'affaires DPAM</i> Se termine à 13h30 | Session ends / Fin de la session DCMMP Business Mtg Ends at 13h30 <i>Réunion d'affaires DPMCM</i> Se termine à 13h30 | MO-A13 C ASCA JCMT User's Meeting / <i>Réunion des utilisateurs du TJCM de la CASCA</i> Chair: L. Knee, NRC Ends at 13h20 / Se termine à 13h20 | Session ends / Fin de la session DTP Business Mtg Ends at 13h30 <i>Réunion d'affaires DPT</i> Se termine à 13h30 | 12h30 |

| Strathcona | Westminster | Campaign A | Victoria | Albert | Campaign B | TIME HEURE |
|---|-------------|---|---|---|---|------------|
| | | | | | MO-P1 (CASCA) Herschel Space Observatory Information Session / <i>Session d'information sur l'observatoire spatial Herschel</i> Chair: M. Fich, U.Waterloo | 13h25 |
| MO-P4 (CASCA) Demonstration of the Karma Visualization Software / <i>Démonstration du logiciel de visualisation Karma</i> GOOCH, R. , U.Calgary (ends at 14h00 / se termine à 14h00) | | | MO-P3 Plenary Session plénière (CAP/INO Médal winner - <i>récipiendaire de la médaille ACP/INO</i>) Chair: P. Galameau, INO NICOLAS JAEGER UBC <i>Optical Sensors for Power Utility Applications (MO-P3-1)</i> | | Ends at 14h15 / Se termine à 14h15 ↓ | 13h30 |
| | | MO-P8 (DNP/DPN) SYMMETRIES IN NUCLEAR PHYSICS / <i>LES SYMÉTRIES EN PHYSIQUE NUCLÉAIRE</i> Chair: W. van Oers, U. Manitoba | ↓ | MO-P9 (DIMP-DMBP/DPIM-DPMB) INSTRUMENTATION AND TECHNIQUES IN BIOMEDICAL PHYSICS / <i>INSTRUMENTATION ET TECHNIQUES EN PHYSIQUE BIOMÉDICALE</i> Chair: A. Mandelis, U. Toronto | ↓ | |
| | | OELERT, Walter Forschungszentrum Juelich <i>Observation of Cold Antihydrogen - Perspectives for Testing Fundamental Symmetries (MO-P8-1)</i> | | BOCCARA, Claude ESPCI <i>Optical Imaging in Turbid Media: New Developments (MO-P9-1)</i> | MO-P11 (DCMMP/DPMCM) CUPRATES IN THE EXTREME UNDERDOPED LIMIT / <i>LES CUPRATES DANS LA LIMITE EXTRÊME SOUS-DOPÉE</i> Chair: I. Herbut, SFU | 14h15 |
| | | ↓ | | ↓ | BONN, Douglas UBC <i>Dying Gasps of a d-Wave Superconductor (MO-P11-1)</i> | 14h30 |

| TIME HEURE | Other Locations Autres endroits | Ballroom A | Ballroom B | Ballroom C | Colbourne | Kildonan |
|---------------|------------------------------------|---|--|--|---|--|
| 14h45 | | MILDENBERGER, Joseph L. TRIUMF <i>Latest Results from the Search for $K^+ \rightarrow \pi^+ \nu \bar{\nu}$</i> (MO-P7-2) | MO-P12 PANEL ON SCIENTIFIC IMAGES IN THE PUBLIC SPHERE / DISCUSSION SUR LES IMAGES SCIENTIFIQUE DANS LA SPHERE PUBLIQUE - Chair: J. English, U.Manitoba Panel comprised of F. Peter Ottensmeyer, Austin Roorda, Michael J. Bronskill, Carol A. Christian, and Peter Calamai (Ends at 15h45 / Se termine à 15h45) | | ↓ | SANDERS, Barry C. U.Calgary <i>Quantum Information Processing with Continuous Variables</i> (MO-P10-2) |
| 15h00 | | | ↓ | | ↓ | ↓ |
| 15h15 | | S. Brunet (c) U.Montreal <i>Measurement of the $B \rightarrow \pi / \pi^0 / \eta / \nu$ Branching Ratios Using Semileptonic Tags in the BaBar Experiment</i> (MO-P7-3) | ↓ | | ↓ | ↓ |
| 15h30 | | D. Cote (c) U.Montreal <i>Determination of V_{ub} from the Measurement of $B \rightarrow \pi^+ / \pi^0 / \eta / \eta' / \rho^+ / \rho^0 / \omega / \nu$ Branching Fractions and Form Factors at BaBar</i> (MO-P7-4) | ↓ | | Session Ends / Fin de la session | KOBES, Randy U.Winnipeg <i>Exploring Paths in Adiabatic Quantum Computing</i> (MO-P10-3) |
| 15h45 | | P. Jackson (c) U.Victoria <i>A Search for $B^+ \rightarrow K^+ \nu \bar{\nu}$</i> (MO-P7-5) | ↓ | ↓ | | ↓ |
| 16h00 | | C. Brown (c) TRIUMF/U.Victoria <i>A Search for Lepton-Flavor Violation at BaBar</i> (MO-P7-6) | ↓ | MO-P15 (ALL ORGS) SCIENTIFIC IMAGING AND VISUALIZATION - CONTRIBUTED / IMAGERIE ET VISUALISATION SCIENTIFIQUES - PRÉSENTATIONS CONTRIBUTÉES Chair: M.J. Bronskill, U.Toronto | | STAMP, Philip UBC <i>Decoherence Mechanisms and the Dynamics of Decoherence in Qubit Networks</i> (MO-P10-4) |
| 16h15 | | D. Fortin (c) U.Victoria <i>Determination of V_{ub} in the BaBar Experiment Using the Lepton Invariant Mass Squared</i> (MO-P7-7) | | G. Joncas (c) U. Laval <i>The Square Kilometre Array</i> (MO-P15-1) | | ↓ |
| 16h30 | | S. McLachlin (c) McGill U. <i>Search for the Rare Decay $B^0 \rightarrow J/\psi \gamma$</i> (MO-P7-8) | | J. Fiege (c) NRC-HIA <i>Evolution Meets Astrophysics: Using Advanced Genetic Algorithms to Search and Visualize Large Parameter Spaces</i> (MO-P15-2) | | KEMPF, Achim U.Waterloo <i>Towards a Notion of Qubit Density for Quantum Fields in Curved Spacetime</i> (MO-P10-5) |
| 16h45 | | M. Quraan (c) TRIUMF <i>A High Precision Measurement of Muon Decay Parameters</i> (MO-P7-9) | | M. Boileau (c) Laurentian U. <i>Energy Dispersive X-Ray Diffraction Measurements Using a Cadmium Zinc Telluride Detector</i> (MO-P15-3) | MO-P16 (CEWIP/CEFEP) IMPROVING THE CLIMATE FOR WOMEN IN PHYSICS / AMÉLIORATION DU CLIMAT POUR LES FEMMES EN PHYSIQUE Chair: B. Frisken, SFU | ↓ |
| 17h00 | | K. Olchanski (c) TRIUMF <i>Data Analysis Techniques for High Precision Measurement of Muon Decay Parameters</i> (MO-P7-10) | | A. Faust (c) Deference R&D Canada <i>Application of X-Ray Backscatter Imaging to Explosive Device Detection</i> (MO-P15-4) | WHITTEN, Barbara Colorado College <i>What Works for Women in Undergraduate Physics?</i> (MO-P16-1) | Session Ends / Fin de la session |

| Strathcona | Westminster | Campaign A | Victoria | Albert | Campaign B | TIME HEURE |
|--|-------------|--|--|---|--|------------|
| | | GWINNER, Gerald U.Manitoba <i>A New Test of the Special Theory of Relativity with the Heidelberg Test Storage Ring (MO-P8-2)</i> | | MANDELIS, Andreas U.Toronto <i>Laser Photo-Thermo-Acoustic Frequency Swept Heterodyned Lock-in Depth Profilometry for Three-Dimensional Sub-Surface Tissue Imaging (MO-P9-2)</i> | | 14h45 |
| | | ↓ | | ↓ | Coffee Break / Pause café | 15h00 |
| | | Coffee Break / Pause café | MO-P13 (DMBP-DCMMP DPMB-DPMC) GENETICS NETWORKS / RÉSEAUX GÉNÉTIQUES Chair: P. Higgs, McMaster U. | Coffee Break / Pause café | ↓ | 15h15 |
| | | ↓ | SWAIN, Peter McGill U. <i>Stochastic Gene Expression in Single Cells (MO-P13-1)</i> | ↓ | FRANZ, Marcel UBC <i>Nodal Protectorate in Underdoped Cuprates (MO-P11-2)</i> | 15h30 |
| | | BACHER, Andrew Indiana U. <i>Observation of Charge Symmetry Breaking in the Reaction $d-d \rightarrow {}^4\text{He}-\pi^0$ (MO-P8-3)</i> | ↓ | H. Dobrovolny (c) Duke U. <i>Conduction Velocity Dispersion in Cardiac Tissue (MO-P9-3)</i> | ↓ | 15h45 |
| MO-P14 (CAP/ACP) NSERC Information Session for Existing Grant Holders / Session d'information du CRSNG pour les détenteurs actuels de bourses | | ↓ | KAERN, Mads Boston U. <i>Gene Regulatory Systems: Roles of Physics in Post-Genomic Biology (MO-P13-2)</i> | C. Kumaradas (c) Ryerson U. <i>Magnetocarcinotherapy: A Novel Method for the Detection and Treatment of Cancer Using Magnetic Nanoparticles (MO-P9-4)</i> | SUTHERLAND, Michael U.Toronto <i>Nodal Metallic Phase in Underdoped Cuprates (MO-P11-3)</i> | 16h00 |
| ↓ | | HASINOFF, Michael UBC <i>A Test of Time Reversal Invariance in Stopped Kaon Decay (MO-P8-4)</i> | ↓ | D. Cote (c) Ontario Cancer Inst. <i>Polarimetry in Turbid Media for Robust Determination of Concentration of Optically Active Molecules: Modelling, Experiments, and Application to Biophotonics (MO-P9-5)</i> | ↓ | 16h15 |
| ↓ | | ↓ | NOIREAUX, Vincent The Rockefeller U. <i>From In Vitro Genetic Circuits to an Artificial Cell (MO-P13-3)</i> | J. Grinyer (c) McMaster U. <i>In Vivo Cadmium Measurement by Prompt Gamma Neutron Activation Analysis (MO-P9-6)</i> | BUYERS, William J.L. NRC <i>Spins and Paired Carriers in a Superconductor that is Nearly an Antiferromagnet - Who Pushes Whom? (MO-P11-4)</i> | 16h30 |
| ↓ | | J.W. Martin (c) California Inst. Tech. <i>Beta-Decay of Ultracold Neutrons (MO-P8-5)</i> | ↓ | R. Korol (c) UWO <i>Optical Analysis of Carotid Atherosclerotic Plaque using Laser Induced Fluorescence (MO-P9-7)</i> | ↓ | 16h45 |
| Session Ends / Fin de la Session | | Session Ends / Fin de la Session | WESTWOOD, Tim U.Toronto <i>Using DNA Microarrays for Functional Genomic Studies (MO-P13-4)</i> | Session Ends / Fin de la Session MO-STUD (CAP/ACP) Best Graduate Student Paper Competition / Concours de la meilleure communication étudiante | Session Ends / Fin de la Session | 17h00 |

| TIME HEURE | Other Locations Autres endroits | Ballroom A | Ballroom B | Ballroom C | Colbourne | Kildonan |
|------------|---|--|--|------------|--|----------|
| 17h15 | | S. Robertson (c) IPP/McGill U. <i>Future High Luminosity Scenarios for the BaBar Experiment (MO-P7-11)</i> | E. Galiano (c) Laurentian U. <i>The Digital Radiographic and Computed Tomography Imaging of Two Types of Explosive Devices (MO-P15-5)</i> | | ↓ | |
| 17h30 | | A. Aleksejevs (c) U.Manitoba <i>Parity-Violating Hard Photon Bremsstrahlung in Electron-Proton Scattering (MO-P7-12)</i> | Session Ends / Fin de la session | | (30 min. discussion plus 1 hour CEWIP meeting - Session ends at 19h00) | |
| 17h45 | | J. Lu (c) TRIUMF <i>Measurement of Azimuthal Asymmetries Associated with Deeply-Virtual Compton Scattering (MO-P7-13)</i> | | | ↓ | |
| 18h00 | CJP Editorial Board Meeting / Réunion du Comité de rédaction de la RCP (Heartland Bdrm) | Session Ends / Fin de la session | | | | |

19h00

Poster Session, with Beer

Winnipeg Convention Centre

Canadian Astronomical Society / Société canadienne d'astronomie

Atmospheric and Space Physics / Physique atmosphérique et de l'espace

Atomic and Molecular Physics / Physique atomique et moléculaire

Condensed Matter and Materials Physics / Physique de la matière condensée et matériaux

Nuclear Physics / Physique nucléaire

Optics and Photonics / Optique et photonique

MO-POS-1 - 68

MO-POS-69 - 70

MO-POS-71 - 80

MO-POS-81 - 95

MO-POS-96 - 101

MO-POS-102

Tuesday, June 15

| TIME HEURE | Other Locations Autres endroits | Ballroom A | Ballroom B | Ballroom C | Colbourne | Kildonan |
|------------|--|------------|---|------------|-----------|----------|
| 07h00 | Meeting of the Canadian National IUPAP Liaison Committee (07h00-09h00) - Private Dining Room (TU-A1) | | | | | |
| 08h30 | | | TU-A2 (CAP/ACP) Plenary Session plénière Chair: M. Paranjape, U.Montreal NIMA ARKANI-HAMED Harvard U. <i>The Crises of Frontier Physics: From the Hubble Length to the Planck Length (TU-P1-1)</i> | | | |
| 08h45 | | | ↓ | | | |
| 09h00 | | | ↓ | | | |

| Strathcona | Westminster | Campaign A | Victoria | Albert | Campaign B | TIME HEURE |
|------------|--|------------|---|--|---|------------|
| | | | ↓ | ↓ | | 17h15 |
| | Physics in Canada Editorial Board Meeting <i>Réunion du Comité de rédaction de La Physique au Canada</i> (Ends at 19h00 / Se termine à 19h00) | | HIGGS, Paul McMaster U. <i>Bacterial Phylogenetics and Horizontal Gene Transfer (MO-P13-5)</i> | ↓ | MO-P17 (CASCA) NSERC GSC-017: Possible Change to Funding Envelope in Astronomy / Modification possible du financement d'enveloppe pour l'astronomie Chair: G. Harris, U. Waterloo | 17h30 |
| | | | ↓ | ↓ | ↓ | 17h45 |
| | | | Session Ends / Fin de la Session | Session ends at 19h00 / Session se termine à 19h00 | Session ends at 18h15 / Session se termine à 18h15 | 18h00 |

19h00
Session d'affiches, bière servie
Winnipeg Convention Centre

| | | | | | |
|--|---|--|--|---|---|
| <i>Physics Education / L'enseignement de la physique</i> | <i>Theoretical Physics / Physique théorique</i> | <i>Industrial and Applied Physics / Physique industrielle et appliquée</i> | <i>Instrumentation and Measurement Physics / Physique des instruments et mesures</i> | <i>Medical and Biological Physics / Physique médicale et biologique</i> | <i>Canadian Organization of Medical Physicists / L'Organisation des physiciens médicaux</i> |
| MO-POS-103 | MO-POS-104 - 114 | MO-POS-115 | MO-POS-116 - 117 | MO-POS-118 - 124 | MO-POS-125 - 149 |

Mardi, le 15 juin

| Strathcona | Westminster | Campaign A | Victoria | Albert | Campaign B | TIME HEURE |
|--|-------------|------------|----------|--|--|------------|
| (TU-A1) Réunion du comité de liaison national Canadien (IUPAP) (07h00-09h00) - Private Dining Room | | | | | | 07h00 |
| | | | | TU-A3 (COMP-DMBP/OCMP-DPMB) YOUNG INVESTIGATORS IN MEDICAL AND BIOLOGICAL PHYSICS / JEUNES CHercheurs(Ses) EN PHYSIQUE MÉDICALE ET BIOLOGIQUE Chair: L.J. Schreiner, Queen's U. | TU-A4 (CASCA) IMAGING WITH ALMA / IMAGERIE À L'AIDE DE L'ALMA Chair: L. Knee, NRC | |
| | | | | B. Warkentin (c) Cross Cancer Inst. 3-D Verification of IMRT Treatments Using a Flat-Panel EPID (TU-A3-1) | To be announced / à venir Imaging Star and Galaxy Formation with ALMA (TU-A4-1) | 08h30 |
| | | | | G. Cranmer-Sargison (c) U. Victoria Benchmarking a Multi-Leaf Collimator Particle Transport Algorithm for IMRT Field Verification (TU-A3-2) | ↓ | 08h45 |
| | | | | B. Schaly (c) London Reg. CancerCentre Dose Tracking for Adaptive Radiation Therapy (TU-A3-3) | ↓ Session Ends at 09h15 / Session se termine à 09h15) | 09h00 |

DETAILED CONGRESS PROGRAM - TUESDAY, JUNE 15

| TIME HEURE | Other Locations Autres endroits | Ballroom A | Ballroom B | Ballroom C | Colbourne | Kildonan |
|---------------|------------------------------------|--|--|---|--|---|
| 09h15 | | | TU-A5 Plenary Session plénière (CAP Medal of Achievement winner - Récipiendaire de la médaille ACP) Chair: B. Joos, U.Ottawa MICHAEL THEWALT SFU <i>Optical Spectroscopy in Semiconductors (TU-A5-1)</i> | | | |
| 09h30 | | | ↓ | | | |
| 09h45 | | | ↓ | | | |
| | | TU-A14 (DAMP/DPAM) ATOMIC AND MOLECULAR SPECTROSCOPY AND DYNAMICS I / SPECTROSCOPIE ET DYNAMIQUE ATOMIQUE ET MOLECULAIRE I Chair: P. Zetner, U.Manitoba | TU-A7 (DCMMP/DPMC) IMPACT OF HIGH PERFORMANCE COMPUTING ON MATERIALS RESEARCH / IMPACT DE L'INFORMATIQUE À HAUTE PERFORMANCE SUR LA RECHERCHE SUR LES MATÉRIAUX Chair: G. Slater, U.Ottawa | TU-A11 (DNP-CASCA/ DPN-CASCA) NOVAE AND SUPERNOVAE / NOVAS ET SUPERNOVAS Chair: S. Safi-Harb, U.Manitoba | TU-A13 (DCMMP/DPMC) CORRELATED ELECTRONS/MAGNETISM / ÉLECTRONS CORRÉLÉS/ MAGNÉTISME Chair: W.J.L. Buyers, NRC | TU-A9 (DTP-PPD DPT-PPD) PARTICLE-STRINGS-FIELDS / PARTICULES-FICELLES-CHAMPS Chair: R. MacKenzie, U.Montreal |
| 10h00 | | HEPBURN, John UBC <i>Spectroscopy and Dynamics of Threshold Ionization of Clusters and Small Molecules (TU-A14-1)</i> | COTE, Michel U.Montreal <i>Virtual Experiments: Applications of Density Functional Theory on Large-Scale Computational Facilities (TU-A7-1)</i> | HWANG, Una NASA/GSFC <i>Windows into Nucleosynthesis from X-Ray Observations of Supernova Remnants (TU-A11-1)</i> | CHAKRABORTY, Tapash U.Manitoba <i>How to Probe a Fractionally-Charged Quasihole? (TU-A13-1)</i> | HOLDOM, Bob U.Toronto <i>Ghostly Tales (TU-A9-1)</i> |
| 10h15 | | ↓ | ↓ | ↓ | ↓ | ↓ |
| 10h30 | | JAEGER, Wolfgang U.Alberta <i>Spectroscopy of He_N- Molecule Clusters: A Probe of the Onset of Superfluidity? (TU-A14-2)</i> | SORENSEN, Erik McMaster U. <i>Kondo Effect and Persistent Currents in Quantum Dot Systems (TU-A7-2)</i> | MATZNER, Christopher U.Toronto <i>Energy Feedback in Core- Collapse Supernovae (TU-A11-2)</i> | C. Doiron (c) U.Sherbrooke <i>Transport Gap in Quantum Hall Bilayers at Total Filling Factor $\nu = 5$ (TU-A13-2)</i> | LEE, Taejin UBC <i>Free Field Representation of Rolling Tachyon (TU-A9-2)</i> |
| 10h45 | | ↓ | ↓ | ↓ | A. Faribault (c) U.Sherbrooke <i>Pinning Mode of the Electron Crystals in Higher Landau Levels (TU-A13-3)</i> | ↓ |
| 11h00 | | VAN WIJNGAARDEN, William York U. <i>Bose-Einstein Condensation in a QUIC Trap (TU-A14-3)</i> | WHITMORE, Mark MUN <i>High Performance Computing: The New and Growing Environment in Canada (TU-A7-3)</i> | Coffee Break / Pause café | Coffee Break / Pause café | BERNSEN, Aaron CHEP, McGill <i>Aspects of Brane-Gas Cosmology (TU-A9-3)</i> |

| Strathcona | Westminster | Campaign A | Victoria | Albert | Campaign B | TIME HEURE |
|------------|--|--|--|---|--|------------|
| | | | | ↓ | TU-A6 (CASCA) NEWS FROM SPACE - CONTRIBUTED TALKS / NOUVELLES DE L'ESPACE - PRÉSENTATIONS CONTRIBUÉES Chair: M. Fich, U. Waterloo | |
| | | | | W. Song (c) London Reg. Cancer Centre <i>Limitations of a Convolution Method for Modeling Geometric Uncertainties in Radiotherapy: The Biologic Dose-Per-Fraction Effect (TU-A3-4)</i> | C. Wilson (c) McMaster U. <i>Odin Upper Limits on Water Emission in Starburst Galaxies (TU-A6-1)</i> | 09h15 |
| | | | | A. McNiven (c) London Reg. Cancer Centre <i>On the Use of Plane Parallel Chambers for the Verification of Dose in Small Radiation Fields (TU-A3-5)</i> | P. Barmby (c) Harvard-Smithsonian CfA <i>Deep Mid-Infrared Imaging with the Spitzer Space Telescope (TU-A6-2)</i> | 09h30 |
| | | | | N. Venugopal (c) U. Manitoba <i>Fast Three Dimensional Non-Linear Warping: Target Localization of Intraprostatic Lesions Using Magnetic Resonance Spectroscopic Images (TU-A3-6)</i> | Session Ends / Fin de session Coffee Break / Pause café | 09h45 |
| | TU-A8 (DTP/DPT) MATHEMATICAL PHYSICS / PHYSIQUE MATHÉMATIQUE Chair: I. Affleck, UBC | TU-A12 (DIMP/DPIM) TECHNIQUES AND MEASUREMENTS IN SEMICONDUCTOR PHYSICS AND TRANSPORT PHENOMENA / TECHNIQUES ET MESURES EN PHYSIQUE DES SEMICONDUCTEURS ET PHÉNOMÈNES DE TRANSPORT Chair: A. Mandelis, U. Toronto | TU-A10 (DAMP-DOP DPAM-DOP) COHERENT INTERACTIONS OF LASERS / INTERACTIONS COHÉRENTES DES LASERS Chair: J. Martin, U. Waterloo | ↓ | ↓ | |
| | WALTON, Mark U. Lethbridge <i>Finding NIM-reps (TU-A8-1)</i> | GARCIA, Jose Photo-Thermal Diagnostics <i>Photo-Carrier Radiometry of Semiconductors: Instrumentation and Ion-Implantation Studies (TU-A12-1)</i> | HAUGEN, Harold McMaster U. <i>Selected Studies of Femtosecond Laser Ablation and Modification of Semiconductors (TU-A10-1)</i> | Session Ends / Fin de session Coffee Break / Pause café | TU-A15 (CASCA) NEWS FROM SPACE - THE MOST SATELLITE / NOUVELLES DE L'ESPACE - LE SATELLITE MOST Chair: C. Robert, U. Laval | 10h00 |
| | ↓ | ↓ | ↓ | TU-A16 (COMP-DMBP) YOUNG INVESTIGATORS IN MEDICAL AND BIOLOGICAL PHYSICS II / JEUNES CHERCHEURS(S) EN PHYSIQUE MÉDICALE ET BIOLOGIQUE II Chair: J.P. Bissonnette Princess Margaret Hospital | JAYMIE MATTHEWS UBC <i>Space Science in a Suitcase: Early Results from MOST (TU-A15-1)</i> | 10h15 |
| | SNIATYCKI, Jędrzej U. Calgary <i>Gauge Symmetries in Yang-Mills Theory (TU-A8-2)</i> | GUREVICH, Yuri Cinvestav <i>The Transport of Nonequilibrium Carriers in Semiconductor Structures (New Point of View) (TU-A12-2)</i> | M. Cowan (c) U. Toronto <i>Diffractive Optics Based 2-D IR Spectroscopy: A New Probe of Hydrogen Bonded Networks (TU-A10-2)</i> | S. White (c) Carleton U. <i>Absolute Volume Estimation from 3D Hyperpolarized Xenon Images - A Monte Carlo and Phantom Study (TU-A16-1)</i> | ↓ | 10h30 |
| | ↓ | ↓ | Coffee Break / Pause café | M. Gordon (c) U. Toronto <i>Doppler Optical Coherence Tomography for Monitoring Anti-Cancer Therapies (TU-A16-2)</i> | ↓ | 10h45 |
| | ROWE, David U. Toronto <i>Quasi-Dynamical Symmetry in the Approach to a Second-Order Phase Transition (TU-A8-3)</i> | Coffee Break / Pause café | ↓ | K. Nakonechny (c) U. Alberta <i>Scatter Tails in CT Single Scan Dose Profiles Measured with a Diamond Detector (TU-A16-3)</i> | TU-A17 CASCA Plaskett Award Conference Plaskett CASCA Chair: R. Taylor, U. Calgary JO-ANNE BROWN U. Calgary <i>Visualizing the Invisible Using Polarization Observations (TU-A17-1)</i> | 11h00 |

| TIME HEURE | Other Locations Autres endroits | Ballroom A | Ballroom B | Ballroom C | Colbourne | Kildonan |
|------------|------------------------------------|--|--|--|---|--|
| 11h15 | | ↓ | ↓ | ↓ | K.J. Vos (c) U.Lethbridge <i>The Formation of Stripes and the Enhancement of Pairing in the Anisotropic t-J Model (TU-A13-4)</i> | ↓ |
| 11h30 | | GRIFFIN, Allan U.Toronto <i>Molecular BEC Condensate vs a BCS Superfluid in a Trapped Atomic Fermi Gas (TU-A14-4)</i> | S. Bekhechi (c) U.Manitoba <i>Short-time Dynamics of Stacked Triangular Antiferromagnets (TU-A7-4)</i> | SCHATZ, Hendrik Michigan State U. <i>Nuclear Physics on Accreting Neutron Stars - From X-Ray Bursts to Superbursts (TU-A11-3)</i> | B.W. Statt (c) U.Toronto <i>Pseudogap in Ortho-II YBCO: NMR vs. INS (TU-A13-5)</i> | GREGOIRE, Thomas CERN <i>Little Higgs Models and Electroweak Precision Measurements (TU-A9-4)</i> |
| 11h45 | | | B. Joos (c) U.Ottawa <i>Viscoelastic and Thermodynamic Properties of Short Chain Polymer Melts with van der Waals Interactions Near the Glass Transition (TU-A7-5)</i> | ↓ | K.C. Hewitt (c) Dalhousie U. <i>Continuous Map of the Phase Diagram of High Temperature Superconductors Using a Composition Spread Approach (TU-A13-6)</i> | ↓ |
| 12h00 | | A. Madej (c) INMS - NRC <i>Measuring a Single Ion at the Limits of Time (TU-A14-5)</i> | J. Polson (c) UPEI <i>Simulation Study of Equilibrium Polymer Dynamics (TU-A7-6)</i> | D. Ballantyne (c) CITA <i>Visualizing the Inner Regions of Accretion Disks around Neutron Stars Using Superbursts (TU-A11-4)</i> | M.P. Bourgeois (c) U.Laval <i>Unbiased Laser Detection in Uncooled YBCO Thin Films (TU-A13-7)</i> | POSPELOV, Maxim U.Victoria <i>Search for Dark Matter in $b \rightarrow s$ Transition with Missing Energy (TU-A9-5)</i> |
| 12h15 | | N. Moazzen-Ahmadi (c) U.Calgary <i>High Resolution Laser Spectroscopy of CCO in the C-C and C-O Stretching Regions (TU-A14-6)</i> | S. Ferdous (c) MUN <i>Ab Initio Polarizabilities of Conducting Polymers (TU-A7-7)</i> | L.R. Buchmann (c) TRIUMF <i>The $^{12}\text{C}(\alpha, \gamma)^{16}\text{O}$ Reaction: Overview and Results of DRAGON (TU-A11-5)</i> | R.A. Lessard (c) U.Laval <i>Fabrication et caractérisation de couches minces de YBaCuO : optimisation de la cristallisation (TU-A13-8)</i> | ↓ |
| 12h30 | | Session Ends / Fin de la session | Session Ends / Fin de la session | Session Ends / Fin de la session | Session Ends / Fin de la session DNP Business Mtg (with lunch) - Ends at 13h30 Réunion d'affaires DPN (lunch compris) - Se termine à 13h30 | Session Ends / Fin de la session |
| 13h15 | | | | | | |
| 13h30 | | | TU-P3 Plenary Session plénière (CAP Herzberg Medal winner - récipiendaire de la médaille Herzberg de l'ACP) Chair: B. Joos, U.Ottawa KASPI, Victoria McGill U. <i>Revolutions in Neutron Star Astrophysics (TU-P3-1)</i> | | | |
| 13h45 | | | | ↓ | | |

| Strathcona | Westminster | Campaign A | Victoria | Albert | Campaign B | TIME HEURE |
|---|--|---|--|--|---|------------|
| | ↓ | HALLEN, Hans North Carolina State U. <i>Electron-Induced Motion of Atoms: Mechanisms and Insights about Hot Electron Transport (TU-A12-3)</i> | SIPE, John U.Toronto <i>Optically Injected Spin Currents in Semiconductors (TU-A10-3)</i> | X. Wu (c) U.Toronto <i>Development of Novel Multi-Focus Acoustic Lens Transducer Systems for Ultrasound Thermal Therapy (TU-A16-4)</i> | ↓ | 11h15 |
| | EDERY, Ariel Bishop's U. <i>Compact Formulas for Casimir Energies in D-Dimensions via Operator Technique (TU-A8-4)</i> | ↓ | ↓ | A. Tunis (c) U.Toronto <i>High Frequency Ultrasound Monitoring of Structural Changes in Cells and Tissues (TU-A16-5)</i> | Session Ends at 11h45 / Session se termine à 11h45 TU-A18 (CASCA) IMAGING IN THE SUBMILLIMETRE WINDOW / IMAGERIE DANS LA FENÊTRE SOUS-MILLIMÉTRIQUE Chair: P. Martin, U.Toronto | 11h30 |
| | ↓ | E. Blackmore (c) TRIUMF <i>Ground-Based Testing of Electronic Devices for Space Radiation Effects (TU-A12-4)</i> | S. Peles (c) Georgia Inst. of Tech. <i>A Theoretical Model of Synchrony for Coupled Fiber Lasers (TU-A10-4)</i> | K. Surry (c) Robarts Res.Inst. <i>Three Dimensional Ultrasound and Stereotactic Mammography Guided Biopsy: A Dual Modality System (TU-A16-6)</i> | R. Taylor (c) U.Calgary <i>Cold Hydrogen Clouds in the Milky Way: An Evolutionary Missing Link? (TU-A18-1)</i> | 11h45 |
| | PATERA, Jiri U.Montreal <i>Orbit Functions of Compact Lie Groups and Their Applications (TU-A8-5)</i> | V. Kovaltchouk (c) U.Regina <i>Silicon Photomultiplier as a Readout System for a Barrel Calorimeter (GlueX Project) (TU-A12-5)</i> | Session Ends / Fin de la session | Session Ends / Fin de la session | T. Webb (c) Leiden Observatory <i>A Submm Survey of High-Redshift Clusters: A submm Butcher-Oemler Effect? (TU-A18-2)</i> | 12h00 |
| | ↓ | K.M. Cheng (c) U.Manitoba <i>Dynamic Response of a Pair of Electrostatically Coupled Cantilevers: Experimental Characterization and Modelling (TU-A12-6)</i> | | | C. Borys (c) Caltech <i>Sub-millimetre Science with the New Generation of Total-Power, CCD-Style Bolometer Arrays (TU-A18-3)</i> | 12h15 |
| DPP Business Mtg Ends at 13h30 <i>Réunion d'affaires DPP Se termine à 13h30</i> | Session Ends / Fin de la session DOP Business Mtg (with lunch) - Ends at 13h30 <i>Réunion d'affaires DOP (lunch compris) - Se termine à 13h30</i> | Session Ends / Fin de la session DMBP Business Mtg (with lunch) - Ends at 13h30 <i>Réunion d'affaires DPMB (lunch compris) - Se termine à 13h30</i> | | | Session Ends / Fin de la session TU-A19 (CASCA) ALMA Information Session / Session d'information sur l'ALMA Chair: C. Wilson, McMaster U | 12h30 |
| | | | TU-P2 (COMP-DMBP/OCPPM-DPMB) MICROIMAGING / MICROIMAGERIE Chair: A. Pejovic-Milic Ryerson U. | TU-P1 (COMP-DMBP/OCPPM-DPMB) RADIOBIOLOGY AND TISSUE CHARACTERIZATION / BIOLOGIE RADIOLOGIQUE ET CARACTÉRISATION DES TISSUS Chair: D.E. Wilkins Ottawa Reg.CancerCen. | ↓ | |
| | | | K. Whittingstall (c) Dalhousie U. <i>Localization of Neural Activity in the Human Brain (TU-P2-1)</i> | M. Carloni (c) Ottawa Reg. Cancer Centre <i>Parameter Correlation for a Fully Heterogeneous Tumour Control Mode (TU-P1-1)</i> | ↓ | 13h15 |
| | | | M. Martin (c) Caltech <i>Visualizing Myelin Disorders in Vivo (TU-P2-2)</i> | N. Ahmed (c) Mount Allison U. <i>Radiation Energy Deposition Calculations Using Monte Carlo Simulations in K-shell X-ray Fluorescence Bone Lead Measurements (TU-P1-2)</i> | Session Ends / Fin de la session | 13h30 |
| | | | W. Ens (c) U.Manitoba <i>Molecular Imaging Using an Orthogonal-Injection Time-of-Flight Mass Spectrometer with a Matrix-Assisted Laser Desorption Ionization Source (TU-P2-3)</i> | J. Hayward (c) Juravinski Cancer Centre <i>Monitoring the Response of Mycosis Fungoides to Total Skin Electron Irradiation with Optical Coherence Tomography (TU-P1-3)</i> | | 13h45 |

| TIME HEURE | Other Locations Autres endroits | Ballroom A | Ballroom B | Ballroom C | Colbourne | Kildonan |
|---------------|--|--|---|--|--|----------|
| 14h00 | | | | ↓ | | |
| | | TU-P10 (DOP-CASCA) ADAPTIVE OPTICS IN ASTRONOMY, BIOLOGY, MEDICINE, AND PHYSICS / OPTIQUE ADAPTATIVE EN ASTRONOME, BIOLOGIE, MÉDECINE ET PHYSIQUE Chair: M. Campbell, U.Waterloo | TU-P4 (DCMMP/DPMC) YOUNG INVESTIGATORS IN CONDENSED MATTER PHYSICS I / JEUNES CHERCHEURS(SES) EN PHYSIQUE DE LA MATIÈRE CONDENSÉE I Chair: H. Kreuzer, Dalhousie U. | TU-P9 (DAMP/DPAM) ATOMIC AND MOLECULAR SPECTROSCOPY AND DYNAMICS II / SPECTROSCOPIE ET DYNAMIQUE ATOMIQUE ET MOLÉCULAIRE II Chair: W. van Wijngaarden York U. | TU-P8 (DIMP/DPIM) GENERAL MEASUREMENT PHYSICS / PHYSIQUE DES MESURES GÉNÉRALES Chair: A. Mandelis, U.Toronto | |
| 14h15 | | DAVIDGE, Tim NRC <i>Adaptive Optics Systems on Canadian Telescopes (TU-P10-1)</i> | WICKHAM, Robert St. Francis Xavier U. <i>Kinetics of Self-Assembly in Block Copolymer Melts (TU-P4-1)</i> | DRAKE, Gordon U.Windsor <i>Exotic Nuclear Size Measurements from High Precision Atomic Theory (TU-P9-1)</i> | KOLIOS, Michael Ryerson U. <i>Micrometer Particle Sizing Using High Frequency Ultrasound with Biological Applications (TU-P8-1)</i> | |
| 14h30 | | ↓ | ↓ | ↓ | ↓ | |
| 14h45 | | M. Campbell (c) U.Waterloo <i>Adaptive Optics: Implications to Diagnosis and Treatment of Eye Disease (TU-P10-2)</i> | DENNISTON, Colin UWO <i>Dynamic Boundaries in Complex Fluids (TU-P4-2)</i> | ZETNER, Peter U.Manitoba <i>Progress in the Investigation of Electron Collisions with Laser Excited Atoms (TU-P9-2)</i> | D. Dahn (c) UPEI <i>A Capacitance-Based Detector for Monitoring Bumblebees (TU-P8-2)</i> | |
| 15h00 | (TU-P15) Heartland Boardroom World Year of Physics Committee Meeting / Réunion du Comité pour l'Année mondiale de la physique | Coffee Break / Pause café | ↓ | ↓ | Coffee Break / Pause café | |
| 15h15 | | ↓ | Coffee Break / Pause café | Coffee Break / Pause café | ↓ | |
| 15h30 | | MUNGER, Rejean U.of Ottawa Eye Inst. <i>Adaptive Optics: Implications to Optical Correction of the Eye (TU-P10-3)</i> | ↓ | J. Cooper (c) U.Calgary <i>Ab Initio Determination of Molecular Parameters for Ethane-Like Molecules (TU-P9-3)</i> | HALLEN, Hans North Carolina State U. <i>Electric Field Effects in Nanoscale Raman Spectroscopy (TU-P8-3)</i> | |
| 15h45 | | ↓ | KILFOIL, Maria McGill U. <i>Consequences of Being Soft: Equilibrium Concepts in Nonequilibrium, Soft Materials Using Real Space Imaging (TU-P4-3)</i> | L.-H. Xu (c) UNB <i>Rotational Spectra, Conformational Structures and Dipole Moments of Thiodiglycol by Jet-Cooled FTMW and Ab Initio Calculations (TU-P9-4)</i> | ↓ | |
| 16h00 | | E. Borra (c) U.Laval <i>Nanoengineered Adaptive Optics (TU-P10-4)</i> | ↓ | Z. Abusara (c) U.Calgary <i>Infrared Laser Spectroscopy of CCO: The ν_3 Band of the α' Δ Electronic State (TU-P9-5)</i> | E. Galiano (c) Laurentian U. <i>Theoretical Estimates of the Solid Angle Subtended by a Dual Diaphragm-Detector Assembly for Alpha Sources (TU-P8-4)</i> | |
| 16h15 | | Session Ends / Fin de la session | HILL, Ian G. Dalhousie U. <i>Contact Resistance in Organic Thin-Film Transistors (TU-P4-4)</i> | N. Moazzen-Ahmadi (c) U.Calgary <i>The $\nu_9 + \nu_4 - \nu_4$ Band of Ethane (TU-P9-6)</i> | D. Hoult (c) NRC <i>The Quantum Origins of the NMR Signal: A Paradigm for Faraday Induction (TU-P8-5)</i> | |

| Strathcona | Westminster | Campaign A | Victoria | Albert | Campaign B | TIME HEURE |
|---|---|--|---|--|--|------------|
| | | | Session Ends / Fin de la session | R. LeClair (c) Laurentian U. <i>Identification of Breast Specimens via Low-Angle X-Ray Scatter Measurements with a Digital Imaging System (TU-P1-4)</i> | | 14h00 |
| TU-P11 (DPE/DEP) NEW DIRECTIONS IN THE PHYSICS CURRICULUM / NOUVELLES ORIENTATIONS DANS LES PROGRAMMES D'ÉTUDES EN PHYSIQUE Chair: S.P. Goldman, UWO | TU-P6 (DTP/DPT) PARTICLE PHYSICS II / PHYSIQUE DES PARTICULES II Chair: M. Shegelski, UNBC | TU-P5 (PPD) THE ENERGY FRONTIER IN PARTICLE PHYSICS / LA FRONTIÈRE DE L'ÉNERGIE EN PHYSIQUE DES PARTICULES Chair: P.W. Krieger, U.Toronto | TU-P7 (DTP-DCMMP/DPT-DPMC) STATISTICAL PHYSICS / PHYSIQUE STATISTIQUE Chair: J. Patera, CRMJU/Montreal | ↓ | TU-P12 (CASCA) MEASURING HIDDEN PARTS OF GALAXIES / MESURE DES PARTIES CACHÉES DES GALAXIES Chair: A. Gulliver, Brandon U. | |
| W. Baylis (c) U.Windsor <i>Teaching Relativity in Introductory Physics (TU-P11-1)</i> | DUTTA, Bhaskar U.Regina <i>Minimal SO(10) Model for Neutrinos and Its Implications (TU-P6-1)</i> | KORDAS, Kostas U.Toronto <i>Recent Results from the Collider Detector at Fermilab (TU-P5-1)</i> | AFFLECK, Ian UBC <i>Field-Induced Phase Transition in Anisotropic Haldane Gap Antiferromagnetic Chains (TU-P7-1)</i> | TU-P13 (COMP-DMBP/OCPM-DPMB) MEDICAL APPLICATIONS OF SOUND: IMAGING AND BEYOND / APPLICATIONS MÉDICALES DU SON : L'IMAGERIE ET AU-DELÀ Chair: W.M. Whelan, Ryerson U. | C. Ryan (c) Sunnybrook/UToronto <i>Are the Central Engines in Narrow-Line Seyfert Is Fundamentally Different? (TU-P12-1)</i> | 14h15 |
| D. Mathewson (c) Kwantlen U. College <i>A Conceptual Treatment of Gauss' Law (TU-P11-2)</i> | ↓ | ↓ | ↓ | BRONSKILL, Michael U.Toronto <i>MRI Guidance for the New Sounds of Tumour Therapy (TU-P13-1)</i> | K. Douglas (c) U.Calgary <i>Analysis of Gas and Dust Emission in the Interstellar Medium of the Outer Galaxy with the Canadian Galactic Plane Survey (TU-P12-2)</i> | 14h30 |
| G. McGuire (c) UCFV <i>Novel Computer Algebra Physics Problems (TU-P11-3)</i> | MARLEAU, Luc U.Laval <i>Revisiting the Skyrme Model (TU-P6-2)</i> | MAZINI, Rachid U.Toronto <i>The ATLAS Detector Physics Potential (TU-P5-2)</i> | HERBUT, Igor SFU <i>Theory of Underdoped Cuprates as Strongly Fluctuating d-wave Superconductors (TU-P7-2)</i> | ↓ | TU-P14 (CASCA) Outgoing President's Talk / Conférence du président sortant Chair: J. Hesser, NRC GRETCHEN HARRIS U.Waterloo <i>CASCA 1971-2004: The Story So Far (TU-A14-1)</i> | 14h45 |
| A. Rogers (c) U.Manitoba <i>Magical Squares in University Physics Education (TU-P11-4)</i> | ↓ | ↓ | ↓ | CLARKE, Robert Carleton U. <i>High Intensity Focused Ultrasound for Non-Invasive Therapy (TU-P13-2)</i> | ↓ | 15h00 |
| Session Ends / Fin de la session | Coffee Break / Pause café | CORRIVEAU, Francois IPP/McGill U. <i>Recent ZEUS Results at HERA (TU-P5-3)</i> | Coffee Break / Pause café | ↓ | Coffee Break / Pause café | 15h15 |
| | TROTTIER, Howard SFU <i>Perturbation Theory for High-Precision Lattice QCD (TU-P6-3)</i> | ↓ | OSHIKAWA, Masaki Tokyo Inst. of Tech. <i>Junctions of Three Quantum Wires and the Dissipative Hofstadter Model (TU-P7-3)</i> | BROWN, J.A. Queen's U. <i>Development and Applications of High Frequency Ultrasound Imaging Systems (TU-P13-3)</i> | ↓ | 15h30 |
| | ↓ | Coffee Break / Pause café | ↓ | ↓ | TU-P16 (CASCA) Long Range Plan Review / Examen du plan à long terme Chair: R.Pudritz, McMaster U (ends at 16h30 / se termine à 16h30) | 15h45 |
| | DATTA, Alakabha U.Toronto <i>Getting CP Violating Phase Information From $b \rightarrow d$ Penguins (TU-P6-4)</i> | ↓ | TREMBLAY, Andre-Marie U.Sherbrooke <i>Two Ways to Destroy a Fermi Liquid (TU-P7-4)</i> | KOLIOS, Michael Ryerson U. <i>High Frequency Ultrasound Imaging and Spectroscopy for the Imaging of Cell Damage and Death (TU-P13-4)</i> | | 16h00 |
| | ↓ | B. Vachon (c) Fermi Nat'l Accel.Lab. <i>Search for the Production of Single Top Quarks in High Energy Proton-Antiprotons Collisions (TU-P5-4)</i> | ↓ | ↓ | | 16h15 |

| TIME HEURE | Other Locations Autres endroits | Ballroom A | Ballroom B | Ballroom C | Colbourne | Kildonan |
|---------------|------------------------------------|------------|----------------------------------|------------|---|--|
| 16h30 | | | | ↓ | D. Tokaryk (c) UNB <i>High Resolution Laser Spectroscopy of Magnesium Monoacetylide (TU-P9-7)</i> | A. Liptak (c) UBC <i>Modulation of Partial Internal Reflection at an Optical Interface (TU-P8-6)</i> |
| 16h45 | | | Session Ends / Fin de la session | | L-H. Xu (c) UNB <i>Lamb-Dip Observations and Assignments of Some Compact Q-Branches in the 11 μm Region for 1,3 Butadiene (TU-P9-8)</i> | Session Ends / Fin de la session |
| 17h00 | | | | | Session Ends / Fin de la session | |
| 17h15 | | | | | | |
| 17h30 | | | | | | |
| 19h00 | Banquet Reception | | | | | Ballrooms A/B/C |
| 19h30 | Banquet | | | | | |

Wednesday, June 16

| TIME HEURE | Other Locations Autres endroits | Ballroom A | Ballroom B | Ballroom C | Colbourne | Kildonan |
|---------------|--|------------|---|------------|-----------|----------|
| 07h00 | (WE-A1) - Meeting of the CAP-NSERC Liaison Committee (07h00-09h00) - Heartland Boardroom (WE-A2) - DPE Breakfast Business Meeting (07h00 - 08h15) - Private Dining Room | | | | | |
| 08h30 | | | WE-A3 CAP Plenary Session plénière ACP Chair: M. Morrow, MUN AARON FENSTER Robarts Research Institute <i>Use of 3D Ultrasound Imaging in Diagnosis, Treatment and Research: Advances and Opportunities (WE-A3)</i> | | | |
| 0845 | | | | ↓ | | |
| 09h00 | | | | ↓ | | |

| Strathcona | Westminster | Campaign A | Victoria | Albert | Campaign B | TIME HEURE |
|------------|--|--|--|---|---|------------|
| | DICK, Rainer U.Saskatchewan <i>Theoretical Aspects of Ultra-High Energy Cosmic Rays (TU-P6-5)</i> | O. Stelzer-Chilton (c) U.Toronto <i>Measuring the W Boson Mass with CDF in Run IIa (TU-P5-5)</i> | SAINT-AUBIN, Yvan U.Montreal <i>Behavior of the Two-Dimensional Ising Model at the Boundary of a Half-Infinite Cylinder (TU-P7-5)</i> | G. Spirou (c) U.Toronto <i>Photoacoustic Imaging in Biological Tissues for Monitoring Thermal Lesions (TU-P13-5)</i> | TU-P17 CASCA Annual General Meeting / Assemblée générale de la CASCA Chair: G. Harris, U.Waterloo | 16h30 |
| | ↓ | R. Moore (c) U.Alberta <i>Searches for SUSY at D0 (TU-P5-6)</i> | ↓ | R. Vlad (c) Ontario Cancer Inst. <i>High Frequency Ultrasound in Monitoring Liver Suitability for Transplantation (TU-P13-6)</i> | | 16h45 |
| | Session Ends / Fin de la session | S. Sabik (c) U.Toronto <i>Study of Jet Fragmentation for the Measurement of the Top Mass with CDF (TU-P5-7)</i> | Session Ends / Fin de la session | Session Ends / Fin de la session | | 17h00 |
| | | K. Garrow (c) TRIUMF <i>Observation of a $S =1$ Baryon State at a Mass of 1.528-GeV in Quasi-Real Photoproduction (TU-P5-8)</i> | | | | 17h15 |
| | | Session Ends / Fin de la session | | | | 17h30 |

| | | | |
|-------|-----------------------------|--|-----------------|
| 19h00 | Réception du banquet | | Ballrooms A/B/C |
| 19h30 | Banquet | | |

Mercredi, le 16 juin

| Strathcona | Westminster | Campaign A | Victoria | Albert | Campaign B | TIME HEURE |
|--|-------------|------------|----------|---|--|------------|
| (WE-A1) - Réunion du comité de liaison ACP-CRSNG (07h00-09h00) - Heartland Boardroom | | | | | | 07h00 |
| (WE-A2) - Réunion d'affaires DEP (07h00 - 08h51) - Private Dining Room | | | | | | |
| | | | | WE-A5 (COMP/OCPM) RADIATION TREATMENT PLANNING / PLANIFICATION D'UNE RADIOTHÉRAPIE Chair: W. Beckham, BC Cancer Agency | WE-A4 (CASCA) PORTRAITS AT MULTIPLE WAVELENGTHS / PORTRAITS À LONGUEURS D'ONDES MULTIPLES Chair: I. Short, Saint Mary's U. | |
| | | | | P. Potrebko (c) CancerCare Manitoba <i>A Broad Beam Analytical Photon Scatter Model Employing Convolution Techniques (WE-A5-1)</i> | M. Bietenholz (c) York U. <i>Time-Evolution and Radio-Optical Correlations in the Synchrotron Emission of The Crab Nebula (WE-A4-1)</i> | 08h30 |
| | | | | N. Blais (c) Hopital Maisonneuve-Rosemont <i>Evaluation of the Rectangular Scatter Integration Model (RSI) (WE-A5-2)</i> | A. Moffatt (c) U.Montreal <i>Wind-Wind Collisions from X-Ray to Radio: The Massive Prototype Binary WR140 (WE-A4-2)</i> | 08h45 |
| | | | | L. Buckley (c) Carleton U./NRC <i>A Correlated Sampling User-Code for the EGSnrc System (WE-A5-3)</i> | WE-A6 (CASCA) DATA MINING AND ARCHIVING / EXPLOITATION ET ARCHIVAGE DES DONNÉES Chair: R. Bochonko, U.Manitoba DAVID SCHADE NRC <i>Data Mining and the Virtual Observatory (WE-A6-1)</i> | 09h00 |

DETAILED CONGRESS PROGRAM - WEDNESDAY, JUNE 16

| TIME HEURE | Other Locations Autres endroits | Ballroom A | Ballroom B | Ballroom C | Colbourne | Kildonan |
|---------------|------------------------------------|---|--|---|--|---|
| 09h15 | | | WE-A7 CAP/COMP Plenary Session plénière ACP/OCPM Chair: C. Arseneault, Dr. Georges L. Dumont Hospital DAVID ROGERS Carleton U. <i>Monte Carlo Simulation of Electron-Photon Transport: From Particle Physics to Cancer Radiotherapy (WE-A7-1)</i> | | | |
| 09h30 | | | ↓ | | | |
| 09h45 | | | ↓ | | | |
| | | | Session Ends at 10h00 / Session se termine à 10h00 | | | |
| | | WE-A9 (DCMMP/DPMCM) YOUNG INVESTIGATORS IN CONDENSED MATTER PHYSICS II / JEUNES CHERCHEURS(S) EN PHYSIQUE DE LA MATIÈRE CONDENSÉE II Chair: M. Cote, U.Montreal | | WE-A8 (DIAP-DIMP/ DPIA-DPIM) INSTRUMENTATION AND TECHNIQUES IN BIOMEDICAL PHYSICS II / INSTRUMENTA- TION ET TECHNIQUES EN PHYSIQUE BIOMÉDICALE II Chair: R. Maev, U.Windsor | WE-A13 (DTP/DPT) GENERAL RELATIVITY AND GRAVITATION I / RELATIVITÉ GÉNÉRALE ET GRAVITATION I Chair: A. Kempf, U. Waterloo | |
| 10h00 | | ROSEI, Federico U. Quebec <i>Critical Issues in Ge/Si Nanostructures: Positioning, Intermixing and Ripening (WE-A9-1)</i> | | KRULL, Ulrich U. Toronto <i>Genomic Target Identification Using Imaging of Distributed Gradients of Oligonucleotide Probes in Conjunction with Microfluidics (WE-A8-1)</i> | KUNSTATTER, Gabor U. Winnipeg <i>Vibrational Modes of Black Holes and Their Quantum Gravitational Microstates (WE-A13-1)</i> | |
| 10h15 | | ↓ | WE-A17 (COMPOCPM) RADIATION DOSIMETRY / DOSIMÉTRIE DES RAYON- NEMENTS Chair: K. Sixel, Sunnybrook/UToronto | WE-A16 (DOP-DAMP/ DOP-DPAM) ULTRAFAST LASER APPLICATIONS / APPLICATIONS DES LASERS ULTRA-RAPIDES Chair: W.-K. Liu, U. Waterloo | ↓ | ↓ |
| 10h30 | | KNOBEL, Robert Queen's U. <i>Integrated Mechanics and Electronics at the Nanoscale (WE-A9-2)</i> | J. Battista (c) London Reg. Cancer Centre <i>Accuracy in Dose Calibration of Fricke- Xylenol Gels Using Optical CT Scanning (WE-A17-1)</i> | FORTIER, Tara U. Colorado <i>Carrier-Envelope Phase Stabilized Modelocked Lasers (WE-A16-1)</i> | ALVARADO-GIL, Juan U. Guelph <i>Study of Blood Sedimentation by Photothermal and Optical Techniques (WE-A8-2)</i> | MANN, Robert U. Waterloo <i>Mass Conjectures, Entropy Bounds and the ds/CFT Correspondence (WE-A13-2)</i> |
| 10h45 | | ↓ | S. Babic (c) Queen's U./KRCC <i>NMR Relaxometry Study and Gravimetric Analysis of an Aqueous Polyacryla- mide Dosimeter Without Gelatin (WE-A17-2)</i> | ↓ | ↓ | ↓ |
| 11h00 | | Coffee Break / Pause café | M. Nielsen (c) Sunnybrook/UToronto <i>Preliminary Study of the MAGIC Gel Dosimeter Using X-Ray Computed Tomography (WE-A17-3)</i> | R. Hostenstein (c) U. Alberta <i>Simulation of Femtosecond Laser Ablation of Silicon (WE-A16-2)</i> | Coffee Break / Pause café | PAGE, Don U. Waterloo <i>Particle Production in a Tunneling Universe (WE-A13-3)</i> |
| 11h15 | | ↓ | L. Beaulieu (c) Centre Hospitalier Univ. <i>Comparison of Scintillating Fibers for Increasing the Signal to Noise Ratio of Scintillator Dosimeters (WE-A17-4)</i> | Coffee Break / Pause café | ↓ | ↓ |

| Strathcona | Westminster | Campaign A | Victoria | Albert | Campaign B | TIME HEURE |
|--|-------------|--|--|---|---|------------|
| | | | | S.P. Goldman (c) UWO <i>Fast Inverse Dose Optimization (FIDO) for IMRT via Matrix Inversion with no Negative Intensities (WE-A5-4)</i> | ↓ | 09h15 |
| | | | | A. Bergman (c) Vancouver CancerCentre <i>Improved Calculation Accuracy for IMRT Using Modified Single Pencil Beam Calculation Kernels (WE-A5-5)</i> | ↓ | 09h30 |
| | | | | S. Yartsev (c) London Reg. CancerCentre <i>Virtual Organs as a Tool in Inverse Planning of IMRT (WE-A5-6)</i> Session ends at 10h00 / Fin de la session à 10h00 | Session Ends / Fin de la session Coffee Break until 10h00/ Pause café jusqu'à 10h00 | 09h45 |
| WE-A12 (DIMP/DPIM) IMAGING WITH PHOTOACOUSTIC AND PHOTOTHERMAL NDE TECHNIQUES AND MICROSCOPIES / IMAGERIE À L'AIDE DE TECHNIQUES END ET DE MICROSCOPIES PHOTOACOUSTIQUES ET PHOTOTHERMIQUES Chair: A. Mandelis, U.Toronto | | WE-A11 (DNP-DAMP/DPN-DPAM) ION TRAPS IN ATOMIC AND NUCLEAR PHYSICS / PIÈGES À IONS EN PHYSIQUE ATOMIQUE ET NUCLÉAIRE Chair: K. Sharma, U.Manitoba | WE-A10 (PPD) PARTICLE ASTROPHYSICS / ASTROPHYSIQUE DES PARTICULES Chair: W. Trischuk, U.Toronto | WE-A14 (BSC/SBC) SYNCHROTRON BIOPHYSICS: THE CANADIAN LIGHT SOURCE / BIOPHYSIQUE AU SYNCHROTRON : LA SOURCE DE LUMIÈRE CANADIENNE Chair: J. Lepock, U.Waterloo | ↓ | |
| MICHAELIAN, Kirk Natural Resources Cda <i>Disperse Photoacoustic Spectroscopy of Hydrocarbons (WE-A12-1)</i> | | PEARSON, Matthew TRIUMF <i>Nuclear Physics from Cold, Trapped Atoms (WE-A11-1)</i> | GRAHAM, Kevin Queen's U. <i>Recent Results from the Sudbury Neutrino Observatory (WE-A10-1)</i> | THOMLINSON, William CLS <i>The Canadian Light Source: Opportunities in Biomedical Research (WE-A14-1)</i> | WE-A15 (CASCA) IMAGING MULTIPLE WAVELENGTHS / IMAGERIE DANS DES LONGUEURS D'ONDES MULTIPLES Chair: R. Bond, CITA | 10h00 |
| ↓ | | ↓ | ↓ | ↓ | M. Sawicki (c) NRC <i>The Evolution of the Galaxy Luminosity Function and Cosmic Star Formation History from z~4 to z~1.7 Using Multiwavelength Imaging (WE-A15-1)</i> | 10h15 |
| SHEN, Jun NRC <i>Photothermal Beam Deflection Techniques Applied to the Non-Destructive Measurements of Thermophysical Properties (WE-A12-2)</i> | | MARTIN, James U.Waterloo <i>Dipole-Dipole Interactions between Ultracold Rydberg Atoms (WE-A11-2)</i> | RAGAN, Kenneth McGill U. <i>STACEE Continues – VERITAS Lives! (WE-A10-2)</i> | CHAPMAN, Dean U.Saskatchewan <i>New Sources of X-Ray Imaging Contrast (WE-A14-2)</i> | C. Willott (c) HIA <i>Multi-Waveband Imaging of the Most Distant Black Holes (WE-A15-2)</i> | 10h30 |
| ↓ | | ↓ | ↓ | ↓ | H. Yee (c) U.Toronto <i>The Red-Sequence Cluster Surveys (WE-A15-3)</i> | 10h45 |
| Coffee Break / Pause café | | Coffee Break / Pause café | Coffee Break / Pause café | Coffee Break / Pause café | WE-A18 (CASCA) Prix Beals Award Chair: G. Harris, U.Waterloo ERNEST SEAQUIST U.Toronto <i>The Galaxy M82 - a Rosetta Stone for the Starburst Phenomenon (WE-A18-1)</i> | 11h00 |
| ↓ | | ↓ | E. Rollin (c) Carleton U. <i>Wavelength Shifter in the Heavy Water of the Sudbury Neutrino Observatory (WE-A10-3)</i> | ↓ | ↓ | 11h15 |
| | | | | | Session ends at 11h45 / La session se termine à 11h45 | |

| TIME HEURE | Other Locations Autres endroits | Ballroom A | Ballroom B | Ballroom C | Colbourne | Kildonan |
|------------|---|---|---|--|---|--|
| 11h30 | | EMBERLY, Eldon SFU <i>The Smallest Molecular Switch (WE-A9-3)</i> | P. Petric (c) BC Cancer Agency <i>A Tissue Equivalent Plastic Scintillator Based Dosimetry System for Verification of IMRT Dose Distributions (WE-A17-5)</i> | ↓ | KOTLICKI, Andrzej UBC <i>Applied Research at the Structured Surface Physics Laboratory at UBC (WE-A8-3)</i> | POISSON, Eric U.Guelph <i>The Gravitational Self-Force (WE-A13-4)</i> |
| 11h45 | | ↓ | K. Stewart (c) McGill U. <i>Development of a Novel Liquid Ionization Chamber for Radiation Dosimetry (WE-A17-6)</i> | SHAPIRO, Evgeny NRC <i>Arbitrary Shaping of Molecular Wavepackets by AC Stark Shifts (WE-A16-3)</i> | ↓ | ↓ |
| 12h00 | | ZHOU, Fei UBC <i>Spin Correlated Ultra Cold Atoms (WE-A9-4)</i> | L. Archambault (c) U.Laval <i>Response of a MOSFET for 50 keV to 5 MeV Incident Radiation and Its Impact in Radiotherapy Measurements (WE-A17-7)</i> | ↓ | BEAULIEU, Luc U. Laval <i>Scintillating Optical Fibers as High Precision, Small Area Dosimeters in Radiation Therapy (WE-A8-4)</i> | LAKE, Kayll Queen's U. <i>Recent Developments in Computer Algebra Applied to General Relativity (WE-A13-5)</i> |
| 12h15 | | ↓ | N. Videla (c) Sunnybrook/UToronto <i>Evaluation of the Water Equivalence of Solid Water Model 457 for Photon and Electron Measurements in TG-51 Protocol (WE-A17-8)</i> | B.J. Siwick (c) U.Toronto <i>Femtosecond Electron Diffraction and the Quest for the "Molecular Movie" (WE-A16-4)</i> | ↓ | ↓ |
| 12h30 | Private Dining Room WE-A20 New Faculty Luncheon / Déjeuner pour les nouveaux professeurs | Session Ends / Fin de la session | Session Ends / Fin de la session | Session Ends / Fin de la session | Session Ends / Fin de la session DIMP/DIAP Business meeting (ends at 13h30) / Réunion d'affaires DPIM/ DPIA (se termine à 13h30) | Session Ends / Fin de la session |
| 12h45 | | | | | | |
| 13h30 | | | | | | |
| 13h45 | | | | | | |
| 14h00 | | | | | | |

| Strathcona | Westminster | Campaign A | Victoria | Albert | Campaign B | TIME HEURE |
|--|-------------|---|---|---|--|------------|
| BAESSO, Mauro U.Maringa <i>Time-Resolved Thermal Lens for Thermo-Optical Measurements in Transparent Materials During Phase Modification (WE-A12-3)</i> | | DILLING, Jens TRIUMF <i>Ion Traps in Nuclear Physics: The Ultimate Tool for Precision Experiments (WE-A11-3)</i> | C.J. Virtue (c) Laurentian U. <i>SNO, SNEWS, and the Next Galactic Supernova (WE-A10-4)</i> | JALILEHVAND, Kenneth U.Calgary <i>X-Ray Absorption Spectroscopy in Natural Sciences: Exploring New Possibilities (WE-A14-3)</i> | WE-A19 (CASCA) NEW DIRECTIONS IN IMAGING / NOUVELLES ORIENTATIONS EN IMAGERIE Chair: T. Landecker, NRC | 11h30 |
| ↓ | | ↓ | P.J. Watson (c) Carleton U. <i>Possible Tests of Universal Gravitation at Short Distances (WE-A10-5)</i> | ↓ | I. Cameron (c) U.Manitoba <i>Crossing the Disciplines: Using Medical Imaging Software for Doing Astronomical Image Analysis (WE-A19-1)</i> | 11h45 |
| BRIGGS, Matthew Los Alamos Nat'l Lab <i>Optical Velocity-Measurement Techniques for Supersonic Surfaces (WE-A12-4)</i> | | K. Sharma (c) U.Manitoba <i>Recent Atomic Mass Measurements on Nuclei Far From Stability with the Canadian Penning Trap Mass Spectrometer (WE-A11-4)</i> | Session Ends / Fin de la session PPD Business meeting (ends at 12h15) / Réunion d'affaires PPD (se termine à 12h15) | NG, Kenneth U.Calgary <i>Protein Crystallography and Antiviral Drug Design (WE-A14-4)</i> | R. Reid (c) DRAO/HIA/NRC <i>Smear Fitting: A New Deconvolution Method for Interferometry (WE-A19-2)</i> | 12h00 |
| ↓ | | T.J. Harmon (c) U.Calgary <i>Tripartite Entanglement of a Trapped Atom in an Optical Cavity (WE-A11-5)</i> | | ↓ | P. Martin (c) CITA <i>On Predicting the Polarization of Low-Frequency Emission by Diffuse Interstellar Dust (WE-A19-3)</i> | 12h15 |
| Session Ends / Fin de la session | | M.C. Fujiwara (c) RIKEN/TRIUMF <i>Casting Light on Antimatter: Cold Antihydrogen with ATHENA (WE-A11-6)</i> | | Session Ends / Fin de la session | Session Ends / Fin de la session WE-A21 Chair: R. Bond, U.Toronto CITA AGM / Assemblée générale CITA (ends at 13h30 / se termine à 13h30) | 12h30 |
| | | Session Ends / Fin de la session | | | | 12h45 |
| | | | | WE-P2 (COMP/OCPM) RADIATION TREATMENT DELIVERY / EXÉCUTION DE LA RADIOTHÉRAPIE Chair: D. Viggars, CancerCare Manitoba | | |
| | | | WE-P1 (CAP-COMP/ACP-OCPM) Plenary Session plénière (Kirkby Medal winner / Récipiendaire de la médaille Kirkby) Chair: M. Steinitz, St. F-X U. ROBERT BARBER U.Manitoba <i>IUPAP - A Brief Introduction (WE-P1-1)</i> | J. Chow (c) Grand River Reg.CancerC. <i>Surface and Peripheral Surface Dose on the Prostate IMRT Treatment (WE-P2-1)</i> | | 13h30 |
| | | | ↓ | G.N. Grigorenko (c) Grand River Reg.CancerC. <i>Mixed IMRT and Conventional Four-Beam Box Treatment on Prostate Cancer (WE-P2-2)</i> | WE-P3 (CASCA) VISUALIZING THEORY: SIMULATIONS IN COSMOLOGY / THÉORIE DE VISUALISATION : SIMULATIONS EN COSMOLOGIE Chair: C. Kerton, Iowa State U. | 13h45 |
| | | | ↓ | F. Vallejo (c) Juravinski CancerCentre <i>Parameters Affecting the Spurious Variation of Photon Fluence in IMRT (WE-P2-3)</i> | DUBINSKI, John U.Toronto <i>A Universe in Motion: Dynamical Evolution of Galaxies in the New Cosmological Paradigm (WE-P3-1)</i> | 14h00 |

| TIME HEURE | Other Locations Autres endroits | Ballroom A | Ballroom B | Ballroom C | Colbourne | Kildonan |
|---------------|------------------------------------|---|---|--|---|---|
| | | WE-P6 (DIMP-CASCA/ DPIM-CASCA) IMAGING IN THE STARS AND ON EARTH / IMAGERIE DANS LES ÉTOILES ET SUR TERRE Chair: J. Rice, Brandon U. | WE-P8 (DIAP-DPIA) INDUSTRIAL AND APPLIED PHYSICS GENERAL SESSION / SESSION GÉNÉRALE SUR LA PHYSIQUE INDUSTRIELLE ET APPLIQUÉE Chair: G. Beer, U. Victoria | WE-P5 (DNP/DPN) RADIOACTIVE BEAM - HEAVY ION PHYSICS / PHYSIQUE DES FAISCEAUX RADIOACTIFS/ D'IONS LOURDS Chair: C. Svensson, U. Guelph | | WE-P10 (DTP/DPT) GENERAL RELATIVITY AND GRAVITATION II / RELATIVITÉ GÉNÉRALE ET GRAVITATION II Chair: M. Paranjape, U. Montreal |
| 14h15 | | D. Scott (c) UBC <i>Dusty Corners of the Universe (WE-P6-1)</i> | BATTISTA, Jerry London Reg. Cancer Centre <i>On-Line CT Imaging for Precision Radiotherapy (WE-P8-1)</i> | GALINDO-URIBARRI, Alfredo Oak Ridge Nat. Lab. <i>Nuclear Spectroscopy with Radioactive Ion Beams: Latest Results from HRIBF (WE-P5-1)</i> | | DAS, Saurya U. Lethbridge <i>Black Holes in Future Colliders (WE-P10-1)</i> |
| 14h30 | | SHEPARD, Steven Thermal Wave Imaging <i>Pulsed Thermography: Perspectives on the Evolution from Qualitative to Quantitative Application (WE-P6-2)</i> | ↓ | ↓ | | ↓ |
| 14h45 | | ↓ | HALLIN, Emil CLS <i>The Applied Science Program at the Canadian Light Source (WE-P8-2)</i> | HACKMAN, Greg TRIUMF <i>TRIUMF-ISAC Gamma-Ray Escape Suppressed Spectrometer (TIGRESS) (WE-P5-2)</i> | | HUSAIN, Viqar UNB <i>Singularity Resolution in Quantum Gravity (WE-P10-2)</i> |
| 15h00 | | Coffee Break / Pause café | ↓ | ↓ | | ↓ |
| 15h15 | | ↓ | Coffee Break / Pause café | ANDREIOU, Corina U. Guelph <i>Doorway States in the Gamma Decay-Out of the Yrast Superdeformed Band in ⁵⁹Cu (WE-P5-3)</i> | | Coffee Break / Pause café |
| 15h30 | | WADE, Gregg RMC <i>Imaging the Surfaces of Stars (WE-P6-3)</i> | J. Aggarwal (c) UBC <i>Fluid Motion Induced by Sequential Interface Deformation (WE-P8-3)</i> | ↓ | | WOOLGAR, Eric U. Alberta <i>The Poincaré Conjecture, Ricci Flow, and the Renormalization Group (WE-P10-3)</i> |
| 15h45 | | ↓ | FENSTER, Aaron Robarts Res. Inst. <i>From Concept to Product: 3D Ultrasound Imaging for Diagnosis and Treatment (WE-P8-4)</i> | BEAULIEU, Luc U. Laval <i>The Dynamics of Neck Formation and Its Isospin Dependence (WE-P5-4)</i> | WE-P13 (PPD-CASCA) DARK MATTER AND DARK ENERGY / MATIÈRE ET ÉNERGIE NOIRES Chair: D. Scott, UBC | ↓ |
| 16h00 | | ANTONIOW, Jean- Stephane Reims U. <i>(Photo)thermal Imaging Using a Modified Atomic Force Microscope (AFM) Combined with Pyroelectric Detection (WE-P6-4)</i> | ↓ | ↓ | HOEKSTRA, Henk CITA <i>Astrophysical Evidence for Dark Matter (WE-P13-1)</i> | UNRUH, William UBC <i>Dumb Holes - Black Holes in the Lab? (WE-P10-4)</i> |
| 16h15 | | ↓ | RUTH, Thomas TRIUMF <i>Production of Radioisotopes for Research in Bioscience and Physical Science (WE-P8-5)</i> | G. Grinyer (c) U. Guelph <i>High Precision Beta Decay Measurements of ²⁶Na at ISAC (WE-P5-5)</i> | ↓ | ↓ |

| Strathcona | Westminster | Campaign A | Victoria | Albert | Campaign B | TIME HEURE |
|--|-------------|--|---|---|---|------------|
| WE-P9 (DPP) PLASMA PHYSICS / <i>PHYSIQUE DES PLASMAS</i> Chair: C. Boucher, INRS | | WE-P7 (DOP) PHOTONICS DEVICES / <i>DISPOSITIFS PHOTONIQUES</i> Chair: M. Campbell, U. Waterloo | WE-P4 (DCMMP/DPMCM) MATERIALS AND MAGNETISM / <i>MATÉRIAUX ET MAGNÉTISME</i> Chair: R. Roshko, U. Manitoba | ↓ | ↓ | |
| HIROSE, Akira U. Saskatchewan <i>Anomalous Electron Thermal Conduction in Tokamaks (WE-P9-1)</i> | | J. Mihaychuk (c) NRC <i>Broad-Spectrum Light Emission in Silicon Tunnel Diodes (WE-P7-1)</i> | QUIRION, Guy MUN <i>Investigation of the Phase Diagram of UNi_2Si_2 (WE-P4-1)</i> | W. Beckham (c) BC Cancer Agency <i>Clinical Implementation of a 3-D Monte Carlo Based Validation Process for IMRT (WE-P2-4)</i> | ↓ Session Ends at 14h45 / La session se termine à 14h45 | 14h15 |
| ↓ | | L. Poirier (c) U. Calgary <i>Computational Analysis of Group Velocity in Periodic Media (WE-P7-2)</i> | ↓ | D. Scora (c) Sunnybrook/UToronto <i>Radiation Spot Position Non-Coincidence on Dual Energy Linacs: Implications for Precision Therapies (WE-P2-5)</i> | WE-P11 (CASC) VISUALIZING CONCEPTS IN THEORY / <i>VISUALISATION DES CONCEPTS THÉORIQUES</i> Chair: J. Fiege, NRC-HIA | 14h30 |
| A. Ito (c) U. Saskatchewan <i>Discrete Alfvén Wave Spectra Due to Hall Current (WE-P9-2)</i> | | S. Yang (c) U. Toronto <i>Focusing of Light in a 3D Inverse Ferroelectric Photonic Crystal (WE-P7-3)</i> | C. Dean (c) Queen's U. <i>Formation of Nickel-Graphite Intercalation Compounds on Silicon Carbide (WE-P4-2)</i> | M. Tambasco (c) Sunnybrook/UToronto <i>Optimization of Imaging Geometry for Megavoltage Cone-Beam CT (WE-P2-6)</i> | J. O'Neill Hurry (c) U. Toronto <i>Observing Simulated Galaxies (WE-P11-1)</i> | 14h45 |
| M.P. Bradley (c) U. Saskatchewan <i>Joint Plasma/Thermal Model for Plasma Ion Implants of Photonic Materials (WE-P9-3)</i> | | Session Ends / Fin de la session | Coffee Break / Pause café | Session Ends / Fin de la session Coffee Break to 15h30 Pause café jusqu'à 15h30 | E. Thommes (c) CITA <i>Dynamics of Young Planetary Systems (WE-P11-2)</i> | 15h00 |
| P. Dobias (c) U. Alberta <i>Observation Constrained Equilibria, Plasma Instabilities, and Substorm Intensification Phase (WE-P9-4)</i> | | | ↓ | WE-P12 (COMP/OCPM) RADIATION TREATMENT VERIFICATION / <i>VÉRIFICATION DE LA RADIOTHÉRAPIE</i> Chair: C. Arseneault Dr. Georges L. Dumont Hospital | D. McNeil (c) Queen's U. <i>Sliding Into Home: Terrestrial Formation and Type I Migration (WE-P11-3)</i> | 15h15 |
| Session Ends / Fin de la session | | | P. Bronsveld (c) U. of Groningen <i>Ordered Co_3W (WE-P4-3)</i> | B. McCurdy (c) CancerCare Manitoba <i>Daily Targeting of Prostate Through EPID Visualization of Implanted Markers (WE-P12-1)</i> | Session Ends / Fin de la session Coffee Break to 16h00 Pause café jusqu'à 16h00 | 15h30 |
| | | | A. Polomska (c) MUN <i>Brillouin Light Scattering from Ordered Carbon Nanotube Arrays (WE-P4-4)</i> | K. Sixel (c) Sunnybrook/UToronto <i>Measurement of Intra- and Inter-Fraction Prostate Motion Using Electronic Portal Imaging of Implanted Radio-Opaque Markers (WE-P12-2)</i> | WE-P14 (CASC) IMAGING THE INVISIBLE SPECTRUM / <i>IMAGERIE DANS LE SPECTRE DE L'INVISIBLE</i> Chair: M. Bielenholz, York U. | 15h45 |
| | | | A. Sarkissian (c) Plasmionique Inc. <i>Plasma-Assisted Deposition of Advanced Carbon-Based Coatings (WE-P4-5)</i> | K. Jabbari (c) U. Manitoba <i>Automatic Extraction of Patient Out-of-Plane Rotation Using Portal Images (WE-P12-3)</i> | R. Brar (c) Queen's U. <i>Cold Dust - Radio Continuum Correlation in Spiral Galaxies (WE-P14-1)</i> | 16h00 |
| | | | W.L. Li (c) U. Manitoba <i>Coincident First- and Second-Order Magnetic Transitions in Single Crystal $La_{0.73}Ca_{0.27}MnO_3$ (WE-P4-6)</i> | C. Kirkby (c) U. Alberta <i>Removing Blur from Energy Fluence Measurements Made Using Varian's aS500 Electronic Portal Imaging Device (WE-P12-4)</i> | J. Hessels (c) McGill U. <i>Imaging of the Young, Energetic Radio Pulsar J2021+3651 with the Chandra X-Ray Observatory (WE-P14-2)</i> Session Ends at 16h30 / Fin de la session à 16h30 | 16h15 |

| TIME HEURE | Other Locations Autres endroits | Ballroom A | Ballroom B | Ballroom C | Colbourne | Kildonan |
|---------------|------------------------------------|----------------------------------|----------------------------------|--|--|---|
| | | ↓ | ↓ | ↓ | ↓ | ↓ |
| 16h30 | | Session Ends / Fin de la session | ↓ | A. Olin (c) TRIUMF <i>Simulation of the DRAGON Recoil Mass Separator Using GEANT (WE-P5-6)</i> | WICHOSKI, Ubi U.Montreal <i>Status of the Dark Matter Search (WE-P13-2)</i> | DASGUPTA, Arundhati U.Libre de Bruxelles <i>Entropy of a Black Hole Apparent Horizon (WE-P10-5)</i> |
| 16h45 | | | Session Ends / Fin de la session | R. Roy (c) U.Laval <i>Target Proximity Effect in Heavy-Ion Collisions (WE-P5-7)</i> | ↓ | ↓ |
| 17h00 | | | | Session Ends / Fin de la session | L. Parker (c) U.Waterloo <i>Weak Lensing by Galaxy Groups at Intermediate Redshift (WE-P13-3)</i> | Session Ends / Fin de la session |
| 17h15 | | | | | M. Landry (c) Hanford U./Caltech <i>Results from LIGO's Second Science Run: A Search for Continuous Gravitational Waves (WE-P13-4)</i> | |
| 17h30 | | | | | Session Ends / Fin de la session | |

Thursday, June 17

TOURS FOR THE OBSERVATORY AND PLANETARIUM (CASCA)

U. of Manitoba Physics Alumni Reunion Events (to celebrate the 100th anniversary of the department)

Meeting of the CAP/NSERC Liaison Committee (09h00 - 12h00) - Strathcona Room, Delta Hotel

Next CAP Annual Congress

2005 June 18-21

at the University of British Columbia, Vancouver, BC

-- CAP's 60th Anniversary and World Year of Physics --

| Strathcona | Westminster | Campaign A | Victoria | Albert | Campaign B | TIME HEURE |
|------------|-------------|---|---|---|--|------------|
| | | | ↓ | ↓ | WE-P15 (CASCA) MISCELLANEOUS INTRIGUES / INTRIGUES DIVERSES Chair: D. Hanes, Queen's U. | |
| | | | Session Ends / Fin de la session | T. Stanescu (c) CrossCancer Inst. <i>Lag Mechanism in Amorphous Selenium Radiation Detectors (WE-P12-5)</i> | J. Kalirai (c) UBC <i>The Initial-Final Mass Relationship (WE-P15-1)</i> | 16h30 |
| | | | | J. Battista (c) London Reg.CancerCentre <i>Fundamental Spatial Resolution Limits in Megavoltage X-Ray Detectors (WE-P12-6)</i> | A. Sajina (c) UBC <i>Simulating Spitzer 3-24 micron colour-colour Diagrams Including Redshift Evolution (WE-P15-2)</i> | 16h45 |
| | | WE-P16 (CAP/ACP) New and Old Council Meeting / Réunion du Conseil (nouveau et ancien) | | Session Ends / Fin de la session | I.H. Stairs (c) UBC <i>Geodetic Precession and the System Geometry of PSR B1534+12 (WE-P15-3)</i> | 17h00 |
| | | | | | WE-P17 (CASCA) Closing and Awards Given for Best Student Presentations / Clôture et remise des prix aux meilleurs présentations d'étudiants | 17h15 |
| | | | | | Session Ends / Fin de la session | 17h30 |

Jeudi, le 17 juin

TOURS FOR THE OBSERVATORY AND PLANETARIUM (CASCA)

U. of Manitoba Physics Alumni Reunion Events (to celebrate the 100th anniversary of the department)

Meeting of the CAP/NSERC Liaison Committee (09h00 - 12h00) - Strathcona Room, Delta Hotel

Prochain Congrès annuel de l'ACP

18-21 juin 2005

à l'Université de la Colombie-Britannique, Vancouver, BC

-- le 60^e anniversaire de l'ACP et l'année mondiale de la physique --

2004 CONGRESS ORAL SESSION ABSTRACTS RÉSUMÉS DES SESSIONS ORALES - CONGRÈS 2004

The oral session abstracts presented here are organized by session codes (SU-A1 to WE-P6). Each presentation is cross-referenced in the Author Index (pg. 113). *Les résumés des sessions orales ci-après sont par code (SU-A1 à WE-P6). L'index des auteurs (pg. 113) établit des renvois à cette liste de présentations.*

Please see the Congress Program Summary for details on the times and locations of each of the sessions as well as all other (non-session) meetings organized in conjunction with the 2004 Congress. *Veillez vous référer au résumé du programme du congrès pour les heures et endroits de chaque session ainsi que pour toutes les autres rencontres organisées en conjonction avec le congrès 2004.*

[SU-A1]**Enriching Our Teaching Through Integration****SUNDAY, JUNE 13**(CAP-CASCA-
COMP/ACP-CASCA-
OCPM)**Enrichissement de notre enseignement par l'intégration****DIMANCHE, 13 JUIN****08h00 - 12h30****[Rooms/Salles : Victoria/Albert]****Chair: J.R. Percy, U. of Toronto at Mississauga****SU-A1-1 08h00**

Astronomy, Biology, Chemistry, Geology and Physics Integrated in a Newly Developed Course "Science: World Views". Vesna Milosevic-Zdjelar, *University of Winnipeg* — Educational Research showed alarming discrepancy between the education of elementary teachers and requirements of science curricula in Canadian schools. At the University of Winnipeg, we launched as experimental, the course that integrates natural sciences. Our aim is to offer to future teachers a broad education about variety of scientific concepts that they will be required to teach in elementary schools. As a six credit hour science requirement towards Bachelor of Education degree, Early Years stream, students choose from a variety of specialized courses that are being offered by science departments. Choosing any one, (physics, chemistry, biology, geology, etc), students are provided with education related to only that particular science. Through a multidisciplinary and curriculum oriented course "Science: World Views", education students can obtain a broad awareness and understanding of issues and concepts covered in elementary school curriculum. The course is also offered to students of other streams.

SU-A1-2 08h15

Integrating a Lab Experience with an Astro 101 Class*, Charles Kerton, Gary Cameron, David Oesper and Lee Anne Willson, *Iowa State University* — A common problem with the large first-year survey class in astronomy for non-science students ("Astro 101") is how to provide students with some sort of lab experience where they can explore certain topics in more detail or perhaps even get a chance to see the night sky! To address this problem the ISU Department of Physics and Astronomy has developed a one-credit stand-alone lab course that is available to students taking our introductory astronomy course. Available resources limit the number of students to approximately 60 out of a typical enrollment of 350 in our first-year survey class; however, experience shows that we tend to attract the more motivated students. Students complete a series of "Indoor" and "Outdoor" labs over the semester. Indoor labs include a mix of relatively simple (senior high-school level) labs along with computer-based labs using commercially available planetarium software. Outdoor labs involve both naked-eye projects (identifying stars, making angular measurements, tracking lunar phases) and telescope-based projects (viewing double-stars, tracking the Galilean satellites). This contribution will describe the practical working of the class in more detail and present examples of the various labs done by the students.

*This work is being supported by ISU.

SU-A1-3 08h30

The Big Questions: Integrating Science at the Undergraduate Level. William E. Harris, J. Waddington, A. Chen, and P. Higgs, *McMaster University* — In September 2003, we introduced a new course called « The Big Questions » to the McMaster undergraduate curriculum which is deliberately designed to present the basic nature of science, and some of its current frontier questions, to the most diverse possible audience. It is open for credit to any student at 2nd year level or higher, from any faculty or program in the university. Our material builds on four related topics: (1) The nature of space and time, (2) The origin of the universe, (3) The origin of the elements, and (4) The origin of life. Our team of instructors, all from the Department of Physics and Astronomy at McMaster, consists of an astronomer, an experimental nuclear physicist, a nuclear astrophysicist, and a biophysicist. We use the course material to present the origin of structure in the universe as an ongoing timeline, and to deal with the students' hidden questions and concerns about the nature of science. We strongly reinforce the students' natural urge to ask large-scale questions rather than details; and we promote class discussion and free exchange of student ideas and opinions, to take advantage of their very diverse backgrounds. Regular lectures are held, but much of the impact of the course comes from frequent meetings of small (20-25 person) tutorial groups into which the class is divided. All students carried out term projects and group presentations and were encouraged to pick topics and approaches which suited their particular backgrounds. We also required the students to post their thoughts and questions on a « topic of the week », and to keep a weekly journal. The students took everything on enthusiastically, and their responses proved to be surprisingly informative for us. This has been an exciting course to give, and seems to fill a basic curiosity-oriented need for students from all across campus. In a way that integrates key concepts about the nature of science with contemporary learning models. We will discuss what other lessons we learned from giving this course: what went well, what we intend to revise, and what challenges we face in this kind of audience. We would like to thank Paul Francis and Craig Savage from the Australian National University, whose own « Big Questions » course at ANU was our inspiration.

SU-A1-4 08h45

Crossing the Disciplines: Using Medical Imaging Software for Teaching Astronomy. Jennifer West and I.D. Cameron, *University of Manitoba* — Image processing and analysis are essential tools common to both astronomy and medical physics. We describe the use of the medical image processing package, ImageJ, distributed by the National Institutes for Health, for teaching astronomy. ImageJ is a particularly adaptable program, allowing the user to easily implement custom functionality through a very well supported "plugin" interface and a macro language, in addition to an impressive list of built-in visualization and analysis tools. The software is very well suited to use in astronomical applications. Its intuitive user-interface makes it particularly good for students first learning these concepts.

SU-A1-5 09h00**DANIEL W RICKEY, CancerCare Manitoba***Medical Physics at the Undergraduate and High School Levels*

Traditionally, only a relatively small number of students are interested in graduate-level medical physics training. This is partially due to the low profile of medical physics as a career path. In Manitoba we have taken a number of steps to increase awareness of medical physics at pre-graduate levels. A number of approaches are used. Presentations on imaging, radiation therapy, and radiation protection have been given to high school teachers at in-services and conferences. Tours have been provided to high school students. We are also involved in a job-shadowing programme where each year, a single (lucky) high-school student sees most areas of medical physics over 15 3-hour visits. Consequently, steps have been taken to incorporate medical physics directly into the high-school physics curriculum. At the university under-graduate level, a course on medical physics is offered annually and is aimed at physics and engineering students. The aim of this talk is to share our experiences and to outline the advantages and disadvantages of these approaches. Specifically, we will highlight those that give the greatest return.

SU-A1-6 09h30

CORINNE A. MANOGUE, Oregon State University

Revitalizing the Upper-Division Physics Curriculum

The Paradigms in Physics Program at Oregon State University has totally reformed the entire upper-division curriculum for physics and engineering physics majors. This has involved both a rearrangement of content to better reflect the way professional physicists think about the field and also the use of a number of reform pedagogies which place responsibility for learning more firmly in the hands of the students. Along the way we are learning about what it takes to successfully design and implement large scale modifications in curriculum and to institutionalize and disseminate them. The particular emphasis will be on how reforms have influenced how we teach quantum mechanics. I will share some of our joyful experiences and hard-learned lessons.

10h00 Coffee Break / Pause café

SU-A1-7 10h30

JAYMIE MATTHEWS, University of British Columbia

Distance Learning from 820 km Straight Up: The Educational Potential of the MOST Space Telescope

The MOST (Microvariability & Oscillations of STars) mission is the first all-Canadian scientific satellite in over 30 years. It is a small but powerful optical telescope and photometer in polar orbit, capable of detecting variations in the brightnesses of stars down to a few parts per million. It is searching for acoustic oscillations and convection in stars, and reflected light from planets outside the Solar System. MOST offers a great opportunity to introduce a wide range of physical, astronomical, technological and even political concepts in the classroom, all packaged in a "Humble" suitcase-sized observatory. MOST science is a springboard to areas as diverse as: acoustics (especially the refraction of sound in stars and elsewhere in nature), planetary science, nuclear reactions, thermal physics and convection, and the laws of light, gravity and dynamics. MOST technology illustrates in a topical and accessible way: digital electronics and detectors, momentum and gyroscopic motions, solar energy conversion, and magnetic fields. The MOST lift-off aboard a former Soviet ICBM can launch discussions about Cold War politics and the space race, and the advantages and challenges of international scientific cooperation. And MOST itself may become the ultimate virtual field trip for you students, since the MOST Team hopes to offer Canadian astronomy enthusiasts and students the chance to submit their own proposals for scientific projects using this unique instrument.

SU-A1-8 11h00

ARTHUR O. STINNER, University of Manitoba

*Using the History of Science to Present the Evolution of Major Concepts in Physics**

We will present the rationale and give a description of two history science courses that we have developed at the University of Manitoba. These are offered to physics as well as science education students. The first course discusses the major ideas and discoveries in science from the Early Greeks to the beginning of the 19th century. The second course uses a thematic approach that traces the evolution of the periodic table from the early ideas of Dalton in the first decade of the 19th century, to the discovery of the neutron in 1932. Three phases of this development are, first, from Dalton's atomic theory to Mendeleev periodic table, the second from Rutherford's discovery of the nucleus and Moseley's experiments to Bohr's periodic table of 1922, and the third phase includes the ideas and discoveries of quantum mechanics and the discovery of the neutron. We will discuss the second course in detail. Our objective for these courses is twofold: to present the major ideas of physics in a historical and contextual way and to attract science students to consider science teaching through a two year post B.Sc program in education.

*In collaboration with P. Loly, University of Manitoba

11h45 Session Ends / Fin de la session

[SU-A2] COMP Business Meeting / Réunion d'affaires de l'OCPM

(COMP/OCPM)

**SUNDAY, JUNE 13
DIMANCHE, 13 JUIN
08h00 - 12h30**

[Room/Salle : Campaign B]

Chair: C. Arsenaault, Dr. Georges L. Dumont Hospital

**[SU-CHAIRS] CAP - Physics Department Heads/Chairs Workshop /
ACP - Réunion des directeurs de départements de physique**

(COMP/OCPM)

**SUNDAY, JUNE 13
DIMANCHE, 13 JUIN
08h30 - 12h30**

[Room/Salle : Paragon Restaurant, then Colbourne Rm, Delta Hotel]

Chair: G. Williams, U.Manitoba

**[SU-A3] IPP Board of Trustees Meeting / Réunion du conseil d'administration
de l'IPP****SUNDAY, JUNE 13
DIMANCHE, 13 JUIN
09h00 - 12h00**

[Room/Salle : Campaign A]

Chair: C. Picciotto, U.Victoria

**[SU-A4] Single-Molecule Polymer Physics: Fundamental Questions /
Physique des polymères monomoléculaires: questions fondamentales**

(DCMMP/DPMCM)

**SUNDAY, JUNE 13
DIMANCHE, 13 JUIN
09h30 - 12h30**

[Rooms/Salles : Ballrooms B/C]

Chair: J.L. Bechhoefer, Simon Fraser U.

SU-A4-1 09h30

EDIT M. SEVICK, Australian National University

*The Fluctuation Theorem as a Generalised Second-Law for Nanomachines and Single Biopolymer Manipulations: Optical Tweezers Experiments and Beyond**

The puzzle of how time-reversible microscopic equations of mechanics lead to the time-irreversible macroscopic equations of thermodynamics has been a paradox since the days of Boltzmann. Boltzmann simply side-stepped this enigma by stating "as soon as one looks at bodies of such small dimension that they contain only very few molecules, the validity of this theorem [the Second Law of Thermodynamics and its description of irreversibility] must cease." Today we can state that the Transient Fluctuation Theorem (TFT) of Evans & Searles is a generalised, Second-Law like theorem that bridges the microscopic and macroscopic domains and links the time-reversible and irreversible descriptions. In this talk we apply this theorem a colloidal particle in an optical trap, and demonstrate that this system can evolve reversibly and "violate" the Second Law over experimentally realisable time and length scales. Moreover, we show how the theoretical Fluctuation Theorem (FT) formalism can be rigorously re-framed in stochastic dynamics. This is important as the dynamical responses of polymer and biophysical systems are often well-described by stochastic dynamics and this suggests new applications of the FT.

* In collaboration with J.C. Reid¹, D.M. Carberry¹, G.M. Wang¹, D.J. Searles² and D.J. Evans¹, ¹ Australian National University and ² Griffith University.

SU-A4-2 10h15

NANCY FORDE, UC Berkeley

*Using Optical Tweezers to Study Single-Molecule Reactions in Real Time**

The ability to exert force on single molecules offers an experimental means to probe mechanical processes and to see beyond ensemble-averaged behaviours. Optical tweezers, which use a focused laser beam to manipulate micron-sized refractive particles with nanometer precision, allow us to exert and detect forces on the piconewton scale. By attaching molecules of interest to these particles, we can determine molecular response to applied mechanical force. In this talk, I will discuss our recent experiments that take advantage of previously characterized elastic properties of DNA in order to follow the movement of RNA polymerase along DNA in real time. RNA polymerase is a molecular motor that catalyzes synthesis of an RNA polymer chain, converting chemical energy into mechanical force causing directed movement along the DNA template. By studying this transcription reaction by single molecules of RNA polymerase, and applying a mechanical force to assist or oppose translocation along DNA, we have been able to follow, and in some cases alter, the reaction kinetics in real time.

* In collaboration with C. Bustamante^{1,2,3}, D. Izhaky¹, ¹Howard Hughes Medical Institute, ²Department of Molecular and Cell Biology, and ³Department of Physics, University of California, Berkeley.

SU-A4-3 11h00

BAE-YEUN HA, University of Waterloo

Statics and Dynamics of Biopolymers: Theory and Biological Relevance

In this talk, I will discuss conformational and dynamical properties of biomolecules with an emphasis on their biological implications. I will first present simple theoretical models for describing loop formation of DNA, both double-stranded (ds) and single-stranded (ss) DNA. In the case of dsDNA (or other semiflexible polymers), large loops are entropically disfavored, while small-loop formation costs bending energy. This results in an optimal loop size at which the closing time is shortest. In contrast, the looping kinetics of short ssDNA is mainly controlled by stacking-breakage probability and shows loop-composition sensitivity. Finally, I will discuss polyelectrolyte aspects of DNA, especially the electrostatic mechanism behind DNA packaging by polyvalent counterions.

SU-A4-4 11h45

HANS JUERGEN KREUZER, Dalhousie University

Stretching and Confinement of Single Polymer Molecules and the Growth of a Polymer Brush: a First Principles Theory

A first principles theory based on (i) *ab initio* (density functional theory) calculations of the potential energy surfaces of the polymer conformers, and (2) the proper statistical mechanics (including the intricacies of the AFM), allows the parameter-free calculation of the thermodynamic properties of single polymer strands and polymer brushes. For the statistical mechanics we succeeded to formulate and solve a Green's function approach (transfer matrix method) in the presence of an external force field. Applied to poly(ethylene glycol) molecules we achieve quantitative agreement with experimental data, both in hexadecane and in water. Results for the confinement of single polymer molecules in pores and for the constrained adsorption of a polyelectrolyte on a self-assembled monolayer will be presented. A theory of the growth of a polymer brush from solution will be developed.

12h15 Session Ends / Fin de la session.

[SU-P1]

(CAP-IACP)

Brockhouse Medal Winner Récipiendaire de la médaille Brockhouse

SUNDAY, JUNE 13
DIMANCHE, 13 JUIN

13h30 - 14h15

[Rooms/Salles : Ballrooms B/C]

Chair: J. Bechhoefer, Simon Fraser U.

SU-P1-1 13h30

MICHAEL THEWALT, Simon Fraser University

Redefining the Limits of Semiconductor Spectroscopy

I will describe recent advances in the ultrahigh resolution spectroscopy of isotopically enriched ²⁸Si, including results for the near-gap bound exciton transitions and the mid-infrared donor and acceptor absorption transitions. While it has long been known that the average isotopic mass of a semiconductor can have a small effect on the low-temperature band gap energy, it is only the recent results for Si which reveal the effects of the isotopic randomness present in samples having the natural isotopic composition. The common assumption that many of these spectroscopies had reached their ultimate limits in high quality natural Si samples is shown to be quite incorrect – these older results were all limited by inhomogeneous isotope broadening. The elimination of this inhomogeneous broadening in ²⁸Si reveals many new features, and new physics, and allows for the determination of previously inaccessible quantities, such as the temperature dependence of the Si band gap below 4.2 K.

14h15 Session Ends / Fin de la session

[SU-P2]

(COMP-OCPM)

Brachytherapy and Thermal Therapy Curiethérapie et thérapie thermique

SUNDAY, JUNE 13
DIMANCHE, 13 JUIN

13h30 - 15h00

[Room/Salle : Campaign B]

Chair: J. Bews, CancerCare Manitoba

SU-P2-1 13h30

Space Distribution Analysis of the Attenuation in Lead and Steel of the Scattered Radiation in a Maze of a High Dose Rate (Iridium 192) Brachytherapy Suite., Noël Blais, Maryse Mondat, Patrice Munger and Wieslaw Wierzbicki, Hôpital Maisonneuve-Rosemont — When a new high dose rate (Iridium 192) brachytherapy suite is built with a maze, the knowledge of the half value layer (HVL) and the tenth value layer (TVL) for the scattered radiation is necessary for evaluating the door composition. The recommended HVL and TVL values for the primary radiation are easily found in the literature. However, the corresponding values of HVL and TVL for the scattered radiation are practically non-existent. In this study, measurement of the attenuation of the primary and the scattered radiation was done for steel and lead. The measured attenuation was compared to the calculated one using a simple theoretical model. The scattered radiation is calculated using the Compton probability of a photon to be scattered by the concrete wall, reaching the detector. Results show that, for the primary radiation, the maximum difference between the calculated and the measured values is 1.1 mm for the second TVL in lead. For the scattered radiation, the maximum difference between calculated and measured values is 4.2 mm for the second TVL in steel. Also, a space distribution analysis of the hot and cold regions in the maze is presented and shows their dependence on the source position in the treatment room. The hot region is defined by the scattered radiation that has a higher TVL than the one in the cold region.

SU-P2-2 13h45

*Yttrium-90 Microspheres for the Treatment of Hepatocellular Carcinoma**, Muthana Al-Ghazi and D. Imagawa, University of California, Irvine — Treatment modalities for unresectable hepatocellular carcinoma (HCC) have been limited in their ability to effectively target large or multifocal lesions. TheraSphere® treatment involves arterial administration

of Yttrium-90 microspheres designed to embolize capillaries within the HCC and provide local radiation therapy. Y-90 microspheres are composed of a biocompatible glass matrix with approximate diameters of 25 μm . Y-90 is a pure β -emitter with an average β -energy of 0.94 MeV. Prior to treatment, a $^{99\text{m}}\text{Tc}$ -MAA scan is performed to determine tumor to normal liver tissue perfusion and detect vascular shunting. Patients having a lung shunt of more than 20% are at high risk for radiation pneumonitis and are excluded. Liver volumes are determined by CT or MRI imaging. Intra-arterial administration of Y-90 microspheres is performed under standard interventional radiology suite conditions. A closed loop apparatus is used to deliver the microspheres to the tumor site via an intra-arterial catheter. An in-house quality assurance protocol is established to deliver a prescription dose in the range of 100 Gy-150 Gy. A brachytherapy scan is performed post-procedure to ascertain delivery of the microspheres to the intended treatment area. To date a total of 11 patients have been treated under a clinical study approved by the Institutional Review Board. Nine of these had failed prior therapy. The Therasphere[®] procedure is delivered for palliation. All of the patients in this study received their treatment on an outpatient basis with no serious side effects. Preliminary results have been encouraging vis-à-vis symptom control, quality of life and increased survival.

* On behalf of the Therasphere Group

SU-P2-3 14h00

Cs-137 Dosimetry Using GAFchromic[®] Film, Martin G. Shim, Lisa Gamble, Tom J. Farrell, and Joseph E. Hayward, *Juravinski Cancer Centre* — Low dose rate (LDR) brachytherapy via remote afterloading of ^{137}Cs seeds is a standard therapy for gynecological cancers. In most treatment planning systems a simple point source model is used to calculate the dose distribution for seed combinations. Neglecting the attenuation from the applicator, stopping screw and adjacent seeds/spacers has the effect of overestimating dose. Attenuation data is obtained from the literature or empirically if more accurate dosimetric calculations are required, but these are only suitable for simple geometries. The most relevant data available for more complex geometries are based on measurements of high dose rate ^{60}Co seeds with an activity 20-40 times greater than the seeds used for LDR brachytherapy. Secondly, no near-field dosimetry is available. In this work we have used GAFchromic film to measure the dose around Selectron applicators loaded with ^{137}Cs seeds. Films were exposed to single-seed loadings and the optical density maps were analyzed in Matlab. Film dosimetry at 1 cm from the seed centre, perpendicular to the applicator axis, was consistently 15% lower than calculated values. This was attributed to a film-cutting artifact that introduced a spatial shift of 1 mm in the high dose gradient region. This error was characterized in detail and accurate dose distributions were measured for ^{137}Cs . These results can be modeled in dosimetry software and treatment can be performed with the revised model. In this talk, the accuracy of GAFchromic film dosimetry will be discussed in addition to the clinical implications of the revised dose model.

SU-P2-4 14h15

Dynamical Post-Implant Dose Calculation for Permanent Prostate Implants: Taking Edema into Consideration, Ghyslain Leclerc^{1,2}, Dragan Tubic^{2,3}, Marie-Claude Lavallée^{1,2}, Éric Vigneault², René Roy¹ and Luc Beaulieu^{1,2}, ¹Université Laval and ²CHUQ (Hôtel-dieu) — Purpose: An algorithm is proposed which allows a dynamic dose evaluation that takes the volume and seed position variations, caused by edema, into account. Materials and Methods: Post-implant edema of 57 clinical cases implanted (^{125}I) between 2000 and 2001 has been evaluated using a combination of CT images and fluoroscopic images acquired a few hours after the implant and 40 days post-implant. An exponential volume resorption scenario was implemented and the prostate contours and seed positions were allowed to dynamically change from $t=0$ and extending to 244 days (about 6 times more than the edema half-life) in steps of 1 day. DVHs were generated at each step and convoluted with a weight equal to the fraction of the total dose delivered in that particular step. This time-integrated DVH was compared to the standard clinical one. Results: The mean initial increase of the volume is 51%. Considering the exponential decay model for edema, the mean half-life of the volume decrease is 33.6 days, which is much higher than the accepted value. With dynamic dosimetry, a representative time (t_w) for an implant can be evaluated and its average is found to be 45 days. The differences with the clinical dosimetry, for D_{90} , is small on average (3%) but differences up to 15 Gy (11%) are found. The observations are similar for V100, V150 and V200. Conclusion: The dosimetric effect of post-implant edema is non negligible and the proposed algorithm correctly takes it into account to first order. Further extension will be discussed.

SU-P2-5 14h30

Interstitial Optical-based Reconstruction of Thermal Coagulation During Microwave Thermal Therapy*, Lee Chin¹, W.M. Whelan², S.R.H. Davidson¹ and I.A. Vitkin¹, ¹Princess Margaret Hospital / University Health Network and ²Ryerson University — Interstitial microwave thermal therapy (IMTT) is a minimally invasive technique currently under investigation for the treatment of solid tumors. Thin microwave applicators are inserted directly into the target site to deliver microwave energy and raise the temperature of the tumor to $> 55\text{ }^\circ\text{C}$, thereby inducing coagulative necrosis. Point temperature measurements currently provide a practical method for monitoring IMTT. However such temperature monitoring methods are indirect, relying on thermal dosimetry models to predict the extent of thermal coagulation. An alternative strategy, made possible by the significant coagulation-induced changes in optical scattering, involves illuminating the tissue with a non-heating optical source and measuring interstitial changes in light intensity using point optical sensors. This may provide a direct means for determining the extent of thermal coagulation. In this work we utilize interstitial light intensity data across multiple projections (i.e. source-detector scans) in the tissue, to reconstruct 2D maps of thermal coagulation. As rectilinear back projection approaches are unsuitable due to the diffuse nature of light in tissue our reconstruction is based on weight matrices obtained from a first order perturbation expansion of the diffusion equation. Singular value analysis of weight matrices for different source-sensor spacing and field of view was performed to obtain an experimental configuration that maximized image resolution and minimized scanning time. The optimized configurations were confirmed by performing reconstructions using forward optical intensity data generated using a heterogeneous finite-element light diffusion model. Finally, using the optimized geometry, experimental optical intensity data was acquired during IMTT of ex vivo bovine liver and used to reconstruct maps of thermal coagulation.

* This work is being supported by NCIC.

SU-P2-6 14h45

A Gel Phantom for MR Calibration of Thermal Therapies*, Shanna Lochhead, Shanna Lochhead, Mark McDonald, Rajiv Chopra and Michael J. Bronskill, *Sunnybrook and Women's College Health Sciences Centre* — Thermal therapy, the application of heat to coagulate tissue, is a rapidly developing therapeutic technique for soft tissue tumor treatment. Sources of heat include radiofrequency (RF), laser, microwave and ultrasound devices. These treatments tend to be less invasive than conventional surgical resection and can sometimes offer an alternative when surgery is not feasible. Magnetic resonance (MR) imaging is useful throughout thermal therapy for tumor visualization and device guidance, the non-invasive measurement of temperatures during heat delivery, and to distinguish between regions of thermal damage and normal tissue. A phantom material with tissue-mimicking thermal properties is essential for the development and characterization of thermal therapy devices, and for clinically related activities such as quality assurance, device comparisons, and treatment verification. Key requirements for such a material are (a) heat absorption and conduction properties similar to tissue; (b) stability over the range of temperatures experienced in thermal therapy; (c) accurate delineation of the volume that is thermally coagulated; and (d) coagulation temperature similar to that of tissue. A tissue-mimicking phantom material has been developed for use with ultrasound thermal therapy devices and techniques. This material has MR properties that change drastically upon thermal coagulation. Consequently, simple T_2 -weighted images can provide a complete three-dimensional picture of the coagulated region. The acoustical properties of the material match those of tissue and the coagulation temperature of the phantom can be adjusted to simulate various tissues. This material also has potential for use with other thermal therapy modalities (laser and RF).

* This work is being supported by Terry Fox / NCIC.

15h00 Session Ends / Fin de la session

[SU-P3]

**Enriching Our Teaching Through Integration
Enrichissement de notre enseignement par l'intégration**

(CAP-CASCA-
COMP/ACP-CASCA-
OCPM)

**SUNDAY, JUNE 13
DIMANCHE, 13 JUIN**

14h15 - 16h15

[Rooms/Salles : Victoria/Albert]

Chair: R. Hawkes, Mount Allison U.

SU-P3-1 14h15

Bringing the Stars to the Students, Heather R. Scott, *Ridley College* — Astronomy, unlike most other branches of science, has relatively few labs that can be performed in a classroom, or even during the day. The beauty of astronomy, however, is in the true discovery at all levels – elementary grades to university research – that can only take place

outdoors, studying the stars under a darkened sky. For many teachers, this raises the issue of assembling students after school hours, and in some cases transporting them to suburban locations. This is often compounded with the fact that few teachers are comfortable navigating the stars and designing a lesson around these observations. This presentation will "bring to light" several easy observing projects that teachers can use including alternative projects for those who cannot get out at night (or who are plagued by cloudy skies!). Connections to the national curriculum will be highlighted, as well as links to other areas of science. An extensive list of astronomy teaching resources will be available.

SU-P3-2 14h30

CAROL A. CHRISTIAN, Space Telescope Science Institute

Putting Research Science and Education Together: Lessons Learned from HST

Incorporating current research results into educational resources that adhere to appropriate standards and uphold pedagogy can enhance learning, yet success at crafting usable materials for pre-college education and informal science represents a significant challenge. Within the Hubble Space Telescope project, we developed a successful model for research scientists to participate in educational content creation by creating teams with teachers, graphic artists, writers and multi-media Web developers. We created multi-media resources designed to improve science and mathematics skills in students and improve public perception of science. A systematic production cycle including specification, project definition, frequent reviews and several testing periods resulted in robust but flexible resources for curriculum support materials, a traveling museum exhibit, press releases and a website for the public.

15h00 Coffee Break / Pause café

SU-P3-3 15h30

JOHN R. PERCY, University of Toronto at Mississauga

Variable Stars: Dynamic Tools for Hands-On Astronomy and Physics Education

Variable stars are stars which change in brightness. They provide important information about the nature and evolution of the stars. I will share my experience in supervising research projects on variable stars by senior high school and undergraduate students. These projects introduce students to most of the basic aspects of the research process. In the course of their background reading, they encounter a variety of fundamental concepts in the physical sciences. Time-series analysis of variable star data then introduces them to further concepts in math, statistics, and computation. Students are motivated by doing real science, with real data! Almost every project results in a published research paper or conference presentation. Hands-On Astrophysics (hoa.aavso.org), which was developed by Janet Mattei and me, is a related project which was targeted at high school students. My students have created a simple web page (www.astro.utoronto.ca/~percy/index.html) with information and links to software and data, to support individual student research projects. Recently, as a result of massive sky surveys, thousands of new variable stars have been discovered — but not yet analyzed. Since most of the data is available on-line, there is a golden opportunity for students to "solve" these stars.

SU-P3-4 16h00

Reaching Out From the Centre of the Universe: A Report from Canada's Astronomy Interpretation Centre. **Margaret L. Milne**, *The Centre of the Universe* — The Centre of the Universe (CU) is an astronomy interpretation centre located in Victoria, BC at the Herzberg Institute of Astrophysics - Dominion Astrophysical Observatory. Open since the summer of 2001, the CU is the first and only outreach centre of the National Research Council of Canada. This presentation will briefly describe the CU facility and its history, highlight the regular programs and special events the CU offers, and discuss the challenges and rewards of interpreting Canadian astronomy to the public.

16h15 Session Ends / Fin de la session

[SU-P4]

(DCMMP/DPMCM)

Single-Molecule Polymer Physics: Biophysical Applications
Physique des polymères monomoléculaires: applications en biophysique

SUNDAY, JUNE 13
DIMANCHE, 13 JUIN

14h15 - 17h30

[Rooms/Salles : Ballrooms B/C]

Chair: J. Bechhoefer, Simon Fraser U.

SU-P4-1 14h15

JOHN MARKO, University of Illinois at Chicago

Micromanipulation Study of Chromatin Fibers and Whole Chromosomes

Although a tremendous amount is known about the structure of DNA and the proteins which organize it at scales of a few angstroms, the structure of chromosomes at larger length scales remains rather poorly understood. I will describe how piconewton and nanonewton-scale force measurements can be used to examine two problems of chromosome structure. First, I will discuss experiments examining the self-assembly of DNA and histone proteins into chromatin fiber, with a focus on the role of ATP hydrolysis in chromatin assembly. Then, I will discuss the use of combined biochemical-micromechanical techniques to analyze the large-scale structure of the mitotic chromosome. I will emphasize experiments which show that DNA itself is the contiguous structural elements of the folded chromosome, rather than a protein 'scaffold'.

15h00 Coffee Break / Pause café

SU-P4-2 15h30

GARY W. SLATER, Université d'Ottawa

*Single-Molecule Polymer Physics: The Role of Molecular Dynamics Simulations**

Molecular Dynamics (MD) computer simulations can help us understand most single-molecule problems currently under investigation in experimental polymer physics. One of the great advantages of MD simulations is that they include both hydrodynamics and excluded volume interactions, two effects that are not easily dealt with using theoretical models, especially in non-equilibrium and non-steady-state situations. In this presentation, I will discuss three different problems that we have studied using this powerful computational tool: 1) the deformation of a polymer pulled at constant velocity in a tube; 2) the cyclic motion of a polymer chain attached to a wall and subjected to a strong shear flow; 3) the collision between a polymer and a post in a microfluidic system.

* In collaboration with M. Kenward, Y. Gratton and S. Hubert, Université d'Ottawa.

SU-P4-3 16h15

ANDRÉ MARZIALI, University of British Columbia

A Single-Molecule Nanosensor For Oligonucleotide Identification

We present the construction and operation of a self-assembling nanosensor for sequence-specific detection of nucleotides across a membrane. The probe is constructed of two main components: a single alpha-hemolysin nanopore self-assembled into a lipid bilayer, and a DNA probe tethered to avidin at one end and complementary to the analyte nucleotide at the other end. The sensor is assembled by electrophoretic insertion of the probe into the cis- side of the nanopore (observable as an increase in electrical impedance). Hybridization of the probe to analyte on the trans- side of the pore traps the probe in place, and increases the time constant for probe exit on subsequent voltage reversal.

Using this sensor, we can uncover the energy landscape of binding interactions between single DNA molecules on the trans side of the membrane and the probe strand. This allows us to detect and identify single base mutations in short oligonucleotide strands specifically targeted based on the sensor probe sequence. The nanosensor shows promise for applications such as single nucleotide polymorphism detection, and potentially, for in vivo detection of specific RNA sequences.

17h00 Session Ends / Fin de la session

[SU-P5] IPP General Meeting / Assemblée générale (IPP)

SUNDAY, JUNE 13

DIMANCHE, 13 JUIN

14h30 - 17h30

[Room/Salle : Campaign A]

Chair: C. Picciotto, U. Victoria

[SU-P6] Radiation Treatment Devices / Appareils de radiothérapie

SUNDAY, JUNE 13

DIMANCHE, 13 JUIN

15h30 - 17h00

(COMP/OCPM)

[Room/Salle : Campaign B]

Chair: P. Dunscombe, Tom Baker C.C.

SU-P6-1 15h30

Licensing, Construction and Radiation Safety of Canada's First Gamma Knife(R)*, Harry Johnson and A. Berndt, *CancerCare Manitoba* — The Department of Neurosurgery, Winnipeg Regional Health Authority and University of Manitoba, installed Canada's first Leksell Gamma Knife® in 2003. This unique stereotactic radiosurgery tool uses 201 cobalt-60 capsules (initial activity 244 TBq) to treat inaccessible cranial lesions in a single session. Source collimators are aligned to a common isocentre. Patients are positioned within a collimating helmet fixed to the bed such that their cranial target coincides with isocentre. Following remote opening of the shielding doors, bed, helmet and patient move into alignment with the source collimators to deliver doses up to 140 Gy. The design, construction, radiation protection measurements and radiation safety experience will be reviewed. The dedicated single-story GK® suite consists of concrete walls and concrete ceiling. Shielding was based on the vendor's radiation field data. A single lead-lined door (1 cm) permits patient entry in line with the self-shielding of the irradiator unit and perpendicular to the bed direction. Licensing followed CNSC C-120. CNSC officers attended to observe the source loading. The vendor's team loaded the sources using a special loading cell mated to the source-shipping flask. Source capsules were remotely transferred to collimation channels using a detailed loading procedure to balance the field at isocentre. Radiation protection tests yielded radiation fields well within design targets, and less than anticipated at the shielded doors due to newly improved irradiator internal shielding.

* The authors acknowledge J. Sandeman's shielding and initial licence documentation.

SU-P6-2 15h45

Gamma Knife® Commissioning Report, Anita Berndt and J. Beck, *CancerCare Manitoba* — The Gamma Knife® (GK) provides a minimally invasive treatment alternative for patients with brain tumors, vascular malformations and some debilitating functional conditions. Radiation is delivered with sub-millimeter accuracy to the affected region, allowing doses ranging from 10 – 140 Gy to be safely administered, even near critical structures. This presentation summarizes the measurements made during commissioning of the first Canadian GK. The GK is very different from conventional radiotherapy equipment in that it consists of 201 fixed radiation sources rather than a single source on a moving gantry. In addition, only four fixed field sizes ranging from 6 to 24 mm in diameter are available. Dose profiles were measured at the center of an 8 cm radius plastic phantom (dosimetry sphere) using EDR-2 films. The 50% isodose line was found to agree with the treatment planning system calculations to within 0.4 mm. The agreement between the mechanical and radiation isocentre was measured using a precisely machined test tool which pricks a film at mechanical isocentre; the agreement between the center of the 4 mm collimator helmet profile (radiation isocentre) and the pinprick was found to be within 0.11 mm. Helmet factors which determine the relative output for different field sizes were measured using individually calibrated TLDs placed at the center of the dosimetry sphere, resulting in agreement of better than 3% with the helmet factors used by the planning system. Absolute calibration was performed by applying the TG21 formalism to ionization measurements at the center of the dosimetry sphere.

SU-P6-3 16h00

An Algorithm for Independent Verification of Gamma Knife® Treatment Plans, James Beck and Anita Berndt, *CancerCare Manitoba* — A formalism for independent treatment verification has been developed for Gamma Knife® radiosurgery in analogy to the second checks being performed routinely in the field of external beam radiotherapy. A verification algorithm is presented, and evaluated based on its agreement with treatment planning calculations for the first 40 Canadian Gamma Knife® patients. The algorithm is used to calculate the irradiation time for each shot, and the value of the dose at the maximum dose point in each calculation matrix. Data entry consists of information included on the plan printout, and can be streamlined by using an optional plan import feature. Calculated shot times differed from those generated by the treatment planning software by an average of 0.3%, with a standard deviation of 1.4%. The agreement of dose maxima was comparable with an average of -0.2% and a standard deviation of 1.3%. Consistently accurate comparisons were observed for centrally located lesions treated with a small number of shots. Large discrepancies were almost all associated with dose plans utilizing a large number of collimator plugs, for which the simplifying approximations used by the program are known to break down.

SU-P6-4 16h15

Initial Experiences with a Commercial Helical Tomotherapy Unit, Marc MacKenzie, G.C. Field and B.G. Fallone, *Cross Cancer Institute, University of Alberta* — Helical tomotherapy (HT) is a modality which represents a convergence of diagnostic imaging and radiation therapy, with the potential for enabling a highly integrated approach to image guided adaptive radiotherapy in the clinic. This device has integrated megavoltage CT (MVCT) capability, as well as being inherently a platform for delivering inverse planned Intensity Modulated Radiation Therapy (IMRT). Our institution has recently had one of the two original HT units (Hi-Art 1) upgraded to the latest commercial version (TomoTherapy Hi-Art IEC System). The implementation of this system has spurred on a number of research projects locally, such as Monte Carlo simulations for absolute dose calibration of the unit, novel approaches to small field dosimetry as well as alternate MVCT detectors. In this presentation, we shall describe clinical aspects of implementation, which have employed several new software tools; some developed and provided by the manufacturer (TomoTherapy Inc.), and some developed in house. As well, there are a number of clinical trials which will begin shortly, and these will also be described.

SU-P6-5 16h30

Helical Tomotherapy Fan Beams and Craniocaudal Penumbra Improvement, Adam Gladwish, Tomas Kron, Andrea McNiven, Glenn Bauman and Jake VanDyk, *London Health Sciences Centre* — In helical tomotherapy (HT), an intensity modulated fan beam with fixed thickness delivers radiation dose to a patient in a helical beam trajectory. The most significant limitation with a constant fan beam thickness (FBT) is the penumbra width in the craniocaudal direction, which, due to a 'ramp up effect' is equivalent to the FBT. We propose to employ a half-blocked fan beam at the start and stop locations of treatment delivery to reduce the penumbra width by half. The choice of starting with a half-blocked beam rather than a completely shut collimator maintains the same constant couch movement as in standard HT and results in a minimum FBT of half the normal treatment FBT. We studied the impact of this technique on dose distributions in phantoms and a patient using a HT beam model implemented on a commercial treatment planning system (Theraplan Plus v3.0). We show that the dose distribution delivered using a 25mm fan beam can be improved significantly, resulting in a dose reduction of ~30% just superiorly and inferiorly of the target. In a sample brain cancer patient, we demonstrate that this approach could reduce the probability of cataract formation dramatically.

SU-P6-6 16h45

Using Isocentre Corrections in Treatment Planning to Improve Accuracy in Stereotactic Radiosurgery, Jason Schella and J.I. Robar, *Nova Scotia Cancer Centre* — One of the limitations in linear accelerator based Stereotactic Radiosurgery/Radiotherapy (SRS/SRT) is the mechanical accuracy of the treatment unit. Gantry, couch, and collimator should rotate about a single point in space. In reality, however, the centres of rotation for each of these motions differ slightly. Typical tolerances for this "wobble" of the isocentre are on the order of ±1mm for SRS/SRT. However, ±1mm is still a relatively large variation for some targets treated with SRS. When treating such functional disorders as trigeminal neuralgia a 1 mm shift in a 1-5mm diameter target may certainly compromise the treatment. In other treatments, critical structures may closely abut the target. In such cases a shift of 1mm toward the structure could deliver unwanted dose to this structure. When such factors are deemed critical one solution would be to re-centre the patient for every treat-

ment port. This can be very time consuming and could significantly increase the time required to treat a patient. Another option would be to account for these uncertainties when developing the treatment plan. By modeling the mechanical isocentre location for gantry, couch, and collimator rotations one can then modify the treatment plan by placing the isocentre of each beam at the "actual" position. The shielding is then modified appropriately. An overall improvement in the accuracy of dose delivery was shown. In one case, volume receiving 50% dose was reduced from 56% to 22%. The volume of the target receiving 80% dose was increased from 95% to 98.6%.

17h00 Session Ends / Fin de la session

| | | |
|------------------------|---|---|
| [SU-P7] (CCMP/CCPM) | CCPM Business Meeting / Réunion d'affaires du CCPM | SUNDAY, JUNE 13 DIMANCHE, 13 JUIN 17h00 - 18h30 |
|------------------------|---|---|

[Room/Salle : Campaign B]

Chair: B. Clark, BC Cancer Agency

| | | |
|---|---|---|
| [SU-KEY] (CAP-CASCA-COMP/ACP-CASCA-OCPM) | CAP Herzberg Memorial Public Lecture - Conférence publique commémorative Herzberg de l'ACP / CASCA Public Lecture in Astronomy - Conférence publique plénière en astronomie de CASCA | SUNDAY, JUNE 13 DIMANCHE, 13 JUIN 19h00 - 20h00 |
|---|---|---|

[Rooms/Salles : Ballrooms A/B/C]

Chair: B. Joos, U. d'Ottawa

SU-KEY 19h00

P. JAMES E. PEEBLES, Princeton University

A Cosmic Picture Show: Images from Astronomy

Some of the astronomical images I will present are meant to illustrate what we know about the large-scale nature of the world around us and how we have gone about discovering it; others are chosen just because they're pretty. Some of the images are close to what you can see with a pair of binoculars; others are numerical representations of what you would 'see' if you had Superman's X-ray eyes, or eyes sensitive to radio waves or neutrinos. I'll show historical examples of the learning process in astronomy, both good — Hubble's classification of the galaxies — and not so good — Lowell's idea that he was seeing canals on Mars — and illustrations drawn from current debates about what is happening on scales ranging from black holes in the centers of galaxies to the expansion of the universe.

20h00 Session Ends / Fin de la session

| | | |
|------------------------|---|--|
| [MO-A1] (CAP-I ACP) | CAP's Friends Breakfast / Déjeuner des "Ami(e) de l'ACP" | MONDAY, JUNE 14 LUNDI, 14 JUIN 07h00 - 08h30 |
|------------------------|---|--|

[Room/Salle : Private Dining Room]

Chair: M. Steinitz, St. Francis Xavier U.

| | | |
|-----------------------|--|--|
| [MO-A2] (DPE-IDEP) | High School Teacher Workshop / Atelier pour les enseignant(e) de physique (see page 18 for details / voir page 18 pour le programme) | MONDAY, JUNE 14 LUNDI, 14 JUIN 08h00 - 12h30 |
|-----------------------|--|--|

[Room/Salle : Colbourne]

Chair: P. Mitchler, Manitoba

| | | |
|------------------------|--|--|
| [MO-A3] (CAP-I ACP) | CAP Teaching Medal Winner Médaille de l'ACP pour l'excellence en enseignement | MONDAY, JUNE 14 LUNDI, 14 JUIN 08h30 - 09h15 |
|------------------------|--|--|

[Rooms/Salles : Ballrooms B/C]

Chair: R. Hawkes, Mount Allison U.

MO-A3-1 08h30

HELMY S. SHERIF, University of Alberta

A Discussion of Spin: From Teaching to Research

The subject of spin occupies a prominent place in many discussions of physical phenomena. I shall use the discussion of spin-1/2 particles as a connecting thread from class room teaching to research. Starting with the treatment of spin-1/2 in a first course on Quantum Mechanics, I shall point out where I believe the students begin to accept some of the basic principles of the subject. A discussion of the Dirac Equation and its role in enriching our understanding of spin is followed by an account of the role it plays in recent discussions of nuclear structure and reactions, including some aspects of my own research. Some personal reflections on physics and teaching will be given.

09h15 Session Ends / Fin de la session

| | | |
|--------------------------|---|--|
| [MO-A4] (COMP-I OCPM) | Diagnostic Imaging / Imagerie diagnostique | MONDAY, JUNE 14 LUNDI, 14 JUIN 08h30 - 09h45 |
|--------------------------|---|--|

[Room/Salle : Albert]

Chair: J.A. Rowlands, Sunnybrook and Women's College Health Sciences Center/U.Toronto

MO-A4-1 08h30

Experimental Verification of Sinogram Merging Technique to Reduce Limited Field-Of-View Artifacts in CT Imaging. A. Kress, R. Hooper and G. Fallone, Cross Cancer Institute, University of Alberta, — Spiral CT truncation artifacts caused by a limited detection field-of-view (FOV) can be reduced by merging two truncated fan-beam sinograms, where the sinograms are acquired with the patient shifted to two different lateral positions within the gantry. This work outlines experimental verification of this sinogram merging technique. Axial and spiral fan-beam sinograms of a phantom were acquired using a Picker PQ5000 CT scanner, with the phantom positioned left and right of isocenter. Fan-beam sinograms were artificially truncated to smaller FOVs. Sagittal lasers were used to align the phantom at the offset locations, and lateral shifts were verified using cross correlation techniques. In spiral scanning the z-axis start location for each scan was determined by placing a fiducial marker on the phantom and reconstructing slices at a small index.

Images reconstructed from the merged sinograms were compared to images reconstructed from single non-shifted, non-truncated sinograms. Qualitative analysis consisted of viewing the images at different window settings to look for artifacts created by the merging technique, and also comparing profiles through images. Quantitative comparisons of reconstructed images were also performed. For both axial and spiral data the sinogram merging technique substantially reduced the artifacts produced by the limited FOV.

MO-A4-2 08h45

Abdominal Three Point Dixon Imaging with Self Calibrating Parallel MRI. Charles McKenzie¹, S.B. Reeder², A. Shimakawa³, N.J. Pelc² and J.H. Brittain^{3,1} *Beth Israel Deaconess Medical Center and Harvard Medical School*; ² Stanford University Medical Center; and ³ GE Medical Systems — The three point Dixon technique can provide excellent separation of fat and water signals. This has a variety of potential applications, such as identification of fatty deposits in the liver. However, application of the technique to abdominal imaging has been severely limited by the requirement that three images, each with a different fat-water phase shift, must be collected, thus tripling acquisition time relative to an equivalent non-Dixon sequence. This work evaluates the feasibility of using self calibrated parallel MRI to accelerate abdominal three point Dixon imaging. *In vivo* fat/water separated images were reconstructed from accelerated and fully gradient encoded Fast Spin Echo Dixon data. By using self calibrated parallel imaging we have been able to accelerate Dixon imaging in the abdomen without encountering artifacts in the parallel MRI reconstruction from misregistration of the calibration and imaging data. Dixon water-fat separation is SNR efficient, so SNR losses from the parallel reconstruction were mitigated by the gains from the extra scan time of the Dixon acquisition. The accelerated images had minimal artifact, good SNR and image quality comparable to the images produced from fully sampled data sets.

MO-A4-3 09h00

Pinhole SPECT with Iterative Reconstruction and the Median Root Prior Filter. Andrew F. Wind¹, Barry T. McKee^{1,2}, and Michael J. Chamberlain^{2,1} *Carleton University* and ²Division of Nuclear Medicine, Ottawa Hospital — This study explores the clinical feasibility of Pinhole SPECT with iterative reconstruction. The Median Root Prior (MRP), a Bayesian Maximum A Posteriori iterative filter, is used to reduce high frequency noise while preserving edges. Capillary tubes were imaged in three orientations with high concentrations of Tc-99m to measure the system resolution. A 4 mm pinhole at a 10.7 cm radius of rotation was used to acquire 128 projections from which subsets of data could be extracted and analyzed. Images were reconstructed using 128 projections over 360 degrees as well as 64 projections over 180 degrees. The images were also reconstructed with increasing amounts of filtering to explore the effect of the MRP filter. A clinical image of a wrist was acquired under realistic conditions to demonstrate the clinical feasibility. The FWHM of the reconstructed capillary tubes was 6.0 mm on average, varying less than 10% in most circumstances. The iterative reconstruction with the MRP filter proved to be robust, yielding the correct geometry without obvious artefacts and only a small increase in noise as the number of projections was reduced. The MRP filter seems to be an excellent filter for controlling noise without smoothing edges. Limiting the acquisition to 180 degrees only shows a loss of resolution with increasing distance from the pinhole. The wrist image, although count limited, demonstrates a clinical potential for pinhole SPECT. In addition to wrists, there should be potential for elbows and ankles, which are not currently well imaged.

MO-A4-4 09h15

3D Mammography - A Single Projection Compton Scatter Imaging Technique*. Eric Van Uytven¹, S. Pistorius¹ and R. Gordon^{2,1} *CancerCare Manitoba* and ² University of Manitoba — Screening mammography is the current gold standard in detecting breast cancer. However, its fundamental disadvantage is that it translates a 3D object into a 2D image. Small lesions are difficult to detect when superimposed over layers of normal tissue. Computed Tomography (CT) produces a true 3D image yet has a limited role in mammography due to low resolution and contrast. As a first step in 3D mammography we have developed a sensitive Compton-scatter based low dose technique which can produce a 3D image of the breast with a single projection. Imaging an object with x-rays produces a characteristic scattered photon spectrum at the detector plane. A known incident beam spectrum, beam shape and arbitrary 3D matrix of electron density values enables a theoretical scattered photon distribution to be calculated. An iterative minimization algorithm is used to make changes to the electron density voxel matrix to reduce regular differences between the theoretical distribution and the experimentally measured distribution. The object is characterized by the converged electron density distribution. This technique has been validated using data produced by the EGSncr Monte Carlo code system. A scanning polychromatic x-ray pencil beam is used to irradiate a cylindrically symmetric slab of breast tissue containing multiple inhomogeneities. The resulting Monte Carlo data is processed using a Nelder-Mead iterative algorithm (MATLAB) to produce the 3D matrix of electron density values. Resulting images have been able to detect 0.5mm calcifications with a voxel resolution of 0.5cm with precision < 5% and accuracy < 4%.

* This work is being supported by CancerCare Manitoba Foundation.

MO-A4-5 09h30

Unintentional Human Skeletal Imaging With 99mTc-Methylene Diphosphonate 45 Months Beyond Expiration. Eduardo Galiano, *Laurentian University* — Eight planar, whole body skeletal scintigraphy patients were inadvertently administered, and imaged with, ^{99m}Tc-labeled Methylene-Diphosphonate (MDP) which was 45 months expired. All patients were subsequently imaged with normal MDP. Laboratory methods employed in the study of the long term stability of the MDP molecule have determined that the efficiency and strength of the labeling bond tend to degrade as a function of MDP age^[1,2]. This may result in the collection of free pertechnetate in the thyroid gland^[3]. The images obtained with expired MDP were clinically acceptable. No differences in scan abnormalities were observed compared with normal MDP for any of the patients. None of the patients suffered any side effects attributable to the expired MDP. These results suggest that it may be possible - but not recommendable - to safely obtain clinically acceptable images with expired MDP.

1. G. Subramanian, J.G. McAfee, R.J. Blair, "Pharmaceutical toxicity as a function of biodegradability", *J Nucl Med*, **14**: 719-722, 1973.

2. H.K. Genant, G.J. Bentovich, M. Singh, *et al.*, "Bone seeking radionuclides: An *in-vivo* study of the factors affecting skeletal uptake", *Radiology*, **113**: 373-376, 1974.

3. R.E. Henkin, A. Woodruff, W. Chang, A.M. Green, "The effect of radiopharmaceutical incubation time on bone scan quality", *Radiology*, **135**: 463-465, 1980.

09h45 Session Ends / Fin de la session

[MO-A5] Plenary Session / Session plénière

(CAP-CASCA-
COMP-J ACP-
CASCA-OCPM)

MONDAY, JUNE 14

LUNDI, 14 JUIN

09h15 - 10h00

[Rooms/Salles : Ballrooms B/C]

Chair: J. Bechhoefer, Simon Fraser U.

MO-A5-1 09h15

DAVID BENSIMON, École normale supérieure

The Elastic Behaviour of a Real Polymer: The Case of ssDNA

The possibility to manipulate single molecules has opened a new vista on the study of their physical properties. It has thus been shown that the elastic behaviour of double stranded DNA (dsDNA) is very well described by the Worm Like Chain model of an ideal (non-interacting) polymer. That excellent agreement is the fortuitous result of the unusually large rigidity (persistence length) of dsDNA. For more usual polymer chains (single stranded DNA (ssDNA), proteins and artificial polymers such as polyethylene or polystyrene) whose persistence length is of the same order of magnitude as the monomer size, the WLC model cannot provide a good description of their behaviour under stress. We have used ssDNA as a model to investigate the elastic behaviour of these polymers, both experimentally and theoretically. We will show that the response to stress of ssDNA can be well described by a more refined model of a polymer (an elastic Freely Jointed Chain) that takes into account electrostatic repulsion and basepairing interactions between complementary nucleotides. This model allows a parameter free description of the elastic behaviour of ssDNA over a wide range of ionic conditions and over 4 orders of magnitude of force. Similar results have been observed on the stretching of proteins where the WLC model is usually (but wrongly) used to fit the data.

10h00 Session Ends / Fin de la session

[MO-A6]

Visualization in Planetary Sciences
Visualisation en science planétaire

(CASCA)

MONDAY, JUNE 14

LUNDI, 14 JUIN

09h15 - 10h00

[Room/Salle : Campaign B]

Chair: S. Safi-Harb, U. of Manitoba

MO-A6-1 09h15

PAUL WIEGERT, University of Western Ontario

Visualizing Dynamics in the Solar System

Computers have long been used to study the behaviour of dynamical systems. Despite this fact, the potential to use computer animations to display and examine the results of such investigations have remained to a large extent unexploited. Advances in processor speed and software now make it possible to display the results of simulations much more easily on a computer screen, in some cases with real-time control of details such as the viewpoint. These developments provide new opportunities for Solar System studies as well as to astronomy in general, both in a research and a teaching context.

10h00 Session Ends / Fin de la session

[MO-A7]

Soft Matter / Matière molle

(DCMMP/DPMCM)

MONDAY, JUNE 14

LUNDI, 14 JUIN

10h00 - 12h30

[Room/Salle : Victoria]

Chair: B. Joos, U. d'Ottawa

MO-A7-1 10h00

Temperature-Sensitive Size of Microgel Particles. Barbara Joan Frisken¹, Y. Sun¹ and A. Bailey^{2,1} *Simon Fraser University* and ² Scitech Instruments — We have been investigating properties of microgel particles made by free-radical polymerization of N-isopropylacrylamide (NIPAM) in water. Usually, these particles are formed during polymerization in the presence of an added crosslinker, typically N,N'-methylene bis(acrylamide), but we have also found that we can make stable particles in the absence of added crosslinker. In a water dispersion, these particles decrease in size upon heating. We have measured the temperature-dependence of particles made with different amounts of crosslinker with both dynamic light scattering and static light scattering techniques. The ratio of the sizes measured by these two techniques is not constant but depends on temperature and on the amount of added crosslinker. This variation is strongest near the volume phase transition in samples with no added crosslinker. Sources of this variation will be discussed.

MO-A7-2 10h15

Spontaneous Formation of Monodisperse Small Unilamellar Vesicles – Kinetically Trapped or Thermodynamically Stable? M.-P. Nieh, V.A. Raghunathan, T.A. Harroun and J. Katsaras, *National Research Council* — The structural phase diagram of the long-chain phospholipid dimyristoyl phosphatidylcholine (DMPC) with the short-chain lipid dihexanoyl phosphatidylcholine (DHPC) doped with charged species was recently constructed. Spontaneously forming unilamellar vesicles (ULV) were found at low concentrations (< 2 wt.%) and temperatures > 23 °C. Using small-angle neutron scattering we have investigated ULV formation on diluting lamellar stacks at 45 °C to determine whether the ULV formed are kinetically trapped or thermodynamically stable.

MO-A7-3 10h30

Phase Behaviour of Aqueous Solutions of Short and Long Chain Phospholipids. V.A. Raghunathan, M.-P. Nieh, T.A. Harroun, and J. Katsaras, *National Research Council* — Mixtures of short and long chain lipids have been shown to be promising matrices to orient membrane proteins for NMR experiments. We have studied the phase behaviour of mixtures of dihexanoyl phosphatidylcholine (DHPC) and dimyristoyl phosphatidylcholine (DMPC), using optical microscopy and neutron scattering techniques. An isotropic phase, consisting of disc-like micelles or so-called bicelles, is observed below the chain melting transition of DMPC. At higher temperatures, a nematic phase made up of long worm-like micelles is formed. Addition of the charged lipid, dimyristoyl phosphatidylglycerol (DMPG), destabilizes the nematic phase, and the system exhibits a lamellar phase made up of bilayers. The influence of molecular chirality on the structure of the different phases has also been investigated.

MO-A7-4 10h45

Novel Finite-Size Effects in Biomimetic Smectic Films. J. Katsaras, T.A. Harroun, V.A. Raghunathan, M.-P. Nieh, *National Research Council* — Thin stacks of lipid multibilayers supported on rigid silicon and mica substrates are found to exhibit novel finite-size effects. Using neutron diffraction we find that the repeat spacing (d), of stacks containing up to a few tens of bilayers, depends on their thickness (D), with d increasing with decreasing D . These results contradict the general belief that thinner stacks have a lower d , due to the suppression of thermal bilayer undulations by the interfaces of the film, which lowers the steric interbilayer repulsion. However, the present experimental results have been envisaged by a recent theoretical analysis of finite-size effects in bilayer stacks at interfacial tensions below a critical value.

MO-A7-5 11h00

Studies of Banded Spherulites in Ethylene-Carbonate-Polymer Mixtures. John Lawrence Bechhoefer, B. Sadlik and L. Talon, *Simon Fraser University* — Banded spherulites appear generically when materials with viscous melts are frozen at high under-coolings. The characteristic striped pattern observed in thin samples is believed to reflect a rotation of crystalline axes that occurs as the front propagates radially away from a nucleation site. Common features include an onset of banding at finite under-cooling and a divergence of the wavelength near this critical under-cooling. Despite much speculation, there is little agreement as to the mechanisms responsible for the twist. We have studied this instability in mixtures of a low-molecular-weight material (ethylene carbonate) and a polymer (polyacrylonitrile). Varying the concentration of polymer changes the wavelength and onset temperature of the bands. An observed scaling with respect to the fluid viscosity suggests a possible hydrodynamic mechanism for the instability. As in other systems, the banded-unbanded transition is observed to be analogous to a second-order transition.

MO-A7-6 11h15

Development of a GISAXS Furnace for In-Situ Polymer Film Characterization*, Marsha Singh¹, G. Beydaghyan¹, Q. Rao (formerly of Queen's University) and D. Schneider², ¹ *Queen's University* and ² *Brookhaven National Laboratory* — A sample chamber for grazing incidence small angle x-ray scattering (GISAXS) characterization of polymer films as a function of temperature and incident angle was constructed for synchrotron measurements at the National Synchrotron Light Source (NSLS) of Brookhaven National Laboratory (NY). The design assumes a horizontal sample surface and utilizes a flat (50.8 mm) mica heater in contact with a cylindrical Cu base to achieve temperatures up to 220.0 °C with a precision of ± 0.1 °C. In addition, a transmission stage has been designed to be mounted on the same Cu base to enable complementary bulk phase measurements, where applicable. A cylindrical enclosing cap with 23 mm high Kapton windows provides nearly 360° visibility access to the sample surface for incoming and scattered x-ray beams while maintaining a low He flow through rate. Heating was controlled using a Eurotherm 818P4 controller interfaced to a PC via a LabVIEW instrumentation program. Preliminary GISAXS measurements have been obtained at beamline X12B of NSLS for diblock styrene-butadiene polymer films indicating the effect of temperature on the observ-

able microstructure. The polymer was also prepared for transmission mode measurements to allow comparison of the thermal evolution of polymer microstructure in both bulk, surface, and near surface phases.

* This work is being supported by NSERC.

MO-A7-7 11h30

Diffusion of Ultrasonic Waves in Porous Glass Bead Sinters*, John H. Page¹, J. Beck², R. Holmes³, J. Bobowski⁴, ¹ University of Manitoba, ² CancerCare Manitoba, ³ Princeton University and ⁴ University of British Columbia — Sintered networks of glass beads form an interesting example of a porous medium in which very strong multiple scattering of elastic waves is observed when the ultrasonic wavelength is comparable with the size of the pores. Because of its relatively simple structure, this material may be an ideal system for probing the diffusion of elastic waves, where diffuse waves have mixed character consisting of both longitudinal and transverse polarizations. To investigate the diffusive transport of energy by multiply scattered waves, the diffusion coefficient D , as well as the absorption time, was determined by fitting the predictions of the diffusion approximation to the time-of-flight profiles in pulse transmission experiments. The frequency dependence of the diffusion coefficient was measured over an extended range of frequencies, and compared with estimates of D from ballistic measurements of the scattering mean free path and group velocity. We find that D exhibits a plateau for frequencies above a crossover frequency determined by the condition $k\xi \sim 1$, where k is the wave vector and ξ is the structural correlation length (equal to the radius of the largest pores). Insight into this behaviour is provided by numerical simulations of phonon transport in a model three-dimensional lattice percolation system, originally performed to elucidate the low temperature thermal conductivity of glasses^[1]

1. Ping Sheng, Minyao Zhou and Zhao-Qing Zhang, *Phys. Rev. Lett.* **72**, 234 (1994).

* This work is being supported by NSERC

MO-A7-8 11h45

Resonant Tunneling of Ultrasound in Phononic Crystals*, Alexey Sukhovich¹, J.H. Page¹, A. Tourin², F. van der Biest², M. Fink², B. van Tiggelen³ and Z. Liu⁴, ¹ University of Manitoba, ² ESPCI, Paris, ³ Université J. Fourier, Grenoble and ⁴ Wuhan University, China — In the band gap of a phononic crystal, wave propagation is forbidden and wave transport takes place by tunnelling^[1]. Here we investigate the resonant tunnelling of ultrasonic waves through a pair of phononic crystals separated by a uniform medium, which acts as a resonant cavity. The transmission coefficient exhibits a narrow peak when the cavity thickness is approximately a half-integer multiple of the wavelength, an effect that is analogous to the resonant tunnelling of a particle through a double potential barrier in quantum mechanics. We also investigate the dynamics of resonant tunnelling by measuring the group velocity. At resonance, the group velocity is remarkably slow and is even predicted to decrease exponentially with the thickness of the crystals in the absence of absorption, while off resonance the velocity is ultra-fast, as is characteristic of tunneling.

1. S. Yang, J.H. Page, Z. Liu, M.L. Cowan, C.T. Chan and Ping Sheng, *Phys. Rev. Lett.* **88**, 104301 (2002).

* This work is being supported by NSERC.

MO-A7-9 12h00

Direct Vibrational Density of States Measurements in Strongly Scattering Media*, William Kurt Hildebrand, J.R. Pitcairn and J.H. Page, *University of Manitoba* — Using ultrasonic techniques, we are directly investigating the behaviour of the vibrational density of states in disordered porous media when the wavelength is of the same scale as the pore size of the sample. By observing the Fourier transform of an ultrasonic pulse transmitted through small samples, the normal modes of elastic waves in the structure can be counted, providing a direct measurement of the density of states as a function of frequency. Since the density of states is proportional to the volume of the sample, the samples must be sufficiently small to allow the individual modes to be resolved. Our samples are random sintered networks of glass beads, which are constructed in a way that corresponds to random three-dimensional percolation. These samples are relatively simple examples of porous materials that may serve as mesoscopic models of amorphous atomic materials. These experiments are providing new information on the nature of wave propagation through random media in this strong scattering regime, and may also help to elucidate two classic problems in low temperature physics: the universal plateau in the thermal conductivity of amorphous materials near 20 K and the properties of low temperature heat exchangers at 1 mK.

* This work is being supported by NSERC.

MO-A7-10 12h15

Nonlinear Dissipation In Brownian Motion*, Alexander Plyukhin, *University of Saskatchewan* — The central point of the Brownian motion theory is the assumption of wide separation of time scales for a heavy Brownian particle and light molecules of surrounding bath. A parameter which governs this separation is usually thought to be the ratio of the mass of a bath molecule to that of the particle, $\lambda = m / M$. In the ultimate limit $\lambda \ll 1$ the conventional Langevin equation with dissipative force linear in particle's momentum can be recovered from underlying equations of motion. In certain situations this approximation is not sufficient and one needs to keep terms of higher orders in λ . In this case the dissipative terms non-linear in particle's momentum appear in the Langevin equation. Using the projection-operator technique, we express the nonlinear dissipative force in terms of microscopic correlation functions. Explicit analytical expressions are found for a specific model of the particle interacting with ideal gas molecules via quadratic repulsive potential. When the particle size and the range of interaction are sufficiently large, the particle interacts simultaneously with $N \gg 1$ bath molecules. Under these circumstances the actual small parameter controlling separation of time scales is found to be $\lambda = m / M$.

* In collaboration with J. Schofield, University of Toronto.

12h30 Session Ends / Fin de la session

[MO-A8]

Advances in Instrumentation / Progrès en instrumentation

MONDAY, JUNE 14

LUNDI, 14 JUIN

(PPD-DNP
/PPD-DPN)

10h00 - 12h30

[Room/Salle : Kildonan]

Chair: F. Corriveau, McGill U.

MO-A8-1 10h00

SCOTT MICHAEL OSER, University of British Columbia

Long-Baseline Neutrino Oscillations at K2K and J-PARC

Intense neutrino beams produced by accelerators can be exploited by long-baseline oscillation experiments to measure neutrino mixing parameters. By comparing the flux and flavour content of the beam at its production site to the beam composition at a far detector located hundreds of kilometers away, transition probabilities between neutrino flavours can be measured as a function of neutrino energy, probing the oscillation pattern. The K2K experiment uses a muon neutrino beam produced at KEK, Japan and directed towards the Super-Kamiokande detector to measure neutrino masses and mixing angles associated with atmospheric neutrino oscillations. A future long-baseline experiment will direct a high-intensity beam from the J-PARC proton driver in Tokai, Japan towards Super-Kamiokande, with the goal of measuring the muon neutrino to electron neutrino conversion probability. The J-PARC neutrino project was funded in December 2003. A future phase of the J-PARC project will attempt to observe CP violation effects in neutrino oscillations by comparing the muon neutrino to electron neutrino oscillation probability with the oscillation probability for antineutrinos. CP violation by neutrinos may have produced the matter-antimatter asymmetry observed in the universe today by a leptogenesis mechanism.

MO-A8-2 10h30

PETER W. KRIEGER, University of Toronto

The ATLAS Detector at the Large Hadron Collider

The ATLAS detector is one of two general-purpose detectors that will record the products of collisions of 7 TeV beams of protons at the Large Hadron Collider at CERN, beginning in 2007. After many years of R&D and construction, the project is now at the start of the assembly phase, in which sub-detectors built at institutions all over the world are beginning to be integrated into the final detector. In particular, years of work on the Canadian-built components of the ATLAS liquid argon calorimeter are now approaching completion. This talk will review the Canadian contributions to ATLAS as well as the status of the detector integration at CERN.

11h00 Coffee Break / Pause café

MO-A8-3 11h15

DEAN KARLEN, University of Victoria / TRIUMF

The Future Linear Collider Project

A linear electron positron collider operating with a centre-of-mass energy between 500 GeV and 1 TeV would provide essential information to understand the way the symmetry between the electromagnetic and weak forces is broken and point to a more complete theory of particle physics. In the recent years, the worldwide particle physics community has come together to agree that this is the top priority for new facilities in this field. This presentation will review the physics goals, the current status, and Canada's involvement in the linear collider project.

MO-A8-4 11h45

Radiation Tolerant Microelectronics by Design, Douglas M. Gingrich and L. Chen, *University of Alberta/TRIUMF* — The radiation environment of high-energy physics experiments have recently become a major concern. Special precautions need to be taken to ensure that the front-end readout electronics will perform reliably over the lifetime of the experiment. Using advanced commercial microelectronics fabrication facilities, along with radiation tolerant circuit designs, has proven to be an effective solution to the radiation problem. Ionizing radiation causes leakage currents within and between the transistors comprising the circuits. By making a modification to the conventional transistor geometry, it is possible to eliminate these radiation-induced current leakage paths. We demonstrate the effectiveness of the radiation-tolerant by design approach. The performance of single transistors, as well as, complete application specific integrated circuits before and after being subjected to ionizing radiation will be presented.

MO-A8-5 12h00

BaF₂ Detector Development, Jérôme Gauthier et le Groupe de Recherche en Physique des Ions Lourds, *Université Laval* — In the heavy ion collisions physics domain, one of the most important points is the quality and the efficiency of the detectors used to detect and identify the reaction products. We work presently on a detector using BaF₂ scintillator for the detection and identification of the isotopes from Z=1 to 3 or more down to low energy range ($E < 5$ MeV/A). Our technique will be to use PMT fitting with the low spectral range of the fast and slow components of the crystal and by combining the pulse shape discrimination and time of flight technique. We project to upgrade our detector array with this type of detectors combined with the phoswich technique to achieve an isotopic resolution up to Z=16 for future experiments with ISAC-II exotic beams.

MO-A8-6 12h15

HERACLES Multidetector Calibration*, René Roy, Josiane Moisan and le Groupe de recherche en physique des ions lourds, *Université Laval* — HERACLES is a 4π multi detector made of 7 rings of detectors. It was used in a heavy-ion collisions experiment at Texas A&M University in 2001. The detectors are made of scintillator material, phoswich for forward rings and CsI for backward rings. Scintillators emit light when charged particles penetrate them. It is important to know the energy of a particle corresponding to a certain amount of light emitted in order to analyse the data collected in the experiment. Therefore we have to use the Parlog parameterization formula which is the best one found up to now for this kind of work.

* This work is being supported by CRSNG.

12h30 Session Ends / Fin de la session

[MO-A9] Semiconductors / Semiconducteurs

(DCMMP/DPMCM)

MONDAY, JUNE 14

LUNDI, 14 JUIN

10h00 - 12h30

[Room/Salle : Ballroom A]

Chair: M. Thewalt, SFU

MO-A9-1 10h00

Dilute Nitride Multiple-Quantum-Well Light Source for Optical Coherence Tomography*, Scott Webster¹, D.A. Beaton¹, E. Nodwell¹, T. Tiedje¹, E.C. Young¹, N.R. Zangenberg¹ and A.F. Umyskov², ¹University of British Columbia and ²Zecotek Innovations — Optical coherence tomography (OCT) is an emerging medical imaging technique that is presently limited by the lack of an inexpensive light source of suitable brightness, with a wide spectrum (>100 nm) in the near infrared (800-1500nm). We are exploring a new type of semiconductor light source, based on Ga_{1-y}In_yN_xAs_{1-x} dilute nitride multiple-quantum-well structures, that has the potential to solve this problem. Our design concept involves an optically pumped semiconductor waveguide device consisting of a series of de-coupled quantum wells of differing composition to achieve the necessary spectral range. In order to maximize the brightness, the source will be operated at low temperature (100K), in a super luminescent mode. Dilute nitride quantum wells are ideally suited to this application as a wide range of quantum well binding energies can be obtained while maintaining a lattice match with GaAs substrates. Samples containing GaInNAs quantum wells have been grown at 450C by RF plasma assisted molecular beam epitaxy with and without a Bi surfactant^[1]. The photoluminescence spectra of these samples have been measured as a function of temperature from 20-300K for both pulsed and CW excitation. In and N concentrations ranged from 3-28% and 0-1% respectively with quantum well emission wavelengths from 820 to 1160nm. Changing the temperature and pump wavelength controls the distribution of carriers in the wells and the shape of the emission spectrum. A three-quantum-well structure has been fabricated with an emission spectrum centred at 1000nm with 110nm FWHM at 100K.

1. S. Tixier *et al.*, *J Cryst Growth* **251**, 449 (2003).

* This work is being supported by NSERC.

MO-A9-2 10h15

Clustering of Ga on GaAs (100)*, Kelly A.L. Shorlin and M. Zinke-Allmang, *University of Western Ontario* — Thin film formation is an important field of study both for the fundamental physics and the technological applications. In many systems the thermodynamic equilibrium is clusters on the substrate rather than the formation of a uniform film and the study of the growth parameters is needed to determine the conditions which result in film formation. An overview of clustering of Ga on GaAs (100) is presented. A shape cycle between round and rectangular clusters is observed and the thermodynamics driving this cycle is discussed. The cluster size and spatial distributions are determined and compared to theoretical predictions.

* This work is being supported by University of Western Ontario.

MO-A9-3 10h30

Change in Photoluminescence Spectrum of Infrared Coupled Multiple Quantum Wells*. Hadi Rastegar-Moghaddam¹, Jochen Meyer¹ and Shane Johnson², ¹University of British Columbia and ²Arizona State University — Change in the photoluminescence (PL) spectrum of multiple quantum wells (MQW) under the influence of intense infrared (IR) laser was investigated. Two Al_xGa_{1-x}As/GaAs MQW samples, one symmetric and one asymmetric, were designed in such a way that their two conduction subbands would have an energy difference close to CO₂ laser that used as source of IR field. The samples were then grown by Dr. S. Johnson and his colleagues at the MBE laboratory of the Arizona State University. Using an amplified, frequency doubled Nd:YAG laser pulse, electrons were excited to the conduction band and with the help of CO₂ laser light the two conduction subbands were IR-coupled to each other. Synchronization of visible and IR laser was achieved by designing a special electronic circuit. The samples were placed at the end of cold finger of a cryostat that was kept in 77 K. Collected PL light was sent to a monochromator and the desired wavelength was guided to a photomultiplier tube (PMT). Using an integrator and computer the collected data were stored in specified files. First the symmetric sample was used and alteration of PL spectrum was investigated. For this sample because of parity, only transition from the first conduction subband (E1) to the first heavy hole valance subband (HH1) was allowed (E1-HH1 emission). To our knowledge for the first time the doublet structure in PL spectrum of QW in presence of IR fields was observed. For the asymmetric sample both e1-hh1 and e2-hh1 were allowed and in experiment both of them were analyzed. Again for the first time "emission hole" or "dark line" effects for e2-hh1 emission were observed. Also the effects of detuning, to positive and negative energy shifts and the relationship between the peak of PL spectrum and the intensity of IR laser were studied and compared to the theory.

* This work is being supported by NSERC.

MO-A9-4 10h45

Controlled Modification of Quantum Heterostructures by Ion Implantation Induced Defects*. Francois Schiettekatte¹, M. Chicoine¹, S. Chevobbe², D. Barba², V. Aimez², C. Dion³, P. Desjardins³, S. Raymond⁴, ¹Université de Montréal, ²Université de Sherbrooke, ³École Polytechnique de Montréal and ⁴Conseil National de Recherche du Canada — Defects generated by low energy ion implantation can be used to controllably blueshift the emission wavelength of InP-based heterostructures intended for optoelectronic applications. Results obtained for both quantum well and self-assembled quantum dot structures are presented and compared. The quantum well structures, grown by chemical beam epitaxy, consist of a lattice-matched 5 nm InGaAs quantum well in between 20 nm InGaAsP barriers on InP(001). P and As ions are implanted at 200 keV in the 1- μ m-thick InP cladding layer. Intermixing starts to be observed during thermal annealing at temperatures about 50°C below that for thermally induced intermixing (~700°C). The maximum blueshift (~100 nm) is obtained for ion fluences above 1×10^{14} at/cm² and implant temperature of 200°C. While intermixing only occurs at elevated temperatures, channeling measurements after implantations at 200°C indicate a long dechanneling tail, attributed to a significant in-depth diffusion of the defects during the implantation. The quantum dot structures consist of self-assembled InAs quantum dots, 3-5 nm thick and 18-42 nm in diameter, grown by metal-organic chemical vapour deposition on InP(001), capped with 200 nm InP, and implanted with 30 keV P ions. This time, a fluence of 1×10^{12} P/cm² and annealing temperatures of only 500°C are sufficient to induce a 370 nm blueshift, the quantum dots then emitting at a wavelength close to that of their wetting layer. This blue shift can namely be explained by an optimal ratio between the inter-diffusion length and the structures size, and a three-dimensional geometry for which diffusion produces more intermixing. Still, these results give an important insight into the role played by ion implantation generated defects at relatively low temperature in InP-based structures.

* This work is being supported by CRSNG & FQRNT.

11h00 Coffee Break / Pause café

MO-A9-5 11h30

Tailoring the Dimensionality of Gold Chains on Silicon. Mark Gallagher¹, Jason Crain², Jessica McChesney², Fan Zheng², Franz Himpsel², Paul Snijders³ and Steve Irwin⁴, ¹Lakehead University, ²University of Wisconsin-Madison, ³Delft University, The Netherlands and ⁴Naval Research Laboratory, Washington — For observing the exotic properties predicted for electrons in one-dimension, it is desirable to have one-dimensional solids with tunable electronic properties. We have explored gold atom chains on stepped silicon surfaces using a combination of scanning tunneling microscopy and angle-resolved photoemission^[1]. It is shown that the interchain coupling and the band filling can be adjusted systematically by varying the step spacing via the tilt angle from Si(111). Vicinal Si(111) surfaces with odd Miller indices, such as Si(335), Si(557), Si(553), Si(775), and others, form regular chain structures upon deposition of a fraction of a monolayer of gold. These chains exhibit metallic bands with nearly one-dimensional Fermi surfaces. From a tight binding fit to the data we find that band filling and inter-chain coupling can be varied from an intra-/inter-chain coupling ratio of 10:1 to >70:1. These findings suggest that self-assembled atomic chains represent a highly-flexible class of solids that approach the one-dimensional limit.

1. Crain *et al.*, *Phys Rev B* **69**, 125401 (2004).

MO-A9-6 11h45

STM of Gold Induced Chains at Stepped Silicon Surfaces. Laura Pedri, Mark Gallagher and Laura Topozini, Lakehead University — It has been predicted for some time that electrons confined to move in a single dimension will exhibit exotic behaviour. Recently, it has been demonstrated that gold induced chains on vicinal Si(111) may provide a model system with which to investigate many of these predictions^[1]. These photoemission experiments have shown that the chain structures exhibit metallic bands with highly 1-d Fermi surfaces. To complement k-space measurements, we have used scanning tunneling microscopy to investigate the real space atomic and electronic properties of several gold induced chains. Structures with different chain spacing are produced by varying the miscut angle and gold coverage. For example, the evaporation of 0.25 ML of gold onto a Si(775) surface produces chains running along the [110] direction spaced 2.13 nm apart.

1. Crain *et al.*, *Phys. Rev. Lett.*, **90**, 176805 (2003).

MO-A9-7 12h00

GISAXS Characterization of Nanostructures in Glancing Angle Deposited Films*. Gisia Beydaghyan¹, K. Robbie¹, D. Schneider² and M.A. Singh¹, ¹Queen's University and ²Brookhaven National Laboratory — The grazing incidence small angle x-ray scattering (GISAXS) technique was used to probe the nanostructure of glancing angle deposited (GLAD) silicon thin films. GLAD is a fabrication technique that combines oblique vapor incidence with dynamic control of substrate motion to make possible the design and engineering of new materials with tailored structural details at the nanometer scale. The films of interest have been characterized using scanning electron microscopy and are known to exhibit pillar-like structures. GISAXS measurements were used for determination of pillar spacing, porosity, and average thickness. Synchrotron GISAXS measurements were performed at beamline X12B of the National Synchrotron Light Source (NSLS) of Brookhaven National Laboratory. The data were corrected for background and refraction effects, and clearly show sample scattering superimposed on the so-called Yoneda peaks from the film-substrate interface. Scattering in the direction parallel to the sample surface (q_{\parallel}) indicates the presence of an interaction peak while scattering perpendicular to the sample surface (q_{\perp}) exhibits Bragg-like peaks due to density variation in the sample thickness. The GISAXS data are used to complement and extend existing information on the GLAD samples obtained from electron microscopy and ellipsometry measurements.

* This work is being supported by NSERC.

MO-A9-8 12h15

Damage in Self-Implanted Si: Channeling Compared to Nanocalorimetry. R. Karmouch, J-F. Mercure, Y. Anahory and F. Schiettekatte, *Regroupement Québécois sur les Matériaux de Pointe (RQMP)*, Département de physique, Université de Montréal — Nanocalorimetry measurement of the ion-implanted defect dynamics in polycrystalline Si is presented. 30 keV Si⁻¹⁵ keV Si⁻ and 15 keV C⁻ implantations have been performed at fluences ranging from $6 \cdot 10^{11}$ to $8 \cdot 10^{14}$ Si/cm², and the heat released as a function of temperature during scans between 30 and 450°C are presented. It is shown that the heat released has the same shape in all cases, indicating that kinetics of ion implantation defects annealing is independent of dose and implantation energy. It is also shown that the heat release starts to saturate around a fluence $1 \cdot 10^{14}$ Si/cm² while for similar fluences, the damage in mono-crystalline Si is far from being saturated, according to channeling measurements. This would imply that further lattice disorder does not occur at the expense of more stored energy. The effect of changing of the fluence rate and time evolution on the released heat is also discussed.

12h30 Session Ends / Fin de la session

[MO-A10] Particle Physics I / Physique des particules I

(DCMMP/DPMCM)

MONDAY, JUNE 14

LUNDI, 14 JUIN

10h00 - 12h30

[Room/Salle : Albert]

Chair: R. Mann, U. Waterloo

MO-A10-1 10h00

MARGARET CARRINGTON, Brandon University

Transport Theory Beyond Binary Collisions

Transport theory provides a practical method to study many-body nonequilibrium systems, both relativistically and nonrelativistically. The contribution of two-loop self-energy diagrams to the collision term in the transport equation can be understood physically in terms of binary collisions. Consequently, it's sufficient to work at 2-loop order only if it's true that dissipation processes are dominated by binary collisions. When dealing with a relativistic system at high energy and density, multi-particle interactions and production processes will be present, and thus the binary collision approximation will not be adequate. The quark-gluon plasma is a prominent example of such a system. We calculate contributions to the collision term from self-energy diagrams at three loops, and show that these contributions correspond to multi-particle collisions and production processes.

MO-A10-2 10h30

CHARLES GALE, McGill University

Electromagnetic Signals From Matter Under Extreme Conditions

Relativistic nuclear collisions offer the unique opportunity of creating and studying matter under extreme conditions of temperature and density, in the laboratory. Penetrating probes are a great asset in the interpretation of the strongly-interacting many-body states thus created. We will discuss what has been learnt through measurements of electromagnetic radiation in relativistic heavy-ion reactions. We shall also outline some of the predictions that will soon be tested at RHIC, and at other upcoming facilities.

MO-A10-3 11h00

RANDY LEWIS, University of Regina

Lattice QCD Phenomenology and its Limits

The structure and properties of hadrons can be studied computationally using lattice field theory. Comparison to nature comes after extrapolations toward the chiral limit, the continuum limit and the infinite volume limit. Lattice QCD results for specific hadron form factors will be presented, and extrapolations will be discussed in the context of effective field theory.

MO-A10-4 11h30

GUY MOORE, McGill University

Strong Bounds on Lorentz Symmetry Violation

The highest energy cosmic rays observed are hadrons, with energies in excess of 10^{11} GeV. I show how the existence of such hadrons (with the assumption that they got their energy through acceleration by ordinary electromagnetic fields) very strongly constrains Lorentz symmetry violation. The difference in maximum propagation speeds of different Standard Model particles are generally constrained to be less than about 10^{-22} . Non-renormalizable, CPT conserving (dimension 6) Lorentz violating operators are constrained to arise at a scale over an order of magnitude above the Planck scale.

* In collaboration with O. Gagnon, McGill University.

MO-A10-5 12h00

ROBERT B. MANN, University of Waterloo

Revised Radiative Electroweak Symmetry Breaking: Further Results^{1},*

In the absence of a scalar field mass term, the full set of leading logarithm terms for the (single Higgs-doublet) Standard-Model's effective potential involving the dominant three contributing standard model couplings (λ , g , α_s) has been extracted via renormalization-group methods to all orders of perturbation theory. Radiative symmetry breaking occurring within this effective potential has been shown to lead to a mass of 216 GeV for the Higgs particle. The resulting all-orders summation-of-leading-logs effective potential can be obtained analytically in the limit QCD is turned off, and is seen to require an onset of new physics at the 5 TeV scale. Incorporation of the set of additional leading logarithm contributions sensitive to the electroweak gauge coupling constants ($g_{2,g}$) is shown to elevate the predicted value for the Higgs mass to 224 GeV.

* In collaboration with V. Elias¹, D.G.C. McKeon¹ and T.G. Steele², ¹University of Western Ontario, and ²University of Saskatchewan

** This work is being supported by NSERC.

12h30 Session Ends / Fin de la session

[MO-A11] Opening Greetings for Imaging Session / Accueil pour la session sur l'imagerie

(All orgs.)

MONDAY, JUNE 14

LUNDI, 14 JUIN

10h20-10h30

[Room/Salle : Ballrooms B/C]

Chair: J. English, U. Manitoba

[MO-A12] Scientific Images in the Public Sphere / Les images scientifiques dans la sphère publique

(DCMMP/DPMCM)

MONDAY, JUNE 14

LUNDI, 14 JUIN

10h30 - 12h30

[Room/Salle : Ballrooms B/C]

Chair: M. Campbell, U. Waterloo

MO-A12-1 10h30

F. PETER OTTENSMEYER, University of Toronto

Images of the Invisibly Small: from Atoms to Biomacromolecular Structure and Function

In the last four decades developments in instrumentation in electron microscopy, in techniques and in specimen preparation have made it possible to image proteins such as the insulin receptor, nucleic acids, peptides such as vasopressin, and even individual atoms such as palladium, iodine and sulphur. While some of the images of these small things are spectacular, and even beautiful, it is another challenge to derive the 3D structure of biomacromolecules and their complexes from such 2D representations of reality. Over the years a number of image processing approaches for 3D reconstruction were developed, and are still being improved, for structures with high internal symmetry, or lateral 2D symmetry, or one or a few highly preferred orientations, or for structures that were completely randomly oriented when imaged. In some instances the images were sufficient to derive atomic coordinates, such as for bacteriorhodopsin; but such resolution detail has not been achieved in general. Nevertheless, even at lower resolution, the structures derived serve as crucially important 3D templates of the complexes into which to fit smaller component domains for which the structures have been solved by x-ray crystallography or NMR. While such a construct is still a static entity, for some the structure itself has led to an understanding of their function, and of the chemistry and the mechanics by which that function is carried out. From initial microscopy to the final 3D mechanism, this process of discovery is driven by images, and so is accessible and understandable in principle by all.

MO-A12-2 11h00

AUSTIN ROORDA, University of Houston College of Optometry

From Telescopes to Ophthalmoscopes: Adaptive Optics for Microscopic Imaging of the Living Eye

Adaptive optics (AO) describes a set of techniques to measure and compensate for optical aberrations that cause blur in images. AO was invented to remove the blur in astronomical images from ground based telescopes caused by phase distortions caused by turbulence in the earth's atmosphere. In the last decade, the same techniques have been applied in ophthalmoscopes to correct for optical aberrations of the human eye. Using AO, microscopic features, such as single cone photoreceptors and dynamic blood flow in the smallest capillaries, are revealed in the eye. The most important aspect of AO imaging is that it offers noninvasive imaging for living, functioning eyes, which facilitates efforts to relate structure to function. Applications range from the study of basic visual processes to the identification of phenotypes for specific genotypes of blinding eye diseases. In this talk, will describe the techniques, discuss the applications and, of course, display the images.

MO-A12-3 11h30

CAROL CHRISTIAN, Space Telescope Science Institute

Public Impact of Scientific Images: Examples from Space Science

Public interest in scientific findings can be greatly enhanced through the use of imagery augmented with suitable background materials. As an example, Space Scientists (astronomers, solar system experts, etc.) have learned that persistent dissemination of new results, showcased through imagery, can have a positive effect on the support of their discipline by federal agencies. Today, the physical sciences must compete with healthcare, security, and social science issues to obtain suitable funding. The use of imagery is one powerful tool that can be used to raise public awareness, improve public perception of science and thereby garner fiscal stability for basic research.

MO-A12-4 12h00

MICHAEL BRONSKILL, Sunnybrook and Women's College Health Sciences Centre, University of Toronto

Imaging Physics Meets Public Perception: Is Private MRI Bad?

The clinical applications of NMR in the form of magnetic resonance imaging (MRI) have now matured over twenty years. Their impact and significance have already been recognized with two Nobel Prizes in Medicine. Originally implemented to provide detailed anatomical images of soft tissues, clinical MRI is now developing capabilities for obtaining much more sophisticated information about the human body by measuring physiological functions and by providing guidance and monitoring of interventions and therapies. These capabilities will be illustrated briefly with some examples of MR angiography, functional MRI of the brain, and monitoring of temperature during experimental thermal therapy. Despite these remarkable capabilities, MRI remains a curiously restricted resource in the Canadian health care system. The history and logic behind this fairly rigid control of MRI systems will be examined, using the situation in Ontario as the prime example. At a time when public expectations of high technology medical imaging are fueled by instant Internet knowledge, does this pattern of restriction make sense? Is there economic evidence that MRI is too expensive for mainstream Canadian medical practice? In particular, the media representation of "private" MRI as a potential violation of the universality of Canadian health care became a political issue in the recent Ontario provincial election. This concept will be explored in an attempt to determine whether private MRI really is bad.

12h30 Session Ends / Fin de la session

[MO-A13]

**CASCA JCMT User's Meeting /
Réunion des utilisateurs du TJCM de la CASCA**

(CASCA)

MONDAY, JUNE 14

LUNDI, 14 JUIN

12h30 - 13h20

[Room/Salle : Campaign B]

Chair: L. Knee, NRC

[MO-A14]

Past Presidents' Lunch / Déjeuner des anciens présidents

(CAPI/ACP)

MONDAY, JUNE 14

LUNDI, 14 JUIN

12h30 - 13h30

[Room/Salle : Heartland Boardroom]

Chair: W.J. McDonald, U.Alberta

[MO-P1]

Herschel Space Observatory Information Session / Session d'information sur l'observatoire spatial Herschel

(CASCA)

MONDAY, JUNE 14

LUNDI, 14 JUIN

13h25 - 14h15

[Room/Salle : Campaign B]

Chair: M. Fich, U.Waterloo

[MO-P2]

CAP-CRM Medal Winner / Récipiendaire de la médaille ACP-CRM(CAP-CRM/
ACP-CRM)

MONDAY, JUNE 14

LUNDI, 14 JUIN

13h30 - 14h15

[Room/Salle : Ballroom A]

Chair: W.J. McDonald, U.Alberta

MO-P2-1 13h30

JIRI PATERA, Université de Montréal

Deterministic Aperiodic Multidimensional Point Sets, Their Properties And Exploitation

Invented originally as models of quasicrystals, such point sets have been studied in recent years. They closely resemble lattices in spite of a complete lack of periodicity; they contain no periodic subsets. Their applications are so far few even if wide ranging. Some of them will be described in the talk.

14h15 Session Ends / Fin de la session

[MO-P3]

CAP-INO Medal Winner / Récipiendaire de la médaille ACP-INO

(CAP-INO/ACP-INO)

MONDAY, JUNE 14

LUNDI, 14 JUIN

13h30 - 14h15

[Room/Salle : Victoria]

Chair: P. Galameau, INO

MO-P3-1 13h30

NICOLAS JAEGER, University of British Columbia

Optical Sensors for Power Utility Applications

It is clear that optical sensors and sensor systems will increasingly find applications in power transmission systems due to the numerous advantages that they can offer over conventional systems. These advantages typically include small size, light weight, high accuracy, low cost, immunity to electromagnetic interference, and compatibility with the digital substation of the future. Additionally, optical instrument transformers can offer much wider bandwidths, are lighter and therefore easier to install, and are more environmentally friendly than conventional instrument transformers. Fiber-optics-based sensors, a subset of optical sensors, typically provide the most reduction in size, complexity, and cost as well as increased performance as compared to bulk-optic devices. As optical sensors are gaining ground in revenue metering, equipment monitoring, protection, and control applications, their compactness is allowing designers to combine multiple sensors into a single unit reducing per unit and installation costs while occupying less real estate in the substation. For example, designers have been able to combine voltage and current instrument transformers in a single unit and incorporate either or both in other substation equipment such as power circuit breakers. It is increasingly apparent that, due to their improved performance and other advantages, optical sensor systems will play a large role in the power utility industry of the future.

14h15 Session Ends / Fin de la session

[MO-P4]

Demonstration of Karma Visualization Software / Démonstration du logiciel de visualisation Karma

(CASCA)

MONDAY, JUNE 14

LUNDI, 14 JUIN

13h30 - 14h00

[Room/Salle : Strathcona]

Chair: J. English, U.Manitoba

[MO-P5]

High School Teachers' Workshop / Atelier pour les enseignant(e)s de la physique

(CAP/ACP)

(see page 18 for details / voir page 18 pour le programme)

MONDAY, JUNE 14

LUNDI, 14 JUIN

13h35 - 15h30

[Room/Salle : Colbourne]

Chair: P. Mitchler, Manitoba

[MO-P6]

Scientific Imaging in the Public Sphere / L'imagerie scientifique dans la sphère publique

(All Orgs)

MONDAY, JUNE 14

LUNDI, 14 JUIN

14h15 -14h45

[Rooms/Salles : Ballrooms B/C]

Chair: J. English, U.Manitoba

MO-P6-1 14h15

PETER CALAMAI, The Toronto Star

Don't Overlook Images Created with Words

Many newsworthy developments in different fields of physics don't readily lend themselves to an illustration easily understood by the general public. In some instances the use of an illustration can actually be misleading. It's a safe bet that the planetoid Sedna doesn't actually look much like the artist's drawings widely used with the discovery announcement. Nor did Beagle 2 actually float unharmed to the surface of Mars, the image that most people still have in their minds. Some images can also be little more than pretty wallpaper, conveying no information by themselves, i.e. people don't know what they are seeing until they are told in a caption or even in a separate article. Astronomical images often fall in this category. For these reasons it's important to remember that the words in a media account can also be used to convey powerful images to the public. For mass market, daily newspapers in Canada, I estimate that is the case in at least two-thirds of published accounts about developments in physics. My remarks will offer guidelines for deciding when word images are more appropriate (than picture images) and techniques for researchers to help journalists paint physics in words

14h45 Session Ends / Fin de la session

[MO-P7]

The Precision Frontier in Particle Physics / *La frontière de la précision en physique des particules*

(All Orgs)

MONDAY, JUNE 14

LUNDI, 14 JUIN

14h15 -18h00

[Room/Salle : Ballroom A]

Chair: D. Karlen, U. Victoria

MO-P7-1 14h15

J. MICHAEL RONEY, University of Victoria

Recent Results from the BaBar Experiment

The Babar experiment has accumulated ~200/fb of e+e- collision data at or near the $\Upsilon(4S)$ resonance on SLAC's PEP-II storage rings. PEP-II continues to reliably deliver increasing levels of luminosity in excess of twice the design. The currently analyzed data provides samples of $O(10^6)$ BB and $\tau^+\tau^-$ events. We will report on recent results from BaBar including measurements of the CP asymmetries and the $|V_{ub}|$ CKM matrix element as well as results of searches for rare and standard model-forbidden decays of the B-meson and τ -lepton.

MO-P7-2 14h45

JOSEPH LLOYD MILDENBERGER, TRIUMF

Latest Results from the Search for $K^+ \rightarrow \pi^+ \nu \bar{\nu}$

Brookhaven experiment E949 continues the search for the rare decay $K^+ \rightarrow \pi^+ \nu \bar{\nu}$, predicted by the Standard Model to occur at a branching ratio of $(0.77 \pm 0.11) \times 10^{-10}$. This talk describes the latest results from data taken in 2002 and provides an updated branching ratio in combination with previously reported data from E787.

MO-P7-3 15h15

Measurement of the $B \rightarrow \pi / \pi^0 / \eta / \eta' \nu \bar{\nu}$ Branching Ratios Using Semileptonic Tags in the BaBar Experiment. Sylvie Brunet, Université de Montréal — The branching ratio measurement of the rare semileptonic decays $b \rightarrow u l \nu$ can lead to a more precise extraction of $|V_{ub}|$, one of the less known elements of the CKM matrix. This analysis uses a new and clever way of measuring these channels by using **semileptonic tags**. That technique leads to a much cleaner sample than the traditional neutrino reconstruction method at, however, a cost in statistics that can be compensated by the high luminosity provided by PEP-II at the Stanford Linear Accelerator Center. At the $\Upsilon(4S)$ used in BaBar, B mesons are always produced in pair. The semileptonic tag technique consists in reconstructing (tagging) one of the Bs in one of its more abundant semileptonic $b \rightarrow c$ decays ($D/D^* l \nu$) and to look for the wanted signal ($\pi / \pi^0 / \eta / \eta' \nu \bar{\nu}$) in the remaining B. This leads to an efficient rejection of non-B backgrounds ($C\bar{C} \tau^+ \tau^-$, ...) as well as most B backgrounds since no charged track or neutral energy should remain in the event after the tag side and the signal side selections. This technique is particularly interesting for the $\pi^0 l \nu$ channel since charged B mesons are easier to tag than the neutral ones. This presentation will give an overview of the analysis as well as the results that can be achieved at the BaBar experiment concerning these three semileptonic $b \rightarrow u l \nu$ channels

MO-P7-4 15h30

Determination of $|V_{ub}|$ from the Measurement of $B \rightarrow \pi^+ \pi^0 / \eta / \eta' / \rho^+ / \rho^0 l \nu$ Branching Fractions and Form Factors at BaBar. David Côté¹, S. Brunet¹, J.C. Dingfelder², M. Simard¹, B.F. Viaud¹ and P. Taras¹, ¹ Université de Montréal and ² (SLAC) — BaBar's Runs 1-4 data sample will contain approximately 480 million B decays and several tens of thousands of each of the lower mass exclusive $B \rightarrow Xu l \nu$ decays. The combination of this unprecedented large data set with an improved version of the "neutrino reconstruction" technique will allow a measurement of the $B \rightarrow \pi^+ \pi^0 / \eta / \eta' / \rho^+ / \rho^0 l \nu$ branching fractions and form factors in a model independent way. This is achieved by maximizing the signal extraction efficiency at the cost of accepting more of the well-understood $B \rightarrow Xc l \nu$ and continuum backgrounds. The cross-feeds arising from the various $Xu l \nu$ decays will be taken into account by a simultaneous fit of all the lower mass exclusive $B \rightarrow Xu l \nu$ branching fractions and form factors. These will provide valuable information about QCD and semileptonic $b \rightarrow u l \nu$ decays. By excluding or validating specific form factor models, the theoretical uncertainty in determining $|V_{ub}|$ from exclusive $B \rightarrow Xu l \nu$ decays will be greatly reduced and should be competitive with the most precise measurements to date. This would be specially true in the framework of improvements in unquenched lattice QCD. We will present an overview of this complex but very promising analysis that is well underway as well as some preliminary results.

MO-P7-5 15h45

A Search for $B^+ \rightarrow K^+ \nu \bar{\nu}$. P.D. Jackson, University of Victoria — We present results of search for the rare B decays mode $B^+ \rightarrow K^+ \nu \bar{\nu}$ with the BaBar detector at the SLAC B factory. This is a theoretically clean flavour changing neutral current decay which proceeds in the Standard Model through loop and box diagrams and which is potentially sensitive to contributions from heavy virtual particles internal to these loops. In this analysis we search for a high momentum signal track and significant missing energy recoiling against \bar{B} charged B which is exclusively reconstructed either hadronically or semileptonically. A 90% confidence limit is quoted based on analyses of a sample of approximately $90 \times 10^6 \Upsilon(4S) \rightarrow B\bar{B}$ decays.

MO-P7-6 16h00

A Search for Lepton-Flavor Violation at BaBar. Chris Brown, University of Victoria, BaBar Collaboration — A search for lepton-flavor violation has been performed in the tau decay modes $\tau \rightarrow \mu \gamma$ and $\tau \rightarrow l l l$ by the BaBar collaboration. The observed rates in all decay modes are consistent with background expectations. Upper limits at 90% confidence level on the allowed branching fractions are found to be $Br(\tau \rightarrow \mu \gamma) = 2.0 \times 10^{-6}$ and range from $(1 - 3) \times 10^{-7}$ for the six different τ to $l l l$ final states.

MO-P7-7 16h15

Determination of $|V_{ub}|$ in the BaBar Experiment using the Lepton Invariant Mass Squared. D. Fortin, University of Victoria — A measurement of the CKM matrix element $|V_{ub}|$ is performed using charmless semileptonic B decays from a sample of 88 million $B\bar{B}$ events recorded with the BaBar detector. Decays are primarily identified by the presence of a high momentum electron and a neutrino inferred from the missing momentum. Further selection requirements are made on the electron energy and the invariant mass squared of the neutrino-electron pair to suppress the dominant background from semileptonic B decays to charm. Signal efficiency and background estimates derived from Monte Carlo simulations are adjusted using a control sample in the data and then used to measure a partial branching fraction for $B \rightarrow X_u e \nu$. Combining this measurement with the B lifetime and using theoretical input allows for the determination of the CKM matrix element $|V_{ub}|$.

MO-P7-8 16h30

Search for the Rare Decay $B^0 \rightarrow J/\psi \gamma$. Sheila McLachlin, McGill University, (On behalf of the BaBar Group) — With the advent of the B-factories at SLAC and KEK, it is now possible to investigate some very rare processes to probe Physics beyond the Standard Model. I will present the results of a search for the rare decay $B^0 \rightarrow J/\psi \gamma$ conducted at the BaBar experiment. The data set used an integrated luminosity of $125 fb^{-1}$. Current theoretical estimates, using leading order Feynman annihilation diagrams suggest a branching ratio of the order of 10^{-8} . The possibility of intrinsic charm in the B^0 meson will, of course, modify these estimates.

* This work is being supported by NSERC.

MO-P7-9 16h45

A High Precision Measurement of Muon Decay Parameters. Maher Quraan, for the TWIST collaboration, TRIUMF — The TRIUMF Weak Interaction Symmetry Test (TWIST) is an experiment designed to perform a high precision simultaneous measurement of the muon decay parameters ρ , δ , and $P_{\mu} \xi$. The ultimate goal of the experiment is to measure these parameters to a precision of few parts in 10^4 , thereby decreasing their uncertainty by almost an order of magnitude over current values. At this level TWIST is sensitive to

physics beyond the standard model, and can impose limits on the validity of several proposed extensions to the standard model. The TWIST spectrometer consists of 56 low mass planar wire chambers positioned inside a 2 T magnetic field. A highly polarized muon beam is stopped in a thin foil at the center of the spectrometer, allowing a measurement of the energy and emission angle of the decay positrons over a wide range. Since the high rate at which data can be acquired allows the collection of 10^9 events in a few weeks, the precision is limited by systematic uncertainties rather than the statistical accuracy of the measurement. To date, TWIST has acquired several high statistics data sets aimed at tackling the various systematics to an accuracy of 10^{-3} . The availability of Western Canada Research Grid (Westgrid) in the past few months has allowed the analysis of almost all data sets acquired in 2002 and 2003, as well as the generation of Monte Carlo runs with statistics adequate for determining systematic effects at the same level. In this talk the TWIST experiment will be described, and the techniques used to tackle the various systematics will be presented.

MO-P7-10 17h00

Data Analysis Techniques for High Precision Measurement of Muon Decay Parameters. Konstantin Olchanski, TRIUMF — The TRIUMF Weak Interaction Symmetry Test (TWIST) is investigating the space-time structure of the charged-current weak interaction. We look for deviations from the predictions of the "V-A" submodel of the Standard Model in the dominant decay mode of the muon, the purely leptonic decay $\mu^+ \rightarrow e^+ \nu_e$. By improving the world-best measurements of the muon decay by a factor of 10, we hope to open (or close) the window on physics possibilities beyond the Standard Model. TWIST is a systematics-dominated experiment. We have developed techniques for using special data runs and special simulations to measure the impact of systematic effects on the overall error, rank the effects by importance, and to eliminate some effects as sources of systematic error. TWIST uses a system of very low mass planar wire chambers. Still, multiple Coulomb scattering and energy loss effects are significant and require careful handling. We have adopted the kink method (G. Lutz, etc) for handling multiple scattering and perform a self-consistent positron energy scale calibration to handle energy loss. In any high-precision experiment, it's important to minimize the potential for subjective bias, typically through blind analysis techniques. TWIST has developed a novel procedure utilizing public-key cryptography to extract the muon decay parameters in a blind manner. This talk will describe the data analysis procedures used by TWIST.

MO-P7-11 17h15

Future High Luminosity Scenarios for the BABAR Experiment. S.H. Robertson, IPP, McGill University — Over the last several years the BABAR experiment at SLAC has succeeded in demonstrating that the Standard Model (SM) mechanism for CP violation, described by a single irreducible phase in the CKM matrix, is essentially correct. This is, however, not the end of the story as there may be additional "New Physics" contributions which could appear in precision CP-asymmetry or branching ratio measurements. Even if evidence for New Physics is discovered first at a high energy hadron collider, the comparatively clean environment and variety of accessible final states suggest that precision B physics measurements performed at the $\Upsilon(4S)$ resonance can play an important role in clarifying the nature of the underlying physics. However, such studies will require data samples 1 - 2 orders of magnitude greater than those currently available. Some possible scenarios for a high luminosity "Super B factory" will be presented.

MO-P7-12 17h30

Parity-Violating Hard Photon Bremsstrahlung In Electron-Proton Scattering. Aleksandrs Aleksejevs¹, Svetlana Barkanova² and Peter Blunden^{1,1} University of Manitoba and² Acadia University — One way to treat the infrared divergences of the electroweak radiative corrections to parity-violating (PV) electron-proton scattering is by adding PV soft-photon emission graphs. Although reasonable, the results are left with a logarithmic dependence on the photon detector acceptance, which can only be eliminated by considering PV hard photon bremsstrahlung (HPB) graphs. We have computed PV HPB differential cross sections for electron-proton scattering using the experimental values of form factors in the diagram vertices. The final results are conveniently expressed through kinematical parameters, making it possible to apply the computed HPB asymmetries for a virtually any PV electron-nucleon scattering process.

MO-P7-13 17h45

Measurement of Azimuthal Asymmetries Associated With Deeply Virtual Compton Scattering. Jiansen Lu, HERMES Collaboration/TRIUMF — Asymmetries in beam helicity and beam charge have been measured for hard exclusive electroproduction of photons scattering off a nucleon/nucleus target. The asymmetries appear in the distribution of the photons in the azimuthal angle around the virtual photon direction, relative to the lepton scattering plane. The asymmetries result from interference of Bethe-Heitler process and the deeply virtual Compton scattering process, which depend on the Generalized Parton Distribution s (GPDs) of nucleon/nucleus. GPDs contain information on two-parton correlations, quark transverse momentum distributions and orbital angular momentum distributions. The experiment is performed at DESY laboratory, Germany, using 27.5 GeV positron/electron incident nucleus target.

18h00 Session Ends / Fin de la session

[MO-P8]

Symmetries in Nuclear Physics / Les symétries en physique nucléaire

(DNP/DPN)

MONDAY, JUNE 14

LUNDI, 14 JUIN

14h15 -17h00

[Room/Salle : Victoria]

Chair: W. van Oers, U.Manitoba

MO-P8-1 14h15

WALTER OELERT, Forschungszentrum Juelich

Observation of Cold Antihydrogen - Perspectives for Testing Fundamental Symmetries

The ATRAP experiment at the CERN antiproton decelerator AD aims for a test of the CPT invariance by a comparison of the hydrogen to anti-hydrogen atom spectroscopy. To achieve the required high precision in the measurements of atomic transitions cold atoms of anti-hydrogen are essential. Trapped neutral anti-hydrogen atoms, up to now not available, have to be used. The anti-hydrogen production via 3-body recombination routinely operated at ATRAP^[1,2] is studied in more detail in order to characterize this production mechanism in view of future trapping of neutral anti-hydrogen atoms. Shape parameters of the antiproton and positron clouds and the anti-hydrogen production probability as a function of relevant parameters have been measured. The N-state distribution of the produced Rydberg anti-hydrogen was analyzed and first measurements of the anti-hydrogen velocity have been performed. Furthermore an alternative production mechanism via double charge exchange has been studied^[3]. The results achieved in 2003 and further steps towards the trapping of anti-hydrogen atoms will be discussed.

1. G. Gabrielse et al., *Phys. Rev. Lett.* **89**, 213401 (2002).
2. G. Gabrielse et al., *Phys. Rev. Lett.* **89**, 233401 (2002).
3. E.A. Hessels et al., *Phys. Rev. A* **57**, 1668 (1998).

MO-P8-2 14h45

GERALD GWINNER, University of Manitoba

A New Test of the Special Theory of Relativity with the Heidelberg Test Storage Ring

An improved test of time dilation in special relativity has been performed using laser spectroscopy on fast ions at the heavy-ion storage-ring TSR in Heidelberg. The Doppler-shifted frequencies of a two-level transition in ${}^7\text{Li}^+$ ions at $v = 0.064c$ have been measured in forward and backward direction to an accuracy of $\Delta v/v = 1 \cdot 10^{-9}$ using collinear saturation spectroscopy. The result confirms the relativistic Doppler formula and sets a new limit of $2.2 \cdot 10^{-7}$ for deviations from the time dilation factor γ_{SR} , a tenfold improvement over other methods. Currently, work is in progress to improve this limit further.

15h15 Coffee Break / Pause café

MO-P8-3 15h45

ANDREW D. BACHER,* Indiana University and IUCF

Observation of Charge Symmetry Breaking in the Reaction $d-d \rightarrow {}^4\text{He}-\pi^0$

Charge symmetry breaking (CSB) in the strong interaction arises from the difference in the masses of the up and down quarks ($m_d > m_u$) and from electromagnetic interactions. These effects cause the neutron to be heavier than the proton and nuclear mass differences within isospin multiplets. Other independent experiments in light systems are needed to separate the hadronic and electromagnetic terms in the effective chiral Lagrangian. The long-sought $d-d \rightarrow {}^4\text{He}-\pi^0$ reaction is forbidden by charge symmetry; its observation would be a measurement of the square of a CSB matrix element with a different combination of hadronic and electromagnetic terms. Our group at the Indiana University Cyclotron Facility recently made the first unambiguous observations of the $d-d \rightarrow {}^4\text{He}-\pi^0$ reaction at two energies just above the π^0 production threshold (225.5 MeV) using the IUCF electron-cooled storage ring. The forward-going cone of ${}^4\text{He}$ nuclei was separated from the circulating deuteron beam in a 6° bending magnet and captured and identified in a magnetic channel consisting of a septum magnet followed by three magnetic quadrupoles. The two photons from π^0 decay were observed in two arrays of Pb-glass Čerenkov detectors that surrounded the cold D_2 gas jet target. While the cross section was very low (~ 10 pb), a three-fold coincidence removed essentially all background. Separation of the CSB ${}^4\text{He}-\pi^0$ events from the allowed continuum of double radiative capture ${}^4\text{He}-\pi^0$ events depended on a reconstruction of the pion mass from channel position and time of flight. The results show a π^0 production cross section that is small but rising with energy in a manner consistent with s-wave production.

* For the Cooler-CSB Collaboration

MO-P8-4 16h15

MICHAEL D. HASINOFF, University of British Columbia

A Test of Time Reversal Invariance in Stopped Kaon Decay

The transverse muon polarization (P_T) in K^+ decay is an excellent CP- or T-violating observable to study since any non-zero value $> 10^{-5}$ would imply new physics beyond the minimal standard model. Furthermore, since P_T involves phases between both the quark-quark and lepton-lepton couplings it probes a different region of parameter space than the neutron dipole moment or K^0 decay experiments. We have measured the T-violating triple product correlation between the μ^+ spin and the π^0 and μ^+ momenta in stopped K^+ decays at the 12 GeV PS at the National Laboratory for High Energy Physics in Tsukuba, Japan. An analysis of our complete data set (11.8 million good K^+ decays) indicates no evidence for any T-violation ($P_T < 0.0051$ at the 90% confidence level). The details of our experiment and the various systematic errors will be presented along with our new constraints on extensions to the standard model.

MO-P8-5 16h45

Beta-Decay of Ultracold Neutrons*, Jeffery William Martin, *California Institute of Technology* for the UCNA Collaboration — Recent advances in the production of ultracold neutrons (UCN) have made possible a new generation of precision measurements of the fundamental properties of the neutron. A new experiment (called UCNA) is in the process of completing construction and commissioning at the Los Alamos Neutron Science Center, located in Los Alamos, New Mexico. The aim of the experiment is to measure the "beta-asymmetry", the asymmetry in the emission of decay electrons relative to the neutron spin, to the level 0.2%. Such a precise measurement, when combined with previous measurements of the neutron's mean lifetime, can be used to determine the Cabibbo-Kobayashi-Maskawa (CKM) matrix parameter V_{ud} . This parameter governs weak transitions between down and up quarks. Combining this measurement with extractions of V_{us} (the same quantity for weak transitions between strange and up quarks) from kaon decay allows a precise test of the unitarity of the CKM matrix. Current extractions of this sort show that the matrix might not be unitary, and may be an indication for new physics beyond the standard model. The current status of the UCNA experiment, along with plans for future experiments, will be presented.

* In collaboration with the UCNA.

17h00 Session Ends / Fin de la session

[MO-P9]

Instrumentation and Techniques in Biomedical Physics I / *Instrumentation et techniques en physique biomédicale I*

(DIMP-DMBP/
DPIM-DPMB)

MONDAY, JUNE 14

LUNDI, 14 JUIN

14h15 -17h00

[Room/Salle : Albert]

Chair: A. Mandelis, U.Toronto

MO-P9-1 14h15

CLAUDE BOCCARA, École Supérieure de physique et chimie industrielles, Paris, France

Optical Imaging in Turbid Media: New Developments

The use of light to generate an imaging process able to reveal in-depth structures and to quantify them in terms of geometrical (size, position) and optical (absorption, scattering) properties is a new goal for a larger and larger community of physicists. We will recall the main approaches which have been used to overcome the strong loss of the photons directional memory in highly scattering media and their limitations in terms of depth and resolution: Optical coherence tomography or microscopy which selects ballistic photons through an interferometric detection but can be perturbed by multiscattered ones. Time and frequency methods for detecting the first photons emerging from the structure by using fast detectors or optical gates. DC or quasi DC approaches in which the source-detector symmetry plays an important role in revealing local changes in optical properties. Opto-acoustics (often called Photoacoustics) where a locally absorbed laser pulse generates an acoustic signal whose position and depth can be localized by an array of piezo-electric detectors. Acousto-Optics where a localized ultrasonic field modulates the speckle distribution, coupling light and sound in a very different way than the preceding technique. We will particularly describe in more detail the techniques used in our laboratory which take advantage of multiple detectors such as CCD sensors working in parallel for faster acquisition times or better signal-to-noise ratios.

MO-P9-2 14h45

ANDREAS MANDELIS, University of Toronto

*Laser Photo-Thermo-Acoustic Frequency Swept Heterodyne Lock-in Depth Profilmetry for Three-Dimensional Sub-surface Tissue Imaging**

In conventional biomedical photoacoustic imaging systems, a pulsed laser is used to generate time-of-flight acoustic information of the subsurface features. This paper reports the theoretical and experimental development of a new frequency-domain (FD) photo-thermo-acoustic (PTA) principle featuring frequency sweep (chirp) and heterodyne modulation and lock-in detection of a continuous-wave laser source at 1064 nm wavelength. PTA imaging is a promising new technique, which is being developed to detect tumor masses in turbid biological tissue. Owing to the linear relationship between the depth of acoustic signal generation and the delay time of signal arrival to the transducer, information specific to a particular depth can be associated with a particular frequency in the chirp signal. Scanning laser modulation with a linear frequency sweep method preserves the depth-to-delay time linearity and recovers FD-PTA signals from a range of depths. Preliminary results performed on rubber samples and solid tissue phantoms indicate that the FD-PTA technique has the potential to be a reliable tool for biomedical depth-profilometric imaging.

* In collaboration with Ying Fan, Gloria Spirou and Alex Vitkin

15h15 Coffee Break / Pause café

MO-P9-3 15h45

Conduction Velocity Dispersion in Cardiac Tissue*. Hana Dobrovolny¹, R.A. Oliver², S. Kalb², E. Tolkacheva¹, W. Krassowska² and D.J. Gauthier^{1, 1} *Department of Physics and* ²*Department of Biomedical Engineering, Duke University* — Conduction velocity dispersion and action potential restitution play a crucial role in determining the stability of waves of electrical activity through cardiac tissue. Recent experimental work has confirmed that action potential restitution is rate-dependent, that is, the restitution properties are dependent on the specific pacing protocol used to measure them. We hypothesize that conduction velocity dispersion shows similar rate-dependence. We will discuss progress on our experiments to determine the rate dependence of conduction velocity restitution.

* This work is being supported by NIH, NSF

MO-P9-4 16h00

Magnetocarcinotherapy: A Novel Method for the Detection and Treatment of Cancer using Magnetic Nanoparticles*. Carl Kumaradas¹ and Robert Kraus Jr.^{2, 1} *Ryerson University and* ²*Los Alamos National Laboratory* — Magnetocarcinotherapy (MCT) is a new and innovative approach that combines the detection and treatment of cancer into a single modality. This approach involves binding magnetized nanoparticles (SmCo₅, Fe₃O₄) to monoclonal antibodies and other molecules that selectively target cancer cells. These nanoparticles are systemically delivered into a patient through intravenous injection and will preferentially collect in tumours due to their binding to receptors uniquely expressed by cancer cells. Focal concentrations of these particles in tissue will be detected and imaged using a Superconducting Quantum Interference Device (SQUID) array or Magnetic Resonance Imaging (MRI) systems. Once detected, the tumours will be immediately destroyed by applying a rotating external magnetic field that causes the nanoparticles to rotate resulting in thermal energy deposition localized at the tumor site (primarily as a consequence of viscous heating). A 2D finite element model of the coil system for generating the driving magnetic field was developed to predict the field pattern produced in a patient. A 3D finite difference model of the motion of the particles in the presence of the rotating external field, including the effect of particle-particle magnetic interactions, was developed to predict the heat deposition rate in tissue as a result of the particle motion. Finally, a 1D finite element model was developed to predict the thermal damage produced in the tumour and its surrounding tissue. Predictions of the ability of optimized MCT system to target the treatment to a tumour while minimizing the dose to normal tissue will be presented.

* This work is being supported by Los Alamos National Laboratory.

MO-P9-5 16h15

Polarimetry in Turbid Media for Robust Determination of Concentration of Optically Active Molecules: Modelling, Experiments, and Application to Biophotonics*. Daniel Côté and I.A. Vitkin, *Ontario Cancer Institute and University of Toronto* — Various non invasive optical methods have been proposed to monitor glucose concentration in biological tissue. Polarimetry is particularly attractive among these because certain measurable polarization properties (e.g., optical rotation) are directly related to the glucose concentration. However, in turbid materials such as biological tissue, the range of validity of this direct relationship, and the effective path length sampled by the optical beam, are unknown. We have developed a polarization-sensitive Monte Carlo statistical simulation model to examine in detail the polarization effects in turbid tissue-like media containing glucose. Specifically, we examine the effects of incident polarization states, source/sample/detection geometries, and scattering properties of the media on the polarization properties of detected light. Our simulation results, corroborated by experiments, show that there is a glucose-unrelated optical rotation of the linear polarization in geometries other than the forward-scattering geometry. We also present a method to determine the path length from the directly measurable linear polarization fraction, and show both theoretically and experimentally that the optical rotation is not proportional to the path length in highly scattering situations. Such fundamental studies are necessary if turbid polarimetry is to be developed into a quantifiable *in vivo* tool for glucose level determination in humans.

* Financial support from NSERC is gratefully acknowledged.

MO-P9-6 16h30

***In Vivo* Cadmium Measurement by Prompt Gamma Neutron Activation Analysis**. Joanna Grinyer, Soo-Hyun Byun and David R. Chettle, *McMaster University* — The monitoring of cadmium levels in occupationally exposed persons is important, as this element is known to cause several health effects. Cadmium is known to accumulate in the kidneys and the liver so a non-invasive technique of detection is required in order to monitor accumulated levels. An *in vivo* prompt gamma neutron activation analysis previously developed at McMaster University was tested and used in the measurement of cadmium in kidney and liver phantoms. The measurement of cadmium is based on the detection of 559 keV g-rays from the ¹¹³Cd(n,g)¹¹⁴Cd reaction *in vivo*. In order to lower the detection limit, a comparison was made between the use of two large surface area planar germanium detectors (51 mm diameter × 21 mm length) and a single coaxial germanium detector (47 mm diameter × 42 mm length). The positioning of the neutron source, phantoms and detectors was optimized to lower the detection limit further. Calibrations were performed using aqueous kidney and liver phantoms of known concentrations in order to determine the amounts of cadmium present in the liver and kidneys of an occupationally exposed individual.

MO-P9-7 16h45

Optical Analysis of Carotid Atherosclerotic Plaque using Laser Induced Fluorescence. Renee Korol^{1,2}, Alexandra Lucas^{2,3}, Gary Ferguson^{2,4}, Rob Hammond⁵, Helen Finlay¹ and Peter Canham^{1, 1} *Department of Medical Biophysics, University of Western Ontario, 2 Vascular Biology Research Group, Roberts Research Institute, 3 Department of Microbiology and Immunology, University of Western Ontario, 4 Department of Clinical Neurological Sciences, University of Western Ontario and 5 Department of Pathology, University of Western Ontario* — Background: Laser induced fluorescence (LIF) spectroscopy is a nondestructive optical diagnostic technique. Arterial bifurcations are associated with increased incidence of later atherosclerotic plaque growth and cerebral aneurysm formation, two vascular pathologies that initiate arterial occlusions and rupture (myocardial infarctions and strokes); Purpose: Our objective is to investigate regional compositional differences of atherosclerotic plaques from patients undergoing a carotid endarterectomy; Materials and methods: Arterial wall was cut open longitudinally along the 'saddle' region of the bifurcation and pinned to a mounting card. Using an optical multi-channel analyzer, we recorded 10 fluorescence spectra for each position during excitation of the arterial surface with an argon ion laser (351.1-363.8nm). Measurements included extracted protein (elastin, collagen type I & III), 10 normal arteries taken from coronary bypass surgery and 16 carotid endarterectomy specimens. Spectra were normalized to maximum intensity. Statistical analysis included ANOVA and multi-regression analysis. Tissue sections were fixed in formalin, sectioned and stained with Hematoxylin & Eosin, and Movat's Pentachrome for histological analysis; Results: Atherosclerotic plaque measurements were cross-examined with conventional histologic techniques and morphometric analysis, which allows characterization of different plaque constituents: fibrous tissue, elastin, foam cells/cholesterol crystals, calcifications and thrombus/hemorrhage. Formulae for quantification of compositional changes have been developed based upon results of fluorescence emission spectra using multiple regression analysis; Conclusions: Laser induced fluorescence spectroscopy provides an effective method for detecting regional differences in vascular structure as it pertains to late atherosclerotic plaques and their bifurcations. It has the potential for discriminating between stable and unstable plaque *in vivo*.

17h00 Session Ends / Fin de la session

[MO-P10] Quantum Information Theory / Théorie de l'information quantique

(DTP/DPT)

MONDAY, JUNE 14

LUNDI, 14 JUIN

14h15 -17h00

[Room/Salle : Kildonan]

Chair: R. Mann, U.Waterloo

MO-P10-1 14h15

RAYMOND LAFLAMME, Institute for Quantum Computing, University of Waterloo

NMR And Quantum Information Processing

Advances in computing are revolutionizing our world. Present day computers advance at a rapid pace toward the barrier defined by the laws of quantum physics. The quantum computation program short-circuits that constraint by exploiting the quantum laws to advantage rather than regarding them as obstacles. Quantum computer accepts any superposition of its inputs as an input, and processes the components simultaneously, performing a sophisticated interference experiment of classical inputs. This "quantum parallelism"

allows one to explore exponentially many trial solutions with relatively modest means, and to select the correct one. This has a particularly dramatic effect on factoring of large integers, which is at the core of the present day encryption strategies (public key) used in diplomatic communication, and (increasingly) in business. As demonstrated approximately five years ago, quantum computers could yield the most commonly used encryption protocol obsolete. Since then, it was also realized that quantum computation can lead to breakthroughs elsewhere, including simulations of quantum systems, implementation of novel encryption strategies (quantum cryptography), as well as more mundane applications such as sorting. I will describe recent work done in quantum computation, in particular I will give a critical review of the NMR implementation, its achievements and future prospect.

MO-P10-2 14h45

BARRY C. SANDERS, University of Calgary

Quantum Information Processing with Continuous Variables

Quantum information theory is built on creating, manipulating and reading qubits yet some of the dramatic experimental successes, such as unconditional quantum teleportation, quantum cryptography with coherent states, and threshold quantum secret sharing, have been achieved for continuous variables. I will explain continuous variable quantum information processing, discuss its realizations as quantum optics experiments, expose the weaknesses, extol the strengths, and consider its future. The field of continuous variable quantum information processing is exciting on several levels. The mathematics is elegant, and the quantum optics experiments can be understood in terms of Hamiltonians that obey the symplectic algebra. The experiments make use of sophisticated, yet well-developed, technology such as the ability to squeeze the vacuum fluctuations of light, perform balanced homodyne detection, and prepare highly coherent states of light. Decoherence is often negligible in these settings. These advantages make continuous variable quantum information processing the best avenue for first proofs-of-concept. The field faces formidable challenges, including encoding quantum information into continuous variables allowing for robust error correction, achieving nonlinear transformations outside the symplectic transformations that allow universal unitary transformations of the field without significant decoherence, and security proofs for quantum cryptography. These challenges are not insurmountable; rather they add to the excitement of the field, which I will discuss.

15h15 Coffee Break / Pause café

MO-P10-3 15h30

RANDY KOBES, University of Winnipeg

Exploring Paths in Adiabatic Quantum Computing

Many systems, such as quantum computers, can be formulated in terms of networks of a large number of coupled two-level quantum systems. Due to the complex interactions, however, it is difficult to infer general properties about the evolution of the system. In such cases it is often useful to consider the behaviour of the system when a degree of randomness is introduced in the interactions, the hope being that, when averaged over large classes of randomness, some qualitative information about the evolution of the system can be deduced. Here we describe one such study, with particular emphasis on seeing the difference between short and long range interactions.

MO-P10-4 16h00

PHILIP STAMP, University of British Columbia

Decoherence Mechanisms And The Dynamics Of Decoherence In Qubit Networks

The major problem confronting the construction of quantum information processing networks of any kind is decoherence, caused either by the interactions of the network with the surrounding environment, or from the time-dependent changes in the network parameters as computations or processing are carried out. To quantify decoherence we need (i) realistic physical models of what causes it, and (ii) means of calculating network dynamics. The main decoherence in solid-state qubit networks at low T comes from localized excitations in the environment (the 'spin bath'). How this works is discussed quantitatively for superconducting and magnetic qubit networks, and compared with experiment. In optical systems the decoherence comes from unwanted photon modes. The problem of network dynamics raises a second fundamental question- how do decoherence rates increase with the number of entangled qubits? This question can be answered in detail with models incorporating spin and oscillator baths acting on 'quantum memory' networks. If there is time I will also discuss decoherence for topological quantum computer designs.

MO-P10-5 16h30

ACHIM KEMPF, University of Waterloo

Towards a Notion of Qubit Density for Quantum Fields in Curved Spacetime

In the literature, there is much discussion as to whether spacetime is discrete or continuous. In information theory, the link between continuous information and discrete information is established through well-known sampling theorems. Sampling theory explains, for example, how frequency-bounded music signals are reconstructible perfectly from discrete samples. I will present a generalization of sampling theory to pseudo-Riemannian manifolds. The aim is to provide a new set of mathematical tools for the study of spacetime at the Planck scale: theories formulated on a differentiable space-time manifold can be completely equivalent to lattice theories. There is a close connection to generalized uncertainty relations which have appeared in string theory and other studies of quantum gravity.

17h00 Session Ends / Fin de la session

[MO-P11] Cuprates in the Extreme Underdoped Limit / *Les cuprates dans la limite extrême sous-dopée*

(DCMMPIDPMCIM)

MONDAY, JUNE 14

LUNDI, 14 JUIN

14h15 -17h00

[Room/Salle : Campaign B]

Chair: I. Herbut, SFU

MO-P11-1 14h30

DOUGLAS BONN, Simon Fraser University

Dying Gasps of a d-Wave Superconductor

In the cuprate superconductor $\text{YBa}_2\text{Cu}_3\text{O}_{6+x}$, hole doping in the CuO_2 layers is controlled by both oxygen content and the degree of oxygen-ordering. At the composition $\text{YBa}_2\text{Cu}_3\text{O}_{6.35}$, the ordering can occur at room temperature, thereby tuning the hole doping so that the superconducting critical temperature gradually rises from zero to 20 K. Here we exploit this to study the electromagnetic penetration depth as a function of temperature and doping. The temperature dependence shows the d-wave superconductor surviving to very low doping, with no sign of another ordered phase interfering with the nodal quasiparticles. The only apparent doping dependence is a smooth decline of superfluid density as T_c decreases.

15h00 Coffee Break / Pause café

MO-P11-2 15h30

MARCEL FRANZ, University of British Columbia

Nodal Protectorate in Underdoped Cuprates

Amidst the complexity characterizing the behavior of the high temperature cuprate superconductors several features have recently emerged that appear universal (or nearly so) across all families of materials. One such feature is the d-wave symmetry of the superconducting order parameter and the associated "nodal protectorate" of coherent low-energy quasiparticle excitations that appear to persist down to strongly underdoped and perhaps even non-superconducting regions of the phase diagram. In this talk I will outline some general ramifications of this physical picture and discuss constraints that it imposes on the candidate microscopic theories of cuprate superconductors.

MO-P11-3 16h00

MICHAEL L. SUTHERLAND, University of Toronto

Nodal Metallic Phase in Underdoped Cuprates

Electrons in cuprates adopt a remarkable sequence of ground states as one varies the density of charge carriers. At zero hole density, the material is a Mott insulator with static long-range antiferromagnetic order. At high density, it is a normal metal with the basic signatures of a Fermi liquid. At intermediate density, it is a superconductor with d-wave symmetry. A central outstanding question is: what is the nature of the underdoped phase that lies between the insulator and the superconductor? Recent measurements of low temperature thermal transport offer new insight into this question. We track the evolution of the residual electronic contribution to the thermal conductivity, κ_0/T , across the cuprate phase diagram. In the extreme underdoped limit, we observe delocalized fermionic excitations at zero energy in the non-superconducting state of strongly underdoped $\text{YBa}_2\text{Cu}_3\text{O}_y$. This reveals that the ground state of clean underdoped cuprates is metallic, and we argue that this metallic phase has a nodal spectrum akin to the superconductor and is therefore distinct from the metallic phase in the overdoped regime. This contrasts with the insulating ground state observed in underdoped $\text{La}_{2-x}\text{Sr}_x\text{CuO}_4$, likely caused by the spin-density-wave order present in that system.

MO-P11-4 16h30

WILLIAM J.L. BUYERS, National Research Council

Spins and Paired Carriers in a Superconductor that is Nearly an Antiferromagnet - Who Pushes Whom?

Near the onset of superconductivity, where there is competition with the nearby antiferromagnetic phase, we find that the spin resonance in YBCO_{6+x} , for $x = 6.35$ ($T_c = 19$ K) is at low energy, is intense and is overdamped. Its relaxation rate slows to ~ 3 meV below T_c , an order of magnitude lower than the resonance energy in $x = 6.50$ ($T_c = 59$ K). It appears that this spectral feature will turn into the spin wave of the antiferromagnetic insulator once it is no longer held up by interaction with the gapped quasiparticles. At a further order of magnitude lower in energy we find a hitherto unobserved non-divergent central peak. Although we expect it to be related to the AF Bragg peak of the undoped insulator, there is no long-range order since the spins at all energies are spatially confined to a region with a correlation range of 2 nm or about 5 cells. Despite the low $\sim 6\%$ doping of holes the superconducting order causes a gradual freezing of the spins, but without a sudden onset at T_c . The results demonstrate the strong interaction between spins and carriers, and suggest that they spontaneously reassemble to cause spin confinement.

1. C. Stock, W.J.L. Buyers, *et al.*, *Phys. Rev. B* 69, 014502 (2004)

17h00 Session Ends / Fin de la session

[MO-P12]

Panel on Scientific Images in the Public Sphere / Discussion sur les images scientifique dans la sphère publique

(All Orgs)

MONDAY, JUNE 14

LUNDI, 14 JUIN

14h45 -15h45

[Rooms/Salles : Ballrooms B/C]

Chair: J. English, U.Manitoba

[MO-P13]

Genetic Networks / Réseaux génétiques

(DMBP-DCMMP/
DPMB-DPMC)

MONDAY, JUNE 14

LUNDI, 14 JUIN

15h30 -18h00

[Room/Salle : Victoria]

Chair: P. Higgs, McMaster U.

MO-P13-1 15h30

PETER SWAIN, McGill University

Stochastic Gene Expression In Single Cells

Generation of variability in populations of cells, all of which have the same genome, is essential for many biological processes. Such heterogeneity is conjectured to arise from stochasticity, or noise, in gene expression. We show theoretically that noise can be decomposed into an intrinsic piece, particular to a given gene, and an extrinsic term, common to all genes in a cell, but variable from one cell to another. Using specially constructed strains of *Escherichia coli*, we are able to discriminate between, and measure, both types of noise. We demonstrate that intrinsic noise indeed exists *in vivo* and accounts for a substantial portion of cell-cell variation. An analytical description of gene expression is also presented, which contains all the major biochemical steps in transcription and translation. As transcription rate is varied, this model confirms experimental findings that the amplitudes of both noise components vary over a wide range. These results reveal how low intracellular copy numbers can fundamentally limit the precision of gene expression.

MO-P13-2 16h00

MADS KAERN, Boston University

Gene Regulatory Systems: Roles Of Physics In Post-Genomic Biology

Advances in high throughput methods have enabled the identification of the majority of genes and of the interactions between their products in a number of model organisms. The next level in genomics and proteomics will be to use this qualitative information to gain quantitative insight into the function and characteristics of cell regulatory systems. In this talk, I will show how techniques and concepts from physics and mathematics can be combined with biological knowledge to provide quantitative understanding of control mechanisms at two distinct levels of organization: the formation of spatial patterns in developing embryos and in the regulation of cell-cell variability arising from the inherent stochastic nature of gene expression. I will also discuss ongoing efforts to explore the consequences and potential benefits of gene expression noise in cellular regulation.

MO-P13-3 16h30

VINCENT NOIREAUX, The Rockefeller University

From In Vitro Genetic Circuits To An Artificial Cell

A cell-free expression extract has been used to assemble genetic circuits *in vitro*. The extract, which does not contain endogenous DNA and RNA, is used as a source of energy to carry out transcription and translation of plasmid genes. Expression stops after 6 hours due to energy consumption, the maximum protein production is two micromolar. In a

ten microliters reaction volume, we engineered transcriptional activation and repression cascades, in which the protein product of each stage is the input required to drive or block the following stage. Substantial time delays and dramatic decreases in output production are incurred with each additional stage, due to a bottleneck at the translation machinery. Faster turnover of messengers RNA can relieve competition between genes and stabilize output against variations in input and parameters. To bring the system at the scale of the cell, the cytoplasmic extract has been encapsulated in phospholipids vesicles from one to a few tens of micrometers diameter. Accumulation of the GFP reporter protein shows that the expression is confined into the vesicles. A membrane pore has been expressed inside the vesicle to permeabilize the bilayer and allow a subsequent feeding of the vesicles with nutrients. With a continuous bioreactor, one can then develop functions to build a minimal cell.

MO-P13-4 17h00

TIM WESTWOOD, University of Toronto

Using DNA Microarrays for Functional Genomic Studies

The sequencing of an organism's genome is only the first step in the functional analysis of the genetic information it contains. Technological advances have allowed genome-wide analysis of such phenomena as: gene function, gene transcription and detection of genetic abnormalities and pathological states. One of the most powerful and exciting of these advances is DNA array based parallel genome analysis. This technique involves the immobilization of specific DNAs corresponding to hundreds or thousands of gene sequences onto glass in a small area to produce a "micro array". Typically, RNA (or DNA) is isolated from control and experimental cells and detectable cDNAs are made from it using fluorescent nucleotides. The cDNAs are then hybridized to the array, and the amount of hybridization quantified and compared between the different conditions. Both the publication of complete annotated genome sequences and the availability of Expressed Sequence Tag cDNA collections have made the construction of "whole genome" microarrays possible for a number of model organisms (e.g. yeast, worms, fruit flies (*Drosophila*), and humans). The Canadian *Drosophila* Microarray Centre provides DNA microarrays, experiment and analysis services for academic researchers and our current microarray represents about 85% of the estimated 14,000 genes in *Drosophila*. The talk will briefly outline how these arrays are constructed and provide a few examples on how they can be used in functional genomic studies including ascribing functions to previously unknown genes.

MO-P13-5 17h30

Paul Higgs, McMaster University

Bacterial Phylogenetics and Horizontal Gene Transfer

We have developed RNA-specific phylogenetic methods that take account of the conserved secondary structure of RNA sequences during construction of evolutionary trees. Our method uses Monte Carlo simulations to generate a representative sample of evolutionary trees (analogous to an equilibrium ensemble in physics). The current picture of bacterial evolution is based largely on studies of ribosomal RNA. However, this is just one gene. It is known that horizontal gene transfer can occur between bacterial species, although the frequency and implications of this are not fully understood. If horizontal transfer were frequent, there would be no single evolutionary tree for bacteria because each gene would follow a different tree. We studied ribosomal and transfer RNA genes from Proteobacteria - a diverse group for which many complete genome sequences are available. We compared trees for 16S rRNA and 23S rRNA with those derived from concatenated alignments of many tRNA genes. The tRNA genes are scattered throughout the genomes, and would not follow the same evolutionary history if horizontal transfer were frequent. Nevertheless, the tRNA tree is consistent with the rRNA tree in most respects. Minor differences can almost all be attributed to uncertainty or unreliability of the phylogenetic method. We therefore conclude that tRNA genes give a coherent picture of the phylogeny of the organisms, and that horizontal transfer of tRNAs is too rare to obscure the signal of the organismal tree. Some tRNA genes are not present in all species. We discuss possible explanations for the observed patterns of presence and absence of genes: these involve gene deletion, gene duplication, and mutations in the tRNA anticodons.

* In collaboration with Bin Tang and Philippe Boisvert, McMaster University

18h00 Session Ends / Fin de la session

[MO-P14]

(CAP/ACP)

NSERC Information Session for Existing Grant Holders / Session
d'information du CRSNG pour les détenteurs actuels de bourses
(See page 20 for details / Voir page 20 pour description)

MONDAY, JUNE 14

LUNDI, 14 JUIN

16h00 - 17h00

[Room/Salle : Strathcona]

Chair: M. Morrow, MUN

[MO-P15]

(All Orgs)

Scientific Imaging and Visualization - contributed / Imagerie et
visualisation scientifiques - contribuées

MONDAY, JUNE 14

LUNDI, 14 JUIN

16h15 - 17h30

[Rooms/Salles : Ballrooms B/C]

Chair: M. Bronskill, U.Toronto

MO-P15-1 16h15

The Square Kilometre Array, Gilles Joncas, Université Laval — Advances in observation and theory have brought the current generation of astronomers to the brink of understanding the origin and evolution of the Universe. The next major step, to explore the earliest epochs of the evolution of the Universe before and during the dawn of first light, and to trace the subsequent formation and evolution of primordial galaxies, will require a giant telescope operating at radio wavelengths. Scientists and engineers from thirty-four institutes in fifteen countries have joined together to design and construct a radio telescope having a total collecting area of one million square meters. Technological advances make it possible to build such a telescope – the Square Kilometre Array (SKA) – in the next decade, at a cost of about 1 billion dollars. Canada has played a leading role in the SKA initiative since its inception, and Canadian technological innovation has generated one of the leading concepts for the SKA technology, the Large Adaptive Reflector. A consortium of universities, in partnership with the National Research Council and Industry, is developing this technology with plans to build a demonstrator telescope, the Canadian Large Adaptive Reflector (CLAR). Until the completion of the SKA, the CLAR will be the largest telescope in the world. Its unique capabilities will allow Canadian scientists to lead the world in key areas of high sensitivity astrophysics, for example measuring the equation of state of the Universe, charting the large scale structure of the Universe and the Cosmic Web, and mapping the pulsar population in the Milky Way.

MO-P15-2 16h30

Evolution Meets Astrophysics: Using Advanced Genetic Algorithms to Search and Visualize Large Parameter Spaces*. Jason Fiege, NRC Herzberg Institute of Astrophysics — Astrophysical data modeling often requires large-scale multi-dimensional parameter searches to find classes of models that best represent heterogeneous, and often noisy, data sets. I introduce an extremely general computational technique based on an advanced multi-objective genetic algorithm that is well suited for difficult parameter exploration and optimization problems that are often encountered in the physical sciences. I present results from two different astrophysical research problems. The first application is a genetic algorithm-based modeling system for polarization data, which forms the core component of an automated theoretical data-modeling pipeline that I am building for archival JCMT SCUBA data and future SCUBA-2 molecular cloud polarization surveys. I conclude with a discussion of new models of the internal structure of the Jovian moon Europa, where I have coupled my multi-objective genetic algorithm to a planetary structure code to find the class of all models that agrees with data obtained by the Galileo orbiter. I show that most models are consistent with deep oceans of liquid saltwater encrusted by a rather thin surface ice layer.

* This work is being supported by NRC/HIA.

MO-P15-3 16h45

Energy Dispersive X-Ray Diffraction Measurements Using a Cadmium Zinc Telluride Detector*. M.M Boileau and R.J. Leclair, Laurentian University — An energy dispersive x-ray diffraction technique is used to measure the total differential scattering cross section m_s [$\text{m}^{-1}\text{sr}^{-1}$] of a small 100 μL H_2O sample using a cadmium zinc telluride detector of

dimensions 3 mm x 3 mm x 2 mm. Our semianalytic x-ray diffraction model reveals that μ_s can be extracted as follows: the scatter data is normalized by the incident spectrum and corrections for attenuation are applied. Verification of the technique is performed using water since its diffraction signal is well known. A 70 kV beam with 1.35 mm Al filtration was used. In the measured spectrum we observe distortions that are mainly caused by hole trapping. In the energy range 25 to 40 keV, however, the response of the detector is good. For the scatter measurements, a 1 mm diameter pencil beam is incident on a 5 mm thick sample of H₂O. We chose to extract μ_s with an average resolution of 0.14 nm⁻¹ in the momentum transfer argument, $x=\lambda^{-1}\sin(\theta/2)$. The measurement times were 21 minutes and the average entrance exposure at the target was 420 R. The scatter signal at $\theta=6.2^\circ$ and in the range $1.1 \text{ nm}^{-1} < x < 1.7 \text{ nm}^{-1}$ yielded a $\chi^2=2.35$ while scatter at 9.3° in the range $1.6 \text{ nm}^{-1} < x < 2.6 \text{ nm}^{-1}$ gave $\chi^2=1.73$. A 28 minute measurement at 9.3° with a 3 mm thick sample gave a similar signal with $\chi^2=2.48$. We will use this technique for the characterization of breast tissue.

* This work is being supported by NSERC.

MO-P15-4 17h00

Application of X-ray Backscatter Imaging to Explosive Device Detection. Anthony A. Faust, *Defence R&D Canada* — Defence R&D Canada (DRDC) has an active research and development program on detection of explosive devices using nuclear methods. One system under development is a coded aperture-based X-ray backscatter imaging detector designed to provide sufficient speed, contrast and spatial resolution to detect antipersonnel landmines and improvised explosive devices (IED). Coded aperture imaging has been used by the observational gamma astronomy community for a number of years. However, it has been advances in the field of medical nuclear imaging and X-ray detector construction that have made a coded aperture hand-held imaging system only a recent possibility. While the final objective is to field a hand-held detector, the scope of this research effort is currently constrained to a design that can be fielded on a small robotic platform. The successful development of a hand-held imaging detector requires, among other things, a light-weight, ruggedized detector with low power requirements, supplying high spatial resolution. The University of California, San Diego (UCSD) designed HEXIS detector provides a modern, large area, high-temperature CZT imaging surface, robustly packaged in a lightweight housing with sound mechanical properties. Based on the potential for the HEXIS detector to be incorporated as the detection element of a hand-held imaging detector, the author initiated a collaborative effort with the UCSD to demonstrate the capability of a coded aperture-based X-ray backscatter imaging detector. This presentation will discuss the landmine and IED detection problem and review the coded aperture technique. Results from initial proof-of-principle experiments will then be reported.

MO-P15-5 17h15

The Digital Radiographic And Computed Tomography Imaging Of Two Types Of Explosive Devices. Eduardo Galiano, *Laurentian University* — Since the terrorist attacks on the World Trade Center on 9/11/01, governments and the general public have focused significant attention on the issue of airport security [1]. Two well established medical imaging methods, digital radiography (DR), and computed tomography (CT) were employed to obtain images of two types of explosive devices- miniature rocket engines and shotgun shells [2]. The images were evaluated from an airport security perspective where one challenge is that of detecting explosive devices clandestinely introduced inside checked baggage [3]. In terms of geometrical shape, the detection probability of the explosive devices appears to be higher with DR imaging, but in terms of the actual explosive compounds in the devices, CT appears to offer a higher detection probability. DR imaging offers a low detection probability for the explosive powder in the shotgun shells, but a rather significant detection probability for the explosive propellant in the rocket engines.

1. Croft, J. "Baggage deadline to refocus standards", *Aviation Week & Space Technology*, 01/17/02 pp 51-52, (2002).

2. Stine, G.H., "Model rocket motors", in *The handbook of model rocketry 6th Ed.*, John Wiley & Sons, New York, pp 68-69, (1994).

3. Williams, G., "A substantial number of inspectors will have to be trained worldwide to ensure that safety oversight obligations are met", *ICAO Journal* 55, 8, pp 14-18, (2000).

17h30 Session Ends / Fin de la session

[MO-P16]

**Improving the Climate for Women in Physics /
Amélioration du climat pour les femmes en physique**

(CAPI/ACP)

MONDAY, JUNE 14

LUNDI, 14 JUIN

17h00 - 19h00

[Room/Salle : Colbourne]

Chair: B. Frisken, SFU

MO-P16-1 17h00

BARBARA L. WHITTEN, Colorado College

What Works for Women in Undergraduate Physics?

The participation of women in physics has increased in recent years, but the percentage of women in undergraduate physics is still less than half that in mathematics and chemistry. This is due in large part to the "leaky pipeline"—women become more scarce in physics with every step up the academic ladder. The largest decrease occurs between high school physics and college graduation, so it is worthwhile to look at how undergraduate physics departments try to make women comfortable. With a team of women physicists, I visited nine undergraduate physics departments in the US. We compared those that are successful in producing a large percentage of women majors (about 40%) with those that are more typical of the national average (about 20%). We found that the most important factor is a warm and female-friendly department culture that reaches out to introductory students. I'll discuss the factors that make up a female-friendly culture, and describe other results of our research.

18h00 Discussion

19h00 Session Ends / Fin de la session

[MO-STUD]

Best Student Paper Competition / Concours de la meilleure communication étudiante

(CAPI/ACP)

MONDAY, JUNE 14

LUNDI, 14 JUIN

17h00 - 19h00

[Room/Salle : Albert]

Chair: M. Morrow, MUN

[MO-PiC]

**Physics in Canada Editorial Board Meeting /
Réunion du Comité de rédaction de La physique au Canada**

(CAPI/ACP)

MONDAY, JUNE 14

LUNDI, 14 JUIN

17h30 - 19h00

[Room/Salle : Westminster]

Chair: J.S.C. McKee, U.Manitoba

[MO-P17]

NSERC GSC-017: Possible Change to Funding Envelope in Astronomy / CRSNG GSC-017 : Modification possible du financement d'enveloppe pour l'astronomie

(CASCA)

MONDAY, JUNE 14

LUNDI, 14 JUIN

17h30 - 18h15

[Room/Salle : Campaign B]

Chair: G. Harris, U.Waterloo

[MO-CJP] CJP Editorial Board Meeting / Réunion du Comité de rédaction de la
(CJP/IRCP) RCP

MONDAY, JUNE 14
LUNDI, 14 JUIN
18h00 - 20h30

[Room/Salle : Heartland Boardroom / Private Dining Room]

Chair: G.W.F. Drake, U.Windsor

[MO-POS] Poster Session, with Beer / Session d'affiches, bière servie
(All Orgs)

MONDAY, JUNE 14
LUNDI, 14 JUIN
19h00 - 21h00

[Room/Salle : Winnipeg Convention Centre]

Chair: n/a

Tuesday, June 15

Mardi, 15 juin

[TU-A1] Meeting of the Canadian National IUPAP Liaison Committee /
(CNILC/CLNC) Réunion du comité de liaison national canadien (IUPAP)

TUESDAY, JUNE 15
MARDI, 15 JUIN
07h00 - 09h00

[Room/Salle : Private Dining Room]

Chair: G.W.F. Drake, U.Windsor

[TU-A2] Plenary Session / Session plénière

TUESDAY, JUNE 15
MARDI, 15 JUIN
08h30 - 09h15

[Room/Salle : Ballroom B]

Chair: M. Paranjape, U.Montreal

TU-A2-1 08h30

NIMA ARKANI-HAMED, Harvard University

The Crises of Frontier Physics: From the Hubble Length to the Planck Length

Our description of the basic interactions in nature, based on the standard model of particle physics and general relativity, is in spectacular agreement with all known experiments. However, it is almost certainly fundamentally incomplete. At very short distances, violent quantum-mechanical fluctuations imply a breakdown in our notion of space-time. Meanwhile, two striking clues from Nature suggest that we are missing important new physical principles: the extreme weakness of gravity relative to the other forces, as well as the extraordinary flatness of our observable universe, appear to require absurdly finely adjusted choices for various parameters of the theory. In this talk I will review attempts at addressing these mysteries, and discuss the ways in which these ideas will be tested experimentally in the coming decade.

09h15 Session Ends / Fin de la session

[TU-A3] Young Investigators in Medical and Biological Physics; Part I /
(COMP-DMBP/ OCPM-DPMB) Jeunes chercheurs(es) en physique médicale et biologique I

TUESDAY, JUNE 15
MARDI, 15 JUIN
08h30 - 10h00

[Room/Salle : Albert]

Chair: L.J. Schreiner, Queen's U.

TU-A3-1 08h30

3-D Verification of IMRT Treatments using a Flat-Panel EPID*. Brad Warkentin^{1,2}, S. Steciw¹, S. Rathee^{1,2}, B.G. Fallone^{1,2,1} Cross Cancer Institute and ² University of Alberta — A 3-D IMRT verification procedure based on use of the Varian aS500 EPID to measure incident fluence profiles is described. Fluences are extracted from raw EPID images by applying a deconvolution method employing kernels used to describe the dose-deposition and scattering properties determining the EPID's dose-response. Good agreement has been shown between profiles measured with the EPID and in-air measurements made with a diamond detector. In our 3-D technique, EPID images of the MLC step-and-shoot delivery and the corresponding "open-field" are acquired for each IMRT field. The measured fluence modulations are imported into our commercial treatment planning system (TPS), which is then used to calculate a 3-D dose distribution. The verification consists of comparing this "measured" dose distribution, based on EPID-measured fluences, to the original "calculated" dose distribution, based on fluences modeled by the TPS. The advantage of this 3-D technique is that dosimetric errors can be quantified and displayed with respect to the 3-D patient anatomy, in contrast to conventional 2-D verification techniques where 2-D dose errors at a single depth in a homogeneous phantom are calculated. The 3-D technique also allows estimation of cumulative uncertainties arising from all fields comprising an IMRT treatment. A preliminary 3-D verification showed a negligible difference between "measured" and "calculated" mean doses in the tumor volume, but "measured" doses that were up to 5 Gy larger in certain critical structures. Such information, unavailable with 2-D techniques, suggests that 3-D verification may provide useful additional insight into the clinical significance of IMRT delivery uncertainties.

* This work is being supported by ACB and AHFMR.

TU-A3-2 08h45

Benchmarking A Multi-Leaf Collimator Particle Transport Algorithm For IMRT Field Verification*. Gavin Cranmer-Sargison, I.A. Popescu, W.A. Beckham, S. Zavgorodni, University of Victoria — As intensity modulated radiation therapy techniques have become clinically viable the need for accurate dose calculations has never been so great. With the recent increase in computing power many investigators have worked to develop accurate Monte Carlo (MC) methods for modelling IMRT treatment plans. The goal of this project was to implement and benchmark one such Monte Carlo multi-leaf collimator (MLC) particle transport algorithm. Benchmark data included both static and dynamic MLC sequences and culminated with dose calculations being performed for individual IMRT patient fields. Modelled dose distributions were compared with film measurements and analysed using an in-house software package. The results showed that for various fields the MC calculated dose distributions were within 2% of the film data and revealed details unresolved by a commercial treatment planning system.

* This work is being supported by NSERC.

TU-A3-3 09h00

Dose Tracking for Adaptive Radiation Therapy. Bryan Schaly¹, Jerry J. Battista² and Jake Van Dyk^{3,1} *London Regional Cancer Centre,² London Health Sciences Centre and³ University of Western Ontario* — The goal of this work is to provide a method of tracking the dose distribution throughout a course of radiation treatment, by accounting for the patient setup uncertainty and ongoing changes in anatomy. We have developed a 3D "dose-warping" algorithm based on a deformable model (thin-plate spline) along with a conventional treatment planning system for dose calculations. In this work, we determine the magnitude of dose differences from the planned dose distribution for three setup scenarios for prostate cancer treatment using a six-field 18 MV conformal technique: (1) Alignment of the treatment beams to external markers in the patient CT scans thus representing a treatment without image guidance, (2) daily alignment to the bony anatomy to minimize setup error (*i.e.*, portal imaging) and (3) daily alignment to the prostate to minimize inter-fraction tumour motion (*i.e.*, ultrasound or CT image guidance). Our results show that the dose delivery to the prostate improves with daily geometric treatment adjustments; the largest negative dose difference in the prostate improves by ~5%. Also, the largest positive dose difference in the rectum improves by ~25% (to less than 10%) when aligning the treatment beams to the prostate. However, normal tissue sparing may not improve in some critical organs depending on the required shift of the treatment beams. Our methodology shows quantitatively the improvements of daily realignment of the treatments to the prostate target, combined with reduction of margins and/or treatment modification. This research enables the development of guidelines for the implementation of high-precision adaptive radiation treatments.

TU-A3-4 09h15

Limitations of a Convolution Method for Modeling Geometric Uncertainties in Radiotherapy: the Biologic Dose-Per-Fraction Effect. William Song, Jerry Battista and Jake Van Dyk, *London Regional Cancer Centre, and the University of Western Ontario* — Convolution method can be used to model the effect of random geometric uncertainties on planned dose distributions. This is effectively done by linearly adding infinitesimally small doses over an infinite number of fractions. This process inherently ignores radiobiological dose-per-fraction effects since only the final total dose distribution is generated. The error on predicted biological outcome (*i.e.* Tumor Control Probability (TCP) and Equivalent Uniform Dose (EUD)) resulting from this assumption has not been quantified. In this work, a Monte Carlo direct simulation method is compared to Convolution predictions using random geometric uncertainties of 0, 1, 2, 3, 4 and 5mm (SD) on a four-field prostate treatment plan. a/b ratios of 0.8, 1.5, 3, 5 and 10Gy are used for biological normalization. For treatment fraction number ≥ 15 or 20 (depending on margin size and uncertainty), the average difference in TCP and EUD calculated from Convolution and Monte Carlo methods diminished to less than 0.5% and 0.2Gy, respectively. However, for fraction numbers ≤ 15 or 20, the difference in TCP and EUD quickly rose with a maximum difference observed to be 17.8% and 9.3Gy, respectively, for one fraction. In this clinical example, for all fraction numbers considered (1 – 50), TCP and EUD calculated with Convolution overestimated those calculated by Monte Carlo simulation. In the range of fraction numbers normally used clinically (≥ 20), Convolution method can safely be used to estimate effects of geometric uncertainties on biological outcomes. For low fraction numbers (≤ 20), careful validation is necessary prior to clinical application.

TU-A3-5 09h30

On the Use of Plane Parallel Chambers for the Verification of Dose in Small Radiation Fields. Andrea McNiven^{1,2}, Matt Mulligan¹, and Tomas Kron^{1,2}, *London Regional Cancer and the University of Western Ontario* — Modern radiotherapy is characterised by the use of many small radiation fields which, when combined, allow great flexibility in shaping dose distributions. It is common practice to verify the dose delivered in these fields prior to irradiating the patient, using film to determine the 2D dose distribution, and an ionisation chamber measurement to determine absolute dose per monitor unit at one or more reference point. The aim of the present study was to determine the suitability of plane parallel chambers for this purpose. A set of four chambers with identical air cavities (diameter 28.6mm; plate separation 2mm) was used. Changing the ratio of guard ring width and collecting electrode radius resulted in active volumes varying from 2 to 20mm in diameter. Measurements were performed in circular 6 MV x-ray fields (0.5 to 4cm diameter) defined by a collimator designed for stereotactic radiosurgery. As expected, the chamber readings reduced dramatically once the field size was comparable with the diameter of the collecting electrode. A further decrease in reading, as compared to pin point chamber, diodes and film, was observed in small fields (compared to the air cavity diameter) due to secondary electrons scattered laterally out of the field in the 2mm thick air cavity. The effect could be modeled using Monte Carlo calculations (BEAMnrc). We conclude that plane parallel ion chambers must be used with caution in small fields or strong dose gradients, particularly if a wide guard ring is employed, as is generally recommended for this type of chamber

TU-A3-6 09h45

Fast Three Dimensional Non-Linear Warping: Target Localization of Intraprostatic Lesions using Magnetic Resonance Spectroscopic Images*, Niranjan Venugopal¹ and B.M.C. McCurdy^{2,1} *University of Manitoba and CancerCare Manitoba.* — Image registration is an important step in the radiotherapy treatment planning process. It provides a method of incorporating different types of diagnostic imaging information. One such application is to combine magnetic resonance spectroscopic images (MRSI) of the prostate with computed tomography images that are routinely used in the radiation treatment planning of prostate cancer. MRSI provides *in vivo* information related to the underlying metabolic activity of tissues, and can be related to the presence of cancer. However, the endorectal coil required during MRS imaging poses a potential problem by deforming the prostate when it is filled with ~100cc of air during image acquisition. This pushes the prostate superiorly/anteriorly, and deforms the prostate and consequently the spectroscopic imaging data in a non-linear manner. Since patients receiving radiation treatment for prostate cancer will not have their prostate deformed in this way, we propose the application of a non-linear mapping to the MRS image data, in order to localize this information accurately. In this application, the coil-deformed MRS images are warped back to a non-deformed state. In this work we present a non-linear warping algorithm to achieve this, developed using a high level programming language. Results indicate that the algorithm attains an accuracy of 97% (3 cc difference) when reproducing the total prostate volume compared to a Radiation Oncologist defined prostate volume. This difference is smaller than the measured intra-operator variance of 7.4 cc (deflated coil) and the measured algorithm variance of 4.0 cc.

*This work is being supported by CancerCare Manitoba

10h00 Session Ends / Fin de la session

[TU-A4] Imaging with ALMA / Imagerie à l'aide de l'ALMA

(CASCA)

TUESDAY, JUNE 15

MARDI, 15 JUIN

08h30 - 09h15

[Room/Salle : Campaign B]

Chair: L. Knee, NRC

TU-A4-1 08h30

To be announced / à venir

Imaging Star - and Galaxy Formation with ALMA

To understand the formation of galaxies, stars, planets and (ultimately) life in the Universe is among the most fundamental interests of modern astrophysics. It has recently been realised that many of the stars which presently exist, were formed in gigantic bursts of star-formation ("starbursts") when the Universe was only 10 % of its current age. Through studying nearby starburst galaxies and high-mass star forming regions in our own Galaxy, we will hope to understand the underlying mechanisms behind the starburst process - knowledge that we can also apply to the more distant super-starbursts that occurred when the Universe was young.

The submillimetre wavebands are unique in astronomy in containing thousands of radio spectral lines of interstellar and circumstellar molecules as well as the thermal continuum spectrum of cold dust in space. They are the only bands in the electromagnetic spectrum in which we can detect cold dust and molecules far away in galaxies in the early Universe, and nearby in the low-temperature shrouds of stars about to be born. The technological and scientific progress in submillimetre astronomy will soon take a giant step with the advent of ALMA - the Atacama Large subMillimetre Array. ALMA is an interferometer-array consisting of sixty-four 12-meter antennas for submillimetre wavelength observations and will be placed at 5000 meters altitude in the the Chilean Andes. ALMA is expected to bring major advances in our understanding of the history of star formation in the Universe and of the physics and chemistry underlying the formation of galaxies, stars and planetary systems. Observing with ALMA also offers new interesting imaging challenges.

09h15 Session Ends / Fin de la session

[TU-A5] Medal of Achievement Winner / Récipiendaire de la médaille ACP

(CAPI/ACP)

TUESDAY, JUNE 15

MARDI, 15 JUIN

09h15 - 10h00

[Room/Salle : Ballroom B]

Chair: B. Joos, U.Ottawa

TU-A5-1 09h15

MICHAEL THEWALT, Simon Fraser University

Optical Spectroscopy in Semiconductors

Optical spectroscopy has been one of the most important tools for advancing our understanding of semiconductor physics and materials science, and it is an area in which Canada has a long and distinguished history. I will review my own experiences in this field, beginning with bound multiexciton complexes in silicon, and describing along the way aspects of double acceptors, compound semiconductors, alloys, heterostructures, and polyexcitons. Finally, I will explain how it is that after ~30 years I am excited to again be studying the fundamental properties of silicon.

10h00 Session Ends / Fin de la session

[TU-A6] News from Space - Contributed Talks / Nouvelles de l'espace - présentations contribuées

(CASCA)

TUESDAY, JUNE 15

MARDI, 15 JUIN

09h15 - 09h45

[Room/Salle : Campaign B]

Chair: M. Fich, U.Waterloo

TU-A6-1 09h15

Odin Upper Limits on Water Emission in Starburst Galaxies, C. Wilson¹, Amy Mason¹, Roy Booth², Henrik Olofsson², Michael Olberg² and Carina Persson^{2,1} McMaster University and ² Onsala Space Observatory — Starburst galaxies contain large quantities of molecular hydrogen gas and display bright emission lines from a wide variety of molecular and atomic species such as CO, HCO⁺, [C], and NH₃. We have used the Odin satellite to search for the 557 GHz water line in five nearby starburst galaxies: NGC 253, M82, Cen A, NGC 4258, and IC342. With typically 20 hours integration on each source, only upper limits to the strength of the H₂O line have been obtained to date. We use these upper limits to compare the H₂O/CO ratios in starburst galaxies with regions of high-mass star formation such as W3 in the Milky Way. Odin is an astronomy/aeronomy mission that is a collaboration between Sweden, Canada, France, and Finland.

TU-A6-2 09h30

Deep Mid-Infrared Imaging with the Spitzer Space Telescope, P. Barmby, J.-S. Huang, G.G. Fazio, M.A. Pahre, S.P. Willner, *Harvard-Smithsonian Center for Astrophysics* — One of the major science themes of the Spitzer Space Telescope is the exploration of the high-redshift universe. One way to understand the assembly history of present-day galaxies is through the study of distant galaxies still in the process of formation. The IRAC instrument on *Spitzer* has four mid-infrared bands (3–9.5 μm) which are sensitive to the light of old stellar populations over the redshift range $z=0.5-3$. This completely covers the redshift range where the cosmic star formation rate undergoes major evolution; IRAC observations are therefore powerful probes of the galaxy stellar mass evolution over this important period of cosmic history. I will present results from several deep imaging surveys carried out with IRAC, including deep galaxy number counts and properties of Lyman-break galaxies, sub-millimeter and X-ray sources.

09h45 Session Ends / Fin de la session

[TU-A7] The Impact of High-Performance Computing on Materials Research / Impact du calcul à haute performance sur la recherche sur les matériaux

(DCMMP/DPMC/M)

TUESDAY, JUNE 15

MARDI, 15 JUIN

10h00 - 12h30

[Room/Salle : Ballroom B]

Chair: G. Slater, U. Ottawa

TU-A7-1 10h00

MICHEL COTE, Université de Montréal, Regroupement québécois sur les matériaux de pointe (RQMP)

Virtual Experiments: Applications Of Density Functional Theory On Large-Scale Computational Facilities

The recent installations of high performance computational facilities have greatly affected the way we do scientific research. Whereas before, we were restricted to the experimental way, or the theoretical pen-and-paper way, these installations have permitted the event of the third way of theory/simulations that may be called: virtual experiments. Condensed matter has from the beginning adopted this new paradigm. And yet, the availability of this increased computational power would not have an important impact if it had not been accompanied by the development of theoretical methods. In this respect, the development of density functional theory was crucial to study condensed matter systems. This first-principles approach is an ideal tool to study new materials and it can also be used to make prediction on systems that have not been synthesised yet. In this presentation, the results of calculations based on density functional theory that were obtained with the facilities of the Réseau québécois de calcul de haute performance (RQCHP) will be presented. I will review the results on the now technological important GaAsN semiconductor where our calculations give us a microscopic picture of this system which permitted us to understand the experimental observations. I will also highlight the results on novel material that combine C60 and hybrid compound, an exercise in the design of a novel material. The challenges in the implementations of this method to the large-scale computation facilities presently available in Canada will also be discussed.

TU-A7-2 10h30

ERIK SORENSEN, McMaster University

Kondo Effect and Persistent Currents in Quantum Dot Systems

Quantum dots can be created not only in semiconductors but also in carbon nanotubes by artificially introducing kinks. Transport through such a system shows a very rich structure. In some cases transport is blocked due to charging effects, the so-called Coulomb blockade. Most interestingly, this blockade phenomenon is sometimes overcome by an effect entirely due to the electron spin, the famous Kondo effect. This effect is most prominently present when the behavior of the quantum dot can be modelled as a single magnetic impurity and is due to the formation of a cloud of electrons screening the magnetic impurity. A neat way of studying this phenomenon is by measuring the persistent current induced by a magnetic field when the system forms a closed ring. The induced persistent current will be strongly modified by the magnetic impurity. The sizable cloud of electrons trying to screen the magnetic impurity will give rise to specific finite-size corrections to the persistent current in such a mesoscopic systems. Calculations of transport properties are notoriously difficult and after an introduction to the underlying physics I will present numerical results from large-scale parallelized density matrix renormalization group and exact diagonalization studies of these systems, obtained using the SHARCnet facilities at McMaster.

TU-A7-3 11h00

MARK WHITMORE, Memorial University of Newfoundland

High Performance Computing: The New and Growing Environment in Canada

Beginning in about 1995, Canadian scientists have been working on a coordinated national project to build, operate, and support high performance computing and visualization facilities across the country. The result is an unprecedented set of computers that are available for use by researchers anywhere in Canada, and accessible via Canada's Can*net 4 network. Users are supported by a national network of Technical Analyst Support Personnel. Funding and support for this infrastructure and personnel come from CFI, NSERC, CANARIE, provincial government programs, computer vendors, and other partners. In this talk, I will outline this overall infrastructure, how it is organized, and how to access it, and briefly discuss the ongoing work to develop a Long Range Plan for High Performance Computing in Canada. Time permitting, I will provide some illustrative condensed matter physics research examples.

TU-A7-4 11h30

Short-time Dynamics of Stacked Triangular Antiferromagnets*, Smaine Bekhechi^{1, 2}, B.W. Southern¹ and A. Peles³, ¹University of Manitoba, ²University of Ottawa and ³Georgia Institute of Technology — Critical scaling and universality in the short-time dynamics of antiferromagnetic models on a three-dimensional stacked triangular lattice are investigated using Monte Carlo simulation. We have measured the critical exponents and, by searching for the best power law behaviour, determined the critical point. Our results indicate that it is possible to distinguish weak first-order from second-order phase transitions.

* This work is being supported by NSERC and UofM.

TU-A7-5 11h45

Viscoelastic and Thermodynamic Properties of Short Chain Polymer Melts with van der Waals Interactions Near the Glass Transition*, Bela Joos¹, Matthew L. Wallace¹, Michael Plischke², ¹ University of Ottawa and ² Simon Fraser University — We present a bead-spring model, where all beads interact with Lennard-Jones potentials, for a thorough characterization of the gelation of a short, non-entangled polymer melt. We first monitor quantities such as the heat capacity (const. P), the diffusion constants and the viscosity to describe the onset of a glass transition (GT). Whenever possible, the properties of the system are examined above and below the GT. In order to accomplish this, we propose a method whereby the glass phase is entered via isothermal compression in order to minimize high cooling-rate effects and computational times. Further insight into the GT is obtained via the time-dependent shear modulus $G(t)$, which is compared with the shear modulus obtained from an externally applied instantaneous shear. It is found that the polymeric glass only displays fully gel-like properties at a temperature below the GT. We also look at the shear rate dependence of the viscosity both above and below the glass transition using a non-equilibrium molecular dynamics approach.

* This work is being supported by NSERC.

TU-A7-6 12h00

Simulation Study of Equilibrium Polymer Dynamics, James Munro Polson, University of Prince Edward Island — We employ computer simulation methods to study hydrodynamic effects in the equilibrium internal dynamics of a polymer in dilute solution. Using Molecular Dynamics (MD), we measure the time auto-correlation functions of the Rouse modes of a simple bead-spring model polymer in a Lennard-Jones solvent. The results are analyzed in the context of a refined version of the Zimm theory of polymer dynamics. We compare the effects of chain length, solvent viscosity and system size on the correlation times measured in the simulation with those predicted by the theory. Finally, we compare the results of the MD simulations to preliminary results obtained using two alternative simulation methods, each of which employs a coarse-grained description of the solvent in a manner designed to preserve the solvent hydrodynamic modes.

TU-A7-7 12h15

Ab Initio Polarizabilities of Conducting Polymers, Sultana Ferdous and Jolanta B. Lagowski, Memorial University of Newfoundland — Polarizabilities and first order hyperpolarizabilities of thiophene, fulvene and cyclopentadiene conducting oligomers and polymers and their cyano derivatives have been calculated using the Hartree-Fock (HF), configuration interaction (singles) (CIS) and density functional (DF) theories with 3-21G* basis using Gaussian 94, 98 and 03 softwares. The main motivation of this investigation is to determine the correlation between the excitation energies and polarizabilities and hyperpolarizabilities for the conjugated systems studied. It has been found that HF and DF approaches give similar magnitudes for polarizabilities whereas CIS theory provides results that are considerably different. All three methods predict similar trends in polarizabilities as a function of oligomer length and bond alternation along the backbone of the oligomers. It has also been observed that the end groups and the number of 'double' bonds have a significant effect on the magnitude of polarizability per C-C bond. To eliminate the need for end groups, solid state calculations (using the periodic boundary condition (PBC option in Gaussian 03)) are performed for some systems. Comparison with experimental results will be made when it is possible.

12h30 Session Ends / Fin de la session

[TU-A8] Mathematical Physics / Physique mathématique

(DTP/DPT)

TUESDAY, JUNE 15

MARDI, 15 JUIN

10h00 - 12h30

[Room/Salle : Westminster]

Chair: I. Affleck, UBC

TU-A8-1 10h00

Mark Walton, University of Lethbridge

Finding NIM-reps

In two-dimensional conformal field theory, bulk primary fields obey an operator product algebra following the fusion algebra. Consistent sets of boundary conditions are in correspondence with the Non-negative Integer Matrix representations (NIM-reps) of this fusion algebra. Methods of constructing NIM-reps will be reviewed, as well as their relation to D-brane charges.

TU-A8-2 10h30

JEDRZEJ SNIATYCKI, University of Calgary

Gauge Symmetries in Yang-Mills Theory

For Yang-Mills equations on the Minkowski space-time, we identify a space P of Cauchy data which admit global solutions, the gauge symmetry $GS(P)$ group of P , and its connected subgroup $GS_0(P)$ consisting of the localized gauge transformations that give rise to the constraints of the theory. We show that the constraint set C has a manifold structure, but it is not a submanifold of P . The group $GS_0(P)$ acts freely and properly on P . The reduced phase space $R=C/GS_0(P)$, consisting of $GS_0(P)$ orbits in C is a quotient manifold of C and it inherits the structure of a symplectic manifold with an exact symplectic form. The colour group $GS(P)/GS_0(P)$ has a Hamiltonian action on R . We conclude that, for the Yang-Mills theory in the Minkowski space, geometric quantization commutes with reduction.

TU-A8-3 11h00

DAVID JOHN ROWE, University of Toronto

Quasi-Dynamical Symmetry In The Approach To A Second-Order Phase Transition

Attempts to understand phase transitions have profited considerably from the study of models with symmetry. Landau stated that two phases of matter with different symmetries (which cannot change continuously from one to the other) must be separated by a line of transition. Some interesting symmetry concepts emerge from the study of how this can happen in practice. Consider a system x which likes to reside in a phase with a symmetry group G_1 when a control parameter has value $x=0$ and in a phase with symmetry group G_2 when it has value $x=1$. The question then is what happens when x is varied continuously from 0 to 1? It transpires, in a number of model investigations of such situations, that the model exhibits a second order phase transition from a phase characterized by one symmetry to a phase characterized by the other in accordance with Landau's principle. However, a closer examination reveals that a more detailed description is that, in the phase characterized by the G_1 symmetry, the symmetry of the system is increasingly distorted by the forces that favour the competing phase until a point comes at which they can be distorted no further and a flip occurs. A complementary behaviour may be observed when the critical point is approached from the other side. The distorted symmetries, called quasi-dynamical symmetries, have an elegant expression in the language of group theory and lead to interesting new concepts in representation theory of considerable significance for understanding why simple models with symmetries are often more successful in practice than they apparently have any right to be.

TU-A8-4 11h30

ARIEL A. EDERY, Bishop's University

Compact Formulas For Casimir Energies In D-Dimensions Via Operator Technique

An operator technique is derived for the multi-dimensional application of the Euler-Maclaurin formula to the Casimir energy problem. We obtain compact formulas for the Casimir energy of a scalar field confined to a D -dimensional hypercube with von Neumann or Dirichlet boundary conditions. The formulas are conveniently expressed as a finite sum of the well-known gamma and Riemann zeta functions and allow for quick numerical calculations at higher values of D . The case of the Dirichlet energy reveals a critical dimension at $D = 36$. We briefly discuss the connection between the Casimir energy in D -dimensions and the $rD(n)$ arithmetic function (where $rD(n)$ represents the number of ways a positive integer n can be expressed as a sum of D integer squares).

TU-A8-5 12h00

JIRI PATERA, Université de Montréal

Orbit Functions of Compact Lie Groups and their Applications

An orbit function is the contribution to an irreducible character of a compact semisimple Lie group G , from one Weyl group orbit. Such functions are much simpler than the characters, but they carry most of the practically useful properties of the characters. Moreover, their versatile discrete orthogonality on certain finite Abelian subgroups of G , makes them particularly suitable for digital data processing.

12h30 Session Ends / Fin de la session

[TU-A9]

Particles/Strings/Fields / *Particules/ficelles/champs*(DTP-PPD/
DPT-PPD)

TUESDAY, JUNE 15

MARDI, 15 JUIN

10h00 - 12h30

[Room/Salle : Kildonan]

Chair: R. MacKenzie, U.Montreal

TU-A9-1 10h00

BOB HOLDOM, University of Toronto

Ghostly Tales

I discuss fields with negative kinetic energy terms in the context of various cosmological puzzles.

TU-A9-2 10h30

TAEJIN LEE, University of British Columbia

Free Field Representation of Rolling Tachyon

We apply the fermionization to the rolling tachyon system, which describes a fate of the unstable D-brane. The boundary state for the unstable D-brane is explicitly constructed and its exact evolution in time is obtained. The free fermion representation of the rolling tachyon system is found useful to understand how the openstring tachyon potential deforms the perturbative basis of closed string.

TU-A9-3 11h00

AARON BERNDSEN, CHEP, McGill University

*Aspects of Brane-Gas Cosmology**

Brane-Gas Cosmology (BGC) is an approach to pre-Big Bang cosmology that attempts to reconcile several problems with standard cosmology through a setup based on string theory. The original idea, qualitatively laid out by Brandenberger and Vafa, has been employed to avoid the initial singularity, to explain why only three of nine spatial dimensions predicted by string theory grow large, and to explore the effects of branes and topology on the Universe, to mention only a few. We review these results and explore further aspects of the BGC setup, such as the stability of the dilaton, the dependence of string interaction rates on the number of dimensions, and the scale of the hierarchy.

* This work is being supported by McGill, NSERC and was in collaboration with J. Cline, CHEP, McGill University.

TU-A9-4 11h30

THOMAS GREGOIRE, CERN

Little Higgs Models And Electroweak Precision Measurements

Little Higgs models stabilize the weak scale with weakly coupled new physics at the TeV scale. In contrast with supersymmetry, quadratic divergences to the Higgs mass are cancel by "partners" of the same statistic. In this talk I will discuss the general mechanism at work in little Higgs models, and discuss their general features. If time permit, I will then review the different kinds of little Higgs models and their consequences for electroweak precision measurements.

TU-A9-5 12h00

MAXIM POSPELOV, University of Victoria

Search For Dark Matter In $B \rightarrow S$ Transition With Missing Energy

We show that the decay of B mesons to K (K^*) and missing energy in the final state can be an efficient probe of dark matter in the mass range $0 < m_S < 2.4$ GeV where the decay into a pair of dark matter particles S is kinematically allowed. We analyze a model with the scalar dark matter coupled to the Standard Model sector via the Higgs boson to show that the width of the Higgs penguin-mediated decay mode $B \rightarrow KSS$ may exceed the decay width in the Standard Model channel, $B \rightarrow K_V \bar{\nu}$, by up to two orders of magnitude if the required cosmological abundance of scalars is achieved through the annihilation at the freeze-out. Existing data from B physics experiments exclude scalar dark matter with $m_S < 430$ MeV and 510 MeV $< m_S < 1.1$ GeV. Expected data from B factories will probe the range of dark matter masses up to 2 GeV.

* In collaboration with C. Bird, P. Jackson and R. Kowalewski, University of Victoria.

12h30 Session Ends / Fin de la session

[TU-A10]

Coherent Interactions of Lasers / *Interactions coh rentes des lasers*

TUESDAY, JUNE 15

MARDI, 15 JUIN

10h00 - 12h00

(DAMP-DOP/
DPAM-DOP)

[Room/Salle : Victoria]

Chair: J. Martin, U.Waterloo

TU-A10-1 10h00

HAROLD HAUGEN, McMaster University

*Selected Studies of Femtosecond Laser Ablation and Modification of Semiconductors**

Femtosecond lasers have become important tools for the micro-modification and micro-machining of materials. We outline a number of recent developments in our laboratory including the formation of sub-wavelength periodic structures on surfaces, the measurement of the ablation thresholds and ablation depths for InP over a wide range of laser wavelengths, and studies of the sub-surface modification of semiconductors using polarized photoluminescence (DOP) and cross-sectional transmission electron microscopic (TEM) techniques. Our work has demonstrated that high spatial frequency periodic structures significantly smaller than the light wavelength can be obtained in ultrafast laser irradiation of semiconductors, analogous to recent results reported in the literature for dielectrics. In addition, in experiments on the laser ablation of InP over a wide wavelength range, we have found a sudden increase of the crater depth with laser fluence near threshold, similar to spallation effects obtained via recently published theoretical models. Finally, observations using DOP and TEM revealed significant differences between nanosecond and femtosecond laser micro-machining of InP. In particular, ultrafast laser interactions lead to substantial damage in the vicinity of the laser-ablated features. Future directions for these on-going investigations will be discussed.

* Conducted in collaboration with A. Borowiec, G.A. Botton, D.M. Bruce, D.T. Cassidy, M. Couillard, and T.H.R. Crawford; McMaster University

TU-A10-2 10h30

*Diffraction Optics Based 2-D IR Spectroscopy: A New Probe of Hydrogen Bonded Networks**. M.L. Cowan¹, B.D. Bruner¹, N. Huse², T. Elsaesser², R.J. Dwayne Miller¹, and E.T.J. Nibbering², ¹ University of Toronto and ² Max Born Institute for Nonlinear Optics and Short Pulse Spectroscopy, Berlin — Recent developments in IR laser technology has made possible the development of optical analogues of multi-dimensional NMR spectroscopy, such as 2D-vibrational spectroscopy. These techniques make possible the disentanglement of complicated vibrational spectra, and the measurement of coupling dynamics between neighboring vibrators on femtosecond time scales, by expanding the spectra into two frequency dimensions. Using phase-locked sequences of sub-100 fs, 3 micron pulses we have performed 2D-vibrational spectroscopy on the O-H vibrational stretch mode of acetic acid dimers in CCl₄, a system with strong hydrogen bonding. The 2D spectra allow us to gain insight into the effects of hydrogen bonding on the dynamics of the dimers, through measurements of the coupling between O-H stretch modes.

* This work is being supported by NSERC, PRO.

10h45 Coffee Break / Pause caf 

TU-A10-3 11h15

JOHN E. SIPE, University of Toronto

Optically Injected Spin Currents In Semiconductors

It has been widely known since the 1980's that carriers with a net spin polarization can be optically injected in semiconductors, such as GaAs, simply by irradiation with circularly polarized light at energies above the band gap. Indeed, such injection followed by acceleration of the injected carriers by an applied DC field is nowadays a standard approach to generating a spin-polarized current. But only recently has it been appreciated that spin currents themselves can be optically injected in semiconductors directly, in the absence of a bias field. Our work has focused on optical injection across the band gap, using quantum interference effects associated with different pathways connecting the same initial and final states. Simultaneous irradiation by beams at ω and 2ω , where 2ω crosses the band gap, allows for the interference of one- and two-photon absorption processes. With a proper choice of a relative phase parameter net currents can be injected in the crystal; this injected current can be spin-polarized. In a difference scenario, carriers injected at k are injected preferentially with one spin polarization, and those at $-k$ with the opposite. No net electrical current or spin is injected into the crystal, but a *pure spin current* is. Theoretical and experimental work will be reviewed, and new scenarios involving laser light of only one frequency will be discussed.

* In collaboration with R.D.R. Bhat¹, Ali Najmaie¹, F. Nastos¹, Y. Kerachian¹, and H.M. van Driel¹, A.L. Smirl², M.J. Stevens², and X.Y. Pan², ¹ University of Toronto and ² University of Iowa.

TU-A10-4 11h45

A Theoretical Model of Synchrony for Coupled Fiber Lasers. Slaven Peles¹, Jeffrey Rogers² and Kurt Wiesenfeld¹, ¹ Georgia Institute of Technology and ² HRL Laboratories — One of the main goals of laser physics is how to increase the intensity of a laser beam. Using an array of lasers is one way to do this, but it has proven to be very difficult to get coherent and in phase behavior. Recent experiments showed that small groups of coupled fiber lasers synchronize under certain circumstances. As a result the output intensity grows as a power law and not linearly with the number of fibers. At the moment, the mechanism as to how these lasers synchronize is not understood. We model the experimental system using a nonlinear map array with a particular symmetry. Our analysis of primary and secondary instabilities provides insight into the system's behavior, and perhaps how to improve its performance.

12h00 Session Ends / Fin de la session

[TU-A11] Novae and Supernovae / *Novas et supernovas*(DNP-CASCA/
DPN-CASCA)TUESDAY, JUNE 15
MARDI, 15 JUIN
10h00 - 12h30

[Room/Salle : Ballroom C]

Chair: S. Safi-Harb, U.Manitoba

TU-A11-1 10h00

UNA HWANG, NASA/GSFC

Windows into Nucleosynthesis from X-ray Observations of Supernova Remnants

A new era in X-ray astronomy was launched by the Chandra and XMM-Newton observatories. Chandra's exquisite angular resolution in particular provides the means to isolate and analyze spectra on small angular scales—a capability that is essential to the study of the nucleosynthesis products in supernova remnants. In this review I will survey the current status of such studies for remnants of both core-collapse and thermonuclear supernovae. These results give hints on the effect of the explosion mechanism in thermonuclear supernovae, on the amount of mixing in core-collapse remnants and asymmetries both in the distribution of the ejecta and the explosion energy. Kinematic information and reliable estimates of the X-ray emitting masses are also now being obtained. Even relatively old remnants are revealing their ejecta to Chandra's scrutinizing eye in surprising ways. The next few years should bring many continuing advances in this exciting field.

TU-A11-2 10h30

MATZNER, Christopher, University of Toronto

Energy Feedback in Core-Collapse Supernovae

In core collapse supernovae, energy released by gravity unbinds the stellar envelope. gravitational energy feedback, which appears also in accreting stars and black holes, plays a controlling role in the explosion mechanism. I briefly review ideas for the mechanism of feedback in supernovae, and go on to discuss some of the spectacular aftereffects of explosive energy deposition within stellar envelopes, touching on envelope ejection, x-ray flashes, relativistic motion, and gamma-ray bursts.

11h00 Coffee Break / Pause café

TU-A11-3 11h30

HENDRIK SCHATZ, Michigan State University

Nuclear Physics on Accreting Neutron Stars - from X-Ray Bursts to Superbursts

We are entering a new era of precision and long-term observations of X-ray binaries with telescopes such as XMM-Newton, the Chandra X-ray observatory, and the Rossi X-ray Timing Explorer. Of particular interest are burst phenomena on accreting neutron stars, which are powered by nuclear physics processes on the surface of the neutron star such as the rp-process. Once well understood, these systems could serve as unique laboratories for matter under extreme conditions. Simultaneous progress in nuclear physics is needed for an interpretation of the observational data and to address the many open questions. With new radioactive beam facilities it becomes now possible to study the exotic nuclei that form the reaction chains in X-ray bursts. I will review the open questions, recent observations, new experimental approaches as well as advances in modelling. In particular I will discuss the recently discovered extremely rare, but 1000 times more powerful superbursts. I will also present first results from a new experimental approach to rp-process physics using radioactive beams at the NSCL's Coupled Cyclotron Facility at Michigan State University.

TU-A11-4 12h00

*Visualizing the Inner Regions of Accretion Disks around Neutron Stars using Superbursts**, David Ballantyne¹ and T.E. Strohmayer², ¹Canadian Institute for Theoretical Astrophysics and ²NASA/GSFC — Accretion from a disk onto a collapsed, relativistic star - a neutron star or black hole - is the mechanism widely believed to be responsible for the emission from compact X-ray binaries. Because of the extreme spatial resolution required, it is not yet possible to directly visualize the evolution or dynamics of the inner parts of the accretion disk where general relativistic effects are dominant. We show that the bright X-ray emission from a superburst on the surface of a neutron star can act as a spotlight to illuminate the disk surface. The X-rays cause iron atoms in the disk to fluoresce, allowing a determination of the ionization state, covering factor and inner radius of the disk over the course of the burst. The time-resolved spectral fitting shows that the inner region of the disk may be disrupted by the burst, allowing us to visualize the evolution of the inner regions of an accretion disk in real-time.

* This work is being supported by NSERC.

TU-A11-5 12h15

The $^{12}\text{C}(\alpha, n)^{16}\text{O}$ Reaction: Overview and Results at DRAGON, Lothar R. Buchmann, TRIUMF -- The $^{12}\text{C}(\alpha, n)^{16}\text{O}$ reaction is arguably the most important reaction yet to be determined on Nuclear Astrophysics. A status report on present determinations of the cross section will be given, together with some results of measurements done at the TRIUMF recoil separator DRAGON at high energies. The importance of cascade transitions will be discussed in addition.

12h30 Session Ends / Fin de la session

[TU-A12] Techniques and Measurements in Semiconductor Physics and Transport Phenomena / *Techniques et mesures en physique des semiconducteurs et phénomènes de transport*

(DIMP/DPIIM)

TUESDAY, JUNE 15
MARDI, 15 JUIN
10h00 - 12h30

[Room/Salle : Campaign A]

Chair: A. Mandelis, U.Toronto

TU-A12-1 10h00

JOSE A. GARCIA, Photo-Thermal Diagnostics Inc.

Photo-Carrier Radiometry of Semiconductors: Instrumentation and Ion-Implantation Studies

Non-contact, non-intrusive photo-carrier radiometry (PCR) was used for monitoring the ion implantation of (p-type) industrial-grade silicon wafers. The silicon wafers were implanted with different species (Boron, Phosphorus) in the dose range of 1×10^{11} -to- 1×10^{16} ions/cm² at different implantation energies (10 keV-to-180 keV). The PCR 100 system from Photo-Thermal Diagnostics Inc, Toronto, Canada was used to perform the measurements. Various aspects of the instrumentation as well as quantitative results of the sensitivity to the implantation doses and energies and the physics of signal dependence on dose will be presented. This laser-based carrier-wave technique monitors harmonically photoexcited and recombining carriers and shows great potential advantages over existing methodologies for characterization of multiple semiconductor processes such as ion implantation and other Si wafer process steps.

* In collaboration with X. Guo, A. Mandelis and A. Simmons, Photo-Thermal Diagnostics Inc.

TU-A12-2 10h30

YURI GUREVICH, Cinvestav del I.P.N.

The Transport of Nonequilibrium Carriers in Semiconductor Structures (New point of view)

The role of nonequilibrium electrons and holes in linear and nonlinear transport is discussed. It is shown that the thermo-emf, electrical and thermal resistance in semiconductor structures depend on the rate of surface and bulk recombination of nonequilibrium carriers. The transition to the general case takes place only when the recombination rate is infinite. It is shown that the well known concepts of life-time of nonequilibrium carriers contradict the Maxwell's equations. Life-times of nonequilibrium carriers can be correctly defined only at equality of nonequilibrium concentration of electrons and holes. The correct definition of recombination rates of nonequilibrium electrons and holes is discussed. In the general case, these recombination rates depend on external generation rates, effective electron, hole and phonon temperatures and on their spatial inhomogeneity. The question about the formation of quasineutral packets of nonequilibrium carriers is studied. New current boundary conditions at the border of two conducting media were formulated taking into account surface resistance and surface recombination. The above stated questions are of great importance to design solid state electronic devices, to interpret experimental results of nonequilibrium charge carriers transport and for the measuring of kinetic characteristics of conducting media.

11h00 Coffee Break / Pause café

TU-A12-3 11h15

HANS D. HALLEN, North Carolina State University

*Electron-Induced Motion Of Atoms: Mechanisms And Insights About Hot Electron Transport**

Few-electron-volt energy electrons can induce motion of atoms in metals. We have observed oxygen motion in YBCO films with near-field optical microscopy (NSOM) and gold atom/vacancy motion in gold thin films using ballistic electron emission microscopy (BEEM). This somewhat surprising result can be attributed to localized bond breaking. The process results in an increased local diffusivity of oxygen in YBCO, and to subsurface terrace growth and/or mound formation in gold films. Tunnel electron energy dependence is measured. The threshold behavior is consistent with expectations from band structure. The effect is limited to a single grain in both cases, implying that these hot electrons do not cross grain boundaries — the electrons lose their excess energy first.

* In coordination with Suzanne Heurth, SPAWAR

TU-A12-4 11h45

Ground-Based Testing of Electronic Devices for Space Radiation Effects. Ewart W. Blackmore, TRIUMF — Spacecraft systems are exposed to energetic charged particles that can cause problems for on-board electronics and devices, such as single-event effects (SEEs), transient ionization effects and in some cases failure from total dose. The space radiation environment consists of three components — galactic cosmic rays, particles from solar events and particles trapped in planetary magnetospheres. For many situations the radiation problems are predominantly caused by energetic protons with energies ranging from a few MeV to hundreds of MeV, the same energy range as the TRIUMF cyclotron. In 1995 a dedicated test facility was developed using TRIUMF beams to enable space electronics designers to test individual devices or circuits for radiation effects. A 10-year mission dose can be delivered in a matter of minutes. This facility is in frequent use by space companies, universities and laboratories in Canada, United States and Europe. The beams are also useful for testing electronics for particle physics experiments at colliders where the radiation dose is significantly higher than in space. The proton test facility and a recent development of a neutron test facility for terrestrial applications and avionics will be described and some typical results will be presented.

TU-A12-5 12h00

Silicon Photomultiplier as a Readout System for a Barrel Calorimeter (GlueX Project). Vitali Kovaltchouk, Z. Papandreou, G. Lolos, University of Regina — Photomultiplier tubes (PMT), hybrid photodiodes (HPD) and silicon photomultipliers (SiPM) have been investigated under laboratory conditions as candidates for the readout system of the HallD/GlueX barrel calorimeter at Jefferson Lab. The shapes of pulses among those readout systems are presented here, with emphasis on the rise time and the pulse duration. The energy and timing spectra for a minimum ionizing particle traversing a scintillating fiber (SCSF-38) were measured with a photomultiplier tube and a silicon photomultiplier. From these tests, it can be concluded that it is feasible to use a silicon photomultiplier as a readout system for the barrel calorimeter. SiPM's have better energy and time resolutions in comparison with PMT's and HPD's and are not sensitive to a high magnetic field.

TU-A12-6 12h15

Dynamic Response Of A Pair Of Electrostatically Coupled Cantilevers: Experimental Characterization And Modelling*. K.M. Cheng, D.R. Oliver, G.E. Bridges and D.J. Thomson, University of Manitoba — Micro-electro-mechanical systems (MEMS) technologies use integrated circuit fabrication techniques to produce three-dimensional structures with micron-scale dimensions. An application of MEMS technology is in the design of mechanical RF resonators and filters. Compared to their electronic counterparts, such structures can have larger Q values and smaller power requirements. However, characterizing the vibration modes of these structures presents interesting challenges. As an alternative to interferometry, our technique derives from non-contact scanning probe microscopy (SPM). This technique has been adapted to examine isolated resonators, enabling modeling of their character without loading due to drive electronics. We demonstrate the technique using two free-standing cantilevers, one is the SPM probe the other acting as the target resonator. A modulated RF source is applied to the probe cantilever (resonant frequency of 14kHz) and actuates the modes of a stationary, grounded test cantilever with a resonant frequency of 80kHz. The electrostatic interaction experienced between the probe tip and the test cantilever results in an attractive force (experienced at the probe tip), the resulting deflection is detected with a beam bounce system and a lock-in amplifier. Fundamental and higher (longitudinal) mode frequencies for the test cantilever were predicted using eigenvalue relations and detected electrostatically using this technique. The response amplitudes detected for higher modes successively decreased indicating larger effective spring constants. While the "free vibration" character of the grounded cantilever is evident from the data, characteristics relating to the coupled system were also found. The analysis includes discussion of a suitable coupled model for this system.

* In collaboration with D.R. Oliver, G.E. Bridges and D.J. Thomson, ECE, University of Manitoba.

** This work is being supported by NSERC.

12h30 Session Ends / Fin de la session

[TU-A13]

Correlated Electrons - Magnetism / Électrons corrélés - Magnétisme

TUESDAY, JUNE 15

MARDI, 15 JUIN

10h00 - 12h30

(DCMMP/DP/MCM)

[Room/Salle : Colbourne]

Chair: W.J.L. Buyers, NRC

TU-A13-1 10h00

TAPASH CHAKRABORTY, University of Manitoba

How to Probe a Fractionally-Charged Quasihole?

A curious anomalous dispersion of charged excitons in photoluminescence experiments on a two-dimensional electron gas subjected to a quantizing magnetic field at and around 1/3 filling of the lowest Landau level was observed experimentally. The anomaly exists only at a very low temperature and an intermediate electron density of the electron gas. We explained the anomaly as due to a perturbation of the incompressible liquid at the 1/3 filling factor, induced by the close proximity of a localized charged exciton which creates a fractionally-charged quasihole in the liquid. The intriguing experimentally observed puzzle that the anomaly can be destroyed by applying a very small thermal energy is thereby resolved, as this energy is found to be enough to close the quasihole energy gap. This work is the first ever probe of the quasihole gap in a quantum Hall system.

TU-A13-2 10h30

Transport Gap in Quantum Hall Bilayers at Total Filling Factor $\nu = 5^*$. C.B. Doiron and R. Côté, *Université de Sherbrooke* — At total filling factor $\nu = 5$, the ground state of two coupled bidimensional electron gases in a perpendicular magnetic field is predicted to be a stripe phase for interlayer distance $d > d_c$. This system presents unidimensional coherent channels where the electrons are totally delocalized across both wells. The lowest-energy charged excitations supported in the stripe phase are pseudospin solitons localized in these coherent channels. The soliton's energy is thus directly related to the transport gap of such a system, one of the properties of the stripe phase that is most open to experimental study. Working in the Hartree-Fock approximation, we have investigated the phase diagram of quantum Hall bilayers at filling factor $\nu = 5$ and have computed the soliton's energy for a wide range of interlayer distances and tunnelings.

* This work is being supported by NSERC.

TU-A13-3 10h45

Pinning Mode of the Electron Crystals in Higher Landau Levels*. Alexandre Faribault¹, R. Côté¹, M. Li¹, H.A. Fertig² and H. Yi³, ¹Université de Sherbrooke, ²University of Kentucky and ³Korea Institute for Advanced Studies — In Landau level $N > 0$, mean-field theory predicts that a two-dimensional electron gas will go through several structural transitions as the partial filling factor is increased. It will evolve from a Wigner crystal (WC) at low filling, through various bubble phases (WC with n electrons per lattice site) at intermediate filling and then to a stripe phase close to a half filling. The electron crystals (WC and bubbles) will be pinned in the presence of disorder and therefore will show a peak in the conductivity at a finite frequency. The behaviour of the pinning peak with filling factor is studied by building an elastic model whose parameters are extracted from the numerical results of the time dependant Hartree-Fock approximation. The disorder is then treated by using the replica theory and gaussian variational method. The results of this calculation are then compared with recent microwave experiments.

* This work is being supported by FCAR, CRSNG.

11h00 Coffee Break / Pause café

TU-A13-4 11h15

The Formation of Stripes and the Enhancement of Pairing in the Anisotropic $t - J$ Model*. Ken Vos, J.M. Tipper and C. Genert, *University of Lethbridge* — We have examined the formation of stripes and pairing in the anisotropic $t - J$ model. We have used exact diagonalization methods on several different cluster sizes to examine the underdoped region. We have found that as the values of the long-range hopping parameters increase, the holes are found to separate while enhancing the strength of the binding, resulting in a bi-directional stripe-like configuration of charge carriers. Evidence of unidirectional stripe formation in the hole and spin correlations is found upon consideration of the phase transition between the high-temperature tetragonal and low-temperature orthorhombic phases of Sr-doped La-214, represented by an anisotropic next-nearest neighbor hopping parameter. Upon examination of the magnetic structure factor, the values closest to (π, π) are found to increase rapidly as a function of doping, indicative of the formation of incommensurate peaks. We have determined that the formation of stripes parallel to the Cu-O-Cu bonds enhances pairing and in the bulk limit there is a finite range of doping concentrations where hole pairs will form. These results are consistent with the experimental data. The computational infrastructure was provided by MACI and WESTGRID.

* This work was supported by NSERC of Canada.

TU-A13-5 11h30

Pseudogap in Ortho-II YBCO: NMR vs. INS*. Bryan W. Statt and Z. Yamani, *University of Toronto* — The pseudogap as measured by Cu NMR for Ortho-II YBCO is presented here. The pseudogap can be seen in the Knight Shift and the Spin-Lattice Relaxation rate ($1/T_1$). The Knight Shift is proportional to the $q=0$ susceptibility whereas $1/T_1$ is predominantly the imaginary susceptibility at $q=(\pi, \pi)$. By contrast, recent Inelastic Neutron Scattering experiments [1] on Ortho-II YBCO reveal no sign of the pseudogap. This discrepancy will be discussed in terms of the different time scales of NMR and INS measurements.

1. C.Stock, PRB 69, 014502 (2004).

* This work is being supported by NSERC.

TU-A13-6 11h45

Continuous Map of the Phase Diagram of High Temperature Superconductors Using a Composition Spread Approach*. Kevin C. Hewitt, R.J. Sanderson, *Dalhousie University* — The physical properties of cuprate superconductors are very sensitive to small changes in hole or electron doping. Up to now, the phase diagram has been mapped discretely. We have developed a method of synthesizing the entire phase range, from the antiferromagnetic insulating phase through to the overdoped phase, in a single experiment using thin film sputter deposition combined with physical masking techniques. The technique enables us to measure, in a truly continuous manner, the physical properties of the cuprates. X-ray photoelectron spectroscopy, Raman spectroscopy, X-ray diffraction, Wavelength Dispersive spectroscopy and high throughput resistivity are used to characterize the resulting films for, respectively, average Cu valence, opto-electronic properties, structure, composition, and electronic transport. Results from our first system $[\text{Bi}_2\text{Sr}_2\text{Ca}_{1-x}\text{Y}_x\text{Cu}_2\text{O}_{8+\delta} \text{ (} 0 \leq x \leq 1)]$ of study will be presented.

* This work is being supported by NSERC.

TU-A13-7 12h00

Unbiased Laser Detection In Uncooled YBCO Thin Films*. Martin Paul Bourgeois¹, P. Mérel², C. Lavigne², A.J.-B. Kpetsu¹, R. Provencher² and R.A. Lessard¹, ¹Université Laval and ²Gentec-EO — It has been shown in the last decade that YBCO, a material mostly known for its outstanding superconducting properties, can also be used as a radiation detector. Both amorphous and crystalline films have been shown to be of interest for this application, and both pyroelectricity and thermoelectricity have been proposed to explain the observed response. In this work, we attempt to optimize YBCO film properties by annealing RF-sputtered films. As various film annealing conditions are experimented with, x-ray diffraction, spectrophotometry, resistivity measurements and laser response are used to evaluate film quality and to better explain the observed effect.

* This work is being supported by NSERC.

TU-A13-8 12h15

Fabrication et caractérisation de couches minces de YBaCuO : optimisation de la cristallisation*. A.K.J.B. Kpetsu, M. Bourgeois, C. Lavigne, P. Mérel, R.A. Lessard et R. Provencher, *Université Laval* — Le YBaCuO ou YBCO ($\text{YBa}_2\text{Cu}_3\text{O}_7$) est une céramique connue pour ses propriétés supraconductrices à 'haute température' ($T_c \approx 93$ K). Outre cette caractéristique, le YBCO a une structure qui le rend très intéressant pour plusieurs applications, notamment pour la fabrication de détecteurs optiques. Dans cette perspective, nous procédons d'abord au dépôt de couches minces de Y-Ba-Cu-O par pulvérisation cathodique RF sur des substrats de MgO et de SrTiO₃, ensuite à leur cristallisation dans diverses conditions de traitement thermique et enfin à leur caractérisation. Cette étude de caractérisation vise d'une part à comprendre les changements des propriétés des couches déposées en fonction de leurs conditions de préparation et d'autre part à permettre ainsi un certain contrôle de la structure cristalline obtenue afin d'optimiser en particulier la cristallisation de couches épitaxiales de YBCO pour les applications souhaitées en détection. Ce projet est réalisé en collaboration avec la compagnie Gentec Electro-Optique inc. à Québec.

* Travail réalisé grâce à : NSERC : CG0589, et à FQRT : FR051731, FT073270.

12h30 Session Ends / Fin de la session

[TU-A14]

(DAMP/DPAM)

Atomic and Molecular Spectroscopy and Dynamics I /
Spectroscopie et dynamique atomique et moléculaire I

TUESDAY, JUNE 15

MARDI, 15 JUIN

10h00 - 12h30

[Room/Salle : Ballroom A]

Chair: P. Zetner, U.Manitoba

TU-A14-1 10h00

JOHN W. HEPBURN, University of British Columbia

*Spectroscopy and Dynamics of Threshold Ionization of Clusters and Small Molecules**

In this talk, recent results on threshold photoionization and photoion-pair production will be discussed. In these experiments, coherent vacuum ultraviolet radiation is used to excite small molecules or clusters to highly excited states, which can result in the formation of conventional or ion-pair Rydberg states, which can be detected by pulsed-field ionization. This threshold spectroscopy allows us to probe the energetics, spectroscopy, and dynamics of photoionization and photoion-pair production.

* In collaboration with Q. Hu, University of British Columbia.

TU-A14-2 10h30

WOLFGANG JAEGER, University of Alberta

Spectroscopy of He_N-Molecule Clusters: A Probe of the Onset of Superfluidity?

High resolution molecular spectroscopy holds great promise to bridge the gap in our knowledge about microscopic, molecular-scale systems on one side and the bulk phase on the other. Spectroscopy of weakly bound complexes has recently been pushed into a new size regime with the investigation of medium-sized He_N-molecule clusters. The successive solvation of the molecular chromophores with helium atoms promises to shed light on the microscopic evolution of the bulk phase property superfluidity. In this talk, rotational spectra of medium sized He_N-molecule clusters will be presented (molecule = carbonyl sulfide, nitrous oxide, carbon monoxide, cyanoacetylene). The corresponding spectroscopic constants will be compared with results from theoretical simulations. There is indication, from the N-dependences of the moments-of-inertia, that the helium atoms begin to decouple from the rotational motion of the monomers. It will be explored how the trends in the spectroscopic constants of the quantum solvated systems can be used to trace the onset of 'microscopic superfluidity'.

TU-A14-3 11h00

WILLIAM VAN WIJNGAARDEN, York University

Bose Einstein Condensation in a QUIC Trap

The apparatus and procedure required to generate a pure Bose Einstein Condensate (BEC) is described. The atoms are first laser cooled in a vapour cell magneto-optical trap (MOT) and subsequently transferred to an ultralow pressure MOT. The atoms are loaded into a QUIC trap consisting of a pair of quadrupole coils and a Ioffe coil that generates a small finite magnetic field at the trap energy minimum to suppress Majorana transitions. Evaporation induced by an RF field lowers the temperature permitting the transition to BEC to be observed by monitoring the free expansion of the atoms after the trapping fields have been switched off.

TU-A14-4 11h30

ALLAN GRIFFIN, University of Toronto

Molecular BEC Condensate vs a BCS Superfluid in a Trapped Atomic Fermi Gas

Recently, there has been enormous interest in trapped ultra cold two component atomic Fermi gases. In the last year, several groups (JILA, MIT, Innsbruck) have produced a Bose condensate of stable dimer molecules by working close to Feshbach resonance. In this review talk, I will discuss these experiments and the physics of the BCS-BEC crossover in the presence of a Feshbach resonance. I will argue that there is no essential difference between the theory of a molecular BEC in a Fermi gas and the more traditional BCS state associated with the formation of Cooper pairs. Both limits are described by a BCS-type mean field theory, but now with a composite order parameter describing both a BEC of molecules and Cooper pairs. By ramping through the Feshbach resonance, one should soon be able to make a complete study of both the quasiparticle spectrum and the collective modes in the crossover region of such Fermi superfluids.

TU-A14-5 12h00

*Measuring a Single Ion at the Limits of Time**. Alan A. Madej, P. Dubé, J.E. Bernard and L. Marmet, *INMS, National Research Council* — Recent experiments using single, laser cooled ions held in electrodynamic trapping fields have produced one of the closest approximations of an isolated quantum system at rest. These systems form a unique test-bed to study atomic physics and spectroscopy at the limit of the highest accuracy and precision and have been applied to measure the time variation of fundamental constants. In the last few years, such trapped ion samples have been studied as the potential reference frequency for a new generation optical atomic clocks whose accuracy have the potential to outperform the current Cs atom based realization of the SI second. This talk will present our recent results at NRC examining a single ion of ⁸⁸Sr⁺ held in a miniature Paul type electrodynamic trap and laser cooled to mK kinetic temperatures. A new 674 nm (445-THz) laser system for probing the ultra narrow 5s ²S_{1/2} - 4d ²D_{5/2} reference transition (0.4 Hz natural linewidth) has been constructed which provides Hz level stabilities over hour periods. Line widths of the reference transition of 50 ± 9 Hz have been observed. Linking the stabilized probe laser to the NRC optical frequency comb has enabled us to count the cycles of radiation and compare the single ion frequency relative to the NRC ensemble of Cs atomic clocks and hydrogen masers. Recent results show that the accuracy of the present results appears to be primarily limited by the current realization of the SI second at our laboratory (2 × 10⁻¹⁴).

* This work is being supported by NRC, CIPI/ICIP.

TU-A14-6 12h15

*High Resolution Laser Spectroscopy of CCO in the C-C and C-O Stretching Regions**, Nasser Moazzen-Ahmadi and Z. AbuSara, *The University of Calgary* — Spectroscopic information regarding the energetics of the electronic states of CCO is essential for establishing the most likely reaction mechanisms in combustion, interstellar clouds, and photodissociation dynamics of carbon suboxide. For example, the photodissociation of C₃O₂ (with ¹Σ⁺ ground electronic state) is still the subject of considerable debate. The question of which electronic state, X³Σ⁻ or $\hat{a}^1\Delta$, the CCO fragment will be in after the dissociation of C₃O₂ still remains unanswered. Over the past few years, studies by our group have resulted in the observation of 10 vibrational bands of CCO in the C-C and C-O stretching fundamental regions. Over 1000 transitions belonging to eight vibrational bands in the ground electronic state and two in the metastable electronic state $\hat{a}^1\Delta$, have been measured. The data were analysed to obtain the most comprehensive set of spectroscopic parameters for the stretching bands of CCO. Because the vibronal bands of X³Σ⁻ and $\hat{a}^1\Delta$ overlap, it is possible to obtain time resolved data on the singlet and the triplet species of CCO and to determine the electronic state of the CCO fragment after the dissociation of C₃O₂. In this talk, I will discuss the analysis of the data as well as some future directions.

* This work is being supported by NSERC.

12h30 Session Ends / Fin de la session

[TU-A15] News from Space - The MOST Satellite / Nouvelles de l'espace - Le satellite MOST

(CASCA)

**TUESDAY, JUNE 15
MARDI, 15 JUIN
10h15 - 11h00**

[Room/Salle : Campaign B]

Chair: C. Robert, U.Laval

TU-A15-1 10h15

JAYMIE MATTHEWS, University of British Columbia

Space Science in a Suitcase: Early Results from MOST

Viewing the Universe in new ways has always yielded surprising discoveries. Astronomers are accustomed to extending the limits of wavelength coverage, light-gathering power, and angular resolution. The MOST (Microvariability & Oscillations of STars) space instrument - an optical photometer of small (15-cm) aperture which deliberately blurs its stellar images for stability - forges its advances in totally different regions of parameter space. MOST is the only existing observatory which can monitor stars several times per minute with almost no interruptions for weeks at a time, reaching photometric precisions of a few micromagnitudes (ppm). This is at least 25 times better than ever achieved before from Earth or space. These demonstrated levels of time sampling and ultraprecise photometry enable the MOST Science team to explore with unprecedented sensitivity acoustic (p-mode) oscillations and granulation behaviour in other stars, reflected light from giant close-in exoplanets, and other phenomena associated with stellar variability. I will summarise the first year of the MOST mission, including results on Sun-like stars such as Procyon and beta Virginis, a "young" counterpart to the Sun (κ 1 Ceti), newly discovered pulsators caught in the nets of MOST's Secondary Science and Guide Star fields, and — I expect, by the time of this meeting — a few other surprises.

11h00 Session Ends / Fin de la session

[TU-A16] Young Investigators in Medical and Biological Physics, Part II / Jeunes chercheurs(es) en physique médicale et biologique II
(COMP-DMBPI
OCPM-DPMB)
**TUESDAY, JUNE 15
MARDI, 15 JUIN
10h30 - 12h00**

[Room/Salle : Albert]

Chair: J.P. Bissonnette, Princess Margaret Hospital

TU-A16-1 10h30

Absolute Volume Estimation from 3D Hyperpolarized Xenon Images: a Monte Carlo and Phantom Study*. Steven White¹, A. Cross² and G. Santyr¹, ¹ Carleton University and ² University of Lethbridge — The development of hyperpolarized ³He and ¹²⁹Xe has made it feasible to image gas spaces in the body as well as provide functional lung information using nuclear magnetic resonance imaging (MRI) systems. The purpose of this study was to ascertain the feasibility of measuring gas volumes with fast 3D imaging of hyperpolarized xenon (H-Xe) gas. Voxel intensities in MRI are usually estimated by calculating the magnitude of the real and imaginary components in a 3D data set. Each component is degraded by Gaussian distributed noise, and as a result of the non-linear square-root operation, the intensity noise is Rice-distributed. While most segmentation analysis attempts to distinguish between two signals at high signal-to-noise ratios (SNR) using Gaussian statistics, in gas space imaging the analysis must distinguish between background noise and the ¹²⁹Xe signal. As such H-Xe images have a continuum of SNR ranging from zero to the SNR of filled voxels, requiring consideration of the Rice distribution. Numerical methods have been developed to estimate MRI signal intensities based on the expectation curve for a Rice distribution at the appropriate SNR. Monte Carlo simulations and *in vitro* phantom work show that in images with little or no partial volume effects, the conventional magnitude and Rician estimators yield equivalent results. However, in images dominated by partially filled voxels the conventional estimator under-estimates low SNR voxels, and subsequently, gas volume, while the Rician estimator yields significantly more accurate results.

* This work is being supported by NSERC.

TU-A16-2 10h45

Doppler Optical Coherence Tomography for Monitoring Anti-Cancer Therapies*, Maggie L. Gordon¹, Victor X.D. Yang¹, Brian C. Wilson^{1,2,3,4}, I. Alex Vitkin^{1,2,3}, ¹ University of Toronto, ² Ontario Cancer Institute / Princess Margaret Hospital, ³ University Health Network, ⁴ Photonics Research Ontario — Doppler optical coherence tomography (DOCT) is a novel imaging technique that permits high-resolution structural and functional imaging in intact tissues. DOCT is an optical analog to Doppler ultrasound imaging, a familiar clinical tool. We have constructed a DOCT system that is capable of high-resolution (~ 15 μ m) structural imaging to depths of about 2 mm in tissues. Subsurface blood flow detection has both high sensitivity (as slow as 30 μ m/s) and wide dynamic range (up to 10 cm/s). Our system has been used in a variety of biomedical and clinical contexts, including tadpole cardiac imaging and *in vivo* human gastrointestinal imaging during endoscopy. In addition to diagnostics, non-invasive DOCT, with its high spatial resolution, high blood flow sensitivity, low cost, and convenience, is a promising technology for *in vivo* monitoring of treatments of all kinds. Our group has looked at the subsurface microstructural changes caused by a cutaneous lymphoma and its response to electron radiation therapy. With the realization that angiogenesis is a critical factor in cancer progression and with the increasing clinical emphasis on anti-angiogenic treatments, DOCT may prove to be an important diagnostic and / or treatment monitoring tool in oncology. We have used DOCT to image the blood flow in cancerous and normal tissues before, during, and after photodynamic therapy and anti-vascular chemotherapy. It is feasible to use DOCT to monitor structural and functional changes during treatments and in the future, DOCT may enable real-time diagnosis and treatment adjustments

* This work is being supported by NSERC, CIHR, NCIC, CFI, PRO.

TU-A16-3 11h00

Scatter Tails in CT Single Scan Dose Profiles Measured with a Diamond Detector, Keith Nakonechny, B.G. Fallone and S. Rathee, Cross Cancer Institute, University of Alberta — Computed tomography dose index (CTDI) conventionally specifies the patient dose in CT studies. It is measured as the integration of the longitudinal single scan dose profile (SSDP) by using a 10 cm long pencil ionization chamber. The assumption that most of the SSDP is contained within the chamber length may not be valid even for thin slices. This assumption is based on SSDPs measured using TLDs in cylindrical phantoms of 15 cm length. In this work we introduce a new method of obtaining the SSDP. The SSDPs for two CT scanners were measured using a diamond detector (PTW Type 60003) in a 30 cm long CIRS phantom for several slice widths. The shape of one SSDP was verified using a pin-point ion (PTW Type 31006) chamber and LiF TLDs. Numeric integration and convolution methods were then applied to the SSDPs measured with the diamond detector to predict the relative accumulated dose. The integrals over 25 cm length of the SSDPs, measured along the phantom (rotational) axis, were approximately 25-30% higher than the integrals over 10 cm length for almost all slice widths on both scanners. This difference was up to 22% for off-axis points. Dose equilibrium along the phantom axis was only achieved for scan lengths >35 cm, suggesting the need for longer phantoms and new measuring techniques to account for the non-negligible dose in the extended scatter tails of the profiles.

TU-A16-4 11h15

Development of Novel Multi-Focus Acoustic Lens Transducer Systems for Ultrasound Thermal Therapy, Xia Wu¹, Arthur E. Worthington¹, John W. Hunt¹, Michael A.S. Jewett² and Michael D. Sherar^{1,3,4}, ¹ Department of Medical Biophysics, ² Department Surgery (Urology) and UroOncology Program, ³ Department Radiation Oncology, University of Toronto, ⁴ Division of Medical Physics, Ontario Cancer Institute and Princess Margaret Hospital — Ultrasound thermal therapy is a promising technique for noninvasive treatment of solid tumours. Focused ultrasound beams are delivered by an external applicator to the target site through overlying tissue layers. Thermal lesions are created in the target due to the energy deposited. The feasibility and safety of this treatment modality have been investigated in breast, liver, kidney, bladder and prostate. The drawback with conventional therapeutic ultrasound applicators is that treatment times are excessively long, because only small thermal lesions are created by these systems. Scanning is therefore required to cover the entire tumour volume. The treatment time, however, can be shortened if novel multi-focus applicators, such as phased arrays or lens transducer systems, are adopted because these applicators produce significantly larger thermal lesions. The lens system is an attractive approach because it is inexpensive and simple to manufac-

ture. We designed and built a prototype of 9-focus lens transducer system. Using this prototype system, we created large thermal lesions in freshly excised porcine kidney tissue. Since overlying tissue layers could potentially degrade the incident beams, preventing the formation of the multi-focus field, we performed experiments and computer simulations to investigate this effect. Results showed that the multi-focus field suffered negligible changes after traveling through representative porcine tissue layers (skin-fat-muscle-fat-muscle). This work indicates that the novel multi-focus lens transducer system may be a useful tool for ultrasound thermal therapy.

TU-A16-5 11h30

High Frequency Ultrasound Monitoring of Structural Changes in Cells and Tissues, A.S. Tunis^{1,2}, G.J. Czarnota^{3,4}, A. Giles², M.D. Sherar^{2,3}, J.W. Hunt^{1,2}, and M.C. Kolios^{1,4},
¹ Department of Medical Biophysics, University of Toronto; ² Ontario Cancer Institute, University Health Network; ³ Department of Radiation Oncology, University of Toronto; ⁴ Department of Mathematics, Physics and Computer Science, Ryerson University — To monitor cell structure changes *in vitro* and *in vivo*, we investigate the use of probability density function fits to histograms of the high frequency ultrasound (HFUS) backscatter signal envelope. To evaluate the technique *in vitro* we first examine cell pellets formed with a mixture of acute myeloid leukemia cells treated with cisplatin (a chemotherapy drug) and untreated cells. Pellets were formed with concentrations of 0% to 100% treated cells; following data acquisition pellets were fixed for histology. To evaluate the technique *in vivo* we examine non-Hodgkin's Lymphoma tumours implanted in mice and monitor the response to chemotherapy up to 96 hours. Following data acquisition, animals were sacrificed and tissue taken for histology. Images and radio frequency (RF) data were collected from 100 independent locations within the cell pellet and the tumour tissue using a HFUS imaging device (VisualSonics VS-40B) with a 20MHz f#2.35 transducer. Simulated RF data was generated to model the pellet data. The envelope of the RF data was computed using the Hilbert transform method; and the Rayleigh and generalized gamma (GG) probability density functions were fit to the data using the maximum likelihood method, with goodness of fit evaluated by the Kolmogorov-Smirnov test. Results indicate that the GG fit parameters are sensitive to the changes that occur to cell structure during cell death. The changes to the fit parameters are in agreement with theoretical predictions and respond to changes in cell structure both *in vitro* and *in vivo*. Further development of the simulations will provide insight into the origin of the changes to the statistics.

TU-A16-6 11h45

Three Dimensional Ultrasound and Stereotactic Mammography Guided Biopsy: a Dual Modality System*, Kathleen J.M. Surry, Greg R. Mills, Donal B. Downey, Aaron Fenster, *Imaging Research Laboratory, Robarts Research Institute* — A three-dimensional ultrasound-guided biopsy system was developed to be integrated with, and to supplement stereotactic mammography (SM) imaging. Our goal is to be able to biopsy a larger percentage of suspicious masses using ultrasound (US), by clarifying ambiguous structures with mammographic imaging. Features from SM and US guided biopsy were combined, including breast stabilization, a confined needle trajectory and dual modality imaging. The 3D US guided biopsy system was designed to be mounted on an upright mammography machine for pre-procedural SM imaging. Intra-procedural targeting and guidance was achieved by real-time 2D and near real-time 3D US imaging. Post-biopsy 3D US imaging allowed for confirmation that the needle was penetrating the target. We evaluated the ultrasound guided biopsy accuracy of our system using breast phantoms. Our system was capable of placing the needle tip with 0.85 mm accuracy at a target identified in the 3D image. We also showed that 3.2 mm diameter lesions could be biopsied with a 96% success rate, *in vitro*. In order to use mammographic imaging information, we registered the SM and 3D US coordinate systems. The 3D positions of targets identified in the SM projection images were determined with a target localisation error of 0.49 mm. SM imaging was then registered to 3D US, with a target registration error of 0.98 mm. As an adjunct to stereotactic mammography, this 3D US guided biopsy system provides more complete imaging information for target identification as well as real-time monitoring of needle insertion and biopsy success.

* This work is being supported by CIHR Doctoral Fellowship.

12h00 Session Ends / Fin de la session

| | | |
|---------------------|---|--|
| [TU-A17] (CASCA) | CASCA-RAS J.S. Plaskett Medal Lecture / Conférence de la Médaille J.S. Plaskett de CASCA-SRA | TUESDAY, JUNE 15 MARDI, 15 JUIN 11h00 - 11h45 |
|---------------------|---|--|

[Room/Salle : Campaign B]

Chair: R. Taylor, U.Calgary

TU-A17-1 11h00

JO-ANNE C. BROWN, University of Calgary

The Magnetic Field in the Outer Galaxy

Observations of synchrotron radiation demonstrate that galaxies have magnetic fields. Our own Galaxy is no exception. The Galactic magnetic field is thought to play a role in both matter and cosmic ray confinement, and hence in overall pressure balance. It is not known how the magnetic field of our Galaxy is generated, nor what its overall structure is. Determining the large scale structure would help identify the origin of the field. Magnetic field reversals (regions of magnetic shear across which the field direction changes by 180 degrees) provide important clues about this large scale structure. Superposed on the large scale magnetic field are smaller scale fluctuations (on the order of 50 parsecs) related to localised motions in the interstellar medium (ISM). In magnetohydrodynamic (MHD) models of the ISM, the assumption is usually made that these small scale fluctuations are isotropic with respect to the large scale field. The polarisation angle of linearly polarised radiation rotates in a predictable way as it propagates through a magnetized plasma. The process, known as Faraday rotation, is characterized by the measurable quantity of rotation measure (RM), which is determined as the slope of the graph of polarisation angle versus the square of the wavelength. By measuring the RM of polarised compact sources (pulsars, external galaxies, and quasars), we are essentially probing the magnetic field along their lines-of-sight; the more probes there are, the easier it is to reconstruct the intervening field. As part of my thesis work, I calculated the rotation measure for 380 extragalactic sources in the Canadian Galactic Plane Survey (CGPS; $145 > l > 75, -3.5 < b < 5.5$), using the 21 cm polarisation data from the synthesis array at the Dominion Radio Astrophysical Observatory (DRAO). These sources have an average solid angle density of about 1 source per square degree - more than 10 times greater than any previous survey in the Galactic plane. Using these data, the primary goals of my thesis research were to identify reversals in the outer Galaxy (at galactocentric radii greater than that of the Sun), and to test the assumption of isotropy in the small scale field. In my talk I will review my PhD work, with a specific focus on the questions I addressed, their significance, and the conclusions I was able to reach. I will end with an outline of my more recent work which builds on my PhD studies, by exploring the magnetic field in other parts of the Galaxy.

11h45 Session Ends / Fin de la session

| | | |
|---------------------|--|--|
| [TU-A18] (CASCA) | Imaging in the Submillimetre Window - contributed / Imagerie dans la fenêtre sous-millimétrique - contribuées | TUESDAY, JUNE 15 MARDI, 15 JUIN 11h45 - 12h30 |
|---------------------|--|--|

[Room/Salle : Campaign B]

Chair: P. Martin, U.Toronto

TU-A18-1 11h45

Cold Hydrogen Clouds in the Milky Way: An Evolutionary Missing Link?, Russ Taylor¹, S.J. Gibson¹ and S.T. Strasser², ¹University of Calgary and ²University of Minnesota — The high angular resolution of the International Canadian Galactic Plane Survey has revealed a wide-spread, cold atomic hydrogen component of the interstellar medium in the form of dark self-absorption cloud complexes. These clouds resemble molecular cloud complexes in structure and trace the spiral arm structure of the Galaxy. While they occupy an l, b, v space similar to that of CO clouds, there is no strict correlation between cold atomic hydrogen clouds and CO emitting gas. Nevertheless, continuum absorption studies show that some of the cold atomic hydrogen clouds have temperatures as low as 15–20 K – similar to dense molecular clouds. We examine the hypothesis that cold atomic hydrogen revealed by these observations represents a phase in the evolution of the ISM marking the transformation of warm diffuse atomic hydrogen gas to molecular clouds, perhaps triggered by compression from the passage of spiral arm density waves.

TU-A18-2 12h00

A Submm Survey of High-Redshift Clusters: A submm Butcher-Oemler Effect?*. Tracy Webb¹, H. Yee², H. Hoekstra² and M. Gladders³, ¹Leiden Observatory; ²University of Toronto and ³Carnegie Observatories — We present the first results of a submm survey designed to investigate star-formation in high-redshift clusters. Recently, an excess of submm-luminous galaxies (SMGs) in high-redshift cluster fields has been reported. If real, this excess can be attributed to an exceptionally high lensing cross-section for a subset of high-redshift clusters, or as an increase in the number of dusty star-forming galaxies in clusters at higher redshift. This second scenario is essentially a submm Butcher-Oemler effect, perhaps due to accretion of field galaxies, or major cluster mergers. To verify the excess of SMGs and to differentiate between the two scenarios, we have begun a submm survey using SCUBA at JCMT of a sample of $0.6 < z < 1.1$ clusters drawn from the Red-Sequence Cluster survey. We have selected clusters which show multiple strong optical arcs, and a control sample of equally rich clusters which do not exhibit strong lensing. We will discuss the preliminary results and implications of the survey, based on the first half of the sample.

* This work is being supported by Leiden Observatory.

TU-A18-3 12h15

Sub-Millimetre Science With the New Generation of Total-Power CCD-Style Bolometer Arrays, Colin Borys, *California Institute of Technology* — The development of close-packed bolometric arrays was responsible for a renaissance in sub-millimetre astronomy. Highly successful imaging campaigns using the SCUBA and MAMBO cameras have discovered a cosmologically significant population of dust enshrouded galaxies that contribute as much to the energy density of the Universe as optical light. Within our own galaxy, sub-mm surveys reveal sites of vigorous star-formation that are practically invisible otherwise. The next step in detector development follows a common theme in astronomy: large format cameras with a wide field of view and increased detector sensitivity. However unlike most optical CCDs, the new generation of sub-mm cameras also have to contend with a paradigm shift in data reduction approaches in addition to new detector technologies. Here I report on the trials and triumphs with the first facility, total-power CCD style sub-mm camera: SHARC-II. Commissioned at the Caltech Submillimeter Observatory in 2003, SHARC-II now routinely detects objects both at high redshift and locally. The data acquisition and image reduction approaches are similar to what will be required for the next leap in CCD-style sub-mm cameras: SCUBA-2. Canada plays a strong role in developing this instrument, and for good reason: with its unprecedented field of view and mapping speed, SCUBA2 will dramatically improve our understanding of the sub-mm Universe.

12h30 Session Ends / Fin de la session

[TU-A19] ALMA Information Session / Session d'information sur l'ALMA

(CASCA)

TUESDAY, JUNE 15

MARDI, 15 JUIN

12h30 - 13h30

[Room/Salle : Campaign B]

Chair: C. Wilson, McMaster U.

[TU-P1] Radiobiology and Tissue Characterization /
Biologie radiologique et caractérisation des tissus(COMP-DMBP/
OCPM-DPMB)

TUESDAY, JUNE 15

MARDI, 15 JUIN

13h15 - 14h15

[Room/Salle : Albert]

Chair: D.E. Wilkins, Ottawa Regional Cancer Centre

TU-P1-1 13h15

Parameter Correlation for a Fully Heterogeneous Tumour Control Model, Marco Carlone, David Wilkins, Balazs Nyiri and G. Peter Raaphorst, *Ottawa Regional Cancer Centre* — There has been considerable interest lately in using clinically measured tumour control data to estimate radiobiological parameters for the linear quadratic model. It is likely that this practice will become more important in the future since there is increasing interest in biologically based treatment planning for radiotherapy. In a previous publication (Carlone et al, *Med. Phys.* **30**, pp. 2832-2848), we introduced a scaling theory to simplify a tumour control model that includes a heterogeneous distribution of radiosensitivity. This scaling theory is further developed in this work. The enhanced theory forms the basis of a procedure that can be used to estimate radiobiological parameters using a heterogeneous tumour control model without construction of a fit statistic, or the subsequent minimization of a statistical function. This procedure yields equivalent parameter estimates as other, statistically based methods, but with a computational efficiency several orders of magnitude faster than the statistically based method. This improved theory also shows that when modeling clinical data with a population tumour control model, the slope of the correlated parameters, a and $\ln(k)$, is an estimate of the reciprocal of the dose of 50% tumour control. This result shows that a bias in estimates of radiobiological parameters will be introduced depending on the mean survival level of the clinical data. It is also shown how the same form of parameter scaling can be applied when the tumour control model is expanded to the general case, which includes inter-patient heterogeneity in clonogen number and tumour growth rate.

TU-P1-2 13h30

Radiation Energy Deposition Calculations using Monte Carlo Simulations in K-shell X-ray Fluorescence Bone Lead Measurements*, Naseer Ahmed¹, David E.B. Fleming¹ and Joanne M. O'Meara², ¹Mount Allison University and ²University of Guelph — Recent applications of K-shell x-ray fluorescence (KXRF) bone lead measurement have used a shorter source-to-sample (S-S) distance than the traditionally used standard value of 20mm, in order to improve measurement precision and decrease minimum detectable limit. This alteration to the standard S-S distance has been made without consideration of the impact on the subject dose. Therefore, Monte Carlo simulation has been used to calculate the energy deposition in a soft-tissue/bone model, simulating the lower part of the leg during KXRF bone lead measurements. The simulations were run for models representing both young and adult subjects, assuming lead concentrations of 10 µg/g in bone and tracing 500 million photons in each simulation. Trials were performed over a wide range of 5–40 mm source to sample (S-S) distances. The energy deposition due to the Compton and the photoelectric (for both x-ray and non x-ray events) processes occurring in the bone and the soft tissue are presented. The ratios of the energies deposited in the bone and in the soft tissue with respect to the total energy deposited in the sample are calculated. Potential implications for the choice of an appropriate source-sample distance in KXRF bone lead analysis are discussed.

* This work is being supported by NSERC.

TU-P1-3 13h45

Monitoring the Response of Mycosis Fungoides to Total Skin Electron Irradiation with Optical Coherence Tomography, Joseph E. Hayward¹, Pawel P. Malysz¹, Glenn W. Jones¹, Maggie L. Gordon², Victor X.D. Yang¹, I. Alex Vitkin^{2,3}, ¹Juravinski Cancer Centre, ²University of Toronto and ³University Health Network — Optical coherence tomography (OCT) is a novel imaging technique that is like ultrasound imaging with light waves, as opposed to sound waves. OCT can acquire subsurface images of tissues with microscopic resolution (~ 15 µm). Microstructural information can be obtained up to ~ 2 mm in depth in tissues like skin. Imaging is completely non-destructive and can be done without touching the tissue surface. Mycosis fungoides (MF) is a cutaneous T-cell lymphoma that is commonly treated with total skin electron irradiation (TSEI). The subsurface margin of the disease beyond the superficial lesion edge is unknown, and its regression dynamics during and following TSEI are poorly understood. The purpose of this study was to determine whether OCT is capable of MF lesion characterization and radiation treatment response monitoring in a selected group of patients undergoing TSEI. Several patients were imaged with OCT before, during, and after TSEI. Similar to histological analysis, it was observed that OCT images of MF lesions usually appeared less structured than MF images of normal, healthy skin. In one patient, OCT images of normal-looking skin had the disordered characteristics of MF lesions. Weeks later, the previously normal-looking area had become part of a large MF lesion, suggesting that OCT may be useful for predicting the subsurface spread of MF.

TU-P1-4 14h00

Identification of Breast Specimens via Low-Angle X-Ray Scatter Measurements with a Digital Imaging System*. Robert LeClair, *Laurentian University* — The information carried by the x rays diffracted from breast specimens could be useful for diagnosing breast cancers. Our research program is focused on determining whether we can identify breast biopsy specimens (e.g. malignant tumor, benign tumor, normal breast tissue) via the use of a pencil beam delivery/low angle x-ray scatter digital imaging system. Suppose we wish to measure the scatter profiles of 5 mm thick samples of carcinoma and fibro-glandular tissue with a 2 in by 2 in charged coupled device (CCD) camera using a 30 kV beam. Each sample is sequentially placed at 2 in above the center of the CCD and interrogated by a 1 mm diameter pencil beam. For an entrance exposure of 120 mR, the signals simulated with scatter between 13 and 15 degrees give a false negative probability of 1.7×10^{-11} and a false positive one of 2.3×10^{-10} . These small values encourage us to quantify the potential applications of the scatter technique. Experimental data obtained for plastics with our digital specimen radiography system indicate that the dark current is too high to acquire diffraction signals. Therefore work is under way to cool our detector. The predicted probabilities quoted above are based upon using preliminary diffraction data from the literature. In our lab, we are in the process of measuring the x-ray diffraction signals of all breast tissue types via energy dispersive x-ray diffraction measurements.

* This work is being supported by NSERC and CIHR, Institute of Cancer Research.

14h15 Session Ends / Fin de la session

[TU-P2] Microimaging / Microimagerie

(COMP-DMBP/
OCPM-PPMB)TUESDAY, JUNE 15
MARDI, 15 JUIN
13h15 - 14h00

[Room/Salle : Victoria]

Chair: A. Pejovic-Milic, Ryerson U.

TU-P2-1 13h15

Localization of Neural Activity in the Human Brain*. Kevin Whittingstall and G. Stroink, *Dalhousie University* — With recent technological advances, there has been a great effort put into the non-invasive localization and imaging of neural activity in the human brain. Tools such as the electroencephalogram (EEG) and functional magnetic resonance imaging (fMRI) measure electrical activity at the scalp and change in hemodynamic activity, respectively. fMRI activity can be investigated via visual inspection of the MR images, whereas the localization of EEG activity is estimated by solving the so-called inverse problem. Factors such as head and source modeling errors can lead to significant localization errors and therefore need to be resolved before a direct comparison between the sources of the EEG and fMRI are made. Although the EEG and fMRI measurements are sensitive to completely different physiological phenomena, their origins are thought to be closely co-localized. The EEG and fMRI activity from several healthy subjects was measured sequentially using the same visual stimulus for both experimental sessions. Topographic maps of the measured electric potential due to stimulus onset were constructed. Using a dipolar source model along with a realistic model of the subject's head, an inverse solution was solved using the Boundary Element Method (BEM). These sources were then compared to the peak fMRI activity of the same subject on the MR image. Preliminary results show that reconstructed dipolar sources are near the location of peak fMRI activation. This suggests a relationship between the localization of neural and hemodynamic activity in humans.

* This work is being supported by NSERC.

TU-P2-2 13h30

Visualizing Myelin Disorders *In Vivo*. Melanie Martin¹, Samuel D. Reyes², Robin Fisher², Anthony T. Campagnoni², Timothy D. Hiltner³, J. Michael Tyszka³, Scott E. Fraser³, Russell E. Jacobs³, Carol Readhead³, ¹ *California Institute of Technology*, ² *UCLA Medical School* and ³ *Caltech* — Our objective was to follow the course of myelin diseases in transgenic mice using non-invasive high-resolution (50 μm – 150 μm) magnetic resonance (μMRI) and Visually Evoked Potential latency (VEPL) techniques. Data presented are from three mutant mouse models. The shiverer, with little or no CNS myelin, has a significantly longer VEPL ($39 \pm 1\text{ms}$) than wildtype mice ($30 \pm 2\text{ms}$). Consistent with this significant difference ($p < 0.0001$), clearly visible changes in the T2-weighted μMR images (T2WI) are seen. A second mouse model, (MBP::J37) ectopically over expresses a variant of a myelin basic protein gene. We followed individual MBP::J37s and their unaffected siblings from 21 until 73 days old using VEPLs and 3D T2WI on an 11.7 T scanner. When myelination is not yet complete all mice show an increased VEPL as compared to a mature, fully myelinated mouse. The μMRI , and the VEPL and histological data, show global a delay of CNS myelin development and persistent hypomyelination in mature MBP::J37. Their VEPLs were close to normal and their tremor had abated. The third mouse model develops Experimental Allergic Encephalomyelitis relapsing-remitting disease course. VEPL measurements and T2WI show varying results between animals even within the same disease stage confirming that it is important to follow the same subject through a disease course in order to find a relationship between symptomology and pathology. These data support the potential of using MRI to follow demyelinating lesions *in vivo* to determine the exact relationship among VEPs and lesions.

TU-P2-3 13h45

Molecular Imaging using an Orthogonal-Injection Time-of-Flight Mass Spectrometer with a Matrix-Assisted Laser Desorption Ionization Source*. Werner Ens, G. Piyadasa, J.R. McNabb, V. Spicer and K.G. Standing, *University of Manitoba* — An orthogonal-injection MALDI TOF instrument is well-suited for obtaining mass-selected 2d images from tissue sections because the source is decoupled from the mass measurement. The mass spectral quality is thus independent of variations in sample properties (such as thickness), and the target may be held at low voltage and in a modest vacuum. Moreover it allows greater flexibility for the incident laser optics and also allows the possibility to perform MS/MS measurements on selected peptides or proteins. We have constructed a new MALDI source for orthogonal TOF in which the ions are ejected perpendicular to the axis of the collisional cooling ion guide. This allows normal incidence for the desorbing laser, and much closer placement of the final focusing optic, both of which are essential for high-resolution imaging. Desorbed ions are drawn into the ion guide by gas flow. For the present experiments, a high-repetition rate Nd-Yag laser is coupled to a 10-micron optical fibre. The output is imaged one-to-one on the sample and rastered at a uniform rate to obtain an image. A continuous data log of flight times is acquired along with real-time markers to coordinate the position of the laser spot. The source and software have been tested with a 500 lines-per-inch grid, coated with angiotensin and placed on a target coated with C60. Mass selected images for both species clearly show spatial resolution of 10 microns or better. With a 500 Hz repetition rate laser, the images can be acquired at 10 pixels per second, although with tissue samples, the rate will likely be determined by the abundance of the protein of interest. Preliminary images of small proteins up to m/z 4000 have been obtained at this rate from some plant tissues. The limits of spatial resolution of imaging MALDI will be tested by focusing the laser directly onto the target with a lens placed about 1 cm from the surface. This is expected to produce spot sizes less than 2 microns in diameter.

* This work is being supported by Genome Canada.

14h00 Session Ends / Fin de la session

[TU-P3] CAP Herzberg Medal Winner /
Récipiendaire de la médaille Herzberg de l'ACP

(CAP/ACP)

TUESDAY, JUNE 15
MARDI, 15 JUIN
13h30 - 14h15

[Room/Salle : Ballrooms B/C]

Chair: B. Joos, U.Ottawa

TU-P3-1 13h30

VICTORIA M. KASPI, McGill University

Revolutions in Neutron Star Astrophysics

Neutron stars, like their black hole cousins, embody physics of the extreme: their physical properties and environments are not merely unrealizable in Terrestrial laboratories but indeed are extreme even when compared with the known Universe's vast zoo of bizarre objects. Interestingly, research into neutron stars has been punctuated, arguably more so

than in any other astrophysical field, by surprising "revolutions," in which major unpredicted and/or unexpected discoveries shock even the most seasoned of scientists. In this talk, we discuss some of the most recent major discoveries, including the existence of "magnetars," young neutron stars having Universal record-holding magnetic field strengths, as well as the very recent discovery of the first double pulsar system, and its amazing radiative and relativistic properties.

14h15 Session Ends / Fin de la session

[TU-P4]

**Young Investigators in Condensed Matter Physics I /
Jeunes chercheurs(es) en physique de la matière condensée I**

(DCMMP/IDPMCJM)

TUESDAY, JUNE 15

MARDI, 15 JUIN

14h15 - 16h45

[Room/Salle : Ballrooms B/C]

Chair: H. Kreuzer, Dalhousie U.

TU-P4-1 14h15

ROBERT WICKHAM, St. Francis Xavier University

Kinetics of Self-Assembly in Block Copolymer Melts

The ability of block copolymer melts to spontaneously organize, or self-assemble, into structures on a scale of tens of nanometers makes these materials attractive for applications requiring such resolution, such as nanofabrication and lithography. When processing these materials it is important to understand the mechanisms and timescales involved in the formation of these structures, that is, the kinetics of self-assembly. The kinetics of nucleation at order-order transitions, where a metastable structure overcomes an energetic barrier and decays by nucleating a droplet of the stable structure is a topic of current interest. I will discuss recent theoretical developments that have enabled the calculation of the critical nucleus size and shape, and the size of the nucleation barrier for the lamellar-to-cylinder and sphere-to-cylinder transitions in diblock copolymer melts. In general, the nucleus shape is non-spherical due to an anisotropy in the free-energy for interfaces between structures of different symmetry. I will compare these results with relevant experiments and discuss future directions.

TU-P4-2 14h45

COLIN DENNISTON, University of Western Ontario

Dynamic Boundaries In Complex Fluids

In a simple fluid the boundary between the fluid and any solid surface is normally a static quantity defined by boundary conditions given at the beginning of the problem. Complex fluids, however, allow greater control of interfacial phenomena via the extra degrees of freedom associated with their internal structure and composition. I will illustrate how this allows the boundary conditions to be manipulated both spatially and temporally. This effect can then be used to design microfluidic and optical devices.

15h15 Coffee Break / Pause café

TU-P4-3 15h45

MARIA KILFOIL, McGill University

Consequences of Being Soft: Equilibrium Concepts in Nonequilibrium, Soft Materials Using Real Space Imaging

'Soft' condensed matter refers to the very small elastic constants — typically nine to ten orders of magnitude smaller than those of atomic and molecular solids — conferred to these materials by their large mesoscopic basic building blocks: colloids, polymers, and biomolecules are examples. These materials are easily driven out of equilibrium. They may also be "quenched" to form nonequilibrium structures through the introduction of an interparticle attraction that is strong relative to the thermal energy. One of the unifying aspects of this research is the search for ways to extend well-developed ideas of statistical mechanics to non-equilibrium systems. In this talk, I will discuss our recent experiments using colloidal systems as models for atoms, and real space imaging for full three-dimensional structure, using this data to measure spatial correlations over time. I will present experimental measurements of translational order in colloidal gels of PMMA colloids with polymer added to induce a controlled attraction. These results are the first to quantify the microscopic disorder in non-equilibrium solids using model colloidal systems. In doing so, I will introduce a new translational order parameter that is sensitive to long range order in these non-random packings, and should be sensitive to a changing characteristic length scale with age, and, importantly, is also sensitive to anisotropy. I will further show the first experimental measurements of the equation of state in a system with short range attractions using the same colloid-polymer model system.

TU-P4-4 16h15

IAN G. HILL, Dalhousie University

Contact Resistance in Organic Thin-Film Transistors

Organic electronics have reached the early stages of commercial viability. Personal electronic devices incorporating small displays based on organic light emitting devices (OLEDs) are now available. Many key challenges still remain, however, which are currently hindering wide-ranging adoption of organic electronic devices. Shortcomings of present day devices include, but are not limited to, poor charge carrier mobilities, high contact resistance at metal/organic interfaces, poor device stability and a lack of inexpensive patterning techniques that do not degrade the electrical properties of the organic films. Organic thin-film transistors (OTFTs) exhibit performance similar to their amorphous silicon (a-Si) counterparts, leading many researchers to suggest that OTFTs may replace a-Si as the technology of choice for active-matrix display backplanes. OTFTs can be fabricated on flexible, plastic substrates that may enable continuous roll-to-roll fabrication. Such techniques can be more than an order of magnitude less expensive than traditional batch processing of glass-based a-Si devices. Recent studies have cited evidence of large source/drain contact resistance in OTFTs. This resistance may limit the current-carrying ability of the devices, lead to underestimates of important device parameters, such as the semiconductor mobility, and restrict their utility in active-matrix backplanes, due to the resulting R-C charging time of an individual pixel. The evidence of contact resistance, and its interpretation, will be presented and discussed in the context of metal/organic interface formation. Recent results of physical device simulations will be presented and compared with published data.

16h45 Session Ends / Fin de la session

[TU-P5]

**The Energy Frontier in Particle Physics / La frontière de l'énergie en
physique des particules**

(PPD)

TUESDAY, JUNE 15

MARDI, 15 JUIN

14h15 - 17h30

[Room/Salle : Campaign A]

Chair: PW. Krieger, U.Toronto

TU-P5-1 14h15

KOSTAS KORDAS, University of Toronto

Recent Results From The Collider Detector At Fermilab

The Tevatron collider at Fermilab is currently providing collisions of protons and anti-protons at a center-of-momentum energy of 1.96 TeV, which is the highest energy ever studied. The Collider Detector at Fermilab (CDF) is one of the two multipurpose detectors observing the outcome of such collisions. After the major upgrades to the collider and the

detectors, the Fermilab "Run II" period of operations is well underway. The CDF II collaboration is collecting physics-quality data for the last two years and has now at hand a dataset which is more than a factor of four larger than the one used to establish the existence of the top quark in 1995. The key upgrades and the performance of the CDF detector will be presented briefly. The bulk of the talk will be devoted to the discussion of recent results from the CDF II collaboration, with an emphasis in the areas where the Canadian group is contributing. Finally, the prospects for several other interesting measurements will be discussed.

TU-P5-2 14h45

RACHID MAZINI, University of Toronto

The ATLAS Detector Physics Potential

The high energy and high luminosity of the LHC pp collider should offer a very rich physics programme. The Standard Model Higgs boson should be discovered over the full range of allowed masses, and its mass and coupling parameters should be measured with a sufficient accuracy. Theories beyond the SM, such as Supersymmetry, Technicolour, new gauge bosons, compositeness and Extra dimensions will also be probed. Several precision measurements will be made in the B-physics sector, in the top sector and in the electroweak sector (W mass, Triple Gauge Couplings, etc.) leading to significant improvements on the precision achieved by previous experiments. This talk will highlight some of the recent studies performed by ATLAS in the context of new theoretical development and detector performance studies.

TU-P5-3 15h15

FRANCOIS CORRIVEAU, IPP/McGill University

Recent ZEUS Results at HERA

The ZEUS experiment at the HERA accelerator observes collisions of electrons with protons and pursues a wide range of studies on the structure of hadronic matter, QCD and several other phenomena. After the major 2001 upgrade of the HERA luminosity, the new experimental run is underway. The status of the machine will be briefly presented, followed by some of the most recent ZEUS results and an outlook at the long-range measurements.

15h45 Coffee Break / Pause café

TU-P5-4 16h15

Search for the Production of Single Top Quarks in High Energy Proton-Antiproton Collisions*, **B. Vachon**, DO Experiment, *Fermi National Accelerator Laboratory* — The top quark, the heaviest of all the known quarks that make up our Universe, was discovered at the Fermi National Accelerator Laboratory in 1995. In high energy proton-antiproton collisions, top quarks are predominantly produced in pairs via the strong interaction. The Standard Model of particle physics also predicts the electroweak production of events containing a single top quark. Due to its small expected cross-section and large background contamination, the production of single top quarks has never been observed. The Fermi National Accelerator Laboratory, near Chicago, is home of the highest energy proton-antiproton collider in the world. The Tevatron collider is the only facility in the world capable of directly producing top quarks. Given the current collision centre-of-mass energy and the considerable data sample foreseen, the production of single top events is expected to be observed for the first time at the Fermi National Accelerator Laboratory. The DO experiment is one of two large multi-purpose detectors recording the results of these high energy proton-antiproton collisions. A brief overview of the DO experiment will be presented. Details of the ongoing data analyses searching for evidence of single top quark production in the current data sample recorded will be discussed. Preliminary results and outlook will be presented.

* This work is being supported by Fermilab.

TU-P5-5 16h30

Measuring the W Boson Mass with CDF in Run IIa, **Oliver Stelzer-Chilton**¹, **William Trischuk**¹ and **Ashutosh Kotwal**², ¹*University of Toronto* and ²*Duke University* — The mass of the W boson is a fundamental parameter of the Standard Model. Through radiative corrections, the mass of the top quark and the W mass are connected to the mass of the Higgs boson, the last missing particle of the Standard Model. As the Higgs boson has not yet been observed experimentally, more precise measurements of the W mass and the top quark mass will further constrain the mass of the Higgs boson. At the Collider Detector at Fermilab (CDF), the W mass can be obtained from a binned maximum likelihood fit to the transverse mass spectrum. Over the last three years CDF has accumulated a high statistics dataset of leptonic W boson decays and we expect an even larger dataset to be collected by the end of this year. Since most of the systematic uncertainties involved scale with available data statistics, a substantial increase in precision on the measured mass can be achieved. This talk will present current studies on the W mass measurement in the muon decay channel and prospects for an improved measurement in Run IIa.

TU-P5-6 16h45

Searches for SUSY at D0*, **Roger Moore**, *University of Alberta* — The Fermilab Tevatron provides proton-antiproton collisions at 1.96 TeV centre-of-mass energy and unparalleled luminosity. The D0 experiment has been collecting data in this environment since early in 2001 and has now accumulated a dataset which exceeds that of previous Tevatron runs. This provides a unique opportunity to search for physics beyond the Standard Model including Supersymmetry (SUSY). I will present the status of SUSY searches at D0 with emphasis on the so-called "golden mode" of tri-lepton signatures of mSUGRA SUSY models.

* This work is being supported by NSERC.

TU-P5-7 17h00

Study of Jet Fragmentation for the Measurement of the Top Mass with CDF, **Simon Sabik**, *University of Toronto* — The measurement of the top quark mass is a vast and important effort in the Collider Detector at Fermilab collaboration. A large number of high energy scientists work on the many instrumental and analytical issues in order to improve this measurement, which will lead to a test of the Standard Model. I will present an overview of the top mass measurement analysis, while keeping an emphasis on the aspects in which I am most directly involved. I will discuss how the study of the fragmentation of jets leads to an improved jet energy calibration, which is crucial to a precise determination of the top quark mass.

TU-P5-8 17h15

Observation of a $|S|=1$ Baryon State at a Mass of 1.528-GeV in Quasi-real Photoproduction, **Ken Garrow**, *HERMES Collaboration/TRIUMF* — The predictions for exotic baryon states consisting of a five quark structure have existed for some two decades. Up until the past couple of years no evidence of such exotic ($uudd\bar{s}$) baryon configurations had been observed. Recently several photoproduction experiments and an experiment using the K^+Xe reaction have reported the observation of an exotic baryon state. In the HERMES experiment, using quasi-real photo-production on a deuterium target, a narrow baryon state has been observed in the $p\bar{K}_S^0 \rightarrow p\pi^+\pi^-$ decay channel. The HERMES contribution to the existing world's data set of this exotic baryon, now referred to as the q^+ , is the most accurate mass determination and the first indication of a finite width.

17h30 Session Ends / Fin de la session

[TU-P6]

**Particle Physics II /
Physique des particules II**

(DTP/DPT)

TUESDAY, JUNE 15

MARDI, 15 JUIN

14h15 - 17h00

[Room/Salle : Westminster]

Chair: M. Shegelski, UNBC

TU-P6-1 14h15

BHASKAR DUTTA, University of Regina

Minimal SO(10) Model for Neutrinos and Its Implications

The minimal renormalizable SO(10) models with one 10 and one 126 Higgs multiplet is considered. The primary goal is to reconcile the CKM CP violation with successful neutrino predictions. The most general type II and type I seesaw formula for neutrino masses that includes the effect of the right handed neutrino mass matrix are used. The potential problems and the solutions are discussed. The type I model is found to require an intermediate ν_R scale, which is lower than the standard GUT scale, however it is compatible with gauge coupling unification which happens around $10^{15.5}$ GeV and it requires a value of the super symmetry parameter $\tan\beta$ larger than 30 to be compatible with the present neutrino data. The phenomenological implications of both type I and II models for neutrino mixings, lepton flavor violation, lepton edms and leptogenesis are presented. These predictions provide a new way to test these models.

TU-P6-2 14h45

LUC MARLEAU, Université Laval

Revisiting the Skyrme Model

Proposed more than four decades ago, the Skyrme model was revived in the 80's in the context of the $1/N_c$ expansion and more recently, have regain attention since it could provide an explanation for newly discovered hadronic states. As a non-linear theory of pions, it provides an approximate description of hadronic physics in the low-energy limit. In this theory, the nucleon emerges as a non perturbative solution of the field equations, or more precisely as a soliton. It is also seen as a prototype model in various physical contexts (e.g. condensed matter, wrapped branes) where one could expect soliton solutions to occur. The original Skyrme Lagrangian is a naive extension of the non-linear sigma model consisting of a fourth-order field derivatives term. This is nonetheless sufficient to stabilize the soliton against scale transformations and to reach at least a 30% accuracy with respect to physical observables. In order to incorporate effects due to higher-spin mesons and improve the fit on most observables a number of alternative Skyrme-like models which preserved the form of the original Lagrangian while extending it to higher orders has been proposed and analyzed. We describe some of these extensions of the model and several attempts to obtain single- and multi-skyrmion solutions.

15h15 Coffee Break / Pause café

TU-P6-3 15h30

HOWARD TROTTIER, Simon Fraser University

Perturbation Theory for High-Precision Lattice QCD

Recent developments suggest that lattice QCD is now capable of few-percent calculations for a variety of important nonperturbative quantities. The main bottleneck slowing lattice results now is a lack of high-order calculations in (lattice) perturbative QCD. This talk will review the recent breakthroughs in lattice QCD, their implications for particle physics, and the essential role of perturbation theory in future progress.

TU-P6-4 16h00

ALAKABHA DATTA, University of Toronto

*Getting CP Violating Phase Information from $b \rightarrow d$ Penguins**

We present a method to extract CP violating phase using $b \rightarrow d$ penguin decays. This method can be used with many decay modes allowing for a clean measurements of the angles of the unitarity triangle. The method can also be turned around to measure new CP violating phases in the case where new physics affects only the $b \rightarrow s$ penguin decays.

* In collaboration with D.L. David London, University of Montreal.

TU-P6-5 16h30

RAINER DICK, University of Saskatchewan

Theoretical Aspects of Ultra-High Energy Cosmic Rays

After a brief review of the experimental facts, I will outline theoretical attempts to explain the origin of ultra-high energy cosmic rays. This will focus on top-down models involving the decay or collisional annihilation of super heavy dark matter particles. These models can be identified and differentiated by their anisotropy signatures, and (contrary to a common prejudice) domination of photon primaries need not be a generic prediction of top-down models. I will also outline a possible connection to black holes.

17h00 Session Ends / Fin de la session

[TU-P7]

Statistical Physics /
Physique statistique(DTP-DCMMP/
DPT-DPMCM)

TUESDAY, JUNE 15

MARDI, 15 JUIN

14h15 - 17h00

[Room/Salle : Victoria]

Chair: J. Patera, CRM/U.Montreal

TU-P7-1 14h15

IAN AFFLECK, University of British Columbia

*Field-Induced Phase Transition In Anisotropic Haldane Gap Antiferromagnetic Chains**

Integer spin antiferromagnetic chains, which exhibit the Haldane gap, undergo a zero temperature phase transition at a critical magnetic field at which the Zeeman energy equals the Haldane gap. This transition was shown to correspond to Bose condensation. In this seminar I will discuss this transition in the presence of anisotropic exchange interactions which change the transition to Ising type. The behavior of the energy and width of various excitations with field will be analysed using field theory, exact integrability and renormalization group techniques.

* In collaboration with F.H.L. Essler, Oxford University

TU-P7-2 14h45

IGOR HERBUT, Simon Fraser University

Theory of Underdoped Cuprates as Strongly Fluctuating d-Wave Superconductors

I will discuss the general theory of two dimensional d-wave superconductors subject to strong quantum phase fluctuations. Such fluctuations arise due to Coulomb repulsion near half-filling in doped Mott insulator, and one may expect the theory to describe the underdoped high-temperature superconductors at low temperatures. The behavior of superfluid

density at both zero and finite temperatures will be addressed, in particular the vanishing of its slope at low temperatures due to a strong charge renormalization, one of the key predictions of the theory. In the spin sector, the theory leads to an intricate incommensurate-commensurate-incommensurate spin response with change of energy, and sheds new light on the famous 41 meV resonance in the superconducting state. Detailed comparison with the measurements on underdoped YBCO will be discussed.

References: I. Herbut, *Phys. Rev. Lett.* **88**, 047006 (2002); *Phys. Rev. B* **66**, 094504 (2002); I. Herbut and D. Lee, *Phys. Rev. B* **68**, 104518 (2003).

15h15 Coffee Break / Pause café

TU-P7-3 15h30

MASAKI OSHIKAWA, Tokyo Institute of Technology

Junctions of Three Quantum Wires and the Dissipative Hofstadter Model

A junction of three quantum wires enclosing a magnetic flux is studied. Each wire contains a one-dimensional Tomonaga-Luttinger liquid of spinless electrons. Unlike the junction of two wires, which has been well understood, Fermi statistics of electrons has non-trivial consequences for the present problem. We present a direct connection between this problem and the dissipative Hofstadter problem, or quantum Brownian motion in two dimensions in a periodic potential and an external magnetic field, which is also related to open string theory in a background electromagnetic field. We find non-trivial fixed points corresponding to a chiral conductance tensor. It implies an asymmetric flow of the current.

* In collaboration with C. Chamon¹ and I. Affleck², ¹ Boston University and ² University of British Columbia.

TU-P7-4 16h00

ANDRÉ-MARIE TREMBLAY, Université de Sherbrooke

Two Ways To Destroy A Fermi Liquid

The Fermi liquid concept is at the basis of much of our understanding of Solid State Physics. I will briefly review the main properties of a Fermi liquid and show that both electron and hole-doped high-temperature superconductors near their parent insulating phase are not Fermi liquids. Many probes, and especially photoemission, reveal the existence of a "pseudogap". I will argue that there are two ways to destroy a Fermi liquid. A strong- and a weak-coupling way. The latter is much better understood and applies to electron-doped high-temperature superconductors. One can even understand the origin of *d*-wave superconductivity in this limit.

TU-P7-5 16h30

YVAN SAINT-AUBIN, Université de Montréal

*Behavior of the Two-Dimensional Ising Model at the Boundary of a Half-Infinite Cylinder**

The two-dimensional Ising model is studied at the boundary of a half-infinite cylinder. The three regular lattices (square, triangular and hexagonal) and the three regimes (sub-, super- and critical) are discussed. The probability of having precisely $2n$ spinflips at the boundary is computed as a function of the positions k_i 's, $i = 1, \dots, 2n$, of the spinflips. The limit when the mesh goes to zero is obtained. For the square lattice, the probability of having $2n$ spinflips, independently of their position, is also computed. These results are obtained as consequences of Onsager's solution and are rigorous. In the special case of precisely 4 spinflips, we use conformal field theory to give a prediction for the following probability. Let $\theta_1, \theta_2, \theta_3$ and θ_4 be the positions of the flips along the boundary. We give the probability distribution that the contour leaving θ_1 ends at θ_2 instead than at θ_4 . The behavior of this function when $\theta_2 - \theta_1 \rightarrow 0$ is described by a power law with an exponent $(\frac{1}{3})$ that belongs to the Kac table but that corresponds to a non-unitarizable highest-weight representation. We check that this prediction agrees with a Monte-Carlo simulation.

* In collaboration with L.P. Arguin¹ and H. Aurag², ¹ Princeton University and ² CAE.

17h00 Session Ends / Fin de la session

| | | |
|-------------------------|---|---|
| [TU-P8] (DIMP/DPIIM) | General Measurement Physics / Physique des mesures générales | TUESDAY, JUNE 15 MARDI, 15 JUIN 14h15 - 16h45 |
|-------------------------|---|---|

[Room/Salle : Kildonan]

Chair: A. Mandelis, U.Toronto

TU-P8-1 14h15

MICHAEL C. KOLIOS, Ryerson University

Micrometer Particle Sizing Using High Frequency Ultrasound with Biological Applications

High frequency ultrasound imaging, using frequencies in the range of 20-60MHz and thus offering better resolution than conventional ultrasound (1-10MHz), has found applications in small animal imaging and the imaging of superficial human tumors. Recent work has shown that ultrasound parametric images based on the frequency dependence of ultrasound backscatter can be used to differentiate between normal and tumor tissue, and also between different tumors types. We have found ultrasound backscatter to increase with cell death (due to chemotherapeutic exposure or ischemic injury) at these frequencies, however the mechanisms responsible for the increase are not well understood. In order to better understand the physics of the interactions between ultrasound and particles in the micrometer range (such as eukaryotic cells), we have examined the ultrasound backscatter from 2-100 micrometer diameter polystyrene microspheres. Polystyrene microspheres can support shear waves, providing resonance rich spectra for the ka values of interest, as predicted by acoustic resonance spectroscopy. We show that using the broadband pulses used for imaging and by analyzing the backscatter from polystyrene spheres we can detect the resonances predicted. Gradients of 10dB/MHz were measured, in good agreement with theory. When the microspheres are embedded in cell pellets used to emulate tissues, the resonances could still be observed. Furthermore, we are investigating techniques using acoustic mirrors to near-simultaneously measure the forward-scatter and backscatter from these particles. This allows us to compare the signals with the theoretical values and obtain accurate measurements of particle size non-invasively.

TU-P8-2 14h45

A Capacitance-Based Detector for Monitoring Bumblebees. Jennifer M. Campbell¹, Randy L. Harper¹, Douglas C. Dahn¹ and Daniel Ryan², ¹ Department of Physics and ² Department of Mathematics and Statistics, University of Prince Edward Island — We have developed a new method for detecting and monitoring the foraging activities of bees. A small sensor is placed in front of the opening to a beehive. Bees pass between a set of electrodes, and are detected using a low-voltage high-frequency circuit that responds to the resulting change in the electrical capacitance. This poster describes the sensor, laboratory tests of the system, and preliminary field trials with bumblebees (*Bombus impatiens*). The sensor has significant advantages over existing bee activity monitors based on optical detection, such as the ability to distinguish between insects of different sizes. It can also be used to determine the direction (in or out), and the velocity of a bee. We expect it to be a valuable tool for researchers studying bees as pollinators of commercially important agricultural crops.

15h00 Coffee Break / Pause café

TU-P8-3 15h30

HANS D. HALLEN, North Carolina State University

Electric Field Effects in Nanoscale Raman Spectroscopy

The nanoscale metal object locally concentrates the electric field. As these evanescent fields decay on a nanometer length-scale, strong field gradients are produced. These gradients have profound effects on the Raman spectra of samples within them, leading to a "Gradient-Field Raman" (GFR) effect. It leads to new selection rules for surface enhanced Raman spectroscopy (SERS), and also to differences between far-field and near-field Raman spectroscopy measured with a metal-apertured near-field optical microscope (NSOM). We describe how a strong gradient of the electric field can alter the Raman spectra, and investigate its implications on selection rules. Heuristically, the field gradient causes the Coulomb force on a polarized bond to vary during the vibration, providing a new coupling mechanism between the field and the vibration. These selection rules differ markedly from the usual Raman selection rules, and allow Raman-like observation of strong IR (not normally Raman) vibrations. The presence of the metal probe near the Raman-emitting dipole also causes plasmons to be created on the tip. We show evidence of this by tracking Raman emission as a function of NSOM tip-sample distance.

TU-P8-4 16h00

Theoretical Estimates of the Solid Angle Subtended by a Dual Diaphragm-Detector Assembly for Alpha Sources. Eduardo Galiano¹ and J. Aguiar^{2,1} *Laurentian University and* ² *Comision Nacional de Energia Atomica* — A vertically oriented, dual opposed, diaphragm-detector assembly has been built for the calibration of circular, planar, α emitting radioactive sources. Knowledge of the solid angle subtended by the diaphragm-detector assembly is essential for the determination of the absolute activity of the sources. To accurately determine the subtended solid angle, the diaphragm diameter r , the source to diaphragm distance d , and the source diameter x , must all be known with an accuracy at least equal to that of the desired accuracy for the solid angle. The advantage of this geometry with respect to a conventional single detector is that for a given source to diaphragm distance, the geometric efficiency is doubled with an improvement in statistics. In this work, the influence of the geometric parameters r , d , and x , on the subtended solid angle are investigated. Expressions published by Segre, Ruby, and others, and the Monte Carlo method, are used^[1,2,3]. The analytical expressions consistently produced higher estimates than the Monte Carlo method for the subtended solid angle.

1. Burt, B.J., 1949. Absolute beta counting. *Nucleonics* 5, 28.2. Segre, E., 1959. *Experimental Nuclear Physics*, Vol III, pp. 435-438.3. Ruby, L., 1995. Further comments on the geometrical efficiency of a parallel disk-source and detector system. *Nucl. Instr. & Meth. Phys. Res. A* 337, 531-533.

TU-P8-5 16h15

The Quantum Origins of the NMR Signal: a Paradigm for Faraday Induction. David Hoult, *Institute for Biodynamics, National Research Council* — Since Dicke's classic 1954 paper, the pulsed NMR signal (FID) from a simple two-level quantum system (protons) has for most physicists been explained by coherent spontaneous emission (CSE, *i.e.* radio waves). Likewise, spin noise is supposedly caused by high-Q tuned circuit-enhanced spontaneous emission. Electrical engineers disagree, but are beaten into submission by the "big gun" of quantum mechanics. However, we have performed careful experiments where the FID was 100 x CSE's predictions and spin noise was easily detected with a circuit of Q-factor ~1. We have made little progress in formulating a full quantum theory, but interesting insights and philosophy have emerged. Faraday induction explains the results, but in an open circuit it takes no energy and so any involved photons can transfer no energy (c.f. Heisenberg on Bohr's atomic theory). Measuring the FID with a voltmeter needs and must cause (how?) directed energy to flow through space from nuclei to conductor. Now emission of real photons from an object moving at relativistic speeds bunches forwards (headlight effect). The electric field from a charge moving similarly (the genesis of magnetic fields and Faraday induction) bunches perpendicular to the motion - as do photons emitted with no energy but momentum (same formula): evidence that the NMR FID (and by extension Faraday induction) is caused by an exchange of virtual photons, not CSE. Pleasingly, by the Uncertainty Principle such virtual photons can travel of the order of a wavelength - exactly an engineer's criterion for distinguishing between induction and radio waves.

TU-P8-6 16h30

Modulation of Partial Internal Reflection at an Optical Interface*. Anne Liptak, M.A. Mossman, L.A. Whitehead, *University of British Columbia* — Frustrated total internal reflection (FTIR) is the well known phenomena in which the electromagnetic energy in the TIR evanescent wave is depleted and the degree of reflection is therefore reduced. For example, moving an absorbing medium into and out of the sub-micron evanescent wave region can change the interface from being highly absorptive to highly reflective; a useful effect, particularly given the very small motion required. It has generally been assumed that such highly sensitive reflection control is limited to the case of TIR. To our surprise, we have established that an analogous effect can occur in the case where the incident angle of light is close to, but not beyond the critical angle and where there is therefore only partial internal reflection (PIR) within the medium. Even though the standard EM treatment of this case includes no evanescent wave, we find that moving an absorber into and out of the sub-micron region near the interface does cause modulation of reflection. In this case, the sub-micron dimension is related to the coherence length of broadband light, rather than the mean depth of the evanescent wave, but these are similar. The presentation will focus on a key possible application - flashing the reflectance of a polymeric corner cube retroreflective conspicuity film to improve traffic safety on rural highways. PIR modulation is important for a display using corner-cube based retroreflectors, because the condition for TIR is generally not met on all three facets when electrophoretic control means are used to modulate reflection.

* This work is being supported by NSERC/3M Company.

16h45 Session Ends / Fin de la session

[TU-P9]

Atomic and Molecular Spectroscopy and Dynamics II / Spectroscopie et dynamique atomique et moléculaire II

(DAMP/DPAM)

TUESDAY, JUNE 15

MARDI, 15 JUIN

14h15 - 17h00

[Room/Salle : Colbourne]

Chair: W. van Wijngaarden, York U.

TU-P9-1 14h15

GORDON W.F. DRAKE, University of Windsor

Exotic Nuclear Size Measurements from High Precision Atomic Theory

Recent advances in high precision atomic theory have opened the way to the creation of a new tool for the measurement of the nuclear charge radius from the measured isotope shift. The unique advantage of the method is that it can be applied to short-lived exotic species such as the neutron-rich isotopes helium-6 and lithium-11. The method relies on high precision calculations of atomic transition frequencies, including relativistic and quantum electrodynamic effects, such that residual uncertainties are small compared with the nuclear volume shift. The current status of theory will be reviewed, together with the progress of experiments at Argonne, TRIUMF, and GSI.

TU-P9-2 14h45

P.W. ZETNER, University of Manitoba

Progress in the Investigation of Electron Collisions with Laser Excited Atoms

The history of electron - atom scattering studies is a long one, dating back to the Franck - Hertz experiment carried out early in the twentieth century. The measurement and calculation of cross sections for various collision processes has been the primary focus of these studies not only because of their intrinsic scientific value but also for their practical utility in the modelling of plasma systems. In the past 25 years, experimental techniques and calculational methods have dramatically improved and new insights into the fundamental physics of the electron - atom collisional interaction have emerged. A particular emphasis has been placed on defining, as completely as possible, the initial and final quantum states of a particular collision process. In this talk, I will discuss atomic target preparation by laser excitation as a means to accomplish this quantum state selection for studies of electron impact excitation / de-excitation, ionization - excitation and elastic scattering. In some instances, laser preparation is sufficient to completely characterize the dynamically relevant quantum numbers. Generally, even when a full characterization is not achieved, the selectivity afforded by laser excitation of an atomic collision target intro-

duces an expanded set of scattering observables which can provide deeper insight into the collision process and furnishes a more demanding test of scattering theories. Some of these "deeper insights" will be presented along with references to recent theoretical improvements motivated by the measurements.

15h15 Coffee Break / Pause café

TU-P9-3 15h30

Ab Initio Determination of Molecular Parameters for Ethane-like Molecules. J.R. Cooper¹, L.-H. Xu² and N. Moazzen-Ahmadi¹, ¹ University of Calgary and ² University of New Brunswick — A new method has been developed for the ab initio determination of several vibration-torsion-rotational spectroscopic parameters for a symmetric top molecule with an internal rotor. In contrast to existing methodologies^[1,2] which employ vibrational contact transformations either numerically or algebraically, the present model treats the molecule as vibrationally static but with a density distribution characteristic of the vibrational wavefunction. The second-order rotational constants A and B and torsional constant F , distortion parameters D_J , D_K and D_{JK} , and torsional distortion parameters $D_{m'}$, D_{jm} , and D_{km} have been determined for a series of ethane-like molecules from the results of ab initio calculations done at the CCSD(T) level. The technique has been applied to the molecules CH_2CH_3 , CH_3CD_3 , CD_3CD_3 , and CH_3SiH_3 with very promising results. Preliminary results for the potential constants F_{3J} and F_{3K} are also in excellent agreement with global fit values.

1. Y.-B. Duan, L. Wang, X.T. Wu, I. Mukhopadhyay, and K. Takagi, *J. Chem. Phys.* **111**, 2385 (1999).
2. T.J. Lukka and E. Kauppi, *J. Chem. Phys.* **103**, 6586 (1995).

TU-P9-4 15h45

Rotational Spectra, Conformational Structures and Dipole Moments of Thiodiglycol by Jet-Cooled FTMW and Ab Initio Calculations. LiHong Xu¹, Qiang Liu¹, R.D. Suenram², F.J. Lovas², A.R. Hight Walker², J.O. Jensen³ and A.C. Samuels³, ¹ Physical Sciences Department, University of New Brunswick; ² Optical Technology Division, National Institute of Standards and Technology and ³ Passive Standoff Detection, Edgewood Chemical and Biology Center — The rotational spectra of three low-energy conformers of thiodiglycol (TDG) ($\text{HOCH}_2\text{CH}_2\text{SCH}_2\text{CH}_2\text{OH}$) have been measured in a molecular beam using a pulsed-nozzle Fourier-transform microwave spectrometer. To determine the likely conformational structures with ab initio approach, conformational structures of 2-(ethylthio)ethanol (HOES) ($\text{CH}_3\text{CH}_2\text{SCH}_2\text{CH}_2\text{OH}$) were used as starting points together with the consideration of possible intramolecular hydrogen bonding in TDG. Three lower energy conformers have been found for TDG at the MP2=Full/6311G** level and ab initio results agree nicely with experimentally determined rotational constants. In addition, Stark measurements were performed for two of the three conformers for dipole moment determinations, adding to our confidence of the conformational structure matches between experimental observations and ab initio calculations. Of the three lower energy conformers, one displays a compact folded-like structure with strong hydrogen bonding between the two hydroxyl groups and the central sulfide atom. Two other conformers have relatively open chain-like structures with hydrogen bonding between each of the hydroxyl groups to the central sulfur atom, of which one has near pure b-type dipole moment according to the ab initio results.

TU-P9-5 16h00

Infrared Laser Spectroscopy of CCO: the ν_3 Band of the $\tilde{a}^1\Delta$ Electronic State*. Ziad Abusara, N. Moazzen-Ahmadi and T.S. Sorensen, University of Calgary - The ketenylidene (CCO) radical has been extensively investigated in the ground electronic state due to its importance in interstellar clouds, photodissociation dynamics of carbon suboxide, and as a reaction intermediate in combustion. Less is known about other electronic states of CCO. *Ab initio* calculations and photoelectron spectroscopy indicate that CCO has several low-lying singlet states. In this talk I will discuss the observation of the rotationally resolved infrared spectrum of the ν_3 fundamental band of the long-lived $\tilde{a}^1\Delta$ electronic state. The measurements were carried out between 1030 and 1105 cm^{-1} using a tunable diode laser spectrometer. Metastable CCO was produced in a discharge through a flowing mixture of carbon suboxide and helium. Forty-six rovibrational transitions in the P- and R-branches and the four lowest J-lines in the Q-branch were measured. The band origin was determined to be 1082.03134(19) cm^{-1} .

* This work is being supported by NSERC.

TU-P9-6 16h15

The $\nu_9 + \nu_4 - \nu_4$ Band of Ethane*. Nasser Moazzen-Ahmadi, University of Calgary — The ν_9 fundamental band of ethane occurs in the 12 μm region of the electromagnetic spectrum. It is the strongest band of ethane in a terrestrial window and is commonly used for the identification of ethane in the Jovian planets. The abundance determination of ethane in the planetary atmospheres relies on the laboratory intensity measurements which are then used to extract mixing ratios and abundances from astrophysical spectra. The ν_9 and $\nu_9 + \nu_4 - \nu_4$ bands both occur in the same region and neither can be analysed as isolated bands because these small amplitude vibrations are embedded in the torsional bath of the ground vibrational state. The effect of the torsional bath on the small amplitude vibrational bands is to enhance torsional tunneling splitting. Several years ago, we reported the analysis of the ν_9 band. In that study, it was shown that the observed torsional splittings can be explained by Coriolis-like interactions with the main interacting partners from the ground state being $\nu_4 = 1$, where the coupling matrix element is large, and $\nu_4 = 3$, where the energy gap is small. The analysis of $\nu_9 + \nu_4 - \nu_4$ band shows that the much larger observed torsional splitting can be largely explained by the same Coriolis-like interactions.

* This work is being supported by NSERC.

TU-P9-7 16h30

High Resolution Laser Spectroscopy of Magnesium Monoacetylide. Dennis W. Tokaryk¹, Allan G. Adam² and W.S. Hopkins², ¹ Physics Department, and ² Chemistry Department, University of New Brunswick — Both atomic magnesium and the polyatomic radical CCH are abundant species in the atmospheres of cooler stars, and in the interstellar medium. The magnesium monoacetylide radical MgCCH is therefore of potential astrophysical significance. The microwave spectrum of this species^[1] has established that the ground electronic state $X^2\Sigma^+$ is linear, and low-resolution dispersed fluorescence spectra of the $A^2\Pi - X^2\Sigma^+$ electronic transition near 437 nm have been observed by another group^[2]. We have observed the 0_0^0 and 3_0^1 bands of the $A^2\Pi - X^2\Sigma^+$ transition of MgCCH in a laser ablation molecular beam spectrometer, both at low resolution (with a pulsed dye laser) and at high resolution (with a continuous wave ring dye laser). These data provide a detailed picture of the nature and structure of the upper states, as well as an accurate line list for possible identification of this species in astrophysical sources through its optical spectrum.

TU-P9-8 16h45

Lamb-Dip Observations and Assignments of Some Compact Q-Branches in the 11 μm Region for 1,3 Butadiene. Zhen-Dong Sun¹, LiHong Xu¹, R.M. Lees¹ and Norman C. Craig², ¹ University of New Brunswick and ² Oberlin College, Ohio — The CH_2 -wagging vibrational mode of 1,3 butadiene centred at 908 cm^{-1} or 11 μm is a well defined c-type band. The Fourier transform spectrum of this band was recently recorded at 0.00184 cm^{-1} resolution in the Giessen laboratory. Apart from some unresolved Q-branch heads for medium to high-K Q-branches, analysis is at an advanced stage with energy levels observed up to K_{max} of about 10 and J_{max} near 70 for unperturbed infrared transitions. With 9 parameters (ν_0 , A, B, C, dJ, dK, DJ, DJK, DK), assignments have been fit to a Watson-type asymmetric rotor Hamiltonian in A-reduction to experimental accuracy^[1]. We have recently carried out Lamb-dip measurements for some unresolved Q-branch heads. Our motivations are (i) to test the performance of our newly built CO_2 -laser/microwave sideband spectrometer in the 11 μm region, (ii) to resolve these overlapped features in the FTS (Doppler limited) with sub-Doppler technique (Lamb-dip) in order to provide accurate line positions and assignments for these components, and (iii) to obtain an estimate of the transition dipole moment for this band. The latter is an important piece of information needed for possible cigarette smoke detection with a tunable diode laser system^[2]. Under broad band scanning mode at Doppler limited resolution, we have observed $K = 10 \leftarrow 9$, $9 \leftarrow 8$, $8 \leftarrow 7$, $7 \leftarrow 6$, $6 \leftarrow 5$, and $5 \leftarrow 4$ Q-branch heads. They are strong features in the spectrum. In order to resolve these heads, sub-Doppler Lamb-dip experiments were performed. So far, we have resolved $K = 9 \leftarrow 8$, $8 \leftarrow 7$, and $7 \leftarrow 6$ Q-branch heads with the Lamb-dip technique. Our fully resolved components are consistent with line predictions based on a previous FT analysis^[1]. From comparison of the weakest Lamb-dip signals observed in our experiment for this molecule with those of other molecules (such as CH_3OH and OCS), we have deduced a very rough estimate of about 0.5 Debye $\Delta\mu_c$ transition dipole moment for this band. Work is in progress for sub-Doppler observations of other K value Q-branch heads.

1. C. Craig, J.L. Davis, K.A. Hanson, M.C. Moore, K.J. Weidenbaum, and M. Lock, *J. Mol. Struct.*, 2004, in press.
2. Q. Shi, D.D. Nelson, J.B. McManus, M.S. Zahniser, C.N. Harward, "Quantum Cascade Infrared Laser Spectroscopy for Real-Time Cigarette Smoke Analysis", *Anal. Chem.* **75**, 5180-5190 (2003).

17h00 Session Ends / Fin de la session

[TU-P10]

(DOP-CASCA)

Adaptive Optics in Astronomy, Biology, Medicine, and Physics / *Optique adaptative en astronomie, biologie, médecine et physique*

TUESDAY, JUNE 15

MARDI, 15 JUIN

14h15 - 16h15

[Room/Salle : Ballroom A]

Chair: M. Campbell, U. Waterloo

TU-P10-1 14h15

TIM DAVIDGE, National Research Council of Canada, Herzberg Institute of Astrophysics

Adaptive Optics Systems on Canadian Telescopes

The atmosphere distorts the wavefronts of astronomical sources, and this causes a degradation in angular resolution. The wavefront distortions can be partially corrected with Adaptive Optics (AO) systems. Canadian astronomers have been pioneers in the use of AO systems for astronomical observations. In this talk I will focus on 3 AO systems that have been available to Canadian astronomers : (1) HRCAM, which was used on the Canada-France Hawaii Telescope (CFHT) during the late 1980s and early 1990s and laid the foundation for subsequent AO development, (2) the CFHT AO Bonnette, which has been in use at CFHT for almost a decade, and (3) the Gemini ALTAIR system, which was commissioned in 2003. Plans for future AO systems on existing facilities, and for the next generation of large telescopes will also be discussed.

TU-P10-2 14h45

Adaptive Optics: Implications to Diagnosis and Treatment of Eye Disease*, Melanie C.W. Campbell, *University of Waterloo* — As adaptive optics is developed for use with the eye, it will become increasingly important to the diagnosis and treatment of a number of eye diseases. Age related macular degeneration is the leading cause of new blindness over the age of 50. Adaptive optics will allow the visualization of low contrast structures in conjunction with functional testing of vision. It is also necessary to the exploration of a number of novel light based therapies. Adaptive optics will increase our understanding of the underlying mechanisms of both the disease and the therapies. In the diagnosis and tracking of glaucoma progression, polarization imaging combined with adaptive optics holds much promise. I will review the potential of AO and the techniques being developed in my laboratory.

* This work is being supported by NSERC/Photonics Research Ontario.

15h00 Coffee Break / Pause café

TU-P10-3 15h30

REJEAN MUNGER, University of Ottawa Eye Institute

Adaptive Optics: Implications to Optical Correction of the Eye

Over the last few decades, improvements in technologies such as aspheric lenses, contact lens materials and shapes, laser refractive surgery and wavefront sensing have had a great impact on our ability to correct the optical aberrations of human eyes. These technologies have also been critical to simultaneously improve our understanding of the optical properties of human eyes and their impact on visual performance. Despite these improvements, the ophthalmology clinic still finds itself dealing with a significant number of patients whose optically based visual problems cannot be satisfactorily explained and/or corrected with current technology. Could adaptive optics be the technology that will help us resolve these issues at least in some of these cases? Strategies in which current adaptive technology can be used to assess and treat optical and visual problems in human eyes will be discussed. New approaches to constructing adaptive elements optimized for the human visual system and their novel uses in the treatment of optical problems in human eyes will also be discussed.

TU-P10-4 16h00

Nanoengineered Adaptive Optics*, Ermanno F. Borra, P. Laird, R. Bergamasco, J. Gingras, L. Da Silva, L. Truong, A. Ritcey, and S. Senkow, *COPL, Université. Laval* — We shall report on the current status of our research on nanoengineered liquid optics. We are developing this new technology to make inexpensive high-performance adaptive mirrors as well as large parabolic mirrors. Adaptive mirrors are made by coating a ferrofluid with a reflective layer of self-assembling nanoparticles. The optical-quality liquid surfaces are deformed by applying external magnetic fields. We shall discuss experimental results obtained with a 110-actuators mirror. We shall also briefly present some results obtained with liquid mirrors deformed with a laser beam and rotating parabolic mirrors.

* This work is being supported by NSERC.

16h15 Session Ends / Fin de la session

[TU-P11]

(DPE/DEP)

New Directions in the Physics Curriculum / *Nouvelles orientations dans les programmes d'études en physique*

TUESDAY, JUNE 15

MARDI, 15 JUIN

14h15 - 15h15

[Room/Salle : Strathcona]

Chair: S.P. Goldman, Univ. of Western Ontario

TU-P11-1 14h15

Teaching Relativity in Introductory Physics*, William E. Baylis, *University of Windsor* — In work about a century ago, Einstein, together with Lorentz, Poincaré, and others, established special relativity as a major paradigm shift in physics that describes fundamental symmetries of electromagnetic phenomena and much of modern physics. Relativity changes our concepts of space and time and the way we approach many problems, often simplifying the computations, and it is frequently important even at low ("nonrelativistic") velocities. Yet, it is still commonly taught as a complicating correction to Newtonian mechanics. Is it not time to integrate relativity more tightly into the early physics curriculum? The talk shows how this can be accomplished with a simple algebraic extension of vector formalism that enables quantitative relativistic calculations without matrices or tensors. The covariant formalism is part of a comprehensive geometric algebra with applications in many areas of physics.

* This work is being supported by NSERC.

TU-P11-2 14h30

A Conceptual Treatment Of Gauss' Law, Donald Mathewson, *Kwantlen University College* — Gauss' Law is a topic now currently covered in many first year, second semester courses. This topic is very difficult for students to grasp. It does not help that most textbooks present Gauss' Law in its integral form which is very intimidating for students who are barely familiar with integration, let alone surface integration. A student-friendly, conceptual development of Gauss' Law will be presented along with a easily understood, simplified notation.

TU-P11-3 14h45

Novel Computer Algebra Physics Problems, George McGuire, *UCFV* — One of my pedagogical goals has been to design novel nonlinear physics problems. My design parameters were predicated upon a number of conditions: first, a computer algebra system would be an indispensable tool in the setting-up, manipulating, and solving of all the equations; second, the underlying physics must be at the undergraduate level, third, the analytical solutions have to be unknown; fourth, spectacular visualizations and animations

would be needed and created to foster a better understanding of the solutions. One or two of these unique computer algebra problems will be showcased in this session.

TU-P11-4 15h00

Magical Squares in University Physics Education*, Adam Rogers and P. Loly, *University of Manitoba* — In a first encounter with the topic of moment of inertia, magic squares, treated as rigid body mass distributions, can be included as an amusing example. A theoretically inclined student can then obtain a general result for any order magic square. At the sophomore level of classical mechanics the full inertia tensor of magic cubes shows maximal symmetry. Further opportunities to use magical squares in physics connections will be given.

* This work is being supported by Winnipeg Foundation.

15h15 Session Ends / Fin de la session

[TU-P12] **Measuring Hidden Parts of Galaxies /**
Mesure des parties cachées des galaxies

(CASCA)

TUESDAY, JUNE 15
MARDI, 15 JUIN
14h30 - 17h00

[Room/Salle : Campaign B]

Chair: A. Gulliver, Brandon U.

TU-P12-1 14h15

Are the Central Engines in Narrow-Line Seyfert 1s Fundamentally Different?*, Christopher Ryan¹, M.M. DeRobertis¹, S. Virani², A. Laor³ and P. Dawson⁴, ¹York University, ²Chandra X-ray Observatory Center, CfA, ³Technion, Israel and ⁴Trent University — Narrow-line Seyfert 1 galaxies (NLS1s) are a sub-class of active galactic nuclei whose emission-line characteristics are similar to Seyfert 1s except that they have relatively narrow permitted emission lines. Based on strong observational evidence, in particular x-ray properties, the accepted model to account for this postulates a relatively low-mass black hole accreting material at a significant fraction of its Eddington limit. To investigate this hypothesis, we have analyzed high-spatial resolution NIR data obtained at CFHT with the KIR/AOB. By employing the two-dimensional fitting algorithm GALFIT, as well as an empirical technique for removing the nuclear light, galaxy bulge luminosities were determined for a sample of 11 NLS1s to an accuracy of ten percent. Assuming the established relation between the black hole mass and the bulge luminosity holds for this sample, we have determined that the mass of compact objects at the centres of galaxies in our sample are indeed systematically less than black hole masses in "normal" Seyfert 1s. We have also found that the relative accretion rates for the sample are up to an order of magnitude higher than that for their broad-line counterparts.

* This work is being supported by NSERC.

TU-P12-2 14h30

Analysis of Gas and Dust Emission in the Interstellar Medium of the Outer Galaxy with the Canadian Galactic Plane Survey, K.A. Douglas and A.R. Taylor, *University of Calgary* — The Canadian Galactic Plane Survey (CGPS) probes the interstellar medium in the Outer Galaxy at arcminute resolution scales. The use of IRAS dust emission datasets to trace dust column density is achieved by determining the optical depth at 100 μm , τ_{100} . We compare τ_{100} to other datasets of the CGPS, including the molecular gas traced by carbon monoxide (CO) using the Five Colleges Radio Astronomy Observatory, and atomic hydrogen measured with the Dominion Radio Astrophysical Observatory (DRAO). Ionised hydrogen can be inferred from thermal radio continuum images produced using the DRAO 1420 and 408 MHz continuum observations. I will describe an analysis of the interstellar components, leading to a method of detecting excess infrared emission that may trace molecular hydrogen not traced by the surrogate species. A catalogue of these infrared excess regions will be presented.

14h45 Session Ends / Fin de la session

[TU-P13] **Medical Applications of Sound: Imaging and Beyond /**
Applications médicales du son : l'imagerie et au-delà

(COMP-DMBP/
OCPM-DPMB)

TUESDAY, JUNE 15
MARDI, 15 JUIN
14h30 - 17h00

[Room/Salle : Albert]

Chair: W.M. Whelan, Ryerson U.

TU-P13-1 14h30

MICHAEL BRONSKILL, Sunnybrook & Women's, University of Toronto

*MRI Guidance for the New Sounds of Tumour Therapy**

The diagnostic uses of ultrasound have become well known. Many parts of the body are routinely examined using diagnostic levels of ultrasound which produce no known bioeffects. Specialized ultrasound imaging systems have now been developed which tailor the ultrasound frequency and pattern to image many organs throughout the body, from microscopic intravascular imaging of arterial plaque to whole organ abdominal imaging. Recently, ultrasound has been investigated for possible therapeutic uses, where high levels of sound energy are deposited in a specific region of the body to heat tissue to the point of coagulation causing cell death. This presentation will review some of the current approaches to thermal therapy using ultrasound. An important component in many cases is the use of magnetic resonance (MR) imaging to target the region for thermal coagulation, to guide the delivery of the energy pattern, and to monitor the effectiveness of the treatment. In particular, MR imaging has a unique ability to measure temperatures accurately in tissue during heating. Examples will be given of our work using an interstitial probe which transmits energy at two different frequencies in order to achieve both large regions of coagulation and tight margins around the targetted region. This device is designed to be MR compatible enabling MR temperature measurements to be taken during treatment and used to control the device.

* In collaboration with Rajiv Chopra, Sunnybrook & Women's.

TU-P13-2 15h00

ROBERT L. CLARKE, Carleton University

High Intensity Focused Ultrasound for Non-Invasive Therapy

The last decade has seen significant advances in the application of high intensity focused ultrasound (HIFU) for the treatment of deep-seated localized cancer. Beams of up to several hundred watts, 1 to 3 MHz, can be focused to elliptical volumes, 0.2 cm diameter by 2 cm long, and directed to sites up to 8 cm below the skin surface, without superficial damage. The resulting intensities can completely destroy cancer tissue within a few seconds. By stepping the beam over the extended region, complete destruction can be achieved. Liver, prostate and pancreas have been the sites most often partially or wholly treated. Phase II trials of about 100 patients in the UK, more in the US and Europe, and more than 1000 in China are now complete. Treatment is essentially conformal, and depends to a great degree on the associated imaging techniques, mainly MRI and ultrasound.

TU-P13-3 15h30

JEREMY A. BROWN, Queen's University

Development and Applications of High Frequency Ultrasound Imaging Systems

The non-destructive nature of ultrasonic waves has made ultrasound imaging one of the most popular diagnostic tools in medicine. Most commercial ultrasound systems operate in the frequency range from 3 to 5 MHz and can resolve structures approximately 1 mm in size. By increasing the frequency, the ultrasound wavelength is decreased and finer resolution can be obtained. Several high frequency (30100 MHz) ultrasound systems have recently been developed for imaging the eye, skin, and vascular system with microscopic resolution (< 100 microns). Despite the improved resolution, high frequency systems are not routinely used in clinical practice or biological studies. A major problem is that the single element transducers that are currently available for high frequency imaging are geometrically shaped to focus the ultrasound energy. This introduces a tradeoff between the image resolution and depth of field. A significant improvement in image quality can be achieved by replacing the single element transducer with a transducer array and an electronic beamformer. This combination allows the ultrasound energy to be optimally focused at each depth within a tissue. Unfortunately, fabricating a high frequency transducer array is difficult since the dimensions of the array scale with the ultrasound wavelength. We have recently developed a technique for fabricating transducer arrays using a simple photolithographic process. The process is relatively simple and has allowed us to reproducibly fabricate miniature arrays. In this talk, I will provide a brief overview of high frequency ultrasound imaging and then describe our work in developing high frequency transducer arrays and beamformers.

* In collaboration with F.S. Foster¹ and G.R. Lockwood², ¹Sunnybrook Health Sciences Centre and ²Queen's University.

TU-P13-4 16h00

MICHAEL KOLIOS, Ryerson University

High Frequency Ultrasound Imaging and Spectroscopy for the Imaging of Cell Damage and Death

In high frequency ultrasound imaging, compressional waves (20-60MHz) are used to interrogate tissue structure. While even at these frequencies individual cells cannot be resolved, the speckle pattern produced from cell ensembles can be analyzed and changes due to treatment visualized. We have shown that i) the ultrasound backscatter intensity, ii) the statistics of the backscatter envelope and iii) the power spectra of the backscatter change when cells and tissues are damaged. In this presentation we will present some of our recent data for our effort to explain the nature of these changes. It is shown that cell size is a major determinant of backscatter for cell ensembles both *in-vivo* and *in-vitro*. The mid-band fit (a measure of backscatter intensity) from cell pellets of a prostate cancer cell line (diameter ~30 microns) is 12dB greater than the MBF of cell pellets using an acute myeloid leukemia (AML) cell line (diameter ~10-15 microns). The measured spectral slope (with no compensation for attenuation) was 0.43 dB/MHz for the prostate cell line vs. 0.75 dB/MHz for the AML cell line, consistent with the smaller diameter of the AML cell. To determine whether treatment effects can be detected *in-vivo*, we have grown non-Hodgkin's lymphoma tumors in mice (14 to date), which were then treated using CHOP chemotherapy. The ultrasound backscatter increased in the treated tumors in a time-dependent fashion, peaking at 24-48h after exposure. The kinetics and etiology of the increase will be discussed.

TU-P13-5 16h30

Photoacoustic Imaging in Biological Tissues for Monitoring Thermal Lesions*. G.M. Spirou¹, Y. Fan², A. Mandelis², W.M. Whelan¹ and A.I. Vitkin^{1,4,5}, ¹Department of Medical Biophysics, University of Toronto, ²Department of Mechanical and Industrial Engineering, University of Toronto, ³Department of Mathematics, Physics and Computer Science, Ryerson University, ⁴Ontario Cancer Institute/Princess Margaret Hospital/University Health Network, Medical Physics Division and ⁵Department of Radiation Oncology, University of Toronto — Photoacoustic imaging is a non-invasive technique that differentiates between materials with different optical absorption properties. This approach may be suitable for detecting thermal lesion boundaries created during thermal therapy, a method used to coagulate a targeted volume (for example, a tumour). The photoacoustic effect is the process whereby light absorbed by a material creates a temperature change resulting in a pressure change. If the incident light is modulated, the resulting periodic pressure change creates an acoustic wave, which propagates from the absorption location and may be detected by a transducer. The strength of the emitted acoustic signal is dependent on the absorption of light within the sample. During thermal therapy, as tissues are thermally damaged, changes in tissue optical absorption occur. Such changes may be detectable photoacoustically and therefore photoacoustic imaging may provide a means to monitor the extent of thermal damage. Changing the frequency of the modulation of light allows one to image different depths using signal-processing analysis. Preliminary tests in turbid biological-like media indicate different absorptions display different signal intensities, demonstrating the dependence of the photoacoustic effect on the optical absorption. We are currently exploring the sensitivity of the system in turbid media, and identifying resolution, contrast, and depth of imaging of this approach, and evaluating its suitability for monitoring the extent of thermal damage to improve tissue targeting.

* This work is being supported by University of Toronto

TU-P13-6 16h45

High Frequency Ultrasound in Monitoring Liver Suitability for Transplantation. R. Vlad¹, G.J. Czarnota^{1,2}, A. Giles^{1,2}, J.W. Hunt^{1,2}, M.D. Sherar^{1,2} and M.C. Kolios^{1,3}, ¹Department of Medical Biophysics, University of Toronto; ²Ontario Cancer Institute, ³Department of Mathematics, Physics and Computer Science, Ryerson University — It has been previously shown that high frequency ultrasound (HFU), 20 to 60 MHz, can be used to detect structural changes in tissue and cell ensembles during cell death. In this project we investigate the potential of HFU to assess liver damage during preservation, prior to transplantation. After 8-24h of cold storage, irreversible injury occurs, leading to liver transplant failure. We hypothesize that the changes in ultrasound back scatter (UB) in liver ischemia are related to the changes in viscoelastic properties of the cell cytoskeleton, induced by osmotic stress, following ATP depletion. In our experiments, we use ischemic Wistar rat livers. Organs from Wistar rats (n=10) are surgically excised, immersed in phosphate buffer saline (PBS) and stored at 4°C for 24h or left to decay at room temperature. In the preservation experiments, organs from Wistar rats (n=4), are surgically excised, flushed with University of Wisconsin (UW) solution and stored at 4°C for 24h. Preservation injury is simulated by either not flushing the organs (n=2) with UW solution or by allowing the organs (n=2) to reach room temperature. Ultrasonic images and the corresponding raw radio frequency (RF) data are collected over the ischemia period from a region located within the transducer focal zone. Samples are fixed for Hematoxylin&Eosin and Electron Microscopy staining at the end of the experiment. For organs prepared using standard preservation conditions there is a slight increase in UB (~2.5dB). UB increases by 4-10dB in the ischemia models demonstrating kinetics dependent on storage conditions. The results demonstrate the potential of HFU imaging to assess liver suitability for preservation.

17h00 Session Ends / Fin de la session

[TU-P14] CASCA Outgoing President's Talk /
Conférence du président sortant de la CASCA

(CASCA)

TUESDAY, JUNE 15
MARDI, 15 JUIN
14h45 - 15h15

[Room/Salle : Campaign B]

Chair: J. Hesser, NRC

TU-P14-1 14h45

GRETCHEN L.H. HARRIS, University of Waterloo

*CASCA 1971-2004: The Story So Far**

CASCA has changed a great deal over the past three decades from relatively modest beginnings to a society which is known and respected both in Canada and around the world. As our community grows and our discipline becomes more diverse, CASCA will continue to evolve. How did we get where we are now? Where will we be in another 30 years and how will we get there? Can we keep the friendly, personal, and diverse environment we value today? How will our demographics and our meetings change? Who will be our leaders in 2031 and what will they be expected to do? What will we expect of CASCA? I will look at our past and provide some ideas for your consideration.

* This work is being supported by NSERC.

[TU-P15] World Year of Physics 2005 Committee Meeting /
Réunion du Comité pour l'Année mondiale de la physique
(All Orgs.)

TUESDAY, JUNE 15
MARDI, 15 JUIN
15h00 - 16h30

[Room/Salle : Heartland Boardroom]

Chair: M. Steinitz, St. Francis Xavier U.

[TU-P16] CASCA - Long Range Plan Review /
Examen du plan à long terme de la CASCA
(CASCA)

TUESDAY, JUNE 15
MARDI, 15 JUIN
15h45 - 16h30

[Room/Salle : Campaign B]

Chair: R. Pudritz, McMaster U.

[TU-P17] CASCA Annual General Meeting /
Assemblée générale de la CASCA
(CASCA)

TUESDAY, JUNE 15
MARDI, 15 JUIN
16h30 - 18h00

[Room/Salle : Campaign B]

Chair: G. Harris, U. Waterloo

[TU-P18] CAP Annual General Meeting /
Assemblée générale de l'ACP
(CAP/ACP)

TUESDAY, JUNE 15
MARDI, 15 JUIN
17h00 - 18h30

[Room/Salle : Victoria]

Chair: B. Joos, U. Ottawa

[TU-P19] COMP Annual General Meeting /
Assemblée générale de l'OCPM
(COMP/OCPM)

TUESDAY, JUNE 15
MARDI, 15 JUIN
17h00 - 18h30

[Room/Salle : Albert]

Chair: C. Arsenault, Dr. Georges L. Dumont Hospital

[TU-P20] Banquet Reception / Réception du banquet
Banquet
-- Ballrooms A/B/C --
(All Orgs.)

19h00 - 19h30
19h30 - 22h30

TUESDAY, JUNE 15
MARDI, 15 JUIN

Wednesday, June 16

Mercredi, 16 juin

[WE-A1] Meeting of the CAP-NSERC Liaison Committee /
Réunion du comité de liaison ACP-CRSNG
(CAP/ACP)

WEDNESDAY, JUNE 16
MERCREDI, 16 JUIN
07h00 - 09h00

[Room/Salle : Heartland Boardroom]

Chair: K. Ragan, McGill U.

[WE-A2] DPE Business Meeting /
Réunion d'affaires DEP
(CAP/ACP)

WEDNESDAY, JUNE 16
MERCREDI, 16 JUIN
07h00 - 08h15

[Room/Salle : Private Dining Room]

Chair: R. Hawkes, Mount Allison U.

[WE-A3] Plenary Session /
Session plénière
(CAP-COMP/
ACP-OCPM)

WEDNESDAY, JUNE 16
MERCREDI, 16 JUIN
08h30 - 09h15

[Rooms/Salles : Ballrooms B/C]

Chair: M. Morrow, MUN

WE-A3-1 08h30

AARON FENSTER, Robarts Research Institute, London, Ontario

Use of 3D Ultrasound Imaging in Diagnosis, Treatment and Research: Advances and Opportunities

2D viewing of 3D anatomy, using conventional ultrasound, limits our ability to quantify and visualize the anatomy and guide therapy, because multiple 2D images must be integrated mentally. This practice is inefficient, and leads to variability and incorrect diagnoses. Over the past 2 decades, investigators have addressed these limitations by developing 3D ultrasound techniques. In this paper we describe our developments of 3D ultrasound imaging instrumentation and techniques for diagnosis, image-guided therapy and use in

basic biomedical research. Examples will be given for imaging various organs, such as the prostate, carotid arteries, and breast, and for the use in 3D ultrasound-guided brachytherapy and cryosurgery. In addition, we describe 3D segmentation methods that can be used for quantitative analysis of disease progression and regression in humans as well as research animal models.

09h15 Session Ends / Fin de la session

**[WE-A4] Portraits at Multiple Wavelengths - Contributed /
Portraits à longueurs d'ondes multiples - contribuées**

(CASCA)

WEDNESDAY, JUNE 16
MERCREDI, 16 JUIN
08h30 - 09h00

[Room/Salle : Campaign B]

Chair: I. Short, Saint Mary's U.

WE-A4-1 08h30

Time-Evolution and Radio-Optical Correlations in the Synchrotron Emission of the Crab Nebula, Michael Bietenholz¹, J.J. Hester², D.A. Frail³, N. Bartel¹, ¹York University, ²Arizona State University and ³NRAO — I present a series of new, high-resolution VLA radio images of the Crab nebula, which were taken simultaneously with HST optical and Chandra X-ray observations as part of a unique observing campaign which obtained simultaneous, time-resolved, high-resolution imaging of the Crab at all three wavelengths. The radio images show that there is systematic variability in the Crab's radio synchrotron emission throughout the region near the pulsar. I discuss the visualization of the variability, and the comparative visualization of the radio and the optical emission. The principal geometry of the both the radio and optical variable features is that of elliptical ripples, called wisps. The radio wisps are seen to move systematically outward with projected speeds of up to 0.3c. Comparing the radio images to the optical ones, we find that the radio wisps are sometimes displaced from the optical ones, or have no optical counterparts. We also find that some optical wisps in particular, the brightest optical wisps near the pulsar, do not seem to have radio counterparts. We discuss implications on our understanding of the pulsar outflow and particle acceleration processes.

WE-A4-2 08h45

Wind-Wind Collisions from X-Ray to Radio: The Massive Prototype Binary WR140, Anthony Moffat, Université de Montréal — Since the discovery in the 1980's of huge cyclic variations in its infra-red flux, we now know that WR140 is a binary system (C-rich Wolf-Rayet star plus a main-sequence O4V-type companion) in a highly elliptical 8-year orbit, in which the hot and dense supersonic winds of the stars collide. The variable IR flux, now imaged with high spatial resolution at 8-10 m telescopes, comes from the hot carbon-based dust formed in the shock-compression zone associated with the collision and ejected by the winds themselves. The collision is most energetic during the rapid periastron passage, resulting in highly variable flux on an orbital time-scale at radio and X-ray wavelengths. This places the system among the brightest X-ray/radio sources among the galactic WR population. This system serves as a unique laboratory for in-depth studies of the mass-loss phenomenon in massive stars.

09h00 Session Ends / Fin de la session

**[WE-A5] Radiation Treatment Planning /
Planification d'une radiothérapie**

(COMPOCPM)

WEDNESDAY, JUNE 16
MERCREDI, 16 JUIN
08h30 - 10h00

[Room/Salle : Albert]

Chair: W. Beckham, BC Cancer Agency

WE-A5-1 08h30

A Broad Beam Analytical Photon Scatter Model Employing Convolution Techniques*, Peter Potrebko, S. Pistorius and B. McCurdy, CancerCare Manitoba / The University of Manitoba — Accurate dosimetry requires a fundamental understanding of the complex interactions that occur in photon radiotherapy. This work attempts to derive from first principles an analytical equation to describe the transport of a broad, parallel, mono energetic beam of photons in a homogeneous water phantom. The Reciprocity Theorem was used to replace a broad beam incident on a central axis point detector by a central axis pencil beam (scatter kernel) integrated over an infinite plane (extended detector) under radiation equilibrium. The scatter kernel was analytically integrated over photon energy by the use of two reasonable assumptions: 1) Forward scatter resulting from first order Compton scattering dominates the interactions in water for energies of 1-10 MeV. 2) The attenuation coefficient of the scattered photons is proportional to the attenuation coefficient of the primary photons with an energy-dependent proportionality constant. The Kinetic Energy Released in the Medium originating from scattered photons was then calculated as a function of depth in the phantom from the analytical convolution of the primary photon fluence with the scatter kernel. The analytic equation was compared to Monte Carlo and numerical convolution data at clinical photon energies of 1.5, 3, and 6 MeV to determine the accuracy of the model. The model promises to be useful for extracting the narrow beam attenuation coefficient under broad beam conditions where we can approximate radiation equilibrium. For 3 MeV, the narrow beam attenuation coefficient was calculated to be $0.0385 \pm 0.0001 \text{ cm}^{-1}$ which compares well to the published value of 0.0395 cm^{-1} .

* This work is being supported by NSERC.

WE-A5-2 08h45

Evaluation of the Rectangular Scatter Integration Model (RSI), Noel Blais, W. Wierzbicki and P. Munger, Hôpital Maisonneuve-Rosemont — The scatter integration model (RSI) is proposed to describe head scatter data. This model is relatively simple and straightforward. Mathematically, the RSI model introduces a multi-variable function to define head scatter dependency on the X₁, X₂, and Y jaw positions. This method, characterized by high mathematical flexibility precisely describes head scatter data for symmetric, asymmetric, open and wedged fields. The RSI model requires numerical integration of the head scatter in the X and Y directions using small strips defined by the MLC leaves (no radial integration involved). The validity of the RSI model was verified against two other models: the equivalent square field method (ESF) and the circular scatter integration method (CSI). The set of head scatter data was measured for a 25 MV RX beam from an Elekta SL-25. The three models above were systematically applied to a measured set of 234 open fields and to a set of 175 wedged fields. Both sets of data included symmetric and asymmetric fields. The results obtained show that the RSI model produced an excellent description for head scatter data since practically all calculated ionizations approximate the measured ones within to $\pm 0.5\%$ for the open fields and within to $\pm 1.0\%$ for the wedged fields. The corresponding errors produced by the ESF and the CSI models were as follows: $\pm 3.0\%$ and $\pm 1.5\%$ for the open fields and $\pm 3.5\%$ and $\pm 3.0\%$ for the wedged fields. Similar results were observed with irregular fields.

WE-A5-3 09h00

A Correlated Sampling User-Code for the EGSnrc System, Lesley A. Buckley¹, I. Kawrakow² and D.W.O. Rogers¹, ¹Carleton University and ²NRC INMS — The implementation of a correlated sampling variance reduction technique into a user-code for the EGSnrc Monte Carlo code system is described. This technique is particularly effective for in-phantom ion chamber calculations or other situations where the difference between quantities of interest is due to small differences between the simulation geometries. For such cases, conventional variance reduction techniques require a prohibitively large number of histories in order to achieve reasonable statistical uncertainties. In the 1990's, Ma and Nahum described, in a series of papers, a correlated sampling technique implemented in the EGS4 Monte Carlo code. The present paper discusses improvements in, and changes to their correlated sampling technique. This code is being used to study the wall effects in ion chambers and the energy response of dosimeters such as Al₂O₃, alanine and TLDs. In this study, the calculation of absorbed dose ratios is used to discuss the efficiency and accuracy of the EGSnrc correlated sampling technique relative to conventional variance reduction techniques. It is shown that for typical ion-chamber calculations, efficiency gains of up to a factor of 45 are achieved. The gain is highest when there is a high degree of correlation between the geometries. For weakly correlated geometries, the time savings alone increase the efficiency of in-phantom calculations by slightly better than a factor of 2 for studies with two geometries.

WE-A5-4 09h15

Fast Inverse Dose Optimization (FIDO) for IMRT via Matrix Inversion with no Negative Intensities. S.P. Goldman¹, J.Z. Chen² and J.J. Battista², ¹ *University of Western Ontario* and ² *London Regional Cancer Centre* — A fast optimization algorithm is very important for inverse planning of Intensity Modulated Radiation Therapy (IMRT), and for adaptive radiotherapy of the future. Conventional numerical search algorithms such as the conjugate gradient search with positive beam weight constraints, generally require many iterations and may produce suboptimal results due to trapping in local minima. A direct solution of the inverse problem using conventional quadratic objective functions without positive beam constraints is more efficient but results in unrealistic negative beam weights. We present here a direct solution of the inverse problem which does not result in unacceptable negative beam weights. The objective function for the optimization of beam intensities for large number of beamlets is reformulated such that the optimization problem is reduced to a linear set of equations. The optimal set of intensities is found through a matrix inversion, and negative beamlet intensities are avoided without the need for externally imposed constraints. The method has been applied to a test phantom and to a few clinical cases. We were able to achieve highly conformal dose distributions with very short optimization times. Typical optimization times for a single anatomical slice using a single processor PC and a standard matrix inversion routine are: 0.2 sec. for 400 beamlets; 8 sec. for 1,000 beamlets; 40 sec. for 2,000 beamlets and 2.5 min for 3,000 beamlets. In conclusion, the new method provides a fast and robust technique to find a global minimum that yields excellent results for the inverse planning of IMRT.

WE-A5-5 09h30

Improved Calculation Accuracy for IMRT using Modified Single Pencil Beam Calculation Kernels*, Alanah Bergman, K. Otto and C. Duzenli, *University of British Columbia / Vancouver Cancer Centre* — Intensity Modulated Radiation Therapy (IMRT) is used to deliver highly conformal radiation doses to tumours while sparing nearby sensitive tissues. Discrepancies between calculated and measured dose distributions have been reported for regions of high dose gradients corresponding to complex radiation fluence patterns. For the single pencil beam superposition/convolution dose calculation algorithm, the ability to resolve areas of high dose structure is partly related to the shape of the pencil beam dose kernel (similar to how a photon detector's point spread function relates to imaging resolution). Improvements in dose calculation accuracy have been reported when the treatment planning system (TPS) is re-commissioned using high-resolution measurement data as input. This study proposes to further improve the dose calculation accuracy for IMRT planning by optimizing readily available clinical dose kernel shapes already present in the TPS, thus avoiding the need to re-commission. The in-house optimization program minimizes a cost-function based on a 2D composite dose subtraction / distance-to-agreement gamma analysis. The final optimized kernel shapes are re-introduced into the treatment planning system and improvements to the dose calculation accuracy for complex IMRT dose distributions evaluated.

* This work is being supported by Michael Smith FHR.

WE-A5-6 09h45

Virtual Organs as a Tool in Inverse Planning of IMRT. Slav Yartsev, Jeff Chen, Tomas Kron, Terry Coad, Kris Trenka and Edward Yu, *Integrated Cancer Care Program / London Health Science Centre / University of Western Ontario* — Inverse treatment planning has become a routine practice in modern radiation therapy. A quadratic objective function with dose-volume constraint violation factors and importance factor for each structure is used in inverse planning for intensity-modulated radiation therapy (IMRT) with Dose Calculation Module (DCM 2.0, MDS Nordion). The objective function defined this way does not sufficiently penalize low doses in small areas (cold spots) of the planning target volume (PTV) and high doses in organs at risks (OARs). The cold spots are usually located close to the boundary of PTV: in the regions with high gradients of dose distribution. In order to ensure acceptable minimal irradiation dose in all voxels of PTV, a virtual PTV with contours outlined with a 3 mm margin around PTV in three dimensions is used either instead of PTV or as an additional target for optimization. This approach was tested in the planning of patients with non-small-cell lung cancer. In addition, gross tumour volume may be used either as a target to increase a relative importance of PTV or as an OAR to have a control on the maximum dose delivered to PTV. We examine merits of both options for modification of dose distribution in the case of large brain tumour. The use of additional structures increases the flexibility of inverse planning procedure in IMRT and could be applicable also to helical tomotherapy.

10h00 Session Ends / Fin de la session

| | | |
|--------------------|--|---|
| [WE-A6] (CASCA) | Data Mining and Archiving / Exploitation et archivage des données | WEDNESDAY, JUNE 16 MERCREDI, 16 JUIN 09h00 - 09h45 |
|--------------------|--|---|

[Room/Salle : Campaign B]

Chair: R. Bochonko, U.Manitoba

WE-A6-1 09h00

DAVID SCHADE, Canadian Astronomy Data Centre, Herzberg Institute of Astrophysics, National Research Council Canada

Data Mining and the Virtual Observatory

Extracting scientific understanding from large, multi-wavelength data collections is the primary motivation of the Virtual Observatory movement. Scientific data mining can be done using either catalogues of derived parameters such as flux, spectral energy distribution shape, and source morphology or it can be done through the application of user-defined algorithms directly on the pixel data. In either case, existing data collections are large enough to require massive processing power. In addition, the data need to be very carefully engineered and organized to allow the execution of either database queries or pixel-level processing across multi-wavelength datasets. This engineering and organization task is the primary challenge of the Virtual Observatory. It is a fact, at present, that even large-scale science projects typically develop their own information technology infrastructure. But at some point in the near future the scale and complexity of available datasets will exceed the capabilities of individuals or small groups of researchers to handle them. At that point the Virtual Observatory capabilities for enabling data mining will become a necessity.

09h45 Session Ends / Fin de la session

| | | |
|------------------------------------|---|---|
| [WE-A7] (CAP-COMPI ACP-OCPI) | Plenary Session / Session plénière | WEDNESDAY, JUNE 16 MERCREDI, 16 JUIN 09h15 - 10h00 |
|------------------------------------|---|---|

[Rooms/Salles : Ballrooms B/C]

Chair: C. Arsenault, Dr. Georges L. Dumont Hospital

WE-A7-1 09h15

DAVID W.O. ROGERS, Carleton University

Monte Carlo Simulation of Electron-Photon Transport: From Particle Physics to Cancer Radiotherapy

Monte Carlo simulation of the transport of electrons and photons plays a central role in modern radiotherapy research and will soon be in routine use in many clinics. The EGS (Electron Gamma Shower) Monte Carlo code system, which is one of the most widely used codes in medical physics applications, was originally developed at the Stanford Linear Accelerator Center for applications in high-energy physics. With various extensions to lower energies it has been used for applications ranging from diagnostic imaging to radiation dosimetry to dose calculations in the treatment of cancer with radiation. With the development of much faster yet accurate codes for radiotherapy treatment planning, Monte Carlo techniques are being extensively developed commercially for radiotherapy applications and continue to be widely used for research. Coming full circle, the extensions of EGS to lower energies led to it being used for simulating electron transport in the SNO neutrino detector and hence it is again a front line particle physics tool.

10h00 Session Ends / Fin de la session

[WE-A8]

**Instrumentation and Techniques in Biomedical Physics II /
Instrumentation et techniques en physique biomédicale II**
(DIAP-DIMP/
DPIA-DPIM)WEDNESDAY, JUNE 16
MERCREDI, 16 JUIN
10h00 - 12h30

[Room/Salle : Colbourne]

Chair: R. Maev, U.Windsor

WE-A8-1 10h00

ULRICH J. KRULL, University of Toronto at Mississauga

Genomic Target Identification using Imaging of Distributed Gradients of Oligonucleotide Probes in Conjunction with Microfluidics

The detection of nucleic acids using biosensors and microarray chips is now used in many applications such as forensic identification, screening of genomes for mutations, and detection and identification of bacteria and viruses. One important finding is that the control of the density of immobilized single stranded probe molecules can be used to tune selectivity to facilitate detection of even single base pair mismatches. The results are now being implemented to develop new device technologies. One approach provides for a multi-dimensional distribution of selective chemistry at a surface, but in such a way that the coatings of probe molecules are continuous, and operate to provide gradients of selectivity in one or more directions. Such a Gradient Resolved Information Platform (GRIP) is based on a surface that is coated with a continuous gradient of density and/or sequence and/or orientation and structure of ssDNA. The location, extent of hybridization, and speed of hybridization on such a surface by a target sequence can be used to identify and quantitatively measure the target. The goal of this research is to combine quantitative microfluidics using electrokinetic flow with this novel form of biochip to create a quantitative sensing system that is suitable for concurrent rapid analysis of multiple nucleic acid targets. We are developing a microfluidics package that quantitatively delivers target oligonucleotide to a GRIP chip, with detection of hybridization being done in pseudo-real-time using epi-fluorescence, confocal fluorescence and time-resolved fluorescence methods.

WE-A8-2 10h30

JUAN J ALVARADO-GIL, University of Guelph

Study of Blood Sedimentation by Photothermal and Optical Techniques

Blood sedimentation rate is a usual indicator in clinical diagnosis, being especially helpful as an auxiliary method in the determination of diseases. The use of new techniques in the study of these phenomena would permit to establish more adequate methodologies as well as new applications of this clinical indicator. The dynamics of fish blood sedimentation is studied at real time using photoacoustic, photopyroelectric and optical techniques. In the case of photothermal techniques two configurations are shown, direct illumination of the sample and illumination of the substrate in which the blood is standing. It is shown that the time evolution of the signal follows a second order kinetics, dominated by the change of the optical properties in the first case and by the thermal ones in the second. In the case of the optical techniques the study is based on the analysis of light transmission through the blood. The transmitted light is simultaneously monitored by a vertical arrangement of optical fibres connected to photodiodes. This technique permits us to study the dynamics of sedimentation at real time and at different heights. It is shown that the results for the parameters of sedimentation depend strongly on the height at which the optical fibres are positioned. This allows us to find the optimal height at which this kind of studies could provide consistent and precise results. Results for fish belonging to three experimental groups treated with different substances are presented. The differences observed in the sedimentation rates are discussed.

11h00 Coffee Break / Pause café

WE-A8-3 11h30

ANDRZEJ KOTLICKI, University of British Columbia

*Applied Research at the Structured Surface Physics Laboratory at UBC**

We are going to describe the projects that constitute the research currently being performed in the Structured Surface Physics Laboratory at UBC. There are three major projects, two of which are quite advanced and are being partially developed by a UBC spin-off company. They are as follows: 1) The Charged Liquid Electro-Active Response Display (CLEAR) is a new reflective display technology with dramatically increased reflectance difference between black and white states in all lighting conditions (compared to a more traditional LCD display); 2) The High Dynamic Range (HDR) display is capable of displaying light intensity over five orders of magnitude, compared to a regular TV set with a range of only 2 orders of magnitude; and 3) The new "green" triple illumination system uses alternative light sources: solar light and the light that is normally lost from gas furnaces, as well as electric fluorescent light. We will also shortly introduce several other projects: the "Millisun," an illuminator that produces a wide light beam with the angular characteristic of solar light; a new kind of integrating sphere; an electrostatic air pump; an electrostatic liquid pump, and a Protein Adsorption Sensor.

* In collaboration with L.A. Whitehead, M. Mossman and H. Seetzen, University of British Columbia.

WE-A8-4 12h00

LUC BEAULIEU, Université Laval et Centre Hospitalier Universitaire de Québec

*Scintillating Optical Fibers as High Precision, Small Area Dosimeters in Radiation Therapy**

Radiotherapy treatment planning aims at delivering a high and uniform dose to the target volume while sparing surrounding normal tissues as much as possible. With the advent of Intensity Modulated Radiation Therapy (IMRT) the tumors can be literally dose-"painted". However with such a precision, quality assurance (QA) has become a long and tedious process. IMRT involves a large number (over 100) of small segments. Each segment can have low (1 cGy) to high (few tens of cGy) dose levels. While QA processes are necessary to experimentally confirm the dose predicted by treatment planning algorithms, only a limited number of solutions are available for the simultaneous measurement of the absolute dose in multiple points with a high spatial resolution. We are proposing a new solution to this problem by building an absolute dose detection system based on scintillating optical fibers. Such detectors can have a very small detection volume, can be used in various geometries and can be scaled up to easily include a few hundreds individual units. Moreover, scintillating fibers are water-equivalent (the medium of reference in radiation therapy) and cost only a few cents per mm. A consistent and elegant solution to the problem of subtracting the Cerenkov light production (noise on the measurements) has been found. The method is based on the simultaneous measurement of the light output using color filters. Furthermore, using a CCD camera solves the problem of reading hundreds of such detectors in a simple and easy-to-use form.

* In collaboration with L. Archambault^{1,2}, L. Gingras^{1,2}, and R. Roy¹, ¹ Université Laval et ² Centre Hospitalier Universita.

12h30 Session Ends / Fin de la session

[WE-A9]

**Young Investigators in Condensed Matter Physics II /
Jeunes chercheurs(es) en physique de la matière condensée II**

(DCMMP/DPMC)

WEDNESDAY, JUNE 16
MERCREDI, 16 JUIN
10h00 - 12h30

[Room/Salle : Ballroom A]

Chair: M. Cote, U.Montreal

WE-A9-1 10h00

FEDERICO ROSEI, IINRS-EMT, University of Quebec

Critical Issues in Ge/Si Nanostructures: Positioning, Intermixing and Ripening

The growth of Ge on Si surfaces proceeds according to the Stranski-Krastanow mode: after the formation of a 3-5 monolayer thick wetting layer, 3D islands nucleate to partially relieve the strain due to the 4.2% lattice mismatch. This growth mode is common in heteroepitaxy, and Ge-Si is a good model system for studying island growth in lattice-mis-

matched heterostructures^[1]. We monitored the growth process *in situ*, taking Scanning Tunneling Microscopy and Low Energy Electron Microscopy (LEEM) movies. Critical issues include the controlled positioning of Ge/Si islands^[2], Ge–Si interdiffusion processes^[3], and ripening processes that affect islands after growth^[4]. In this presentation I will address all three issues:

- (i) By using step-bunched Si(111) surfaces as templates, we demonstrate the self-assembly of an ordered distribution of Ge islands *without* lithographic patterning^[2].
- (ii) Ge/Si intermixing has been shown to be significant^[3], but the composition of single islands remains unknown. Here I describe Ge–Si intermixing from *individual* islands measured *in situ* using X-Ray Photoemission Electron Microscopy.
- (iii) Finally, LEEM movies taken *in situ* during post-deposition annealing, reveal a surprising phenomenon of metastability^[4].

1. F. Rosei, R. Rosei, *Surf. Sci.* **500**, 395 (2002).
2. A. Sgarlata, P.D. Szkutnik, A. Balzarotti, N. Motta, and F. Rosei, *Appl. Phys. Lett.*, **83**, 4002 (2003).
3. F. Boscherini, G. Capellini, L. Di Gaspare, N. Motta, F. Rosei, S. Mobilio, *Appl. Phys. Lett.* **76**, 682 (2000).
4. F. Ratto, N. Motta, A. Sgarlata, P.D. Szkutnik, S. Cherifi, S. Heun, A. Locatelli, M. De Crescenzi, and F. Rosei, in preparation.

WE-A9-2 **10h30**

ROBERT KNOBEL, Queen's University

Integrated Mechanics and Electronics at the Nanoscale

Exciting new advances in fabrication technology are allowing researchers to start making mechanical devices at the nanoscale. The simplest of such devices, tiny flexing beams, will respond to vanishingly small forces at frequencies up to the microwave range. These can form the heart of novel force sensors, more sensitive scanning probe microscopes and integrated radio-frequency filters. One intriguing possibility is that nanomechanical resonators at cryogenic temperatures may allow the detection of quantum mechanical effects in a macroscopic mechanical object. A critical challenge to reach this limit is the measurement of the displacement, since existing techniques are either not sensitive enough or do not scale well to sub-micron structures and sub-Kelvin temperatures. The exquisite charge sensitivity of the Single Electron Transistor (SET), as an integrated nano-electronic device, is well suited to measurements of quantum systems. I will present measurements exploiting the SET to detect the displacement of a nanomechanical resonator^[1]. This close coupling of a quantum electronic system with a (possibly) quantum mechanical system suggests a fascinating laboratory for studies of decoherence, quantum control and measurement. I will survey experiments proposed to reach these limits.

1. R.G. Knobel and A.N. Cleland, *Nature* **424**, 291 (2003).

11h00 **Coffee Break / Pause café**

WE-A9-3 **11h30**

ELDON G. EMBERLY, Simon Fraser University

The Smallest Molecular Switch

The field of molecular electronics concerns itself with the study of the electronic properties of single molecules attached to external voltage sources. Molecular wires display an assortment of conductance behaviour and it is thought that they may someday replace conventional semiconductor devices. In this talk, I will discuss the theoretically predicted switching behaviour of the smallest molecular switch, namely a benzene-dithiolate molecule bonded between a gold electrode and a scanning tunneling microscope. Remarkably, the molecule can exist in two different low energy configurations - one conducting and the other not. Flipping between these states is predicted to be induced via lateral motion of the STM tip or voltage pulses. Such a mechanism might explain recent experiments that have seen STM induced switching using similar molecular components.

WE-A9-4 **12h00**

FEI ZHOU, University of British Columbia

Spin Correlated Ultra Cold Atoms

Recent experiments on cold atoms in optical traps and optical lattices have revealed many exciting properties of correlated atoms which are beyond the scope of condensation of spinless atoms. In this talk I offer an introduction to various spin correlated states of cold atoms recently investigated. I will focus on Ising symmetries in many-body wave functions and discuss consequences in spin nematic Mott states (SNM), Spin Singlet Mott (SSM) states and Dimerized Valence Bond Crystal states (DVBC) found in various limits.

12h30 **Session Ends / Fin de la session**

[WE-A10] **Particle Astrophysics /**
Astrophysique des particules

(PPD)

WEDNESDAY, JUNE 16
MERCREDI, 16 JUIN
10h00 - 12h00

[Room/Salle : Victoria]

Chair: W. Trischuk, U.Toronto

WE-A10-1 **10h00**

KEVIN GRAHAM, Queen's University

Recent Results from the Sudbury Neutrino Observatory

From measurements of the flux of 8B solar neutrinos, the Sudbury Neutrino Observatory has now made significant contributions to solar and neutrino physics from both the initial 'pure D₂O' and second 'salt' phases. A summary of results to date will be provided along with some details of the experimental procedures utilized. A description of detector calibration and systematic uncertainty evaluations for the salt phase will be given including energy, reconstruction, and background evaluations and with some emphasis placed on the differences between neutron response in the first and second phases of data taking. The impact of SNO results will be discussed with particular focus placed on the impact of the flux results on neutrino parameters. A brief account of the current phase of operation and future expectations will conclude the session.

WE-A10-2 **10h30**

KENNETH J. RAGAN, McGill University

STACEE Continues — VERITAS Lives!

We will discuss the current status of the STACEE and VERITAS ground-based gamma-ray astrophysics projects. Both are based on the proven Atmospheric Cherenkov Technique (ACT) in which high-energy gamma-rays are detected by observation of the Cherenkov light produced by their cascades in the upper atmosphere. STACEE samples the resulting Cherenkov wavefront using the large mirrors of a solar research facility, in principle allowing lower thresholds than hitherto obtained from first-generation ACT instruments. STACEE is complete and operating and results will be presented from the data taken to date. VERITAS is an array of 4 imaging telescopes, each of which creates an image of the Cherenkov shower in a pixelated camera. It is now under construction in Arizona and scheduled for completion in early 2006. We will present the current status of the detector and its foreseen capabilities, as well as data from the prototype which has been recently commissioned.

11h00 **Coffee Break / Pause café**

WE-A10-3 11h15

Wavelength Shifter in the Heavy Water of the Sudbury Neutrino Observatory, Etienne Rollin, Carleton University — In order to have access to the lower energy part of the Boron-8 solar neutrino energy spectrum, a proposal has been made to add wavelength shifter molecules (WLS) to the heavy water of the Sudbury Neutrino Observatory (SNO). WLS should increase the number of photons detected per event while keeping the external backgrounds at a low level. This has the potential to lower the energy threshold cut currently used by the SNO collaboration. Montecarlo studies show that using a Carbostyryl-124 solution at a concentration of 1 ppm, one can lower the energy threshold from 5.5 to 3.5 MeV. The physics implications of such a reduction will be discussed.

WE-A10-4 11h30

SNO, SNEWS, and the Next Galactic Supernova, Clarence J. Virtue, Laurentian University, for the SNO Collaboration — A type II supernova releases 99% of its energy in the form of neutrinos over a brief timescale of tens of seconds. These neutrinos escape from the proto-neutron star following core collapse and are an excellent window into the dynamics of the supernova process itself, whose detailed understanding is seen as one of the remaining "grand challenges" of computational physics. The Sudbury Neutrino Observatory (SNO) is one of several detectors worldwide capable of observing galactic supernovae, through the detection of hundreds to thousands of neutrino interaction events. Current models of the supernova process have robust and distinguishing features in their neutrino energy, flavour and luminosity spectra. SNO's capabilities to extract neutrino energy and flavour distributions are therefore important tools in providing experimental constraints to supernovae theory. A tantalizing aspect of supernova neutrino detection is that the neutrinos precede, by up to 10 hours, the visible eruption of the mantle of the star. This potentially allows for an alert to be issued before the supernova is otherwise detectable. Though galactic supernovae are rare events, occurring approximately every 10-50 years, a false announcement from a neutrino detector would be very disruptive to the observing programs of astronomical instruments around the world. However, a prompt announcement following on the real-time observation of a supernova neutrino signal would also be a unique opportunity for the astronomical community to observe a near-by supernova with modern instruments from the earliest possible moment. In order to ensure a prompt and positive alert several neutrino detectors have formed the Supernova Early Warning System (SNEWS). This presentation will outline the potential of SNO for supernova physics and the techniques in place to maximize this scientific opportunity by providing a reliable and timely alert to the astronomical community through SNEWS.

WE-A10-5 11h45

Possible Tests of Universal Gravitation at Short Distances, Peter Watson, Carleton University — A number of recent theories have suggested that the inverse-square law may be modified at short distances. Current experimental limits show that it is valid down to at least 150 μ ; but there are effectively no limits below 10 μ . We show that it is possible to obtain a very weak limit for shorter distances, and suggest that it may be possible to use a "quantum pendulum" to go below 1 μ .

12h00 Session Ends / Fin de la session

**[WE-A11] Ion Traps in Atomic and Nuclear Physics /
Pièges à ions en physique atomique et nucléaire**

(DNP-DAMP/
DPN-DPAM)WEDNESDAY, JUNE 16
MERCREDI, 16 JUIN
10h00 - 12h45

[Room/Salle : Campaign A]

Chair: K. Sharma, U.Manitoba

WE-A11-1 10h00

MATTHEW PEARSON, TRIUMF

Nuclear Physics From Cold, Trapped Atoms

Neutral atom traps provide a well localised, backing free sample of cold atoms. In addition the sample is both isotopically and isomerically pure and held within a highly controllable environment. When coupled, on-line to a radioactive beam facility this allows for precision atomic spectroscopy to be performed along a chain of isotopes. These measurements can yield detailed information on the ground state nuclear moments and nuclear spin as well as the charge and magnetisation distributions within the nucleus. Recent measurements on Potassium isotopes performed at TRIUMF's TRINAT facility will be shown along with future plans.

WE-A11-2 10h30

JAMES D.D. MARTIN, University of Waterloo

*Dipole-Dipole Interactions Between Ultracold Rydberg Atoms**

Highly excited Rydberg atoms may strongly interact through dipole-dipole coupling. Thus, temporary excitation to Rydberg states has been proposed for implementing quantum gates between single neutral atoms storing qubits^[1], and as a means to encode qubits in small clouds of neutral atoms (such as in magnetic microtraps)^[2]. To investigate the feasibility of these proposals we have experimentally studied the dipole-dipole interactions between cold Rydberg atoms. Cold Rubidium atoms from a magneto-optical trap are excited to Rydberg states using a novel modeless dye laser. The dipole-dipole interactions are then probed using microwave transitions and selective field ionization. Both resonant and non-resonant dipole-dipole interactions have been studied.

1. Jaksch *et al.*, Phys. Rev. Lett., v. **85**, 2208 (2000).2. Lukin *et al.*, Phys. Rev. Lett., v. **87**, 37901 (2001).

* In collaboration with K. Afrousheh, P. Bohlouli-Zanjani, M. Fedorov and D. Vagale and supported by NSERC, Canada Foundation for Innovation, and Ontario Innovation Trust.

11h00 Coffee Break / Pause café

WE-A11-3 11h30

JENS DILLING, TRIUMF

Ion Traps in Nuclear Physics: The Ultimate Tool for Precision Experiments

Ion traps were originally developed for atomic physics purposes, but were quickly adapted by the nuclear physics community due to its unique features and strait forward compatibility. Some of the most attractive attributes is that these traps allow one to store a sample over an extended period of time in a very well defined environment. This permits long observation times, hence leads to better precision in the measurements, or provides for addition manipulation, often necessary to carry out the procedure of interest. Ion traps in nuclear physics are therefore mostly used for either high precision experiments, or serve as intermediate steps where additional manipulation techniques, like cooling or accumulation, can be applied. An additional asset is the general applicability of ion traps to all charged particles, particularly important in nuclear physics, where one has for example excess to a broad variety of different isotopes. This talk reviews the various trapping techniques as currently used in nuclear physics and shows, how and why some of the best precision experiments, like CPT-tests and weak-interaction Standard model test employ ion traps. An overview of present world-wide activities is given.

WE-A11-4 12h00

Recent Atomic Mass Measurements on Nuclei Far From Stability with the Canadian Penning Trap Mass Spectrometer, K.S. Sharma¹ and J.A. Clark^{1,2}, R.C. Barber¹, B. Blank^{2,3}, C. Boudreau^{2,4}, F. Buchinger⁴, J.E. Crawford⁴, S. Gulick⁴, J.C. Hardy⁵, A. Heinz^{2,6}, J.K.P. Lee⁴, A.F. Levand², B. Lundgren², R.B. Moore⁴, G. Savard², N. Scielzo², D. Seweryniak², G.D. Sprouse⁷, W. Trimble², J. Vaz^{1,2}, J.C. Wang^{1,2}, Y. Wang^{1,2}, Z. Zhou², ¹ University of Manitoba, ² Argonne National Laboratory, ³ Centre d'Etudes Nucléaires de Bordeaux-Gradignan, ⁴ McGill University, ⁵ Texas A&M University, ⁶ Yale University and ⁷ Stony Brook University — The Canadian Penning Trap (CPT) mass spectrometer, installed at the ATLAS facility of the Argonne National Laboratory, was designed to be able to measure the masses of a wide variety of nuclides, having half-lives as low as 50ms, to an accuracy approaching 1ppb of the mass. Such data are important because they provide input to astrophysical theories of nucleosynthesis, allow

tests of fundamental symmetries in the standard model for particle physics and provide stringent constraints on theories that predict nuclear masses. Recent enhancements to the instrument together with the results of recent precision mass measurements among proton and neutron rich nuclei will be discussed.

WE-A11-5 12h15

Tripartite Entanglement of a Trapped Atom in an Optical Cavity*. T.J. Harmon, R.I. Thompson and B.C. Sanders, *University of Calgary* — Single-atom cavity quantum electrodynamics (QED) is important at a scientific level as a testbed for atom-field coupling in combined systems and to explore atom-field entanglement, which is important for tests of QED and applications to quantum information science. At a technological level, single-atom cavity QED offers the prospect of single-photon sources, quantum memory storage, and quantum computing. The theory of the atom in the cavity is well described by the Jaynes-Cummings model, which treats the atom as an electric dipole interacting with a single mode of the cavity field. However, recent progress with trapping neutral atoms and ions allows quantum features of the motion to arise. The resultant electron-photon-phonon entanglement is especially interesting as a manifestation of tripartite entanglement, which can now be investigated in cavity QED. We are particularly interested in probing this tripartite entanglement and propose the method of photon coincidence spectroscopy (PCS), which combines features of spectral hole burning and photon correlation measurements, for probing this entanglement. In the specific case of a trapped ion, cooled below the Lamb-Dicke limit and positioned inside a cavity, we have developed an exact, analytical solution for the coupling of the sinusoidally-oscillating atom to the cavity modes in the adiabatic approximation. This result allows a determination of the spectrum atom-cavity system. PCS techniques are then employed to observe two-photon spectral signatures of tripartite entanglement. We discuss the feasibility of this scheme in the context of current experimental capabilities.

* This work is being supported by NSERC.

WE-A11-6 12h30

CASTING LIGHT ON ANTIMATTER: COLD ANTIHYDROGEN WITH ATHENA. Makoto C. Fujiwara, *RIKEN/TRIUMF* — Testing fundamental symmetries plays an important role in our understanding of Nature. The ATHENA experiment, located at CERN's Antiproton Decelerator (AD) facility, aims to make a precision test of CPT symmetry by comparing the properties of hydrogen with those of its antimatter counterpart, antihydrogen. After several years of development, we have achieved our initial goal in 2002: production of antihydrogen at low velocity^[1] (see for a review [2]). With our results subsequently confirmed by another AD experiment, a next major goal is laser spectroscopy of cold antihydrogen. I will discuss our first production, together with the subsequent progress^[3] and the prospects for antihydrogen spectroscopy.

1. M. Amoretti *et al.*, *Nature* (London) 419, 456 (2002).
2. M.C. Fujiwara *et al.*, *Nucl. Instrum. Method. B* 214, 11 (2004).
3. M.C. Fujiwara *et al.*, *Phys. Rev. Lett.* 92, 065005 (2004).

12h45 Session Ends / Fin de la session

[WE-A12]

(DIMP/DPIIM)

Imaging with Photoacoustic and Photothermal NDE Techniques and Microscopies / Imagerie à l'aide de techniques END et de microscopies photoacoustiques et photothermiques

WEDNESDAY, JUNE 16

MERCREDI, 16 JUIN

10h00 - 12h30

[Room/Salle : Strathcona]

Chair: A. Mandelis, U.Toronto

WE-A12-1 10h00

KIRK H. MICHAELIAN, Natural Resources Canada

Disperse Photoacoustic Spectroscopy of Hydrocarbons

A dispersive photoacoustic (PA) spectroscopy system was constructed from a 450-W Xe lamp, a 0.19-m monochromator fitted with three interchangeable gratings, a mechanical chopper, and a commercial PA cell. After preamplification, signals were detected with a lock-in amplifier. Magnitude and phase spectra of a series of opaque, viscous hydrocarbon liquids revealed the existence of near-ultraviolet absorption edges. The wavelengths of these features depended on sample boiling point and were consistent with data from conventional transmission spectroscopy. Dispersive visible and near-infrared PA spectra contained additional bands of interest.

WE-A12-2 10h30

JUN SHEN, National Research Council Canada

Photothermal Beam Deflection Techniques Applied to the Non-Destructive Measurements of Thermophysical Properties

Photothermal beam deflection (PBD), namely optical beam deflection, is a remote (noncontact) technique, which is suitable for studying samples in a severe environment. In the transverse PBD (or mirage effect) spectrometry, a probe beam probes the gradient of the optical refractive index in the deflecting medium adjacent to a sample surface, resulting in the deflection of the probe beam. The gradient of the optical refractive index is induced by the temperature gradient from the sample surface to the medium, and the temperature rise in the sample is the result of the conversion of the absorbed electromagnetic excitation radiation into heat. The optical and thermophysical properties of the sample, therefore, can be measured by monitoring the frequency dependence (for frequency-modulated excitation) or the time dependence (for pulsed excitation) of the PD signal. In this presentation, different configurations of PBD are introduced, and the experimental results with these configurations are presented. Thermal effusivities of different materials are obtained using frequency-modulated excitation method, and thermal diffusivities are measured with our recently developed step excitation technique. Thermal conductivity and unit volume specific heat then can be deduced from thermal diffusivity and thermal effusivity. Considerations in designing these configurations and performing experiments are also discussed.

11h00 Coffee Break / Pause café

WE-A12-3 11h30

MAURO M. BAISSO, University of Maringa

*Time Resolved Thermal Lens for Thermo-Optical Measurements in Transparent Materials During Phase Modification**

The fortieth anniversary of the first observation of the thermal lens effect will occur in 2004 and certainly is a time for reflection on the contribution of this phenomenon to the study of transparent materials. As a troublesome effect during the operation of many lasers or as a high sensitive tool for non-destructive characterization of any kind of highly transparent samples, including solids, liquids and gases, the thermal lens spectrometry has provided substantial information regarding the thermo-optical properties of the studied materials. Measurements of the optical absorption coefficient, the temperature coefficients of refractive index and optical path length, the fluorescence quantum efficiency, the thermal diffusivity, the thermal conductivity, etc, have been performed. The evolution of the thermal lens methods for non-destructive studies has allowed new insights in recent years as a consequence of the introduction of several modifications in their experimental set up. Exploring the remote nature of the technique, several works have focused on the ability of the method to evaluate the samples during the temperature scanning, the application of external field and also during the occurrence of photochemical reaction. The aim of this presentation is to highlight the ability and the accuracy of the thermal lens method for spectroscopic measurements performed during the samples phase modification. Quantitative measurements during phase transitions in biomaterials, glass transitions in polymers and the photochemical reaction in Cr6+-complex solution will be discussed. The focus will be the resolution of the method as compared to conventional measurements. Finally, together with the new perspectives of future work, the recent improvement in the thermal lens data acquisition procedure will be discussed.

* In collaboration with P.R.B. Pedreira and J. Mura, Departamento de Física, Universidade Estadual de Maringá, Brazil.

WE-A12-4 12h00

MATTHEW E. BRIGGS, Los Alamos National Lab

Optical Velocity-Measurement Techniques For Supersonic Surfaces

Interferometric techniques have been used routinely for more than 20 years to measure velocities of explosive shock-fronts. Recently, structured-light measurements have been used for the same purpose. Explosions accelerate surfaces to as much as 15 km/sec in a nanosecond or less, often generating much light, large changes in reflectivity, and ejecting particles or layers at different speeds. I will describe the current performance of fiber-optic displacement-interferometers, Fabret-Perot interferometers, velocity interferometers (VISAR), and structured light, in this interesting physical space.

12h30 Session Ends / Fin de la session

[WE-A13] **General Relativity and Gravitation I /**
Relativité générale et gravitation I

(DTP/DPT)

WEDNESDAY, JUNE 16
 MERCREDI, 16 JUIN
 10h00 - 12h30

[Room/Salle : Kildonan]

Chair: A. Kempf, U.Waterloo

WE-A13-1 10h00

GABOR KUNSTATTER, University of Winnipeg

Vibrational Modes of Black Holes and their Quantum Gravitational Microstates

The quasi-normal modes (QNM) are classical vibrational modes of black holes that play an important role in predictions for gravitational wave experiments. A few years ago, Hod used semi-classical arguments to derive the energy/area spectrum of quantum black holes from numerical observations about their QNM spectrum. More recently Dryer used arguments similar to those of Hod in order to fix the elusive Immirzi parameter in loop quantum gravity. I review a generalization of Hod's arguments that seems to suggest the fact that the QNM spectrum may be providing clues about black hole quantum microstates at least for the case of Schwarzschild black holes. I will also review some of the evidence that this relationship does not hold for more complicated black holes, and speculate on the reasons for this apparent discrepancy.

WE-A13-2 10h30

ROBERT BRUCE MANN, University of Waterloo

*Mass Conjectures, Entropy Bounds and the dS/CFT Correspondence**

We consider the class of four-dimensional Taub-Bolt(NUT) spacetimes with positive cosmological constant and non-zero NUT charge. We show that such spacetimes can be thermodynamically stable and have entropies that are greater than that of de Sitter spacetime, in violation of the entropic N-bound conjecture. We also show that the maximal mass conjecture, which states "any asymptotically dS spacetime with mass greater than dS has a cosmological singularity", can be violated as well. Our calculation of conserved mass and entropy is based on an extension of the path integral formulation to asymptotically de Sitter spacetimes.

* In collaboration with R. Clarkson¹ and M. Ghezelbash², ¹University of Waterloo and ²University of Waterloo.

WE-A13-3 11h00

DON N PAGE, University of Alberta

Particle Production in a Tunneling Universe

Rubakov and Vilenkin, and their collaborators, have debated whether there is catastrophic particle production in a tunneling universe. Here we examine the toy model in which one has a quantized scalar field evolving in a classical FRW spacetime which has a real Lorentzian evolution followed by a real Euclidean evolution followed by a final real Lorentzian evolution (an L-E-L model). We find that if one chooses the vacuum state in the asymptotic past, then for modes with sufficiently large spatial momentum, the quantum state diverges within the Euclidean region. Therefore, the asymptotic past vacuum would not give a physical state in the asymptotic future in this L-E-L model.

* In collaboration with S.P. Kim, Kunsan National University.

WE-A13-4 11h30

ERIC POISSON, University of Guelph

The Gravitational Self-Force

The gravitational self-force describes the effect of a particle's own field on its motion; while the motion is geodesic in the test-mass limit, it is accelerated to first-order in the particle's mass. I will review the foundations of the self-force, and show how an infinite field can be unambiguously decomposed into a singular piece that exerts no force, and a smooth remainder that is responsible for the acceleration. The context of this work is provided by the Laser Interferometer Space Antenna, which will be sensitive to low-frequency gravitational waves. Among the sources for this detector is the motion of small compact objects around massive (galactic) black holes. To calculate the waves emitted by such systems requires a detailed understanding of the motion, beyond the test-mass approximation.

WE-A13-5 12h00

KAYLL LAKE,, Queen's University

Recent Developments in Computer Algebra Applied to General Relativity

I review some recent developments in computer algebra and visualization applied to general relativity. As an example, the classical notions of "R" and "T" regions of spacetime are given invariant definition and explored away from spherical symmetry.

12h30 Session Ends / Fin de la session

[WE-A14] **Synchrotron Biophysics: The Canadian Light Source /**
Biophysique au synchrotron : La source de lumière canadienne

(BSC/SCB)

WEDNESDAY, JUNE 16
 MERCREDI, 16 JUIN
 10h00 - 12h30

[Room/Salle : Albert]

Chair: J. Lepock, U.Waterloo

WE-A14-1 10h00

WILLIAM THOMLINSON, Canadian Light Source

The Canadian Light Source: Opportunities in Biomedical Research

The Canadian Light Source (CLS) is in the early phase of operations. Located on the campus of the University of Saskatchewan, the CLS is Canada's national synchrotron radiation facility serving the Canadian academic, industrial and government scientific communities. The facility is a 3rd generation high brightness source operating at 2.9 GeV.

Commissioning of the facility started in the autumn of 2003. Seven experimental beamlines are in the commissioning or construction phase, with full operation of the scientific programs commencing by the end of 2004. These beamlines include: two infrared beamlines for spectroscopy and microscopy, three soft x-ray beamlines for spectroscopy and microscopy, and two hard x-ray lines for protein crystallography and micro-EXAFS. This talk is an overview of the CLS facility, the present status of the storage ring performance and a summary of the Phase I beamlines. In addition, the Canada Foundation for Innovation has recently agreed to fund additional experimental facilities and these will be presented as well, with emphasis on those of direct interest to biomedical research. Several examples of synchrotron radiation biomedical research will be given to highlight the types of programs to be carried out at the CLS in medical imaging and radiation therapy.

WE-A14-2 10h30

DEAN CHAPMAN, Anatomy and Cell Biology, University of Saskatchewan

New Sources of X-Ray Imaging Contrast

New sources of x-ray contrast that rely on phase or phase related effects have been developed in the past several years. One of the techniques that exploit these contrast mechanisms is Diffraction Enhanced Imaging. This method develops contrast from x-ray refraction and ultra-small angle scattering and is easily applied using synchrotron x-ray sources. These contrast mechanisms have been shown to be particularly useful for soft tissue imaging. The physics of these mechanisms will be discussed along with experimental verification. Examples of the contrast and applications to mammography and other soft tissue imaging problems will be presented. A new method of extracting more information from a series of images is also presented. This method independently extracts scatter information and also improves the refraction and absorption images. Also, progress and future plans for in-laboratory systems will be briefly discussed.

11h00 Coffee Break / Pause café

WE-A14-3 11h30

FARIDEH JALILEHVAND, University of Calgary

X-Ray Absorption Spectroscopy in Natural Sciences; Exploring New Possibilities

Extended X-ray absorption fine structure (EXAFS) spectroscopy is an element-specific technique, providing information on average interatomic distances, the number and chemical identities of near neighbors around absorber. The hydration of the biologically important Ca^{2+} ion is notoriously difficult to study in solution because of the flexible and dynamic coordination environment. By combining EXAFS results with molecular dynamics simulations we could obtain precise mean Ca-O bond distances, the hydration number, and the geometry of the $\text{Ca}^{2+}(\text{aq})$ species. In living organisms the synthesized proteins are translocated across cell membranes. The translocation is catalyzed by the preprotein translocase, where *SecA ATPase* is a central component. In a recent study on the structure of the zinc-binding domain of *Sec A*, we could clarify the local zinc site environment by Zn K-edge EXAFS. The zinc atom coordinates two cysteine thiolate groups, an imidazole group of histidine, and a water molecule. X-ray absorption near edge structure (XANES) spectroscopy is a non-destructive technique, giving information on the oxidation state, electronic configuration and bonding of the absorber. By applying sulfur XANES on wooden cores from the 17th century Swedish warship *Vasa*, we could reveal the cause of high acidity and salt precipitation on the wood (*Nature* **2002**, *415*, 893-897). Our results show that large amounts of sulfur in reduced forms within the moist wood are being oxidized to sulfuric acid, which eventually will cause wood degradation. Sulfur XANES spectroscopy can also reveal, on a molecular basis, the effects of sour gas exposure on sulfur metabolism in intact plant leaves.

WE-A14-4 12h00

KENNETH K.S. NG, University of Calgary

Protein Crystallography and Antiviral Drug Design

A wide range of viruses are responsible for medically and economically important diseases in plants and animals. The positive-strand RNA viruses constitute a evolutionarily related group of organisms, including the pathogens responsible for polio, hepatitis A, C and D, viral gastroenteritis (Norwalk Virus), viral meningitis (West Nile Virus) and Severe Acute Respiratory Syndrome (SARS Coronavirus). Novel antiviral drug treatments are urgently needed for most of these diseases, because existing or alternative therapeutic approaches are not effective. Our approach to the development of novel antiviral drug treatments is through the structural analysis of viral proteins using X-ray crystallography. By obtaining structures of viral proteins and their complexes with substrates or binding partners at nearly atomic resolution, it is possible to infer many of their important chemical and biological functions. Understanding the structure and mechanism of viral proteins in turn allows for the design and synthesis of novel chemical molecules that bind to the protein and interfere with a function of the protein that is important for the life cycle of the virus. If effective in a biological setting, these compounds can be considered candidate antiviral drugs. Crystallographic analysis of complexes formed between viral proteins and these novel, designed chemical compounds allows for the refinement and further improvement of the design of second-generation compounds, and further iterations of this cycle of design, synthesis and analysis hopefully leads to the production of therapeutically effective antiviral drugs. Current work on the Norwalk Virus polymerase will be discussed in relation to this overall scheme.

12h30 Session Ends / Fin de la session

[WE-A15]

(CASCA)

**Imaging in Multiple Wavelengths - Contributed /
Imagerie dans des longueurs d'ondes multiples - contribuées**

WEDNESDAY, JUNE 16

MERCREDI, 16 JUIN

10h15 - 11h00

[Room/Salle : Campaign B]

Chair: R. Bond, CITA

WE-A15-1 10h15

The Evolution of the Galaxy Luminosity Function and Cosmic Star Formation History from $z \sim 4$ to $z \sim 1.7$ using Multiwavelength Imaging. **Marcin Sawicki**, *National Research Council* — I will present results from an extremely deep UGRI ground-based imaging survey on Keck. These multiwavelength observations use the identical filter set and well-characterized selection techniques employed by Steidel and collaborators to select star-forming galaxies at $z \sim 4$ and $z \sim 3$, and include a very recent extension of the technique into the "redshift desert" at $z \sim 2.2$ and $z \sim 1.7$. In contrast to previous work, our survey reaches typically ~ 1.5 magnitudes, or a factor of 4, deeper, and so probes well into the faint end of the galaxy luminosity function. We present the first robust measurements of the UV galaxy luminosity function at $z \sim 2$, and of the faint end of the luminosity function at $z \sim 4$. Our data show that the faint end of the luminosity function appears to be evolving with lookback time, while the bright end remains virtually unchanged. I will discuss this differential evolution of the luminosity function and the possible mechanisms that can be responsible for it.

WE-A15-2 10h30

Multi-Waveband Imaging of the Most Distant Black Holes*, **Chris Willott**, *Herzberg Institute of Astrophysics* — The high optical luminosities of the most distant quasars known infer black hole masses greater than a billion solar masses powering these objects. If local correlations between black hole mass and dark matter halo mass extend to redshift 6, then these quasars pinpoint the locations of the first massive structures to have formed. I will discuss how imaging observations at various wavebands ranging from the optical through the sub-millimetre to the radio enable us to infer physical parameters of these systems such as black hole mass, star formation rate and dark matter halo mass.

* This work is being supported by NR.

WE-A15-3 10h45

The Red-Sequence Cluster Surveys*, **Howard Yee**, *University of Toronto* — Galaxy clusters at high redshift provide the largest leverage in both the determination of cosmological parameters and the study of cluster formation and evolution. The Red-Sequence Cluster Survey 1 (RCS1) is a completed 100 sq. deg. optical imaging survey designed to create a large sample of galaxy clusters at $z \sim 1$, with the primary goal of measuring the mass density and σ_8 parameters. With the new CFHT MegaCam camera and the suc-

successful demonstration of the red-sequence method used for RCS1, we have begun the next generation optical cluster survey, the RCS2 — a 1000 sq. deg. survey with the goal of measuring the equation of state parameter w , via the evolution of the cluster mass function. This survey will potentially create a sample of a few times 10,000 clusters up to the redshift of 1, providing constraints in the w - Ω_m plane with similar uncertainties as that of SNe projects such as CFH-LS. A secondary benefit will be the discovery of 50-100 new strong lensing clusters — an important new tool for studying reionization and the very early stages of galaxy formation. I will describe some results from the RCS1, and the prospects for the RCS2.

* This work is being supported by NSERC, U of Toronto, CRC.

11h00 Session Ends / Fin de la session

[WE-A16]

**Ultrafast Laser Applications /
Applications des lasers ultra-rapides**

(DOP-DAMPI
DOP-DPAM)

WEDNESDAY, JUNE 16

MERCREDI, 16 JUIN

10h30 - 12h30

[Room/Salle : Ballroom C]

Chair: *W.-K. Liu, U.Waterloo*

WE-A16-1 10h30

TARA M FORTIER, University of Colorado

Carrier-Envelope Phase Stabilized Modelocked Lasers

By drawing on the techniques of single-frequency laser stabilization and on improvements of ultrafast lasers, phase stabilization of Ti:sapphire lasers has led to great advances in both the fields of optical frequency metrology and ultrafast science. I will speak about the development of the technology and the application of modelocked laser stabilization to both these domains. Towards the latter, the highly phase-coherent pulse train of the laser has been employed in the exploration of quantum interference control in semiconductors, with the aim of developing a phase sensitive photodetector for simplification of the laser stabilization scheme. As an application to the former I will a phase stable octave spanning Ti:sapphire laser that is a possible candidate as a transfer oscillator for an all-optical clock.

WE-A16-2 11h00

Simulation of Femtosecond Laser Ablation of Silicon. Roman Holenstein, R. Fedosejevs and Y.Y. Tsui *University of Alberta* — Femtosecond laser ablation is an important process in the micromachining and nanomachining of microelectronic, optoelectronic, biophotonic and MEMS components. The process of laser ablation of silicon is being studied on an atomic level using molecular dynamics (MD) simulations. We present on ablation thresholds for Gaussian laser pulses of 700 – 800 nm and in the range of a few hundred femtoseconds in duration. Absorption occurs into a hot electron bath which then transfers energy into the crystal lattice. The simulation box is a narrow column approximately 6 nm x 6 nm x 80 nm with periodic boundaries in the x and y transverse directions and a 1-D heat flow model at the bottom coupled to a heat bath to simulate an infinite bulk medium. A modified Stillinger-Weber potential is used to model the silicon atoms.

11h15 Coffee Break / Pause café

WE-A16-3 11h45

EVGENY A. SHAPIRO, National Research Council

Shaping Molecular Wavepackets by AC Stark Shifts

From a wavepacket perspective, quantum dynamics are viewed as a flow of probability and phase - in contrast with a few-level dynamics. Trying to control such processes, we have to think in terms of applying coordinate-dependent potentials rather than in terms of level-by-level addressability. I shall describe control of quantum wavepackets using the combination of coordinate-dependent AC Stark shifts induced by short laser pulses (phase kicks) and free evolution. This approach resembles shaping wavepackets of light in optics. Like spatial light modulators in optics, the tools used allow arbitrary shaping of molecular wavepackets via interference of effective eigenstates of the so-called revival-scale evolution. The number of such eigenstates is determined by the accuracy of control we are interested in. Numerical and experimental examples show how this technique allows one to control molecular alignment and orientation. Next, I shall discuss relation of the wavepacket control to quantum information processing. It will be shown how several quantum bits can be encoded in the shape of a single wavepacket, and how the control can be implemented as a quantum computation.

WE-A16-4 12h15

Femtosecond Electron Diffraction and the Quest for the "Molecular Movie". Bradley J. Siwick, Jason R. Dwyer, Robert E. Jordan, Christoph Hebeisen, R.J. Dwayne Miller, *University of Toronto* — One of the great experimental challenges in physics and chemistry is to obtain a real-time view of chemical reactions by resolving the nuclear motions that accompany the breaking and making of chemical bonds in the transition state region between reactant and product surfaces. The recent development of time-resolved diffraction techniques — both x-ray and electron — with ultrafast temporal resolution has opened up such a direct window on the time-evolving atomic configuration of molecules and solids. Our group has developed a photo-activated electron source capable of producing sub-500 femtosecond electron pulses that contain sufficient numbers of electrons to allow the study of even irreversible structural dynamics. The first study employing this 'electron gun' was to investigate the strongly-driven, laser induced solid-liquid phase-transition in polycrystalline aluminum as a model transition state process. We are able to see, in real-time, the loss of the long-range order present in the crystalline phase and the emergence of the liquid structure where only short-range atomic correlations are present. The sensitivity and temporal resolution was sufficient to capture the time-dependent radial distribution function of the material as it evolved from the solid to liquid state in 3.5 ps. The rapidity of the structural transition in aluminum contrasts strongly with the case of gold, where the time-scale for the phase transition, under equivalent conditions, is longer than 10 ps. These observations provide an atomic-level description of the melting process and represent the first instance of electron diffraction performed with subpicosecond temporal resolution.

* This work is being supported by Bradley Siwick.

12h30 Session Ends / Fin de la session

[WE-A17]

**Radiation Dosimetry /
Dosimétrie des rayonnements**

(COMPI/OCPM)

WEDNESDAY, JUNE 16

MERCREDI, 16 JUIN

10h30 - 12h30

[Room/Salle : Ballroom B]

Chair: *K. Sixel, Sunnybrook/U.Toronto*

WE-A17-1 10h30

Accuracy in Dose Calibration of Fricke-Xylenol Orange Gels using Optical CT Scanning. K. Jordan and J.J. Battista, *London Regional Cancer Centre, London Health Sciences Centre, and University of Western Ontario* — Three-dimensional (3D) dosimetry is used more frequently to verify dose distributions produced by conformal radiotherapy techniques. In our work, we record dose distributions in Fricke-Xylenol Orange gelatine and then use optical CT scanning to read the exposed gel. The best accuracy is currently obtained with a pencil beam laser scanner ($\lambda = 594$ nm). We are also developing a faster rotate-only system with a planar diffuse LED light source ($\lambda = 590$ nm), and CCD camera for capturing optical transmission data. The entire gel cylinder (10 cm diameter x 10 cm long) is scanned in 40 minutes with an isotropic spatial resolution of 0.5 mm (i.e. 200 dose slices). Our dose calibration procedure involves (a) good control of the thermal history of the gels during fabrication and storage, (b) independent calibration of the

optical scanner in terms of reconstructed attenuation coefficients (μ) using reference liquid solutions (agreement $\leq 1\%$), and (c) using the depth-dose curve of a 12 MeV electron beam to provide a single self-consistent calibration with a wide range of doses traceable to a standard ionization chamber. This procedure also determines the gel sensitivity and linearity ($\Delta\mu / \Delta D = 0.1 \text{ cm}^{-1}$ per Gy), assesses spatial uniformity and temporal response (*i.e.* dose rate and fractionation effects). We achieve good agreement in local absolute dose ($\leq 3\%$ of D_{max} of 3 Gy, and $< 1 \text{ mm}$ offset in electron depth-dose curves). In conclusion, we demonstrate clinical applications of 3D gel dosimetry to megavoltage x-ray IMRT, including tomotherapy.

WE-A17-2 10h45

NMR Relaxometry Study and Gravimetric Analysis of an Aqueous Polyacrylamide Dosimeter Without Gelatin*, S. Babic and L.J. Schreiner, *Queen's University/KRCC* — In conformal radiation therapy, a high dose is given specifically to a target volume to increase the probability of cure, and care is taken to minimize the dose to surrounding healthy tissue. The techniques used to achieve this are very complicated and the precise verification of the resulting three-dimensional (3D) dose distribution is required. Polyacrylamide gelatin (PAG) dosimeters with MRI and optical CT provide the required 3D dosimetry with high spatial resolution. The study of the fundamental properties of the radiation-induced polymerization in PAG dosimeters is complicated by the presence of the background gelatin matrix. We have developed a gelatin-free model system for the study of the basic radiation-induced polymerization in PAG. In this presentation, we show results of investigations on gelatin-free dosimeters containing equal amounts of acrylamide and N,N'-methylene-bisacrylamide (named Aqueous Polyacrylamide, APA). The APA dosimeters were prepared with four different total monomer concentrations (2, 4, 6, and 8% by weight). NMR spin-spin and spin-lattice proton relaxation measurements at 20 MHz, and gravimetric analyses performed on all four dosimeters, show a continuous degree of polymerization over the range of dose 0-25 Gy. The polymer fraction measurements are supported by gas chromatography spectrometry measurements on the non-polymerized monomer components in a 2% by weight APA dosimeter. The developed NMR model explains the relationship observed between the relaxation data and the amount of cross-linked polymer formed at each dose. This model can be extended with gelatin relaxation data to provide a fundamental understanding of radiation-induced polymerization in the conventional PAG dosimeters.

* This work is being supported by CIHR, OCITS, CCO/Nordion.

WE-A17-3 11h00

Preliminary Study of the MAGIC Gel Dosimeter Using X-ray Computed Tomography, Michelle Nielsen and B. Keller, *Toronto Sunnybrook Regional Cancer Centre* — This study presents some feasibility investigations of MAGIC gel used along with x-ray CT as the read-out technique. It has been established that CT can be used to readout polyacrylamide gels (PAGs). MAGIC (methacrylic and ascorbic acid in gelatin initiated by copper) gel is a relatively new, easy to manufacture normoxic polymer gel formulation. The gels were manufactured and irradiated using either a 6MV photon beam or an Ir^{192} HDR source. The gels were imaged pre and post irradiation using a Picker CT simulator and software was developed to filter and subtract the pre-irradiated images from post-irradiated image. For the external beam irradiation, 20 ml plastic cylindrical vials containing the gel were irradiated to varying doses using a parallel opposed irradiation geometry with the vials immersed in a water filled container. Dose response curves were generated where a change in CT number was plotted as a function of radiation dose. The sensitivity of the gel was measured to be $0.25 \pm 0.01 \text{ DHU Gy}^{-1}$. The HDR gels were irradiated with either a point or line source geometry. Calibration curves were generated where the change in CT number was plotted as a function of distance away from the HDR catheter. Issues of CT dose and gel sensitivity will be discussed. Future studies will focus on sensitizing gel dosimeters to x-ray CT in order to make this readout technique clinically viable.

WE-A17-4 11h15

Comparison of Scintillating Fibers for Increasing the Signal to Noise Ratio of Scintillator Dosimeters*, Luc Beaulieu¹, L. Archambault¹, S. Lambert-Girard¹, J. Arseneault¹, L. Gingras¹, S.A. Beddar², M.D. Anderson² and R. Roy^{3, 1}, *Centre Hospitalier Universitaire de Québec, 2 Cancer Center and 3 Université Laval* — Purpose: plastic scintillators display excellent properties that could suits the most demanding applications (IMRT, radiosurgery, 4D radiotherapy) with sensitive volumes as low as 0.001 cm^3 . The limitation of scintillating systems is the low signal to noise ratio (SNR) mostly resulting from the undesired Cerenkov radiation in the light guide linking the scintillator to the photodetector. Methods and materials: Theoretical evaluation of scintillating fibers compared to simple scintillators was done, followed by an experimental comparison of light production and emission spectrum. It was done with fibers from Bicron and Kuraray manufacturers with diameters from 0.5 to 3 mm and scintillation peak between 430 and 530 nm. Results: Water equivalence of scintillating fibers was over 97 % for 1 mm diameter. Collection efficiency for a 1 cm long fiber is between 1.7 and 3.9 times that of a standard scintillator, depending on the light guide numerical aperture. It can be further increased using multicladding. Fibers from both company shows a higher production efficiency for the blue fibers (430 nm) compared to the green ones (530 nm). For the same wavelength peak, the light production for the two companies was comparable even though Kuraray fibers were multiclad. Conclusion: Scintillating fibers are an alternative to standard scintillator. They can increase the light collection efficiency and therefore increase the SNR of such dosimeter. Even if the green fibers produce less light than the blue ones, the highest wavelength allows a better separation between the signal and Cerenkov light which is more intense at lower wavelengths.

* This work is being supported by NSERC.

WE-A17-5 11h30

A Tissue Equivalent Plastic Scintillator Based Dosimetry System for Verification of IMRT Dose Distributions, M. Peter Petric^{1,2}, James L. Robar³, Brenda G. Clark^{1,2, 1}, *University of British Columbia, 2 BC Cancer Agency and 3 Nova Scotia Cancer Centre* — Intensity modulated radiation therapy (IMRT) provides improved target coverage and normal tissue sparing compared with conformal radiotherapy. In spite of these advantages, quality assurance is more challenging for the complex fluence maps used in IMRT and verification of dose distributions can be labour-intensive and time consuming. An IMRT dose verification system has been developed using tissue equivalent plastic scintillator that provides an easy to use, rapid electronic and directly digital dose measurement of a 2D plane perpendicular to the beam. The system consists of a water-filled lucite phantom with a scintillator screen built into the top. The phantom contains a plastic mirror to reflect scintillation light towards a viewing window where it is captured using a CCD camera and a personal computer. This computer is linked to the MU signal of the linear accelerator and the camera integrates the scintillation light and produces a cumulative image for every MU delivered thereby also providing temporal dose deposition information. Optical photon spread is accounted for by de-convolving a glare kernel from the raw images and system calibration is performed using radiation fields of known dose distributions. IMRT dose distributions acquired using the system were verified using film dosimetry and a high resolution mini-ionization chamber. In addition to providing instantaneous digital measurements of the dose distributions with temporal deposition information, the use of tissue equivalent scintillator which does not perturb the radiation beam during measurement means the dose detected by this system is an accurate representation of the dose delivered to the target.

WE-A17-6 11h45

Development of a Novel Liquid Ionization Chamber for Radiation Dosimetry, K.J. Stewart and J.P. Seuntjens, *Montreal General Hospital, McGill University Health Centre* — This work investigates the characteristics of a novel liquid ionization chamber currently under development as a high accuracy reference dosimeter. Liquid-filled ionization chambers have many potential advantages over traditional air-filled chambers. These include allowing for a small sensitive volume while maintaining a high signal, low perturbation effects and very little energy dependence. A dosimeter with such characteristics would be particularly useful in IMRT or small field dosimetry. We have constructed two guarded liquid ionization chambers. The GLIC-02 has C552 conducting plastic electrodes, a sensitive volume of approximately 1 mm^3 and a plane-parallel design. The sensitive liquid used is isoctane. The properties of the GLIC-02 as an air-filled device have been investigated for 6 and 18 MV photon beams. In terms of calibration factor, ion recombination and energy dependence, the GLIC-02 has characteristics equivalent to the Exradin A14P, a commercial air-filled chamber with a similar sensitive volume. As well, the polarity effect of the GLIC-02 is significantly smaller than that of the A14P. We have also filled the GLIC-02 with isoctane and examined the stability of its response in a ^{60}Co beam. Because of variations in the GLIC-02 response, we are investigating a new chamber design, the GLIC-03, which is of similar dimensions but has graphite electrodes. We are determining the effect of several parameters including electrode material, operating conditions such as the length of time voltage is applied to the chamber and the irradiation time and controlled impurities such as oxygen on the stability of the liquid-filled chamber response

WE-A17-7 12h00

Response of a MOSFET for 50 keV to 5 MeV Incident Radiation and its Impact in Radiotherapy Measurements*, Louis Archambault, L. Gingras, J.F. Carrier, R. Roy and L. Beaulieu, *Université Laval, Hôtel Dieu de Québec* — Purpose: With their excellent spatial resolution, MOSFET's are used in the evaluation of IMRT treatments. With the large number of fields, scattered radiation is significantly higher in IMRT than in standard radiotherapy. Those particles are less energetic than the primary contribution and therefore could induce an over response in the silicon sensitive area of a MOSFET. Methods and materials: GEANT4, a Monte Carlo toolkit recently validated for medical physics, was used to analyze dose deposition inside the MOSFET compared to the deposition in a similar water volume. Photon beams between 0.05 and 5 MeV were sent directly or indirectly on the dosimeter. Electron spectra reaching the active area were evaluated for different depths and for different out of field distances. Results: It was found that dose deposi-

tion by electrons inside the MOSFET could be classified according to the electrons energies. For electrons of 1 MeV and higher, the dosimeter operates in optimal conditions with a response similar to water. Between 1 MeV and 100 keV, the difference between water and silicon cross sections generates an increasing over response that reaches 31 % at 100 keV. Below that, the active area thickness begins to play an important role, since more electrons are stopped in it, but not in water, thus causing discrepancies. **Conclusion:** Even if there is an increased presence of low energy radiation in an IMRT treatment, MOSFET's could still be used for verifications, but a cautious calibration is required and users should be aware of an over response to the scattered radiation.

* This work is being supported by NSERC.

WE-A17-8 12h15

Evaluation of the Water Equivalence of Solid Water Model 457 for Photon and Electron Measurements in TG-51 Protocol. N. Videla, D. Beachey, A. Fung, A. Nico and R. Tkaczyk, *Toronto Sunnybrook Regional Cancer Centre* — TG-51 protocol recommends that water be used as the standard phantom material for clinical dosimetry. The use of plastic is not part of the protocol. In this study the water equivalency of solid water for photons (6, 10 and 18 MV) and electrons (5 to 21 MeV) was evaluated using TG-51 protocol. The absorbed dose to water was calculated from ionization measurements performed in both phantoms at a depth of 10 cm for photon beams and at the depth of d_{ref} for electron beams. The detectors consisted of multiple Farmer type cylindrical ion chambers NE-2571-0.6cc for the photon beam measurements. These chambers were cross-calibrated in a Cobalt beam against a primary standard, also a cylindrical NE-2571 ion chamber originally calibrated at NRC. The N_D calibration factors of all the cylindrical chambers used in this study were within 0.5% of the primary standard. For the electron beam measurements, two parallel plane ion chambers: Markus PTWN 23343 and the Attix model 454 were used for detection. Both chambers were also cross-calibrated against the primary standard using the TG-39 protocol of the AAPM. The absorbed-dose ratios (water/solid water) decrease as the photon energy increases. The spread in the ratio remained within $\pm 0.5\%$ for all photon energies. In the case of the electron beam the spread in the ratio of water/solid water is much larger, up to $\pm 3\%$. The electron beam ratio showed an increase as the energy of the electron increases. The conclusion of this work is that those results are consistent and systematic and therefore, solid water can be used as a replacement of water in routine quality assurance work.

12h30 **Session Ends / Fin de la session**

[WE-A18] **CASCA Carlyle S. Beals Award Lecture /**
Conférence du Prix Carlyle S. Beals de la CASCA

(CASCA)

WEDNESDAY, JUNE 16
MERCREDI, 16 JUIN
11h00 - 11h45

[Room/Salle : Campaign B]

Chair: G. Harris, U.Waterloo

WE-A18-1 11h00

ERNEST R. SEAQUIST, University of Toronto

The Galaxy M82 - a Rosetta Stone for the Starburst Phenomenon

Starburst activity in galaxies is currently the focus of much attention, both in the local and early universe. One reason is that it now appears that such activity was the primary mode for star formation in the first generations of galaxies, for example the ultra luminous infrared emitting galaxies detected at high red shift in sub-mm surveys. Though star formation is less common in the universe today, the local universe provides the best means to explore the starburst phenomenon at higher resolution and to understand the detailed processes responsible. The galaxy M82 was known as a nearby peculiar system long before the starburst phenomenon became a player on the cosmological stage. As more and more data emerged to permit an understanding of this peculiar galaxy throughout the 1960's 70's and 80's, it became increasingly clear that the intense activity in this system seen in all wavebands reflect an anomalously high rate of star formation, possibly linked to galaxy interaction. My lecture will trace the milestones during this period, by which we came to understand M82's role as a "Rosetta Stone" of the starburst phenomenon, and how it continues today to set the pace for understanding the mechanisms which promote and inhibit explosive star formation.

11h45 **Session Ends / Fin de la session**

[WE-A19] **New Directions in Imaging /**
Nouvelles orientations en imagerie

(CASCA)

WEDNESDAY, JUNE 16
MERCREDI, 16 JUIN
11h45 - 12h30

[Room/Salle : Campaign B]

Chair: T. Landecker, NRC

WE-A19-1 11h45

Crossing The Disciplines: Using Medical Imaging Software For Doing Astronomical Image Analysis. Ian Cameron and J.L. West, *University of Manitoba* — Though differing in approach, both astronomical and medical image analysis share many common techniques and challenges. Having had experience using the ImageJ program from NIH for CCD camera control and image acquisition, we feel it is worthwhile to further explore the feasibility of using medical imaging software for doing astronomy, and in the process benefiting from new approaches for doing some common astronomical image processing tasks. We present a comparison of the standard astronomical image processing package, IRAF, with the freely available medical image processing package, ImageJ. We compare the image analysis and visualization capabilities as well as the quantitative results produced from these software packages.

WE-A19-2 12h00

Smear Fitting: A New Deconvolution Method For Interferometry. Rob Reid, *DRAO/HIA/NRC* — Interferometers measure the Fourier transform of the image plane, but rarely can a good image be obtained simply by computing the FFT of the measurements, because the measurements are typically an incomplete sample. De-convolution techniques work by incorporating additional constraints, such as locality or smoothness in the final image. Smear fitting is a new de-convolution method that makes its constraints double as a model, with uncertainties, of the source. In fact it can be viewed as a tool for easily, or even automatically, producing and fitting a model for a source. I propose that such model-based constraints are not only more scientifically useful than the ones used in traditional de-convolution methods, but also more appropriate for imaging. An additional benefit of smear fitting is that it typically achieves much sharper (reliable) resolution than CLEAN, while simultaneously avoiding the most serious problems that can arise with CLEAN or traditional maximum entropy or model fitting de-convolution. I will show some examples from radio astronomy, and explain why the famous Rayleigh criterion (resolution = wavelength / baseline) is inappropriate for interferometers.

* This work is being supported by University of Toronto, NRC, and NSERC.

WE-A19-3 12h15

On Predicting the Polarization of Low-frequency Emission by Diffuse Interstellar Dust*, Peter Martin, *CITA, University of Toronto* — Several of the current and next-generation cosmic microwave background (CMB) experiments have polarimetric capability (including the Planck Surveyor for which Canadian participation is funded by the CSA), promising to add to the finesse of precision cosmology. One of the contaminating Galactic foregrounds is thermal emission by dust. Since optical interstellar polarization is commonly seen, from differential extinction by aligned aspherical dust particles, it seems likely that the thermal emission will be polarized. Indeed, in the Galactic plane and in dark (molecular) clouds, dust emission in the infrared and submillimetre has been measured to be polarized. It seems likely that the faint diffuse cirrus emission, of more interest (and nuisance) to CMB experiments, will be polarized too. We discuss how well the amount of polarization of this component can be predicted, making use of what is known about optical (and infrared and ultraviolet) interstellar polarization. Some constraints on anomalous microwave emission from spinning dust can be made through polarimetry as well.

* This work is being supported by NSERC and CSA.

12h30 **Session Ends / Fin de la session**

**[WE-A20] New Faculty Luncheon with NSERC /
Déjeuner pour les nouveaux professeurs avec le CRSNG**

(CAP/ACP)

WEDNESDAY, JUNE 16
MERCREDI, 16 JUIN
12h30 - 13h30

[Room/Salle : Private Dining Room]

Chair: W. Davidson, NRC

**[WE-A21] CITA Annual General Meeting /
Assemblée générale de CITA**

(CASCA)

WEDNESDAY, JUNE 16
MERCREDI, 16 JUIN
12h30 - 13h30

[Room/Salle : Campaign B]

Chair: R. Bond, CITA

**[WE-P1] CAP/COMP P. Kirkby Memorial Medal Winner /
Récipiendaire de la médaille commémorative P. Kirkby de
l'ACP/OCPM**

(CAP-COMPI
ACP-OCPM)

WEDNESDAY, JUNE 16
MERCREDI, 16 JUIN
13h30 - 14h15

[Room/Salle : Victoria]

Chair: M. Steinitz, St. Francis Xavier U.

WE-P1-1 13h30

ROBERT C. BARBER, University of Manitoba

IUPAP - A Brief Introduction

The International Union of Pure and Applied Physics was formed in 1922 and is one of the oldest international scientific organizations. Its main purpose is the promotion of international scientific exchange in physics. It does this by sponsoring international conferences that attract a wider constituency than those of national conferences and by implementing the principle of the free international circulation of scientists. While its organization is centred around a representative set of classic disciplines, it is adapting its structure to respond to a number of new challenges, notably those around big science and international cooperation. An overview of the organization and its current activities will be presented.

14h15 Session Ends / Fin de la session

**[WE-P2] Radiation Treatment Delivery /
Exécution de la radiothérapie**

(COMPI/OCPM)

WEDNESDAY, JUNE 16
MERCREDI, 16 JUIN
13h30 - 15h00

[Room/Salle : Albert]

Chair: D. Viggers, CancerCare Manitoba

WE-P2-1 13h30

Surface and Peripheral Surface Dose on the Prostate IMRT Treatment. James C.L. Chow, Grigor Grigorov and Rob B. Barnett, *Grand River Regional Cancer Center* — Surface and peripheral surface dose of a five-beam prostate Intensity Modulated Radiation Therapy (IMRT) and conventional four-beam box irradiations using multileaf collimator (MLC) were measured. The aim is to investigate how the dynamic movement of MLC varies with the configuration of the linac head. This may affect the head leakage and secondary collimator scattering contributing to the surface and peripheral surface dose of the patient. A typical five-beam prostate IMRT planning and irradiation carried out on a CT scanned Rando Phantom were examined. Calibrated MOSFET detectors were placed with equal distance along a transverse surface line at the central axis of the beam around the phantom surface (left, anterior and right) in order to measure the surface dose. The detectors on the transverse surface line were then shifted towards the inferior to 5 and 10 cm from the central axis of the beam and the measurement was repeated. A conventional four-beam box planning and irradiation were also done on the phantom with the same Patient Target Volume, and the same measurements were carried out for comparison. Peripheral surface doses for the IMRT and conventional four-beam irradiations were measured up to 30 cm inferior from the central axis of the beam along the phantom's sagittal surface line. We found that the five-beam IMRT irradiation gives more surface and peripheral surface doses than those of the conventional four-beam."

WE-P2-2 13h45

Mixed IMRT and Conventional Four-Beam Box Treatment on Prostate Cancer. Grigorov N. Grigor, James C.L. Chow and Rob B. Barnett, *Medical Physics Department, Grand River Regional Cancer Center* — It is well known that the Intensity Modulated Radiation Therapy on prostate cancer can give good conformal dose coverage on the Patient Target Volume (PTV) and reduce the complications to the critical organs such as bladder and rectum. However, such treatment takes a long patient set up and irradiation time and there is a clinical concern in the increase of neutron dose exposure to the patient body. On the other hand, the conventional four-beam box technique is a simple, reliable and quick treatment option, though it cannot give the same desired dose coverage to the prostate PTV as that of the IMRT. To date, it is possible to join both the four-beam box and IMRT technique in the prostate treatment in the treatment planning. The idea is to combine the advantages of the four-beam box (short treatment time and patient immobilization), and the advantages of the IMRT (conformal dose delivery to the target and better complication avoiding of the critical organs). The patient will first go for a conventional four-beam box treatment for a number of fractions and then IMRT will be used to escalate the dose in the PTV. Different planning and irradiations were done with various fractional combinations of IMRT and four-beam box in order to optimize the treatment process. Mean Dose (MD) of the overlapped parts of the rectum and bladder, NTCP and MD of the critical organs in different plans were also calculated and studied to optimize.

WE-P2-3 14h00

Parameters Affecting the Spurious Variation of Photon Fluence in IMRT. Fabiola Vallejo, Thomas J. Farrell, Orest Z. Ostapiak, *Juravinski Cancer Centre and McMaster University* — IMRT optimization yields intensity fluence maps (FM) which specify how the fluence must vary across each beam in order to satisfy planning objectives and constraints. Some of the variation in a FM may be spurious since the optimization algorithm does not favour the smoothest set of FMs from multiple nearly degenerate sets. Nevertheless, a smooth set of FMs is desirable because it is more efficient to deliver, lends itself better to interpolation and simplifies dosimetric verification. We investigated several parameters which are hypothesized to affect spurious variation. Those that had the greatest effect are: the size of the field margin, the separation between the planning target volume (PTV) and the organ at risk (OAR) and the effect of dose calculation grid dimensions. It is found that a margin of less than or equal to 0.5cm from the PTV to the field edge increases the variation within a FM. The separation between the PTV and the OAR is varied in two simplified geometries. It is found that the proximity of a PTV to an OAR affects the variation in a FM in a manner similar to the proximity of a PTV to a beam edge. In our simple phantom, dose grids whose dimensions divide evenly into the pencil beam dimension reduce the amount of spurious variation in a FM compared to those that do not. In both cases, reducing the dose grid dimension decreases the amount of spurious variation.

WE-P2-4 14h15

Clinical Implementation Of A 3-D Monte Carlo Based Validation Process For IMRT, Wayne Beckham, C. Shaw, G. Cranmer-Sargison, D. Wells, S. Zavgorodni, R. Mann and T. Popescu, *BC Cancer Agency, Vancouver Island Centre* — With the recent addition of IMRT treatment at the BCCA, Vancouver Island Centre, it has become necessary to develop independent methods for verifying the accuracy of treatment planning for this procedure. Following extensive benchmarking of a Monte Carlo (MC) based dose calculation process (using BEAMnrc and DOSXYZ) against linac data from our institution, we have developed a method that allows MC calculation of IMRT dose distributions within patient CT data sets. We created specific computer programs that streamline the simulation and analysis of IMRT plans. In addition we adapted the MC model to handle absolute dosimetry for multiple fields, each with a specific number of machine monitor units (MU) associated. For the purpose of analysis, programs were created that convert MC dose distributions to a format readable by our commercial treatment planning system (TPS). This put the various tools available in the TPS, such as dose volume histograms, plan subtractions, and object contours at our disposal. The entire MC IMRT system has been thoroughly benchmarked against experiment and these results will be discussed. We will present the MC derived dose distribution for a patient treated with 7-field sliding window head and neck IMRT in our centre, showing a dose at the ICRU point that is 3% lower than the TPS calculated one. A detailed quantitative analysis of the difference between the MC and the TPS 3-dimensional dose distributions compared to experiment in an anthropomorphic phantom is included.

WE-P2-5 14h30

Radiation Spot Position Non-Coincidence On Dual Energy Linacs: Implications For Precision Therapies, Daryl Scora, *Toronto Sunnybrook Regional Cancer Centre* — Precision therapies such as IMRT, stereotactic radiosurgery, and image-guided therapy are more sensitive to systematic setup errors than conventional treatments. Many of these treatment modalities are being delivered on linear accelerators with two available photon energies. We have observed that the radiation spot positions on our dual energy linacs are not always coincident, particularly in the cross-plane direction where there is no control over the spot position. Deviations of up to 1.5 mm between the radiation spot position (projected to isocentre) and the collimator axis of rotation, 1 mm between the radiation spot positions of different beam energies, and 1 mm between the collimator and gantry mechanical axes of rotation have been observed at the isocentre plane. The measured radiation spot positions and mechanical isocenter alignment on our 6 dual energy linacs are summarized and the implications for machine setup, precision patient treatment, and portal imaging will be briefly discussed. A factory-suggested technique to change the radiation spot positions that was successfully applied to one of our linacs will also be presented.

WE-P2-6 14h45

Optimization of Imaging Geometry for Megavoltage Cone-Beam CT*, Mauro Tambasco, G. Pang, P. O'Brien and J.A. Rowlands, *Toronto-Sunnybrook Regional Cancer Centre* — Our overall goal is to develop mega-voltage cone-beam CT (MVCT) using a flat-panel detector for image-guided radiotherapy. In this work, we have formulated and applied a general signal-to-noise ratio (SNR) index of image quality — the detectability index — to find optimal geometric magnifications required for MVCT using a flat-panel detector. The detectability index incorporates the effects of imager detective quantum efficiency (DQE), x-ray source size, x-ray scatter, and object size and contrast. In this study, we used water phantoms to represent nominal patient thicknesses, and assumed the anatomical structures of interest to be cylindrical objects (of various sizes and densities) embedded in the center of the phantoms. To calculate the detectability index, we computed the detective quantum efficiency (DQE) of the flat-panel from Monte Carlo simulations using doses representative of those in MVCT, and we modeled the effect of finite x-ray source size with a Gaussian function whose width was taken from the literature. The effects of x-ray scatter were derived from measurements of scatter-to-primary ratio acquired with the phantoms. To validate our theoretical predictions of optimal magnification for an object, we compared the optimal magnification derived from the detectability index results with measured output-SNR results computed from flat-panel images of a phantom. Our results show that small structures require smaller optimal magnifications than larger objects. Furthermore, we found the image quality of smaller objects to be much more sensitive to magnification than larger objects, indicating the importance of using the optimal magnification in such cases.

* This work is being supported by Siemens Medical Solutions USA.

15h00 Session Ends / Fin de la session

[WE-P3]

(CASCA)

Visualizing Theory: Simulations in Cosmology / Théorie de visualisation : simulations en cosmologie

WEDNESDAY, JUNE 16

MERCREDI, 16 JUIN

14h00 - 14h45

[Room/Salle : Campaign B]

Chair: C. Kerton, Iowa State U.

WE-P3-1 14h00

JOHN J. DUBINSKI, University of Toronto

A Universe in Motion : Dynamical Evolution of Galaxies in the New Cosmological Paradigm

Interactions and mergers drive galaxy morphological evolution. The galaxies that condense out of the cosmological expansion form in groups and fall into clusters creating opportunities for interactions. Interactions lead to enhanced rates of star formation and starbursts and ultimately lead to mergers – the main mode of formation of the elliptical galaxies.

14h45 Session Ends / Fin de la session

[WE-P4]

(DCMMPIDPMCM)

Materials and Magnetism / Matériaux et magnétisme

WEDNESDAY, JUNE 16

MERCREDI, 16 JUIN

14h15 - 16h30

[Room/Salle : Victoria]

Chair: R. Roshko, U.Manitoba

WE-P4-1 14h15

GUY QUIRION, Memorial University of Newfoundland

Investigation of the Phase Diagram of UNi_2Si_2

It is now well established that the strong anisotropy in the magnetic properties of the intermetallic compounds UT_2Si_2 , where T stand for a transition metal, is responsible for their rich magnetic phase diagram. However, within that series of compounds (URu_2Si_2 , UPd_2Si_2 , URh_2Si_2 just to name a few), UNi_2Si_2 is one that shows an unusual sequence of magnetically ordered states which cannot be accounted for by the axial next-nearest neighbor Ising model (ANNNI). For that reason, UNi_2Si_2 certainly continues to attract much attention. Thus, in order to better understand its unusual magnetic properties, we have investigated, by means of sound velocity measurements, the influence of pressure on its magnetic phase diagram. First of all, our measurements, in the magnetically ordered states, indicate that the temperature dependence of the elastic properties along the c-axis is dominated by magnetoelastic effects. Moreover, the analysis of the temperature dependence for the incommensurate longitudinal spin-density state reveals a $\nu = 0.38$ which is consistent with other type of ν critical exponent measurements. From all these measurements, we derive the magnetic phase diagram of UNi_2Si_2 at different pressures. Our observations clearly indicate that the commensurate longitudinal spin-density wave with a ferromagnetic component ($<12>$ phase below 50 K) is the only phase that sees its stability increase under pressure and magnetic field. Finally, our investigation also reveals that the coordinates of the triple-point (T_p , H_p) decrease with pressure at a rate of $dT_p/dP = -1$ K/kbar and $dH_p/dP = 0.1$ T/kbar, respectively.

WE-P4-2 14h45

Formation of Nickel-Graphite Intercalation Compounds on Silicon Carbide. Cory Dean and K. Robbie, *Queen's University* — Graphite Intercalation Compounds (GICs) are an interesting class of hybrid materials which often have surprising and unique chemical and physical properties. Recent studies have demonstrated a new technique for fabricating transition metal GICs using thin film deposition. In the first ever realization of a pure transition metal-GIC, thin films of Ni were vacuum deposited onto crystalline SiC substrates and annealed to high temperatures. After annealing, the appearance of small islands, observed by scanning tunnelling microscopy (STM), scanning electron microscopy (SEM), Auger electron spectroscopy (AES) and atomic force microscopy (AFM), were shown to be composed of Ni atoms intercalated into a graphite matrix. The nanosized Ni-GIC islands observed in the initial studies were small and dispersed which only allowed for characterization at the atomic level. Current investigations have extended our understanding of the Ni-GIC growth process so that islands of increased size and density have been realized, allowing us to probe the crystal structure of these unique materials using x-ray diffraction. In my talk, a review of the growth and characterization of the first reported pure Ni-GIC structures will be given. Additionally, new findings resulting from current x-ray diffraction studies, and discussion of the Ni-GIC growth mechanism will be presented.

15h00 Coffee Break / Pause café

WE-P4-3 15h30

Ordered Co₃W, P.M. Bronsveld, W.A. Soer, P.A. Carvalho and J.Th. M. De Hosson, *University of Groningen-NL* — Co₃W is formed in a peritectoid reaction below 1093°C from the eutectic phases a-Co and Co₇W₆ solidified at 1471°C. During the transformation two closely related fronts are observed: an fcc > hcp and an hcp > ordered hcp (DO₁₉) front. Such behavior points to a preliminary displacive / diffusional transformation followed by long range ordering. The Co₃W can be considered as an AB₂AB stacking of 2D ordered (111) planes much the same way as Ni₃Al can be considered as an ABC₂ABC stacking of 2D ordered (111) planes. Pure cobalt exhibits a polymorph fcc > hcp transformation at 422°C, meaning that at this temperature the stacking fault energy is zero. Therefore, it is not surprising that local AB₂CB and AB₂CA stacking do occur with small excess ordering energies of D_{ABC} and 2D_{ABC}, respectively. With HRTEM it was possible to prove that in thoroughly annealed sample material only the local AB₂CB stacking sequence remains. Attempts to image these stacking faults in a VG100 FIM/Atomprobe were not yet successful but Time-of-Flight Mass spectra were recorded that showed a wide variety of tungsten nitride ions. Most of the tungsten was detected in the form of WN_n²⁺ ions, where 0 ≤ n ≤ 9. Especially the ions with an odd number of N atoms (n) prevailed in this ion group. This is a remarkable observation, since all other studies of metal nitrides report only even numbers of N atoms.

WE-P4-4 15h45

Brillouin Light Scattering from Ordered Carbon Nanotube Arrays*, A. Polomska¹, C.K. Young¹, G.T. Andrews¹, M.J. Clouter¹, A. Yin² and J. Xu^{2,1} *Memorial University of Newfoundland* and ² *Brown University* — Brillouin light scattering spectroscopy was used to study ordered carbon nanotube arrays exposed to vacuum and various gaseous environments (H₂, air, Ar, and SF₆). The arrays were fabricated on alumina substrates and laser-annealed with an Ar⁺ laser at a power of 4 W for 5 minutes. The exposed length of the nanotubes was 200-300 nm. At least four Brillouin peaks, at frequency shifts of approximately 0.7 GHz, 1.5 GHz, 7 GHz and 32 GHz, were observed in the spectra for free spectral ranges up to 50 GHz; these shifts were found to be independent of the angle of incidence. The intensity of the peak located at 0.75 GHz depended strongly on the environment to which the sample was exposed and was not evident in spectra collected when the sample was in vacuum, but was observed in the presence of H₂, air, Ar, and SF₆ at about 1 atm of pressure. The ratio of the maximum intensity of the 7 GHz mode to that of the 32 GHz mode was found to decrease with increasing angle of incidence.

* This work is being supported by NSERC and CFI.

WE-P4-5 16h00

Plasma-Assisted Deposition of Advanced Carbon-Based Coatings*, Andranik Sarkissian¹, Q. Yang², C. Côté¹, A. Hirose², A. Singh², C. Xiao^{2,1} *Plasmionique Inc.*, and ² *University of Saskatchewan* — Carbon atoms are the building blocks for a variety of important class of advanced materials with numerous demonstrated and potential applications in several technological areas. Carbon nanotubes, nanowalls or nanoflakes, diamond films and diamond-like carbon coatings are some of the most important examples of advanced, carbon-based materials and coatings. Various material synthesis and deposition techniques have been used to produce them. However, plasma assisted techniques offer several advantages due to their versatility. These coatings cover a large spectrum of physical, chemical, electrical and optical characteristics, which are determined by the bonding structure of C – C and C – I, where I represent other atoms introduced into the film structure to engineer the film properties, or represent impurities. In this presentation, we shall discuss the deposited film properties, characterized by using several techniques, and the influence of operation parameters of plasma assisted deposition systems on those properties.

* This work is being supported by Plasmionique Inc. and NSERC.

WE-P4-6 16h15

Coincident First - and Second - Order Magnetic Transitions In Single Crystal La_{0.73}Ca_{0.27}MnO₃, Wei Li¹, H.P. Kunkel¹, X.Z. Zhou¹, Gwyn Williams¹, Y. Mukovskii² and D. Shulyatev^{2,1} *University of Manitoba* and ² *Moscow State Steel and Alloys Institute, Russia* — Detailed measurements of the field and temperature dependent magnetization and ac susceptibility of single crystal LCMO reveal features associated with both first- and second-order magnetic phase transitions. Specifically, magnetic isotherms near 240K exhibit a metamagnetic structure generally linked with a first - order transition, while the ac susceptibility exhibits a series of maxima that move upward in temperature and decrease in amplitude as the applied field is increased. The latter are consistent with predictions arising from the static scaling law for continuous transitions, as well as numerical calculations for both Heisenberg and mean - field (Ising) models. Within experimental uncertainty these features are coincident in the (H – T) plane.

16h30 Session Ends / Fin de la session

[WE-P5]

Radioactive Beam/Heavy Ion Physics /
Physique des faisceaux radioactifs/d'ions lourds

WEDNESDAY, JUNE 16

MERCREDI, 16 JUIN

14h15 - 17h00

(DNP/DPN)

[Room/Salle : Ballroom C]

Chair: C. Svensson, U. of Guelph

WE-P5-1 14h15

ALFREDO GALINDO-URIBARRI, Oak Ridge National Laboratory*

Nuclear Spectroscopy with Radioactive Ion Beams: Latest Results from HRIBF

At the Holifield Radioactive Ion Beam Facility more than 120 beams of p-rich and n-rich radioactive ions with a wide range of intensities, purities and energies are now available to carry out pioneering studies of the study of reactions of far-from-stability nuclei. These radioactive ion beams provide a unique opportunity for a whole class of measurements that could never before be applied. A recent highlight has been the acceleration of "pure" beams of fission fragments such as ⁸²Ge (T_{1/2}=4.6s) and ¹³²Sn (T_{1/2}=40s). These semi-magic and doubly-magic nuclei are important bench marks within the chart of nuclides, because they are constraints for the shell-model parameter sets. We have developed specialized experimental tools and techniques for studies in nuclear astrophysics, reaction spectroscopy, and nuclear structure research with radioactive ion beams. We will discuss some of the challenges encountered in recent experiments in fusion, breakup, Coulomb-excitation, transfer, resonance scattering and mass measurements with radioactive ion beams.

* Managed by UT-Battelle, LLC, for the U.S. Department of Energy under contract DE-AC05-00OR22725

WE-P5-2 14h45

GREG HACKMAN, for the TIGRESS collaboration, TRIUMF

TRIUMF-ISAC Gamma-Ray Escape Suppressed Spectrometer (TIGRESS),

Reactions with high-energy radioactive beams from ISAC-II at TRIUMF populate excited states that subsequently decay by cascades of gamma rays that are broadened by up to 10% due to the Doppler shift of the recoil. The energies, spins and parities, population and decay yields of these excited states probe mesoscopic nuclear matter. In exotic nuclei, breakdown of shell structure, emergence of new "magic" numbers, and formation of neutron-proton pair condensates are all predicted modes of nuclear behaviour that can be probed with ISAC-II beams and an appropriate gamma-ray detector. The TRIUMF-ISAC Gamma-Ray Escape Suppressed Spectrometer (TIGRESS) combines escape-suppressed multi-crystal high-purity germanium (HPGe) detectors with high outer-contact electrical segmentation and digital signal processing to measure gamma ray production in ISAC-II experiments. Initial tests show that a prototype HPGe unit is capable of <2 mm lateral position resolution for single interactions, well within the limits needed for ISAC-II experiments. Following a technical review of the prototype detector, the Natural Science and Engineering Research Council (NSERC) released funds to begin construction of a 12-detector array to be completed in 2009. Physics opportunities with TIGRESS, design considerations, technical developments, timelines and milestones will be discussed.

WE-P5-3 15h15

CORINA ANDREOIU, University of Guelph

Doorway States in the Gamma Decay-Out of the Yrast Super Deformed Band in ^{59}Cu

Nuclei with atomic mass number around 60 are among the fastest rotating nuclei known in Nature. They can spin with an angular velocity of about 1.5-2.0 MeV. At these rotational frequencies, highly- or super-deformed shapes are favored over the normally deformed shapes. For the superdeformed states to be pure they need to be shielded from the normally deformed states by an energy barrier in the deformation coordinates. These states prefer to decay by emitting gamma-ray radiation to the normally deformed states in the same nucleus, or by fast (prompt) particle decays in spherical states of the corresponding daughter nucleus. The shape change occurring in the decay-out implies a substantial rearrangement of nucleonic states. Especially the nucleonic states from higher shells, which are occupied in the super deformed bands, need to be vacated. This process is facilitated by vibrational coupling through the barrier between the super deformed state and doorway states, which in turn typically are coupled to a very large number of normally states. The decay-out process of the yrast super deformed band in ^{59}Cu has been recently investigated and compared with decay-out mechanisms in heavier nuclei. The firm determination of spin, parity, excitation energy, and configuration of the states involved in this process constitutes a unique situation for a detailed understanding of the decay-out mechanism. Doorway states involved in this mechanism have been observed and are classified for the first time.

WE-P5-4 15h45

LUC BEAULIEU, Université Laval

The Dynamics Of Neck Formation And Its Isospin Dependence

Mid-peripheral heavy-ion reactions explore a whole range of reaction features with increasing beam energy, going from deep inelastic scattering to fireball formation. The interplay between mean field interaction and particle-particle collisions leads to interesting phenomena in intermediate energy reactions (20-100 A MeV). Of these, the deformation of the reaction partners leading to the formation of a neck is of interest. During the past few years, our group has been able to characterize a deformation scenario, where the larger of the two colliding nuclei is more affected by deformation than the smaller one. Under these conditions, delayed-aligned particles productions occur in the neck region, possibly early on in the collision history. This would point to a dynamical, rather than statistical, production mode. Furthermore, we are able to show that the neck region is neutron rich, compared to the projectile and target, and that the richness could be dependent on the neutron to proton content of the reaction partners.

WE-P5-5 16h15

High Precision Beta Decay Measurements of ^{26}Na at ISAC. G.F. Grinyer, University of Guelph - High precision measurements of the half-life and beta branching ratios from the beta-minus decay of ^{26}Na to ^{26}Mg have been deduced as part of a broad experimental program taking place at TRIUMF's ISAC facility in Vancouver. Radioactive beams of ^{26}Na produced from the ISAC surface ion source were used in conjunction with a 4B gas proportional counter and the 8B gamma-ray spectrometer. In this talk, I will present a recent determination of the half-life of ^{26}Na deduced from the beta activity, in addition to the beta branching ratio measurements from the gamma activity.

WE-P5-6 16h30

Simulation of the DRAGON Recoil Mass Separator using GEANT*, Arthur Olin, P. Gumpinger, S. Yen, and the DRAGON Collaboration, TRIUMF — Simulations of radiative capture measurements using the DRAGON spectrometer have been undertaken using GEANT3. The starting point of the simulation is the ion beam from the accelerator and the simulation tracks through the gas target and spectrometer through to the end detectors. Within this framework it is possible to add physics processes that would be difficult to simulate in beam transport codes and to study correlated responses of the gamma and recoil product detectors. To accomplish this it was necessary to add to GEANT the ability to track heavy ions through electric and magnetic fields, specification of the spectrometer by a beam optics file based on the MIT-RAYTRACE standard, and a flexible event generator to produce the radiative capture process. The decay scheme and angular distribution of the resonant state is specified in an input file. The simulation is being applied to calculation of the DRAGON acceptance for reactions with very large recoil angles. These tools are of rather general applicability for spectrometer simulations.

*This work is being supported by NSERC.

WE-P5-7 16h45

Target Proximity Effect In Heavy-Ion Collisions*, Rene Roy, (Groupe des ion lourds – dynamique des réactions), Université Laval — Heavy ion collisions in the Fermi energy domain are known to be dominated by deep inelastic scattering, a process leading to the formation of two partners in the reaction exit channel. Their identity (charge, mass, velocity) is closely related to that of the projectile and the target, and they are the so-called quasi-projectile (QP) and quasi-target (QT) fragments. In that process, the initial kinetic energy is transformed into internal excitation energy of the QP and QT, that decay subsequently by binary fission and/or light particle evaporation at low excitations, and by several fragment emission when the multi fragmentation regime is reached at higher excitations. However, the presence of an excess of light fragments at mid-rapidity cannot be explained by the standard decay of the QP and QT. To understand the mechanisms producing such an excess, this work studies more precisely the breakup in two fragments of the QP formed in Ni+C, Mg, Au at 34.5 MeV/nucleon and Ni+Zn at 40 MeV/nucleon. The fragment angular distributions exhibit an anisotropic pattern showing that breakup is aligned with the direction of scattered quasi-projectile (QP). The correlation functions of the two heaviest fragments have been studied as a function of charge asymmetry. They suggest that the QP decays while still in close proximity of the target. The correlation between the charge and velocity of the two heavy fragments shows that the binary breakup of the QP might originate from an important deformation of the projectile by the target, and that the lighter of the colliding partners also contributes to the aligned emission pattern.

*This work is being supported by CRSNG.

17h00 Session Ends / Fin de la session

[WE-P6]

Imaging in the Stars and on Earth /
Imagerie dans les étoiles et sur terre

(DIMP-CASCA/
DPIM-CASCA)

WEDNESDAY, JUNE 16

MERCREDI, 16 JUIN

14h15 - 16h30

[Room/Salle : Ballroom A]

Chair: J. Rice, Brandon U.

WE-P6-1 14h15

Dusty Corners of the Universe*, Douglas Scott, University of British Columbia — The sub-millimetre part of the electromagnetic spectrum has been opening as a new window on the high redshift Universe. For several years the foremost instrument has been SCUBA at the James Clerk Maxwell Telescope. Extracting the most from SCUBA data involves careful data reduction in order to make images which are free of the dominant effects of the atmosphere. I will briefly describe some of these techniques, but focus largely on the exciting scientific results which have been coming from deep SCUBA integrations of "blank sky". These observations have revealed more than 300 sources, representing a popu-

lation of dust-enshrouded starbursting galaxies. I will show some examples of the progress we have been making towards identifying these objects using multiwavelengths campaigns. I will focus on the region of the Hubble Deep Field north, and also show how gravitational lensing through rich clusters of galaxies can act as a natural telescope. Identified SCUBA sources are typically redshift 2.5 ultra-luminous infra-red galaxies, which often show up in radio continuum, sometimes in the X-ray, and occasionally as very red optical galaxies. Circumstantial evidence suggests that they represent a population of proto-ellipticals, which were forming a large fraction of all the stars at those epochs. The biggest unresolved question is: what are the currently unidentified sub-mm sources? Related questions include: what is the cosmic star formation history?; and what sorts of galaxies make up the cosmic far-infrared background. I will indicate how such questions may be answered with current and future sub-mm surveys.

* This work is being supported by NSERC.

WE-P6-2 14h30

STEVEN M. SHEPARD, Thermal Wave Imaging Inc.

Pulsed Thermography: Perspectives on the Evolution from Qualitative to Quantitative Application

Since infrared cameras were first offered commercially in the 1960's, the potential of thermography as a tool for NDE has been widely recognized and investigated. Motivated by the prospect of a safe, wide-area, non-contact inspection technology capable of imaging subsurface defects, researchers and practitioners in the field quickly determined that monitoring the surface temperature response of a sample to a thermal impulse was necessary to achieve a useful degree of sensitivity and repeatability. Although many stimulation methods have been successfully implemented, pulsed thermography, using optical flashlamp excitation, has gradually evolved as the most widely used configuration for manufacturing and maintenance applications in the aerospace and power generation industries. However, in most instances pulsed thermography has only been used as a qualitative adjunct to quantitative inspection technologies, such as ultrasound. For many years, quantitative interpretation of pulsed thermographic data was based on analysis of image contrast, which required a degree of calibration, preparation and inspector involvement that is rarely feasible in an industrial setting. Recently, new approaches to processing and interpreting pulsed thermographic data that do not rely on image contrast or visual analysis have been developed. In these approaches, the entire post-stimulation time evolution of each pixel is analyzed as a separate entity, enabling sensitivity, resolution and measurement accuracy far beyond conventional image processing and previously accepted "rule-of-thumb" limits for thermography. The advent of these new methods, as well as complementary hardware developments, has led to and expansion of the field beyond NDE and into materials characterization. The evolution of pulsed thermography, from its contrast-based roots, to the current state of quantitative analysis will be discussed in detail, with examples spanning a broad range of materials and application.

15h00 Coffee Break / Pause café

WE-P6-3 15h30

GREGG A. WADE, Royal Military College

Imaging the Surfaces of Stars

Indirect (Doppler) mapping techniques represent powerful tools for mapping temperature, abundance, and magnetic field structures in stellar atmospheres. In this talk I will review the basic underpinnings of the Doppler Imaging method, describe recent results reported in the refereed literature, and discuss prospects for future studies of stellar surface structure and variability.

WE-P6-4 16h00

JEAN-STEPHANE ANTONIOW, Laboratoire de Thermophysique

*(Photo)Thermal Imaging Using A Modified Atomic Force Microscope (Afm) Combined With Pyroelectric Detection**

A variety of scanning probe microscopy techniques have been explored since the invention of the scanning tunneling microscope and of the atomic force microscope. Variants of these techniques include the scanning thermal microscopy (SThM) and the scanning near-field optical microscopy (SNOM). In the field of photothermal investigations, we attempted to achieve sub-micron-imaging resolution by combining a localized excitation provided by SNOM or SThM with a pyroelectric (PE) sensor in a *back-detection* configuration. The PE signal measured when the tip is "in contact" with the sample contains several thermal components. The main one is due to heat conduction from the tip right through the contact point. So, the PE signal accounts for the thermal wave propagating across the sample, which carries information on the thermal diffusivity. In the case of SNOM, optical properties at the sample surface may contribute to PE signal formation and the resolution is limited by the size of the optical fibre aperture. Our aim was to map thermal diffusivity in the case of very thin layered samples deposited on a PE sensor used as substrate. We show that spatial integration of thermal effects by the PE sensor allows the use of a simple one-dimensional geometry for the theoretical analysis of several operating modes. Images of PE signals reveal contrast zones due to variations of thermal properties, in particular of the thermal diffusivity of a test sample. The method may open new perspectives for thermal investigations of thin layers in biological or technological domains at a microscopic scale.

* In collaboration with Mihai Chirtoc¹, Franck Lei¹, Nathalie Trannoy¹ and Josef Pelzl^{2,1} Unité de thermique et analyse physique, Reims University, Reims, France and ² Exp. Phys. III, Solid State Spectroscopy, Ruhr-Universität, Bochum, Germany.

16h30 Session Ends / Fin de la session

[WE-P7]

**Photonics Devices /
Dispositifs photoniques**

(DOP)

WEDNESDAY, JUNE 16

MERCREDI, 16 JUIN

14h15 - 15h00

[Room/Salle : Campaign A]

Chair: M. Campbell, U. Waterloo

WE-P7-1 14h15

Broad-Spectrum Light Emission in Silicon Tunnel Diodes. James G. Mihaychuk, M.W. Denhoff, S.P. McAlister, W.R. McKinnon and J. Lapointe, *National Research Council Canada, Institute for Microstructural Sciences* — Light emission in crystalline silicon is not limited to the indirect radiative recombination at the band edge that yields 1.1-eV photons. Hot-carrier luminescence can produce a broad spectrum through a combination of direct and indirect intraband transitions. We measure electro luminescence (EL) spectra in metal-insulator-semiconductor (MIS) tunnel diodes when we inject electrons into crystalline Si. The MIS devices have an indium-tin-oxide transparent electrode, a 1.5-nm to 4-nm thick tunnel barrier, and a p-Si substrate with Al back contact. The tunnel barriers are formed from SiO₂, Al₂O₃ and HfO_xN_y. For devices with an Al₂O₃/SiO₂ barrier, in addition to spatially uniform EL at the band edge, we measure EL with a broad, detector-limited spectrum from 0.7 eV to 2.5 eV (1700 nm to 500 nm) that is emitted from multiple isolated sites. Up to hundreds of such sites, each less than 1 μm in size, appear in a mesa with ~100-μm diameter following thermal annealing and/or high-bias operation. Using electron beam lithography, we can define similar EL sites by forming thin tunnel regions in a ~18-nm thick SiO₂ layer.

WE-P7-2 14h30

Computational Analysis of Group Velocity in Periodic Media. Louis Poirier¹ and A. Haché², ¹University of Calgary and ²Université de Moncton — Imagine receiving a signal through a transmission line before it was sent. The theory for group velocity allows superluminal tunneling times and some believe negative tunneling times as well. We shall discuss experimental results from our own work^[1] and other published materials^[2] that claim to observe both superluminal and negative group velocities in a simple coaxial cable periodic system driven in the MHz regime. Detailed computational analysis of the system reveals that negative velocities are not possible in any simple and practical periodic system. A simple error analysis will show that it is possible to obtain uncertainties as large as the measurements themselves, which can lead to some misleading interpretations of results.

1. A. Haché and L. Poirier, *Phys. Rev. E* **65**, 036608 (2002)

2. J. N. Munday and W. M. Robertson, *App. Phys. Lett.* **81**, 2127 (2002).

WE-P7-3 14h45

Focusing Of Light In A 3D Inverse Ferroelectric Photonic Crystal*. Suxia Yang, S. Yang, N. Matsuura, P. Sun, H.E. Ruda, *University of Toronto* — We present a theoretical study of light focusing phenomena in a pass band above the first stop band in a 3D inverse ferroelectric photonic crystal, fabricated using a self-assembly method followed by infiltration and removal of the initial PhC templates. Wave propagation was found to depend dramatically on both frequency and incident direction. This propagation anisotropy leads to very large negative refraction, which can be used to focus a diverging light beam into a narrow focal spot with a large focal depth.

* This work is being supported by NSERC.

15h00 Session Ends / Fin de la session

[WE-P8]

(DIAP/DPIA)

Industrial and Applied Physics General Session / Session générale sur la physique industrielle et appliquée

WEDNESDAY, JUNE 16

MERCREDI, 16 JUIN

14h15 - 16h45

[Room/Salle : Ballroom B]

Chair: G. Beer, U. Victoria

WE-P8-1 14h15

JERRY J. BATTISTA, London Regional Cancer Centre, University of Western Ontario

*On-Line CT Imaging for Precision Radiotherapy**

Radiation oncology has steadily evolved over the last century. From its beginnings with kilovoltage x and γ -rays (1900's) to megavoltage cobalt radiation (developed in Canada in the 1950's), linear accelerators (1960's) are now used routinely to produce higher energy beams of electrons or x-rays. Further advances have stemmed from: (1) multi-modality 3D imaging, which includes CT, MRI, ultrasound, and PET for better delineation of the targeted disease, (2) automation of beam collimation (MLCs) with programmable field shaping and intensity modulation (IMRT), and (3) image-guidance to verify patient alignment prior to treatment delivery. Current developments are focusing towards providing on-line CT imaging devices mounted "onboard" the gantry of the radiation therapy machine. Two new approaches are being investigated in Ontario: (a) fan-beam CT using a ring gantry design for both imaging and treatment with megavoltage (3.5 MV and 6 MV) x-rays (TomoTherapy Inc.) and (b) cone-beam CT using a standard C-arm gantry (Elekta Synergy System) that rotates an auxiliary x-ray tube (120 kVp) and a flat-panel detector (e.g. $Gd_2O_3S:Tb$, amorphous silicon). In this presentation, the pros and cons of each approach will be reviewed, including the imaging physics at kV and MV energies, image quality parameters, imaging dose, imaging time, and process flow. In the near future, the measured treatment beam transmission fluence will be combined with CT data sets to reconstruct the actual dose distribution delivered to the patient *in vivo*. This exciting development will expand research into adaptive radiotherapy, to allow a treatment fraction to be modified in mid-course as needed. Human radiobiology, that correlates clinical outcomes (i.e. tumour response and treatment complications) with the true dose pattern in tumour and surrounding normal tissues, respectively, becomes possible for the first time.

* In collaboration with: T. Kron¹, G. Hajdok², I. Cunningham³, J. Van Dyk¹ and G. Bauman¹, ¹London Regional Cancer Centre, ²University of Western Ontario and ³Robarts Research Institute.

WE-P8-2 14h45

EMIL HALLIN, Canadian Light Source

The Applied Science Program at the Canadian Light Source

The Canadian Light Source (CLS), a 2.9 GeV synchrotron facility, is currently being constructed at the University of Saskatchewan. The building is complete, the accelerator has been operated at a stored current of 100 mA and the first light from an insertion device has been extracted from the storage ring tunnel. The facility (with seven beamlines) will be operational by the end of 2004. Most of these beamlines and associated endstations will be extremely useful for materials and/or surface analysis – using infrared spectroscopy and spectromicroscopy, an x-ray microprobe and soft and hard x-ray XANES and EXAFS. The Canadian Light Source is broadly focused on research in materials science, environmental sciences and the life sciences. Recent Canadian results at the Canadian Synchrotron Radiation Facility in Madison, and at other foreign sources such as NSLS, APS and Daresbury will illustrate the importance of these measurements for the detailed study of materials and surfaces.

15h15 Coffee Break / Pause café

WE-P8-3 15h30

Fluid Motion Induced by Sequential Interface Deformation*. Januk Aggarwal, Lorne Whitehead and Andrzej Kotlicki, *University of British Columbia* — We present a method for pumping fluid pump along a surface, without moving parts, which may have application in heat transfer. The method involves a surface having a pattern of different wetting characteristics to confine drops of one fluid in another and to facilitate electrostatic deformation of the resultant interface. In current embodiments, printing techniques are used to create lyophilic "tracks" on a comparatively lyophobic substrate, to trap oil drops in a background aqueous solution. By applying localized electrostatic fields between the electrolyte and an underlying conductor, the oil is pinched into well localized drops. Sweeping the field pattern along the tracks drags these drops as well, causing net fluid flow. We have established a way to effectively sweep the field using only 3 conductive segments in one conductive layer, facilitating fabrication. This approach has so far achieved flow rates of 15 cm/s, with drops that are of order 2mm diameter on 2mm wide tracks, which loop back onto themselves but can in principle be any length. Being a purely electrostatic effect, the power used is extremely low. With such flow rates, it is possible to transport heat more effectively than using an equivalent volume of solid copper.

* This work is being supported by NSERC.

WE-P8-4 15h45

AARON FENSTER, Robarts Research Institute

From Concept to Product: 3D Ultrasound Imaging for Diagnosis and Treatment

The last two decades have witnessed unprecedented developments of new imaging systems making use of 3D visualization. These new technologies have revolutionized diagnostic radiology, as they provide the clinician with information about the interior of the human body never before available. Ultrasound imaging is an important cost-effective technique used routinely in the management of a number of diseases. However, technical improvements are needed before its full potential is realized, particularly in applications involving minimally invasive therapy or surgery. 2D viewing of 3D anatomy, using conventional ultrasound, limits our ability to quantify and visualize the anatomy and guide therapy, because multiple 2D images must be integrated mentally. This practice is inefficient, and leads to variability and incorrect diagnoses. Also, since the 2D ultrasound image represents a thin plane at an arbitrary angle in the body, reproduction of this plane at a later time is difficult. We have developed 3D ultrasound imaging techniques that address the problems discussed above. In our approach, the conventional ultrasound transducer is scanned mechanically or with a free-hand technique. The 2D images are digitized and then reconstructed in real-time into a 3D image, which can be viewed and manipulated interactively. Examples will be given for imaging various organs, such as the prostate, carotid arteries, and breast, and for the use in 3D ultrasound-guided brachytherapy and cryosurgery. In this paper we will also describe the path of our developments from concept to product and commercialization. Issues related to protection of intellectual property in the development of our instrumentation will be addressed. In addition, methods we have used to commercialize our innovations, including licensing and formation of a company, will be described.

WE-P8-5 16h15

THOMAS J. RUTH, TRIUMF

Production of Radioisotopes for Research in Bioscience and Physical Science

Radioisotopes have long been used as tracers in the biological and physical sciences. TRIUMF with its 5 cyclotrons represents the most powerful radioisotope production facility in the world. The Life Science Program at TRIUMF has exploited this capability for more than 2 decades in its applications in positron emission tomography with collaborations with the Faculty of Medicine at UBC in studying Parkinson's disease. For the last decade research into the use of nitrogen in various plant systems has been explored with the

tracer N-13. More recently studies in fluid dynamics for the pulp and paper industry have made use of wood fibers labeled with F-18 to study the factors affecting paper quality. The applications of radiotracers to understand fundamental phenomena are almost limitless. However, there are numerous constraints to exploiting this method, not the least of which is communicating across disciplines. Examples illustrating various levels of success will be presented along with possible applications for the future.

16h45 Session Ends / Fin de la session

[WE-P9] Plasma Physics /
Physique des plasmas
(DPP)

WEDNESDAY, JUNE 16
MERCREDI, 16 JUIN
14h15 - 15h30

[Room/Salle : Strathcona]

Chair: C. Boucher, INRS

WE-P9-1 14h15

AKIRA HIROSE, Plasma Physics Laboratory, University of Saskatchewan

Anomalous Electron Thermal Conductivity In Tokamaks.

The electron thermal diffusivity in tokamaks has been known to be anomalously high since the beginning of the tokamak research. As the anomalous ion thermal diffusion is caused by an ion temperature gradient, it is natural to seek instabilities driven by electron temperature gradient (ETG). A toroidicity driven ETG mode has been revisited in tokamak stability analysis based on a fully kinetic, electromagnetic integral equation code recently developed in the Laboratory. The ETG mode is characterized by short wavelengths which can be comparable with the Debye length and charge neutrality often assumed in the analysis of the ETG mode breaks down. For typical tokamak discharge parameters, the maximum growth rate occurs at a wavenumber comparable with the Debye wavenumber. The growth rate is of the order of the electron transit frequency and is proportional to square root of plasma beta factor. The electron thermal diffusivity based on simple mixing length estimate is large enough to be relevant to the experimentally observed values, and it increases with the plasma minor radius [1].

1. A. Hirose, Phys. Rev. Lett. 92, 025001 (2004).

WE-P9-2 14h45

*Discrete Alfvén Wave Spectra Due to Hall Current**, Atsushi Ito¹, S. Ohsaki² and S.M. Mahajan³, ¹ University of Saskatchewan, ² University of Tokyo and ³ University of Texas — Non-ideal effects on inhomogeneous MHD may resolve singularity in the Alfvén continuous spectrum by inducing higher order derivative in the mode equation. It has been shown analytically [1] that the coupling of the Hall current with the sound wave gives rise to discrete spectra, and dominates the electron-inertia (kinetic) effect [2]. A numerical code has been developed to investigate parameter regimes of the ion skin depth, the sound speed, and the wave numbers which allow the presence of discrete Alfvén spectra and radial mode structure.

1. S. Ohsaki and S.M. Mahajan, Phys. Plasmas 11, 898 (2004).

2. S.M. Mahajan, Phys. Fluids 27, 2238 (1984).

* Work supported by NSERC and CRC

WE-P9-3 15h00

Joint Plasma/Thermal Model for Plasma Ion Implants of Photonic Materials, Michael P. Bradley, University of Saskatchewan — Ion implantation is a powerful tool for the modification of materials by the introduction of controlled amounts of impurities at controlled depths. It has great promise for the production of new photonic and optoelectronic materials. In plasma ion implantation the ions to be implanted are extracted from a plasma in contact with the target. Obviously the final material characteristics depend upon the ion species used and the depth of the implants. In addition, the final characteristics of an ion-implanted sample depend significantly upon its thermal history because of the importance of thermally-driven diffusion and activation processes. Because high-dose ion implants (such as those which might be used to produce buried luminescent SiC layers) lead to very rapid target heating, the temperature vs. time history of the target is a critical aspect of any ion implantation process, and must be known and controlled to achieve optimal results. Accurate, predictive modelling of plasma conditions and their effect on target temperature is an important component of my research program in Plasma Ion Implantation at the University of Saskatchewan. In this talk I will present the results of a numerical model which incorporates the coupling between plasma ion implant conditions and target heating, and discuss the implications for my photonics materials research program.

WE-P9-4 15h15

*Observation Constrained Equilibria, Plasma Instabilities, And Substorm Intensification Phase**, Peter Dobias¹, J.A. Wanliss², I.O. Voronkov¹ and J.C. Samson¹, ¹ University of Alberta and ² Embry Riddle Aeronautical University — Dynamics of a substorm onset is one of the most challenging problems in space plasma physics. A sufficient theory must be able to explain the sub-Alfvénic time scales of the onset, and must also provide plausible explanations for the whole series of observed characteristics connected to substorms. We use the Grad-Shafranov equation to define a 3D plasma equilibrium. The theoretical equilibrium is tied to ground-based CANOPUS observations through the proton aurora equatorward boundary as an experimental constraint for the equilibrium. Then we use an energy-based nonlinear stability analysis to follow the stability of the magnetotail during the late growth phase, including periods just prior to and after the onset of the substorm intensification phase. Using various potential sources of a perturbation to plasma equilibrium, we demonstrate that timing of the substorm onset coincides with the transition between nonlinearly stable and unstable configurations of the magnetotail. Possible triggering mechanism for the instability could include field line resonances, shear flow or shear flow-ballooning instability, or a strong external impulse.

* This work is being supported by NSERC.

15h30 Session Ends / Fin de la session

[WE-P10] General Relativity and Gravitation II /
Relativité générale et gravitation II
(DTP/DPT)

WEDNESDAY, JUNE 16
MERCREDI, 16 JUIN
14h15 - 17h00

[Room/Salle : Kildonan]

Chair: M. Paranjape, U.Montreal

WE-P10-1 14h15

SAURYA DAS, The University of Lethbridge

Black Holes In Future Colliders

Brane world models which predict the fundamental higher dimensional Planck scale to be about a TeV, also predict the copious production of black holes in future high energy colliders such as the Large Hadron Collider (LHC). We examine properties of these black holes, their possible experimental signatures and the influence of the Generalised Uncertainty Principle and thermodynamic fluctuations on these signatures.

* In collaboration with M. Cavaglia¹ and R. Maartens², ¹ The University of Mississippi and ² University of Portsmouth.

WE-P10-2 14h45

VIQAR HUSAIN, University of New Brunswick

Singularity Resolution in Quantum Gravity

We examine the singularity resolution issue in quantum gravity by studying a new quantization of Friedmann-Robertson-Walker geometrodynamics. The quantization procedure is based on an alternative to the usual Schrodinger representation used in metric variable quantum cosmology. We show that in this representation there exists a densely defined inverse scale factor operator, and that the Hamiltonian constraint acts as a difference operator on the basis states. We find that the cosmological singularity is avoided in the quantum dynamics. We discuss these results with a view to identifying the criteria that constitute "singularity resolution" in quantum gravity.

15h15 Coffee Break / Pause café

WE-P10-3 15h30

ERIC WOOLGAR, University of Alberta

The Poincaré Conjecture, Ricci Flow, And The Renormalization Group

In a series of papers beginning in the fall of 2002, Grisha Perelman announced what may be a proof of the Poincaré conjecture and, indeed, the much broader Thurston geometrization conjecture for 3-manifolds. His method is based on Hamilton's Ricci flow, which is a sort of heat equation for tensors. References to physics abound in Perelman's work. One example is that the Ricci flow is the renormalization group flow for a nonlinear sigma model (at one loop). Another is that Perelman's results are based on a monotonicity theorem for the Ricci flow, which he shows is in fact the "second law" applied to a certain statistical entropy obtained from a formal partition function (for an unknown statistical ensemble). In this talk, I will describe the geometrization conjecture, Perelman's method, and some of the connections to physics. Finally, I will describe joint work with T. Oliynyk and V. Suneeta wherein we apply Perelman's technique to noncompact manifolds to study the problem of mass decrease in renormalization group flow.

WE-P10-4 16h00

WILLIAM UNRUH, University of British Columbia

Dumb Holes— Black holes in the Lab?

Various condensed matter systems can be shown to mimic the behaviour of black hole, including the quantum emission of radiation with a temperature characteristic of the dimensions of the black hole. These dumb (not-speaking) holes illuminate the theoretical origins of the black hole evaporation radiation, and also offer the possibility of measuring the radiation in the laboratory. This talk will review this field, and outline the promise and difficulties of such measurements.

WE-P10-5 16h30

ARUNDHATI DASGUPTA, Université Libre de Bruxelles

Entropy of a Black Hole Apparent Horizon

Coherent states are determined for the Schwarzschild black hole space-time in the framework of canonical quantisation of general relativity. The degeneracy associated with a density matrix for a given semi classical space-time after tracing over the coherent state wave function inside the apparent horizon is determined. This is shown to give rise to an entropy of the black hole which is proportional to the area of the apparent horizon.

17h00 Session Ends / Fin de la session

[WE-P11]

Visualizing Concepts in Theory - Contributed /
 Visualisation des concepts théoriques- contribuées

(CASCA)

WEDNESDAY, JUNE 16

MERCREDI, 16 JUIN

14h45 - 15h30

[Room/Salle : Campaign B]

Chair: J. Fiege, NRC-HIA

WE-P11-1 14h45

Observing Simulated Galaxies*: Jennifer O'Neill Hurry, *University of Toronto* — Comparisons between hydrodynamical galaxy simulations and observations are becoming more detailed as the resolution increases for both. An inherent problem with these comparisons is the basic unit in each is different - one traces mass, the other, light. By converting stellar mass to light and modelling both dust obscuration and the properties of the telescope, we can directly compare images of simulated galaxies with their observed counterparts. The goal of many observations of galaxies (especially at high redshift) is to discover something of the underlying mass distribution. The obvious benefit to using images from simulations is the mass distribution and dynamics of the galaxy are known; we can then investigate various parameters in observational space to determine what has the best chance of recovering the fundamental properties of the galaxy. One aspect we are currently investigating is morphology. There are currently several quantitative methods of determining a broad definition of morphology. Because we have control over cameras, exposure time, etc, we can determine which parameters most affect the resulting morphology classification and the ideal set of parameters which most closely mimic the underlying mass and dynamical state of the galaxy. One of the results I will present are striking plots showing how a standard morphological classification scheme assigns a very different morphology to the light distribution of a galaxy than the mass distribution, and that this variation continues over a wide range of redshifts.

* This work is being supported by Dr. Roberto Abraham.

WE-P11-2 15h00

Dynamics Of Young Planetary Systems*: Edward Thommes, *CITA* — Early in the life of a planetary system, (proto-) planets gravitationally interact with each other as well as with the gas disk out of which they are born. Using a hybrid N-body code, we examine some of the dynamics which may result. Key features of mature planetary systems like our own, as well as of the growing ensemble of discovered exoplanetary systems, may be the result of the interplay between planet-planet and planet-disk interactions during the first few million years.

* This work is being supported by NSERC.

WE-P11-3 15h15

Sliding into Home: Terrestrial Formation and Type I Migration: Douglas McNeil, and M.J.D. Duncan, *Queen's University* — Terrestrial-mass planetary embryos embedded in a gas disc suffer a decay in semimajor axis - type I migration - due to the asymmetric torques produced by the interior and exterior wakes raised by the body (Goldreich and Tremaine 1980; Ward 1986). This presents a challenge for standard oligarchic approaches to forming the terrestrial planets (Kokubo and Ida 1998) as the timescale to grow the progenitor objects near 1 AU is longer than that for them to decay into the Sun. Using both semianalytic methods and numerical integrations we investigate this problem by varying the gas dispersal rate in different models of the protoplanetary disc. We consider the possibility that the Earth's forebears were immigrants to her current home. Recent results and plans for future work are discussed.

15h30 Session Ends / Fin de la session

**[WE-P12] Radiation Treatment Verification /
Vérification de la radiothérapie**

(COMPIOCPM)

**WEDNESDAY, JUNE 16
MERCREDI, 16 JUIN
15h30 - 17h00**

[Room/Salle : Albert]

Chair: C. Arsenault, Dr. Georges L. Dumont Hospital

WE-P12-1 15h30

Daily Targeting of Prostate Through EPID Visualization of Implanted Markers. Boyd McCurdy, *CancerCare Manitoba* — In this study, we investigated our clinic's ability to accurately deliver dose-escalated, 3D, conformal prostate radiation therapy, using only electronic portal imaging (no film). The implemented protocol requires three gold cylinders (1.3 mm x 3.0 mm) to be inserted into the patients' prostate gland under ultrasound guidance. Conformal treatment planning proceeds as usual, except that points of interest are placed at the location of the cylinders. At the beginning of all 39 treatment fractions, a pre-port image acquisition (~6 MU) was obtained with an amorphous-silicon portal imaging device and a grid tray inserted. The radiation therapists performed on-line analysis of the shifts of all three markers from the central axis, and entered this data into a computerized spreadsheet. The spreadsheet compared the position data to data from the planning DRR. If the discrepancy is more than 5 mm, patient position was corrected before treatment proceeded. Daily positioning information for the first patient was analysed, and setup uncertainties using the geometric centre of the cylinders were found: del (AP) = -0.2 mm +/-1.7 mm; del (SI) = -1.3 mm +/- 1.7 mm, accounting for corrections. Only 4 corrections were needed. A systematic rotation (10.1 + /-4.7 degrees) of the prostate about a lateral axis was also observed. In 2 fractions, significant discrepancies were observed due to rectal gas, despite patient rectal preparation. In these situations, correction based on bony anatomy alone would have been ineffective. This integrated, on-line imaging approach has a minimal impact on the total treatment time for the patient, with most fractions deliverable within 12 minutes.

WE-P12-2 15h45

Measurement of Intra- and Inter-Fraction Prostate Motion Using Electronic Portal Imaging of Implanted Radio-Opaque Markers. Katharina Sixel¹, P. Cheung¹ R. Tirona¹, and G. Pang¹, ¹Toronto Sunnybrook Regional Cancer Centre and ²University of Toronto — Radio opaque markers implanted into the prostate represent a target surrogate that can be imaged directly with a linear accelerator, enabling image guided radiation for prostate cancer. Pre-treatment imaging of the markers and on-line correction for marker position eliminate interfraction motion errors, and offer the opportunity for planning target volume (PTV) reduction. However, this intervention does not eliminate the PTV, as intrafraction motion must still be considered. Gold markers were implanted into the prostate of 33 prostate cancer patients. Anterior and lateral electronic portal images were acquired at the start and at the end of the first 9 fractions of treatment. On-line correction software (PortalNT, Quebec) was used to analyse the images. Comparison of seed positions on pre-treatment images to planning digitally reconstructed radiographs quantified interfraction motion. Comparison of post-treatment images to pre-treatment images allowed the assessment of intrafraction motion. For the population of patients studied, the systematic (average) and random (standard deviation) inter- and intra-fraction errors are listed:

| | Systematic errors (mm) | | | Random errors (mm) | | |
|---------------|------------------------|-----|-----|--------------------|-----|-----|
| | LR | SI | AP | LR | SI | AP |
| Intrafraction | 0.1 | 0.4 | 0.7 | 0.9 | 1.3 | 1.8 |
| Interfraction | 1.4 | 0.4 | 0.3 | 2.5 | 3.3 | 4.9 |

By applying appropriate margin recipes and accounting for seed localization uncertainty, the PTV can be calculated. If on-line correction is used to position the prostate to the treatment isocentre at the start of each fraction, a residual population based PTV of 3.5 mm (LR), 3.5 mm (SI) and 4.1 mm (AP) will ensure that the prostate receives the prescribed dose.

WE-P12-3 16h00

Automatic Extraction of Patient Out-of-Plane Rotation Using Portal Images. Keyvan Jabbari and Stephen Pistorius, *Cancer Care Manitoba* and *University of Manitoba* — Radiation therapy requires accurate treatment set up and patient placement and Electronic Portal Imaging Devices are now commonly used for treatment verification. A number of techniques are available to ascertain patient set up by spatially registering the portal image with its reference image. One problem in many two-dimensional registration methods is due to the assumption that the anatomical structures to be registered, lie in the same plane. These methods cannot account for patient rotations out of the image plane and translation errors can occur. Out of plane rotation results in an apparent distortion of anatomy in the portal image. This distortion can be mathematically predicted with the magnification varying at each point in the image. Whereas an equal change of magnification in both dimensions results from an incorrect SSD setup, a variation of magnification in only one dimension is due to an out-of-plane rotation. Previously we have reported an accurate technique for extracting the in-plane rotation, scale and translation of a portal image. A similar technique can be used to calculate the out-of-plane rotation. Correlating the Fourier Transform of the portal image on a log scale with that of the reference image enables the out of plane rotation to be automatically extracted from a single portal image. This technique is able to identify out-of-plane rotations of up to 25° with an accuracy of ±3°. The ability to detect out-of-plane rotations with a single image will enhance our ability to quickly and accurately account for both in-plane and out-of-plane set-up errors.

WE-P12-4 16h15

Removing Blur From Energy Fluence Measurements Made Using Varian's aS500 Electronic Portal Imaging Device. Charles Kirkby and R. Sloboda, *University of Alberta* — As a result of their linear response to absorbed dose, amorphous silicon electronic portal imaging devices (a-Si EPIDs) have the potential to produce a two-dimensional pixel map of dose or energy fluence within a given therapeutic field. Unfortunately, the image formed by the detector is subject to multiple blurring processes. To produce an accurate energy fluence map, it is therefore necessary to model the blur in order to deconvolve it from the image. We examined the blur kernel of Varian's aS500 EPID, a typical a-Si portal imager. The overall blur kernel is a convolution of two processes: a) the spread of dose deposited in the scintillation screen, and b) the spread of optical photons created in the screen and detected by the amorphous silicon photodiodes. We modelled dose deposition in the aS500 using the EGSnrc Monte Carlo code, which simulates transport of high-energy (MeV) photons and electrons, and optical spreading using the DETECT2000 Monte Carlo code, which tracks optical photon propagation. Convoluting these results yielded robust overall blur kernels for both 6 and 15 MV beams. EPID images deconvolved using these kernels resulted in fluence profiles that conformed with those measured by a diamond detector across a range of standard clinical fields: 4'4 cm², 10'10 cm², 20'20 cm², and a 10'10 cm² 45° wedged field. We used a g-concept test to quantify the improvement introduced after the deconvolution.

WE-P12-5 16h30

Lag Mechanism in Amorphous Selenium Radiation Detectors. Teodor Stanescu¹, Mr. Schroeder², Dr. Rathee¹ and Dr. Fallone¹, ¹Cross Cancer Institute and ²CancerCare Manitoba, — Amorphous selenium (a-Se) active matrix flat panel imagers (AMFPIs) have been studied for applications in medical imaging. We showed that the amorphous selenium photodetectors suffer from lag ^[1] and sensitivity reduction ^[2]. These effects result in reduced contrast in the images subsequently produced by the detector. Lag is determined by the residual signal from previous exposures, and can be seen in subsequently acquired dark images. Although lag is a real problem for a-Se AMFPIs, no theoretical approach has been developed to explain it for externally biased a-Se detectors. We previously modeled the lag effect ^[3]. In this work, the mechanism of lag is investigated from first principles, by solving kinetic equations characterizing, photogeneration, trapping, and release of electrons and holes. The mechanism is described by the density of trapped charge at the end of the irradiation pulse interval, and the current density generated by the charge released from the trapping sites after stopping the irradiation. We have applied this theoretical model to the experimentally measured lag data for several x-rays energies and doses delivered by using a Monte Carlo method.

1. S Steciw, T Stanescu, S Rathee, B G Fallone 2002 J. Phys. D 35 1-7

2. C Schroeder, T Stanescu, S Rathee, G Fallone Med Phys (in press)

3. T Stanescu, C Schroeder, S Steciw, S Rathee, G Fallone 2003 Med Phys 30 1390.

WE-P12-6 16h45

Fundamental Spatial Resolution Limits in Megavoltage X-ray Detectors. Jerry J. Battista¹, G. Hajdok² and I. Cunningham^{3,1}, ¹London Regional Cancer Centre, ²University of Western Ontario and ³Robarts Research Institute — Advancements in high precision radiotherapy have prompted the development of better image guidance systems, such as on-line portal and CT imaging. We present a Monte Carlo study in which the fundamental spatial resolution limits imposed by x-ray interactions were determined for direct con-

version amorphous selenium (a-Se), tungsten (W) and lead iodide (PbI₂), and indirect conversion cesium iodide (CsI) detectors. Using a simulated infinitesimal x-ray beam, the spatial distribution of absorbed energy, or point spread function (PSF), in each detector material was scored within rectilinear bin sizes of $1 \times 1 \text{ mm}^2$ for incident x-ray energies between 1 and 10 MeV. The modulation transfer function (MTF) was determined from each simulated PSF and characterized in terms of the 50% MTF frequency, f_{50} , and the effective sampling aperture, a_{eff} . Each material demonstrates a similar fall-off profile for the spatial resolution degradation with increase in megavoltage x-ray energy. The x-ray interactions responsible for the degradation include Compton scatter and pair/triplet production. The fundamental spread of energy from Compton recoil electrons and the secondary charged particles resulting from pair/triplet production primarily dictate the magnitude of the spread. Once these limits have been reached, further investments in new detector design will not improve image quality any further. In addition, the f_{50} and a_{eff} curves demonstrate that tungsten ($r = 19.3 \text{ g/cm}^3$) offers the best spatial resolution, in comparison with a-Se, CsI, and PbI₂ ($r = 4.20, 4.51, 6.20 \text{ g/cm}^3$ respectively). Therefore, the fundamental spatial resolution limits are independent of atomic number, and dependent on material density.

17h00 Session Ends / Fin de la session

[WE-P13] **Dark Matter and Dark Energy /**
 (PPD-CASCA) **Matière et énergie noires**

WEDNESDAY, JUNE 16
 MERCREDI, 16 JUIN
 16h00 - 17h30

[Room/Salle : Colbourne]

Chair: D. Scott, UBC

WE-P13-1 16h00

HENK HOEKSTRA, CITA

Astrophysical Evidence For Dark Matter

The evidence for dark matter as a significant constituent of the universe based on astronomical observations has been compelling for a long time. Observations of the rotation curves of galaxies and the motion of galaxies and gas in clusters of galaxies provided the first clues about dark matter. More recent probes such as weak gravitational lensing have significantly improved our knowledge about the amount and distribution of dark matter. In this talk I will review the observational evidence for dark matter based on the variety of probes mentioned above, focusing on the most recent developments. I will also demonstrate how new observations are incompatible with alternative theories of gravity, which have been proposed to explain the observations without the need of dark matter.

WE-P13-2 16h30

UBI WICHOSKI, Groupe de Physique des Particule - Université de Montréal

Status of the Dark Matter Search

Our present understanding of the Universe, based on the most recent observations, is that approximately 70% of its energy density is in the form of dark energy and the remaining 30% in the form of gravitating matter. According to the big-bang model of cosmology, only approximately 15% of the gravitating matter in the Universe can be made of baryons. This leads to the conclusion that 85% of the matter content of the Universe is made of non-baryonic and, in the sense that it does not emit nor absorb electromagnetic radiation, dark matter. The first suggestion for the existence of dark matter appeared more than 70 years ago to explain the rotation curves of the spiral galaxies. Nowadays, dark matter is expected to exist in scales ranging from galactic to cosmological. On the theoretical side, there is a profusion of dark matter candidates, the majority coming from extensions of the standard model of particle physics. There is also a wealth of experiments searching for dark matter both directly and indirectly. In this talk we will give an overview and discuss future perspectives in the light of recent developments.

WE-P13-3 17h00

*Weak Lensing by Galaxy Groups at Intermediate Redshift**, Laura Parker, University of Waterloo — I intend to present the results from our weak lensing survey of CNO2 galaxy groups. The detected shear is used to calculate the M/L of these groups and constrain the matter density of the universe. The measured tangential shear is also of sufficient S/N that it allows us, for the first time, to constrain the DM profile of galaxy groups.

* This work is being supported by NSERC, ORDCF.

WE-P13-4 17h15

*Results From LIGO's Second Science Run: A Search For Continuous Gravitational Waves**, Michael Landry for the LIGO Scientific Collaboration, LIGO Hanford Observatory/Caltech — The Laser Interferometer Gravitational Wave Observatory (LIGO) was operated from Feb 14 - Apr 14 2003, comprising the second science run for the project. These data have been analyzed for evidence of gravitational waves emitted by several classes of potential sources, including continuous wave sources such as spinning neutron stars. A brief overview of the interferometers and detection scheme is presented, followed by a discussion of the methodology and results of the search for continuous gravitational waves. Plans for future analyses are outlined.

* This work is being supported by National Science Foundation.

17h30 Session Ends / Fin de la session

[WE-P14] **Imaging the Invisible Spectrum - Contributed /**
 (CASCA) **Imagerie dans le spectre de l'invisible - contribuées**

WEDNESDAY, JUNE 16
 MERCREDI, 16 JUIN
 16h00 - 16h30

[Room/Salle : Campaign B]

Chair: M. Bietenholz, York U.

WE-P14-1 16h00

Cold Dust - Radio Continuum Correlation in Spiral Galaxies, Rupinder Brar and J.A. Irwin, Queen's University — A startling new correlation between meter wavelength radio emission and sub-mm emission, due to cold dust, in the disks and at high-latitudes of a sample of edge-on spiral galaxies is presented. The location and type of emission indicates that the link is not via star formation, other possible explanations are presented. Observations for these results were made with the newly commissioned Giant Metrewave Radio Telescope (GMRT) and the Submillimetre Common-User Bolometer Array (SCUBA) on the James Clerk Maxwell Telescope (JCMT). The techniques required to image and analyze multiple wavelengths with these cutting-edge telescopes is described.

WE-P14-2 16h15

Imaging of the Young, Energetic Radio Pulsar J2021+3651 with the Chandra X-ray Observatory, Jason W.T. Hessels¹, M.S.E. Roberts^{1,2}, S.M. Ransom¹, V.M. Kaspi¹, C.-Y. Ng³, R.W. Romani³, P.C.C. Freire^{4,1}, McGill University,² MIT,³ Stanford University and⁴ NAIC, Arecibo — Rotation-powered pulsars release their spin energy in the form of pulsations and a particle wind. This wind can create striking nebulae around the pulsar. We present imaging and timing observations with the Chandra X-ray Observatory of the young and energetic pulsar PSR J2021+3651. This pulsar is a probable source of gamma-rays, being coincident with the high-energy gamma-ray source GeV 2021+3658 seen by the EGRET instrument onboard the Compton Gamma-Ray Observatory. Our Chandra image reveals a 20 X 10 asec nebula with an embedded point source, likely the

pulsar itself. We discuss the spectrum and morphology of this new pulsar wind nebula and compare it to others. Chandra timing observations show possible X-ray pulsations from the point source at the rotational period predicted by radio timing observations. The point-source emission is most likely thermal, from the neutron-star surface.

16h30 Session Ends / Fin de la session

**[WE-P15] Miscellaneous Intrigues - Contributed /
Intrigues diverses - contribuées**

(CASCA)

WEDNESDAY, JUNE 16
MERCREDI, 16 JUIN
16h30 - 17h15

[Room/Salle : Campaign B]

Chair: D. Hanes, Queen's U.

WE-P15-1 16h30

The Initial-Final Mass Relationship*. Jasonjot Kalirai¹, H. Richer¹, P. Bergeron², G. Fahlman³, B. Gibson⁴, B. Hansen⁵, T. von Hippel^{6,1} *University of British Columbia*, ² *Université de Montréal*, ³ *HIA/NRC*, ⁴ *Swinburne*, ⁵ *UCLA* and ⁶ *University of Texas* — The initial-final mass relationship relates the mass of a white dwarf star to its main sequence progenitor mass. The relationship, despite being poorly constrained, is widely used as input in several important astrophysical areas. These include determining the upper mass limit to white dwarf production, constraining the rates of type II SNe, better understanding star formation rates, determining the chemical enrichment of the ISM, and constraining the birth rates of neutron stars. We will discuss first results from a new program at Gemini to investigate the white dwarf initial-final mass relationship. Preliminary analysis of multi-object spectroscopic observations of very faint candidate white dwarfs in the rich, well studied, open star cluster NGC 2099 will be presented.

* This work is being supported by NSERC.

WE-P15-2 16h45

Simulating Spitzer 3-24Micron Colour-Colour Diagrams Including Redshift Evolution. Anna Sajina¹, M.D. Lacy² and D. Scott¹, ¹*University of British Columbia* and ²*Spitzer Science Center* — We use a simple parametrization of the mid-IR spectra of a wide range of galaxy types in order to predict their distribution in IRAC/MIPS colour-colour diagrams. In particular, we discuss three basic types by the energetically dominant component in the 3-12micron regime: stellar-dominated, PAH-dominated, and continuum-dominated all spread over the range $z \sim 0-1.5$. This allows us to present colour cuts preferably selecting higher redshift sources of specific type, as well as to discuss possible tests for redshift evolution of the average SED. We compare our predictions with Spitzer First Look Survey data released to date.

WE-P15-3 17h00

Geodetic Precession And The System Geometry Of PSR B1534+12. Ingrid Helen Stairs¹, S.E. Thorsett² and Z. Arzoumanian^{3,1} *University of British Columbia*, ² *University of California* and ³ *Goddard Space Flight Center* — We have conducted high-precision Arecibo observations of the relativistic double-neutron-star binary pulsar B1534+12 since 1998, with data being acquired biweekly and in roughly annual 12-day campaigns. These observations show clear evidence of pulse profile and polarization changes due to geodetic precession of the pulsar's spin axis, which is misaligned with the total angular momentum of the system. We have also found evidence for orbital modulation of the pulse profile due to the special-relativistic effect of aberration. The aberration data and polarization changes can be used to calibrate the scale of the long-term precession effects, resulting in the first quantitative test of the geodetic precession rate in a strong-gravity system. In addition, these observations completely constrain the geometry of the binary system, which otherwise suffers from multiple ambiguities. We discuss implications for asymmetries in supernova explosions and prospects for application to other double-neutron-star systems.

17h15 Session Ends / Fin de la session

**[WE-P16] CAP Council Meeting (New and Old) /
Réunion du Conseil (nouveau et ancien) de l'ACP**

(CAP/ACP)

WEDNESDAY, JUNE 16
MERCREDI, 16 JUIN
17h00 - 18h30

[Room/Salle : Campaign A]

Chair: M. Morrow, MUN

**[WE-P17] CASCA Closing and Awards Given for Best Student Presentations /
Clôture et remise des prix aux meilleures présentations d'étudiants
de la CASCA**

(CASCA)

WEDNESDAY, JUNE 16
MERCREDI, 16 JUIN
17h15 - 17h30

[Room/Salle : Campaign B]

Chair: J. English, U.Manitoba

Thursday, June 17

Jeudi, 17 juin

TOURS FOR THE OBSERVATORY AND PLANETARIUM (CASCA)

U. of Manitoba Physics Alumni Reunion Events (to celebrate the 100th anniversary of the department)

Meeting of the CAP/NSERC Liaison Committee (09h00 - 12h00) - Strathcona Room, Delta Hotel

2004 CONGRESS POSTER SESSION ABSTRACTS

RÉSUMÉS DES SESSIONS D’AFFICHES - CONGRÈS 2004

The poster session abstracts presented here will be on display in this order in the Winnipeg Convention Centre in Winnipeg, Manitoba from 19h00 - 22h00 on Monday, June 14th. *Les résumés présentés en affiches publiés ci-après seront en montre de 19h00 à 22h00, le lundi, 14 juin dans le Centre de congrès à Winnipeg, Manitoba.*

[MO-POS] CASCA

Monday
Lundi

MO-POS-1

The Impact of Canadian Astronomy as Measured by Citations. Dennis R. Crabtree *NRC-HIA* — The impact of scientific research is often measured by citation counts. Citations do not measure the quality of the scientific research but are more a measure of the relevance of the research to other researchers. Citation counts are frequently used as one piece of information in tenure decisions and also used to measure the strength of a whole research community (as in the Astronomy Long Range Plan). In this poster I will compare the publication and citation record of Canadian astronomy groups from 1990 onward.

MO-POS-2

‘Lets Talk Science Partnership Program’ Promotes Science in Canadian Schools. Vesna Milosevic-Zdjelar, *University of Winnipeg* — Canadian universities participate in initiative developed to promote science in schools and community. At seventeen universities, graduate students (as well as undergraduate students at the University of Winnipeg), volunteer to share their knowledge, expertise and enthusiasm with elementary and high school students, teachers and wide community. Through partnerships with schools, science and children museums and scout organizations, our program successfully reaches 25 000 children every year. We will describe here our program at the University of Winnipeg and its place in the national picture

MO-POS-3

Doing Science with the Spitzer Space Telescope. P. Barmby, S. Laine, M. Lacy, Spitzer/IRAC Team, *Harvard-Smithsonian Center for Astrophysics, Spitzer Science Center* — The Spitzer Space Telescope, launch in August 2003, is well into normal science operations. Here we give an overview of the capabilities of the three science instruments, science operations, and the long-term schedule. Science projects from the Early Release Observations, First Look Survey, and IRAC instrument team’s Guaranteed Time will be used to illustrate the power of Spitzer observations for the study of Galactic and extragalactic star formation, high-redshift galaxies, and stellar populations.

MO-POS-4

HIFI: The High Resolution Spectrometer for Herschel*. Michel Fich, *University of Waterloo* (on behalf of the HIFI Team) — The Herschel Space Observatory will be a facility-class space observatory operating at wavelengths between 60 and 670 microns. It will be launched, with the Planck satellite, in 2007 to the second Lagrangian point with a minimum lifetime of three years. The Herschel telescope will be 3.5 m in diameter and passively cooled to 80K. HIFI (the Heterodyne Instrument for the Far-Infrared) is a high resolution spectrometer and one of three focal plane science instruments for Herschel. One of the primary purposes of Herschel is to study astrochemistry and HIFI is the main instrument for studying atomic and molecular spectral lines. Together with the Canadian Space Agency, a consortium of approximately 25 Canadian astronomers are contributing a central part of the HIFI instrument (the Local Oscillator Source Unit, or LSU) and, in return, are full partners in the HIFI Science Team. This poster outlines the current status of the instrument development and presents an overview of the science to be carried out with HIFI. It will also describe how interested Canadian scientists can join the Canadian Herschel/HIFI Consortium and become involved in the mission.

* This work is being supported by CSA.

MO-POS-5

Recent Results from the Odin Satellite*. Michel Fich¹ and K.A. Woodley², ¹*University of Waterloo* and ²*McMaster University* — Odin is a mm and submm heterodyne 1.1m radio telescope mounted on a spacecraft launched on 20 February 2001. It has been developed in a partnership between Sweden, Canada, Finland and France. In this poster we report on recent results from Odin, including a sensitive search for molecular oxygen in interstellar clouds, a survey of the Galactic Plane, and a detailed study of molecular processes in several star forming regions.

* This work is being supported by NSERC and CSA.

MO-POS-6

SPIRE: Herschel’s Submillimetre Camera and Spectrometer*. David Naylor¹, P. Davis¹, J. DiFrancesco², M. Halpern³, P. Martin⁴, D. Scott³ and C. Wilson⁵, ¹*University of Lethbridge*, ²*HIA*, ³*University of British Columbia*, ⁴*University of Toronto* and ⁵*McMaster University* — The Herschel Space Observatory is an ESA cornerstone mission due for launch in 2007, which will conduct astronomical observations across the far-infrared and submillimetre waveband. It will carry a passively cooled, low-emissivity, 3.5-m telescope and will operate at the Sun-Earth L2 point for three years, providing a large amount of observing time at wavelengths unrestricted by the terrestrial atmosphere. The instrument payload will be cooled with an on-board supply of liquid helium, which determines the lifetime of the mission. Canada is involved in both the SPIRE and HIFI instruments on Herschel. The main scientific goals of SPIRE are deep extragalactic and galactic imaging surveys and spectroscopy of star-forming regions in our own and nearby galaxies. The SPIRE instrument comprises a 3 and imaging photometer at spectral channels at 250, 350, and 500 μm , and an imaging Fourier transform spectrometer (FTS) covering the range 200-670 μm . The FTS employs a dual-beam configuration with broad-band intensity beam dividers. The SPIRE detectors are feedhorn-coupled neutron transmutation doped (NTD) Germanium spider-web bolometers. The Canadian contributions to the SPIRE instrument are (a) a mid-resolution ($R \gg 1000$) broadband FTS to test and qualify instrument models, (b) software packages to deglitch the signal stream, correct for the spectral response of the instrument, and process the spectrometer data, and (c) staff effort for the Instrument Test Team and Control Centre. Five Canadian researchers participate in the SPIRE Specialist Astronomy Groups as Associate Scientists. The Canadian involvement in the SPIRE project will be described.

* This work is being supported by CSA, NSERC.

MO-POS-7

Protoplanetary Dust Disk Dynamics*. Robin Humble¹, S.T. Maddison² and J.R. Murray², ¹*Canadian Institute for Theoretical Astrophysics* and ²*Swinburne Centre for Astro and Supercomputing* — With a view to investigating planet formation processes we have developed a code for simulating astrophysical dusty-gas flows in protoplanetary disks. Our parallel three dimensional code incorporates gas hydrodynamics, self-gravity and several gas drag prescriptions to follow the dynamical evolution of a two-phase dusty-gas medium. We present results of some calculations with submillimetre, centimetre and metre sized dust. Dust disk lifetimes and possible gas giant and terrestrial planet formation scenarios are discussed.

MO-POS-8

Neptune’s Migration into a Dynamically Hot Kuiper Belt*. Joseph Hahn¹ and R. Malhotra², ¹*Saint Mary’s University* and ²*University of Arizona* — The effects of Neptune’s orbital expansion into a dynamically hot Kuiper Belt is examined numerically. In the model, a torque is applied to Neptune’s orbit causing it to expand 9 AU outwards and into a stirred up Kuiper Belt composed of 10^4 massless particles having initial eccentricities $e \sim 0.1$. This system is integrated over the age of the Solar System, and our results confirm Chiang *et al.*’s (2003) finding that migration into hot Kuiper Belt allows particles to get trapped at weak mean motion resonances like the 5:2. Indeed, our higher-resolution study of this scenario shows particles getting trapped at many of Neptune’s weak resonances, including the 13:6, 9:4, 7:3, 12:5, 8:3, 11:4, 3:1, 7:2, 4:1, all of which reside in the 50- a -80 AU zone. Many of these trapped particles have such high eccentricities that they also inhabit the domain usually identified as the Scattered Disk. Of course, gravitational scattering by Neptune also produces a Scattered Disk of particles, but most of these particles are removed over the age of the Solar System during subsequent encounters with the planets. Indeed, inspection of all particles with semimajor axes 50- a -80 AU and $e > 0.25$ shows that about 90% were trapped at Neptune’s migrating resonances, with only 10% actually being scattered by Neptune. These results may also provide an explanation for the ‘extended’ scattered disk of Gladman *et al.* (2002), namely, that some of these KBOs were trapped at an exotic resonance with Neptune rather than scattered.

* This work is being supported by CFI.

M0-POS-9

Evolutionary Models of the roAp star HR 1217: Magnetic Fields and Pulsation Frequencies. Christopher Cameron¹, J.M. Matthews¹, M.S. Cunha², D.B. Guenther³ and W. Weiss⁴, ¹University of British Columbia, ²Centre for Astrophysics of the University of Port, ³Saint Mary's University and ⁴University of Vienna — Strong magnetic fields measured in the chemically peculiar A stars of the upper main sequence are believed to be intricately linked to observed abundance anomalies. In addition, a small subset of these stars are unstable to high-overtone pulsations. These stars, known as rapidly oscillating Ap (roAp) stars, show evidence that the magnetic field also has a strong influence on the observed oscillation frequencies. We present evolutionary models for the particular case of the roAp star HR 1217 and estimate the effect of the magnetic field on the calculated oscillation frequencies. We also show how the observed abundances influence calculations of the temperature-optical depth relation for this star.

M0-POS-10

Testing Stellar Evolution Theory: Theoretical Luminosity Functions and M92. Brian Chaboyer, S.R. Bjork, N.E.Q. Paust, Dartmouth College — A Monte Carlo simulation exploring uncertainties in standard stellar evolution theory on the red giant branch of metal-poor globular clusters has been conducted. The analysis takes into account uncertainties in the primordial helium abundance, abundance of alpha-capture elements, radiative and conductive opacities, nuclear reaction rates, neutrino energy losses, the treatments of diffusion and convection, the surface boundary conditions, and color transformations. These theoretical luminosity functions are compared the observed luminosity function of M92. The M92 luminosity function was obtained from observations which combine wide field (32 x 32 arc-minute) data from the 2.4m telescope at MDM Observatory with HST ACS images of the central 3 arc-minute core of M92. Accurate photometry of over 25,000 stars are used in the construction of the M92 luminosity function.

M0-POS-11

In Pursuit of the Rotation Rates of Wolf-Rayet Stars. Andre-Nicolas Chene and N.S. St-Louis, Université de Montreal — Les étoiles chaudes et massives ont un taux de perte de masse très important (jusqu'à 10⁻⁵ MSolaire an⁻¹), sous la forme d'un vent stellaire engendré par la pression de radiation (force exercée par la lumière sur la matière). Les étoiles Wolf-Rayet (WR), qui sont les descendantes des étoiles O (les étoiles les plus massives de la Séquence Principale de brûlage d'hydrogène), possèdent les vents stables les plus intenses (voir fig.1). Cette épaisse couche de matière nous empêche de voir l'étoile elle-même, dont il est, par ce fait, difficile d'en déterminer les paramètres. En particulier, le taux de rotation des étoiles WR est pratiquement inconnu. Comme des modèles récents d'évolution stellaire montrent que le taux de rotation est un paramètre crucial dans la vie de ces étoiles (Maeder & Meynet 1996), il est important de le déterminer par des observations. Or, pour certaines étoiles, il est maintenant bien connu que des perturbations à la surface, tel des pulsations stellaires ou des taches magnétiques, se propagent dans le vent en engendrant des structures à grande échelle qui ont une densité inférieure ou supérieure à la moyenne (voir fig.2). La rotation entraîne ces structures, appelées Régions d'Interaction en Co-rotation (CIR en anglais), en générant des spirales dans le vent. Cela se traduit par des variations périodiques dans les raies spectrales d'étoiles apparemment isolées (voir fig.3 tirée de la thèse de T.Morel, 1999). En étudiant ces variations, il est donc possible de déduire le taux de rotation des étoiles WR, tant attendu par les modèles.

M0-POS-12

Defining the Orbit and Distance to WR140. Sean Dougherty¹, N.J. Bolingbroke¹, A.J. Beasley² and M.J. Claussen³, ¹National Research Council, ²OVRO and ³NRAO — Milli-arcsecond resolution VLBA observations of the archetype colliding-wind WR+O star binary system WR140 reveal the wind-collision region as a bow-shaped arc of emission that rotates as the highly eccentric orbit progresses from phase 0.74 to 0.95 (Beasley *et al.*, in prep). Assuming that the arc is symmetric about the line-of-centres of the two stars and "points" at the WR star, this rotation shows the O star moving from SE to approximately E of the WR star between these orbital phases. In conjunction with orbital parameters derived from radial velocity variations (Marchenko *et al.* 2003, *ApJ* 596, 1295) and the recent IOTA observation of both stellar components (Monnier *et al.* 2004, *ApJL* 602, L57), the VLBA observations allow us to constrain, for the first time, the inclination of the orbit plane as 122° ± 5°, the longitude of the ascending node as 353° ± 3°, and the orbit semi-major axis as 9.0 ± 0.3 mas. This leads to a robust distance estimate to WR 140 of 1.8 ± 0.1 kpc and mass estimates for the components of 20 ± 4 M_⊙ for the WR star and 54 ± 10 M_⊙ for the O star.

M0-POS-13

Seeking the Progenitors of Magnetic Ap/Bp stars: Detection of a Magnetic Field in Two HAEBE Stars* Dominic Drouin¹, S. Bagnulo², J.D. Landstreet³, E. Mason², D.N. Monin³ and G.A. Wade¹, ¹Royal Military College of Canada, ²ESO Chile and ³University of Western Ontario — The Herbig Ae/Be (HAEBe) stars are widely thought to be the pre-main sequence progenitors of the magnetic Ap/Bp stars. During a very recent observing run at the ESO VLT, we carried out observations to search for direct evidence of magnetic fields in the envelopes and photospheres of a selected sample of HAEBe stars. The analysis of our data showed a 4σ detection for 2 of the 14 targets observed. These results represent a breakthrough in our understanding of the nature, origin and evolution of magnetic activity in A and B type stars by providing a crucial link between the main sequence magnetic stars and their pre-main sequence counterparts.

* This work is being supported by NSERC.

M0-POS-14

New Insights into Polaris the Cepheid. David G. Turner, Saint Mary's University — The North Star, Polaris, and the anonymous, poorly populated star cluster in which it lies, have been target objects in a newly initiated campaign of photometric observation using the Burke-Gaffney Observatory at Saint Mary's University. Polaris is one of the most curious, overlooked, and misinterpreted objects in the nighttime sky. Even its presently recognized status as the brightest known classical Cepheid variable is of fairly recent origin. Yet for the last twenty years Polaris has presented an enigma of major concern to variable star specialists: its light amplitude has been decreasing at such an alarming rate that concern was expressed that it might cease to pulsate entirely some time in the mid-1990s. As usual, Polaris stubbornly defies all expectations. Recent photometry indicates that it continues to pulsate at its standard rate of once every 4 days, but at an extremely low, perhaps still decreasing, level. The star also exhibits a rapid rate of period change that raises questions about its evolutionary status and pulsation mode: is it in the first crossing of the instability strip or perhaps the fifth crossing, does it pulsate in the fundamental mode or in an excited harmonic? Such questions are not easy to answer with certainty, and the fact that the star's distance inferred from its Hipparcos parallax is probably inaccurate does not help the situation. Main sequence fitting from its cluster membership and new studies of its period changes provide alternate estimates for its basic parameters that appear to resolve many of the questions posed above. And the North Star is also an exciting object of study for avid variable star enthusiasts with proper equipment. Where else can you see stellar evolution occurring right before your eyes?

PO-MOS-15

Synthetic Flux Spectra of Rotationally Deformed Stars. C. Ian Short and Catherine Lovekin, Institute for Computational Astrophysics and Department of Astronomy and Physics, Saint Mary's University — Due to geometrical effects and variation of stellar parameters over the surface, the flux spectrum of a star that is deformed by rapid rotation may differ significantly from that of a spherical star of stellar parameters that are fit to the observed flux spectrum. We have used the shape and variation of stellar parameters computed with a fully 2D stellar evolution code and synthetic intensities computed as a function of emergent angle with a NLTE stellar atmosphere and spectrum synthesis code (PHOENIX) to synthesize the flux spectrum of the rapidly rotating star alpha Eridani. We compare the flux spectrum of the rotationally deformed model to that of a spherical model fit to the observed spectrum and investigate the effect on derived stellar parameters of the more realistic modeling.

PO-MOS-16

Rapid Photometry of Variables in the Globular Cluster M55. Jason Rowe, C. Cameron, J.M. Matthews and M. Huber, University of British Columbia — We present results from photometry obtained with the 8 metre Gemini-South telescope for the core of the globular cluster M55. Over a 6 hour observing run, 2200 images were obtained to measure the light curve shapes of SX Phe type variables. The shape parameters are used to help identify pulsation modes for application to field variables.

M0-POS-17

Spectral Modelisation and Analysis of NGC2363-V1, An Errupting LBV*. Véronique Petit¹, L.D. Drissen¹ and P.C. Crowther², ¹Université Laval and ²University of Sheffield — I will present the results of a follow up study of the LBV star NGC2363-V1 between the years 1997 and 2003. V1, discovered in 1994 by Drissen *et al.*, is presently undergoing a major outburst, associated with an increase in its mass loss rate. Spectra obtained by the Hubble Space Telescope were modeled by the non-LTE line-blanketed model CMFGEN (Hillier and Miller 1998) to obtain the evolution in the physical parameters of this incredible star.

* This work is being supported by Laurent Drissen.

M0-POS-18

Self-Correlation: A Useful New Tool for Analyzing the Photometric Variability of T Tauri Stars*. John Percy¹, W.K. Gryc¹, W. Herbst² and J.C.Y. Wong¹, ¹University of Toronto and ²Wesleyan University, Middletown CT — T Tauri stars are irregular variable stars in an early phase of evolution where gravitational contraction to the main sequence is still taking place. The (photometric) variability is complex, and takes place on a variety of timescales, due to a variety of physical processes. There is low-level periodic photometric variability, due to the rotation of the star with active regions on its surface. The periodicity is usually investigated by Fourier analysis, but, especially if the active regions are non-permanent, this method may fail. In this paper, we use self-correlation analysis as an adjunct to Fourier analysis. Self-correlation analysis determines the cycle-to-cycle behaviour of the star, averaged over all the data. The data come from an on-line archive of T Tauri photometry, maintained by W. Herbst. Using self-correlation, we have reanalyzed T Tauri stars with known periods, to verify the periods and the applicability of the technique. We have then applied self-correlation to T Tauri stars whose periods (if any) are uncertain or unknown. The results will be described.

* This work is being supported by NSERC Canada.

MO-POS-19

Atomic Data for Resonance Lines. Donald C. Morton, *Herzberg Institute of Astrophysics, National Research Council of Canada* — Resonance lines, i.e. those transitions involving the ground state or excited levels of the ground term, have a special role in astrophysics because they will dominate the spectra of regions of low particle and radiation densities such as interstellar and intergalactic gas as well as stellar and QSO winds. Thus having reliable data on the wavelengths and transition probabilities of resonance lines is central to many astrophysical investigations. This paper summarizes the present status of the author's efforts to provide critical compilations of these data. Under the general title of "Atomic data for Resonance Absorption Lines" there are three papers:

II. Wavelengths Longward of the Lyman Limit for Heavy Elements (Ge to U), 2000 ApJS 130, 403;

III. Wavelengths Longward of the Lyman Limit for the Elements Hydrogen to Gallium, 2003 ApJS 149, 205 – an update of Paper I published in 1991; and

IV. Wavelengths between the Lyman Limit and 100 Å for the Elements Helium to Gallium, in preparation.

Experimental transition probabilities (A_{ul}) for the extreme ultraviolet region covered in Paper IV are scarce, but fortunately *ab initio* theoretical multiconfiguration calculations now can accurately predict the laboratory energies and give A -values consistent with laboratory measurements where checks are possible at longer wavelengths. The data in Paper IV are particularly relevant to the study of absorption lines in high-redshift QSOs.

MO-POS-20

The Degree of Contact and Other Properties of Binary Stars with Common Envelopes* Stefan Mochnacki, *University of Toronto* — A compilation of models fitted using both photometric and spectroscopic data is analysed using the concepts of mean density, minimum period and transfer-corrected primary temperature. The tendency of W UMa systems to have common envelopes close to their inner Roche surfaces is shown to be a closeness in radius rather than a function of fill-out factor. This allows the use for evolutionary studies of systems for which only spectroscopic mass ratios are available without photometric solutions; the new DDO sample of spectroscopically observed systems is analysed. An analysis of the recent Pribulla-Kreiner-Tremko catalogue is also presented.

* This work is being supported by NSERC.

MO-POS-21

2D-Modelling of the Rotation of a Rapidly Rotating Be star. C. Lovekin and R.G. Deupree, *Institute for Computational Astrophysics, St Mary's University* — Recent interferometric observations of the Be star Achernar (HD10144) have found it to be extremely oblate, with an axis ratio of $2a/2b = 1.56 \pm 0.05$, where a and b are the best fit to the semimajor and semiminor axes for the surface shape. This ratio is very close to the limit of 1.5 for a solid body at critical rotation. Based on stellar models, Achernar is a late main sequence star and probably should not be expected to be rotating as a solid body. We have modelled rapidly rotating stars to attempt to reproduce the observed properties of Achernar using a 2D stellar evolution code. The surface of the model is assumed to be an equipotential. Calculated models rotating at critical velocity on the ZAMS have appreciably lower surface velocities than the observed T_{eff} and L of Achernar are reached. These models fail to match the observed oblateness, with ratios of $2a/2b$ of 1.27 to 1.36, depending on the inclination. We have also calculated models whose rotation rate increases towards the rotation axis and is constant on cylinders. These laws do make the stellar surface more oblate, although the increase in oblateness is insufficient to match the observations.

MO-POS-22

The Structure of Close Binaries in 2D. A.I. Karakas, and R.G. Deupree, *ICA, Saint Mary's University* — Previous studies of the evolution of close binary systems have assumed that each component is spherically symmetric, even if it fills its Roche lobe. Rotation and tidal interactions will cause the structure to deviate from spherical symmetry but it was not known in detail how large this distortion will be. Using a state-of-the-art 2D stellar structure code, we study the departure from spherical symmetry on the structure of an zero-age main sequence model of solar composition ($Z = 0.02$). We assume that the companion is a gravitational point source and in a circular orbit. We present preliminary results of the structure of an $8M_{\odot}$ primary with a $5M_{\odot}$ point-source secondary companion. We have also begun to study the effect of the primary on the secondary, by calculating the case with $5M_{\odot}$ with an $8M_{\odot}$ companion. In each case we assume that the separation is $20R_{\odot}$. We plan to perform evolutionary calculations on these models, evolving to the point where the primary fills its Roche lobe. At this point this model may serve as a starting point for a study of mass loss from the primary. Future work will be to study the effect each binary star has on the structure of the other by assuming that neither star is a gravitational point source and calculating the structure of both components simultaneously.

MO-POS-23

The Faint End Of The Luminosity Function In The Core Of The Coma Cluster: A Data Mining Case Study. Margaret L. Milne and C.J. Pritchett, *University of Victoria* — We present optical measurements of the faint end of the luminosity function (LF) in the core of the Coma cluster. The archives of the Hubble Space Telescope were mined for images of the Coma cluster and of the field; number counts were determined from these and used with the method of statistical background subtraction to determine the luminosity function to $m_p = 25.75$. This is the faintest determination of Coma's LF to date, and also marks the first time that HST images have been used to construct Coma's LF. Evidence is found for a steep faint end slope with alpha approximately equal to -2. The process of creating the LF and the implications of the result will be discussed, with an emphasis on the role data mining can play in this field of study.

MO-POS-24

Stellar Atmospheres with Abundance Stratifications. Dmitry Monin and F. LeBlanc, *Université de Moncton* — Strong non-uniform distributions of chemical elements as a function of optical depth (i.e. chemical stratification) are observed in some chemically peculiar stars. Diffusion processes acting in their atmosphere is most likely responsible for the stratification. Model atmospheres including self-consistent vertical element abundance gradients produced by diffusion are presented here. These models are based on a modified version of the multi-purpose atmospheric code PHOENIX. The changes to the atmospheric structure due to the abundance gradients are shown. Possible applications to different stars are also discussed.

MO-POS-25

Probing Sunspot Magnetic Fields with Solar Oscillations. Ashley Crouch¹ and P.S. Cally^{2, 1} *Université de Montréal* and ² *Monash University* — Sunspots absorb and scatter incident f- and p-modes. Until recently, the responsible absorption mechanism was uncertain. The most promising explanation appears to be conversion to slow magnetoacoustic-gravity waves and Alfvén waves, which carry energy down the magnetic field lines into the interior. Assuming uniform vertical magnetic field, this mechanism easily explains f-mode absorption, but cannot fully account for observations of (higher order) p-modes. Recent calculations show that p-mode absorption produced by simple sunspot models with non-vertical magnetic fields is ample to explain the observations. In fact, the resultant p-mode scattering by such models is in remarkable agreement with observations. This excellent agreement allows some degree of probing of subsurface magnetic field strengths (i.e., visualizing the invisible). Here, we present results from the best sunspot models currently available and discuss their implications for subsurface magnetic field structure.

MO-POS-26

Models of Rotating Delta Scuti Stars. R. Deupree, *Institute for Computational Astrophysics and Department of Astronomy and Physics, Saint Mary's University* — Delta Scuti stars are viewed as prime candidates for probing the internal structure of stars by matching multiple pulsation modes. The task is formidable because mode identification is not trivial when there are only a comparatively small number of modes observed and because a number of delta Scuti stars rotate sufficiently rapidly that their structure cannot be modeled with the same degree of confidence as can the structure of nonrotating stars. This work presents a first step with the full 2D calculation of rotating models of delta Scuti stars. It is expected that these models will form the basis of calculating rigorous linear, adiabatic, nonradial pulsation periods using the approach of Clement (ApJS, 116, 57). Pulsation mode results for ZAMS models for several rotation rates.

MO-POS-27

Causality and the Collimation of Astrophysical Jets* Heather Cameron and C.D. Matzner, *University of Toronto* — Collimated jet-like outflows are associated with many astrophysical objects, ranging from protostellar objects to active galactic nuclei. Although magnetic fields are implicated in launching and shaping these flows, and many theoretical models have been offered for them, fundamental questions remain to be resolved. What, for instance, is necessary for collimation — would the Solar wind collimate if there were no heliopause? In both Newtonian and relativistic winds, collimation requires causality: information must cross streamlines. At the same time, information flow is restricted by the acceleration that accompanies collimation. We use the method of characteristics to derive preliminary results on the links between collimation, acceleration, and the causal structure of magnetized winds.

* This work is being supported by University of Toronto.

MO-POS-28

The Relation Between Supermassive Black Holes and their Environments* X.Y. Dong and M.M. De Robertis, *York University* — In order to study the origin and maintenance of activity in galactic nuclei, we consider a sample of 118 spiral galaxies from a variety of morphological stages from Ho *et al.* (1997) to search for correlations among active parameters such as emission-line properties, and parameters associated with the host galaxy. After first calibrating a K -band relation between the bulge and central black hole masses: $\log_{10} [M_{\text{BH}} / M_{\text{sun}}] = (-0.413 \pm 0.061) M_K + (-1.704 \pm 1.442)$, we determine the central black hole masses for these galaxies from K -band bulge magnitudes M_K measured from 2MASS data, and using the two-dimensional decomposition routine GALFIT. The parameters that correlate extremely well with black-hole mass include: narrow emission-line width, various emission-line ratios, and the inclination-corrected 21 cm line width for the galactic disk. A list of other pairs of parameters that show good correlations also described. The IRAS 25, 60 and 100 μm luminosities correlate well with the $H\alpha$ (narrow-line) luminosity. There are also interesting correlations between the IR flux ratios and the

$H\alpha$ luminosity. We also present the distributions of active and non-active parameters as a function of morphological type, T . Bulge luminosities (and black hole masses) are larger in early type spiral galaxies, but with a significant scatter. The absolute K -band bulge magnitude is $M_{K_s} = (0.3528 \pm 0.1413) T + (-22.7378 \pm 0.4277)$. As we discuss, this is undoubtedly a major reason why Seyfert galaxies are discovered primarily in early type spirals. The distributions for Sc galaxies are often markedly different from the distributions in earlier types.

* This work is being supported by NSERC.

MO-POS-29

The Optical And Infrared Emission Of The Magnetar 1E 1048*. Martin Durant and M.H. van Kerkwijk, *University of Toronto* — In the magnetar model for anomalous X-ray pulsars (AXPs), the superstrong magnetic field of the neutron star causes currents to traverse the magnetosphere. Optical and infrared emission is produced when ions absorb X-rays from the stellar surface and are promoted into high Landau excitation states, energy which is then released as the ion de-excites. Since the energy of the Landau levels and the radiative timescale both depend on the local magnetic flux density, the magnetic mirroring effect causes a sharp cutoff in the spectrum; and since the current causes the toroidal component of the exterior magnetic field, a relationship between the infrared/optical flux and the X-ray flux and timing torque are expected. I will present photometric data taken with Magellan and the VLT of 1E 1048, and compare these to other AXPs and specifically to the questions raised above.

* This work is being supported by Martin Durant.

MO-POS-30

XMM-Newton Observation of the High Magnetic Field Radio Pulsar B0154+61. Marjorie Gonzalez¹, V.M. Kaspi¹, A.G. Lyne² and M.J. Pivovarov³, ¹McGill University, ²University of Manchester and ³Space Sciences Laboratory, UC Berkeley — We present results from a deep X-ray observation of the radio pulsar B0154+61 performed with the XMM-Newton satellite. The pulsar has a characteristic age of 20.5 kyr, a rotation period of 2.3 seconds and an inferred dipole surface magnetic field strength of 2.1×10^{13} G, some of the highest values in the radio pulsar population. Our analysis shows that no X-ray emission is detected from the position of B0154+61 with XMM-Newton. Using a blackbody model, the derived upper limits on the pulsar's temperature and luminosity are <73 eV and $<1.4 \times 10^{32}$ ergs s⁻¹, respectively (assuming a distance of 1.7-kpc and a column density $N_H < 3 \times 10^{21}$ cm⁻²). When compared to the values predicted by neutron star cooling models, the above limits are found to favor those requiring rapid cooling, especially when corrections for the presence of a light-element atmosphere and relatively high magnetic field on the neutron star are made. However, the uncertainties in distance, column density and atmospheric composition prevent a definite conclusion. In addition, the limits on the temperature and luminosity of B0154+61 are found to be much lower than those exhibited by the "anomalous X-ray pulsars" (AXPs), although their spin characteristics are comparable, thus leaving unanswered the question of a radio pulsar/AXP connection.

MO-POS-31

A Gemini Observation of the Anomalous X-Ray Pulsar 1RXSJ170849-400910*. Jennifer West and S. Safi-Harb, *University of Manitoba* — The anomalous X-ray pulsars (AXPs) represent a growing class of neutron stars discovered at X-ray energies. Unlike the Crab-like pulsars, they are radio-quiet, slow X-ray rotators, and have an X-ray luminosity higher than their rotational spin-down power. The two competing models proposed to explain their anomalous nature invoke either accretion from a low-mass companion on a disk, or an ultra-magnetized neutron star (magnetar). In the past few years, evidence has been accumulating in favor of the magnetar model, making AXPs and the Soft Gamma-Ray Repeaters among the strongest magnets in the Universe. Infrared observations offer a tool to test these models and study the variability of these objects. 1RXSJ170849-400910 is a relatively bright AXP which was discovered with the ROSAT X-ray satellite, and later found to be an 11 s X-ray pulsar by the ASCA X-ray satellite. Recently, Israel *et al.* (2003) reported the detection of the likely IR counterpart to 1RXSJ170849-400910 using a deep observation the ESO and CFHT telescopes. We will here present a Gemini observation of 1RXSJ170849-400910 obtained with Flamingos, the Gemini-South near-IR imager, in J (1.25 μ m), H (1.65 μ m), and K (short) (2.15 μ m), and compare our result with that of Israel *et al.*

* This work is being supported by NSERC and URGF.

MO-POS-32

Near InfraRed Detection of the Anomalous X-Ray Pulsar 1E 2259+586. Cindy Tam¹, V.M. Kaspi¹, M.H. van Kerkwijk² and M. Durant², ¹McGill University and ²University of Toronto — On June 18 2002, the Anomalous X-ray Pulsar AXP 1E 2259+586 underwent a major X-ray outburst that lasted several hours and consequently linked AXP's to another class of high-energy bursting objects, called Soft Gamma-ray Repeaters (SGR). This was predicted uniquely by the "magnetar" model, in which these two classes are ultrahigh magnetic field, isolated young neutron stars. A few days after this outburst, Target of Opportunity observations were obtained with the Gemini North Near-Infrared Imager (NIRI), followed by a longer term monitoring program of the IR variability that spanned nearly one and a half years. It was observed that shortly after the burst, the pulsar's Ks band flux dramatically increased relative to its pre-burst flux level, prompting the question "does the IR luminosity of 1E 2259+586 constantly undergo fluctuations, or can this brightening be undeniably associated with the X-ray outburst?" We present the results of our IR analysis, and relate them to the results of previous X-ray studies. There was no evidence for variability apart from that seen immediately after the outburst, implying the IR fluctuation was definitely associated with the outburst. Also, we discuss the effect that our findings might have on current AXP theoretical models.

MO-POS-33

The Study of a Puzzling Galactic Supernova Remnant and The Discovery of an Active Galactic Nucleus in its background void*. Samar Safi-Harb¹, U. Hwang², R. Petre², S.S. Holt³ and P. Durouchoux⁴, ¹University of Manitoba, ²NASA/GSFC, ³Olin College and ⁴Saclay, France — G41.1-0.3 is an intriguing supernova remnant with an unusual morphology and properties. In our previous X-ray study of this remnant, we suggested that it is the result of a type II supernova explosion; however no pulsar has been yet found to be associated with it. We report on our Chandra spatially resolved spectroscopic study of the remnant, and correlate its X-ray emission with the radio and millimeter observations. We then address its unusual morphology and discuss its properties in the light of a shock wave interacting with an inhomogeneous medium. The burning question about G41.1-0.3 remains: where is its compact stellar remnant? While searching for a compact object, we discovered an X-ray pointsource just outside the remnant. We discuss the nature of this new source and argue that it is a nearby Seyfert II Active Galactic Nucleus.

* This work is being supported by NSERC, NASA.

MO-POS-34

Long Term Timing Observations of the Young, Energetic Pulsar PSR B1509-58. Margaret Livingstone¹, V.M. Kaspi¹ and R.N. Manchester², ¹McGill University and ²ATNF - We present results from the long-term timing observations of the young, energetic pulsar PSR B1509-58. We present a phase-coherent analysis of 21 years of timing data from the Molonglo and Parkes Radio Observatories and the Rossi X-Ray Timing Explorer. We have measured the frequency derivative as well as higher order frequency derivatives to test the conventional model of pulsar spin-down given by $\dot{\nu} = K\nu^n$, where ν is the frequency of the pulsar, $\dot{\nu}$ is the frequency derivative, K is a constant related to the magnetic field of the pulsar and n is the 'braking index'. Using a partially phase-coherent timing analysis, we have measured a braking index consistent with previous measurements. We also measure the value of the third frequency derivative to be inconsistent with the simple spin-down law for pulsars, possibly indicating a time-dependent magnetic field.

MO-POS-35

PSR J1740-5340 Promises and Surprises*. Fernando Pena and M.H. van Kerkwijk, *University of Toronto* — Bright stars which are binary systems where the other component is a neutron star are very useful as a tool to constraint pulsar's masses. Different equations of state (EOS) will give different values slightly greater than the current $1.35 M_{\odot}$ depending in the type of interactions between particles at the core and depending in the mass accreted. In the particular case of the binary system PSR J1740-5340 the companion is a bright ($V \sim 17$) non-MS star (we called it "red straggler") which partially fills its Roche lobe ($R/R_{\text{RocheLobe}} \leq 1$), the orbital period is 1.35 days. The system is in the globular cluster NGC 6397 (mean velocity ~ 18 km/s) and the pulsar has a period of 3.5 ms (MSP). I will present high resolution VLT/UVES spectra (~ 24 nights covering different orbital phases). From these I will show the radial and rotational velocities of the companion star, and assuming some models I will present the mass ratio (already done, $M_{\text{PULSAR}}/M_{\text{COMP}} \sim 5.7$), the inclination angle of the orbit (in progress but will be finished by the time of the congress), and finally the mass of the binary components (MSP and companion). Together with the mass measurement I will discuss some interesting puzzles of this system, most of them related to the lack of heating showed by companion's light curve (which is purely sinusoidal, because of its tidal deformation), strange because we expect some influence of the pulsar's irradiation on the very close-companion's atmosphere.

* This work is being supported by University of Toronto.

MO-POS-36

A Chandra Observation of the W50 Nebula Associated with SS433. A. Moldowan and S. Safi-Harb, *University of Manitoba* — The X-ray binary system SS433/W50 has baffled astrophysicists since its discovery in 1979. W50 has been classified as a Galactic supernova remnant that harbors SS433, an X-ray binary consisting of a compact object accreting matter from a companion star at a super-Eddington rate. The nature of the compact object is still unknown, but it is expelling relativistic jets that interact with W50, causing it to elongate along the jets axis and forming the X-ray lobes. We have studied this system with ROSAT, ASCA, RXTE and, most recently, Chandra. A 75 ksec Chandra observation will be presented for the western lobe of W50. This observation and the corresponding analysis will be compared to the observations made by ASCA and ROSAT of the western lobe, as well as the eastern lobe of W50. The Chandra data will also allow a spatial resolution of thermal and non-thermal emission from the shock-excited regions in the remnant.

MO-POS-37

The Plerionic Supernova Remnant G21.5-0.9: In and Out*. H. Matheson and S. Safi-Harb, *University of Manitoba* — The Crab nebula has been viewed as the prototype for a pulsar-wind nebula or a plerion. Today, we know of about a dozen Galactic plerions. The absence of a supernova remnant (SNR) shell surrounding the Crab and other plerions is still a mystery. G21.5-0.9 is an intriguing plerionic SNR. Early Chandra observations revealed a faint extended X-ray halo, which was suggested to be the missing shell of the

SNR. Safi-Harb *et al.* (2001) show however that the X-ray emission from this extended halo is non-thermal, unlike what would be expected from an SNR shell. They suggested that the extension could be indicative of a larger than previously thought plerion and/or due to a dust scattering X-ray halo. In the former scenario, G21.5-0.9 would be the only plerion which has a larger size in X-rays than in the radio. Since G21.5-0.9 is a calibration target for Chandra, there is a large amount of data available. We will present our analysis of 207 ksec of data obtained with the High-Resolution Camera and 450 ksec of data acquired with the Advanced CCD Imaging Spectrometer. We will show the results of our deep search for thermal emission and discuss the nature of the X-ray halo in the light of the proposed models. We will also put further constraints on the parameters of the putative pulsar powering G21.5-0.9.

* This work is being supported by NSERC.

MO-POS-38

X-Ray Aurora in Magnetosphere of Accreting Neutron Stars*, Vahid Rezanian, John C. Samson and Peter Dobias, *Theoretical Physics Institute* — In this study we propose a new generic model for quasi periodic oscillations (QPOs) based on oscillation modes of neutron star magnetospheres. We argue that the interaction of the accretion disk with the magnetosphere can excite resonant shear Alfvén waves in a region of enhanced density gradients. We demonstrate that depending on the distance of this enhanced density region from the star and the magnetic field strength, the frequency of the field line resonance can range from several Hz (weaker field, farther from star), to approximately kHz frequencies (stronger field, ~6-10 star radii from the star). We show that such oscillations are able to significantly modulate inflow of matter from the high density region toward the star surface, and possibly produce the observed X-ray spectrum. In addition, we show that the observed 2:3 frequency ratio of QPOs is a natural result of our model.

* This work is being supported by NSERC.

MO-POS-39

The Search for Supernova Remnants Using the International Galactic Plane Survey Data*, Ashish Asgekar¹, Samar Safi-Harb² and Roland Kothes^{2, 1}, *University of Manitoba* and ²Dominion Radio Astrophysical Observatory, NRC — The International Galactic Plane Survey (IGPS) has in the past few years demonstrated its remarkable sensitivity towards low-surface brightness, extended structures, like supernova remnants (SNRs). We are searching for new SNRs targeting the positions of already-known pulsars in the IGPS data. Two candidates were identified by comparing the IGPS 20-cm images with the archival images from other surveys, such as the NVSS and IRAS. We will present their polarized intensity and spectral index maps obtained with the archival VLA data, and search for their X-ray counterparts.

* This work is being supported by IGPS.

MO-POS-40

Correlating Dust Properties with Star Formation and the ISM in the BIMA SONG Survey, Scott Brooks and C. Wilson, *McMaster University* — We present preliminary results from the analysis of 450 and 850 micron SCUBA jiggle maps of a selection of galaxies from the BIMA SONG catalog. Our observations are sensitive to the continuum emission due to cool dust, which can be correlated with the gas emission to determine empirically what the relative importance is to the continuum emission of changes in the dust mass versus changes in the dust heating due to nearby star formation.

MO-POS-41

The Spatial Distribution and Extraordinary Extinction Law in Optical Nebulae of the 2nd Quadrant, Tyler Foster¹ and R. Kothes^{2, 1}, *Herzberg Institute of Astrophysics, National Research Council*, ²University of Calgary, HIA/NRC — We have constructed a new map of the Galactic Plane Region $90^\circ \leq \ell \leq 180^\circ$, $-3.5^\circ \leq b \leq 5.5^\circ$ using new non-photometric distances to ~70 HII regions, from the technique of Foster & Routledge (2003). We present new radial velocity measurements for each region using Canadian Galactic Plane Survey HI and ¹²CO data, as well as published Ha line surveys. The most noticeable result is that the clear majority of these optically catalogued nebulae (c.f. Sharpless 1959) are residents are the Perseus Arm, the nearest major spiral arm to the Sun. Many of these regions form a striking "chain" that follows the Arm's inner edge. Some others are Local Arm inhabitants, while Sh-127 ($d = 6.2$ kpc) is likely an Outer Spiral Arm member. Published photometric distances to many HII regions (particularly those near the Galactic anticentre, $150^\circ \leq \ell \leq 180^\circ$) suggest that they are scattered irregularly throughout the disk, a picture inconsistent with the accepted model of their formation in "chains" along Spiral Arms. We show that most of these HII regions are surrounded by layers of dust, and that the value of total-to-selective extinction $R_V = A_V / E(B - V)$ in the involved dust is greater than the canonical ISM value of $R_V = 3.1$. The anomalous photometric distances of these HII regions are likely the result of observing their exciting star(s) through these dense shells of dust, where we measure R_V to range from 3.2 to more than 7. This abnormal extinction law particularly affects the distance moduli of those regions toward the anticentre, where extinction due to associated dust equals or exceeds that due to foreground material.

MO-POS-42

Pulsar-Based Galactic Magnetic Field Mapping: A Small Annulus With An Anti-Clockwise Magnetic Field, In A Large Disk With A Clockwise Magnetic Field, Jacques P. Vallee, *National Research Council Canada - Herzberg Institute of Astrophysics* — A new pulsar-based model for the structure of the Milky Way's magnetic field is obtained, by using both the rotation measure and the dispersion measure of over 350 pulsars in the Milky Way. The model holds true separately for pulsars above the galactic plane, and for pulsars below the plane. In this pulsar-based model, an overall clockwise-going magnetic field (as seen from the North Galactic Pole) extends radially at least from 1 to 12 kpc from the Galactic Center, except for a 2-kpc wide anti-clockwise magnetic field located in a radial annulus between 4 and 6 kpc from the Galactic Centre. Here the magnetic field is not attached to any specific spiral arm. The origin of this unique anti-clockwise annulus could be due to a number of factors (internal or external) or could be primordial (regular or chaotic). The new model has a very special feature in the form of a string of HII regions located in the anti-clockwise annulus, and it may be a new class of "axisymmetric (ASS) magnetic field" models. The new model disagrees with recent pulsar studies that employed several magnetic reversals in the inner Galaxy, and some more in the outer Galaxy [the "bisymmetric (BSS) field" model].

MO-POS-43

Fourier Transform Spectroscopy of Orion Molecular Cloud, D.A. Naylor¹, M.K. Tahic¹, B.G. Gom¹, G.R. Davis² and D. Johnstone^{3, 1}, *University of Lethbridge*, ²JAC and ³Herzberg Institute of Astrophysics — The Orion molecular cloud is the most studied region of star formation in our galaxy. Recent SCUBA images at 450 & 850 mm reveal a variety of structures including candidate pre-stellar cores, cores containing Class 0 protostars, shocks and PDR fronts. In the last few years, we have been using a Fourier transform spectrometer (FTS) at the James Clerk Maxwell Telescope (JCMT) to separate the line and continuum components of emission in the two brightest sources of the Orion Molecular Cloud: KL and S. In December 2000 we obtained complete spectral scans of the 850 mm band of Orion KL and S with the JCMT heterodyne receiver B3. In October 2002 and April 2003 we obtained spectral scans of the 850 mm band of Orion KL with the University of Lethbridge Fourier Transform Spectrometer. These spectra will be compared to determine the potential for measuring, simultaneously, both the line and continuum emission components of galactic sources using the FTS currently under development for use with the SCUBA-2 detector.

MO-POS-44

A Galactic Chimney Over the W47 HII Region Complex, Jeroen Stil, R. Ouyed and A.R. Taylor, *University of Calgary* — We present new 21-cm line and 21-cm continuum from the VLA Galactic Plane Survey (VGPS; Taylor *et al.* 2002) of the Galactic star formation region W47 and the associated worm GW 38.0+1.6. The edge of this region is a 200 pc long vertical filament observed in the 21-cm line and 21-cm continuum. The location of this filament and the radio recombination line velocity of the ionized gas associate the filament with the W47 complex at $V_{LSR} = 50$ km/s. The shape of the filament can be represented by a Kompaneets model with W47 as the source that encloses the GW 38.0+1.6 area. However, the HI filament is detected at $V_{LSR} = 0$ km/s. The location and velocity of the HI suggest a velocity component of 50 km/s perpendicular to the expansion velocity of the super bubble. We have initiated 3-dimensional magnetohydrodynamic simulations of a superbubble bursting out of the Galactic disk to obtain insight into the physics of this surprising result.

MO-POS-45

Imaging Cold Dust in the Galactic Plane, Henry Matthews¹, B. Weferling², A. Evans³, M. Cohen⁴, J. Jackson⁵, R. Simon⁵, D. Johnstone⁶, G. Davis², T. Jenness², D. Pierce-Price², W. Dent⁷, J. Richer⁸ and G. Fuller⁹, ¹National Research Council of Canada, ²JAC Hawaii, ³Keele University, UK, ⁴Berkeley University, ⁵Boston University, ⁶HIA/NRC, ⁷UKATC, UK, ⁸MRAO, UK, ⁹UMIST, UK — We present images of continuum emission at 850 and 1200 microns wavelength from a section of the Galactic Plane centered near longitude 44 degrees. These data were obtained from complementary observations made with the JCMT and SEST bolometer array receivers, with beamwidths of about 14 and 22 arcsec respectively. The features seen arise principally from cold dust in two spiral arms at about 1.5 and 8kpc distant from Earth; dust is optically thin at mm/submm wavelengths. These data are compared with existing spectral line data having similar angular resolution, which allow kinematic distances to be assigned to individual features. Comparison with images at mid-infrared wavelengths is also revealing. These data presage the potential of large-scale survey observations with forthcoming instrumentation such as SCUBA2 and HARPC/ACSIS at the JCMT.

MO-POS-46

HI Shells Surrounding The Cygnus Loop*, Denis Leahy, *University of Calgary* — The Cygnus Loop supernova remnant has been observed in the 21 cm neutral hydrogen (HI) line with the Dominion Radio Astrophysical Observatory's (DRAO) Synthesis Telescope and 26 m Telescope. A search through the dataset reveals large structures associated with the Cygnus Loop in position and velocity. A large ring feature extends from the southeast rim into the center of the Cygnus Loop. Another large structure is found which wraps around the southern and western limb of the southern extension of the Cygnus Loop. Both structures have been identified in the IRAS all-sky survey maps of the region, allowing both HI and dust column densities to be determined as a function of position. The velocity structure of the HI is studied and used to constrain the origin of the HI.

* This work is being supported by NSERC.

MO-POS-47

A Huge Magnetic Bubble In The Anti-Centre Region Of The Milky Way. Roland Kothes, and T.L. Landecker, *Dominion Radio Astrophysical Observatory, University of Calgary* — We present the discovery of a large magnetic bubble in the data of the Canadian Galactic Plane Survey. This structure is revealed by rotating the polarization angle of the smooth Galactic background polarization. The magnetic bubble is surrounded by an HI bubble with a systemic velocity of about -20 km/s implying a Perseus arm location. At this distance the bubble has a diameter of about 300 pc. At the northern edge of the bubble is the SNR VRO 42.05.01, which is the remnant of a supernova that happened just outside the edge of the bubble. This is not only the first time a Faraday screen can be related to an HI structure, but also gives us the opportunity to directly study the interaction of the supernova shock wave with the HI bubble and the embedded magnetic field.

MO-POS-48

Propagating Star Formation Around Single O-star HII Regions. Charles Kerton¹, Lewis Knee² and Christopher Brunt^{3,1} *Iowa State University*,² *HIA* and³ *UMass/FCRAO* — The vast majority of stars of all masses form in regions in which rare but prominent high mass O stars are born. It is thus important to understand the processes and modes of star formation in the harsh environment of HII regions and PDRs around O stars. We present the initial results of our sub-mm (JCMT SCUBA) observations of small angular size HII regions designed to examine how star formation propagates through a molecular cloud surrounding an HII region. Our targets are a carefully chosen sample of eight small (~10 arcmin in diameter) HII regions each excited by a single O star. The SCUBA observations are being combined with near-IR (2MASS), mid-IR (MSX), mm (FCRAO) and cm (DRAO) observations to determine the spatial distribution of the embedded stellar population throughout the surrounding molecular cloud. The small size of the HII regions permits easier acquisition of the multiwavelength data needed to trace all of the relevant physical components (HI, HII, molecular gas, and stars) which enables the entire physical chain from triggering source to emerging stellar population to be investigated.

MO-POS-49

The Kinematics of Massive Star-Forming Region NGC 7538* Michael Reid¹, C. Wilson¹ and B. Matthews^{2,1} *McMaster University* and² *University of California at Berkeley* — Progress in understanding star formation increasingly comes through an understanding of the kinematics of star-forming regions and cores. Much is known about the kinematics of low-mass regions and cores, but less about their higher mass counterparts. One such region in our galaxy, NGC 7538, is the home of a spectacular class 0 core candidate, NGC 7538, which has a young outflow and disk of several hundred solar masses (Sandell, Wright, & Forster 2003, ApJ, 590L, 45). We are studying the massive young cores of NGC 7538, with an eye toward their kinematic properties. We have acquired SCUBA continuum maps at 850 and 450 microns of the entire region, as well as high-resolution BIMA and VLA line maps of select cores in up to seven different molecular kinematic probes. Analysis of this data is proving complex, but we present some preliminary results here.

* This work is being supported by NSERC.

MO-POS-50

Characterizing the Outflow of W28A2. Pamela Klaassen¹, R. Plume¹, R. Ouedy¹ and J. DiFrancesco^{2,1} *University of Calgary* and² *Herzberg Institute of Astrophysics* — The formation of high mass stars is less well understood than that of lower mass stars due to the shorter time scales and larger distances involved. One of the earliest stages of high mass star formation consists of a period of outflow which can be studied through its impact on its environment. We present observations of W28A2, a shell like Ultracompact HII region associated with one of the youngest and most energetic outflows in the Galaxy (O6 star). Using the James Clerk Maxwell Telescope, we have observed the outflow in a number of transitions and have derived the age, mass, extent, and velocity of the outflow. In order to better constrain the driving mechanism of the outflow, we have conducted magneto-hydrodynamic simulations (using Zeus-MP and Jetget) of a high-velocity jet impacting on a surrounding molecular envelope.

MO-POS-51

Mapping the Spiral Structure of the Milky Way Galaxy* Saul Davis¹, H.B. Richer¹, J.S. Kalirai¹, G. Fahlan¹, G. Bono² and M. Cignoni^{3,1} *University of British Columbia*,² *Osservatorio di Roma* and³ *Università degli Studi di Pisa* — The details of the spiral structure of the Milky Way remain poorly understood. This project attempts to provide us with a more complete picture of our own Galaxy - We have obtained images of 19 open clusters in the disk of the Milky Way. These clusters are predominantly in the quadrant of the Galaxy opposite to the Galactic center ($135^\circ < l < 225^\circ$), and over half are at low latitude ($b < 5^\circ$). The images were obtained with CFHT12k, for the CFHT Open Star Cluster Survey, and represent a unique data set in terms of area (0.22 square degrees per image) and depth ($V \sim 23$) in this region of the sky. The colour-magnitude diagrams (CMDs) of the various lines of sight look markedly different. Most obvious, is the difference between the lines of sight with $b > 5^\circ$ and those with $b < 5^\circ$, yet more subtle distinctions appear between the low-latitude lines of sight with are presumably attributable to the presence of spiral arms. By simulating CMDs we hope to be able to constrain various parameters that describe the Galaxy, such as scale-length and scale height of the disk, star formation history of the disk, initial-mass function of the halo, and finally, the precise location and extent of the spiral arms. Early results will be presented.

* This work is being supported by UBC.

MO-POS-52

Infrared Imaging of Protoclusters in the Orion B Molecular Cloud. Ashley J. Ruiter and George F. Mitchell, *Saint Mary's University* — Sub-millimetre mapping of Orion B using SCUBA (Mitchell *et al.* 2001, ApJ, 556, 215) has revealed a large population of compact cores, most of which are clustered in well-separated regions. In three nights in January 2003, we obtained near-infrared images of two of these regions. Using the CFHT-IR camera on the Canada-France-Hawaii telescope, we imaged NGC 2068 and NGC 2071 in a narrow band K-continuum filter, and in a narrow band filter centred on the 2.122 μ m line of H₂. This vibrational H₂ line is a well-known diagnostic for shocked gas and radiatively excited gas. When it is observed in regions of active star formation, the exciting mechanism is often shock excitation by an outflow. The IR images show continuum point sources (stars), and regions of extended molecular hydrogen emission. Some cores show a coincident infrared source, while others show no sign of an associated IR source. The latter situation is an indication that the core in question, if containing a forming star, is deeply embedded. Since deeply embedded pre-stellar cores will have no obvious associated K narrow band emission, the H₂ map and a CO map of high-velocity gas are useful probes of the physical processes which are taking place in the vicinity of each core. We will present the H₂ and K continuum images, comparing the emission with the SCUBA map and with a previously obtained map of CO. In particular, we will discuss the implications of these new observations for the evolutionary state of the SCUBA cores.

MO-POS-53

Starlight Excitation Of Permitted Lines In The Orion Nebula* Kevin Blagrove and P.G. Martin, *CITA, University of Toronto* — Robust abundance calculations for gaseous nebulae require knowledge of line formation mechanisms for a multitude of lines, encompassing both permitted and forbidden. Permitted lines are usually associated with cascades after recombination. However, there is often a sizeable (or even overwhelming) contribution from fluorescence processes (e.g., excitation by starlight). Here, using data from deep optical echelle spectroscopy, we confirm (and extend the analysis of) the line formation mechanisms which had been predicted for permitted lines of several ions. We develop a completely independent method based on the ionization and velocity structure of the Orion Nebula as determined from forbidden lines in the context of photoionization models.

* This work is being supported by NSERC.

MO-POS-54

Molecular Hydrogen in a Sample of Cooling Flow Clusters Louise Edwards¹, C. Robert¹ and F. Marleau^{2,1} *Université Laval* and² *SIRT Science Centre* — We present imaging data of the cooling flow clusters Abell 644, Abell 400 and Abell 1795 taken with CFHT-IR in the infrared. These clusters are all cooling flows of moderate mass deposition rates (200, 100 and 10 solar masses per year, respectively). With proper data reduction, the use of narrow band filters can provide the 1-0 S(1) emission line of molecular hydrogen. For Abell 1795, we report the molecular hydrogen flux of the central dominant galaxy, as well as discuss the first detections of molecular hydrogen emission found in cooling flow cluster galaxy other than the CDG. We describe the emission morphology of the CDG emission found for Abell 1795 and relate it to possible emission mechanisms. We compare our measurements with Donahue *et al.* (2000) who have published similar work for three other cooling flow clusters. For Abell 400 and Abell 644 we present the preliminary results of our data analysis.

MO-POS-55

Studies of an Intergalactic Neutral Hydrogen Cloud. Jayanne English¹, B. Koribalski² and K.C. Freeman^{3,1} *University of Manitoba*,² *Australia Telescope National Facility* and³ *RSAA, Australian National University* — An intergalactic HI cloud of a few billion solar masses, previously detected using the Parkes Radio Telescope and the Australia Telescope Compact Array (ATCA) (English 1994; Freeman *et al.* 1996), has been confirmed in further ATCA observations of the NGC 3256 galaxy group. The group contains the prominent merging galaxy NGC 3256, which is surrounded by a number of HI fragments (English *et al.* 2003), the tidally disturbed galaxy NGC 3263 (Koribalski *et al.*, in prep.), and several other galaxies. Using ATCA HI data we examine the nature of this massive gas cloud and its relationship to the neighbouring galaxies. This could be a primordial "galaxy building block". However the cloud's properties, in conjunction with the spatial extents and velocity behaviours of the group's major galaxies, may indicate that it originated out of tidal debris.

MO-POS-56

A Gallery of Galaxies in the Hubble Deep Field South. Theresa Wiegert^{1,2}, D.F. de Mello³ and C. Horellou^{2,1} *University of Manitoba*,² *Onsala Space Observatory*; and³ *Goddard Space Flight Center* — We have applied a photometric redshift technique using spectral energy distribution templates to the WFPC2 images of the Hubble Deep Field South. As a result, a catalogue of 1142 objects with photometric redshifts and spectral types was produced, showing the redshift distribution of galaxy spectral types. There is a

decrease in early-type galaxies for higher redshifts ($z > 1$), while the amount of irregular and starburst galaxies increases. A subsample of the galaxies is displayed in a gallery, showing the reliability of using spectral energy distributions for calculating photometric redshifts. The work was done as part of a master's thesis project at Onsala Space Observatory.

MO-POS-57

The NOAO Fundamental Plane Survey. Russell Smith¹, M.J. Hudson¹, R.L. Davies², J.R. Lucey³, J.E. Nelan⁴, D. Schade⁵, N.B. Suntzeff⁶ and G.A. Wegner^{4, 1} *University of Waterloo*, ²Oxford University, ³University of Durham, ⁴Dartmouth College, ⁵HIA/CADC and ⁶CTIO/NOAO — The NOAO Fundamental Plane Survey (NFPS) is a wide field imaging and spectroscopic survey of the ~100 nearest X-ray luminous galaxy clusters, with two principal science goals: (1) to measure distances and peculiar velocities through the Fundamental Plane relation, to probe large-scale flows to ~200 h^{-1} Mpc; and (2) to study the structural, morphological and star-formation properties of the cluster galaxy population. Here, I present some preliminary results in each of these categories, and discuss some multi-wavelength follow-up studies based upon the NFPS sample.

MO-POS-58

Changes in the Radio Image of Quasar 3C454.3 and their Possible Effect on the VLBI Astrometry for the Guide Star of the Gravity Probe B Mission*, Ryan Ransom¹, J.I. Lederman¹, N. Bartel¹, M.F. Bietenholz¹, D.E. Lebach², M.I. Ratner², I.I. Shapiro² and J.-F. Lestrade^{3, 1} *York University*, ²Harvard-Smithsonian Center for Astrophysics and ³Observatoire de Paris-DEMIRM — Since 1997 we have observed the quasar 3C454.3 at 3.6 cm with a VLBI array of 12 or more stations about four times per year in support of the NASA-Stanford relativity gyroscope experiment, Gravity Probe B (GP-B). This quasar is a phase reference source for the imaging and astrometry of the mission guide star, HR 8703, which we observed during the same sessions. We present a selection of VLBI images of 3C454.3 produced from observations between January 1997 and December 2003. The images show changes in the region within 1.5 mas of the radio core of the quasar. We also examine the effect of these changes on our astrometric results for HR 8703.

* This work is being supported by NASA, NSERC.

MO-POS-59

A Step Closer to the Detection of the Reionization Epoch. Sasa Nedeljkovic, C.B. Netterfield and U. Pen, *University of Toronto* — Approximately a billion years after the Big Bang, the first stars reionized the universe and ended the so-called Dark Ages. In many models, the reionization occurs rapidly making a sharp step in the spectra from the quenching of the redshifted 21cm line. The step is expected to be visible between 70-240MHz for $Z_{\text{reion}} = 5$ to 20. The step is expected to be around 15mK, which is easily detectable from a signal to noise point of view. However, the signal is 5 orders of magnitude smaller than the foregrounds, complicating the task of detection. With large radio instruments such as PAST, CLAR, LOFAR and ultimately SKA on the way, we give the update of the small instrument built primary for the detection of the reionization step: TREX (21cm Reionization EXperiment). This poster will give an overview of the latest instrument specification.

MO-POS-60

Visualizing the CMB through the Dust : A New Generation of IRAS Maps*, Marc-Antoine Miville-Deschenes¹ and G. Lagache^{2, 1} *Canadian Institute for Theoretical Astrophysics* and ²Institut d'Astrophysique Spatiale — Twenty years ago the IRAS satellite made an all-sky survey in the mid/far-infrared that had a tremendous impact on modern astrophysics. In this contribution I will show that IRAS will still be a crucial element for cosmological missions to come like Planck, an European satellite (with Canadian contribution) that will be launched in 2007 and that will map the whole sky in the submm/mm range. The main scientific goal of Planck is to study the cosmic microwave background but one of the biggest challenge of Planck is to be able to separate the numerous emission components in that frequency range (dust emission, synchrotron, free-free). To tackle this problem, external data sets, which probe specific components, are needed. With its full-sky coverage and arcminute resolution, the IRAS data, that probe the dust emission of the interstellar medium, will be a key player in the analysis of the Planck data. Unfortunately, the available IRAS product suffers from several instrumental effects that prevent its use for detailed CMB analysis. In this context we have performed a totally new reprocessing of the IRAS data, based on the knowledge acquired recently on the behavior of photoconductors and using modern data analysis techniques. In this contribution I will present the image processing techniques we used to improve significantly the quality and reliability of the IRAS data. This new generation of IRAS data opens very exciting new perspectives on the study of the interstellar medium but it will also be essential for the analysis of CMB data.

* This work is being supported by Canadian Space Agency.

MO-POS-61

Distribution of the Submillimetre Population of Galaxies. Vjera Miovic and C.B. Netterfield, *University of Toronto* — The sources detected by the ground-based sub-mm surveys are understood to be dusty galaxies experiencing massive bursts of star-formation. The lack of the precise redshift determination of these sources and of the counterpart identification in radio and other wavebands, prevents a reliable estimate of the evolutionary history of these galaxies. Previous studies have investigated finding the photometric redshifts of identified point sources above the confusion limit^[1]. We investigate the possibility of constraining the luminosity and density evolution of sub-mm galaxies using a different approach – extracting information from the statistics of the unresolved sources detected beyond the "confusion limit". The results from our simulations can be used to analyse the data from sub-mm surveys, such as Spitzer, BLAST or Herschel.

1. Hughes *et al.*, 2002

MO-POS-62

A Deep Near-IR Look At Dusty Submillimetre Galaxies*, Alexandra Pope¹, D. Scott¹ and C. Borys^{2, 1} *University of British Columbia* and ²Caltech — The study of sub-mm galaxies at optical wavelengths is difficult given that the optical images are highly obscured by dust and there are often several possible counterparts. We have been forced to characterize the entire population of sub-mm galaxies by the sub-sample of sources that have radio counterparts. There is a need for deep near-IR images of these dusty galaxies in order to study the radio-undetected sub-sample and thus understand the entire sub-mm population. We have been compiling a sub-mm map of the Great Observatories Origins Deep Survey (GOODS) North field. GOODS is a huge multi-wavelength campaign to unite the deepest observations from NASA's big three space observatories: HST, Chandra and Spitzer, to study galaxy formation and evolution. We have used the ACS HST images from GOODS to study a large sample of 850 micron sources. With the depth achieved by this survey, near-IR counterparts have been found for the majority of the radio-detected sub-mm sources. The colours, morphologies and photometric redshifts of these secure identifications can be used to characterize the optical properties of dusty sub-mm galaxies to help identify counterparts to the blank-field sources. Certain combinations of near-IR properties can be used to successfully identify the counterpart to a sub-mm source.

* This work is being supported by NSERC/NRC.

MO-POS-63

Results from the BOOMERANG 2003 Antarctic LDB Flight. Carrie MacTavish, *University of Toronto / BOOMERANG collaboration* — BOOMERANG is a balloon-borne, microwave telescope with polarisation sensitive bolometric detectors. It is designed to measure the polarization, as well as the small scale temperature anisotropies of the cosmic microwave background. In January of 2003 the experiment mapped over 2000 square degrees of the sky at an angular resolution of approximately 10 arcminutes. The most recent results from the analysis of the data obtained from this flight will be presented.

MO-POS-64

Metallicity Distribution Function of Galaxies Through Infrared Colors. Waldemar Okon¹, W.E. Harris¹ and D. Crabtree^{2, 1} *McMaster University* and ²HIA/NRC — Globular clusters around galaxies provide unique tracers of their merger and formation history as well as the cluster formation itself. The key quantity which is related to the galaxy enrichment history is the metallicity distribution function (MDF). The MDF is of much interest and debate in current literature, and its fine structure, which contains the sequential starburst history of a galaxy, is sketchily known. This is because most of the current MDF work is based on the fundamentally insensitive (V-I) color index. We have undertaken a project which uses the (V-K) color index, which is more than four times more sensitive to metallicity than (V-I), to considerably improve on the current state of the quality of MDFs. This new data will allow us to study the MDFs of galaxies in much greater detail than previously possible, and hence will increase the understanding of galaxy formation. We have been using the CFHT-IR camera on the Canada-France-Hawaii Telescope to obtain deep K-band photometry of globular clusters in the interesting S0 galaxy NGC 1023 (which may have an unusually wide mixture of cluster ages), the giant elliptical M87, NGC 3377, 3379, 3608, M60, M86, M89 and NGC 2768 during three observing runs. Results from data analysis completed to date are presented here. These include the color distribution (which clearly shows bimodality for M87), color-magnitude and color-color diagrams.

MO-POS-65

Dynamical Masses of Galaxy Clusters. Kris Blindert¹, H.K.C. Yee¹, M.D. Gladders² and E. Ellingson^{3, 1} *University of Toronto*, ²Carnegie Observatories and ³University of Colorado — Cosmological simulations predict a universal density profile for galaxy clusters. In order to test this prediction one requires a large sample of galaxy clusters in a wide range of masses. To this end, we are completing a follow-up survey of about forty galaxy clusters selected from the Red-Sequence Cluster Survey (RCS), with redshifts from 0.15 to 0.6, in a wide range of cluster richness. I will present some preliminary results for a subset of the clusters, including the correlation of optical richness with mass, and the mass-to-light ratio as a function of cluster mass.

MO-POS-66

A Peculiar Probe of the Dark Matter Distribution of Large Scale Structure*, Robbi Pike, *University of Waterloo* — Quantifying peculiar motions of galaxies and clusters provides a fundamental tool for probing the mass distribution of large scale structure. It is believed that light traces mass (at least within some biasing scheme), permitting the use galaxies as tracers for the underlying dark matter distribution. Within the confines of linear theory, peculiar motions, due to coherent gravitational pulls from overdense regions can lead to

valuable information pertaining to the cosmological density parameter, Ω_m . The primary goal of this research was to place constraints on Ω_m by modelling the galactic density and velocity fields in the local universe ($cz \sim 8000$ km/s). When comparing observed peculiar velocities to that which is predicted for a given density model ($v-v$ comparisons), the aim is actually to measure the parameter $\beta = \Omega^{0.6} / b$, which depending on how well mass traces light is a degenerate combination of Ω_m and the biasing parameter, b . We have computed the density field from galaxy distributions for both the 2MASS and NOG all sky redshift surveys (magnitude and volume limited samples). These are transformed into real space density fields through an iterative procedure outlined by Yahil *et al.* (1991). We use the VELMOD maximum likelihood technique (Willick *et al.* 1997b), making $v-v$ comparisons with several peculiar velocity datasets (SFI, SBF and SNIa) to constrain β . I will report on our findings and discuss how they fit in the current literature, as well as shed some insight into the morphological dependences for both elliptical and spiral galaxies.

* This work has been supported by Hudson for the completion of a Masters program at the University of Waterloo.

MO-POS-67

SCUBA-2: A Submillimeter Bolometer Array Camera for the JCMT* Michel Fich, (on behalf of the SCUBA-2 Team), *University of Waterloo* — Canadian astronomers have played a large role in the success of SCUBA on the JCMT. SCUBA has had a major impact in many areas of astronomy from solar system research out to large scale cosmology studies. SCUBA has been declared to be the "most successful ground-based instrument" in a recent study. Now Canadian astronomers have an opportunity to participate in the construction of a replacement for SCUBA. SCUBA-2 will be many hundred of times faster than SCUBA. This will generate a new explosion in submillimeter research and discoveries as revolutionary as those found with SCUBA. This poster will discuss the current state of the development of SCUBA-2 and describe a few of the exciting science programs that various groups have proposed for the new instrument.

* This work is being supported by CFA.

MO-POS-68

Initial Observations with the Arecibo Signal Processor, Robert D. Ferdman¹, I.H. Stairs¹, D.J. Nice², D.C. Backer³, R. Ramachandran³ and P. Demorest^{3, 1} *University of British Columbia*, ²Princeton University and ³U.C. Berkeley — The Arecibo Signal Processor (ASP) is a flexible, state-of-the-art wide-bandwidth observing system, for the acquisition and analysis of radio telescope signals. The primary application driving the development of this instrument is high-precision long-term timing of predominantly millisecond pulsars. This is attained through coherent removal of dispersion introduced into pulsar signals as they traverse the interstellar medium. The system will be able to process the incoming data stream in near-real time, through a network of personal computers, over a bandwidth of 64 MHz, in each of two polarisations. This initial implementation of ASP is at the 300-m Arecibo telescope in Puerto Rico, in order to take advantage of its enormous sensitivity. We present preliminary results of timing and flux calibrations with ASP for several pulsars. Comparisons have been made, and are shown, between ASP results and those of several existing pulsar instruments ranging from narrow to wide bandwidths, and which use coherent as well as incoherent de-dispersion. In particular, we show results of parallel timing observations with the Princeton Mark IV instrument, a narrow-bandwidth coherent de-dispersion instrument, and the precursor timing system to ASP. We briefly discuss several upcoming observations with ASP, as well as plans for installation of a twin instrument at the 100-m Green Bank Telescope.

[MO-POS] ATMOSPHERIC AND SPACE PHYSICS **Monday**
PHYSIQUE ATMOSPHÉRIQUE ET DE L'ESPACE **Lundi**

MOPOS-69

Trends in Relative Humidity in Canada from 1953-2003, W.A. van Wijngaarden¹ and L.A. Vincent^{2, 1} *York University* and ²Meteorological Service of Canada — This study reports the analysis of relative humidity data collected at 75 stations throughout Canada. For data at each station, a best fit linear trend estimated the change during 1953-2003 and a statistical t test determined whether the trend was significant. Large decreases in relative humidity occur throughout Canada in winter and spring. These results correlate closely to changes in dew point, temperature and precipitation. This study shows that relative humidity is a potentially useful indicator of climate change

MO-POS-70

A Quantitative Analysis on the Effects of Physical Sputtering in Meteoroid Ablation*, Kyle A. Hill, *Mount Allison University* — Conventional meteor ablation theory assumes that during atmospheric flight, a meteoroid undergoes intensive heating and meteoric atoms evaporate from its surface. Light is then produced as the ablated (evaporated) constituents undergo collisions with the atmospheric molecules and become excited. Our research has investigated whether another process, physical sputtering, could play a significant role as an alternative disintegration process. Using a 4th order Runge-Kutta numerical integration technique, we ran computer simulations which simultaneously solved the ablation and sputtering equations during the atmospheric flight for these meteoroids. We modeled asteroidal, cometary, and porous meteoroids with masses ranging from 10^{-3} kg to 10^{13} kg and velocities ranging from 11.2 km/s to 71 km/s. We find that while in many cases (particularly at low velocities and for relatively large meteoroid masses) sputtering contributes only a small amount of mass loss during atmospheric flight, in some cases sputtering is responsible for a large fraction of the mass loss. The impact of this work will be most dramatic for the very small meteoroids observed with large aperture radars, whose ablation process may possibly be dominated by sputtering. The heights of ablation and decelerations observed using these systems may provide evidence in the future for the importance of sputtering.

* This work is being supported by NSERC.

[MO-POS] ATOMIC AND MOLECULAR PHYSICS **Monday**
PHYSIQUE ATOMIQUE ET MOLÉCULAIRE **Lundi**

MO-POS-71

Torsion-Vibration, Torsion-Rotation, and Vibration-Rotation Interaction Constants for CH₃OH from *Ab Initio* Calculations, Li-Hong Xu¹, J.T. Hougen² and R.M. Lees^{1, 1} *University of New Brunswick* and ²National Institute of Standards and Technology — This is a progress report on our effort to investigate the possibility of obtaining useful spectroscopic information from *ab initio* calculations. Previously, we have shown^[1] that quantum chemistry results for methanol at the top and bottom of the torsional barrier could be used to determine the $\cos 3\gamma$ dependence of the torsional potential energy (*i.e.*, the barrier height) to better than 0.5 %, and the $\cos 3\gamma$ dependence of the rotational constants (three diagonal and one off-diagonal) to accuracies ranging from 7 % to 40 %. Results for acetaldehyde were about ten times worse, though these large discrepancies could be improved significantly by an empirical adjustment procedure. We then have shown^[2] that G98 delivered very smooth force constant plots as a function of angle along the internal rotation coordinate (defined to be 0° at the bottom and 60° at the top of the barrier), and that when symmetrized coordinates (in the permutation inversion group G_6) were used, these plots exhibited the $\sin 3\gamma$ or $\cos 3\gamma$ behavior expected from the symmetry species of the pair of vibrational coordinates multiplied by the force constant. In the present paper we investigate algebraically the meaning of various off-diagonal elements occurring in a Hessian matrix obtained by rotating the Cartesian Hessian matrix (containing second derivatives of the potential surface) to a coordinate system consisting of 3N-7 small-amplitude vibrations (where N is the number of atoms in the molecule), one large-amplitude vibration (the torsion), three overall rotations of the molecule, and three translations of the molecule. We then compute these elements numerically using quantum chemistry methods. Finally we discuss how these elements can be applied to analyses of vibration-torsion-rotation bands of methanol.

1. L.-H. Xu, R.M. Lees, and J.T. Hougen, *J. Chem. Phys.* **110**, 3835-3841 (1999).
2. L.-H. Xu, J.T. Hougen, R.M. Lees, and M.A. Mekhtiev, *J. Mol. Spectrosc.* **214**, 175-187 (2002).

MO-POS-72

Progress Report on the Measurement of Cesium Electron-Impact Cross Sections Using a Magneto-Optical Trap*, T.J. Reddish¹, J.A. MacAskill¹, C. McGrath¹, D.P. Secombe¹, M. Lukomski¹, J. Teeuwen¹, S. Sutton¹, W. Kedzierski¹, J.W. McConkey¹, W.A. van Wijngaarden², I. Bray^{3, 1} *University of Windsor*, ²York University and ³Murdoch University, Australia — A trapped Cesium atom target, prepared using a magneto-optical trap (MOT), is exposed to a broad monochromatic beam of electrons. Since the infrared fluorescence from the trap is directly proportional to the number of atoms in the trap, the measurement of the decrease in the fluorescence signal, due to the interaction of the electron beam, provides a straightforward method of determining electron-impact cross sections. This technique, pioneered by Lin and co-workers^[1], does require knowledge of the absolute target density. The choice of an appropriate pulsing scheme enables one to obtain either the ground state ($Cs\ 6^2S_{1/2}$) total cross section or that for the $6^2P_{1/2}$ excited state; ionisation cross sections may also be determined. The first results (100-400 eV) showed good agreement with convergent close coupling calculations^[2]. Improvements to the experimental setup and new results at lower electron energies will be presented at the conference.

1. R.S. Schapp, *et al* *Phys. Rev. Lett.* **76** (1996) 4328.
2. J.A. MacAskill *et al* *J. Elec. Spec. Rel. Phen.* **123** (2002) 173.

* We gratefully acknowledge CFI and NSERC for their support.

MO-POS-73

Modeling of Collision-Induced Light Scattering using Mathematica/Programme Mathematica pour le calcul de l'intensité de la diffusion de la lumière induite par les chocs*. Andrew Senchuk and George Tabisz, *University of Manitoba* — Collision-induced light scattering has been of great interest for many years due to the insights it gives on the physics of molecular interactions and dynamics. Calculation of the scattered intensities usually involves the manipulation and coupling of Cartesian tensors describing the multi-pole polarizability of the atoms or molecules together with tensors describing their interaction. As more complicated effects between the atoms and the field and/or higher order interactions between the atoms themselves are considered, the ranks of the resulting tensors become large. Consequently the resulting complexity, arising from the sheer number of terms that need to be considered, makes the calculation impractical in all but the lowest order cases. However, the effect of the higher order interactions cannot necessarily be dismissed as being negligible. To make the problem more tractable, one can re-express the theory in terms of irreducible spherical tensors, whose symmetry properties allow only a limited number of terms for a particular polarizability, and couple according to the Wigner coefficients. This is advantageous, as software packages, like Mathematica, exist which are able to calculate these very quickly. Thus we present results of modeling collision-induced light scattering using Mathematica in spherical tensor formalism. Our program handles arbitrary order polarizability tensors and can calculate interactions up to second-order.

* This work is being supported by CIPI.

MO-POS-74

Variational Calculations of Four-Body Molecular Systems. Z.-C. Yan, *University of New Brunswick* — Fully nonadiabatic calculations are performed for various four-body two-center molecular systems, using variational method in Hylleraas coordinates. The systems under study include H_2 , HeH^+ , MuH , and their isotopes. Our studies demonstrate that the traditional Hylleraas coordinates, which has been used widely for one-center atomic systems, can be equally well applied to two-center molecular systems. High-precision energy eigenvalues will be reported.

MO-POS-75

Intensity-Dependent Optical Rotation by Molecules/ Rotation Optique par les Molécules Dépendante sur l'Intensité de la Lumière*. R. Cameron and G.C. Tabisz, *University of Manitoba* — Chiral molecules rotate light through a forward scattering event. Single photon scattering, which is known as ordinary optical rotation, is independent of the light intensity I . We used a polarimeter in a heterodyne experiment to measure the optical rotation of solutions at 308 nm with high-intensity laser pulses. In three of the molecules that we studied (uridine, thymidine and cytidine) we found an intensity-dependent effect. The effect only appeared in molecules that had an absorption line near 308 nm; in other molecules that had no absorption line near 308 nm, such as sucrose, no intensity-dependent effect was observed. The intensity-dependent optical rotation in the three molecules was cumulative with each laser pulse and persisted with a time constant that was on the order of seconds and characteristic of the molecule.

* This work is being supported by NSERC.

MO-POS-76

Atomic Metastable Production Following Fragmentation of S-Containing Molecules*. W. Kedzierski, S. Amlin, X. Liao, R.J. Murray, J. Mutus, and J.W. McConkey, *University of Windsor* — A special xenon-matrix detector which is selectively sensitive to $S^+(S)$ atoms has been used to monitor dissociation of sulfur containing molecules into this fragment following controlled electron impact over an incident energy range from threshold to 400eV. A crossed-beam apparatus with a pulsed electron beam is used to obtain time-of-flight, and hence energy, spectra of metastable S fragments. Cross sections have been made absolute by comparison with previously obtained data from COS targets ^[1].

1. Kedzierski *et al.* *J. Phys. B*, **34**, 4027 (2001).

* Research supported by the Natural Sciences and Engineering Research Council of Canada (NSERC), and the Canadian Foundation for Innovation (CFI).

MO-POS-77

Trace Gas Detection Using Cavity Enhanced Absorption*. Jeff Seabrook and D. Tokaryk, *University of New Brunswick* — This presentation describes our application of an integrated cavity output spectrometer (ICOS) to trace gas detection. The principles behind cavity enhanced absorption and details of our implementation will be presented. In addition, we will discuss this technique's potential for determining number densities of the trace gases we hope to monitor. This technique also shows promise as an easy to use, and highly sensitive absorption spectroscopy tool. The near infrared region offers us the opportunity to detect weak vibrational transitions in many atmospheric species such as CO , CO_2 and H_2S . We will present our preliminary investigations into the detection of the pollutant hydrogen sulfide, and of our spectroscopy of the extremely weak and highly perturbed (012) vibrational transition of this molecule.

* This work is being supported by CIPI, NSERC.

MO-POS-78

An Atomic Source for Degenerate Fermi Gas Experiments*. Swati Singh ¹, S. Aubin ², P. Scrutton ², M. Extavour ², S. Myrskog ² and J.H. Thywissen ², ¹ *McMaster University* and ² *University of Toronto* — Even though all the constituents (electrons, protons, neutrons) of an atom are fermions, fermionic atoms are much less abundant in nature than bosonic atoms. In order to make a degenerate Fermi gas of Potassium 40 ($40K$) atoms, we had to make our own atomic source using potassium enriched to 3% $40K$, instead of the natural 0.01% abundance. We present the experimental challenges faced in building and testing of a "dispenser" source for $K-40$ that can be used for the experiment. We also present recent progress in other areas of the experiment, towards magneto-optical trapping and pure magnetic trapping of potassium.

* This work is being supported by NSERC, CFI, OIT, PRO.

MO-POS-79

Mixed Sample Ion Trapping: Analysis and Evolution of Trapped Species*. Jérémie J. Choquette ¹ and R.I. Thompson ², ¹ *University of Calgary* and ² NSERC — Sympathetic laser cooling of trapped ions shows promise as a tool for low temperature studies of atoms and molecules. However, by its very nature it requires the generation and storage of mixtures of ions. Our work is currently focused on some of the issues and challenges of generating, storing, and analysing mixed samples involving magnesium, noble gas, nitrogen, and carbon monoxide ions. This presentation will outline our techniques for loading and buffer gas cooling of atomic and molecular ions from solid and gas phase sources. It will outline the 'q-scan' ion trap mass spectrometric technique that we use to analyse our trapped samples, and will provide a detailed discussion of the temporal evolution of these mixed samples which results from charge transfer reactions involving the trapped species and background gases in the vacuum system.

* This work is being supported by NSERC.

MO-POS-80

Spectral Clustering in the NMR Spectrum of a Gaseous System*. Geoffrey Archibald, Simon, E. Brief and M.E. Hayden, *Simon Fraser University* — We have observed unanticipated spectral clustering effects in the NMR spectrum of room temperature thermally polarized 3He gas at 1.5 Tesla. At least three distinct lines form when 3He is adulterated with the highly paramagnetic gases NO or O_2 . These lines shift in frequency yet remain remarkably narrow when linear field gradients are applied. Unlike previous reports of spectral clustering, this behaviour cannot be explained solely in terms of the dipolar fields of the 3He atoms. Instead, the effects we observe appear to be mediated by electronic spins associated with the paramagnetic adulterants.

* This work is being supported by NSERC.

[MO-POS] CONDENSED MATTER AND MATERIALS PHYSICS PHYSIQUE DE LA MATIÈRE CONDENSÉE ET DES MATÉRIAUX

Monday
Lundi

MO-POS-81

Effect of Chain Unsaturation on Bilayer Response to Pressure: A Deuterium NMR Study*. Michael R. Morrow, I.D. Skanes, J. Stewart and K.M.W. Keough, *Memorial University of Newfoundland* — The effect of chain unsaturation on bilayer response to pressure has been investigated via wide-line deuterium NMR observations of 16:0-18:1 PC- d_{31} (POPC- d_{31}) and 16:0-18:2 PC- d_{31} (PLPC- d_{31}). For bilayers of each lipid, saturated chain orientational order was measured as a function of pressure for selected temperatures and as a function of temperature for selected pressures up to 193 MPa. For POPC- d_{31} , the main transition temperature increased by ~ 0.18 K/MPa, a rate that is similar to that found for bilayers of disaturated PCs. For PLPC- d_{31} , the increase in transition temperature with pressure was slightly smaller at ~ 0.13 K/MPa. To investigate the isothermal response of chain orientational order parameters to pressure, spectra for each lipid were obtained for three pressures (ambient, 55 MPa, and 110 MPa) at 25°C and for three pressures (ambient, 110 MPa, and 193 MPa) at 40°C. Application of a given pressure was found to increase orientational order for each methylene group on the saturated chain of a particular lipid by roughly similar amounts. This corresponds to an approximately uniform shift of the saturated chain orientational order parameter profile with pressure. Within the liquid crystalline phase, the response to pressure decreased with increasing temperature. Comparison of the responses of POPC and PLPC to pressure at corresponding temperatures relative to their respective ambient pressure transition temperatures showed that PLPC saturated-chain orientational order was less sensitive to pressure than that of POPC.

These observations suggest that increasing levels of chain unsaturation may reduce the sensitivity of bilayer order to variations in pressure.

* Supported by NSERC (MRM) and CIHR (KMWK).

MO-POS-82

Characterization Of Anisotropy In Foams: An Ultrasonic Approach*, Hussein Elmeheidi, J.H. Page AND M.G. Scanlon, *University of Manitoba* — We use low frequency ultrasonic waves (50 kHz) to investigate the mechanical properties of anisotropic freeze-dried bread foams that were prepared by applying uniaxial stress to fresh breadcrumb. Longitudinal ultrasonic velocity and amplitude measurements were taken in directions parallel and perpendicular to the compression direction. The velocity was found to decrease as the amount of compression is increased, with the decrease being greater in the parallel direction. The velocity data were interpreted using two theoretical models, one based on the static compression of a simplified strut model of foams and the other including the effects of tortuosity on wave propagation through anisotropic media. Both models allowed the velocity anisotropy to be directly related to the anisotropy of the foam structure, and give predictions in good overall agreement with the data. The results also allowed us to conclude that there must be a weakening of the cell walls caused by the uniaxial compression in addition to the effects resulting from the anisotropy alone.

* This work is being supported by NSERC.

MO-POS-83

Structure of a Homologue Series of Banana Mesogens Studied By C13 NMR Spectrum*, J. Xu and R.Y. Dong, *University of Manitoba* — C13 NMR spectroscopy was used to obtain the geometrical information in three members of a homologue series of banana molecules, 9CIPBBC, 8DCIPBBC and 9DCIPBBC. The orientational order parameter S, bending angles and tilt angles between the biphenyl rings were determined from the temperature dependent chemical shifts in the nematic phases. Although the temperature dependence of S was found to be different for these molecules, the S values at Tc were almost identical. It was also found that tilt angles depend linearly on temperature, and the bending angle in the mono-substituted molecule is about 14 degree smaller than the di-substituted molecular. A SUPER (Separation of Undistorted Chemical-Shift Anisotropy Powder Patterns) technique was used to determine the chemical shift tensors of carbons of model compounds (e.g. 4-Chlororesorcinol). These tensorial components are required for fitting the temperature dependent chemical shifts in aligned samples.

* Research is supported by NSERC and Brandon University

MO-POS-84

On the Physical Mechanism of Vortex Stirring in MHD-Driven Two-Fluid Molten Metal Flows, David Munger and A. Vincent, *Université de Montréal* — Magnetohydrodynamic (MHD) instabilities such as those observed in aluminum reduction cells have been thoroughly studied, for instance by means of linear analysis by Sneyd (1992) and numerical simulation by Potocnik (1989) using industrial codes, as well as by Gerbeau (2001) using finite elements. Though its understanding is critical for efficient aluminium production, the physical mechanism is still unknown. We focus on the stability of vortex stirring that naturally occurs in MHD-driven systems of two fluids with a large electrical conductivity ratio, traversed by an intense vertical electric current and under a strong background magnetic field. We perform three-dimensional nonstationary numerical simulations of the conservative equations, using a levelset technique to track the position of the interface between the two fluids. Periodic transport of large eddies occurs, in which we observe an oscillation of vortex energy arising from a balance between the dissipation forces and the supply from the imposed electric current. The corresponding frequencies are orders of magnitude smaller than those observed in typical metal pad roll, so that long-lasting simulations are necessary to track slowly growing instabilities. We are able to find a stability threshold in terms of the electrical conductivity of the fluids, and we are currently trying to correlate it with the cell's dimensions. We conjecture that an increase of the latter will compensate a decrease of conductivity in the triggering of instabilities. Simulations are underway and results will be presented at the conference.

MO-POS-85

Spin Wave Dispersion of the 2D Hubbard Model at Intermediate Coupling*, Walter Stephan, *Bishop's University* — The spin wave dispersion relation for the 2D square lattice Hubbard model at half-filling is calculated using an "exact" linked cluster expansion method. The approach used is most reliable at strong coupling, but still converges reasonably well when the Coulomb repulsion is of the same order of magnitude as the band width. Results are compared to those of other approximate calculations as well as neutron scattering measurements of undoped cuprates.

* This work is being supported by NSERC.

MO-POS-86

The Giant Magnetocaloric Effect (GMCE) in Ni-Mn-Ga, Wei Li, Xuezhi Zhou, H P Kunkel and Gwyn Williams, *University of Manitoba* — Several previous investigations have demonstrated that a giant magnetocaloric effect (GMCE) – a large isothermal entropy / adiabatic temperature change associated with the application of an external magnetic field to a system – is most often linked to the substantial entropy change accompanying a first-order phase change. However, it appeared plausible that in systems exhibiting sequential magnetic transitions – specifically a continuous paramagnetic to ferromagnetic transition followed by a first-order / discontinuous (order-order) transition - this effect might be enhanced if these two transitions could be brought into close proximity, or better still, merged. The veracity of this suggestion has been demonstrated in the Ni-Mn-Ga system where such a coincidence can be achieved through careful compositional tuning, thus for Ni_{55.2}Mn_{18.6}Ga_{26.2} an entropy change of $\Delta S_M = -20.4 J kg^{-1} K^{-1}$ is observed at 317K in a field of 5T, one of the larger values measured at or above room temperature.

MO-POS-87

Comparison of Electron Mobility in Zincblende and wurtzite GaInN, A. Somae², M. Sadeghi², H. Arabshahi¹, M. Ghazi²,¹ Tarbiat Moallem University and ² Shahrod University, Shahrod, Iran — GaN has received much attention in recent years because of its potential for a wide range of applications in high power and optoelectronic devices. The demands of device designs have encouraged numerical studies of electron transport in the material. In this research a numerical iteration method has been developed and used to model electron transport in zincblende and wurtzite GaInN at low electric fields. Our results show that the electron drift mobility of wurtzite GaInN is lower than that for the zincblende structure at all temperatures. This is largely due to the higher G valley effective mass and a higher electron scattering rate in the wurtzite phase.

MO-POS-88

Low-Field Electron Transport Calculations in Bulk Wurtzite GaN Using Iterative Technique, Hadi Arabshahi, *Tarbiat Moallem University* — Temperature and electric field-dependent electron transport in bulk wurtzite GaN structure have been calculated using an iterative technique. The following scattering mechanisms, i.e. impurity, polar optical phonon, acoustic phonon, piezoelectric and electron plasmon are included in the calculation. Ionized impurity scattering has been treated beyond the Born approximation using the phase-shift analysis. The low electron drift mobility is calculated for temperatures in the range of 300-600K and for ionized impurity concentrations between 10¹⁶ and 10¹⁸ Cm⁻³. The low temperature value of electron mobility increases significantly with increasing doping concentration. The iterative results are in fair agreement with other recent calculations obtained using the relaxation-time approximation and experimental methods. Compensation effects on the mobility are also examined. Due to the freezeout of deep donor levels the role of ionized impurity scattering in bulk wurtzite GaN is suppressed and the role of phonon scattering is enhanced, compared to zincblende structure. Electron transport properties have been modelled with an electric field applied both parallel and perpendicular to the (0001)c-axis. The extracted model parameters can be used for electron transport simulations in GaN-based transistors.

MO-POS-89

Design and Modelling of Inductively Heated Substrate Holders for Advanced Plasma Materials Processing Applications*, Ajay K. Singh and Michael P. Bradley, *University of Saskatchewan* — Plasma processing of materials will be one of the key enablers for advances in electronics and photonics technology in the 21st century. Effective plasma materials processing requires careful control of process parameters, including the temperature of the target material. For example, a minimum target temperature ~ 800 Celsius is required for plasma deposition of diamond films. Unfortunately, in high pressure (~ 10 Torr) microwave plasma systems (such as the diamond film growth system at the University of Saskatchewan) the ultimate target temperature may be limited to ~ 500 Celsius because ion-neutral collisions limit the amount of heat delivered to the target, and because of relatively high convective cooling rates. Thus it is necessary to directly heat the target to achieve the high temperatures required. Direct heating via heating wire may be difficult to implement because in most cases the substrate must be biased with respect to the grounded chamber walls to achieve good film growth. Inductive eddy current heating provides a solution. Heating energy is efficiently coupled into the substrate via induced eddy currents, providing rapid and potentially highly uniform heating. The purely inductive coupling means that the substrate can be biased to arbitrary voltages as required. This presentation will discuss our design efforts on heated substrate holders. We will present results of thermal modelling calculations (i.e. heating curves, mean temperature, temperature uniformity) and will discuss their implications for advanced target holder design.

* This work is being supported by NSERC.

MO-POS-90

Elastic Fields from Reconstructed Terraces of a Semi-Infinite Solid*, R. Arief Budiman, *University of Calgary* — Two-dimensional problem of a semi-infinite solid with surface reconstruction boundary condition is considered. Surface reconstruction produces sinusoidal displacement fields on a terrace and attractive interaction due to the reconstruction is

found. Stress fields and surface forces due to the surface reconstruction are presented. With the addition of the step-step interaction model by Marchenko and Parshin, the equilibrium surface configuration under the presence of step array and reconstructed terraces is presented.

* This work is being supported by NSERC.

MO-POS-91

High Resolution Oxide Single - Crystalline X-Ray Screens, S. Nedilko, *Kyiv National Taras Shevchenko University, Ukraine* — There are well known applications of scintillating materials in imaging devices: X-ray imaging, X-ray computed tomography (X-ray CT), single photon emission computed tomography (SPECT) and positron emission tomography (PET). Here we will talk only concerning X-ray imaging with micrometer resolution. Decreasing of exposure dose during diagnostics, medical, biological *in vivo* etc., when ionizing irradiation is used, can be achieved by increasing of spatial resolution of the screens used for visualization of X-rays image. At present X-rays screens are made, as a rule, on the polycrystalline powder luminophors base with the 5 – 200 μ grain dimensions which determine spatial resolution of the screens. Essential increasing of spatial resolution became possible by using of screens those are the single crystalline thin film (SCF) scintillator with a high coefficient of X-ray absorption applied on the surface of non-luminescent single crystalline substrate by means of liquid phase epitaxy method. At first, the X-ray image detector with resolution near 1.3 – 1.5 μ with the screen on the doped with Ce ions yttrium aluminum garnet SCF with thickness $h = 5 \mu$ was described by A. Koch *et al.* in 1998. The further increase of resolution can be achieved by thickness decreasing that requires higher SCF X-ray absorption (the last is proportional to effective atomic number of SCF) and by increasing of SCF light output. In this paper the results of investigation the set of doped oxide materials with the garnet and perovskite structure which allow significant improving of the X – ray screens parameters are presented and the perspectives of their using are discussed as well.

MO-POS-92

Thermostimulated Self-Assembled Formation of Semiconductors Micro – Inclusions in Matrices of Oxide Dielectric Sulphate Crystals, V. Sheludko¹ and S. Nedilko², ¹ *Glukhiv Pedagogical University, Ukraine* and ² *Kyiv National Taras Shevchenko University, Ukraine* — Paper reports about formation of the CdS semiconductor micro-inclusions in the dielectric matrix of CdSO₄. The formation of the CdS is a result of the CdSO₄ annealing. Temperature diapasons and atmosphere effects on results of the thermal treatment were established. The excess of the sulfur is necessary condition of the CdS formation. Control of the micro-inclusions formation and determination of their spatial and energy parameters was carried out by observation of the optical (luminescent) properties of the samples. Spectral distribution and decay parameters reveal a recombination character of this emission - luminescence of the donor-acceptor pairs in semiconductors of the A(II)B(VI) group. Obtained results are analyzed from the point of view of formation of other compound micro-inclusions in a volume of the initial crystal matrix. A close similarity of observed characteristics to characteristics of the so called "green" edge emission of very well known material as the cadmium sulfide CdS don't allow any doubts concerning the fact that thermal treatment results the inclusions just of cadmium sulfide semiconductor phase into volume of the CdSO₄. The same luminescence properties had been observed for the K₂SO₄ and Rb₂SO₄ crystals. K₂S and Rb₂S are formed there after thermal treatment. Energy characteristics and the sizes of the clusters (25 - 50 nm) of the inclusions were estimated.

MO-POS-93

Modelling the Magnetic Response of Fe Nanoparticles in Alumina: A Preisach Approach, Candice A.H. Viddal and R.M. Roshko, *University of Manitoba* — Measurements of the field cooled moment, the zero field cooled moment, the isothermal remanent moment, the thermo remanent moment, and hysteresis isotherms, were performed on a thin film of nanodimensional Fe particles embedded in Al₂O₃ over a temperature range 10K \leq T \leq 300K and a field range $|H_s| \leq 2$ kOe. The data were analyzed within the framework of a Preisach model, which assumes that the free energy landscape can be decomposed into an ensemble of bistable Barkhausen elements, each with two moment configurations $\pm \mu$, a dissipation barrier $W_d = \mu H_d$, which measures energy dissipated as heat, and a level splitting $W_s = 2\mu H_s$, which measures energy stored reversibly. Numerical simulations based on the Preisach model, assuming a lognormal distribution of dissipation fields H_d and a Lorentzian distribution of bias fields H_s , were able to replicate all of the principal structural features of the experimental data, and their systematic variation with field and temperature. In particular, fits to the experimental data yield the temperature dependence of the mean dissipation field $H_d(T)$, and the dispersions of dissipation fields $\sigma_d(T)$ and bias fields $\sigma_s(T)$, and show that the magnetic response below T \approx 150K is dominated by field activated transitions over free energy excitation barriers which collapse rapidly with increasing temperature, and which are most likely related to disordered spin configurations on the surfaces of the Fe nanoparticles. By contrast, at temperatures above 150K, the response is dominated by thermal relaxation of Barkhausen elements with an average moment $\mu \approx 10^{-10}$ emu, which probably originates from the ferromagnetic cores of the Fe nanoparticles.

MO-POS-94

Thermally Activated Diffusion of Indium into 2H-TaSe₂, Onkar Rajora, *University College of the Cariboo* — We have studied the thermal diffusion of indium into the layered compound 2H-TaSe₂ single crystals parallel to the layers. Measurements¹ were done *in situ* in a scanning electron microscope equipped with an x-ray energy dispersive system. The distance of the diffusing indium front into the crystal was determined as a function of time from secondary electron image as well as from x-ray line scans for indium taken at different time intervals. The diffusion coefficients D were found by fitting the data to $\langle r^2 \rangle = 2 D t$, where $\langle r^2 \rangle$ is the mean square displacement in time t. The diffusion coefficients thus obtained were 1.5×10^{-12} , 3.8×10^{-12} , 7.7×10^{-12} and 17.5×10^{-12} m²/s with an uncertainty of about 10 percent at 351, 375, 411, and 458 K respectively. The activation energy E₀ of indium diffusion into TaSe₂ using $D = D_0 e^{-E_0/k_B T}$, was calculated to be 0.32 ± 0.04 eV. The results show that diffusing indium atoms put severe stress on the layers as they intercalate between them. This stress is relieved by buckling of the layers and these buckling features are clearly visible in secondary electron images.

1. O. Singh and A.E. Curzon, J. Appl. Phys., 17, 1415, 1984.

MO-POS-95

Magnetic Properties of ErFe₂/DyFe₂ Superlattices Studied by Neutron Diffraction*, Z. Yamani¹, H. Fritzsche¹, W.J.L. Buyers¹, Z. Tun¹, R.A. Cowley² and R.C.C. Ward², ¹ *Neutron Program for Materials Research* and ² *Oxford Physics, Clarendon Laboratory, UK* — Magnetic structure of two superlattices of the form [60Å ErFe₂/60Å DyFe₂]₄₀ and [80Å ErFe₂/40Å DyFe₂]₄₀, prepared by molecular beam epitaxy on a sapphire (1120) substrate, is determined by neutron diffraction technique using the triple-axis spectrometer C5 at the NRU reactor in Chalk River. The experiments were performed at zero field, in a horizontal field of 2.63 T applied along [001] (the easy axis for bulk DyFe₂), along [111] (the easy axis of bulk ErFe₂), and along the surface normal [110]. The temperature dependence of several Bragg reflections both at zero field and non-zero field was determined in the range of 4 K to 250 K. The data analysis shows that the easy magnetization direction is determined by a competition between the Zeeman energy favoring the field direction, the crystalline anisotropy favoring either the [001] or [111] directions, the exchange interaction at the interface favoring a parallel orientation of the magnetizations of both layers, and finally the magnetoelastic energy.

* This work is being supported by NRC.

[MO-POS] NUCLEAR PHYSICS PHYSIQUE NUCLÉAIRE

Monday
Lundi

MO-POS-96

Preliminary Results of the FINUDA Experiment at DAFNE*, George Beer for the FINUDA Collaboration, *University of Victoria* — The FINUDA experiment studies the formation and decay of hypernuclei produced by stopping kaons through the reaction $K_{stop}^- + {}^A_Z \rightarrow {}^A_Z + \pi^-$ FINUDA is a large acceptance spectrometer with resolution below 1 MeV which measures energy levels of the hypernuclei and the particles produced by hypernuclear weak decay. Approximately 250 pb⁻¹ integrated luminosity has been collected in 2003-2004. We present preliminary results concerning detector calibration, spectrometer performance, and hypernuclear formation and decay spectra.

* This work is being supported by Art Olin.

MO-POS-97

Measurement of the Parity Violating Asymmetry in Radiative Neutron-Proton Capture*, Chad Gillis, *University of Manitoba* — The NPDGamma experiment^[1] will measure the parity-violating gamma-ray asymmetry A_γ in the reaction $n + p \rightarrow d + \gamma$ in order to provide a theoretically clean measurement of the pion-nucleon weak coupling constant f_π to high precision. The Los Alamos Neutron Science Centre provides a pulsed cold neutron beam which is then polarized by transmission through polarized ³He and captured in a liquid para-hydrogen target. The 2.2 MeV gamma rays from the capture reaction are detected in an array of CsI(Tl) scintillators which are read out in current mode by vacuum photodiodes. The pulsed nature of the beam provides a crucial capability to distinguish systematic error contributions through their unique time-of-flight dependences. The appa-

ratus is being commissioned during the spring of 2004; initial results from the commissioning data will be discussed.

* Supported by the US DOE, NSF, TRIUMF, and NSERC Canada.

MO-POS-98

Design Optimization of TIGRESS using a GEANT4 Simulation. Michael Schumaker, *University of Guelph* — The TRIUMF-ISAC Gamma-Ray Escape-Suppressed Spectrometer (TIGRESS) will be an important experimental facility for the ISAC-II particle accelerator at TRIUMF. It will consist of twelve Compton-suppressed High-Purity Germanium (HPGe) detectors. A number of design optimization studies were conducted using a software simulation of the TIGRESS array. These studies were carried out using a Monte-Carlo simulation created using the GEANT4 toolkit. The goals of these studies were the improvement of the expected absolute gamma ray efficiency and peak-to-total ratio, and the reduction of experimental error due to Doppler-broadening. In this presentation, I will discuss the results of these simulations, and show how these results have been incorporated into the TIGRESS detector design.

MO-POS-99

Effects of the Symmetry Energy in the Mid-Rapidity Zone*. René Roy and the Heavy-Ion Collision Dynamics Research Team, *Université Laval* — The density dependence of the symmetry term of the equation of state (EOS) is a major point of interest in the heavy-ion dynamics. Using a soft Skyrme-like parametrisation, different symmetry terms are tested in the BUU calculations framework. These terms are constant, linear and quadratic with different compressibility moduli. Their effects are observed in the mid-rapidity zone. The chosen observable is the global N/Z ratio of this zone.

* This work is being supported by CRSNG.

MO-POS-100

Detection Prototype with Position Sensitive Photomultiplier / Prototypage de détection avec photomultiplicateur à position*. R. Roy, *Groupe de recherche en physique des ions lourds, Université Laval* — In the case of heavy-ion collisions physics, the reaction studies must be supported by a good detection matrix with good mass, charge, energy and position resolutions. For this we need a good set of photomultipliers. Then I have chosen to study a position sensitive photomultiplier, which gives great gain and compactness, to improve position resolution. It is giving good results in position, up to 1mm of position resolution. Also, it can be coupled with a large set of different form scintillators, giving unlike resolutions. *Dans le cadre de la physique des collisions d'ions lourds, l'étude des réactions doit être soutenue par une bonne matrice de détection, possédant de bonnes résolutions en masse, charge, énergie et position. Pour cela, nous avons besoin d'un montage adéquat de photomultiplicateurs. Le choix d'utiliser un photomultiplicateur à position, ici, viendra améliorer la résolution en position. Il possède un grand gain et il est intéressant pour son aspect très compact. Les résultats obtenus parlent par eux-mêmes ; j'ai obtenu des résolutions en position allant jusqu'à 1 mm. Il peut aussi être couplé avec des scintillateurs de différentes tailles et formes, donnant évidemment des résolutions propres à chacun des couplages.*

* This work is being supported by CRSNG.

MO-POS-101

Agreement in Supernova Simulations with Boltzmann Neutrino Transport and its Connection to Nuclear Input Physics. Matthias Liebendoerfer, *CITA, University of Toronto* — Three independent supernova groups have built detailed Boltzmann neutrino transport into spherically symmetric supernova simulations^[1,2,3]. In large scale computations, the energy- and angle-dependent distribution functions for the three neutrino flavors are determined during stellar core collapse and post-bounce evolution. The results of the general relativistic Boltzmann solver, Agile-Boltztran, are compared^[4,5] with those of alternative codes that either use approximations for the general relativistic effects or rely on the multi-group flux-limited diffusion approximation for the neutrino transport. The finding that spherically symmetric supernova models with standard input physics do not lead to explosions has settled in qualitative and quantitative agreement. Not so in the dynamically more comprehensive multi-dimensional simulations: they still produce controversial results, as many of them have to rely on severe simplifications in the neutrino treatment. The accurate knowledge of the energy-resolved neutrino abundances throughout the star is a prerequisite to accurately evaluate and improve the underlying nuclear input physics. I point to the dominant reactions and where current supernova models would be most sensitive to changes in the input physics. Some reactions (e.g. electron capture rates on nuclei) are crucial for core collapse while others (e.g. neutrino opacities in hot dissociated matter) may determine the delay and success for the neutrino-driven ejection of the surface layers. The collapse of the inner core and the ejection of the surface layers should be regarded as distinctive physical events.

1. Rampp & Janka, *ApJ*, **539**, L33 (2000)
2. Liebendoerfer, Mezzacappa, Thielemann, Messer, Hix & Bruenn, *Phys. Rev. D*, **63**, 103004 (2001)
3. Thompson, Burrows & Pinto, *ApJ*, **592**, 434 (2003)
4. Liebendoerfer, Rampp, Janka & Mezzacappa, astro-ph/0310662
5. Liebendoerfer, Messer, Mezzacappa, Bruenn, Cardall & Thielemann, *ApJS*, **150**, 263 (2004)

**[MO-POS] OPTICS AND PHOTONICS
OPTIQUE ET PHOTONIQUE**

**Monday
Lundi**

MO-POS-102

Dynamic ¹²⁹Xe NMR Spectroscopy in an Experimental Model of Pneumonitis in Rat Lung Induced by Exposure to *Stachybotrys Chartarum* Spores*. Nishard Abdeen¹, Albert Cross², Tom Rand³ and Giles Santyr¹, ¹ Carleton University, ² University of Lethbridge and ³ St. Mary's University — Hyperpolarized Xenon(H-Xe) NMR spectroscopy demonstrates the dynamics of gas exchange in rat lung *in vivo*, aided by the large chemical shift between gas phase and xenon dissolved in red blood cells and lung parenchyma. By repeating a pulse sequence consisting of selective saturation of the dissolved phase peaks followed by a readout pulse at variable time delay intervals, the time dependence of the exchange between gas phase xenon and xenon dissolved in the lung and red blood cells can be determined within a single lung inflation. This dependence is characterized by a gas transfer time constant which depends on diffusion across the alveoli, lung parenchyma, and blood and is therefore sensitive to changes in gas exchange and compartment effects. In this study, the time constant is measured in a rat model of chronic alveolar inflammation induced by intra tracheal instillation of fungal (*Stachybotrys chartarum*) spores. A significant difference is demonstrated between experimental animals (recovery time 25.1+/- 4.7 ms) and control animals (17.2+/-1.6 ms). These results show promise for detection of subtle alterations in gas exchange in lung disease. The applicability of this technique to other models of lung disease in animal and humans is discussed.

* This work is being supported by NSERC.

**[MO-POS] PHYSICS EDUCATION
ENSEIGNEMENT DE LA PHYSIQUE**

**Monday
Lundi**

MO-POS-103

Ongoing Professional Development Projects – BC Association of Physics Teachers. Donald Mathewson, *Kwantlen University College* — The BC Association of Physics Teachers is a chapter of the American Association of Physics Teachers. Our membership is comprised of a wide cross-section of high school, college and university physics teachers. On behalf of the membership, the BCAPT executive has recently embarked on an ambitious series of professional development projects for teachers. These initiatives have been enthusiastically embraced by the physics teaching community and have positively impacted the BC physics teaching community. For those within CAP and its member institutions interested in outreach, some information about the BCAPT and its professional development programs will be presented.

[MO-POS] THEORETICAL PHYSICS
PHYSIQUE THÉORIQUE
Monday
Lundi
MO-POS-104

Geometric Phase of a System Coupled to a Reservoir*, Karl-Peter Marzlin, S. Ghose and B.C. Sanders, *University of Calgary* - We present a new approach to Berry's phase for mixed states in non-unitary, non-cyclic evolution. Starting from a general system coupled to a reservoir we define Berry's phase using Kraus operators. The mixed-state evolution of Berry's phase is compared to the evolution for a pure state when no coupling to a reservoir is present.

* This work is being supported by iCore Alberta.

MO-POS-105

Axisymmetric Charged Matter Accretion on Kerr Black Holes*, Roman J.W. Petryk and M.W. Choptuik, *University of British Columbia, CIAR* — Accretion and jet formation of charged matter about black holes is not well understood. It is thought that twisting of magnetic field lines within the ergosphere of rotating black holes plays a role in collimating matter and radiation as bipolar jets. We numerically investigate these processes in axial symmetry for scalar fields on Kerr spacetime.

* This work is being supported by CIAR; CFI; NSERC.

MO-POS-106

Cycle Expansion of a Driven Pendulum / L'Expansion Périodique d'Orbite d'un Pendule Conduit, Andrew Penner, Randy Kobes and Slaven Peles, *University of Manitoba* — Chaos is fundamental to nature. Perhaps the most illustrative examples are atmospheric processes, but even further than that, some systems that had been commonly thought to be periodic, such as planetary motion, were recently proven to be chaotic. Chaos refers to a deterministic behavior characterized by a high sensitivity to a change of initial conditions. Due to these qualities any long term predictions are impossible, and consequently any solution of a given initial condition problem is not a physical observable. Calculating expectation values of observables for chaotic systems is usually done numerically and often marred by numerical artifacts. In this presentation we investigate a more subtle approach for evaluating expectation values for a chaotic system. We demonstrate our results in the example of a driven pendulum. Chaotic behavior may be thought of as motion over an infinite number of periodic orbits. A feasible mathematical solution to determine the expectation values is through cycle expansion, where an expectation value is calculated as a statistical average over periodic orbits in phase space. Statistical weight of each orbit is determined by its stability. Ultimately our goal was two fold. First we were to find the periodic orbits that contributed the most to the averages. Second, through use of these relatively few periodic orbits, we were to estimate expectation values for the rotation number and Lyapunov exponent of the driven pendulum to a high level of accuracy, and compare them to the brute force numerical calculations.

MO-POS-107

Dynamical Entanglement in Chaotic Systems, Shohini Ghose¹, Xiaoguang Wang², Ivan Deutsch³ and Barry Sanders¹, ¹*University of Calgary*, ²*Macquarie University* and ³*University of New Mexico* — We analyze the entanglement dynamics of systems that are chaotic in the classical limit using cold atoms trapped in a magneto-optical lattice as a test system. Coupling between the atomic center-of mass motion and spin leads to entangled spinor wave packets. The ability to reconstruct the reduced density matrix of spin subsystem via quantum state tomography makes it possible for entanglement dynamics to be studied in actual experiments. For states initially localized in a regular region of the phase space, the entanglement shows quasi-periodic behavior, whereas for states localized in a chaotic region, the growth of entanglement is faster and no quasi-periodic behavior is present. These features are similar to those seen in other chaotic systems such as the quantum kicked top. We explain the main features by examining the support of the initial state on 'regular' and 'chaotic' eigenstates of the Hamiltonian. Our analysis is general and applicable to other quantum chaotic systems.

MO-POS-108

Surprising Symmetries in Relativistic Charge Dynamics*, William E. Baylis, *University of Windsor* — The eigenspinor approach uses the classical amplitude of the algebraic Lorentz rotation connecting the lab and rest frames to study the relativistic motion of particles. When applied to the dynamics of a point charge in an external electromagnetic field, it reveals surprising symmetries, particularly the invariance of a couple of field properties in the rest frame of the accelerating charge. The symmetries facilitate the discovery of analytic solutions of the charge motion and are simply explained in terms of the geometry of spacetime. The eigenspinor approach also suggests a simple covariant extension of the common definition of the electric field: the electromagnetic field can be defined as the proper spacetime rotation rate it induces in the particle times its mass-to-charge ratio.

* This work is being supported by NSERC.

MO-POS-109

Poissonian Random Process on a Regular Fractal, John M. Nieminen¹ and Jamal Sakhr², ¹*Northern Digital Inc.*, and ²*McMaster University* — A new measure of fractal dimension, based on the nearest-neighbour spacings of a Poissonian random process, is proposed. The validity of this measure is demonstrated by calculating the dimensions of several well-known regular fractals. For all fractals studied, the calculated dimension is within two percent of the accepted fractal dimension. A formal connection between this new measure of dimension and the familiar Brody parameter of Random Matrix Theory is also discussed.

MO-POS-110

Bohmian Trajectories and Numerical Solution of the Schrödinger Equation, Louis Marchildon and Emilie Guay, *Université du Québec à Trois-Rivières* — In Bohmian quantum mechanics, particles follow definite trajectories governed by deterministic laws. The initial conditions of the particles, however, are known only probabilistically. The statistical predictions of quantum mechanics are recovered because the equations of motion of the particles involve the system's total wave function in an essential way. In situations where the wave function is known analytically, the numerical computation of trajectories is rather straightforward and reduces to the integration of first or second-order coupled ordinary differential equations. Where the wave function is not known, however, it must first be obtained by appropriate numerical methods. We investigate the case of two-slit interference involving one particle or two identical particles. Two kinds of methods are considered. The first one, based on the hydrodynamic formulation of the Schrödinger equation, uses either a fixed or a comoving grid. The second one is based on simple splitting of the Schrödinger equation into real and imaginary parts. Although the former (especially with a comoving grid) is computationally effective in many-dimensional problems, we find that the latter is more accurate around near-zeros of the total wave function. Trajectories obtained through the numerical integration of the Schrödinger equation are compared with similar ones computed from exact wave functions.

MO-POS-111

Vector Fields and Topological Counting Numbers, J.G. Williams¹ and Tina A. Harriott², ¹*Brandon University* and ²*Mount Saint Vincent University* — Monopoles, instantons and skyrmions are all topological structures that can be counted by integrating a suitable Jacobian, thereby computing the degree of the mapping represented by the relevant (vector) field. In this paper, the usual Euclidean integral formula is modified to produce a covariant formula that can be applied to general relativistic kinks. The kink number is calculated for some simple-to-visualize examples in 2+1 dimensions.

MO-POS-112

Observable 3-D Boundary in 4-D Space-Time Defined by the Diachronic Now*, Michel A. Duguay and C. Grenon, *Centre d'Optique, Photonique et Laser, Université Laval* — In diachronic time first considered by Einstein^[1] one assigns Greenwich time to astronomical events. In a diachronic representation of 4-D space-time events on our past light cone form a Lorentz invariant 3-D boundary of 4-D space-time characterizing an extended diachronic now^[2]. In the diachronic perspective the conventional speed of light is identified with the flow of time. In this perspective recent speculation about a varying speed of light as a function of cosmological look-distance is equivalent to a varying rate in the flow of remote time relative to us. The observed red-shift of distant galaxies is usually attributed to a Doppler effect, but an alternative explanation is a slower flow of time relative to us, immediately perceived thanks to the infinite diachronic speed of incoming light. In a cosmology built with a single boundary for space-time the need for a second boundary, as

might be defined by the Big Bang theory, would disappear. A straightforward prediction of such a cosmology is that there will be no limit to the look-distance at which distant supernovae or quasars will be discovered in the future.

1. A. Einstein, *Annalen der Physik*, 17, 891-921 (1905).

2. M.A. Duguay, "Diachronic representation of space-time applied to problems in special relativity and in quantum optics", submitted to *The Can. J. Physics*, 27 Feb. 2003.

* This work is being supported by NSERC.

MO-POS-113

Unstable Nuclei / Dialectic Equilibrates: A Violent Collision. William Simmons, David Mu and Reinhardt Bsumek, *Energy Metals Corporation* — Albert Einstein postulated only for maximum mass energy with $E = mc^2$. We present dialectic antithesis for Einstein's Equation with $E_p = m(\lt c^2)$, mass energy at less speed of light is ground state energy potential. For energy of unstable nuclei released in a heterogeneous non-fertile field becomes field energy. We will show further that when a field is a ground state, all radioactive prodigies of the unstable nuclei surcease because primal heritage desists and benign stability results since the energy normally conceived to daughters by natural radioactive decay becomes embryonic energy for the field instead. Profound atypical collision mechanics of quanta structures more efficient than typical collider physics^[1] facilitate heterogeneous nucleation to pattern minority unstable energy to majority stable field energy when unified field force subsides and capture is complete. Energy in entropy fosters field energy equilibrium. Einstein's Equation for, mass/energy (having normal binding energy) increases with velocity. By dialectic equilibrates we will show that mass/energy decreases when velocity is reduced by negating binding energy potential. Hence, unstable mass/energy transforms to rest and precipitates in the capture field stable. Such that matter and energy are interchangeable and different only in form, we simply replicate a phenomenon of unstable energy in extreme atypical violent collisions by antithesis synthesizes to its ground state in one forward non-sustaining reaction and further radioactive decay is eliminated.

1. I.e. Collider/accelerator physics such as that practiced at Fermi Lab, Jlab, ANL, etc.

MO-POS-114

Global Optimization Algorithms and the Sodium Chloride Cluster Problem. Richard Hodgson, *University of Ottawa* — In this work we evaluate and compare the performance of three different global optimization algorithms when applied to the challenging problem of determining the structure of sodium chloride clusters of a given size. In general the task of finding a cluster's global minimum structure is a difficult one. For a simple pair potential which only takes into account the two major interaction effects, the number of local minima on the potential energy hyper-surface grows exponentially with increasing cluster size. The algorithms which are investigated include a) an improved genetic algorithm which makes use of a self-guiding search strategy, using a combination of "traditional" and geometric genetic operators; b) a fast annealing evolutionary algorithm which combines the aspect of population in genetic algorithm and a simulated annealing algorithm; and c) a modification of the standard Lipschitzian approach that removes the need to specify a Lipschitz constant. Instead simultaneous searches are conducted using all possible constants.

[MO-POS] INDUSTRIAL AND APPLIED PHYSICS
PHYSIQUE INDUSTRIELLE ET APPLIQUÉE

Monday
Lundi

MO-POS-115

Characterizing Multiple Bubbles In An Agar Gel With Ultrasonic Spectroscopy And Optical Imaging. K.A. Ross^{1,2}, L.J. Pyrak-Nolte³, and O.H. Campanella^{4,1} *Department of Food Science, University of Manitoba*, ² *Department of Physics and Astronomy, University of Manitoba*, ³ *Department of Physics and Astronomy, Purdue University* and ⁴ *Department of Agricultural and Biological Engineering, Purdue University* — The presence of inhomogeneities, such as bubbles or pores, affects the physical properties of any solid material. This is especially important for food products, whose textural attributes are strongly influenced by bubble/pore size distribution, bubble/pore size orientation, and air volume fraction/porosity. The main focus of this work was to use ultrasonic spectroscopy, based on the frequency dependence of the ultrasonic attenuation, to determine the pore size distribution of air bubbles in an agar gel, which may be considered a model biological system with laboratory, pharmaceutical and food applications. Different bubble size distributions were introduced into the gels by varying the mixing conditions. A fundamental spectroscopic analysis of the ultrasonic attenuation was performed to demonstrate that both the bubble size distribution and the spacing between the bubbles could be successfully determined. Since the gels are transparent, digital imaging of the bubbles could also be performed, allowing the two-point spatial correlation function to be determined and giving a direct measurement of the bubble/pore sizes and porosity. Good agreement was found between the results of ultrasonic spectroscopy and the two-point correlation function, thereby validating the ultrasound bubble sizing data. Overall, this work indicates that these techniques may be applied to a biological system containing polydisperse bubbles/pores in order to determine the structure of the system through effective characterization of bubble/pore size and porosity. This is significant as bubble/pore size and porosity affect mechanical properties and the utility of such materials, which is of technological importance.

[MO-POS] INSTRUMENTATION AND MEASUREMENT PHYSICS
PHYSIQUE DES INSTRUMENTS ET MESURES

Monday
Lundi

MO-POS-116

Submicron Gold Wires Fabricated Via Dielectrophoresis Of A Colloidal Suspension*. C.T. Harrower and D.R. Oliver, *Electrical & Computer Engineering, University of Manitoba* — Sub-micron metallic wires may be fabricated via dielectrophoresis of a colloidal suspension^[1,2]. The goal of this project is to study the conduction character of these wires as the early stages of formation involve very small contact areas. Colloidal gold was prepared by the reduction of tetrachloroauric [III] acid with sodium citrate^[3,4] and the particle sizes obtained depend upon the concentrations. The particle size distribution for the suspensions obtained has been estimated using Mie Theory and extinction measurements obtained with a spectrophotometer. In order to form wires the colloidal solution must be further concentrated by a factor of about 20 before wires could be grown at a reasonable rate. Sub-micron wires were grown between two gold electrodes (0.25 mm diameter wire) and placed in the colloidal solution. The wires were grown over a sub-millimeter electrode spacing using both electrophoresis (DC) and dielectrophoresis (AC). Control of the growth was obtained by varying the electric field strength and, in the case of dielectrophoresis, frequency. The conductivity through the system was studied during and after wire formation.

1. K. Hermanson, et al., *Science* 294 p1082 (2001)

2. R. M. Penner, *J. Phys. Chem. B* 106 p3339 (2002)

3. G. Frens, *Nature* 41 p20 (1973)

4. J.W. Slot & H.J. Geuze, *J. Cell Biol.* 90 p533 (1981)

* This work is being supported by NSERC.

MO-POS-117

Experimental Characterization of an Aerogel Cherenkov Prototype for the G0 Experiment. Marcus J. Steeds¹, J. Birchall¹, B. Clement¹, W. Falk¹, L. Lee¹, S.A. Page¹, W.D. Ramsay¹, W.T.H. van Oers¹, E. Korkmaz², T.A. Porcelli² and C.A. Davis^{3,1} *University of Manitoba*, ² *University of Northern British Columbia* and ³ *TRIUMF* — The G0 experiment in Hall C at Jefferson Lab will determine the strange quark contributions to the vector form factors of the proton. The upcoming back-angle mode will use aerogel Cherenkov detectors for threshold discrimination of an electron signal against a pionic background. The results of electron beam tests of the North American prototype detector conducted at TRIUMF's M11 experimental beamline will be presented.

[MO-POS] MEDICAL AND BIOLOGICAL PHYSICS
PHYSIQUE MÉDICALE ET BIOLOGIQUE

Monday
Lundi

MO-POS-118

Investigation of SNR and SAR for Low-Frequency Polarized Noble Gas MRI of the Lung*. Erin Chapple, C.P. Bidinosti, J. Cha, N.A. David, M.E. Hayden, *Simon Fraser University* — Low-field magnetic resonance imaging (MRI) of human lungs using hyperpolarized noble gases has only recently been demonstrated for the first time. As a result there are still a number of surrounding issues that are poorly characterized at low frequencies, such as fundamental signal-to-noise ratio (SNR) limitations and specific-absorption rates (SARs). Here we present the results of an ongoing study that probes SNR and SAR from 100 kHz – 1 MHz, the range of frequencies relevant to this new MRI technique. Resonant coil structures suitable for the study of each property were constructed, and a determination of the effective coil resistance was made with and without a human subject inside each coil type. For the SNR study, rectangular Helmholtz coils (34 x 40 cm) were placed at the front and back of the chest of the subject. At all frequencies the coil resistance is at least an order of magnitude larger than the effective resistance of the subject, implying that optimal SNR might only be achieved with cryogenically cooled coils. For the SAR study, a birdcage-like transmit (B_1) coil which had a homogeneous field map over the volume of the chest was used. An SAR value of $1.5 \times 10^{-5} / B_1^2$ W/kg (MKS units) was determined. This result is suitable for any body coil of comparable homogeneity, and is useful for determining limits on RF pulse rates.

* This work is being supported by NSERC.

MO-POS-119

A Structural Study of a Myristoylated Membrane Binding Peptide. T.A. Harroun¹, K. Balali-Mood², J.P. Bradshaw² and J. Katsaras¹, ¹National Research Council and ²University of Edinburgh, - Myristoylation is a common post-transcriptional modification to proteins that confers additional membrane binding affinity. The process involves the attachment of the fourteen carbon saturated acyl-chain of myristic acid to the N-terminus of the protein. Such modified proteins include the adenosine ribosylation factor (ARF) family. Using specific deuterium labeling and neutron diffraction, we previously determined that the 15 amino acid peptide from the N-terminal sequence of ARF1 (pARF1) lies parallel to the membrane interface, in the region of the headgroup. We have repeated this experiment with the myristoylated form of the peptide, and found that the effect of myristoylation is to tighten the helical structure of the membrane-binding domain, forming a new hydrophobic face for the protein, increasing its membrane binding capabilities. These results confirm the theoretical prediction that the effect of myristoylation can extend many residues along the amino acid sequence from the terminus.

MO-POS-120

A Method for Concentrating Nucleic Acids by Synchronous Perturbation of Electrophoretic Mobility. A. Marziali¹, J. Pel¹, E. Holtham¹, D. Broemeling¹, R. Coope¹, D. Bizzotto² and L. Whitehead¹, ¹Dept. of Physics and Astronomy and ²Dept. of Chemistry, *University of British Columbia* — Electrophoretic current fields are divergence free, which prevents spatial concentration of DNA by standard electrophoresis in uniform, non-binding media. In this presentation, we demonstrate a general method for achieving electrophoretic concentration of DNA using alternating electric fields and synchronized coefficient of drag alteration. We demonstrate DNA concentration in low (<1%) agarose gel by focussing a uniform DNA solution to a single region in the center of the gel. This is done by applying a mix of dipole and quadrupole electric fields to four electrodes contacting the side of the gel, such that the DNA undergoes oscillatory motion, but its mobility is always higher when moving toward the centre of the gel. Recent results and theory behind this effect will be presented, as well as initial work toward DNA purification applications.

MO-POS-121

Analysis of Nucleic Acid Dissociation Rates using a Trans-membrane Single Molecule Sensor*. Jonathan Nakane, M. Wiggin and A. Marziali, *University of British Columbia* — A self-assembling nanosensor for sequence-specific detection of nucleotides across a membrane has been constructed from a single alpha-hemolysin nanopore self-assembled into a lipid bilayer, and a DNA probe tethered to avidin at one end and complementary to the analyte nucleotide at the other end. By monitoring the dissociation rate of single DNA molecules on the trans side of the membrane after binding to the trapped probe strand, we can uncover the energy landscape of these events, allowing us to detect and identify short (14-mer) perfectly complementary strands and localize regions of single base mutations in strands specifically targeted based on the sensor probe sequence. Further analysis of the energy landscapes reveals that several characteristics of the binding interaction, including the length and number of contiguous regions of complementary nucleotides, and the overall free energy of binding between may be used to distinguish populations of different oligonucleotides.

* This work is being supported by NSERC.

MO-POS-122

A 3D Ultrasound Scanner for Evaluation of Musculoskeletal Disorders. Andrea Lai², Daniel W. Rickey^{1,3,5} and Martin H. Reed^{2,4,5}, ¹Medical Physics, *CancerCare Manitoba*, ²Faculty of Medicine, *University of Manitoba*, ³Dept of Physics, *University of Manitoba*, ⁴Department of Radiology, *Children's Hospital, Winnipeg* and ⁵Department of Radiology, *Health Sciences Centre* — Ultrasound is a primary imaging technique for diagnosis and assessment of musculoskeletal disorders because it gives excellent visualization of soft tissues and cartilaginous components. The common ultrasound method used is conventional 2-dimensional technology. There is much interest in newer 3-dimensional (3D) ultrasound technology. Although, there are many advantages to 3D methods, it has been weak in scanning over the curved surfaces of the body. The goal of this project is to develop and evaluate a novel 3D ultrasound technique that allows scanning over curved surfaces. In this poster we will show ultrasound images of various musculoskeletal anatomy acquired with a diagnostic ultrasound machine coupled to a system that obtains 3D images over curved surfaces. The usefulness of this 3D technique was evaluated by scanning a number of pediatric patients. The technology was found to easily move over the curved surfaces of the subjects. In addition, the 3D images were tested for geometric fidelity. The scanner reproduced image geometry with a high degree of fidelity, i.e., within 0.3 mm. Motion artefacts could be corrected to a certain degree, however some distortion remained in images acquired from neonates and infants who had been in constant motion during the scan.

MO-POS-123

The Effect of Bone Shape and Orientation in X-Ray Fluorescence Bone Lead Measurement. A.F. McDonald, N. Ahmed and D.E.B. Fleming, *Mount Allison University* - Lead is a nonessential trace metal in the human body and has been associated with a variety of adverse health effects. Since the half-life of lead in bone tissue is 10-20 years, measurement of lead concentration in bone allows one to ascertain long-term exposure. Our group uses X-ray fluorescence (XRF) to analyze bone lead levels. This method is performed *in vivo* and is capable of measuring bone lead levels above 5 ppm. The focus of the research project was to investigate some of the factors that may affect precision and accuracy of the technique. The XRF instrument is calibrated using cylindrical bone phantoms doped with known quantities of lead. We constructed additional phantoms of other shapes in order to investigate what effect, if any, bone shape and orientation might have on the technique. Preliminary results are presented and their implications assessed.

MO-POS-124

Localized Ion Depletion And Read Length Degradation In Capillary Electrophoresis For DNA Sequencing*. Robin Coope and Andre Marziali, *University of British Columbia* — We have investigated the performance degradation in capillary sequencing of DNA samples that contain slow-moving contaminant fragments such as genomic DNA. Analysis of current and fluorescence data from a 96 capillary electrophoresis instrument has shown that poor reads are primarily due to low capillary current, resulting in a large increase in run length for some capillaries. While the peak shape of different length DNA bands is maintained, simply not enough bands in the affected capillaries reach the detector during the run. While this effect has been observed for years in production DNA sequencing, no satisfactory explanation has been advanced. The mechanism of current reduction has been identified as the catastrophic development of an ionic depletion region downstream of low mobility DNA fragments remaining from the *e-coli* based DNA preparation protocol. The depletion region, with ~5% the conductivity of the background region, grows over time and as a result, the current declines and read length is reduced. We present experimental results showing the growth and propagation of this depletion region, and present analytic and numerical models of this effect.

* This work is being supported by National Institutes of Health.

MO-POS-125

A Note on Interpolation and Extrapolation Methods in Brachytherapy Dose Calculations*. Jason Sun, Nucletron Canada Inc. — In brachytherapy treatment planning, dose-rate distribution data for a given source, obtained from phantom measurements or Monte Carlo calculations, are usually reported on a polar or Cartesian grid. Interpolation and extrapolation are always required for determining the dose rate on off-grid points. Since the dose rate changes rapidly around a source, there has been a general belief that one would have more accurate results if the inverse-square factor were extracted from the dose-rate distribution before interpolation or extrapolation is performed. This is found to be true for point sources. For line sources, the AAPM TG-43 recommends that a geometric factor, which is different from the inverse-square factor, be separated from other slow-varying factors or functions, e.g., radial dose function and anisotropy function. According to TG-43 and its revised protocol (drafted by the AAPM LIBD subcommittee), for each off-grid point, one should calculate the geometric factor specifically, using the well-defined equation. Interpolation or extrapolation should be made only on other factors. Recently, within the brachytherapy community, there is an open debate on the necessity of making such a separation. This paper clearly shows that, without a proper handling of the geometric factor, i.e., not separating this factor from dose-rate distribution, or simply applying the inverse-square factor for a line-source, the interpolation or extrapolation may certainly result in errors well beyond the acceptable range. The published dosimetric data of Iodine-125 6711 source, commonly used for treating prostate cancer, are used in this study.

* This work is supported by Nucletron Canada Inc.

MO-POS-126

Simulation of a Radioactive Eluting Stent Using Geant4*, Jean-Francois Carrier^{1,2}, L. Beaulieu^{1,2}, R. Roy² and O. Bertrand³, ¹Hôtel-Dieu de Québec, ²Université Laval and ³Hôpital Laval — Radiation therapy has been identified as a promising means of treating coronary restenosis. However, precise dosimetry simulations have to be done in order to make sure the dose deposited in the artery wall is uniformly distributed. The project currently under study is a radioactive eluting stent with a polymer coating. Following stent implantation in the vessel, radioactive 45 isotopes are delivered to the artery wall from the polymer matrix. Numerical simulations were done in order to study the diffusion of the isotopes through the wall. Afterwards, the irradiation of the target volume is studied with Monte Carlo simulations. The Monte Carlo toolkit used for the dosimetry simulations is Geant4, an object-oriented toolkit developed at CERN. Simulations were done for a 2D artery static model for specific parameter values. The parameters are inter-strut spacing, polymer coating thickness and diffusivity coefficients in wall, blood and coating. Dose deposited distributions were also calculated for a dynamic model. The total dose distribution in the artery wall after two weeks of diffusion and radiation will be presented. The dose delivery success is measured using two quantities: the dose homogeneity in the therapeutic region and the percentage of activity remaining in the therapeutic region after a defined duration. A 3D artery model has also been developed and preliminary results will also be presented.

* This work is being supported by FQRNT.

MO-POS-127

Performance Evaluation of a CT/PET Imaging System for Radiation Oncology Treatment Simulation. P.S. Basran¹, C. Caldwell² and K. Mah¹, ¹Department of Medical Physics, Toronto-Sunnybrook Regional Cancer Centre & Department of Radiation Oncology and ²Sunnybrook and Womens College Health Science Centre & Department of Medical Imaging, University of Toronto — Acceptance testing of a new combined Positron Emission Tomography (PET) multi-slice CT scanner (Philips Gemini PET-CT System) dedicated for radiation oncology simulation was undertaken at our institute. Testing was divided into the evaluation of the i) CT-simulator and imaging system; ii) PET-imaging system; and iii) the registration of the PET and CT data. Performance of the CT-simulator system was evaluated with tests described by the American Association of Medical Physicists Task Group Reports 2 and 66, plus some additional tests that examine the multi-slice capabilities of the system. In this poster, we present details on the electromechanical and image quality characteristics of the multi-slice CT scanner. To summarize our results, the performance characteristics of the imaging systems were favourable; however, there were some mechanical challenges when using the system as a radiotherapy simulator due to greater demands in geometrical accuracy when simulating radiation therapy. Some key findings include: a systematic couch tilt with and without the flat-bed top; an (expected) increase in radiation profile thickness for the multiple CT images due to beam divergence; signature image artifacts from multi-slice helical scanning; and, a systematic in-plane rotation in reconstructed images. While many of these findings do not impact radiation therapy simulation significantly, some findings required in-house modifications or other ameliorations. Since November 2003, the CT simulator component of the imaging system has been commissioned for clinical use. In this poster, we describe the major results of these tests along with modifications to the radiation therapy CT simulator.

MO-POS-128

A Bench-top Megavoltage CT Scanner with Cadmium Tungstate-Photodiode Detectors*. D. Tu¹, T.T. Monajemi¹, D. Rickey², B.G. Fallone¹, S. Rathee¹, ¹Medical Physics, Cross Cancer Institute, University of Alberta and ²Medical Physics, CancerCare Manitoba — Imaging patients in treatment position for accurate patient set up and dose delivery verification in radiotherapy is possible with megavoltage computed tomography (MVCT). However, in order to overcome the poor contrast and higher dose resulting from megavoltage photons, the MVCT detector must be designed to provide the optimal detective quantum efficiency (DQE). The aim of the present study is to fabricate a prototype (80-element, 25 cm) fan-beam CT detector using CdWO₄ scintillator and photodiodes. In a previous study, we determined that the zero frequency DQE of an 8-element CdWO₄ array was 26% and 19% in 1.25 MeV and 6 MV photons, respectively. We have designed, fabricated and tested the data acquisition timing control, precision rotary stage control and an analog data multiplexer unit for the prototype 80-element detector array. The data acquisition is synchronized with radiation producing pulses from the linear accelerator. We have tested the linearity of the prototype detector array with respect to the dose rate, and its ability to accurately measure the attenuation of 6 MV photon beam by solid water. The pre-sampled line spread function, modulation transfer function (MTF), the noise power spectrum, and the spatial frequency dependent DQE of the detector have been measured in 6 MV photon beam. In future, this detector, along with the precision rotary stage, will be used for collecting the fan beam projection data for a standard CT phantom (CATPHAN500) in order to assess the basic MVCT image quality. The system block diagram and the preliminary results will be presented.

* This work is being supported by CIHR(MOP 43254), ACB (RE-78).

MO-POS-129

Development of Megavoltage Cone-beam CT for Image-guided Radiotherapy Treatment*. Geordi Pang, J.A. Rowlands, P.F. O'Brien, X. Mei, C. Yeboah, M. Tambasco, Toronto-Sunnybrook Regional Cancer Centre — Soft tissue imaging in the treatment room is one of the main challenges faced today in radiation therapy. Our overall goal is to develop a megavoltage cone beam CT (MVCT) which can be used to image soft tissue targets, such as the prostate, with a low dose (<5% of the treatment dose) so that daily imaging would become feasible and image-guided radiotherapy using MVCT could be realised. The precise knowledge of patient anatomy at the time of treatment obtained with MVCT will permit higher radiation doses to be delivered to the target volume with potentially greater cancer control but without an increase of side effects. Compared to kVCT (i.e., cone beam CT with a kilovoltage x-ray source mounted on the linear accelerator), MVCT has the advantages of simplicity and potentially higher accuracy. A MVCT system has been built which consists of a flat panel detector and a linear accelerator fitted with a low-z target and a removable flattening filter. Effects of various factors on phantom image quality such as the x-ray focal spot, x-ray spectrum, phantom scatter, imaging geometry and detector quality have been investigated. A method aimed to improve the MVCT image quality and reduce the imaging dose has been proposed. This includes the optimization of the beamline components, the reduction of x-ray scatter as well as a significant increase in the quantum efficiency of the flat panel detector for MV x-rays.

* This work was supported by Siemens Medical Solutions USA, Inc.

MO-POS-130

An Empirical Model to Estimate the Mean Square Scattering Angle of Electron Beams for Use in Treatment Planning Systems. Deborah Hodefi, Hôpital Maisonneuve-Rosemont — Electron pencil beam algorithms, such as that employed by CadPlan (Varian), generally rely on the mean square scattering angle (msa) to characterize the beam spread. Usually, one virtual machine is created per electron energy. This practice implies that one value for the msa is sufficient to model dose distributions of any field size. The field size is delimited by the jaw positions, applicator and cut-out. As electrons are easily scattered, variation of these parameters will influence the angular spread. The msa used as input for a treatment planning system may differ considerably from the msa associated with a given set of conditions. Subsequently, error may be introduced into the calculated dose distribution. The objective of this work was to develop an empirical formula, suitable for use in a treatment planning system, which is capable of determining the msa particu-

lar to each case. Measurements were carried out using an Elekta SL25 accelerator. A p-type silicon diode was utilized to measure profiles at the surface of a water phantom for various combinations of energy, applicator, cut-out size and jaw position. The corresponding msa was derived from the penumbra of each profile. For a given energy, the msa has been shown to vary dramatically over the range of applicators used in the clinic. An expression was formulated which predicts the msa, accounting for applicator, cut-out size, energy and jaw effects. By providing a significantly more accurate msa for a given set of conditions, more realistic dose distributions may be generated.

MO-POS-131

Proposed Definitions for Isodose Flatness and Symmetry in Clinical Radiotherapy Beams. Eduardo Galiano¹, T. Joly¹ and F. Wiebe², ¹ Laurentian University and ² Universidad Nacional de Asuncion — In radiotherapy it is important that beam intensity be as homogeneous as possible to reduce the probability of treatment failure. As extensions of the concepts of beam flatness and symmetry, the concepts of isodose flatness (IF) and symmetry (IS) are introduced. An isodose curve is a planar curve across a radiation beam, such that every point on the curve receives the same dose. Using a 10 x 10 cm field, an 80 cm SSD, and a phantom measurement depth of 10 cm, we propose defining isodose flatness for an isodose curve as the maximum absolute spatial deviation from the mean expressed as a percentage of the measurement depth of 10 cm. With identical geometry we propose defining isodose symmetry (IS) as the maximum spatial deviation between any pair of symmetric points about the beam midline expressed as a percentage of the same measurement depth. Mathematically:

$$IF = (\frac{1}{2}x_1 - m \frac{1}{2}x_{max} \times 100\%) / 10 \text{ cm}$$

$$\text{and}$$

$$IS = (\frac{1}{2}x_1 - x_1' \frac{1}{2}x_{max} \times 100\%) / 10 \text{ cm}$$

where x_1 is any point on the isodose curve, x_1' is its symmetric point with respect to the beam midline, and m is the mean of all x_1 's. These definitions were tested with actual data obtained from a Co-60 unit and a linear accelerator, with film. The calculated IF and IS for the Co-60 unit were $3.20 \pm 69\%$ and $3.02 \pm 69\%$ respectively. The calculated IF and IS for the accelerator were $6.11 \pm 2.19\%$ and $11.01 \pm 2.19\%$ respectively.

MO-POS-132

Analytic Expressions for Depth-Dose Curve in a Homogeneous Cylindrical Phantom for Photon Beam Irradiation. Jose M. Martinez-Ortega, Ottawa-Carleton Medical Physics Institute, Carleton University — Analytic expression for dose calculation is quite rare in radiotherapy context. The main reason of that is due to the high complexity of the catastrophic electron-transport mechanism as the electron slowing down in media. Currently condensed histories of MC algorithms have been postulated as the best candidate for dose calculation purposes. The present work is one of the first attempts toward to find analytic solutions for the depth-dose curve in a homogeneous cylindrical phantom irradiated by photon beam. In order to illustrate how this theory works the scatter fluence inside of homogeneous cylinder irradiated by monoenergetic Cobalt-60 beam was determined. The beam was considered a set of parallel photons rays hitting perpendicular to the top of cylinder's surface and the probability of photon scattering was assumed via Thomson. As result a set of fast convergent analytic series were obtained allowing compute the depth-dose curve along the main axis of the cylinder. Due to the simplicity of the photon-electron transport mechanism considered here, this first model has been considered for academic purposes only. However, further development of this theory is an outgoing investigation.

MO-POS-133

Virtual Compensation Compared with Physical Compensation in Head and Neck Radiotherapy. Darcy Mason, C. Araujo, J. Wilson and A. Baillie, BC Cancer Agency - Southern Interior — A common head and neck technique uses parallel opposed lateral fields matched to a supraclavicular field. The lateral fields need tissue compensation in two dimensions; this was formerly achieved at our centre using wedges placed thick end anterior for most fractions, and thick end inferior for the last few fractions. We now use "virtual compensation" provided by beam segments shaped by multi-leaf collimators (MLC). The segments are designed by inspection of a dose distribution on a mid-sagittal slice. Uniform doses can be achieved with three segments per field, and often with only two segments by staggering the shapes from the opposing fields. We compared the virtual compensator (v-comp) technique with physical compensators (p-comps) made of brass. Dose distributions were measured for v-comps and p-comps for an anthropomorphic head phantom and a flat phantom. The two compensator types produced clinically equivalent dose distributions, and the measurements confirmed the dose predictions of the treatment planning system within a few percent. Initially the v-comp technique required a lot of planning time, but we have streamlined the process. Patient treatment times are not significantly different from the previous technique. Unlike inverse-planned intensity modulated radiation therapy (IMRT), our field sizes and shapes fall within the normal parameters of conventional treatment. The only extra work needed was to confirm our linear accelerator stability for the low monitor units used in some segments. Thus the v-comp technique provides a simple but effective IMRT without the complications of special planning software or per-patient measurements.

MO-POS-134

A Dosimetric Comparison of Four External Beam Techniques for Accelerated Partial Breast Irradiation: Set-up of Study and Preliminary Results. Mike Oliver, Jeff Chen, Eugene Wong, Tomas Kron, Jake Van Dyk and Francisco Perera, Department of Medical Biophysics, University of Western Ontario and Department of Physics and Engineering, London Regional Cancer Center — Conventional early breast cancer treatment consists of a lumpectomy followed by whole breast radiation therapy (WBRT). Accelerated partial breast irradiation (APBI) is a method to reduce the irradiation volume to the lumpectomy site only. APBI may deliver more uniform dose to the target, while sparing healthy tissues better than WBRT. In addition, APBI reduces the overall treatment time from 5-6 weeks to 1 week. A treatment planning study was undertaken to compare four external beam techniques for APBI: small-field tangents, conformal radiotherapy (2 and 4-field), intensity-modulated radiation therapy (2 and 4-field) and helical tomotherapy. Critical structures (heart, contra-lateral breast, uninvolved breast, lungs and skin) were contoured on the CT simulator. The gross tumour volume (GTV) was defined as the union of seroma volume and the volume bounding the surgical clips. Clinical target volume (CTV) was defined with a 1.5 cm margin around GTV, constrained to within 5 mm to the skin surface. A further 1 cm uniform expansion was used to create the planning target volume (PTV). Treatment plans were generated using conventional and tomotherapy planning systems with plans normalized to $D_{95}=37.2$ Gy to the PTV. The ratio of CTV to whole breast volume was determined for 13 cases and varied greatly from case to case with an average of $30.1 \pm 13.4\%$ (min: 12.7%, max: 60.1%). Initial dose volume histogram analysis showed that the four APBI techniques produce superior dose distributions compared to WBRT. Results for the superior APBI technique will be presented.

MO-POS-135

Distributed Monte Carlo Calculations in a Multi-Platform Environment. Patrice Munger, Hôpital Maisonneuve-Rosemont — Clinically realistic, Monte Carlo calculations with BEAMnrc and DOSXYZnrc may require large amounts of computing power. In a typical configuration, several computers are used in parallel. In our department, only one Linux workstation is completely dedicated to Monte Carlo calculations. The majority of the other computers in the department run various flavours of Windows operating systems. We also have a few IRIX and HP-UX workstations. In an attempt to make maximum use of this heterogeneous computer park, we have created a distributed job submission system which allows any of the computers present in our department, regardless if the OS it runs, to act as a Monte Carlo computation engine. All components of our system were written in Python, a high-level, object-oriented, multi-purpose language. In addition to allowing compact programs to be written, its multi-platform character is an obvious advantage in an heterogeneous environment like ours. The system was designed to satisfy some important requirements. First, due to the low priority assigned to Monte Carlo processes running on the computation engines, these processes do not disturb users that may be using these computers locally. Also, limits on the number of Monte Carlo processes simultaneously running, and on the maximum memory that they can consume, can be adjusted for every computation engine, preventing Monte Carlo processes to use all the resources of a given computer. Our system has been proven to be efficient at employing the existing computer resources of our department that otherwise would not be fully exploited.

MO-POS-136

Web-based Electronic Physics Database in the Grand River Regional Cancer Center. Rob B. Barnett, James C.L. Chow, David Shenton and Steve Kennedy, Medical Physics Department, Grand River Regional Cancer Center — An "in-house" web-based Physics database was developed and implemented in the Medical Physics Department of the Grand River Regional Cancer Center (GRRCC). The database has a window front-end and web application domain developed by VB.NET and ASP.NET respectively. The database architecture is designed to be easily maintainable and extensible. It also provides an arbitrary file/data format, report generation and graphical analysis tools for analyzing the QA data. The database contains both "static" and "dynamic" records. The "static" records include the treatment unit commissioning data, a physics handbook, the radiation survey/protection data, physics equipment inventory, electronic instrument manuals and manufacturers' contact information. For the "dynamic" records (data varying over time) such as the linac maintenance/repair history, and routine QA test data, the user can submit the information on a computer (desktop or laptop with wireless Internet) through a web interface linked to the Cancer Center network. For example, for routine machine QA, the testing user can input measured results through the web. Physicist can access, investigate and approve the results once data has been entered electronically. Comparison can easily be made between current and previous data, which can be graphically analyzed and printed. Physicist approval is password controlled and can be assigned to specific tasks. Such a web-based database is needed for a "paperless center" which was a principal objective for GRRCC.

MO-POS-137

Characterization of the Energy Spectra of a Cobalt-60 Tomotherapy Beam, Johnson Darko, C.P. Joshi, L.J. Schreiner and A.T. Kerr, *Kingston Regional Cancer Centre and Queen's University* — Tomotherapy is a technique for delivering Intensity Modulated Radiation Therapy based on a rotating fan-beam geometry, analogous to a CT-like delivery. The geometry is ideally suited for CT image acquisition for patient position verification. We have been investigating the feasibility of using a Co-60 source for CT imaging (Co-60CT) in the context of tomotherapy. We have observed that Co-60CT images lack beam-hardening characteristics and thus offer a potential advantage in dose reconstruction analysis. As part of our effort to more carefully quantify this behavior, and to design an optimal detector for Co-60CT imaging, the goal of this work is to model the fluence spectra for our Co-60CT benchtop pencil-beam (1x1cm²) and fan-beam (1x30cm²). The BEAMnrc Monte Carlo code was used to model a realistic Co-60 source and associated collimation and patient geometries. The fluence spectra were scored at the imaging detector plane with and without a typical patient in the beam. In-air simulations (no patient in the beam) yielded spectra with fairly evenly distributed low energy components, forming 30 % of the total fluence. The pencil beam collimator had no significant effect on the in-air spectrum compared to a broad beam. When the beam passes through a typical patient the total low energy component of fluence changes, as does the relative contribution of scatter, depending on the shape and size of the beam. Details of these simulations will be presented. The results obtained from this work form a strong basis for future work designing an optimal detector for Co-60CT imaging.

MO-POS-138

Gantry Angle Optimization for Conventional Radiotherapy*, Peter Potrebko and B. McCurdy, *CancerCare Manitoba/The University of Manitoba* — In conventional radiotherapy, the incident beam orientations are often determined using a manual trial and error search and may not be truly optimal. A fast, 3D-geometric-based optimization algorithm for gantry angle selection is proposed. The algorithm is interfaced with the Pinnacle³ treatment planning system to extract patient contour data. The voxels contained in a particular patient structure are uniquely identified with a tagging index allowing the determination of which structure each voxel is attributed to. The radiation portal is defined by the Beams-Eye-View perspective of the planning target volume (PTV). Each beam portal is divided into a grid of beamlets. A score function is used to measure the 'goodness' of each beamlet at a given gantry angle. The overall score of the beam angle is given by a sum of the scores of all beamlets. The score function contains geometric factors that are taken into account in radiation therapy treatment planning. Such factors include: maximizing irradiation of the PTV, minimizing irradiation of the Organs-At-Risk (OARS), the depth of the OARS with respect to the PTV (avoiding irradiation of OARS upstream of the PTV), minimizing irradiation of other normal tissue both upstream and downstream of the PTV, the incidence angle of the beam (perpendicular incidence is favourable because it creates less skin reaction), and the separation angle of the beams. Once the algorithm populates the solution space, the optimal orientations are input into the Pinnacle³ treatment planning system. Optimal solutions are presented for phantom and patient examples.

* This work is being supported by NSERC

MO-POS-139

Measurement of Beam-Spot Size for Siemens Linear Accelerators, Collins Yeboah, P. O'Brien and G. Pang, *Toronto-Sunnybrook Regional Cancer Centre* — The goal of intensity-modulated radiotherapy is to minimize the volume of normal tissues irradiated to high doses so that the tumour dose may be escalated without increasing normal tissue complications. This necessitates precise localization of tumour and adjacent sensitive structures just prior to delivery of each treatment fraction. To accomplish this, megavoltage cone-beam CT (MV-CBCT) has been proposed for repeatedly imaging and guiding patient positioning throughout the entire course of treatment. For this to be clinically feasible low doses (<5% of treatment dose) must be used for each imaging session. Consequently, stability of the beam-spot size and position during the first few seconds after beam start-up becomes crucial. Therefore, measurement of beam-spot size and motion, assessment of their effects on low-dose MV-CBCT, and methods for minimizing them are of interest. In this work, measurements of the beam-spot size in the two principal planes were performed on a number of Siemens linacs using 20-cm long laminated beam-spot camera and verification films. The measured beam-spot diameters (FWHM) range from 2.0-3.4 mm. In all cases, the in-plane spot size was equal to or larger than the corresponding cross-plane spot size. For machines of the same design, the spot sizes were, in general, not identical but differences of up to 0.7 mm were observed. Comparison of measurements on the old and newer models of the linacs showed that the spot sizes for the latter are not necessarily sharper. For a given dual-energy linac, the spot sizes for the two energies were found to be similar.

MO-POS-140

An Intuitive Algorithm for Converting Electron Beam Ionization Measurements to Absorbed Dose*, Myron Rogers and L.J. Schreiner, *Kingston Regional Cancer Centre* — In medical physics, electron dosimetry with ionization chambers tends to be complicated since the energy spectrum changes so rapidly as electrons travel through a medium. Of particular concern in dosimetry is the depth dependence of the mean restricted stopping power ratios (SPR) between air and water $(L/p)_{air}^w$ that results from this energy loss. Early protocols for electron dosimetry attempted to account for this by correlating the SPR with beam energy for depths in water, although the average beam energies were either crudely estimated using the Harder equation, or lost within look-up tables. Furthermore, the approximations provided by these approaches weren't sufficiently accurate, therefore, current dosimetry protocols (the AAPM TG-51 and the IAEA TRS-398) now use a universal fit to Monte Carlo data to determine the SPR. In this work, we revisit the energy dependence of an electron beam in water using historical work and current modelling within the BEAM/egsnrc Monte Carlo program. We determine the full energy spectra at depth for various monoenergetic beams from 4 MeV to 40 MeV impinging on a water phantom. We show that the complications in some of the earlier approaches arise from the differences in the spectra for beams that have similar average energies. However, with a small correction determined from the initial beam energy, one can approximate the SPR at any depth from the average electron beam energy at that depth.

* This work is being supported by ORDCF (OCITS).

MO-POS-141

Unsettling Behaviour: Pre-irradiation Effects and Long-term Stability of Ionization Chambers, John McCaffrey¹, M. McEwen¹, D. Niven², B. Downton¹ and H. Shen¹, ¹ *National Research Council (NRC)* and ² *Carleton University* — Dosimetry protocols recommend that ionization chambers be pre-irradiated until a stable reading is obtained. Previous studies have shown that a lack of any pre-irradiation could result in errors up to several percent. Recently, data collected for a large number of commonly used ion chambers at the Institute for National Measurement Standards, NRC, Canada and the National Physical Laboratory, UK, have been collated and analysed. With such a data set it is now possible to relate patterns of ion chamber behaviour to design parameters. While several mechanisms seem to contribute, the most obvious correlation relates the extent of collector electrode shielding to settling time. Ion chambers with guarded electrodes up to the active air volume settle quickly (~6 minutes) and the change in response is less (up to 0.2%). For ion chambers where the guard connection around the central collector electrode does not extend up to the active air volume, settling times of 20 minutes (with an associated change in response of up to 1%) are typical. This settling time is not dependent on beam quality. This settling data was combined with a study of long-term stability and it was found that there was no correlation between settling behaviour and stability of response, and a change in settling behaviour was no predictor of chamber failure. The air-kerma to absorbed dose ratio, C_k , is shown to be a very sensitive parameter for monitoring ion chamber response.

MO-POS-142

Fractal Quantification of the Architectural Complexity of Computer Simulated Vasculature, Brian Lim¹ and Ivan Yeung^{1,2}, ¹ *Department of Radiation Physics, Princess Margaret Hospital* and ² *Department of Radiation Oncology, University of Toronto* — It is well known that tumour vascular architecture differs greatly from that of normal tissue, tending to be quite tortuous with seemingly irregular spatial distribution. While the measurement of microvascular density (MVD) has been widely applied to many kinds of tumours, and is generally accepted as having prognostic value for long-term survival, it has been recently suggested that the fractal dimension (FD) is more useful for quantifying the complexity of tumor and normal vascular architecture. In contrast to MVD, which may only be a rough indicator of the complexity of vascular architecture in a 2D cross-sectional slice, the FD is a measure of the vascular network's topology when calculated on a 3D volume. However, the FD is usually measured on 2D sectioned slices. The correlation between the FD of 2D slices and the 3D vascular structure remains unclear, although it is hypothesized that higher 3D complexity should be reflected in the slice FD. The purpose of this computer simulation study was to investigate this hypothesis. Three-dimensional networks representing tumor and normal vasculature were simulated, and the architectural complexity of the resulting networks was then analyzed by calculating the FD. The FD was calculated for the 3D volumes and for orthogonal and oblique slices. The results showed that simulated tumour networks displayed consistently higher slice and volume FDs than for normal vasculature, demonstrating the robustness of the FD as a measure of vascular architecture complexity. The FD promises to be useful for validating functional imaging techniques being developed for vascular characterization.

MO-POS-143

Estimation of X-Ray Dual-Basis-Material Thicknesses from Multiple Energy-Bin Measurements, Yang Cai¹ and Paul C. Johns^{1,2}, ¹ *Dept. of Physics, Carleton University* and ² *Dept. of Radiology, University of Ottawa* — Detectors now under development, capable of counting xray photons and scoring the energy detected at clinical fluence rates, will

facilitate single-exposure dual-energy radiography and CT. The natural logarithm of the patient transmission at energy E is given quite accurately by $T(E) = A_\alpha \mu_\alpha(E) + A_\beta \mu_\beta(E)$, where A_α and A_β are the thicknesses of the equivalent basis materials a , b (e.g., poly methyl methacrylate, aluminum), and μ_α , μ_β are their linear attenuation coefficients. The crux of dual-energy radiography is to determine A_α , A_β for each pixel. Classically, measurements are made with two spectra and an empirical nonlinear transformation is made from the two log transmissions T_1 , T_2 to A_α , A_β . Suppose an energy-scoring detector measures a single spectrum and bins the events into energy intervals $\approx 1, 2, \dots, n$. $\log_2 n$ is the number of bits to which the detector must digitize the energies in real time. At the bin centres, $T_i = A_\alpha \mu_\alpha(E_i) + A_\beta \mu_\beta(E_i)$, $i=1, 2, \dots, n$. Algebraically, write $T=UA$, where T is a vector of length n , A is a vector of length 2 containing A_α , A_β , and U is an $n \times 2$ matrix. In the limit of infinitesimal bin widths, the basis thicknesses are $A=(U^T U)^{-1} U^T T$. In reality the bins are of finite width and the transmission $\exp[-(A_\alpha \mu_\alpha(E) + A_\beta \mu_\beta(E))]$, weighted by the incident spectrum, must be integrated over the bin. We use Taylor expansions of the transmissions about their values at the bin centres E_j . The linear terms in the expansion are sufficient for accurate determination of the basis material thicknesses. For an imaging task in which the patient is 18 cm soft tissue plus 2 cm bone and the final image is to have bone-tissue contrast suppressed, by sorting the transmission of a 140 kV spectrum into 8 bins one can obtain accuracy of 2.3 % in the pixel value. If 16 bins are used, 0.50 % is achieved.

MO-POS-144

Projection Imaging of Plastic Materials using Coherently-Scattered X Rays, Mohammad Nisar¹ and Paul C. Johns^{1,2}, ¹Dept. of Physics, Carleton University and ²Dept. of Radiology, University of Ottawa - The conventional x-ray imaging technique based on the transmission of primary photons works well to distinguish between hard and soft tissues. To distinguish between different kinds of soft tissues the scatter x-ray imaging technique can be used. Low-angle scattered photons can only be distinguished from primary on the basis of direction and consequently a well-collimated x-ray system is required. A hexagonal array of seven pinholes, each with a diameter of 1.5 mm, has been designed and tested to record the diffraction patterns of homogeneous plastic phantoms and of phantoms comprised of slabs of different plastics in a water tank. The phantom materials are amorphous solids and result in rotationally-symmetric diffraction patterns which are characteristic of the materials. The intensities of the diffraction patterns are numerically integrated over concentric rings and the scatter images are made by assigning the ring sums as the pixel values. A finite size (5 x 5 x 5 cm³) water tank containing plastics is scanned to make the scatter images. For these measurements the tube is operated at 100 kV and 800 mAs. A storage phosphor image plate is used to record the scatter patterns. The ultimate goal is to make scatter images of different kinds of tissues for better diagnostic information.

MO-POS-145

Energy-Dispersive Technique to Measure X-Ray Scattering Form Factors over a Wide Momentum Transfer Range, Ziaul Hasan¹ and Paul C. Johns^{1,2}, ¹Dept. of Physics, Carleton University and ²Dept. of Radiology, University of Ottawa — In some particular diagnostic x-ray exams such as neuroradiology and breast imaging, scattered radiation can give more information than conventional transmission imaging. To optimize a scatter imaging system, it is required to know the coherent scattering form factors of biological materials. An energy-dispersive form factor measurement technique has been developed. It uses a geometry that consists of an x-ray tube, target, and high purity germanium detector. The tube and detector are kept fixed and the target is moved transversely to get the desired scatter angles. Geometry was optimized by analyzing the variation of scatter angle with the dimensions of the extended target and with other geometric parameters. To develop the technique, coherent form factors in the range 0.15 nm⁻¹ to 11.87 nm⁻¹ of the momentum transfer parameter $\chi = \lambda^{-1} \sin(\theta/2)$ were measured for lexan, poly methyl methacrylate, polystyrene, polyethylene, nylon, and water. The scatter angles as obtained by geometry optimization and the respective x-ray spectra used were 1.32°, 86 kV; 3.13°, 106 kV; and 15.41°, 121 kV. Weighted averaging was done at the two overlapping regions of the three form factor datasets to get one continuous dataset. Comparison of our data with published data obtained by the angle-dispersive technique using a powder diffractometer shows that the energy-dispersive technique can be used as a substitute for the angle-dispersive technique.

MO-POS-146

An Improved Volumetric (3d) Look-Locker Imaging Method for Longitudinal Relaxation Time (T1) Estimation, Ken Nkongchu, G. Santyr, Carleton University — A three-dimensional (3D) Look-Locker imaging pulse sequence employing a segmented acquisition of k-space with an improved accuracy in the estimation of the longitudinal relaxation time, T_1 , was achieved in this study. To achieve adequate signal-to-noise ratio (SNR), the conventional 3D Look-Locker imaging sequence presented uses a large number (> 150) of small angles of only about 5° and a constant inter-pulse timing through out the image acquisition. In this study, a novel modification of the 3D Look-Locker imaging sequence is described where the inter-pulse timings are not constant. This variable inter-pulse timing allows for the inclusion of an intermediate recovery timing variable, and permits use of tip angles as large as 15° in the k-space acquisition, thereby improving the SNR. The T_1 accuracy of the method was tested for a phantom containing Gd-DTPA doped water with T_1 values varying between approximately 300 ms and 1700ms. For a 10° tip angle, T_1 accuracy was found to be within 3 % compared to conventional inversion recovery estimates. This compares favourably with an accuracy of only 11 % for the conventional 3D Look-Locker imaging sequence using an optimal 5° tip angle pulse.

MO-POS-147

Assessment of Phototimer Operation, Harry Johnson¹, L. Kurjewicz¹ and C. Neduzak², ¹University of Winnipeg and ²CancerCare Manitoba — Phototimer systems provide automatic exposure control (AEC) to terminate the imaging exposure of a diagnostic x-ray beam. Proper functioning of the AEC system is essential to control x-ray image exposure, both for diagnostic image quality and patient dose. Quantitative assessment of the calibration and operability of the photo cells is needed but is time consuming and requires repeated films. Radiation Protection Services, a department of the Medical Physics Division of CancerCare Manitoba regulates x-ray safety and compliance in Manitoba. RPS has undertaken tests of a new quantitative digital tool to measure exposure to the x-ray imaging plane. The device consists of a cassette and a digital readout unit. The cassette contains the sensory components and is placed in the film plane – image plate plane. It measures the exposure (calibrated re mR) required to produce the image and hence also the imaging speed, independent of the processor (either film or computed radiographic plate). In a 400 speed system, the skin entrance dose for a chest x-ray is 0.11 mGy, effective patient dose is 0.03 mSv. This is the average for film systems in Manitoba. CR imaging is at lower speed, higher dose. Our findings indicate: (1) Calibrations of the left-centre-right photo cells vary; (2) Photo cells have been found inoperative, unknown to the technologists; (3) Speed of most film systems is at "400" plus; (4) Speed of CR systems is approximately "200". Data will be provided of the results of surveys and the review will include service-related discussions.

MO-POS-148

Standards for Quality Control for Canadian Radiation Treatment Centres, Peter Dunscombe¹, Clément Arsenault², Jean-Pierre Bissonnette³, Harry Johnson⁴, George Mawko⁵, and Jan Seuntjens⁶, ¹Tom Baker Cancer Centre, ²Hôpital Dr Georges-L. Dumont, ³Princess Margaret Hospital, ⁴CancerCare Manitoba, ⁵QeII Health Sciences Centre and ⁶Montreal General Hospital — The Canadian Association of Provincial Cancer Agencies (CAPCA) has begun a standardisation process for the establishment and maintenance of quality radiation treatment across Canada. A final draft of the "Standards for Quality Assurance at Canadian Radiation Treatment Centers" has been submitted, and the Canadian Organisation of Medical Physicists has been mandated to develop a series of appendices to this final draft to document national quality control standards for the equipment used in Canadian radiation therapy clinics. All documents use a standard format, thereby providing a unique consistency across the entire proposed quality assurance standard. Each document details quality control frequencies, tolerances, and action levels for the given equipment or modality. All quality control procedures echo, where applicable, accepted international standards, such as those endorsed by the AAPM or IPEM, or with other current publications. We have submitted the content of each quality control protocol for review by a recognized Canadian expert. Documents have been drafted so far for simulators, cobalt units, linear accelerator, dosimetry instruments, orthovoltage units, multi-leaf collimators, portal imaging systems, brachytherapy, and intensity-modulated radiotherapy, and will be made available through the COMP/CCPM web site. Other standards are planned for CT simulation, record-and-verify systems, radiosurgery, and prostate implants. These documents reflect the spirit of continuous quality improvement: clinics can use them as templates and revise test frequencies and tolerances based on accumulated evidence. We expect that, upon approval from CAPCA, federal and provincial regulations and accreditations bodies shall require compliance to these quality control standard.

MO-POS-149

The BioMedical Imaging and Therapy Beamline at the Canadian Light Source Inc, Colleen Christensen, Canadian Light Source Inc — The BioMedical Imaging and Therapy (BMIT) Beamline is a multidisciplinary, multiuse facility that is being proposed for the Canadian Light Source, Canada's National Synchrotron Facility. The BMIT Beamline will have two specific research uses, non destructive imaging of tissues and radiation therapy in living organisms. The total cost of this project will be approximately \$17M. Funding for this project will be obtained from the Canadian Foundation for Innovation, the provincial governments and charitable foundations. The BMIT Beamline is projected to be ready for operations in 2006.

Author Index / Index des auteurs

- ABDEEN, N., POS-102
 ABUSARA, Z., TU-A14-6
 ADAM, A.G., TU-P9-7
 AFFLECK, I., TU-P7-1, TU-P7-3
 AGGARWAL, J., WE-P8-3
 AGUIAR, J., TU-P8-4
 AHMED, N., TU-P1-2, POS-123
 AIMEZ, V., MO-A9-4
 AL-GHAZI, M., SU-P2-2
 ALEKSEJEVS, A., MO-P7-12
 ALVARADO-GIL, J., WE-A8-2
 AMLIN, S., POS-76
 ANAHORY, Y., MO-A9-8
 ANDREIOU C., WE-P5-3
 ANDREWS, G.T., WE-P4-4
 ANTONIOW, J., WE-P6-4
 ARABSHAHI, H., POS-87, POS-88
 ARAUJO, C., POS-133
 ARCHAMBAULT, L., WE-A8-4, WE-A17-4, WE-A17-7
 ARCHIBALD, G., POS-80
 ARGUIN, L.P., TU-P7-5
 ARKANI-HAMED, N., TU-A2-1
 ARSENAULT, C., POS-148
 ARSENAULT, J., WE-A17-4
 ARZOUMANIAN, Z., WE-P15-3
 ASGEKAR, A., POS-39
 AUBIN, S., POS-78
 AURAG, H., TU-P7-5

 BACHER, A., MO-P8-3
 BACKER, D. C., POS-68
 BAESSO, M., WE-A12-3
 BAGNULO, S., POS-13
 BAILEY, A., MO-A7-1, POS-133
 BALALI-MOOD, K., POS-119
 BALLANTYNE, D., TU-A11-4
 BARBA, D., MO-A9-4
 BARBER R.C., WE-A11-4, WE-P1-1
 BARKANOVA, S., MO-P7-12
 BARMBY, P., TU-A6-2, POS-3
 BARNETT, R., WE-P2-1, WE-P2-2
 BARTEL, N., WE-A4-1, POS-58
 BASRAN, P., POS-127
 BATTISTA, J.J., TU-A3-3, TU-A3-4, WE-A5-4, WE-A17-1, WE-P8-1, WE-P12-6
 BAUMAN, G., SU-P6-5, WE-P8-1
 BAYLIS, W., TU-P11-1, POS-108
 BEACHEY, D., WE-A17-8
 BEASLEY, A.J., POS-12
 BEATON, D.A., MO-A9-1
 BEAULIEU, L., SU-P2-4, WE-A8-4, WE-A17-4, WE-A17-7, WE-P5-4, POS-126
 BECHHOEFER, J., MO-A7-5
 BECK, J., SU-P6-2, SU-P6-3, MO-A7-7
 BECKHAM, W.A., TU-A3-2, WE-P2-4
 BEDDAR, S.A., WE-A17-4
 BEER, G., POS-96
 BEKHECHI, S., TU-A7-4
 BENSIMON, D., MO-A5-1
 BERGAMASCO, R., TU-P10-4
 BERGERON, P., WE-P15-1
 BERGMAN, A., WE-A5-5
 BERNARD, J. E., TU-A14-5
 BERNDSEN, A., TU-A9-3
 BERNDT, A., SU-P6-1, SU-P6-2, SU-P6-3
 BERTRAND, O., POS-126
 BEYDAGHYAN, G., MO-A7-6, MO-A9-7
 BHAT, R.D.R., TU-A10-3
 BIDINOSTI, C.P., POS-118
 BIETENHOLZ, M.F., WE-A4-1, POS-58
 BIRCHALL, J., POS-117
 BIRD, C., TU-A9-5
 BISSONNETTE, J., POS-148
 BIZZOTTO, D., POS-120
 BJORK, S.R., POS-10
 BLACKMORE, E., TU-A12-4
 BLAGRAVE, K., POS-53

 BLAIS, N., SU-P2-1, WE-A5-2
 BLANK, B., WE-A11-4
 BLINDERT, K., POS-65
 BLUNDEN, P., MO-P7-12
 BOBOWSKI, J., MO-A7-7
 BOCCARA, C., MO-P9-1
 BOILEAU, M., MO-P15-3
 BOISVERT, P., MO-P13-5
 BOLINGBROKE, N.J., POS-12
 BONN, D., MO-P11-1
 BONO, G., POS-51
 BOOTH, R., TU-A6-1
 BOROWIEC, A., TU-A10-1
 BORRA, E.F., TU-P10-4
 BORYS, C., TU-A18-3, POS-62
 BOTTON, G.A., TU-A10-1
 BOUDREAU, C., WE-A11-4
 BOURGEOIS, M., TU-A13-7, TU-A13-8
 BRADLEY, M., WE-P9-3, POS-89
 BRADSHAW, J.P., POS-119
 BRAR, R., TU-A18-1
 BRAY, I., POS-72
 BRIDGES, G.E., TU-A12-6
 BRIEF, E., POS-80
 BRIGGS, M., WE-A12-4
 BRITTAIN, J.H., MO-A4-2
 BROEMELING, D., POS-120
 BRONSKILL, M., SU-P2-6, MO-A12-4, MO-P12, TU-P13-1
 BRONSVELD, P., WE-P4-3
 BROOKS, S., POS-40
 BROWN, C., MO-P7-6
 BROWN, J., TU-A17-1, TU-P13-3
 BRUCE, D.M., TU-A10-1
 BRUNER, B. D., TU-A10-2
 BRUNET, S., MO-P7-3, MO-P7-4
 BRUNT, C., POS-48
 BUCHINGER, F., WE-A11-4
 BUCHMANN, L., TU-A11-5
 BUCKLEY, L., WE-A5-3
 BUDIMAN, R., POS-90
 BUSTAMANTE, C., SU-A4-2
 BUYERS, W.J.L., MO-P11-4, POS-95
 BYUN, S.H., MO-P9-6

 CAI, Y., POS-143
 CALAMAI, P., MO-P6-1, MO-P12
 CALDWELL, C., POS-127
 CALLY, P. S., POS-25
 CAMERON, C., POS-9, POS-16
 CAMERON, G., SU-A1-2
 CAMERON, H., POS-27
 CAMERON, I.D., SU-A1-4, WE-A19-1
 CAMERON, R., POS-75
 CAMPAGNONI, A.T., TU-P2-2
 CAMPANELLA, O.H., POS-115
 CAMPBELL, J.M., TU-P8-2
 CAMPBELL, M., TU-P10-2
 CANHAM, P., MO-P9-7
 CARBERRY, D.M., SU-A4-1
 CARLONE, M., TU-P1-1
 CARRIER, J., WE-A17-7, POS-126
 CARRINGTON, M., MO-A10-1
 CARVALHO, P.A., WE-P4-3
 CASSIDY, D.T., TU-A10-1
 CAVAGLIA, M., WE-P10-1
 CHA, J., POS-118
 CHABOYER, B., POS-10
 CHAKRABORTY, T., TU-A13-1
 CHAMBERLAIN, M.J., MO-A4-3
 CHAMON, C., TU-P7-3
 CHAPMAN, D., WE-A14-2
 CHAPPLE, E., POS-118
 CHEN, A., SU-A1-3
 CHEN, J., WE-A5-4, WE-A5-6, POS-134
 CHEN, L., MO-A8-4
 CHENG, K.M., TU-A12-6

 CHENE, A., POS-11
 CHETTLE, D.R., MO-P9-6
 CHEUNG, P., WE-P12-2
 CHEVOBBE, S., MO-A9-4
 CHICOINE, M., MO-A9-4
 CHIN, L., SU-P2-5
 CHIRTOC, M., WE-P6-4
 CHOPRA, R., SU-P2-6, TU-P13-1
 CHOPTUIK, M.W., POS-105
 CHOW, J., WE-P2-1, WE-P2-2, POS-136
 CHRISTENSEN, C., POS-149
 CHRISTIAN, C., SU-P3-2, MO-A12-3, MO-P12
 CIGNONI, M., POS-51
 CLARK, B.G., WE-A17-5
 CLARK, J.A., WE-A11-4
 CLARKE, R., TU-P13-2
 CLARKSON, R., WE-A13-2
 CLAUSSEN, M.J., POS-12
 CLEMENT, B., POS-117
 CLINE, J., TU-A9-3
 CLOUTER, M.J., WE-P4-4
 COAD, T., WE-A5-6
 COHEN, M., POS-45
 COOPE, R., POS-120, POS-124
 COOPER, J., TU-P9-3
 CORRIVEAU, F., TU-P5-3
 CÔTÉ, C., WE-P4-5
 COTE D., MO-P7-4, MO-P9-5
 COTE, M., TU-A7-1
 CÔTÉ, R., TU-A13-2, TU-A13-3
 COUILLARD, M., TU-A10-1
 COWAN, M., TU-A10-2
 COWLEY, R.A., POS-95
 CRABTREE, D., POS-1, POS-64
 CRAIG, N.C., TU-P9-8
 CRAIN, J. N., MO-A9-5
 CRANMER-SARGISON, G., TU-A3-2, WE-P2-4
 CRAWFORD, J.E., WE-A11-4
 CRAWFORD, T.H.R., TU-A10-1
 CROSS, A., TU-A16-1, POS-102
 CROUCH, A., POS-25
 CROWTHER, P.C., POS-17
 CUNHA, M.S., POS-9
 CUNNINGHAM, I., WE-P8-1, WE-P12-6
 CZARNOTA, G.J., TU-A16-5, TU-P13-6

 DA SILVA, L., TU-P10-4
 DAHN, D., TU-P8-2
 DARKO, J., POS-137
 DAS S., WE-P10-1
 DASGUPTA, A., WE-P10-5
 DATTA, A., TU-P6-4
 DAVID, L., TU-P6-4
 DAVID, N.A., POS-118
 DAVIDGE, T., TU-P10-1
 DAVIDSON, S.R.H., SU-P2-5
 DAVIES, R.L., POS-57
 DAVIS, C.A., POS-117
 DAVIS, G.R., POS-43, POS-45
 DAVIS, P., POS-6
 DAVIS, S., POS-51
 DAWSON, P., TU-P12-1
 DE HOSSON, J.M., WE-P4-3
 DE MELLO, D.F., POS-56
 DEAN, C., WE-P4-2
 DEMOREST, P., POS-68
 DENHOFF, M.W., WE-P7-1
 DENNISTON, C., TU-P4-2
 DENT, W., POS-45
 DEROBERTIS, M.M., TU-P12-1, POS-28
 DESJARDINS, P., MO-A9-4
 DEUPREE, R.G., POS-21, POS-22, POS-26
 DEUTSCH, I., POS-107
 DICK, R., TU-P6-5
 DIFRANCESCO, J., POS-6, POS-50
 DILLING, J., WE-A11-3
 DINGFELDER, J.C., MO-P7-4

- DION, C., MO-A9-4
 DOBIAS, P., WE-P9-4, POS-38
 DOBROVOLNY, H., MO-P9-3
 DOIRON, C., TU-A13-2
 DONG, R.Y., POS-83
 DONG, X., POS-28
 DOUGHERTY, S., POS-12
 DOUGLAS, K., TU-P12-2
 DOWNEY, D.B., TU-A16-6
 DOWNTON, B., POS-141
 DRAKE, G., TU-P9-1
 DRISSEN, L.D., POS-17
 DROUIN, D., POS-13
 DUBÉ, P., TU-A14-5
 DUBINSKI, J., WE-P3-1
 DUGUAY, M., POS-112
 DUNCAN, M.J.D., WE-P11-3
 DUNSCOMBE, P., POS-148
 DURANT, M., POS-29, POS-32
 DUROUCHOUX, P., POS-33
 DUTTA, B., TU-P6-1
 DUZENLI, C., WE-A5-5
 DWYER, J.R., WE-A16-4
- EDERY, A., TU-A8-4
 EDWARDS, L., POS-54
 ELLINGSON, E., POS-65
 ELMEHDI, H., POS-82
 ELSAESSER, T., TU-A10-2
 EMBERLY, E., WE-A9-3
 ENGLISH, J., POS-55
 ENS, W., TU-P2-3
 ESSLER, F.H.L., TU-P7-1
 EVANS, A., POS-45
 EVANS, D.J., SU-A4-1
 EXTAVOUR, M., POS-78
- FAHLMAN, G., WE-P15-1, POS-51
 FALK, W., POS-117
 FALLONE, B.G., SU-P6-4, MO-A4-1, TU-A3-1, TU-A16-3, WE-P12-5, POS-128,
 FAN, Y., MO-P9-2
 FARIBAULT, A., TU-A13-3
 FARRELL, T.J., SU-P2-3, WE-P2-3
 FAUST, A., MO-P15-4
 FAZIO, G.G., TU-A6-2
 FEDOSEJEVS, R., WE-A16-2
 FENSTER, A., TU-A16-6, WE-A3-1, WE-P8-4
 FERDMAN, R., POS-68
 FERDOUS, S., TU-A7-7
 FERGUSON, G., MO-P9-7
 FERTIG, H.A., TU-A13-3
 FICH, M., POS-4, POS-5, POS-67
 FIEGE, J., MO-P15-2
 FIELD, G. C., SU-P6-4
 FINK, M., MO-A7-8
 FINLAY, H. ., MO-P9-7
 FISHER, R., TU-P2-2
 FLEMING, D.E.B., TU-P1-2, POS-123
 FORDE, N., SU-A4-2
 FORTIER, T., WE-A16-1
 FORTIN D., MO-P7-7
 FOSTER, F.S., TU-P13-3
 FOSTER, T., POS-41
 FRAIL, D. A., WE-A4-1
 FRANZ, M., MO-P11-2
 FRASER, S.E., TU-P2-2
 FREEMAN, K.C., POS-55
 FREIRE, P.C.C., WE-P14-2
 FRISKEN, B., MO-A7-1
 FRITZSCHE, H., POS-95
 FUJIWARA, M., WE-A11-6
 FULLER, G., POS-45
 FUNG, A., WE-A17-8
- GAGNON, O., MO-A10-4
 GALE, C., MO-A10-2
 GALIANO, E., MO-A4-5, MO-P15-5, TU-P8-4, POS-131
 GALINDO-URIBARRI, A., WE-P5-1
 GALLAGHER, M.C., MO-A9-5, MO-A9-6
- GAMBLE, L., SU-P2-3
 GARCIA J., TU-A12-1
 GARROW, K., TU-P5-8
 GAUTHIER, D.J., MO-P9-3
 GAUTHIER, J., MO-A8-5
 GENERT, C., TU-A13-4
 GHAZI, M., POS-87
 GHEZELBASH, M., WE-A13-2
 GHOSE, S., POS-104, POS-107
 GIBSON, B., WE-P15-1
 GIBSON, S.J., WE-P14-1
 GILES, A., TU-A16-5, TU-P13-6
 GILLIS, C., POS-97
 GINGRAS, L., TU-P10-4, WE-A8-4, WE-A17-4, WE-A17-7
 GINGRICH, D., MO-A8-4
 GLADDERS, M., TU-A18-2, POS-65
 GLADWISH, A., SU-P6-5
 GOLDMAN, S., WE-A5-4
 GOM, B.G., POS-43
 GONZALEZ, M., POS-30
 GORDON, M.L., TU-A16-2, TU-P1-3
 GORDON, R., MO-A4-4
 GRAHAM, K., WE-A10-1
 GRATTON, Y., SU-P4-2
 GREGOIRE, T., TU-A9-4
 GRIFFIN, A., TU-A14-4
 GRIGOROV, G., WE-P2-1, WE-P2-2
 GRINYER, G., WE-P5-5
 GRINYER, J., MO-P9-6
 GRYC, W.K., POS-18
 GUAY, E., POS-110
 GUENTHER, D.B., POS-9
 GULICK, S., WE-A11-4
 GUMPINGER, P., WE-P5-7
 GUO, X., TU-A12-1
 GUREVICH, Y., TU-A12-2
 GWINNER, G., MO-P8-2
- HA, B., SU-A4-3
 HACHÉ, A., WE-P7-2
 HACKMAN, G., WE-P5-2
 HAHN, J., POS-8
 HADOK, G., WE-P8-1, WE-P12-6
 HALLEN, H., TU-A12-3, TU-P8-3
 HALLIN, E., WE-P8-2
 HALPERN, M., POS-6
 HAMMOND, R., MO-P9-7
 HANSEN, B., WE-P15-1
 HARDY, J.C., WE-A11-4
 HARMON, T.J. WE-A11-5
 HARPER, R.L., TU-P8-2
 HARRIOTT, T.A., POS-111
 HARRIS, G., TU-P14-1
 HARRIS, W., SU-A1-3
 HARRIS, W.E., POS-64
 HARROUN, T.A., MO-A7-2, MO-A7-3, MO-A7-4
 HARROWER, C.T., POS-116
 HASAN, Z., POS-145
 HASINOFF, M., MO-P8-4
 HAUGEN, H., TU-A10-1
 HAYDEN, M. E., POS-80, POS-118
 HAYWARD, J.E., SU-P2-3, TU-P1-3
 HEBEISEN, C., WE-A16-4
 HEINZ, A., WE-A11-4
 HEPBURN, J., TU-A14-1
 HERBST, W., POS-18
 HERBUT, I., TU-P7-2
 HESSELS, J., WE-P14-2
 HESTER, J.J., WE-A4-1
 HEURTH, S., TU-A12-3
 HEWITT, K., TU-A13-6
 HIGGS, P., SU-A1-3, MO-P13-5
 HIGHT WALKER, A.R., TU-P9-4
 HILDEBRAND, W., MO-A7-9
 HILL, I., TU-P4-4
 HILL, K., POS-70
 HILTNER, T.D., TU-P2-2
 HIMPEL, F. J., MO-A9-5
 HIROSE, A., WE-P4-5, WE-P9-1, WE-P9-2
 HODEFI, D., POS-130
- HODGSON, R., POS-114
 HOEKSTRA, H., TU-A18-2, WE-P13-1
 HOLDOM, B., TU-A9-1
 HOLENSTEIN, R., WE-A16-2
 HOLMES, R. ., MO-A7-7
 HOLT, S., POS-33
 HOLTHAM, E., POS-120
 HOOPER, R., MO-A4-1
 HOPKINS, W.S., TU-P9-7
 HORELLOU, C., POS-56
 HOUGEN, J.T., POS-71
 HOULT, D., TU-P8-5
 HU, Q., TU-A14-1
 HUANG, J.-S., TU-A6-2
 HUBER, M., POS-16
 HUBERT, S., SU-P4-2
 HUDSON, M.J., POS-57
 HUMBLE, R., POS-7
 HUNT, J.W., TU-A16-4, TU-A16-5, TU-P13-6
 HUSAIN, V., WE-P10-2
 HUSE, N., TU-A10-2
 HWANG, U., TU-A11-1, POS-33
- IMAGAWA, D., SU-P2-2
 IRWIN, J.A., TU-A18-1
 IRWIN, S., MO-A9-5
 ITO, A., WE-P9-2
 IZHAKY, D., SU-A4-2
- JABBARI, K., WE-P12-3
 JACKSON, J., POS-45
 JACKSON, P., MO-P7-5, TU-A9-5
 JACOBS, R.E., TU-P2-2
 JAEGER, N., MO-P3-1
 JAEGER, W., TU-A14-2
 JALILEHVAND, F., WE-A14-3
 JENNESS, T., POS-45
 JENSEN, J.O., TU-P9-4
 JEWETT, M.A.S., TU-A16-4
 JOHNS P., POS-143, POS-144, POS-145
 JOHNSON, H., SU-P6-1, POS-147, POS-148
 JOHNSON, S., MO-A9-3
 JOHNSTONE, D., POS-43, POS-45
 JOLY, T., POS-131
 JONCAS, G., MO-P15-1
 JONES, G.W., TU-P1-3
 JOOS, B., TU-A7-5
 JORDAN, K., WE-A17-1
 JORDAN, R.E., WE-A16-4
 JOSHI, C.P., POS-137
- KAERN, M., MO-P13-2
 KALB, S., MO-P9-3
 KALIRAI, J.S., WE-P15-1, POS-51
 KARAKAS, A., POS-22
 KARLEN, D., MO-A8-3
 KARMOUCH, R., MO-A9-8
 KASPI, V. M., TU-P3-1, WE-P14-2, POS-30, POS-32, POS-34
 KATSARAS, J., MO-A7-2, MO-A7-3, MO-A7-4, POS-119
 KAWRAKOW, I., WE-A5-3
 KEDZIERSKI, W., POS-72, POS-76
 KELLER, B., WE-A17-3
 KEMPF, A., MO-P10-5
 KENNEDY, S., POS-136
 KENWARD, M., SU-P4-2
 KEOUGH, K.M.W., POS-81
 KERACHIAN, Y., TU-A10-3
 KERR, A.T., POS-137
 KERTON, C., SU-A1-2, POS-48
 KILFOIL, M., TU-P4-3
 KIM, S.P., WE-A13-3
 KIRKBY, C., WE-P12-4
 KLAASSEN, P., POS-50
 KNEE, L., POS-48
 KNOBEL, R., WE-A9-2
 KOBES, R., MO-P10-3, POS-106
 KOLIOS, M., TU-A16-5, TU-P8-1, TU-P13-4, TU-P13-6
 KORDAS, K., TU-P5-1
 KORIBALSKI, B., POS-55

- KORKMAZ, E., POS-117
 KOROL, R., MO-P9-7
 KOTHES, R., POS-39, POS-41, POS-47
 KOTLICKI, A., WE-A8-3
 KOTWAL, A., TU-P5-5
 KOVALTCHOUK, V., TU-A12-5
 KOWALEWSKI, R.V., MO-P7-7, TU-A9-5
 KPETSU, A., TU-A13-7, TU-A13-8
 KRASSOWSKA, W., MO-P9-3
 KRAUS, JR., R., MO-P9-4
 KRESS, A., MO-A4-1
 KREUZER, H., SU-A4-4
 KRIEGER, P., MO-A8-2
 KRON, T., SU-P6-5, TU-A3-5, WE-A5-6, WE-P8-1,
 POS-134
 KRULL, U., WE-A8-1
 KUMARADAS, J., MO-P9-4
 KUNKEL, H.P., WE-P4-6, POS-86
 KUNSTATTER, G., WE-A13-1
 KURJEWICZ, L., POS-147
- LACKER, H., MO-P7-7, WE-P15-2
 LACY M.D., WE-P15-2, POS-3
 LAFLAMME, R., MO-P10-1
 LAGACHE, G., POS-60
 LAGOWSKI, J., TU-A7-7
 LAI, A., POS-122
 LAINE, S., POS-3
 LAIRD, P., TU-P10-4
 LAKE, K., WE-A13-5
 LAMBERT, G., WE-A17-4
 LANDECKER, T.L., POS-47
 LANDRY, M., WE-P13-4
 LANDSTREET, J. D., POS-13
 LAOR, A., TU-P12-1
 LAPOINTE, J., WE-P7-1
 LAVALLÉE, M-C., TU-P2-4
 LAVIGNE, C., TU-A13-7, TU-A13-8
 LEAHY, D., POS-46
 LEBACH, D.E., POS-58
 LEBLANC, F., POS-24
 LECLAIR, R.J., MO-P15-3, TU-P1-4
 LECLERC, G., SU-P2-4
 LEDERMAN, J. I., POS-58
 LEE, J.K.P., WE-A11-4
 LEE, L., MO-POS-117
 LEE, T., TU-A9-2
 LEES R.J., POS-71
 LEES, R.M., TU-P9-8
 LEI, F., WE-P6-4
 LESSARD, R.A., TU-A13-7, TU-A13-8
 LESTRADE, J.-F., POS-58
 LEVAND, A.F., WE-A11-4
 LEWIS, R., MO-A10-3
 LI, M., TU-A13-3
 LI, W., WE-P4-6, POS-86
 LIAO, X., POS-76
 LIEBENDOERFER, M., POS-101
 LIM, B., POS-142
 LIPTAK, A., TU-P8-6
 LIU, Z., MO-A7-8
 LIVINGSTONE, M., POS-34
 LOCHHEAD, S., SU-P2-6
 LOCKWOOD, G.R., TU-P13-3
 LOLOS, G., TU-A12-5
 LOLY, P., SU-A1-8, TU-P11-4
 LOVAS, F.J., TU-P9-4
 LOVEKIN, C., POS-15, POS-21
 LU, J., MO-P7-13
 LU, Q., TU-P9-4
 LUCAS, A., MO-P9-7
 LUCEY, J.R., POS-57
 LUKOMSKI, M., POS-72
 LUNDGREN, B., WE-A11-4
 LYNE, A.G., POS-30
- MAARTENS, R., WE-P10-1
 MACASKILL, J.A., POS-72
 MACKENZIE, M., SU-P6-4
 MACTAVISH, C., POS-63
- MADDISON, S.T., POS-7
 MADEJ, A., TU-A14-5
 MAH, K., POS-127
 MAHAJAN, S.M., WE-P9-2
 MALHOTRA, R., POS-8
 MALYSZ, P.P., TU-P1-3
 MANCHESTER, R.N., POS-34
 MANDELIS, A., MO-P9-2, TU-A12-1
 MANN R. B., MO-A10-5, WE-A13-2, WE-P2-4
 MANOGUE, C., SU-A1-6
 MARCHENKO, S.V., WE-A4-2
 MARCHILDON, L., POS-110
 MARKO, J., SU-P4-1
 MARLEAU, F., POS-54
 MARLEAU, L., TU-P6-2
 MARMET, L., TU-A14-5
 MARTIN, J., MO-P8-5, WE-A11-2
 MARTIN, M., TU-P2-2
 MARTIN, P. G., WE-A19-3, POS-6, POS-53
 MARTINEZ-ORTEGA, J., POS-132
 MARZIALI, A., SU-P4-3, POS-120, POS-121, POS-124
 MARZLIN, K., POS-104
 MASON, A., TU-A6-1
 MASON, D., POS-133
 MASON, E., POS-13
 MATHESON, H., POS-37
 MATHEWSON, D., TU-P11-2, POS-103
 MATSUURA, N., WE-P7-3
 MATTHEWS, B., POS-49
 MATTHEWS, H., POS-45
 MATTHEWS, J., SU-A1-7, TU-A15-1, POS-9, POS-16
 MATZNER, C.D., TU-A11-2, POS-27
 MAWKO, G., POS-148
 MAZINI, R., TU-P5-2
 MCALISTER, S.P., WE-P7-1
 MCCAFFREY, J., POS-141
 MCCHESENEY, J.L., MO-A9-5
 MCCONKEY, J.W., POS-72, POS-76
 MCCURDY, B., TU-A3-6, WE-A5-1, WE-P12-1, POS-
 138
 MCDONALD, A., POS-123
 MCDONALD, M., SU-P2-6
 MCEWEN, N., POS-141
 MCGRATH, C., POS-72
 MCGUIRE, G., TU-P11-3
 MCKEE, B.T., MO-A4-3
 MCKENZIE, C., MO-A4-2
 MCKEON, D.G.C., MO-A10-5
 MCKINNON, W.R., WE-P7-1
 MCLACHLIN, S., MO-P7-8
 MCNABB, J.R., TU-P2-3
 MCNEIL, D., WE-P11-3
 MCNIVEN, A., SU-P6-5, TU-A3-5
 MEI, X., POS-129
 MERCURE, J-F., MO-A9-8
 MÉREL, P., TU-A13-7, TU-A13-8
 MEYER, J., MO-A9-3
 MICHAELIAN, K., WE-A12-1
 MIHAYCHUK, J., WE-P7-1
 MILDENBERGER, J., MO-P7-2
 MILLER, R.J.D., TU-A10-2, WE-A16-4
 MILLS, G.R., TU-A16-6
 MILNE M., SU-P3-4, POS-23
 MILOSEVIC-ZDIJELAR, V., SU-A1-1, POS-2
 MOVIC, V., POS-61
 MITCHELL, G.F., POS-52
 MIVILLE-DESCHÈNES, M., POS-60
 MOAZZEN-AHMADI, N., TU-A14-6, TU-P9-3, TU-P9-
 5, TU-P9-6
 MOCHNACKI, S., POS-20
 MOFFAT, A., WE-A4-2
 MOISAN, J., MO-A8-6
 MOLDOWAN, A., POS-36
 MONAJEMI, T.T., POS-128
 MONDAT, M., SU-P2-1
 MONIN, D.N., POS-13, POS-24
 MOORE, G., MO-A10-4
 MOORE, R., TU-P5-6
 MORROW, M., POS-81
 MORTON, D., POS-19
- MOSSMAN, M.A., TU-P8-6, WE-A8-3
 MUKOVSKII, Y., WE-P4-6
 MULLIGAN, M., TU-A3-5
 MUNGER, D., POS-84, POS-135
 MUNGER, P., SU-P2-1, WE-A5-2
 MUNGER, R., TU-P10-3
 MURRAY, J.R., POS-7
 MURRAY, R.J., POS-76
 MUTUS, J., POS-76
 MYRSKOG, S., POS-78
- NAJMAIE, A., TU-A10-3
 NAKANE, J., POS-121
 NAKONECHNY, K., TU-A16-3
 NASTOS, F., TU-A10-3
 NAYLOR, D.A., POS-6, POS-43
 NEDELJKOVIC, S., POS-59
 NEDILKO, S., POS-91
 NEDUZAK, C., POS-147
 NELAN, J.E., POS-57
 NETTERFIELD, C.B., POS-59, POS-61
 NG, C.-Y., WE-P14-2
 NG, K., WE-A14-4
 NIBBERING, E.T.J., TU-A10-2
 NICE, D.J., POS-68
 NICO, A., WE-A17-8
 NIEH, M.-P., MO-A7-2, MO-A7-4, MO-A7-3
 NIELSEN, M., WE-A17-3
 NIEMINEN, J., POS-109
 NISAR, M., POS-144
 NIVEN, D., POS-141
 NKONGCHU, K., POS-146
 NODWELL, E., MO-A9-1
 NOIREAUX, V., MO-P13-3
 NYIRI, B., TU-P1-1
- O'BRIEN, P.F., WE-P2-6, POS-129, POS-139
 O'MEARA, J.M., TU-P1-2
 O'NEILL HURRY, H.J., WE-P11-1
 OELERT, W., MO-P8-1
 OESPER, D., SU-A1-2
 OHSAKI, S., WE-P9-2
 OKON, W., POS-64
 OLBERG, M., TU-A6-1
 OLCHANSKI, K., MO-P7-10
 OLIN, A., WE-P5-6
 OLIVER, D., TU-A12-6, POS-116
 OLIVER, M., POS-134
 OLIVER, R.A., MO-P9-3
 OLOFSSON, H., TU-A6-1
 OSER, S., MO-A8-1
 OSHIKAWA, M., TU-P7-3
 OSTAPIAK, O.Z., WE-P2-3
 OTTENSMEYER, F., MO-A12-1, MO-P12
 OTTO, K., WE-A5-5
 OUYED, R., POS-44, POS-50
- PAGE, D., WE-A13-3
 PAGE, J.H., MO-A7-7, MO-A7-8, MO-A7-9, POS-82
 PAGE, S.A., POS-117
 PAHRE, M.A., TU-A6-2
 PAN, X.Y., TU-A10-3
 PANG, G., WE-P2-6, WE-P12-2, POS-129, POS-139
 PAPANDREOU, Z., TU-A12-5
 PARKER, L., WE-P13-3
 PATERA, J., MO-P2-1, TU-A8-5
 PAUST, N.E.Q., POS-10
 PEARSON, M., WE-A11-1
 PEDRI, L., MO-A9-6
 PEEBLES, J., SU-KEY-1
 PEIZI, J., WE-P6-4
 PEL, J., POS-120
 PELC, N.J., MO-A4-2
 PELES, A., TU-A7-4
 PELES, S., TU-A10-4, POS-106
 PEN, U., POS-59
 PENA, F., POS-35
 PENNER, A., POS-106
 PERCY, J., SU-P3-3, POS-18
 PERERA, F., POS-134

- PERSSON, C., TU-A6-1
 PETIT, V. P., POS-17
 PETRE, R., POS-33
 PETRIC, M., WE-A17-5
 PETRYK, R., POS-105
 PIERCE-PRICE, D., POS-45
 PIKE, R., POS-66
 PISTORIUS, S., MO-A4-4, WE-A5-1, WE-P12-3
 PITCAIRN, J.R., MO-A7-9
 PIVOVAROFF, M.J., POS-30
 PIYADASA, G., TU-P2-3
 PLISCHKE, M., TU-A7-5
 PLUME, R., POS-50
 PLYUKHIN, A., MO-A7-10
 POIRIER, L., WE-P7-2
 POISSON, E., WE-A13-4
 POLOMSKA, A., WE-P4-4
 POLSON, J., TU-A7-6
 POPE, A., POS-62
 POPESCU, I. A., TU-A3-2
 POPESCU, T., WE-P2-4
 PORCELLI, T.A., POS-117
 POSPELOV, M., TU-A9-5
 POTREBKO, P., WE-A5-1, POS-138
 PRITCHET, C.J., POS-23
 PROVENCHER, R., TU-A13-7, TU-A13-8
 PYRAK-NOLTE, L.J., POS-115
- QUIRION, G., WE-P4-1
 QURAAAN, M., MO-P7-9
- RAAPHORST, G.P., TU-P1-1
 RAGAN, K., WE-A10-2
 RAGHUNATHAN, V.A., MO-A7-2, MO-A7-3, MO-A7-4
 RAJORA, O., POS-94
 RAMACHANDRAN, R., POS-68
 RAMSAY, W.D., POS-117
 RAND, T., POS-102
 RANSOM, R., POS-58
 RANSOM, S.M., WE-P14-2
 RAO, Q., MO-A7-6
 RASTEGAR-MOGHADDAM, H., MO-A9-3
 RATHEE, S., TU-A3-1, TU-A16-3, WE-P12-5, POS-128
 RATNER, M.I., POS-58
 RAYMOND, S., MO-A9-4
 REDDISH, T., POS-72
 REDHEAD, C., TU-P2-2
 REED, M.H., POS-122
 REEDER, S.B., MO-A4-2
 REID, J.C., SU-A4-1
 REID, M., POS-49
 REID, R., WE-A19-2
 REYES, S.D., TU-P2-2
 REZANIA, V., POS-38
 RICHER, H.B., WE-P15-1, POS-51
 RICHER, J., POS-45
 RICKEY, D., SU-A1-5, POS-122, POS-128
 RITCEY, A., TU-P10-4
 ROBAR, J.L., SU-P6-6, WE-A17-5
 ROBBIE, K., MO-A9-7, WE-P4-2
 ROBERT, C., POS-54
 ROBERTS, M.S.E., WE-P14-2
 ROBERTSON, S., MO-P7-11
 ROGERS, A., TU-P11-4
 ROGERS, D., WE-A5-3, WE-A7-1
 ROGERS, J., TU-A10-4
 ROGERS, M., POS-140
 ROLLIN, E., WE-A10-3
 ROMANI, R.W., WE-P14-2
 RONEY, J., MO-P7-1
 ROORDA, A., MO-A12-2, MO-P12
 ROSEI, F., WE-A9-1
 ROSHKO, R.M., POS-93
 ROSS, K., POS-115
 ROWE, D., TU-A8-3
 ROWE, J., POS-16
 ROWLANDS, J.A., WE-P2-6, POS-129
 ROY, R., SU-P2-4, MO-A8-6, WE-A8-4, WE-A17-4, WE-A17-7, WE-P5-7, POS-100, POS-126
- RUDA, H.E., WE-P7-3
 RUITER, A., POS-52
 RUTH, T., WE-P8-5
 RYAN, C., TU-P12-1
 RYAN, D., TU-P8-2
- SABIK, S., TU-P5-7
 SADEGHI, M., POS-87
 SADLIK, B., MO-A7-5
 SAFI-HARB, S., POS-31, POS-33, POS-36, POS-37, POS-39
 SAINT-AUBIN, Y., TU-P7-5
 SAJINA, A., WE-P15-2
 SAKR, J., POS-109
 SAMSON, J.C., WE-P9-4, POS-38
 SAMUELS, A.C., TU-P9-4
 SANDERS, B.C., MO-P10-2, WE-A11-5, POS-104, POS-107
 SANDERSON, R.J., TU-A13-6
 SANTYR, G., TU-A16-1, POS-102, POS-146
 SARKISSIAN, A., WE-P4-5
 SAWICKI, M., WE-A15-
 SCANLON, M.G., POS-82
 SCHADE, D., WE-A6-1, POS-57
 SCHALY, B., TU-A3-3
 SCHATZ, H., TU-A11-3
 SCHELLA, J., SU-P6-6
 SCHIETTEKATTE, F., MO-A9-4, MO-A9-8
 SCHNEIDER, D., MO-A7-6, MO-A9-7
 SCHOFIELD, J., MO-A7-10
 SCHREINER, L.J., WE-A17-2, POS-137, POS-140
 SCHROEDER, M.R., WE-P12-5
 SCHUMAKER, M., POS-98
 SCORA, D., WE-P2-5
 SCOTT, D., WE-P6-1, WE-P15-2, POS-6, POS-62
 SCOTT, H., SU-P3-
 SCRUTTON, P., POS-78
 SEABROOK, J., POS-77
 SEAQUIST, E., WE-A18-1
 SEARLES, D.J., SU-A4-1
 SECCOMBE, D.P., POS-72
 SEETZEN, H., WE-A8-3
 SENCHUK, A., POS-73
 SENKOW, S., TU-P10-4
 SEUNTJENS, J.P., WE-A17-6, POS-148
 SEVICK, E., SU-A4-1
 SHAPIRO, E., WE-A16-3
 SHAPIRO, I.I., POS-58
 SHARMA, K., WE-A11-4
 SHAW, C., WE-P2-4
 SHELUDKO, V., POS-92
 SHEN, H., POS-141
 SHEN, J., WE-A12-2
 SHENTON, D., POS-136
 SHEPARD, S., WE-P6-2
 SHERAR, M.D., TU-A16-4, TU-A16-5, TU-P13-6
 SHERIF, H., MO-A3-1
 SHIM, M., SU-P2-3
 SHIMAKAWA, A., MO-A4-2
 SHORLIN, K., MO-A9-2
 SHORT, I., POS-15
 SHULYATEV, D., WE-P4-6
 SIMARD, M., MO-P7-4
 SIMMONS, A., TU-A12-1
 SIMMONS, W., POS-113
 SIMON, R., POS-45
 SINGH, A., MO-A9-7, WE-P4-5, POS-89
 SINGH, M., MO-A7-6
 SINGH, S., POS-78
 SIPE, J., TU-A10-3
 SIWICK, B., WE-A16-4
 SIXEL, K., WE-P12-2
 SKANES, I. D., POS-81
 SLATER, G., SU-P4-2
 SLOBODA, R., WE-P12-4
 SMIRL, A.L., TU-A10-3
 SMITH, R., POS-57
 SNIATYCKI, J., TU-A8-2
 SNIJDERS, P., MO-A9-5
 SOER, W.A., WE-P4-3
- SOMAE, A., POS-87
 SONG, W., TU-A3-4
 SORESENSEN, E., TU-A7-2
 SORESENSEN, T.S., TU-P9-5
 SOUTHERN, B., TU-A7-4
 SPICER, V., TU-P2-3
 SPIROU, G., MO-P9-2, TU-P13-5
 ST-LOUIS, N.S., POS-11
 STAIRS, I.H., WE-P15-3, POS-68
 STAMP, P., MO-P10-4
 STANDING, K.G., TU-P2-3
 STANESCU, T., WE-P12-5
 STATT, B., TU-A13-5
 STECIW, S., TU-A3-1
 STEEDS, M., POS-117
 STEELE, T.G., MO-A10-5
 STELZER-CHILTON, O., TU-P5-5
 STEPHAN, W., POS-85
 STEVENS, M.J., TU-A10-3
 STEWART, J., POS-81
 STEWART, K., WE-A17-6
 STIL, J., POS-44
 STINNER, A., SU-A1-8
 STRASSER, S.T., WE-P14-1
 STROHMAYER, T.E., TU-A11-4
 STROINK, G., TU-P2-1
 SUENRAM, R.D., TU-P9-4
 SUKHOVICH, A., MO-A7-8
 SUN, J., POS-125
 SUN, P., WE-P7-3
 SUN, Y., MO-A7-1
 SUN, Z.-D., TU-P9-8
 SUNTZEFF, N.B., POS-57
 SURRY, K., TU-A16-6
 SUTHERLAND, M., MO-P11-3
 SUTTON, S., POS-72
 SWAIN, P., MO-P13-1
- TABISZ, G.C., POS-73, POS-75
 TAHIC, M.K., POS-43
 TALON, L., MO-A7-5
 TAM, C., POS-32
 TAMBASCO, M., WE-P2-6, POS-129
 TANG, B., MO-P13-5
 TARAS, P., MO-P7-4
 TAYLOR, A.R., POS-44
 TAYLOR, R., TU-P12-2, WE-P14-1
 TEEUWEN, J., POS-72
 THEWALT, M., SU-P1-1, TU-A5-1
 THOMLINSON, W., WE-A14-1
 THOMMES, E., WE-P11-2
 THOMPSON, R.I., WE-A11-5, POS-79
 THOMSON, D.J., TU-A12-6
 THORSETT, S.E., WE-P15-3
 THYWISSEN, J.H., POS-78
 TIEDJE, T., MO-A9-1
 TIPPER, J.M., TU-A13-4
 TIRONA, R., WE-P12-2
 TKACZYK, R., WE-A17-8
 TOKARYK, D., TU-P9-7, POS-77
 TOLKACHEVA, E., MO-P9-3
 TOPPOZINI, L., MO-A9-6
 TOURIN, A., MO-A7-8
 TRANNOY, N., WE-P6-4
 TREMBLAY, A., TU-P7-4
 TRENKA, T., WE-A5-6
 TRISCHUK, W., TU-P5-5
 TROTTER, H., TU-P6-3
 TRUONG, L., TU-P10-4
 TSUI, Y.Y., WE-A16-2
 TU, D., POS-128
 TUBIC, D., SU-P2-4
 TUN, Z., POS-95
 TUNIS, A., TU-A16-5
 TURNER, D., POS-14
 TYSZKA, J.M., TU-P2-2
- UMYSKOV, A.F., MO-A9-1
 UNRUH, W., WE-P10-4

- VACHON, B., TU-P5-4
 VALLÉE, A., POS-99
 VALLEE, J., POS-42
 VALLEJO, F., WE-P2-3
 VAN DER BIEST, F., MO-A7-8
 VAN DRIEL, TU-A10-3
 VAN DYK, J., SU-P6-5, TU-A3-3, TU-A3-4, WE-P8-1, POS-134
 VAN KERKWIJK, M.H., POS-29, POS-32, POS-35
 VAN OERS, W.T.H., POS-117
 VAN TIGGELEN, B., MO-A7-8
 VAN UYTVEN, E., MO-A4-4
 VAN WIINGAARDEN, W., TU-A14-3, POS-69, POS-72
 VENUGOPAL, N., TU-A3-6
 VIAUD, B., MO-P7-4
 VIDDAL, C., POS-93
 VIDELA, N., WE-A17-8
 VIGNEAULT, E., SU-P2-4
 VINCENT, A., POS-84
 VINCENT, L.A., POS-69
 VIRANI, S., TU-P12-1
 VIRTUE, C., WE-A10-4
 VITKIN, I.A., SU-P2-5, MO-P9-2, MO-P9-5, TU-A16-2, TU-P1-3
 VLAD, R., TU-P13-6
 VON HIPPEL, T., WE-P15-1
 VORONKOV, I.O., WE-P9-4
 VOS, K., TU-A13-4
- WADDINGTON, J., SU-A1-3
 WADE, G.A., WE-P6-3, POS-13
 WALLACE, M.L., TU-A7-5
 WALTON, M., TU-A8-1
 WANG, G.M., SU-A4-1
 WANG, X., POS-107
 WANLISS, J.A., WE-P9-4
 WARD, R.C. C., POS-95
 WARKENTIN, B., TU-A3-1
 WATSON, P., WE-A10-5
- WEBB, T., TU-A18-2
 WEBSTER, S., MO-A9-1
 WEFERLING, B., POS-45
 WEGNER, G.A., POS-57
 WEISS, W., POS-9
 WELLS, D., WE-P2-4
 WEST, J., SU-A1-4, WE-A19-1, POS-31
 WESTWOOD, T., MO-P13-4
 WHELAN, W.M., SU-P2-5
 WHITE, S., TU-A16-1
 WHITEHEAD, L., TU-P8-6, WE-A8-3, WE-P8-3, POS-120
 WHITMORE, M., TU-A7-3
 WHITTEN, B., MO-P16-1
 WHITTINGSTALL, K., TU-P2-1
 WICHOSKI, U., WE-P13-2
 WICKHAM, R., TU-P4-1
 WIEBE, F., POS-131
 WIEGERT, P., MO-A6-1
 WIEGERT, T., POS-56
 WIERZBICKI, W., SU-P2-1, WE-A5-2
 WIESENFELD, K., TU-A10-4
 WIGGIN, M., POS-121
 WILKINS, D., TU-P1-1
 WILLIAMS, G., WE-P4-6, POS-86
 WILLIAMS, J., POS-111
 WILLNER, S.P., TU-A6-2
 WILLOTT C., WE-A15-2
 WILLSON, L.A., SU-A1-2
 WILSON, B.C., TU-A16-2
 WILSON, C., TU-A6-1, POS-6, POS-40, POS-49
 WILSON, J., POS-133
 WIND, A., MO-A4-3
 WONG, E., POS-134
 WONG, J.C.Y., POS-18
 WOODLEY, K.A., POS-5
 WOOLGAR, E., WE-P10-3
 WORTHINGTON, A.E., TU-A16-4
 WU, X., TU-A16-4
- XIAO, C., WE-P4-5
 XU, J., WE-P4-4, POS-83
 XU, L.H., TU-P9-3, POS-71
 XU, L., TU-P9-4, TU-P9-8
- YAMANI, Z., TU-A13-5, POS-95
 YAN, Z., POS-74
 YANG, Q., WE-P4-5
 YANG, S., WE-P7-3
 YANG, V.X.D., TU-A16-2, TU-P1-3
 YARTSEV, S., WE-A5-6
 YEBOAH, C., POS-129, POS-139
 YEE, H., TU-A18-2, WE-A15-3, POS-65
 YEN, S., WE-P5-7
 YEUNG, I., POS-142
 YI, H., TU-A13-3
 YIN, A., WE-P4-4
 YOUNG, C.K., WE-P4-4
 YOUNG, E.C., MO-A9-1
 YU, E., WE-A5-6
- ZANGENBERG, N.R., MO-A9-1
 ZHENG, F., MO-A9-5
 ZAVGORODNI, S., TU-A3-2, WE-P2-4
 ZETNER, P., TU-P9-2
 ZHENG F., MO-A9-5
 ZHOU, F., WE-A9-4
 ZHOU, X.Z., MO-POS-86, WE-P4-6
 ZINKE-ALLMANG M., MO-A9-2

The Editorial Board welcomes articles from readers suitable for, and understandable to, any practising or student physicist. Review papers and contributions of general interest are particularly welcome.

Le comité de rédaction invite les lecteurs à soumettre des articles qui intéresseraient et seraient compris par tout physicien, ou physicienne, et étudiant ou étudiante en physique. Les articles de synthèse sont en particulier bienvenus.

**POSTDOCTORAL RESEARCH ASSOCIATE,
 UNIVERSITY OF VICTORIA**

The University of Victoria Particle Physics Group invites applications for a postdoctoral Research Associate position working on the ATLAS experiment at the CERN LHC. The ATLAS group at Victoria consists of 5 faculty members (Alan Astbury, Richard Keeler, Rob McPherson, Michel Lefebvre and Randall Sobie) making significant hardware and software contributions to ATLAS liquid argon calorimetry, and who are playing a leading role in the development of a computing grid for the analysis of ATLAS data in Canada. The current interests of the group include using upcoming ATLAS data challenges for developing, testing and deploying a large-scale Canadian computing grid, calibration and integration of the ATLAS calorimeter system using beam tests and preparation for ATLAS commissioning with cosmic rays and first beam.

The successful candidate will be expected to take a leading role in general software and computing grid development as well as ATLAS commissioning and physics studies. The candidate should have a PhD in experimental particle physics by the time of the appointment. Experience in particle physics computing, object oriented programming and computing grids would be an asset. The position will be initially based in Victoria with the possibility of relocating to CERN at a later date, subject to mutual agreement.

The candidate should send a CV and arrange to have at least three letters of recommendation sent to:

Professor Randall Sobie
 Dept. of Physics and Astronomy
 University of Victoria
 PO Box 3055 Stn Csc
 Victoria, BC, Canada V8W 3P6

Email: rsobie@uvic.ca

The application should be received by 1 June 2004 in order to ensure full consideration. All qualified candidates are encouraged to apply; however, in accordance with Canadian Immigration requirements, Canadians and permanent residents will be given priority.